bulletin 51

manual – textbook

fib
CEB-FIP

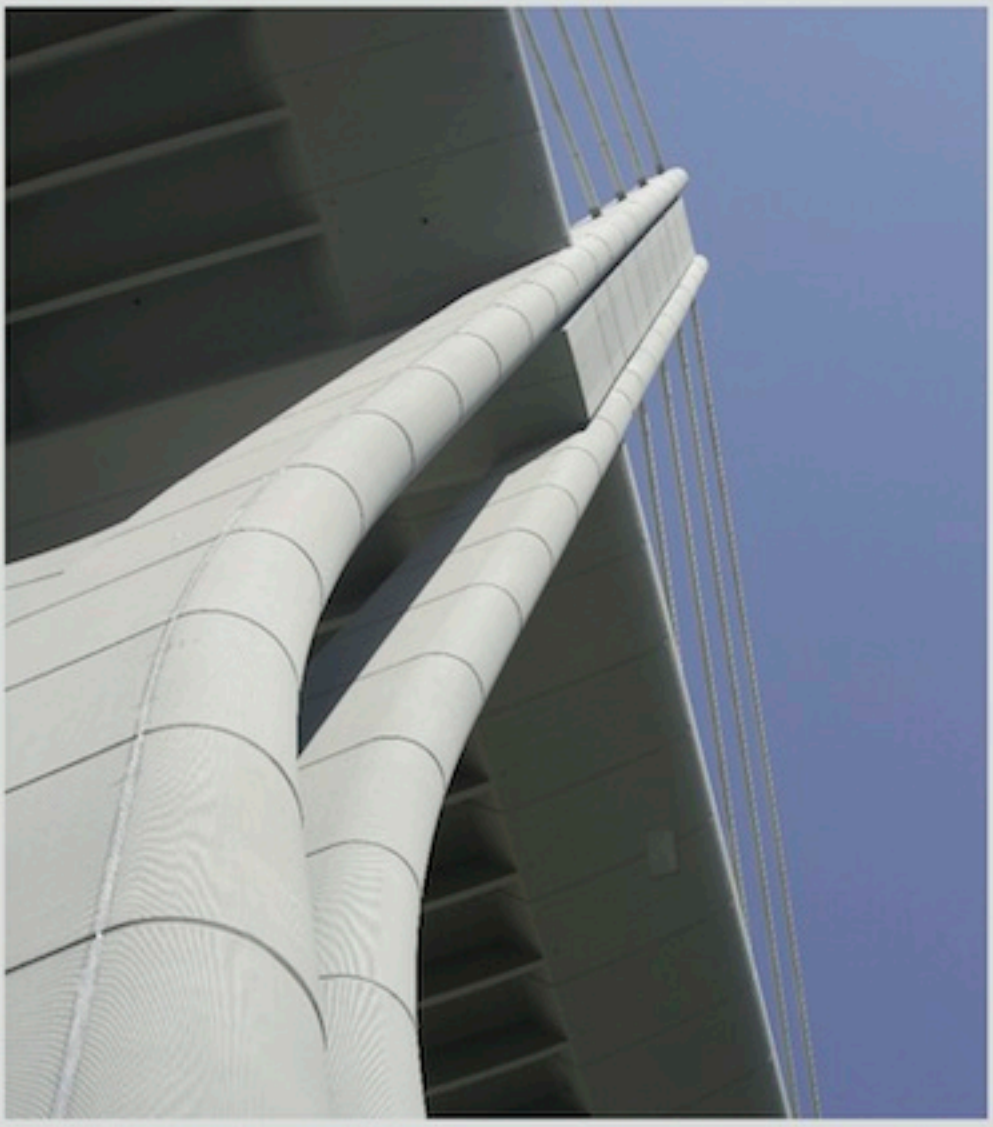

Structural Concrete

Textbook on behaviour, design and performance

Second edition

Volume 1

Structural Concrete

Textbook

on behaviour, design and performance

Second edition

Volume 1

November 2009

Subject to priorities defined by the Technical Council and the Presidium, the results of ***fib***'s work in Commissions and Task Groups are published in a continuously numbered series of technical publications called 'Bulletins'. The following categories are used:

category	minimum approval procedure required prior to publication
Technical Report	approved by a Task Group and the Chairpersons of the Commission
State-of-Art Report	approved by a Commission
Manual, Guide (to good practice) or Recommendation	approved by the Technical Council of ***fib***
Model Code	approved by the General Assembly of ***fib***

Any publication not having met the above requirements will be clearly identified as preliminary draft.

This Bulletin N° 51 was approved as an ***fib*** Manual by the Technical Council in June 2009.

This first volume of the Structural Concrete Textbook was drafted by the following authors:

György L. Balázs* (Budapest Univ. of Technology and Economics, Hungary)	Editor, Convener
Agnieszka Bigaj-van Vliet* (TNO, The Netherlands)	Sections 3.2, 3.3.1, 3.3.2
Hugo Corres Peiretti* (FHECOR/Polytechnic Univ. Madrid, Spain)	Chapter 2
Rolf Eligehausen* (Univ. Stuttgart, Germany)	Sections 3.2, 3.3.1, 3.3.2
Michael Haist (Univ. Karlsruhe, Germany)	Sections 3.1
Javier León (FHECOR/Polytechnic Univ. Madrid, Spain),	Chapter 2
Luis J. Lima* (Argentina)	Sections 3.3.1
Harald S. Müller* (Univ. Karlsruhe, Germany)	Sections 3.1
Alejandro Pérez Caldentey (FHECOR/Polytechnic Univ. Madrid, Spain)	Chapter 2
Norbert Randl (Carinthia University of Applied Sciences, Austria)	Chapter 1
José Romo (FHECOR)	Chapter 2
Joost C. Walraven* (Delft Univ. of Technology, The Netherlands)	Sections 3.3.3, 3.3.4, 3.3.5, 3.3.6
Manfred Wicke (Austria)	Chapter 1

* member of Special Activity Group 2, "Dissemination of knowledge", Working Group "Textbook".

Full address details of Task Group members may be found in the ***fib*** Directory or through the online services on ***fib's*** website, www.fib-international.org.

Cover image: Wadi Abdoun Bridge, Jordan, one of the winners of the 2010 *fib* Awards for Outstanding Concrete Structures [photo courtesy of Dar Al-Handasah (Shair & Partners)].

First published in 2009 by the International Federation for Structural Concrete (*fib*)
Postal address: Case Postale 88, CH-1015 Lausanne, Switzerland
Street address: Federal Institute of Technology Lausanne - EPFL, Section Génie Civil
Tel +41 21 693 2747 • Fax +41 21 693 6245
fib@epfl.ch • www.fib-international.org

ISSN 1562-3610
ISBN 978-2-88394-091-8

Printed by DCC Document Competence Center Siegmar Kästl e.K., Germany

Preface

The three volumes of "Structural Concrete: Textbook on behaviour, design and performance – Updated knowledge of the CEB/FIP Model Code 1990" inaugurated ***fib***'s series of Bulletins in 1999. The first ***fib*** President, Michel Virlogeux, noted in his Preface to these three Bulletins that: "... the decision to publish it first, as numbers 1, 2 and 3, is highly symbolic." Shortly after the dawn of the second decade of ***fib***'s life and the completion of its first 50 Bulletins, numbers 51, 52, 53 and 54 in the series are again devoted to the "Structural Concrete Textbook" in what appear at first sight as its "second edition".

The new volumes go far beyond the minor upgrade that a "second edition" normally entails. The scope and the structure are about the same as in Bulletins 1, 2 and 3, but the new edition contains a wealth of new information. Some chapters have been upgraded and updated, while others are almost fully new in content, reflecting the advances in our knowledge and technology during the past decade. As a matter of fact, some authors of the new edition have not resisted the temptation to go beyond what may reasonably be considered as background documentation of CEB/FIP Model Code 1990. Their chapters epitomise the modern thinking and knowledge that will go into ***fib***'s new Model Code, which is scheduled to appear in 2010 with a scope much wider than that of CEB/FIP Model Code 1990. In this respect the new Textbook presages ***fib*** Model Code 2010.

Like its predecessor, the new Textbook will be essential reading material for graduate students in the field of structural concrete, especially for doctoral ones at the outset of their research work. It will offer them the basics of material and structural behaviour and the fundamental knowledge needed for the design, assessment or retrofitting of concrete structures. It will also help designers and consultants in their quest to know what is behind the – often prescriptive – rules they apply in their everyday practice. In this respect the new Textbook will prove specially valuable to the users of the new European Norms EN 1992-1-1:2003, EN 1992-2:2005 and EN 1992-3: 2006 (i.e. Eurocode 2 for concrete buildings, bridges and container structures, respectively), which are based only partly on CEB/FIP Model Code 1990 and partly on more recent knowledge, not reflected yet in the 1999 edition of the Textbook.

The driving force behind the new Textbook has been György L. Balázs, who succeeded Manfred Wicke as chairman of SAG 2, "Dissemination of Knowledge", and is currently Deputy President of ***fib***. György persistently pursued the upgrade of the older version of chapters, or the drafting of new ones when the original version was out of date or its authors no longer available (as was often the case). Thanks and congratulations are also due to all contributing authors of the Textbook, new or old, for devoting their precious time to its completion, even more so because they have also been contributing at the same time to the draft ***fib*** Model Code 2010 and/or working in ***fib***'s Commissions and Task Groups. ***fib*** is most grateful to them all.

Michael Fardis
President, ***fib***

Editor's remarks

The ***fib*** *Structural Concrete Textbook on behaviour, design and performance* is a unique Textbook that has been written mainly by professors from various universities and some prominent experts from companies who are all strongly involved in the work of ***fib*** (International Federation for Structural Concrete).

The objective of the *Structural Concrete Textbook* is to give detailed information on a wide range of concrete engineering from selection of appropriate structural system as well as materials through design and execution and finally behaviour in use.

The *Structural Concrete Textbook* includes the following main areas:

(1) phases of design process, conceptual design, short and long term properties of conventional concrete (including creep, shrinkage, fatigue and temperature influences), special types of concretes (such as self compacting concrete, architectural concrete, fibre reinforced concrete, high and ultra high performance concrete), properties of reinforcing and prestressing materials, bond, tension stiffening, moment-curvature, confining effect, dowel action, aggregate interlock;

(2) structural analysis (with or without time dependent effects), definition of limit states, control of cracking and deformations, design for moment, shear or torsion, buckling, fatigue, anchorages, splices, detailing;

(3) design for durability (including service life design aspects, deterioration mechanisms, modelling of deterioration mechanisms, environmental influences, influences of design and execution on durability);

(4) fire design (including changes in material and structural properties, spalling, degree of deterioration), member design (linear members and slabs with reinforcement layout, deep beams); management, assessment, maintenance, repair (including, conservation strategies, risk management, types of interventions) as well as aspects of execution (quality assurance), formwork and curing.

The Textbook is directed to advanced studies of those who already have basic concrete engineering knowledge and would like to extend it. These can be both graduate students as well as practicing engineers.

The Textbook was prepared in the intermediate period from the CEP-FIP Model Code 1990 (MC90) to ***fib*** Model Code 2010 (MC2010). Therefore, we were able to incorporate a lot of information that has been already finalized for MC2010, while keeping some materials from MC90 that was not yet modified considerably.

Finally, I would like to express my gratitude to all of the authors of the Textbook for their very valuable work in preparing their contributions. In addition to them my special thanks are directed to Laura Thommen-Vidale at the ***fib*** secretariat in Lausanne for her careful work in finalizing the manuscripts, as well as to Dr. Éva Lublóy at my university in Budapest for providing me with continuous help. I should also recall here the very valuable editorial work done by Manfred Wicke and Norbert Randl when editing the first edition of this Textbook

I hope you will be able to use the *Structural Concrete Textbook* in your studies or work, and also that the *Structural Concrete Textbook* will help the use of both the ***fib*** Model Codes as well as the Eurocodes in related areas.

György L. Balázs, Editor
Convener, SAG 2, *Dissemination of knowledge*
Deputy-President, ***fib***

Contents

1 Design of concrete structures

by Manfred Wicke and Norbert Randl

1.1 Introduction

In the design process for an engineering project various groups of people are involved representing various disciplines. Teamwork and exchange of information are required to bring the project to a satisfactory conclusion within the given parameters. For engineering structures, such as bridges, power plants, chimneys, television towers or industrial facilities, the structural engineer usually leads the team. However, for buildings in general an architect will be the team leader and the structural engineer one of the consultants.

Many fundamental and basic decisions are taken during the initial design phase. Therefore, this stage will greatly affect the likely overall success of the project. The different disciplines should cooperate right from the beginning in order to discuss the requirements and determine a solution acceptable to all parties involved. Civil engineers must take an active part in this process, independent of whether or not they are the team leaders. The requirements of the structures which need to be designed must be well understood so that engineers can contribute to find the optimum solution. Especially in their collaboration with architects civil engineers need to take a proactive position in the improvement process of the initial proposal which often is drafted by the architects. The contribution of civil engineering to this process must be made with an open vision and an integral way of thinking in order to be able to develop the best structural concept for the specific problem, taking into account all aspects: structural typology, choice of materials, construction process, sustainability conditions, durability, maintenance and so on.

The following sections will outline the various aspects to be considered in the different design stages.

1.2 Sequence of activities in the design process

The *starting point* is the decision of a client to construct a civil engineering project to satisfy specified demands. Clients may be for example highway administrations, municipal agencies, insurance companies or private persons. Usually the client is assisted by an architect or an engineering consultant.

Primarily the requirements and needs of the client have to be identified. This may be achieved by discussions of the designing team with the client. At the end of this phase it should be clear how the requirements of the client can be satisfied in the form of buildings or engineering structures. Simultaneously, a feasibility study is needed to clarify the question of financing (payment schedule): financing by user fees (e.g. toll roads), general fund sources, private financing etc.

The *structural design process* is part of the entire design process and may be subdivided into the three stages *conceptual design, preliminary design and detailled design*. In each stage there are finite targets, influences and boundary conditions which should be kept in mind. In the following sections the different aspects in relationship to each phase are presented.

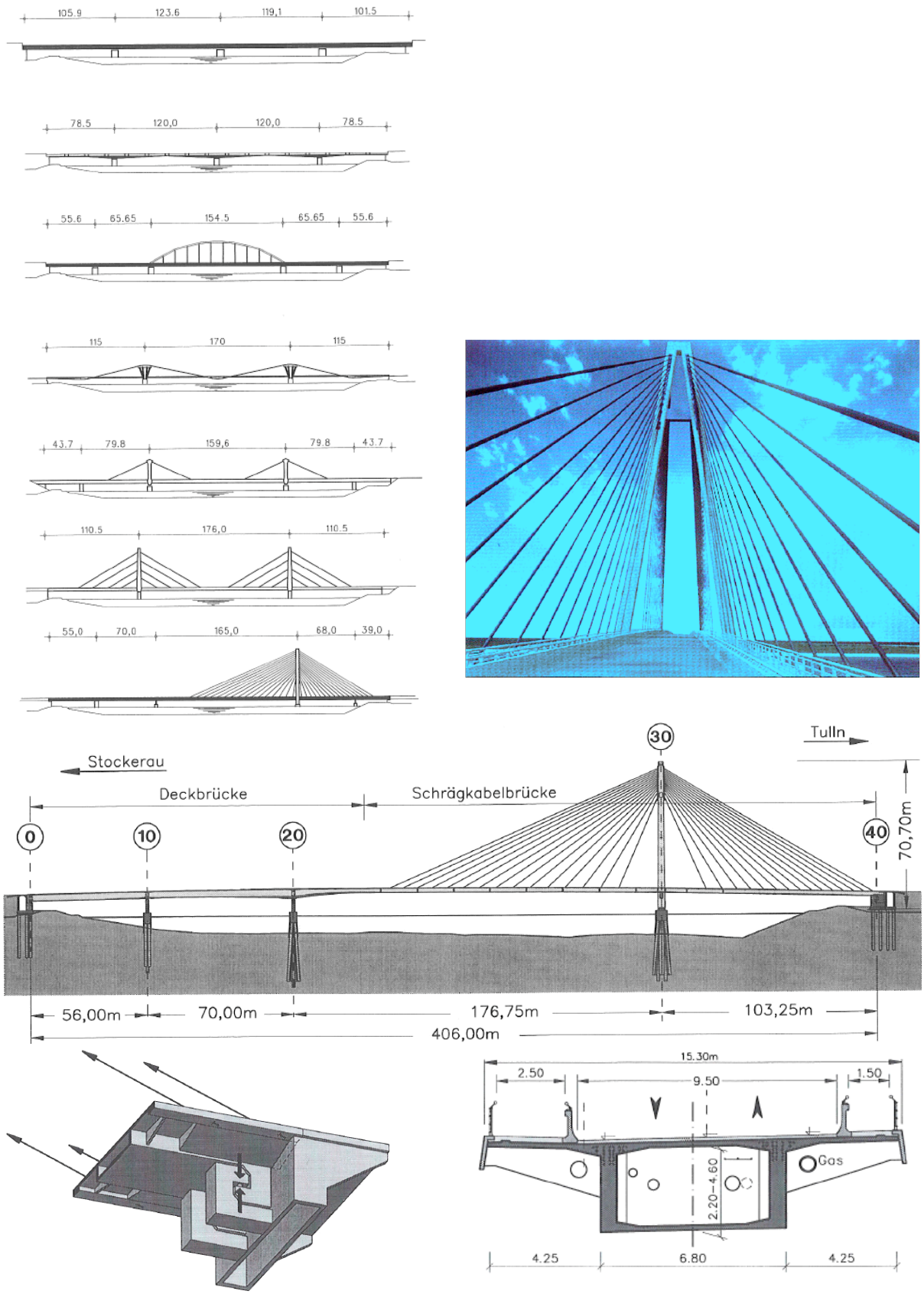

Fig. 1.1-1: Cable stayed bridge over the river Danube in Austria - From conceptual considerations (upper left hand side) to final concept (CAD-modelling upper right hand side) and detailing (central and lower pictures) (Pauser et al., 1996)

1.2.1 Conceptual design

Conceptual design can be defined as the stage in the design process where the basic decisions are made related to the nature and form of a structure. The phase of conceptual design is decisive for the quality of the work and a very important stage in design (therefore chapter 2 is dedicated to that process).

There are some main targets to be achieved in the conceptual design. Of course as a first aim the building or structure, respectively, must render its service well from the engineering point of view. In addition the design process is influenced by many different boundary conditions and interrelated external constraints which have to be satisfied:

- use and functionality;
- form and structural efficiency;
- aesthetics;
- environment (water, de-icing salt, noise, etc.);
- economy.

Economical efficiency has to be considered for the whole lifetime. This means not only low construction and life time costs but also low demolition costs. Depending on the kind of building expenses the following parameters have to be taken into account apart from the mere erection costs:

- maintenance;
- inspection, accessibility;
- repair (changing the structure or replacing elements which are deteriorated);
- replacing;
- demolition;
- recycling.

Therefore, lowest overall costs compared to the potential life expectancy of the work have to be considered and lower initial costs do not necessarily mean that the overall benefit/cost ratio will be enhanced. Nevertheless, economics alone should not be the decisive factor as shown in the following paragraphs.

Conceptual design should result in final decisions on:

- choice of materials [structural steel, reinforced and/or prestressed cast in place concrete (normal-/lightweight, HPC etc.), precast concrete systems, composite systems (steel girders and cast-in-place concrete components), timber (depending also on availability of the different materials)];
- layout of entire structure (structural system), including the definition of reasonable spans;
- layout and member size of important structural elements (reasonable structural dimensions may be determined from experience).

To achieve proper structural performance, from the point of view of analytical detailing, the following aspects have to be taken into account:

- structural configuration with respect to load bearing capacity (including how the form serves its structural purpose) and the stiffness of materials and structural members;
- joining together of superstructure and substructure (i.e. all elements required to support the superstructure like columns, piers, bearings);
- construction method and execution (speed of construction as a boundary condition, the method of construction has influence on the static system);
- flow of forces from the applied load to the foundation (it might be stated as a basic rule that heavy loads should be transferred to the foundations through the shortest path possible – although in a building grid the position of the column is predominantly determined by functional requirements);
- system stability, arrangement of bracing structures and lateral load transfer;
- construction joints, compartmentalization.

Successful conceptual design demands a high level of integral and cross-linked way of thinking, flexibility and engagement from all parties involved. Additionally there are numerous other requirements which can be summarised as follows:

- In general, extensive experience and a broad view of the design and construction process are required as the basis for being capable of regarding all aspects of a project.
- Knowledge of fabrication process and construction methods is expected as well as an understanding of the behaviour of the structure.
- An understanding of the economics of construction and the relative economy of different structural approaches is essential.
- Communication (including the ability to negotiate) and cooperation is required among members of the different disciplines. Respectful and solution-driven communication and cooperation between architects and engineers is desirable in this phase.

At the end of the conceptual design phase a solution should be identified which will be accepted by the client and the other parties involved in the design and construction. For this purpose a reasonable estimate of the total project costs should be possible at this stage.

1.2.2 Preliminary design

This phase of design is the stage where the chosen alternative is designed on a general level using preliminary calculations resulting in appropriate dimensions of members (firm definition of the mechanical and geometrical properties like steel sizes, reinforcement steel area etc.). The structural analyses are based on simplified reasonable models (see following sections) for the overall behaviour.

For the *preliminary design steps* checks for serviceability limit states (SLS) and ultimate limit states (ULS) are needed. SLS checks may be crucial for the entire structure and often govern the depth of slabs and beams. The load bearing capacity is verified by

- loss of equilibrium of the structure or any part of it, considered as a rigid body,
- failure by rupture, excessive deformation, or loss of stability of the structure or any part of it.

The level of sophistication of the calculations depends on the type of the structure and the degree of reliability. Normally at this stage linear elastic analysis with or without moment redistribution are carried out, as related to static behaviour. Simple checks on the basis of the theory of plasticity might also be useful in this phase. Although a computer is not necessarily required in the preliminary design phase, nowadays it will mostly be used right from the beginning resulting in a high level of accuracy. There is however also the risk that the unintelligent use of computer analysis from the beginning might result in poor understanding of the functioning of the structure.

Before starting with the calculations the engineer must carefully consider all relevant *loading* conditions. Referring to the effects on the structure one can distinguish between four kinds of actions: static, long term, cyclic or impact.

Considering the non-linear behaviour of a structure, the response is different according to direct or indirect actions:

- direct: loads and forces
- indirect: imposed or restrained deformations.

The identification of actions by variation in time leads to the following division:

- permanent (dead) loads: self weight of structural elements, self weight of non-structural elements, pressures due to earth or water, prestressing forces
- variable (live) loads: imposed loads, traffic loads, wind actions, snow loads
- accidental actions and hazards: seismic forces, impact, channel forces (stream flow, floating ice etc.), fire exposure
- imposed deformations and restraints: creep, shrinkage, settlement, uplift and thermal effects.

From the relevant combinations of actions, sufficient load cases are taken into account to enable the critical design conditions to be established at all sections within the structure or parts of the structure. The choice of the static system requires knowledge and experience of the actual behaviour of structures in relation to different materials. For instance, in concrete construction good structural modelling results in fewer cracks under external loading.

Having determined the internal forces, the next step is the dimensioning of members in relevant cross-sections. Section analysis (normally by using computer programs or design charts e.g. for beams and columns, even though it is preferable to have the capacity of doing this by hand calculations) is the selection of suitable steel and concrete grade by taking into consideration strength and durability requirements. At this stage the designer should already have in mind important details e.g. in node regions which may govern the cross-section of whole members.

In general, the public trusts that designers utilise and stick to the state-of-the-art technology. Design specifications (design codes) as regulatory documents should ensure the safety of the constructed project and aid engineers in the design and construction of safe and economic structures which perform in a satisfactory manner. **The designer must understand the behaviour for which the rules apply and be aware that codes cannot replace sound engineering judgement.**

1.2.3 Detailled design

In the *detailled design phase* all structural details are designed and calculated, starting with the member sizes from the preliminary design. Normally, this is the phase which entails the greatest amount of work for the civil engineer. The detailled drawings ready for construction have to be prepared (i.e. generating drawings such as formwork drawings, reinforcement drawings), containing specifications for the required types and qualities of the building materials.

As a first step, the distribution of internal forces and moments has to be established for all parts of the structure. The engineer should always keep in mind the flow of forces. All potential modes of failure have to be determined and thoroughly traced in the calculation. Some basic aspects and questions which have to be considered might be the following:

- Depending on the complexity of the problem non-linear analyses could be necessary. In this case it is of utmost importance that the engineer is well aware of the structural behaviour in order to be able to correctly interpret the results of this type of analysis.
- Provided the ductility conditions are satisfied, plastic analyses may be adopted.
- If the material behaviour is idealised elastic, the possibility of a limited redistribution of moments might be taken into consideration.
- If necessary, second order effects have to be taken into account (especially where they may significantly affect the overall stability of the structure or in cases where deformations lead to a significant increase in the internal forces and moments).
- Consideration shall be given to the effects of possible imperfections in the geometry of the unloaded structure (geometric deviation from the vertical line or equivalent lateral forces).
- If considerable cyclic loading has to be taken into account and the structure is sensitive to vibrations, dynamic analyses could be necessary.
- Detailing of the reinforcement should be carried out very carefully with respect to actual structural behaviour and also feasibility on the site. The strut and tie approach can be a very valuable tool as a means of understanding the flow of forces and as a help to define the geometry of the reinforcement.

The use of computer software is inevitable nowadays, however, **a computer cannot replace the experience and intuition of a competent designer**. It is still necessary to judge and evaluate the results and the constructability of a detail.

As a summary the different steps for each member can be listed as follows:

- structural modelling (documented by means of sketches);
- load arrangement and load cases;
- calculation of internal forces (M, N, V, T);
- proportioning of whole members;
- detailing (reinforcement layout and reinforcement drawings).

An essential part of the design process is **quality assurance**. To ensure proper design and construction as specified and expected by the building owner, systematic control and

supervision is needed. This also includes one's own checking as well as supervision through an external check engineer.

Additionally testing might be an option to assist in certain design situations and verify special methods of analysis. In any case feedback from the construction site is required in order to determine that the building is being constructed in accordance with the design assumptions and that behaviour corresponds to that presumed in design.

It must be kept in mind that drawings and Technical Specifications are documents which define many important aspects of the project and are the basis for its realization. Therefore drawings must be sufficiently detailled in order to fully define the structural elements. During the drafting process of the drawings the constructability of the details should be examined and possible construction problems or conditions be identified. A detailled verification of these aspects is essential to guarantee the appropriate definition of the project.

The Technical Specifications complete the definition of the project. Technical Specifications allow the detailled definition of the materials to be used, of the necessary building methods and the project-specific control conditions. All of these must also be properly defined.

Nowadays, the drawings are usually drafted automatically by specific computer programs which can lead to an insufficient definition of structural elements. This automatic process sometimes has the counterproductive effect of generating a lack of interest on structural detailing and the revision of these documents by structural engineers, even though a thorough revision has always been essential for the final definition of the project. It is necessary and worthwhile to give this process the importance it deserves.

1.3 Activities and strategies during the various stages

It is usually the responsibility of the client to define the requirements of the final product, although for this, he might require the help of consulting services. Conceptual and preliminary design may be carried out by the client, depending on the size of the project, if the client is the owner of an in-house design department. Otherwise a consulting firm will be in charge of these first design studies.

Determination of quantities and preparation of bills of quantities enab1ing a detailled calculation of costs are achieved at the end of preliminary design. The client then makes a request for tenders and the project may be listed in an advertisement where several contractors may bid on the job.

Usually, the tender documents contain the following information:

- layout of the whole site including drawings of the planned building or structure;
- soil and foundation conditions;
- special external constraints such as water-level (high water), etc.;
- deadline for completion and other compulsory dates;
- instructions for regulatory documents to be used (specifications, codes);
- bills of quantities.

In the tender period the potential contractors evaluate the project and price the services required. All incoming bids are then opened at a pre-fixed deadline. Usually the contract is awarded by the client to the lowest bidder, although this is not always the case. It has to be mentioned that a choice based solely on the initial cost may result in a problematic project. Such decisions should not be based on cost alone but on the overall solution and its impact on everything from aesthetics to environmental concerns.

Besides the initial costs further life cycle expenses should be considered. Trying to save costs to impress an owner, the engineer may be tempted to sacrifice safety of the structure in order to minimise construction expenses. Lowest first cost as a structural design objective is a destructive goal; the reason that so many structures need rehabilitation today is that cost was the main criterion to receive a contract.

In normal cases detailled design does not start before delivery is at least in sight. Usually detailled design is carried out under pressure from the beginning of the construction. Project speed becomes more and more critical for the success of a project (considering for example the effect of inflation on the costs of a bridge, etc.).

After completion of construction the following issues must be addressed:

- taking over of the structure;
- warranty period;
- monitoring;
- inspection;
- maintenance and repair.

An important point is presentation to the potential client / publics and the following public relations of a project. Efforts to bring elements of the public into the planning process make them feel they had a part in the conception of the project. Public hearings should start as soon as possible, already during the phase of conceptual design.

Presentations may be three-dimensional and show a building from different perspectives with the assistance of CAD-programs. Models, photos and videos are very useful tools for the client as well as for concerned citizens when explaining a project.

1.4 Modelling

The calculation of internal forces which can be done on a computer with a high degree of accuracy requires first an idealisation of the whole structure. Therefore so called *design models* or *engineering models* have to be applied which result in reasonable simplifications of complicated systems. They differ in complexity from *research models* which are much more sophisticated, but not practicable for design.

Design models with a degree of accuracy adequate for the real problem are needed on the resistance side as well as on the action side describing the different loads and how they are applied.

A few examples can illustrate some of the aspects and challenges a designer might encounter on the way to a reasonable model:

- When idealising a complex engineering structure, distinction has to be made between the primary and the secondary members. Primary structural elements are represented by the load bearing parts of a structure whereas secondary members act as bracing between primary members. Secondary members are designed to resist and prevent cross-sectional deformation of the superstructure frame and help to distribute part of the vertical load between stringers. Sometimes it can be very difficult or even impossible to decide which members actually take part in the load transfer. This might of course increase the complexity of the computer analysis considerably.
- The primary structural elements are normally classified by consideration of their nature and function, as beams, columns, slabs, walls, plates, arches, shells etc. To be considered and designed as beam or column, the span or length of the member should not be less than twice the overall section depth. Usually the effective span is introduced as the distance between adjacent support axes. A beam with a span less than twice its depth is considered as a deep beam. For elastic analyses truss-like idealisations of walls, corbels and deep beams are possible.
- Another challenge is the support conditions which are very often not clearly defined. For example in normal building construction continuous beams are usually analysed on the assumption that at least the intermediate supports provide no rotational restraint. End faces of beams or slabs are considered as simply supported or sometimes fully fixed. In reality especially at end supports partial fixation will occur, but is not taken into account in the analysis. Suggestions and rules for adequate reinforcement which has to be provided in such cases are given in the national codes.
- Appropriate models are also needed on the action side for the imposed loads and their arrangement. Nominal loads as well as application rules are normal1y defined in the relevant load standards. Moreover combination models are needed to take into account their compatibility and the relevant conditions. All actions and combinations thereof must be thoroughly examined regarding if the effects are favourable or unfavourable.

The examples show that whenever performing structural analysis, the designer has to make assumptions in each phase and the main question is if they provide a good reflection of the reality. This task is rather difficult in reinforced concrete construction due to the strong dependence of the material behaviour on the load level. The ability to find reasonable models for the analysis of a structure can be partly learned during education, however, feeling for real structural behaviour depends also on the experience from previous completed projects.

References to Chapter 1

Leonhardt, F. (1982), *Bridges - Aesthetics and Design.* Deutsche Verlags-Anstalt GmbH, Stuttgart, 1982.

Menn, Ch. (1990), *Stahlbetonbrücken.* Springer-Verlag Wien-New York, second edition.

Pauser, A., Beschorner, K. et al. (1996), *Donaubrücke Tulln*. Schriftenreihe des Österreichischen Betonvereins. Heft 24, April 1996.

Schlaich, J. (1996), *On the conceptual design of structures - an introduction.* International Symposium on 'Conceptual design of structures', University of Stuttgart, Proceedings Volume 1, Methodology, Stuttgart, Germany, Oct. 1996, pp. 15 - 25.

Watson, St.C. and Hurd, M.K (1990), *Esthetics in concrete bridge design.* Proceedings, ACI Symposium on 'Bridge Esthetics', American Concrete Institute, Detroit, Michigan, 1990.

2 Conceptual design

Hugo Corres-Peiretti, José Romo, Javier León, Alejandro Pérez Caldentey

2.1 Introduction

The objective of this document is to explain some of the essential arguments which lie behind the resisting aspects of structural concrete.

This chapter aims to provide ideas on how to design/create structural solutions for different structural problems, from a global perspective that integrates, among others, the knowledge referenced in the other chapters of this text.

The conceptual design of a construction involves choosing an appropriate solution among many possible which must be studied in order to solve a particular problem. Good projects are characterized by the proposal of outstanding solutions in which it is perfectly clear how the different design conditions of the problem are met:

- functional requirements, related to the purpose of the structure;
- structural requirements aimed at meeting, with safety, the different external actions (gravity loads, climatic loads, etc.);
- environmental requirements, necessary for achieving sustainability, and in consonance with these, durability requirements, that is the satisfaction of the mentioned requirements throughout the lifetime of the structure.

To the above list, which is mainly technical and economic in character, other aspects must be added: aesthetic requirements, which are of a more subjective nature and will generally reflect the *style* of the designer, formed and cultured throughout his professional life; social requirements to which the project must be adapted in order to insure its integration into the medium and culture for which it has been designed; innovations which must be sought and introduced, etc.

It is very difficult to describe the process of conceptual design explicitly. It is not formally defined and in the best of cases is poorly explained in engineering schools, even though it is absolutely necessary for sound engineering.

Conceptual design is an ability which is acquired through time. It requires of the professional engineer **a great effort to understand the requirements**; it requires **a broad engineering and human culture** in order to be sensitive to the many variables involved – to all, if possible – which are implicated by the act of design. It requires **great ambition**, which is a trade mark of those who, in any engineering activity, always seek the optimal solution; it requires **experience**, which is nurtured from successes and failures – the indispensable heritage needed to build a path of continuous evolution until the last minute of the last project. There are probably other requirements besides those mentioned above, but it is certain that without satisfying these it would be difficult to even make a start.

A project has the magic of beginning with a blank piece of paper and a great number of conditions. The first phase generally consists of increasing the number of requirements, many of which have not been explicitly defined by the client. The best phase is that of brain storming, which results in going from a blank piece of paper to many sheets filled with proposals. Since a solution is not unique, any number of solutions is too small. Further proposals can always be found. There will always be some proposals which are not made

explicit. Afterwards comes the phase of selection, decision making, and finally of refining the chosen solutions. There is always room for improvement. Throughout this process there are no computer models, no fine calculations. There is only imagination, the knowledge acquired through experience and the joy of working. This is how a project is brought into being from the ability to imagine, putting calculations in their proper place, that is, as a tool at the service of creativity which will provide an answer to the challenges laid out.

Afterwards comes the detailed development of the project, always starting from a previously conceived and defined idea. This is the time of detailed verifications.

Finally comes the sublime phase of engineering when the ideas are made tangible and real. We engineers have the enormous good fortune to be able to see, materialized, our ideas, both good and bad (Fig. 2-1).

Fig. 2-1: Before design and after construction (Corres et al. 1999)

Engineers of the past have left us a fabulous legacy filled with examples which exhibit great ideas, despite the very limited technological resources at their disposal when compared to those available today.

The Pantheon of Rome (Fig. 2-2) is one of the most outstanding examples of building engineering. The inside of the building is inscribed in a perfect sphere of 150 feet of diameter (43.44 m), a record span in concrete construction, only broken at the beginning of the 20th century by Max Berg with the Centennial Room in Breslau. Rebuilt in the 2nd Century by Apollodorus of Damascus (then at the service of Hadrian), its architectonic configuration is

adapted to the philosophical conception which related human beings with the vault of heaven, whose center, the oculus, is the sun. This is the theme of the architectural configuration from which was built the most outstanding vestige of roman antiquity, filled with excellent engineers. The counterbalance of the dome is formed by a drum of *opera latericia* (brick) 7 m deep, wisely configured with a grid of arches built into the drum walls which allow it to resist both the compressions transmitted by the meridians of the dome as well as the circumferential tension stresses at the spring of the dome. The dome itself has variable depth, ranging from 5.90 m at the dome springs to 1.5 m at the oculus, masterly distributed with recourse to partial waffle-slab-like voids on the inside and a discrete set of rings on the exterior of the building. This is an extraordinary example of a completely satisfactory conceptual design both from the architectural and engineering points of view.

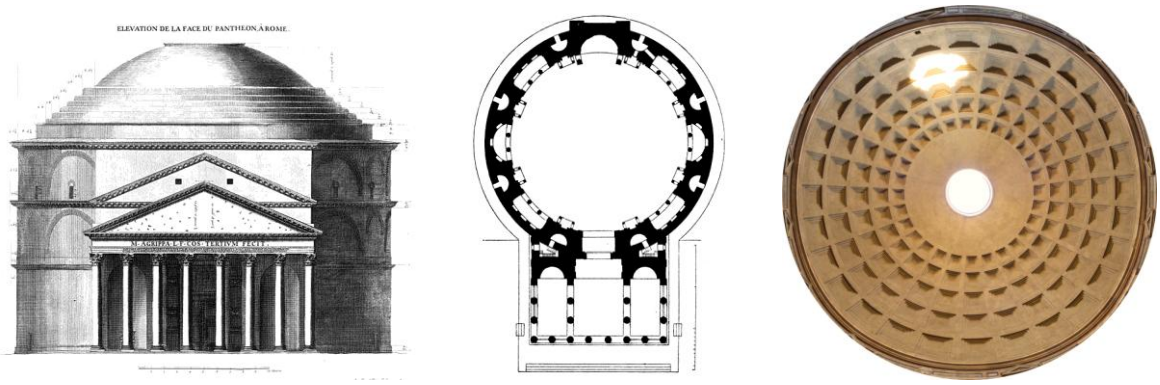

Fig. 2-2: Left: Antoine Desgodetz's elevation of the Pantheon in "Les edifices antiques de Rome", 1779. The grid of arches built into the dome is clearly visible. Center: Pantheon floor plan by Georg Dehio/Gustav von Bezold, 1887-1901. Right: the dome of the Pantheon (photo: Matthias Kabel).

In the field of concrete structures it is indispensible to recall some of the names and high points which have dominated, in a relatively recent past, the process of innovation in construction and which must be regarded as examples from the pedagogic point of view.

Emil Mörsch (1872-1950) (Fig. 2-3), pioneer of knowledge, of design and of normalization of concrete structures was, among many other things, the author of the phrase "*nothing is more practical than a good theory*", which expresses the need for engineers to be well schooled with regard to resistance mechanisms. There is no doubt that a good theoretical and conceptual basis is essential to structural projects.

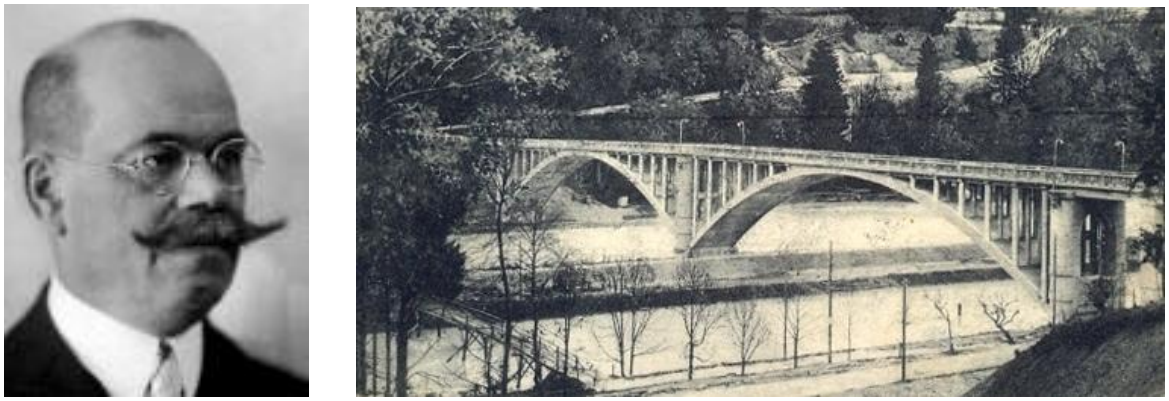

Fig. 2-3: Grünwald Bridge over the Isar River, the work of a young Mörsch (1904). The bridge has two arches of 70 m of span and 8 m of width. Today this bridge may seem conventional, but in its time, it materialized the consecration of structural concrete as a material which could emulate stone and improve on its structural properties and constructive possibilities. (León, 2005)

Robert Maillart (1872-1940) (Fig. 2-4) is one of those brilliant engineers who represents a before and an after in structural engineering. Living a life worthy of the best movie script, Maillart elevated to an art, with its own personality, the design and construction of structural concrete.

a

b)

c)

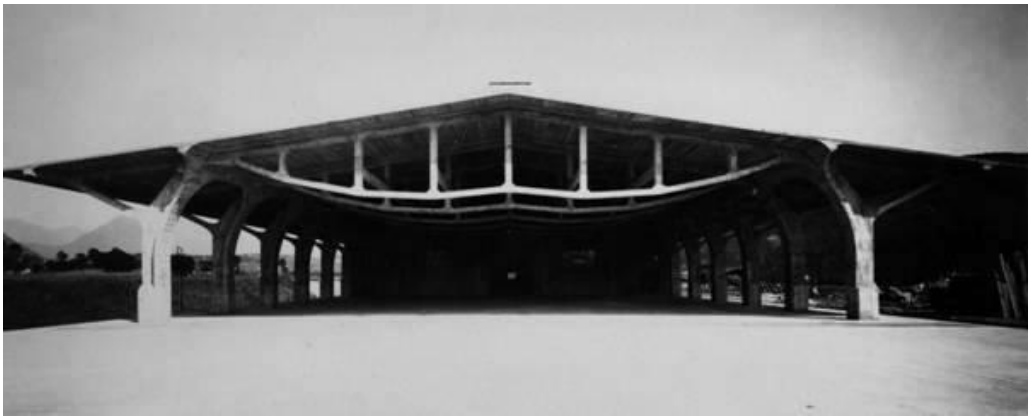

Fig. 2.4: Innovation, talent and structural knowledge are some of the ingredients that contributed to Maillart's impressive engineering output. a) Salginatobel Bridge (1929). It represents the full maturity of its author in the knowledge of structures, the most efficient use of materials and the play between the stiffness of the deck and that of the arch. b) The "slab without beams" of the Giesshübel, Zürich (1910, left) and St. Petersburg (1912, right) warehouses, is a concrete slab of constant depth, supported on pillars with capitals. Its practical application was preceded by an intense and intelligent experimental campaign (1908) which guaranteed both technically and psychologically the invention. c) In the Magazzini Generali in Chiasso (1924), a work of a full creative and intellectual maturity, Maillart amuses himself by proposing a structure with the minimum amount of materials – concrete and steel – which expresses a deep knowledge of the resisting mechanisms of the structure.

Faced with phenomena involving complex analytical formulations, Maillart acted as an engineer, rather than as a scientist, by studying the problem by empirical means, investing important sums of money in the building and testing of prototypes for the experimental validation of his design criteria. The experimental techniques, which he developed very personally, with measuring devices which are still used today for load tests, were not only a solid guarantee of his systems but also magnificent proof of his technical competence.

Eduardo Torroja (1899-1961) is another of those distinguished personalities (Fig. 2-5). Torroja, who stood out as designer, researcher, teacher and author of technical codes, made no concessions to improvisation. The ideas that he made known to the outside world were the mature fruit of deep pondering, of the precise enunciation of the problem and its boundary conditions, as well as the study of different possibilities and alternatives.

a)

b)

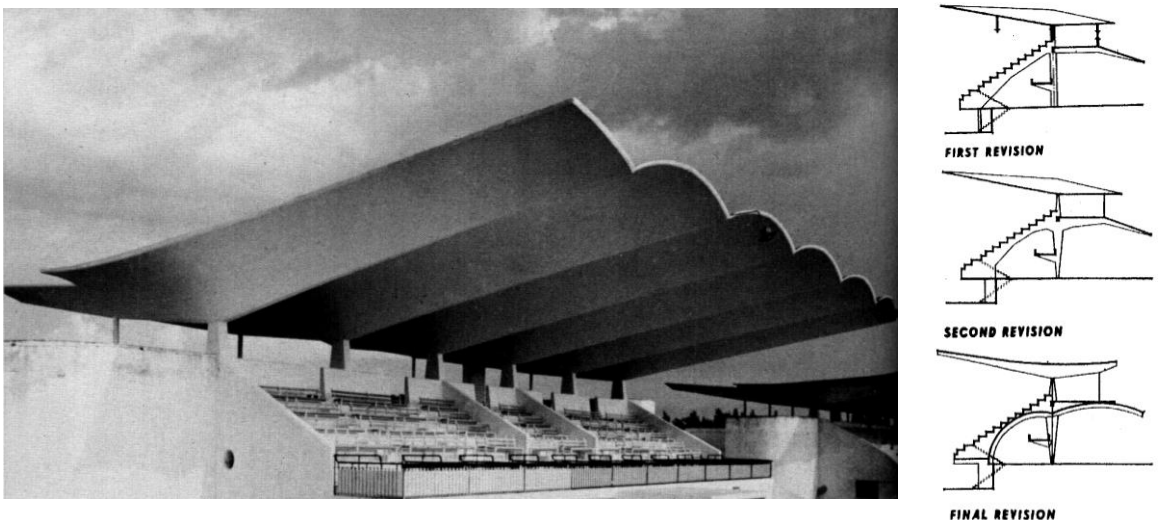

Fig. 2-5: Torroja made a point of uniting form and function, as is very clear not only from his written works but also from his design of ultra-thin shell structures. a) Roof of the Algeciras market (1933) with a span of 47.6 m and a thickness of 8 cm, a slenderness equivalent to that of an eggshell. Torroja was aware that the success of such a structure was heavily dependent on the effective materialization of the assumed boundary conditions which are achieved by an octagonal ring at the roof springs (including stays which prevent the transfer of horizontal forces to the vertical supports) and by the addition of cantilevers which ensure the effective realization of the sought-after membrane state as soon as possible. b) Cover of the stands of the Zarzuela Horse Racing Track (1935). Successive versions of the cross section of the stands and resisting mechanisms revealing a wise distribution of mass and stiffness in mutual equilibrium, the result of a deep study of the structural behaviour. (Torroja, 1958)

The activity of Torroja comprehends all structural typologies, some of which distinguish him in an especially brilliant and pioneering way. This is the case of laminar structures. Torroja, who was very well trained in mathematics and geometry, put his full talent into the design and construction of structures such as the Algeciras market (1933), the stands of the Zarzuela horse racing track (1935) or the Recoletos Fronton (1936) of a staggering slenderness.

Eugène Freyssinet (1879-1962) is an epic figure of French and international engineering (Fig. 2-6). Designer, builder, inventor, businessman and artist, recognized by all, this brilliant engineer, a man of his time, living an intense life, was able to understand the ins and outs of the profession better than others. He has gone down in history as the inventor of prestressing, and as the author of construction techniques which made the building of the structures he designed both possible and economical.

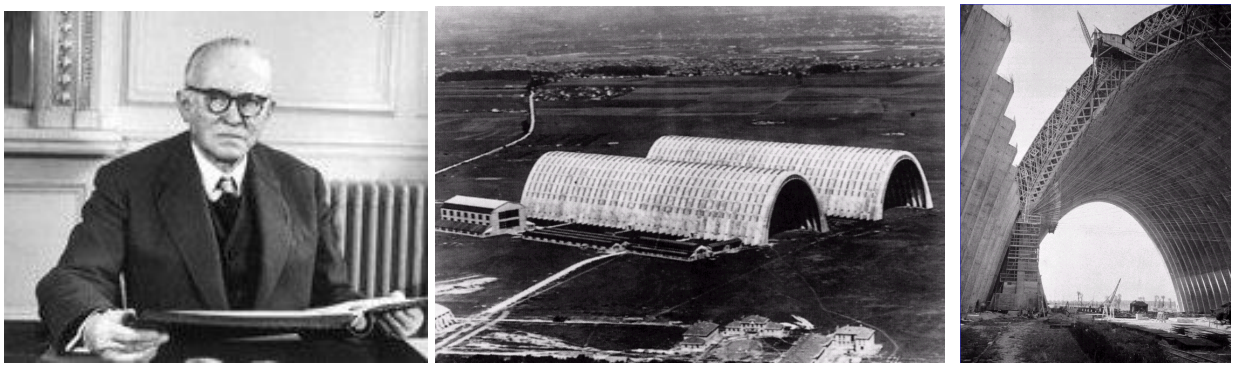

a)

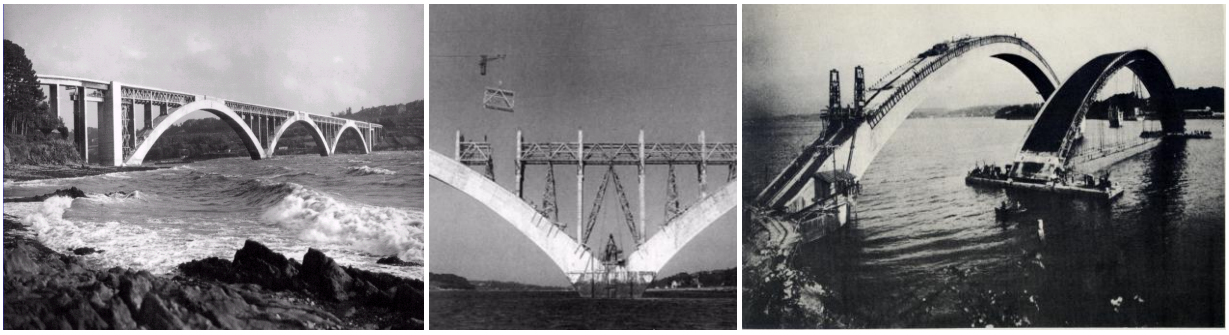

b)

Fig. 2-6: As a builder Freyssinet was very conscious of the need to solve the construction procedures of his works in an economical way. a) The Orly hangars (1923). The triumph of the resisting shapes in concrete and of construction techniques with modular formwork. b) Several aspects of the construction of the Plougaster bridge, over the Elorn Estuary in Brittany in inverted order. The key to the construction of the bridge according to Freyssinet's proposal was the construction sequence involving scaffolding transported by flotation. (Fernández Ordoñez, 1978)

After the above thoughts it must be warned that this text does not aspire to describe in detail the process followed in conceptual design, nor give enough information to guarantee its learning. It only lays out a few ideas, attempts to define the problem and to illustrate it by eloquent examples. This is because the creative act is individual, and requires living experiences, awareness of the examples of brilliant structural concrete designers of the past, and above all, the existence of a guiding idea. Without this idea there is no project. Without this idea structural engineering is not possible.

2.2 What is conceptual design?

During the last decades, this term has been used to refer to many concepts which have not yet been clearly defined.

The symposium on conceptual design, organized at the University of Stuttgart by Prof. Jörg Schlaich in 1996 (University of Stuttgart, 1996), was possibly the first event organized by engineers to analyze this problem. It was the result of a long-time concern of a few professionals.

The preface to the symposium papers states: "The overall quality of many structures today leaves much to be desired. The rapid technological progress does not reflect adequately in their variety, beauty and sensitivity. Too often structural engineers neglect the creative conceptual design phase by repeating standard designs and not sufficiently contributing with own ideas to the fruitful collaboration with architects. Engineers thus often waste the chance to create building culture."

The announcement of the symposium invited participants, who were known to be expert designers, to describe the process of design, of the creation of a solution to a problem. The symposium had a high attendance and was very interesting, but was not conclusive with respect to the definition of conceptual design, nor to the definition of the process leading to the final solution.

Conceptual design is a process or design method which, using the available resources – structural, technological, cultural, creative, etc. – aims at making easier the search for the solutions to a project, to a structural problem, etc. The objective of the process is to find the optimal solution to a multi-variable problem, in which all variables are important.

It must be made clear that this process does not guarantee the quality of the idea. An interesting idea, even a brilliant one, does not come from sudden inspiration. It is the result of a persistent search and of detailed and hard work. We have all sometime seen how hard work, the intelligent and unrelenting search, the tenacious persistence in finding by discarding, ends in yielding results – the best results (Figs. 2-7 and 2-8).

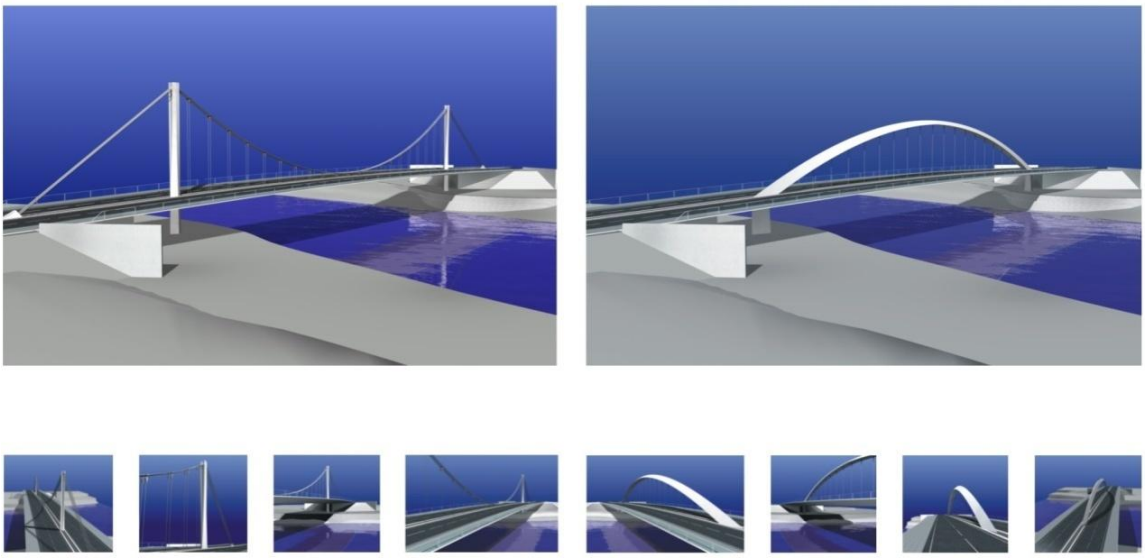

Fig. 2-7: Contest of ideas. Proposed solution for a semi-urban bridge in which road traffic, pedestrian traffic on the bridge and pedestrian traffic along the riverbank had to be integrated in a structure which was to become a central element in the development of this new part of the city. (Corres, 2006)

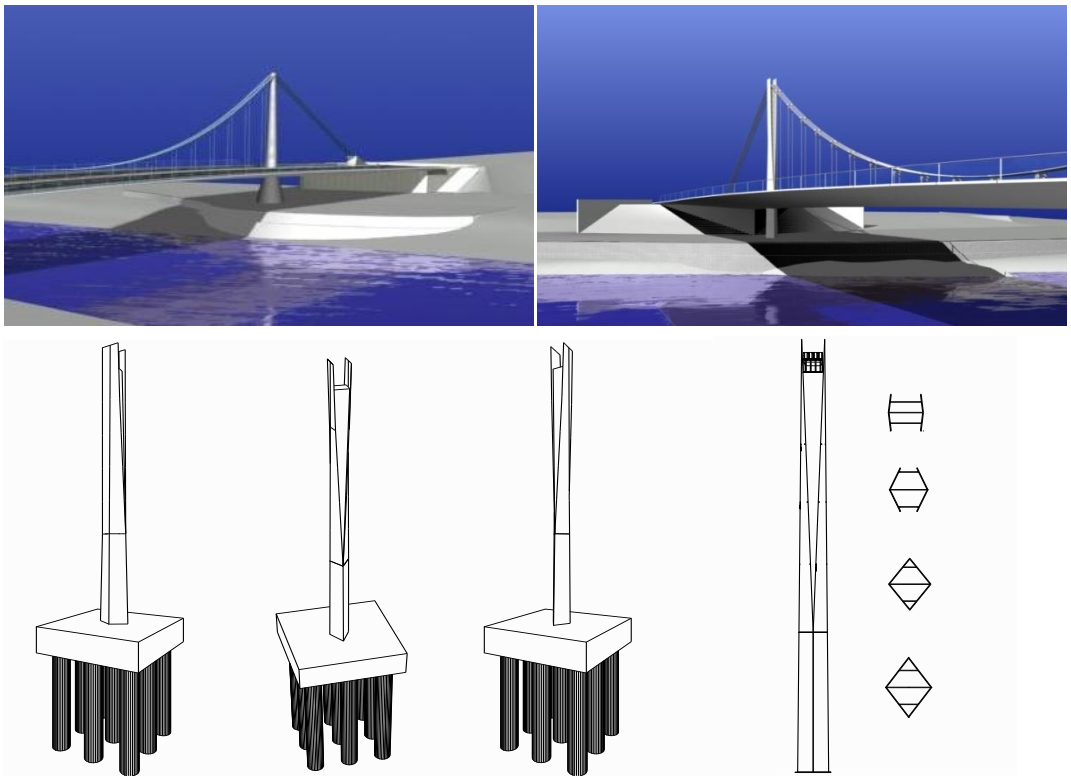

Fig. 2-8: Contest of ideas: evolution of the pylon's form of a small suspended bridge (160 m span) (Corres, 2006)

Conceptual design is a process which can be employed at different levels within a project, in each case involving different resources, as shown in Fig. 2-9.

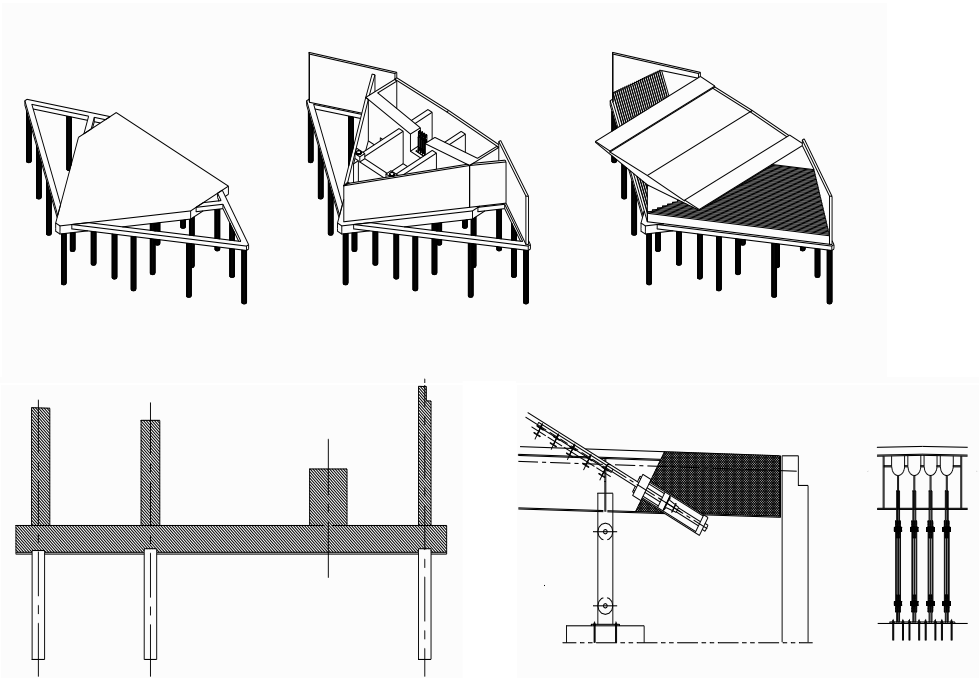

Fig. 2-9: Contest of ideas: study of the anchorage detail of the main cable in the abutment which serves as counterweight (Corres, 2006)

These ideas are also indispensable in the much needed interventions on existing structures (Fig. 2-10). Far from being a second order activity because of the lack of sparkle of new constructions, this type of work allows us to delve into such interesting aspects as the understanding of built works, their historical and construction context, the knowledge of the materials and their degrading mechanisms, which cannot be avoided. They are sources of learning on a scale of one-to-one, which can later be used on new structures. It enables us to understand, because it becomes self-evident, that constructions have a fourth dimension, that of time. The same ideas of conceptual design can be applied to all these activities, which are comprised in this fascinating field: inspection, diagnosis, therapy and the formulation of a prognosis.

Fig. 2-10: Los Santos Bridge (Corres et al., 2008). Existing bridge comprising three 150,00 m spans, built by the cantilever method in the 1980's. The bridge deck was widened from 12,0 to 24,0 m by reinforcing the existing box cross section and using new ideas and materials in order to minimize the impact of the additional loads.

The process proposed by conceptual design is always applicable. To all activities, from the most general ones to the more detailed ones, even to the most exotic. There can be no engineering without an idea. There can be no project without an idea. There can be no details without an idea.

2.3 How is conceptual design carried out?

It is not easy to define the process of conceptual design. Fig. 2-11 is based on a flow chart which was presented by Jean François Klein (Klein, 2004) at a meeting of the ***fib*** Special Activity Group 5, New Model Code, in Lausanne, intended as a basis for the introduction of these concepts into the new Model Code.

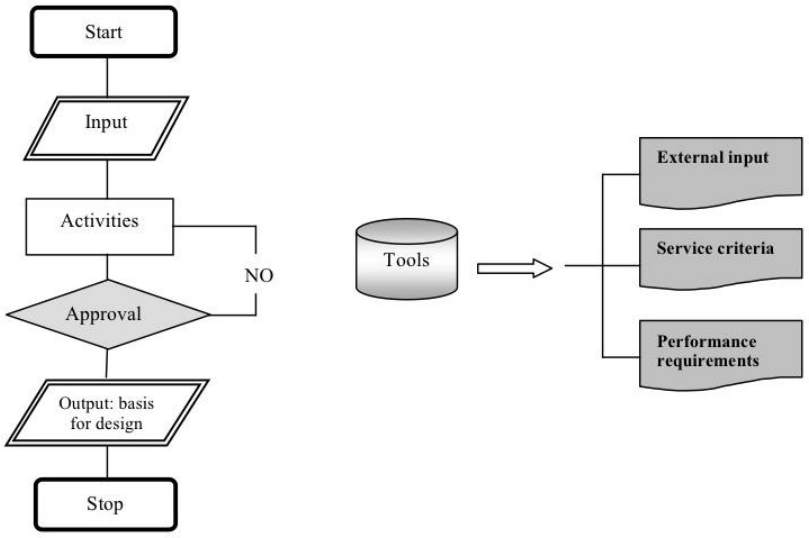

Conceptual design: General process

External input:
- drawings, sketches (from architects, from owner);
- general layout, plans, of site, topography;
- technical data about the site (soil conditions, geology);
- environmental data (weather, wind, floods, earthquake, etc.);
- accessibility and transport facilities;
- local construction rules, pictures of the site.

Service criteria:
- use of structure (efficiency, comfort and safety);
- operational requirements (efficiency, economy);
- maintenance requirements (efficiency, economy);
- upgrading requirements.

Performance requirements:
- service life (temporary, replaceable, evolutive, long term);
- solidity (for determined design values – risk evaluation);
- structural efficiency;
- durability;
- aesthetics;
- integration in its surroundings;
- economy (budget);
- construction method;
- sustainability;
- replacement;
- demolition;
- recycling.

Activities:
- constraints analysis and classification;
- environmental analysis (including local politics and local traditions);
- general conception;
- choice of materials (considering economy and energy consumption for production and elimination);
- structural concept (structural logic, dimensions);
- integration and aesthetics (legibility, simplicity, calm, proportions);
- construction method (sequences):
- rough cost estimate;
- comparison of alternatives;
- successive presentation, explanation and discussions with the owner (architect);
- after acceptance by the owner – preparation of the basis for design (drawings, notes, reports).

Tools:
- experience, background, feedback, database;
- feelings, sensitivity;
- creativity, imagination;
- capacity to simultaneously analyze and integrate all criteria and constraints with their relative weight;
- quick pre-design methods;
- design by sketching (from rough freehand sketches to accurate drawings);
- visualization tools.

Fig. 2-11: Flow chart and tables describing the process of conceptual design (based on Klein, 2004)

In this paragraph the process followed for a contest of ideas for the building of a bridge in a semi-urban area is described as a real example experienced. The conditions of the contest were defined in the competition clauses, which, as is obvious, must be studied in much detail.

It is necessary to visit the site of the future structure. The conditions of the site (Fig. 2-12) must be known close-up and personally, it is necessary to talk to the client, in order to obtain additional information, and to talk to the neighbours, if it is an urban work, etc. This is an essential activity. From each visit much information may be gathered. We engineers must be conscious that we must solve problems aimed at improving the life of people, that we are investing public money, and that we need to study deeply all existing conditions. This deeply social dimension, which has always been present in the activity of engineers, cannot be forgotten. This aspect cannot be tarnished by caprice, a topic which, although it is a point of acute interest, does not fit into the scope of this text.

Fig. 2-12: Conditions of the site

It is necessary to understand and study the social and historical conditions involved. This means that information needs to be gathered from specialists of other disciplines, such as urban planners, historians. It also means to understand the roots and consequences which the political action of promoting a new infrastructure requires from us as engineers. It is not easy, but it is necessary.

Even though the serviceability criteria and the behaviour requirements are closer to the culture of engineers, and are therefore well considered, it must be kept in mind that such requirements are a few of many others which are equally real and important and are also in need of practical engineering consideration (Fig. 2-13).

Fig. 2-13: Bridges in the city of Logroño

After this phase, the guiding ideas of the project must be established. These ideas are a synthesis; they are the main ideas of the beginning of the process of approximation to the problem with which conceptual design is carried out in order to achieve the optimal solution. In the case of this example the guiding ideas can be summarized as follows:

- It should be a rational intervention, with discretion as a priority, as an integrating quality, and of scrupulous elegance so as to guarantee the acceptance of the work by the users and the city as a whole.
- The various uses of the work must be optimally integrated in the final solution. Each use must be defined and solved from the beginning of the study in order to guarantee an adequate solution for each, balanced and compatible with each requirement.
- The integration of the structure into the landscape must be compatible with the general philosophy of the structure, and compatible and harmonious with the general landscape of the town.

Afterwards, the task of searching for the optimal solution can be launched. The bridge layout in plan, elevation and cross section must be established.

In this case, due to the skew of the bridge with respect to the river, a special problem involving the placing of the piers in plan and the design of the abutments was present. Studies were undertaken in order to provide answers to this challenge. A synthesis of this study is shown in Fig. 2-14.

There are several possibilities. It is possible to use a pier with a single shaft or a pier formed by two shafts. In the latter case, the shafts could be placed parallel to the river, thereby obtaining a skew deck and also, skew abutments, with a clear advantage for the relation between the river and the structure. If, on the other hand, the shafts are placed perpendicularly to the bridge axis, the piers and the abutments would be a larger hydraulic obstacle to the passage of the river.

The solution which was finally accepted was that of a single shaft with triangular abutments. In this way both the problem of skew and the problem of hydraulic interaction between river and infrastructure met adequate solutions. This unedited solution has also allowed the solving of other problems as will be presently shown.

For the definition of the layout in elevation, many possibilities were studied. Generally in a work such as this one, the maximum number of possibilities should be studied. The better solutions will come out strengthened and will provide continuity to the search, while the less optimal solutions will point to new ideas, which is what makes their consideration essential.

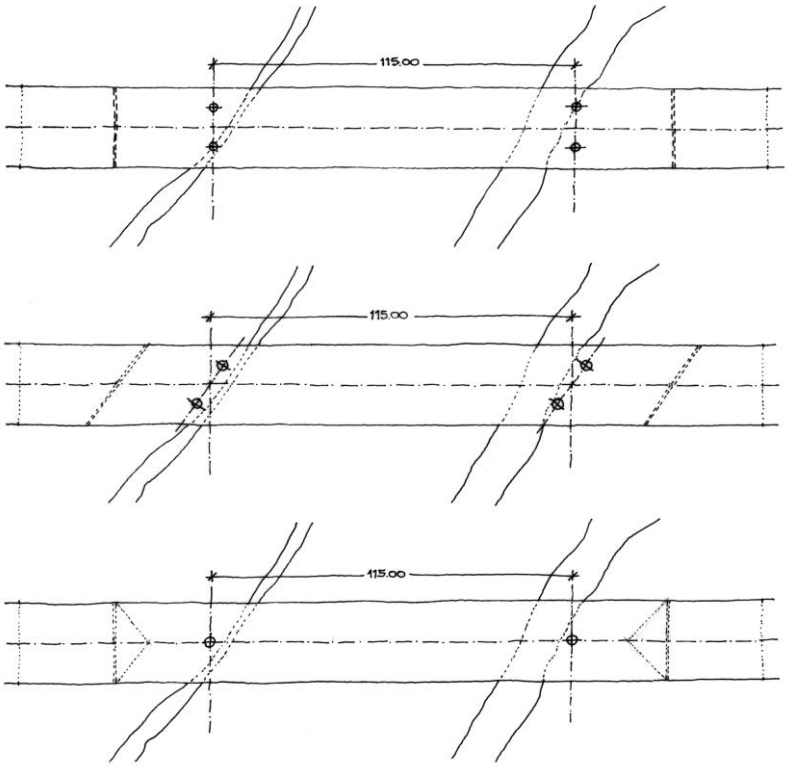

Fig. 2-14: Study of alternatives for piers and abutments

These are still paper and pencil activities in which drawing is the most important language of expression, unfortunately not replaceable by the computer (Fig. 2-15). It is not yet the time for 3-D renderings. The scale of the problem must first be felt and control of the created object attained.

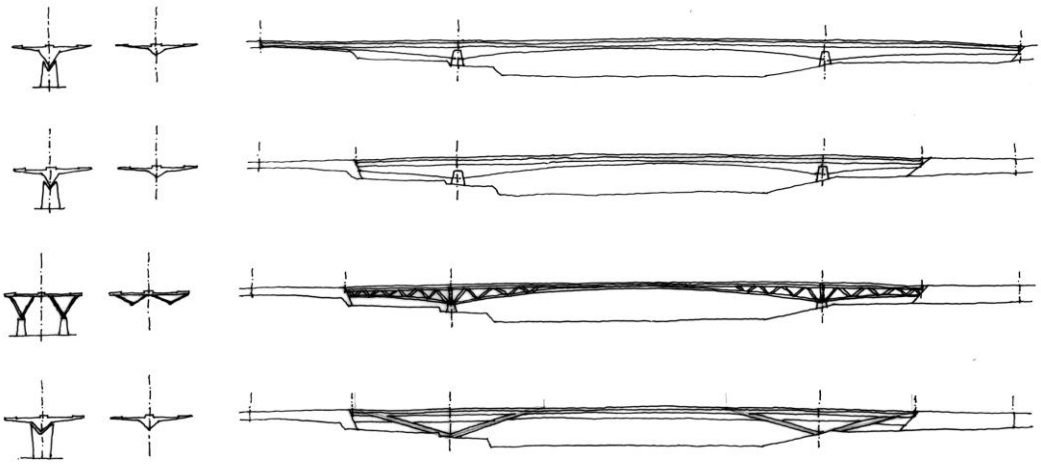

Fig. 2-15: Layout study in elevation, with resisting structure placed under the road (Courtesy of FHECOR Consulting Engineers)

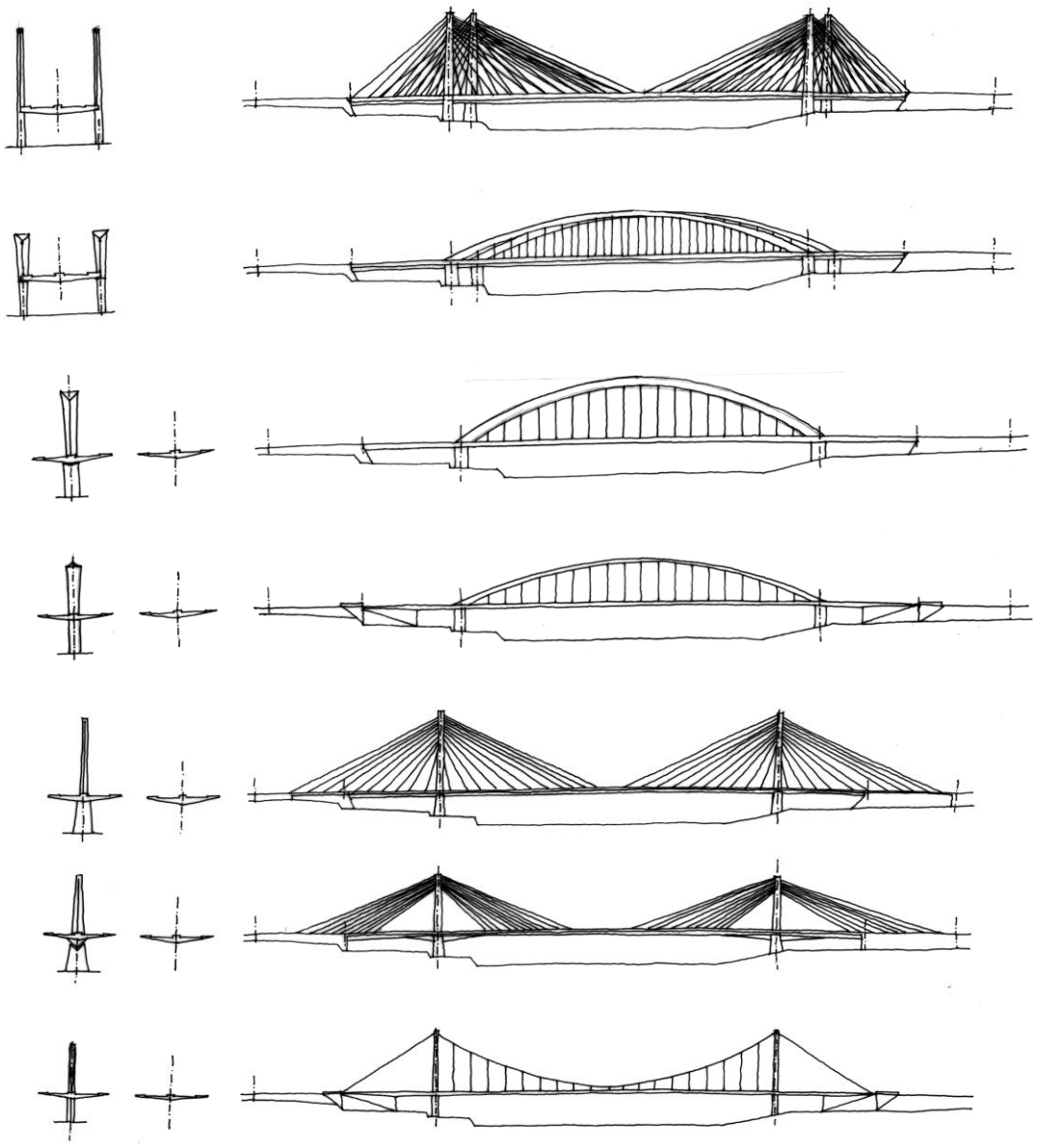

Fig. 2-16: Layout study in elevation, with resisting structure placed over the road (Courtesy of FHECOR Consulting Engineers)

In this phase it was decided to keep two alternatives: an arch solution and a suspended solution, both with a resisting structure placed over the deck and with a single resisting plane (Fig. 2-16).

This was the moment when the first virtual representations were made, before the selection of the final solution. Fig. 2-17 shows the first renderings. It can be seen that the solutions are still at a very primitive stage. These solutions were yet to undergo much improvement.

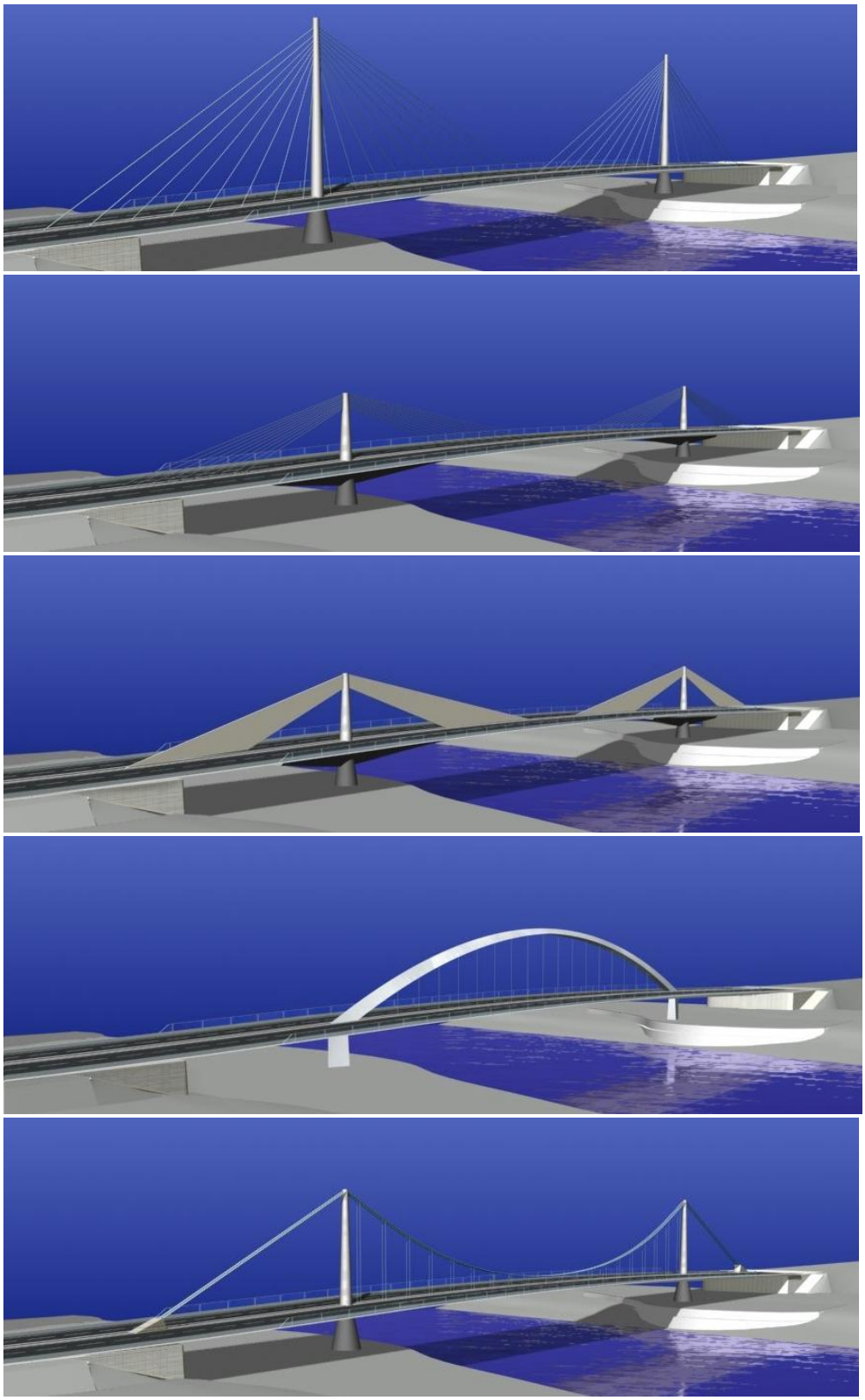

Fig. 2-17: 3-D Studies of the most adequate solutions aimed at choosing the best path to follow

Work must continue. The act of creation requires self-criticism and ambition. The details must be deeply studied. All ideas must be tried. Until the last minute, the best idea, the best proposal must be sought.

Fig. 2-18 shows the final structural layout adopted, which must be consistent, they must show clear evidence of our culture as engineers. Fig. 2-19, shows the construction sequences which were proposed. Fig. 2-20 shows the details of the different structural elements. This type of study is among the most important since it allows refining the proposal up to a degree of detail which good engineering should always achieve. Finally, in Fig. 2-21, the colour studies aimed at deciding the colours to be used in the different elements of the bridge are shown. Different colour ranges have been chosen and for each colour range different colours have been proposed for each structural element. Additionally a work of modern art featuring the same shades is shown in order to convey an idea of the combination possibilities laid out.

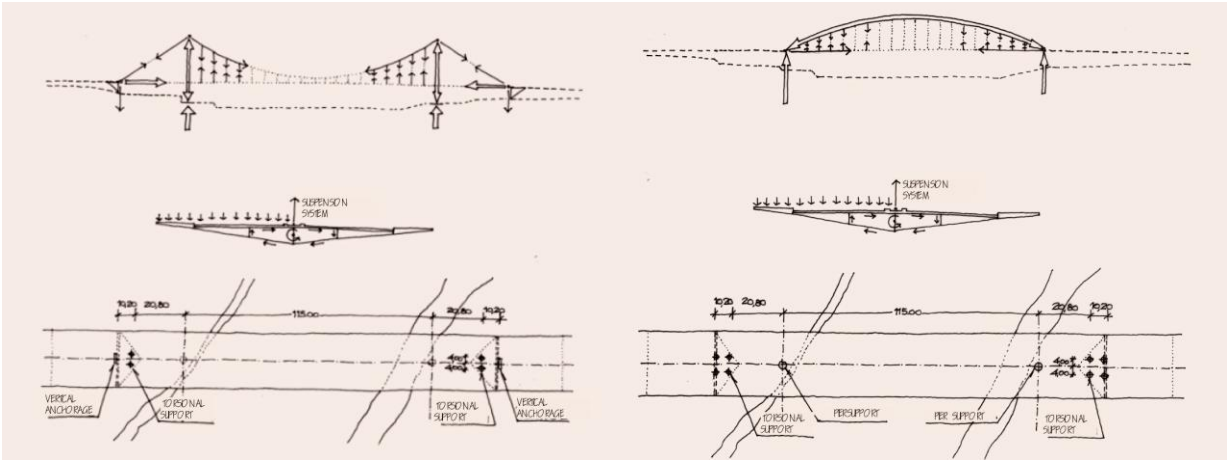

a) *b)*

Fig. 2-18: Structural layout a) Suspended solution with composite deck b) Bow-string type arch solution

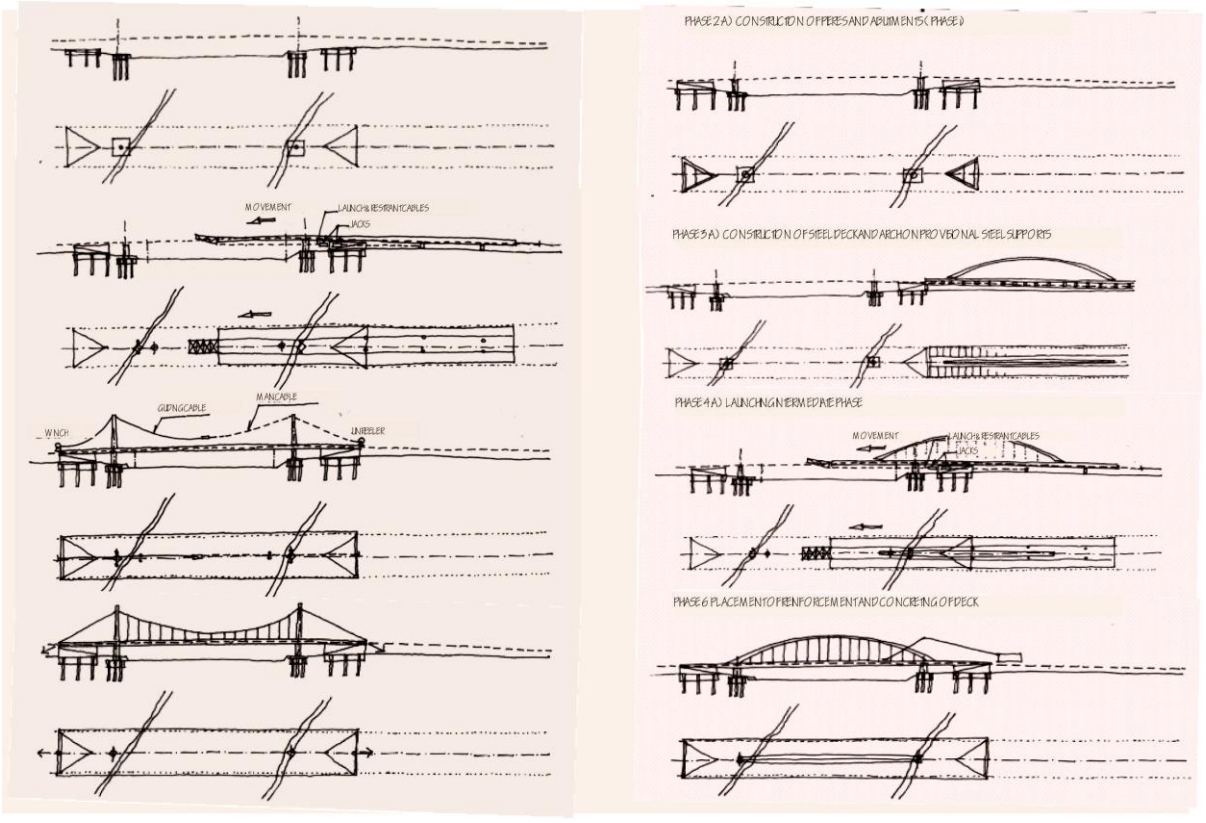

a) *b)*

Fig. 2-19: Construction process. a) Suspended solution with composite deck b) Bow-string type arch solution

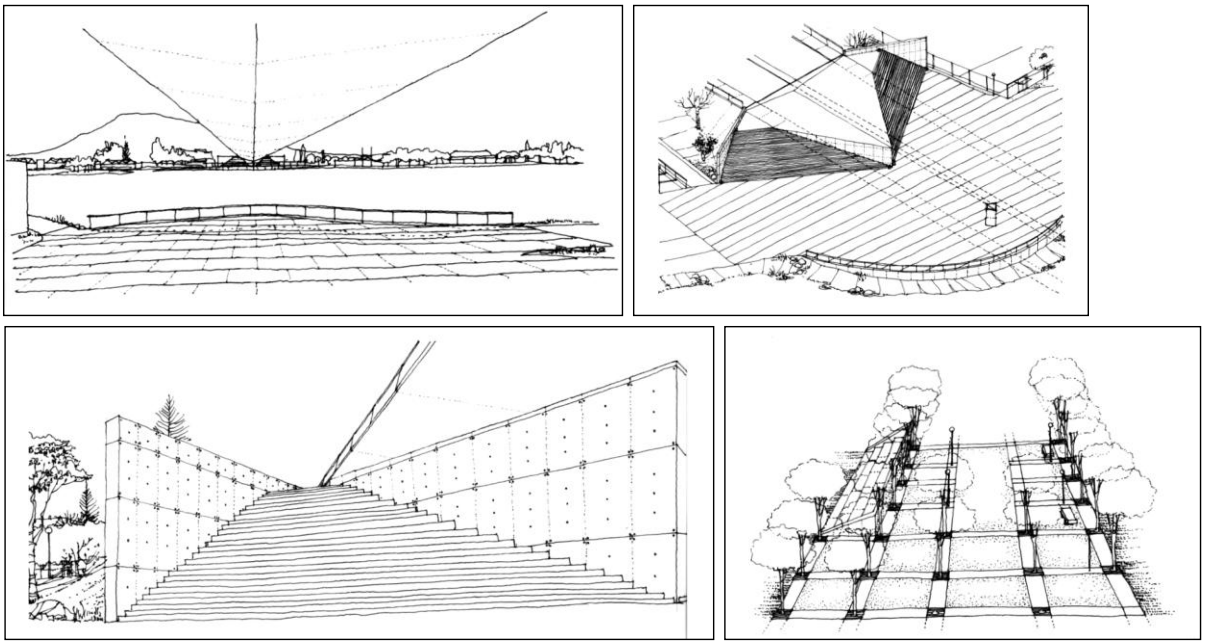

Fig. 2-20: Details of different elements of the proposed solutions

This phase of conceptual design allows defining the idea of the project. It requires the utmost dedication and the greatest attention. It should not be thought resolved with the first idea. It requires the time deserved by good engineering: that needed to review, to permanently question a solution and extract from it with the chisel of self-criticism the best piece.

It must not be thought that this is only done when time is available. The time of other activities must be curbed in order to provide time to this most important activity. A good idea always gives rise to a good project. A project without ideas is always a vulgar and a poor project.

2.4 Some good examples of conceptual design

There have been, as mentioned before, many good examples of creativity, innovation and know-how in many of the works of the great masters of structural engineering, in general, and built of concrete in particular. Unfortunately, and in spite of the great opportunities in the recent past to engineers, when large investments in infrastructures have given work to everybody, there have been only a few examples of creative, innovative and interesting structural engineering.

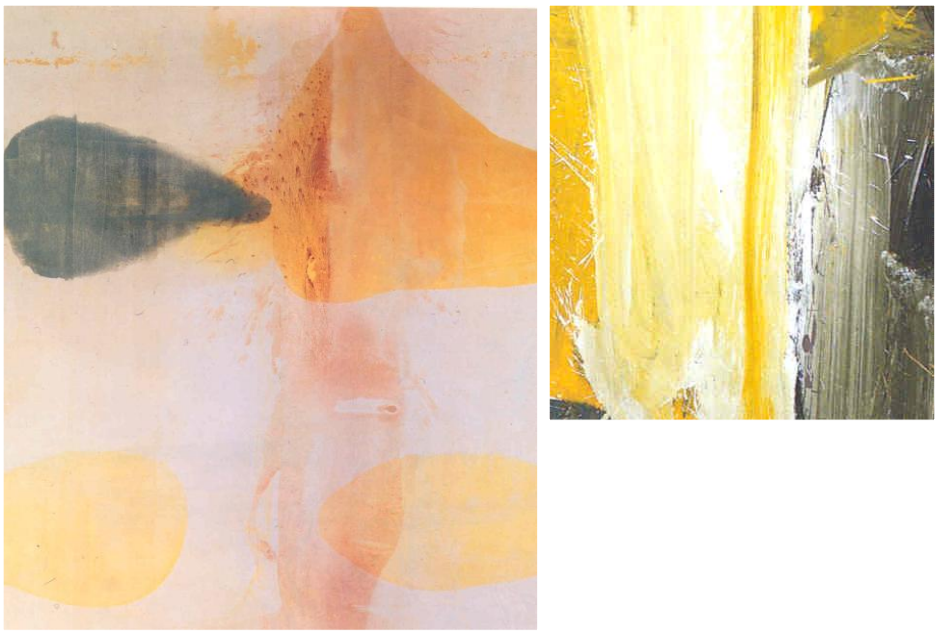

***Flavus** proposal* : Melodic yellow colour scale

	Abutments	Deck	Piers	Cables	Railing
Colour	Ochre	Ochre	Ochre	Metallic	Gold

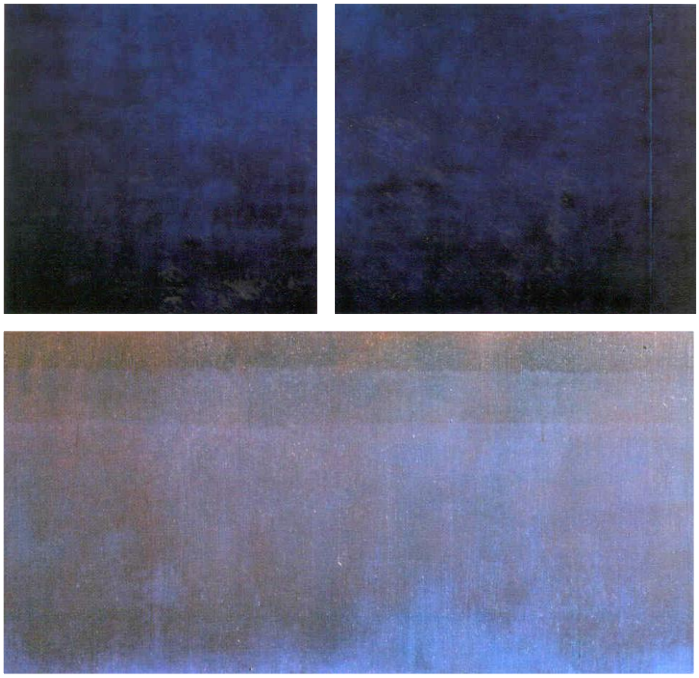

***Cœrulus** proposal* : Melodic blue colour scale

	Abutments	Deck	Piers	Cables	Railing
Colour	Violet	Ultramarine	50% Gray	Metallic	Cobalt b

Fig. 2-21: Colour study featuring two shade ranges

There is no detailed documentation about the way in which the process of conceptual design has been carried out in all the engineering masterworks of structural concrete of the past. This being, as has been expressed, a very personal process, it is not easy to explain the works of others.

In spite of this, two works of the above-mentioned Eduardo Torroja, teacher, researcher and designer, a rare breed, whose creative process fits in perfectly well with the *modus operandi* described above, will be discussed.

When he was 26 years old, Torroja faced the need to solve the problem of the design and construction of the Tempul aqueduct (1925). The diagram in Fig. 2-22 shows, above, the original project, an aqueduct with simply supported spans and two piers placed within the river bed, and below, the constructed solution, in which these piers have been replaced by cable stays.

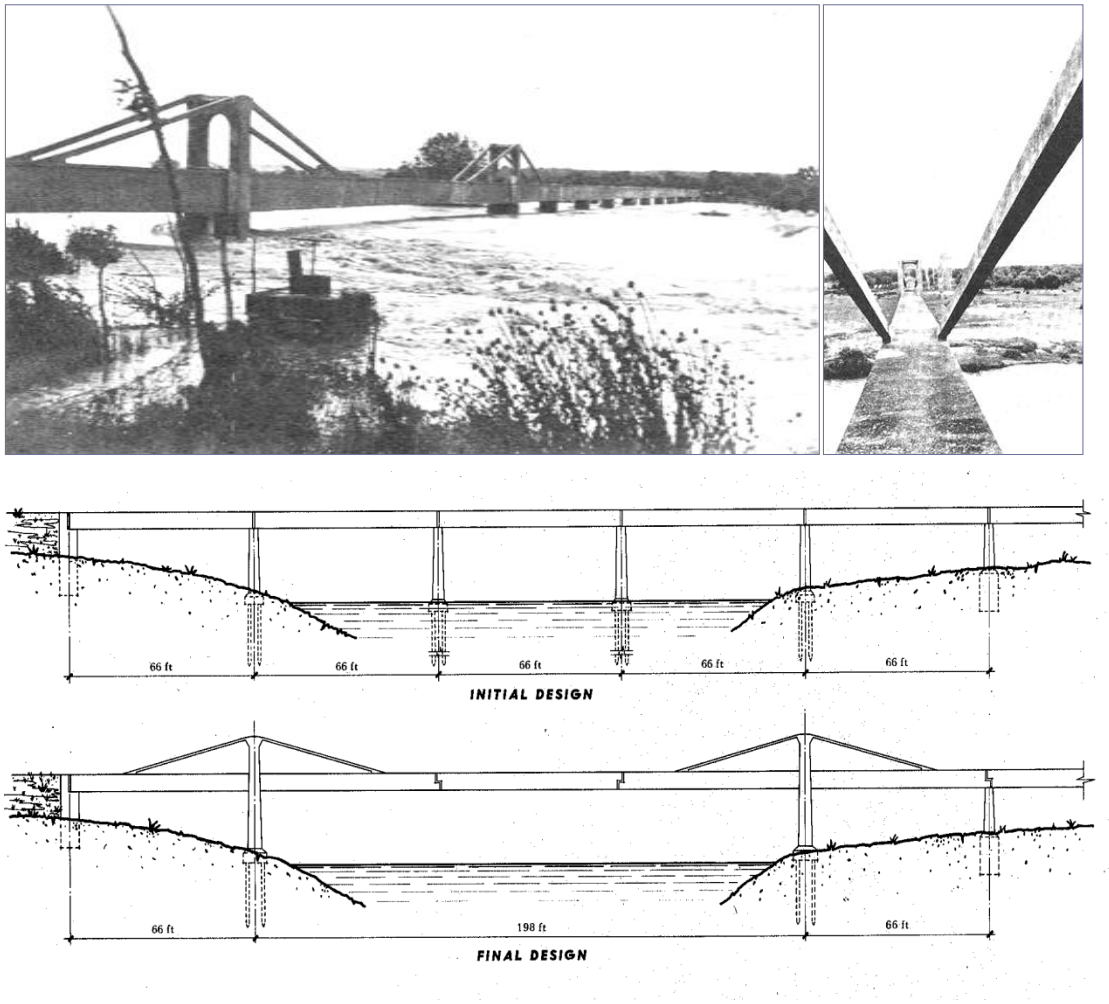

Fig. 2-22: Tempul Aqueduct, 1925 (Torroja, 1958)

At the time of construction, there was no commercial technology for the stays designed by Torroja. He proposed to use closed cables, commonly used in harbors, and in order to stress the stays he proposed to use jacks acting in the vertical direction on the pier tops, as shown in Fig. 2-23. Also, in order to improve the behaviour conditions of the stays, the stressing operation was done with the stays already in tension, supporting the stretch of the U-shaped beams going from the pier to the expansion joints. In this situation the stays were enveloped in concrete, thereby conferring greater stiffness, greater protection and better durability conditions.

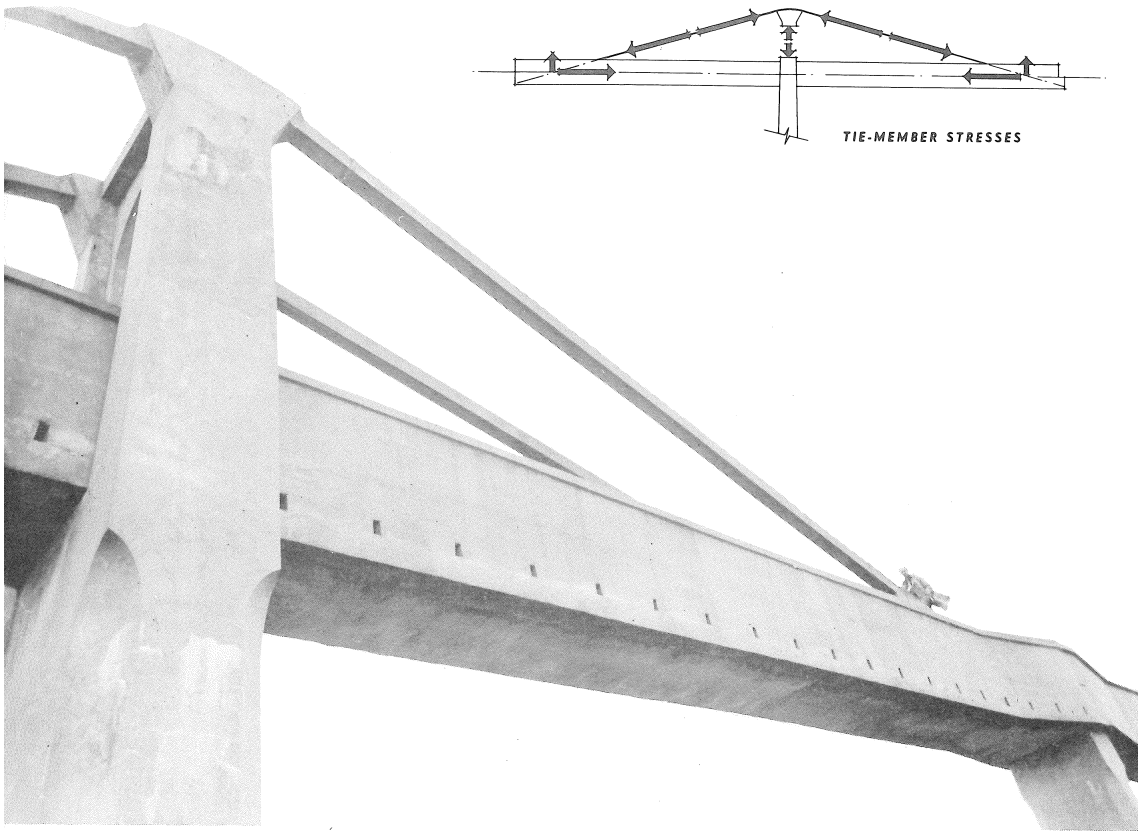

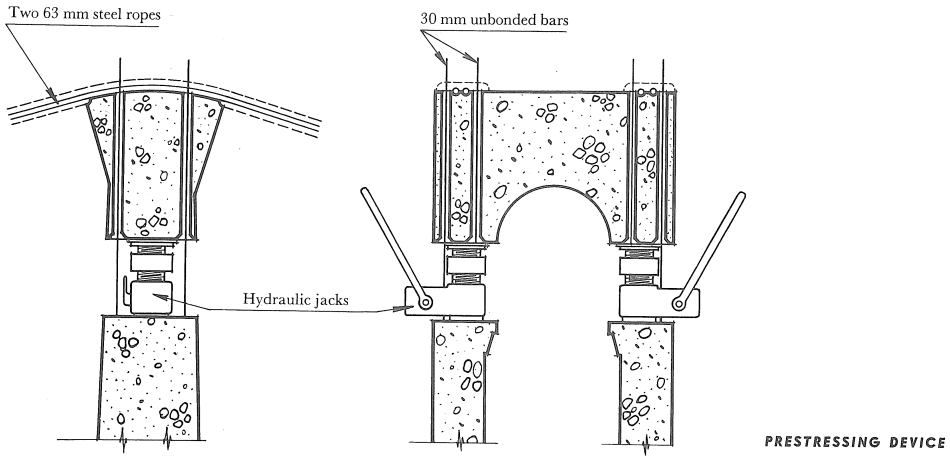

Tempul Aqueduct 51

Fig. 2-23 Detail of the stressing of the stays (Torroja, 1958)

In this example it can be clearly seen how the conceptual solution to the problem, that is the use of stays in order to suppress the piers in the riverbed, is combined with many other ideas aimed at solving the practical problem of stressing and materializing the stays. It sould be noted that, although many fans of Torroja saw in this solution a predecessor of

prestressing, by the compression produced in the deck due to the horizontal component of the stay forces, the great engineer politely declined the honor, and acknowledged his contemporary colleague Freyssinet, saying that he had not deliberately sought to produce a previous and favorable tensional state, as a prestressing concept, but had only solved a construction problem. Thus, great figures are often humble.

One of the most interesting works of Torroja is the Recoletos Fronton, built in 1936 and sadly destroyed shortly after the Spanish Civil War as a consequence of the impacts it suffered (Fig. 2-24). This work, like many others he designed, is the result of a close collaboration with architects and engineers. Generally, good engineers can be good conveyors of good architecture. This is the case, in the past of Torroja, admired by such great architects as Wright, Pier Luigi Nervi, Peter Rice, etc, and can also be the case in the future.

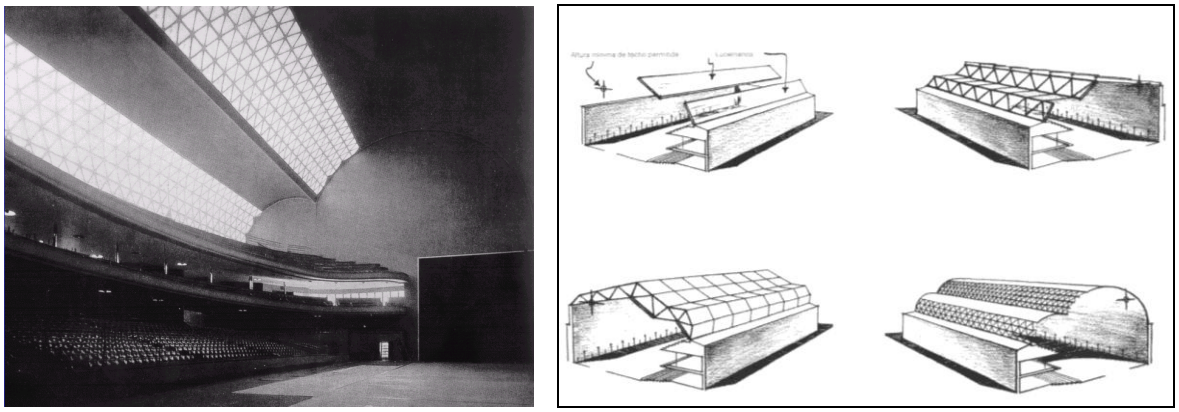

Fig. 2-24: Interior view of the Fronton Recoletos and images of the typological study made for its conception (Torroja, 1958)

In this case, the building requires a playing court, stands, and spaces for various functions of the building. Torroja designed a longitudinal beam supported by the lateral walls, with a transverse cross section involving two circular curves of 6.4 and 12.2 m of radius, with 0.08 m of depth. The slab was substituted by a concrete grid in certain areas in order to allow the entrance of light. Among the possible solutions, which are also shown in Fig. 2-24, Torroja adopted the most peculiar, innovative and beautiful. A choice made, after the search, with ambition.

In the brief and dense preface of "Reason and Being of Structural Types" (Torroja, 1960) he wrote: "Each material has a specific and distinguishing personality, and each form imposes a different stress phenomenon. The natural solution to a problem – art without artifice – , optimum in the face of the previous impositions which originated it, is impressive by its message, satisfying at the same time, the demands of the technician and of the artist. The birth of a structural ensemble, the result of a creative process, escapes the sole domain of logic and penetrates the secret frontiers of inspiration. Before, and above all calculation there is the idea, which shapes the material in a resisting form, in order to comply with its mission."

The authors do not believe that there is a better way to describe and synthesize the process of conceptual design.

2.5 Strengths and weaknesses of current structural engineering and their relationship to conceptual design

Today's situation is filled with so many paradoxes that, at times, it seems unintelligible. We have at our disposal modern design codes, which are the synthesis of our more recent knowledge, powerful and versatile means of calculation, new materials, which are a not so well known, fruit of technological progress (probably because the capacity for amazement of post-modern man has decreased), very powerful means of construction, never before seen, and, in spite of it all, the result of structural engineering is not always up to the standards which would be expected in such favorable circumstances. Possibly the following factors can explain this situation.

The education of engineers, no doubt, an essential factor, has suffered great changes in recent times. It is clear, on the one hand, that universities must provide solid and deep theoretical knowledge, which the engineer must possess, but they should also provide a wide vision of engineering and culture. As is known, and with very few exceptions, the contribution of universities to the humanist education of engineers has become almost non-existent. On the other hand, it is necessary to learn the trade of the structural engineer, which is not acquired during university studies, but rather by professional experience. This requires knowledgeable senior colleagues who can serve as mentors for the younger engineers to be groomed, from whom young engineers must learn and to whom the young engineers must, one day, succeed. Unfortunately this process is not currently taken care of, which is a deplorable waste.

Knowledge has advanced and has become atomized. Too frequently we find that there is no connection, no bridge between the knowledge which is being generated and professional practice. It is obvious that the world of research is far away from the world of design, the languages are different, and they serve interests which are not common, or even clearly divergent, without points of contact.

Codes, which have evolved remarkably, can be, in many occasions, an obstacle to invention. They should be written to provide liberty, not to create restrictions. In this sense, the increasingly performance- and client-oriented character of modern codes contributes encouraging progress which can be made by those who are better prepared and have better control of the art of conceptual design.

Computer resources, which at first glance are a significant step forward, can in fact become traps which imprison the minds of engineers, who can only see though the limited and distorted windows offered by mere modeling, restricting the act of thinking, confusing designers, now young, who use as sources of inspiration what are mere working tools intended to free them from the routine of computation.

Reality is rich and complex. Engineering has always distinguished itself by the capacity to manage uncertainty (in words of our dear colleague Javier Rui-Wamba) and it is clear that computer programs cannot solve the uncertainties we face. For that, it is necessary to be conscious of what these uncertainties are. Today it is frequent to see an engineering of Technicolor, supported by the post-processing of computer programs, in which complex models offer the false hope of solving that which is not known – something which cannot be done, which is not possible. Only knowledge can enable the limits of ideas to be identified, and therefore the limits of computer programs. It is essential to know what can be expected from models; it is essential that, at all times, the intellectual fruit, the idea which comes from

the process of conceptual design, prevails. Computational models must be at the service of this idea, helping to quantify them in a more coherent and rigourous manner.

New technologies must be controlled by designers, at least to a sufficient level as to guarantee adequate mastery of them. New materials, new gadgets, new technological inventions must be assimilated by designers in order to guarantee their optimal use. Many times, the products which are offered in the world of civil engineering have been developed for other applications, and only with sufficient knowledge can engineers use them efficiently.

Finally, knowledge, today, requires teams, because it has become so vast that it cannot fit into the minds of individuals who were all in a past not so far away, but who could not today grasp it all with the required level of detail. This requires a new culture of working together for a common objective: engineering.

2.6 Final remarks

Design is an art which must be cultivated, it is an act of creation, for which conceptual design is an indispensable instrument.

Design is an art which is learned over time; each project is an opportunity which cannot be wasted. Brilliant ideas are not always achieved, but ideas are essential. If they are good, it is magnificent; if they are brilliant, it is an exception.

The development of technology, materials, construction means, etc., offers good possibilities for potential creators.

References to Chapter 2

Corres, H.; Pérez, A. (1999), *Puente Arco Sobre el Embalse del Burguillo (Ávila)*. 1er Congreso de la Asociación Científico-Técnica de Hormigón Estructural (ache) 1999.

Corres, H. (2006), *II Rapporto tra Ingegneria e Architettura nella Progettazione Strutturale*. Alcune Esperienze. Architettura Strutturale, Galileo nº 178, pp 12-20, Italy, October-December 2006.

Corres, H.; Pérez, A.; Romo, J.; León, J.; Prieto, F.; Sánchez, J.; Sisi, D.; Espeche, A. (2008), *The Widening of Los Santos Bridge. A Case Study of a Tailor-Made Structure.* International *fib* Symposium 2008. Amsterdam, 19-22 May 2008.

Escrig, F. (1994), *La cúpula y la torre – The dome and the Tower*. Ed. Fundación Centro de Fomento de Actividades Arquitectónicas, Seville, 1994.

Fernández Ordóñez, J.A (1978), *Eugene Freyssinet*. Revista de Obras Públicas. April, 1978.

Heinle, E. and Schlaich, J.(1996), *Kuppeln aller Zeiten, aller Kulturen*. Stuttgart 1996.

Klein, J.F. (2004), *fib*, SAG 5 New Model Code. Model Code kick-off meeting, Lausanne, 2004.

León, J. (2005), *Notas para una historia del hormigón estructural*. Unidad Docente de Hormigón Estructural, ETS Ingenieros de Caminos, Canales y Puertos, Universidad Politécnica de Madrid. 2005. *Unpublished notes for students*.

Torroja E. (1958), *The Structures of Eduardo Torroja*. Foreword by Mario Salvadori, CEDEX, CEHOPU, Ministerio de Fomento, 1958.

Torroja, E. (1960), *Razón y ser de los tipos estructurales*. EBCOMP, S.A., 1960.

University of Stuttgart (1996), *Proceedings of the Conceptual Design of Structures*. IASS International Symposium organized by the University of Stuttgart, October 7 – 11. 1996.

3 Materials

3.1 Concrete

by Harald S. Müller and Michael Haist

3.1.1 Introduction

The following section primarily deals with the mechanical and other physical properties of normal weight concrete as well as with constitutive relations to describe these properties. For information regarding concrete raw materials, details of concrete composition and the manufacturing of concrete reference is made to the literature such as [CEB-FIP MC90; ACI (2009); Neville (1996); Grübl et al. (2001); Müller and Reinhardt (2010)].

Since the last edition of the *fib* Textbook in 1999 considerable progress in concrete technology has taken place. New types of concrete such as self-compacting concrete, high strength and even ultra high strength concrete are produced in practice on a routine basis. Therefore an additional section on special concretes has been included in this edition of the Textbook. In this new section also architectural and light weight concrete as well as fibre-reinforced concrete are dealt with. However, it is not possible in this book to treat these special concretes in detail. Hence reference is made to the literature where further information may be found. Textile concrete, i.e. concrete being reinforced by the means of textiles, is not dealt with here.

Further it should be mentioned that this Textbook is published before the first draft of the new *fib* Model Code, referred to as "MC2010", is finished and released. When reference is made to the new *fib* Model Code 2010 the authors presume that the existing draft at the time when the Textbook at hand was written will be maintained for the final version of the code. However, this might not happen in some cases, and as a consequence, the given references will turn out to be wrong. Obeying the rule, to give most up-to-date information, this risk is taken.

Note that in the constitutive relations given in the following, tensile stresses and tensile strains (elongation) are positive, whereas compressive stresses and compressive strains (contraction) are negative. Material properties are positive or to be used in absolute terms e.g. compressive strength, $f_{cm} = |f_{cm}|$. When multiaxial stress states are considered then $\sigma_1 > \sigma_2 > \sigma_3$ is valid.

3.1.2 Classification

In national and international codes concrete is generally classified according to its *compressive strength*, such as low strength, normal strength, high strength or ultra high strength concrete. This classification is subdivided into strength classes designated by the 5% fractile value of the compressive strength – generally referred to as characteristic value – determined both on cylinders (d/h = 150/300 mm; f_{ck}) and on cubes (edge length a = 150 mm; $f_{ck,cube}$). This classification thus guarantees that 95% of the tested samples in the defined class exceed the desired minimum strength at the age of 28 days.

The characteristic strength f_{ck} is related to the mean value of compressive strength f_{cm} at an age of 28 days according to eq. (3.1-1).

$$f_{cm} = f_{ck} + \Delta f \tag{3.1-1}$$

where:

Δf $1.64 \cdot \sigma$
σ standard deviation.

In MC2010 it is assumed that Δf = const = 8 MPa and is independent of the grade of concrete.

The strength classes specified in EN 206-1:2001 range from characteristic cylinder strengths of 8 MPa to 100 MPa and thus cover low, normal and high strength concretes. This range is maintained in view of the technical information given in this textbook wherever possible. Table 3.1-1 gives an overview on the available strength classes.

concrete type	strength class $f_{ck}/f_{ck,cube}$						
low strength concrete	C8/10	C12/15	C16/20				
normal strength concrete	C20/25	C25/30	C30/37	C35/45	C40/50	C45/55	C50/60
high strength concrete	C55/67	C60/75	C70/85	C80/95	C90/105	C100/115	
ultra high strength concrete[1)]	> C100/115						

1) not included in EN 206-1:2001

Table 3.1-1: Strength classes for normal weight concrete according to EN 206-1:2001 as well as classification according to concrete type

Concrete may also be classified on the basis of its *unit weight*, as the weight is a key design criterion allowing the determination of loads. Both in MC2010 and in EN 206-1:2001 distinction is made between:

- light weight concrete with an oven-dry density not exceeding 2000 kg/m^3;
- normal weight concrete with an oven-dry density larger than 2000 kg/m^3 but not exceeding 2600 kg/m^3;
- heavy weight concrete with an oven-dry density exceeding 2600 kg/m^3.

The classes named above are again subdivided according to the unit weight of a defined concrete or other criteria, such as the type and properties of the aggregates used or the way the concrete is produced.

As can be seen from Fig. 3.1-1, during the last century most international research efforts were strongly focused on developing concretes with a higher compressive strength. However, beginning in the 1980s other performance criteria, such as the workability at the fresh state or the durability of the concrete gained more and more importance and in turn led to the incorporation of additional classification schemes in international standards. EN 206-1:2001 for example includes a classification system for standard durability exposures and regulations for the mixture composition of such concretes.

In contrast to the classification according to the compressive strength, which serves as a design value in order to determine defined limit states, the durability design according to EN 206-1:2001 is still limited to regulations in view of limiting values regarding the mixture composition. In a next step, durability aspects will also be connected to limit state criteria, thus enabling the planning engineer to conduct a durability or even a service life design based on the load actions (e.g. carbonation or acid attack) and the resistance to this action (e.g. concrete cover, diffusion characteristics etc.). This design concept is presented in the Model Code for Service Life Design (see [*fib* Bulletin 34 (2006)]). Further classification criteria, such as whether the concrete needs compaction work or is self-compacting, architectural and aesthetic aspects, as well as ecological criteria, have been or will be incorporated in international standards.

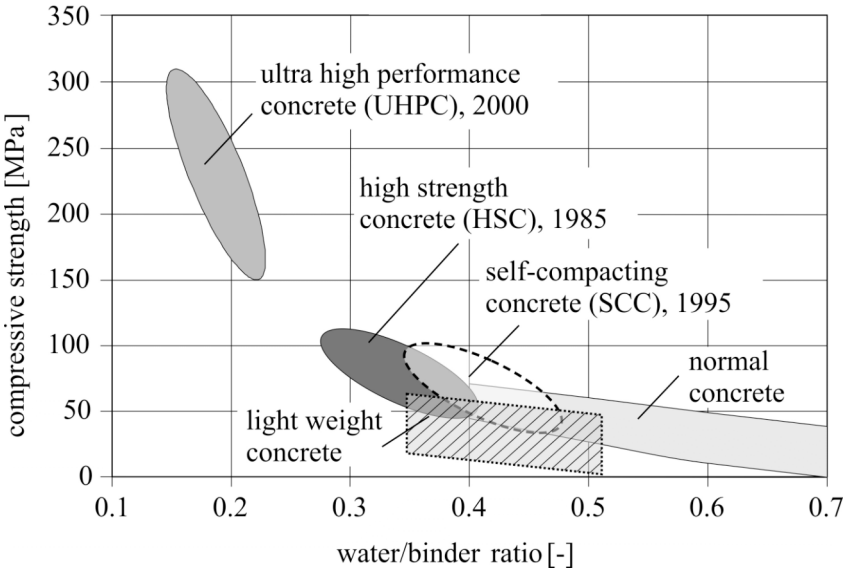

Fig. 3.1-1: Development of the compressive strength of concrete as a function of the water/binder (w/b) ratio for different types of concrete [Müller (2007)]

Today, a combination of different performance classes in the design of a concrete member, such as the combination of low strength and high durability or self-compactability combined with high resistance against acid attack is only possible in a very limited range. Such concretes are addressed as tailored concretes. The problem with such a concrete mix design results from the fact that some major performance criteria are inextricably coupled by certain mixture parameters. For example, the production of a high durable concrete is among other measures primarily realized by a reduction of the water/cement ratio. This reduction in turn causes a high strength concrete which might be of disadvantage depending on the actual design situation. It will be the assignment of future research to investigate and eventually overcome the technical boundaries, limiting this incompatibility.

3.1.3 Concrete composition and properties at the fresh state

Modern structural concrete mixes in general form a five-component composite. They are primarily composed of mineral aggregates (such as natural gravel and sand), cement and water. Further, additions, e.g. fly ash or stone dust, and admixtures are generally used, the latter one only in very small quantities. As the aggregates normally possess a much higher strength, stiffness and durability than the hardened cement paste (i.e. the hydrated cement), it is the primary goal of the mix design process to maximize the aggregate content in the

concrete while maintaining sufficient workability at the same time. As a result structural concrete made without additions usually consists roughly of 70 vol.-% of aggregates and 30 vol.-% of hardened cement paste. For normal strength concrete the water/cement ratio varies roughly between 0.4 and 0.7, depending on the concrete properties, and the cement content ranges mostly between 280 kg to 450 kg per m³ of concrete.

By optimizing the granular packing of the aggregates the void content in the packing and thus the cement paste volume necessary to fill these voids can be minimized by grading the aggregates. This process is normally performed using formalized methods e.g. as proposed by Fuller or Andreasen [Andreasen (1930)] which allow to predict the void content in a granular system on the basis of its grain size distribution. By minimizing the paste content in concrete also the workability is reduced, which may necessitate the application of admixtures like plasticizers.

The hardened state properties of concrete are strongly influenced by air voids unintentionally entrapped in the concrete during the mixing and placing process. Thus the consistency of the concrete must be chosen such that during the compaction process – i.e. facilitated by vibrations – the unintentionally entrapped air rises to the surface and disappears. At the same time the consistency has to obey the condition that no segregation of the aggregates, having a higher unit weight than the cement paste, occurs while the fresh concrete fills a given formwork. As both phenomena, the air void inclusion and the aggregate segregation, strongly deteriorate the hardened concrete properties, these effects must be prevented by ensuring a good workability of the concrete. The mix design of concrete therefore is an optimization process with the aim, to obtain sufficient workability of the concrete at the fresh state in combination with a maximum aggregate content.

The key to designing such a concrete lies in achieving a high packing density of the aggregates while maintaining a sufficiently high amount of paste causing a lubrication film between the aggregates. As can be seen from Fig. 3.1-2, at equal aggregate content per concrete volume but different packing density of the aggregates used, the average clearance between the aggregate grains increases with increasing packing density of the aggregates. In other words, with increasing packing density of the aggregates the cement paste volume needed in order to achieve a defined workability is reduced.

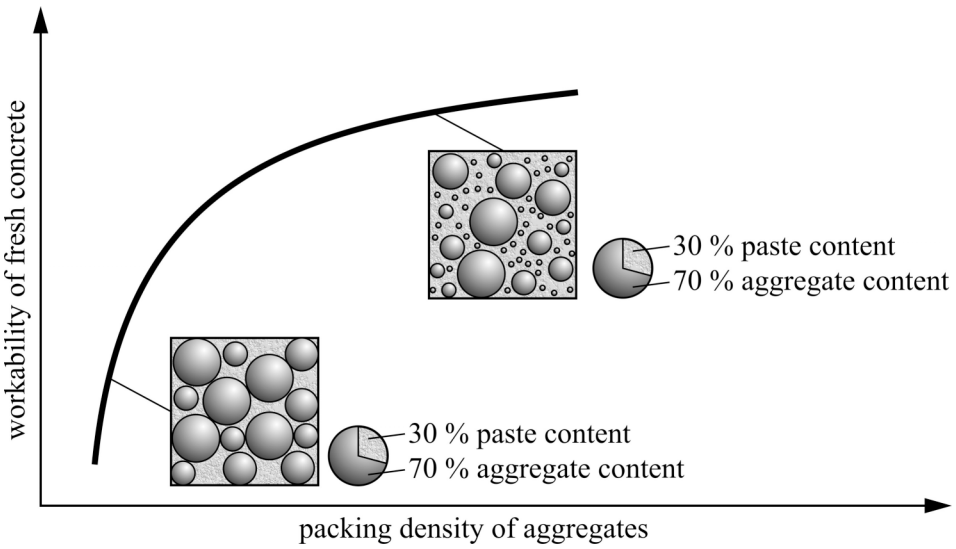

Fig. 3.1-2: Influence of the packing density (achieved by proper grading) on the spacing of the aggregates and the workability of the fresh concrete

Even though the cement paste content of a normal concrete (approximately 27-32 vol.-%) is comparatively low, the composition and the rheological properties of the paste have a significant influence on the workability of the concrete. By adding chemical admixtures which interact with the cement in water, the viscosity of the paste and the concrete can be reduced significantly. As visualized in Fig. 3.1-3 (left) this is necessary to allow for entrapped air voids to escape from the concrete. However, at the same time the aggregates suspended in the paste must be hindered from sinking, Fig. 3.1-3 (middle), and must be transported securely through narrow reinforcement bar layouts Fig. 3.1-3 (right), requiring a sufficient or even a very high viscosity. Cement paste fulfils these at a first glance contradictory requirements, as it is a non-newtonian material, with a strongly shear rate dependent viscosity [Haist (2009)].

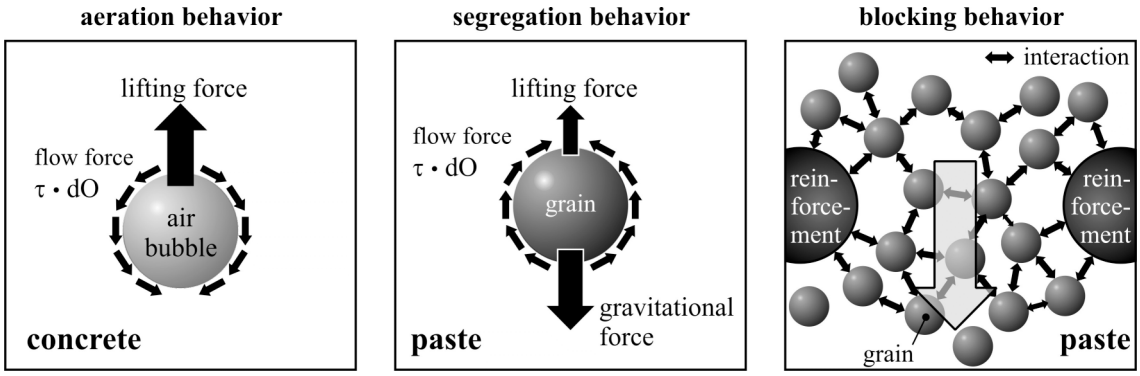

Fig. 3.1-3: Key criteria for the production of concrete: sufficient de-airing behaviour (left), high resistance against segregation (middle) and high resistance against blockage of aggregates between narrowly placed reinforcement bars

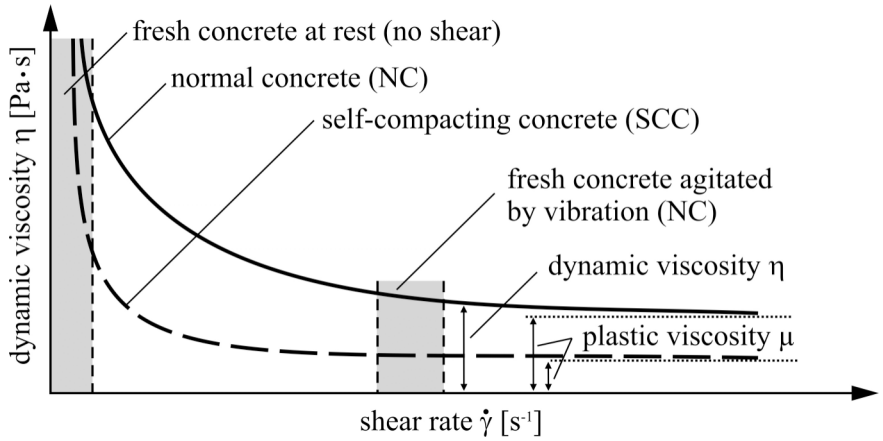

Fig. 3.1-4: Rheological behaviour of fresh normal (conventional) concrete (NC) and self-compacting concrete (SCC) as a function of the shear rate during placing

For very low shear rates or when the concrete is at rest, the concrete has a very high dynamic viscosity, which continuously reduces with increasing shear rate and approaches a final value, the so-called plastic viscosity (Fig. 3.1-4). In order to compact a concrete after placing, the material is subjected to high shear rates using a vibrator-poker. This measure reduces the viscosity of the concrete and minimizes the viscous flow resistance allowing air bubbles to escape. At rest, however, the viscosity instantly regains its previous high value, preventing segregation effects [Haist (2009)].

The invention of modern superplasticizers in combination with the use of additions such as fly ash enabled to design concretes – so-called self-compacting concretes – for which just the flow induced shear during the filling of a formwork is sufficient to facilitate de-airing. These concretes therefore do not need any additional compaction work. In order to get such a good workability, however a very high paste content is required in addition to using modern admixtures (also see Section 3.1.10.1). According to the present state-of-the-art the workability of concrete in practice is described by test results obtained from e.g. the slump test or flow table test, see [CEB-FIP MC90; Müller and Reinhardt (2010)]. Those values are used to classify the fresh concrete on the basis of its workability, see EN 206-1:2001 and EN 206-9:2008.

3.1.4 The structure of concrete

(1) Hydrated cement paste

The physical properties of concrete are to a large extent governed by the microstructure of the hydrated cement paste. After mixing, the unhydrated cement particles are surrounded by a thin layer of water. Its thickness increases with increasing water/cement mass-ratio. As hydration of the cement progresses, the hydration products – primarily calcium silicate hydrates and calcium hydroxide – grow into the space originally occupied by water. For water/cement ratios around 0.40 and a sufficient supply of water, the hydration products may eventually fill the initially water filled space almost completely. For water/cement ratios less than 0.40, there is not enough mixing water for complete hydration of the cement. Consequently, residua of unhydrated cement particles remain within the hydrated cement paste. For water/cement ratios above approximately 0.40 the hydrated cement paste contains spaces which may be filled with water and which become empty upon drying. These spaces form a system of pores generally referred to as *capillary pores* with diameters in the range of 10^{-8} to 10^{-4} m.

The hydration products of the cement do not constitute a solid mass. They consist of the *hydrated cement gel* which is formed primarily by calcium silicate hydrates into which larger crystals of calcium hydroxide are incorporated. The hydrated cement gel contains a system of *gel pores* with diameters in the range of about 10^{-10} to 10^{-8} m. These pores take up about 25 percent of the gel volume. The gel pore volume increases with increasing degree of hydration. However, it is independent of the water/cement ratio and cannot be controlled or influenced by conventional technological means. This does not hold true for the capillary porosity which increases significantly with increasing water/cement ratio *w/c* and decreasing degree of hydration. The relation between capillary porosity V_{cp}, water/cement ratio w/c and degree of hydration *m* may be described by eqs. (3.1-2 a and b). The degree of hydration, m, is defined as the mass fraction of the cement which has hydrated at a given point in time, thus $0 < m < 1.0$ [Müller and Reinhardt (2010)].

$$\frac{V_{cp}}{V_0} = \frac{w/c - 0.36 \cdot m}{w/c + 0.32} \tag{3.1-2 a}$$

taking into account the condition that

$$m_{\max} = \frac{w/c}{0.42} \leq 1.0 \tag{3.1-2 b}$$

In eq. (3.1-2a) V_0 is the initial volume of cement and mixing water. An additional characteristic of the hydrated cement gel is that its volume V_g is about twice the volume of the unhydrated cement from which it has been formed: $V_g = 2.1 \cdot m \cdot c/\rho_c$, where ρ_c is the density of the cement. However, it is less than the sum of the initial volume of unhydrated cement and water from which it has been formed [Powers (1960); Hansen (1986)]. As a consequence, some of the capillary pores become empty during hydration even under sealed conditions, i.e. when the paste neither looses water nor takes up additional water from its surrounding. This leads to internal drying, generally referred to as *self-desiccation* and consequently to shrinkage strains as will be shown in Section 3.1.6 (4). Self-desiccation is of particular significance for the higher strength grades with low water/cement ratios. In this case the internal relative humidity may be reduced to such an extent, that the hydration process is significantly slowed down or stopped entirely even without external drying.

In Fig. 3.1-5 the volume fractions of the main constituents of hydrated paste, i.e. the volume fractions of unhydrated cement residue $v_{nh} = V_{nh}/V_0$, of hydrated cement gel $v_g = V_g/V_0$, and of capillary pores $v_{cp} = V_{cp}/V_0$ are given as a function of the water/cement ratio w/c for degrees of hydration m = 0, m = 0.5 and m = 1.0, respectively. These relations are valid for hydrated cement pastes under sealed conditions.

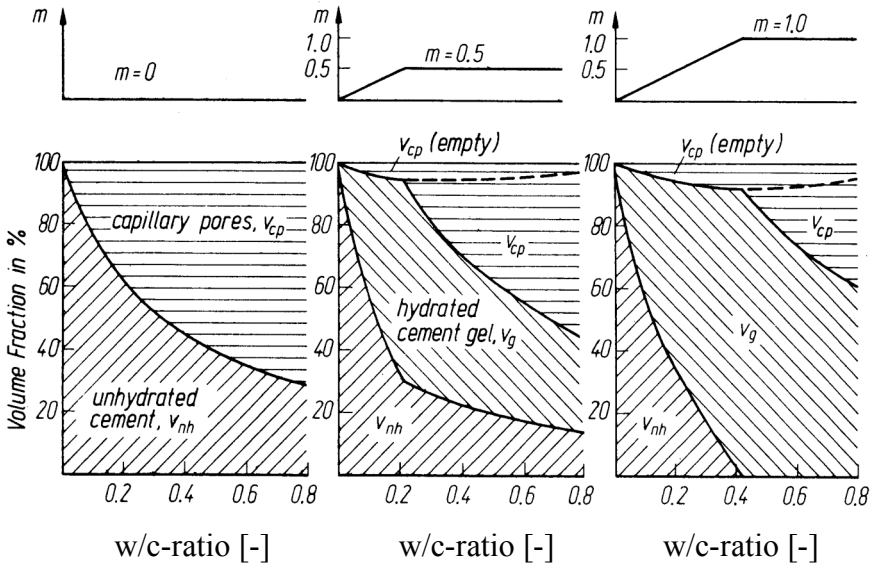

Fig. 3.1-5: The effect of water/cement ratio w/c and degree of hydration m on the volume fractions of the constituents of hydrated cement paste [Müller and Reinhardt (2010)]

As shown in the upper part of Fig. 3.1-5 the maximum degree of hydration which can be reached for lower values of *w/c* depends on the water/cement ratio as expressed by eq. (3.1-2 b). As a consequence, for a water/cement ratio of 0.2 the hydrated cement paste contains a volume fraction of unhydrated cement of more than 30 percent even at high ages. This is of particular significance for the properties of high performance concretes.

With decreasing water/cement ratio and increasing degree of hydration the *pore size distribution* of the paste is shifted to smaller sizes. This follows from Fig. 3.1-6 which shows the distribution of pore sizes in hydrated cement pastes at an age of 28 days for different water/cement ratios.

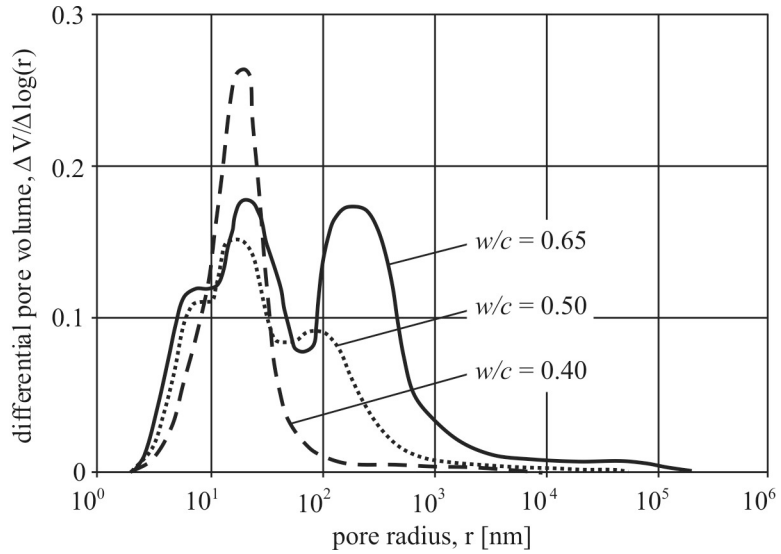

Fig. 3.1-6: Effect of water/cement ratio on the pore size distribution in hydrated cement paste

A further parameter influencing the properties of the hydrated cement paste is the *packing* of the cement grains prior to hydration. An optimum grain size distribution may lead to a close packing and thus to improved properties both with respect to strength and to impermeability of the paste. Packing may be further improved if the empty spaces between the cement grains are filled by so-called *microfillers* e.g. fine fly ash or silica fume particles. This is of particular significance for high performance concrete [Bache (1981)].

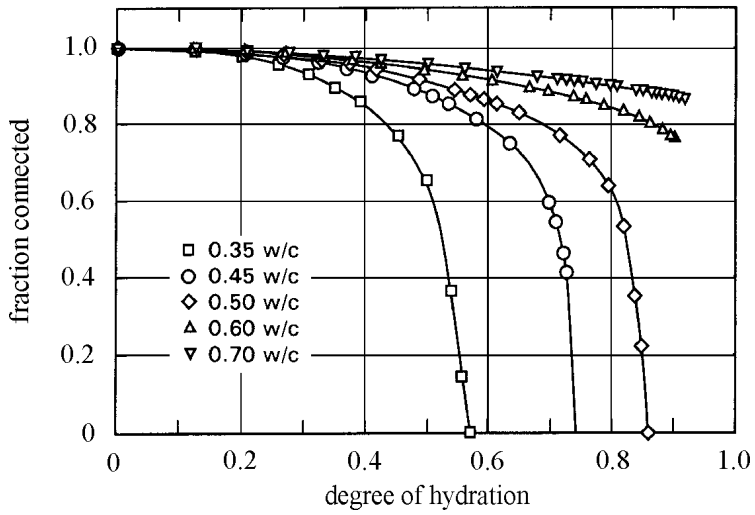

Fig. 3.1-7: Effect of water/cement ratio and degree of hydration on the connectivity of capillary pores in hydrated cement paste [Bentz and Garboczi (1991)]

For durability considerations one of the most significant microstructural parameters of hydrated cement pastes is the *continuity* or *connectivity* of the pore system. Fig. 3.1-7 shows the result of a computer simulation in which by means of the percolation theory the fraction of interconnected capillary pores in hydrated cement pastes made of different water/cement ratios is given as a function of the degree of hydration. Consequently in hydrated cement pastes with low water/cement ratios the continuity of capillary pores is drastically reduced with increasing degree of hydration. However, for $w/c > 0.60$ the capillary pore system never becomes discontinuous even at high degrees of hydration, thus facilitating the penetration of liquids or gases into the concrete (see also Section 3.1.8 and [Bentz and Garboczi (1991);

Garboczi (1992)]). This is supported by experiments from [Powers et al. (1959)] who showed a pronounced increase of water permeability of concrete for cement pastes with $w/c > 0.60$.

The considerations regarding the structure and properties of the hydrated cement paste given above are also valid for the cement paste in concrete. However, in concrete the *microstructure of the interface* between the paste and the aggregates differs significantly from that of the bulk paste. In these regions the paste generally has a higher porosity and a higher content of calcium hydroxide (see e.g. [Larbi (1993)]). In addition, the interface region may be damaged by microcracks, refer to Section 3.1.4 (2). Furthermore, the hydrated cement paste in concrete may contain larger *compaction pores* (i.e. entrapped air which failed to be expelled by the compaction of the fresh concrete) as well as *intentional air voids* to ensure a high frost resistance of the concrete (see Section 3.1.8 (2.1)).

The major parameter controlling the mechanical properties of the hydrated cement paste is its capillary porosity. The relationship between the *compressive strength* of the paste, f_{hp}, and the capillary porosity, V_{cp}/V_0, may be described with acceptable accuracy by eqs. (3.1-3 a and b) [Mindess (1984); Hansen (1986)].

$$f_{hp} = f_{go}\left(1 - a\frac{V_{cp}}{V_0}\right)^n \qquad (3.1\text{-}3\ a)$$

with

$$a = \frac{w/c + 0.32}{w/c + 0.32m} \qquad (3.1\text{-}3\ b)$$

In eq. (3.1-3 a) V_{cp}/V_0 is the volume fraction of the capillary pores. It may be estimated from eq. (3.1-2), and f_{go} is the compressive strength of a hydrated cement paste gel free of capillary pores. Both f_{go} and the power n in eq. (3.1-3 a) depend on the type of cement and other technological parameters. Fig. 3.1-8 shows an evaluation of eqs. 3.1-3 for $f_{go} = 240$ MPa, n = 3 and for m = 0.2, m = 0.5 and m = 1.0, respectively.

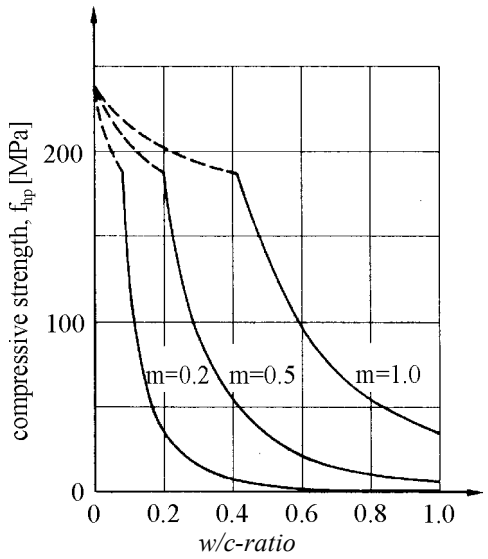

Fig. 3.1-8: Effect of water/cement ratio, w/c, and degree of hydration, m, on the compressive strength of hydrated cement paste according to eqs. (3.1-3) for $f_{go} = 240$ MPa and n = 3 [Müller and Reinhardt (2010)]

The relations shown in Fig. 3.1-8 are very similar to the well known relations between water/cement ratio and compressive strength of concrete. Nevertheless, the range of applicability of eqs. (3.1-3) is limited. According to eqs. (3.1-3 a and b) a reduction of the water/cement ratio below $w/c = 0.42 \cdot m_{max}$ leads only to a small increase of the theoretical strength of the paste. For $w/c = 0$ a limiting value of $f_{hp} = f_{go} = 240$ MPa is reached. In reality, the compressive strength of the paste increases continuously with decreasing water/cement ratio, provided sufficient workability of the paste can be maintained. This is so because at low water/cement ratios the unhydrated cement particles have a substantial strengthening effect which is not taken into account in eq. (3.1-3). Furthermore, in order to apply eq. (3.1-3 a) to the relation between the water/cement ratio and the concrete compressive strength it should be modified to take into account compaction pores as defined above.

Similar to the compressive strength, also the *modulus of elasticity* as well as the *creep* properties of the hydrated cement paste depend on the capillary porosity, and relations similar to eqs. (3.1-3) may be developed, refer to e.g. [Helmuth and Turk (1966)].

The effect of capillary porosity on the *gas* or *water permeability* of the hydrated cement paste is even more pronounced than it is on the compressive strength, because a hydrated cement gel free of capillary pores is almost impermeable to liquids or gases [Powers et al. (1959)]. Empirical relations for these properties may be found e.g. in [Kropp and Hilsdorf (Ed.; 1992)].

More details on the microstructure of hydrated cement paste are given e.g. in [Feldman and Sereda (1968); Wittmann (1977); Mindess and Young (1981); Taylor (1990)].

(2) Hardened concrete

The total porosity of normal weight concrete is in the range of 8 to 15 percent by volume. It generally decreases with decreasing aggregate porosity, decreasing water/cement ratio, increasing degree of hydration and increasing extent of compaction.

It is of particular significance for the properties of hardened concrete to consider that the interfaces between hydrated cement paste and aggregates exhibit a system of microcracks already prior to exposure to external loads or environmental effects. These cracks are the consequence of internal stresses which develop because the stiffer aggregates restrain the free shrinkage strains of the hydrating cement paste. They have a significant effect on strength and deformation characteristics of the hardened concrete as well as on its durability and transport properties. Because of these microcracks the permeability of concrete tends to be higher than that of a bulk paste with the same water/cement ratio and degree of hydration, even if dense aggregates with a very low permeability are used for the concrete.

3.1.5 Strength and deformation under short term loading

(1) Compression

(1.1) Stress state and failure process

Due to the heterogeneity of the concrete a uniform uniaxial stress applied to a concrete member results in a non-uniform, locally multiaxial state of stress. For normal weight concrete the compressive stresses in the direction of the external load are higher in the

aggregates than they are in the cement paste matrix. Perpendicular to the direction of the external load both compressive as well as tensile stresses are generated, which for low loadings are in equilibrium with each other. At a stress corresponding to about 40 percent of the compressive strength the bond cracks already present in the aggregate-paste interface start to grow. At about 80 percent of the compressive strength these cracks propagate into the matrix, predominantly in a direction parallel to the external load. To a large extent this system of microcracks is responsible for the deviation of the concrete's stress-strain diagram from linearity. With a further increase in stress, the cracks continue to grow, and shorter cracks join to form longer ones. The compressive strength is reached as soon as in a critical region the length of one or of several microcracks becomes critical so that a sudden and unstable fracture under a constant stress will occur. If, however, in the case of loading with a constant strain rate the external load is reduced after the ultimate load has been reached, the microcracks continue to grow in a stable fashion, the average strain increases and a descending portion of the stress-strain relationship can be observed. Whereas for lower and medium strength concretes microcracking is concentrated in the hydrated cement paste and in the paste-aggregate interfaces, for higher strength grades microcracks also pass through the aggregates, and different crack patterns may develop [Shah and Winter (1968); Stroeven (1973); Tasdemir et al. (1990)].

Similar to the fracture process in tension, also in compression the development of microcracks is concentrated in a limited region so that in most instances also fracture in compression is a discrete phenomenon [van Mier (1986)].

(1.2) Parameters affecting compressive strength

The compressive strength of lower and medium strength normal weight concretes is controlled primarily by the properties of the hydrated cement paste. Therefore, as a first approximation, the compressive strength of concrete is proportional to that of the hydrated cement paste. Thus concrete strength depends primarily on the water/cement ratio, on the degree of hydration, i.e. on the concrete age and curing, on the type and strength class of the cement, on the type and amount of additions and in some cases on the type of admixtures. For high strength classes, also the strength and stiffness of the aggregates is of significance. Thus the compressive strength of concrete depends primarily on its composition and the conditions during hardening, i.e. curing and environmental effects. In addition, effects of testing such as size and shape of the specimens used have to be taken into account. For further details refer to e.g. [Grübl et al. (2001); Neville (1996)].

(1.3) Stress-strain relations and modulus of elasticity

Fig. 3.1-9 shows compressive stress-strain relations for concrete strength classes ranging from about C20/25 to C80/95 [Nilson (1987)]. These relations have the characteristics already pointed out in Section 3.1.5 (1.1): up to about 40 percent of the ultimate stress, stress and strain are almost proportional, i.e. the modulus of elasticity is constant. The later is defined to be the initial slope of the stress strain curve and increases with increasing strength class. At higher stresses the stress strain relationships increasingly deviate from the linear behaviour and level out at the maximum stress $\sigma_c = - f_{cm}$. The ultimate strain at maximum stress ε_{co} is in the range of $- 0.003 < \varepsilon_{co} < - 0.002$ and increases with increasing compressive strength.

Whereas for lower strength classes the concrete subjected to compression is rather ductile, it becomes more and more brittle as the compressive strength increases. For high strength concretes a very brittle behaviour of the plain concrete has to be taken into account.

As pointed out in Section 3.1.5 (1.1) the formation of microcracks and thus the irreversible strains are often concentrated within a limited region, particularly for strains $\varepsilon_c > |\varepsilon_{co}|$. As a consequence, the descending portion of a stress-strain relationship is not unique, but depends on the gage length for which the concrete strain is recorded. If the strains in the region of concentrated microcracking are taken into account only, then the descending part of the stress-strain relationship is rather flat. For longer gage lengths the strain concentrations become smeared, and the descending portions of the stress-strain relations appear to be steeper [van Mier (1986)].

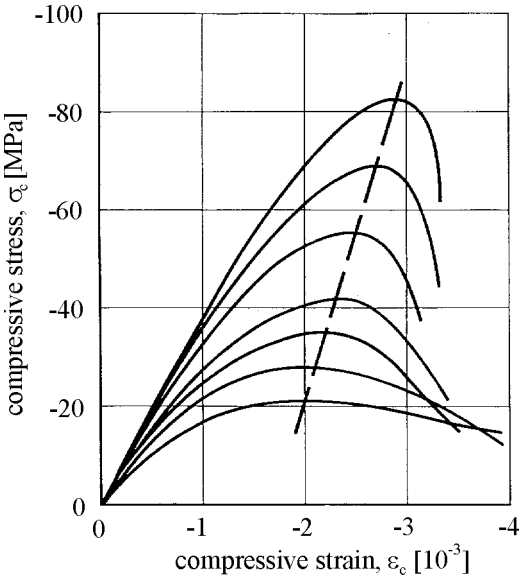

Fig.3.1-9: Stress-strain diagrams for concretes of different strength classes subjected to a constant strain rate [Nilson (1987)]

The *modulus of elasticity* of concrete is controlled by the moduli of elasticity of its components, i.e. the hydrated cement paste and the aggregates. It may be estimated from the moduli of its components on the basis of the theory of composite materials (see e.g. [Hashin (1983); Nilsen and Monteiro (1993)]). A number of empirical relations such as eq. (3.1-4) have been proposed to estimate the modulus of elasticity of a concrete from its compressive strength. This is justified as it takes into account the influence of the modulus of elasticity of the hydrated cement paste which in turn depends on the capillary porosity of the paste in a similar way than does the compressive strength of the paste.

$$E_{ci} = \alpha_E \cdot E_{co} \left(\frac{f_{cm}}{f_{cmo}} \right)^{1/3} \tag{3.1-4}$$

where:

E_{ci} tangent modulus of elasticity at $\sigma_c = 0$ [MPa] and at a concrete age of 28 days
E_{co} $= 2.15 \cdot 10^4$ MPa
f_{cm} mean compressive cylinder strength [MPa]
f_{cmo} = 10 MPa
α_E coefficient to be taken from Table 3.1-2.

The modulus of elasticity E_{ci} obtained from eq. (3.1-4) is the tangent modulus at $\sigma_c = 0$. For an elastic analysis of concrete structures a reduced modulus of elasticity $E_c = \alpha_i \cdot E_{ci}$ may be used in order to take into account initial plastic strains. The coefficient α_i may be estimated from $\alpha_i = [0.8 + 0.2\ (f_{cm} / 88\ \text{MPa})]$ under the condition that $\alpha_i \leq 1.0$.

The prediction of the modulus of elasticity can be considerably improved, if the influence of the modulus of elasticity of a particular type of aggregate is taken into account. To accomplish this, an empirical coefficient α_E has been introduced in eq. (3.1-4) which may be taken from Table 3.1-2.

type of aggregate	α_E
basalt, dense limestone	1.2
quartzitic aggregates	1.0
limestone	0.9
sandstone	0.7

Table 3.1-2: Effect of the type of aggregate on the modulus of elasticity of concrete [MC2010]

Various relations can be found in the literature to describe the stress-strain diagram of concrete in compression. Eq. (3.1-5 a) is based on a relation initially proposed by [Sargin (1971)] which has been extended to take into account the increase of the strain at maximum stress ε_{co} with increasing strength grade.

$$\frac{\sigma_c}{f_{cm}} = -\left(\frac{k \cdot \eta - \eta^2}{1 + (k-2) \cdot \eta} \right) \tag{3.1-5 a}$$

with:

$$\eta = \frac{\varepsilon_c}{\varepsilon_{c1}} \tag{3.1-5 b}$$

$$k = \frac{E_{ci}}{E_{c1}} \tag{3.1-5 c}$$

where:

σ_c compressive stress [MPa]
f_{cm} mean compressive cylinder strength [MPa]
η relative compressive strain according to eq. (3.1-5 b) [-]
ε_c compressive strain [-]
ε_{c1} strain at maximum compressive stress [-]
k plasticity number according to eq. (3.1-5 c)
E_{ci} modulus of elasticity [MPa] at concrete age of 28 days according to eq. (3.1-4)
E_{c1} secant modulus from the origin to the peak compressive stress [MPa].

Eq. (3.1-5 a) describes the ascending and the descending branch of the stress-strain relationship up to stresses $|\sigma_c| > 0.5 \cdot f_{cm}$. The effect of concrete strength grade on the strain at maximum stress may be estimated from eq. (3.1-5 b). Further comments to describe the descending branch for stresses $|\sigma_c| < f_{cm}$ are given in MC2010.

(2) Tension

(2.1) Fracture process

In a concrete member subjected to uniform tension the microcracks which are already present prior to loading start to propagate at stresses equal to about 70 percent of the tensile strength of the concrete. Consequently, the stress-strain relation for concrete subjected to tension is almost linear up to this stress level. At higher stresses the microcracks start to propagate primarily in a direction perpendicular to the external stress. In the vicinity of a notch or of larger flaws a so-called *process zone* starts to develop. Such a process zone consists of a system of more or less parallel but initially discontinuous microcracks. The process zone can still transmit tensile stresses. Therefore, it is also referred to as a *fictitious* or a *cohesive crack.*

The stresses which can be transmitted by such a cohesive crack decrease with increasing crack opening, until a continuous crack with a certain crack opening has formed. The development of a cohesive crack generally is limited to the cross-section with a notch or the largest flaw, so that the fracture process of concrete subjected to tension is even more discrete than the failure process of concrete subjected to compression. As soon as a cohesive crack reaches a critical size, unstable fracture can be avoided only by a reduction of the external stress. Therefore, also the stress-strain relation for concrete subjected to tension has a descending branch. In the band (process zone) in which the cohesive crack has developed, a steady increase of deformations occurs due to gradual opening of the crack, whereas in regions away from this critical cross-section the strains decrease as the tensile stress is reduced. Therefore, in describing the stress-strain behaviour of concrete in tension, distinction has to be made between the cross-section in which fracture develops and the sections outside the fracture zone (see also Section 3.1.5 (2.6)).

For a finite element analysis of concrete members subjected to tension, several cohesive crack models have been developed which take into account the fracture and deformation process described above. The most important are the *fictitious crack model* [Hillerborg et al. (1976)] and the *crack band model* [Bažant and Oh (1983)]. While the fictitious crack model correctly models the existence of a discrete crack it includes the disadvantage that the path of such cracks has to be estimated beforehand so that a suitable finite element net can be chosen. This is not mandatory when using the crack band model, though in this case the crack is partially smeared since its width corresponds to the width of the finite element. In general, the crack band model may be applied more universally and has been used in various commercially available finite element programs.

(2.2) Parameters affecting tensile strength

The tensile strength of concrete depends primarily on those parameters which also influence the concretes compressive strength. However, tensile and compressive strength are not proportional, and particularly for higher strength grades an increase of compressive strength leads only to a minor increase of tensile strength as will be shown in Section 3.1.5 (2.4).

Internal stresses e.g. due to drying shrinkage, which frequently lead to microcracks prior to loading, are of particular significance for the tensile strength of the concrete. As a consequence, the tensile strength may decrease for some time after the end of curing until it continues to increase again. In addition, the tensile strength strongly depends on the particular test method applied. In this context, the tensile strength generally is more size dependent than the compressive strength.

(2.3) Methods to determine tensile strength

Though the *axial tensile strength* of concrete is the most objective characteristic to describe the tensile behaviour of concrete, it is determined almost exclusively in research due to the experimental difficulties in performing such experiments.

Therefore, in many instances the *flexural strength* of concrete is determined. It is generally higher than the axial tensile strength and strongly depends on the size of the beam, particularly on its depth. Eq. (3.1-6) gives the relation between axial tensile strength of a beam and the flexural strength of concrete. According to eq. (3.1-6) this relation also depends on the size of the beam. As the depth of the beam increases, the flexural strength approaches the axial tensile strength. Eq. (3.1-6) is also given in MC2010 and has been deduced from fracture mechanics considerations.

$$f_{ctm} = f_{ct,fl} \frac{\alpha_{fl} \cdot (h_b / h_0)^{0,7}}{1 + \alpha_{fl} \cdot (h_b / h_0)^{0,7}} \tag{3.1-6}$$

where:

f_{ctm}	mean axial tensile strength [MPa]
$f_{ct,fl}$	flexural strength [MPa]
h_b	overall depth of the beam [mm]
h_o	= 100 mm
α_{fl}	= 1.5.

In MC90 a coefficient $\alpha_{fl} = 1.5$ was proposed for normal strength concrete. Since the ratio of flexural strength to axial tensile strength of concrete $f_{ct,fl}/f_{ctm}$ decreases for a given beam depth as the concrete becomes more brittle, α_{fl} depends on the brittleness of the concrete and decreases as brittleness increases. This means that for high strength concrete and for light weight aggregate concrete lower values of the coefficient α_{fl} can be expected.

Another simple method to determine concrete tensile strength is the *tensile splitting strength* which is closer to the axial tensile strength and less size dependent than is the flexural strength. Eq. (3.1-7) has been proposed in MC2010 (note Section 3.1.1, last paragraph) to estimate the mean axial strength f_{ctm} from the tensile splitting strength $f_{ct,sp}$. For further details regarding tensile splitting strength refer to e.g. [Neville (1996); Malárics (2010)].

$$f_{ctm} = 1.0 \cdot f_{ct,sp} \tag{3.1-7}$$

Note that the former relation $f_{ctm} = 0.9 \cdot f_{ct,sp}$, having been applied for many years, proved to be too inaccurate.

(2.4) Relations between tensile strength and compressive strength

Various relations have been proposed to estimate the axial tensile strength of concrete from its compressive strength. Eq. (3.1-8) is based on more recent data including also tests on high strength concretes [König and Grimm (1996)].

$$f_{ctm} = f_{ctmo} \cdot \ln(1 + f_{cm}/f_{cmo}) \quad (3.1\text{-}8)$$

where:

f_{ctm} mean axial tensile strength [MPa]
f_{cm} mean compressive strength [MPa]
f_{ctmo} = 2.12 MPa
f_{cmo} = 10 MPa.

(2.5) Fracture energy and characteristic length

The fracture mode of concrete subjected to tension allows the application of fracture mechanics concepts, i.e. energy considerations. Primarily in research but also in finite element analysis the *fracture energy* of concrete G_F is used as a material characteristic value to describe the resistance of concrete subjected to tensile stresses. The fracture energy is defined as the energy required to propagate a tensile crack of unit area. It has the dimension Nmm/mm^2 or N/mm.

Experimental methods to determine the fracture energy are dealt with e.g. in [Wittmann (Ed.; 1986)]. The fracture energy depends primarily on the water/cement ratio and the age of the concrete [Wittmann et al. (1987)]. In addition, G_F is affected by the size of the structural member and in particular the depth of the ligament in front of a crack or a notch. The influence of the maximum aggregate size is much lower as formerly stated. As a rough approximation the fracture energy may be estimated from the compressive strength of the concrete using eq. (3.1-9) [Hilsdorf and Brameshuber (1991); MC2010]).

$$G_F = 180 - \left(\frac{1385}{f_{cm}} \right) \quad (3.1\text{-}9)$$

where:

G_F fracture energy [N/mm]
f_{cm} mean concrete compressive strength [MPa].

Another useful fracture parameter is the *characteristic length* as defined by eq. (3.1-10). It corresponds to half the length of a specimen subjected to axial tension in which just enough elastic strain energy is stored to create one complete fracture surface. Thus, a decrease of the characteristic length is an indication of increased brittleness.

$$l_{ch} = \frac{E_{ci} \cdot G_F}{f_{ctm}^2} \quad (3.1\text{-}10)$$

where:

l_{ch} characteristic length [mm]
E_{ci} modulus of elasticity [MPa]
G_F fracture energy [N/mm]
f_{ctm} axial tensile strength [MPa].

The characteristic length decreases as the compressive strength increases, i.e. the concrete becomes more brittle as its tensile and compressive strength increase [Hillerborg (1983)].

(2.6) Stress-strain and stress-crack opening relations

As pointed out already, the stress-strain behaviour of concrete subjected to tensile stresses should be expressed by two relations: a stress-strain relation representing the behaviour of the concrete outside the fracture zone and a stress-crack opening relation which describes the deformation occurring within the fracture zone.

The left hand side of Fig. 3.1-10 shows experimentally determined stress-strain relations for increasing stresses as obtained in concentric tension tests on unnotched specimens made of a normal strength concrete (NSC) or of a high strength concrete (HSC), respectively. For the high strength concrete, the σ-ε-relations are almost linear up to the maximum stress, whereas for the normal strength concrete, there is a definite deviation from linearity at stresses above approximately $0.8 \cdot f_{ctm}$. The lack of curing of the unsealed specimens led to a decrease of tensile strength and to an increased non-linearity because of shrinkage stresses and associated microcracking.

For the same concretes stress-crack opening relations are given on the right hand side of Fig. 3.1-10. These were determined on notched specimens, so that the tensile strength is less than that of the unnotched specimens. The notch facilitates the crack opening measurement during a stable crack propagation. Despite of the steeper slope of the σ-w-relation of the high strength concrete, the fracture energy which corresponds to the area under the σ-w-curve, is significantly larger than that of the normal strength concrete.

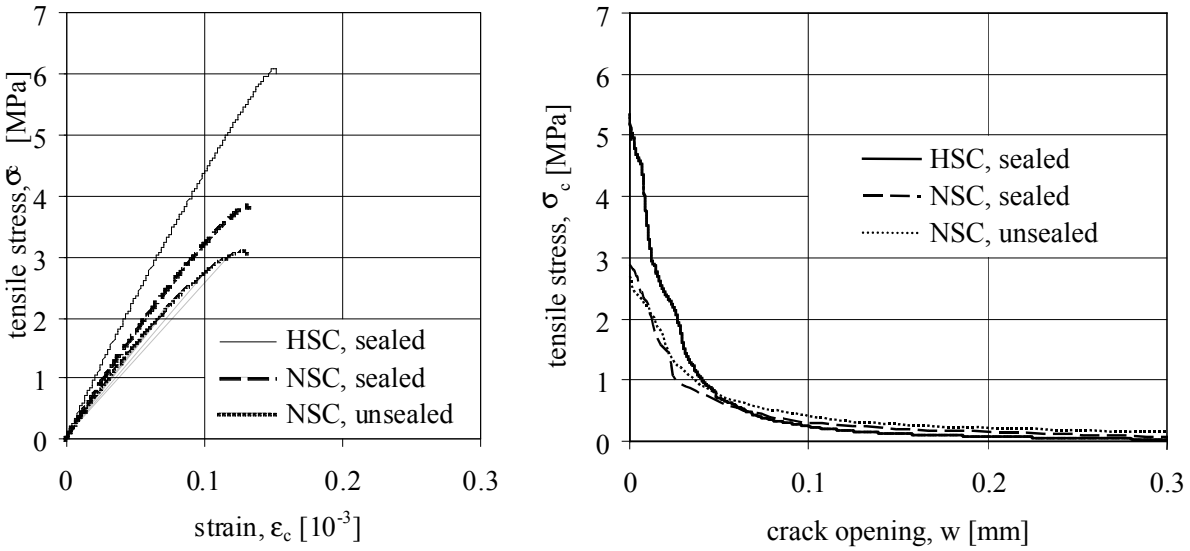

Fig. 3.1-10: Stress-strain and stress-crack opening relations for normal strength concrete (NSC) and for high strength concrete (HSC) subjected to concentric tension [Mechtcherine and Müller (1997)]

In MC2010 bilinear relations are given both for the ascending branch of the σ-ε relationship of the uncracked concrete and for the stress-crack opening relation σ-w of the cracked region. Particularly the shape of the stress-crack opening relation is of considerable importance in an analysis of a concrete member subjected to tensile stresses. The relations

given in MC2010 are in good approximation of experimental data. They correctly predict the decreasing non-linearity of the stress-strain relation with increasing compressive strength as well as the steeper slopes of the stress-crack opening relation and decreasing crack opening w at zero stress $\sigma_c = 0$ with increasing brittleness of the concrete.

(3) Multiaxial stress states

Structural elements such as slabs and shells or thick concrete structures are often subjected to a multiaxial stress state. Even in a beam subjected to bending and shear, the stress state is biaxial. The description of the strength and deformation characteristics of various concretes subjected to multiaxial stress states requires the application of special constitutive relations and strength or yield criteria. MC2010 gives such information.

The strength of concrete subjected to multiaxial states of stress depends on the same parameters which also affect the uniaxial strength of concrete, i.e. the composition and age of the concrete, the moisture state and temperature as well as the specimen size and shape, the method of testing and the loading rate. Therefore, it is generally sufficient to express the multiaxial strength as a fraction of the uniaxial strength, though the ratio of uniaxial tensile to uniaxial compressive strength f_{ctm}/f_{cm} or the ratio of biaxial compressive strength to uniaxial compressive strength f_{2cm}/f_{cm} may enter as additional parameters.

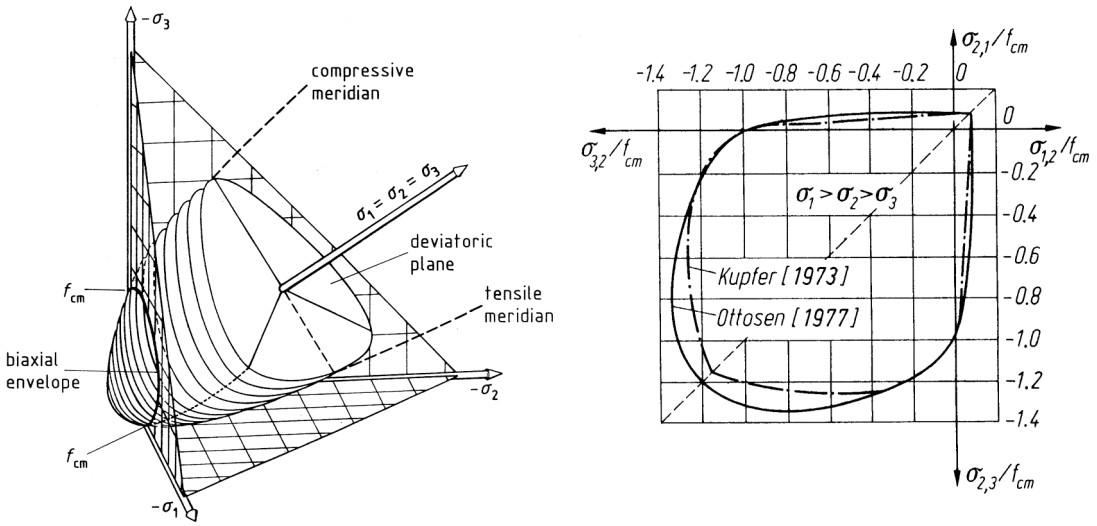

Failure surface Biaxial failure envelope

Fig. 3.1-11: Typical failure surface and biaxial failure envelope for concrete subjected to multiaxial states of stress

The strength of a material under multiaxial states of stress often is presented in terms of a failure surface as shown on the left hand side of Fig. 3.1-11. Of particular significance in such a three-dimensional diagram are the deviatoric planes, which for a given state of stress represent the deviations from a hydrostatic state of stress at failure, the compressive and the tensile meridians, which represent failure for stress states $|\sigma_1| = |\sigma_2| < |\sigma_3|$ and $|\sigma_1| = |\sigma_2| > |\sigma_3|$, respectively, and the failure envelop for biaxial stress states which is also shown on the right hand side of Fig. 3.1-11.

Eq. (3.1-11) describes a failure criterion for concrete which forms the basis of the approach given in the MC2010 and which is based on work of Ottosen [Ottosen (1977)]. For further details also refer to [CEB Bull. No. 156 (1983)].

$$\alpha \cdot \frac{J_2}{f_{cm}^2} + \lambda \cdot \frac{\sqrt{J_2}}{f_{cm}} + \beta \cdot \frac{I_1}{f_{cm}} - 1 = 0 \qquad (3.1\text{-}11)$$

where:

I_i, J_i	invariants i = 1, 2, 3 of the stress tensor and the stress deviator, respectively
f_{cm}	mean compressive strength [MPa]
α, β	coefficients which depend on the ratio f_{ctm}/f_{cm}
λ	coefficient which depends on the invariants of the stress deviators J_2 and J_3 as well as on the ratio f_{ctm}/f_{cm}.

Suitable relations to estimate the coefficients α, β and λ are given in the literature [Ottosen (1977); CEB Bull. No. 156 (1983); MC2010].

MC2010 also contains relations to estimate the *stress-strain behaviour* of concretes subjected to multiaxial states of stresses. For further details regarding the behaviour of concrete subjected to multiaxial stress states refer also to [Chen and Saleb (1994); Speck (2009); CEB Bull. No. 217 (1993)].

3.1.6 Effects of time upon strength and deformation

(1) Development of strength and modulus of elasticity with time

The rate at which the concrete strength increases with time depends on a variety of parameters, in particular the type and strength class of the cement, the type and amount of admixtures and additions, the water/cement ratio and environmental conditions. The development of the *compressive strength* with time may be estimated from eqs. (3.1-12).

$$f_{cm}(t) = \beta_{cc}(t) \cdot f_{cm} \qquad (3.1\text{-}12\ a)$$

with

$$\beta_{cc}(t) = \exp\left\{ s \cdot \left[1 - \left(\frac{28}{t/t_1} \right)^{0.5} \right] \right\} \qquad (3.1\text{-}12\ b)$$

where:

$f_{cm}(t)$	mean compressive strength [MPa] at a concrete age t [days]
f_{cm}	mean compressive strength [MPa] at a concrete age of 28 days
$\beta_{cc}(t)$	function to describe the development of compressive strength with time
t	concrete age [days]
t_1	= 1 day
s	coefficient which depends on the strength class of cement as given in Table 3.1-3.

Strength class of cement	32.5	32.5R 42.5	42.5R 52.5
s	0.38	0.25	0.20

Table 3.1-3: Coefficient s to be used in eq. (3.1-12) for different strength classes of cement [MC2010]

With reference to EN 197-1:2009, which specifies the European CEM cements, the values for the coefficient s may be taken from Table 3.1-3. Eqs. (3.1-12 a and b) are valid for a concrete temperature of 20°C. For temperatures deviating from 20°C a temperature adjusted concrete age according to eq. (3.1-40) should be used, see also Section 3.1.7 (2).

An evaluation of eqs. (3.1-12 a and b) is shown in Fig. 3.1-12 where the ratio $f_{cm}(t)/f_{cm}$ is given as a function of concrete age.

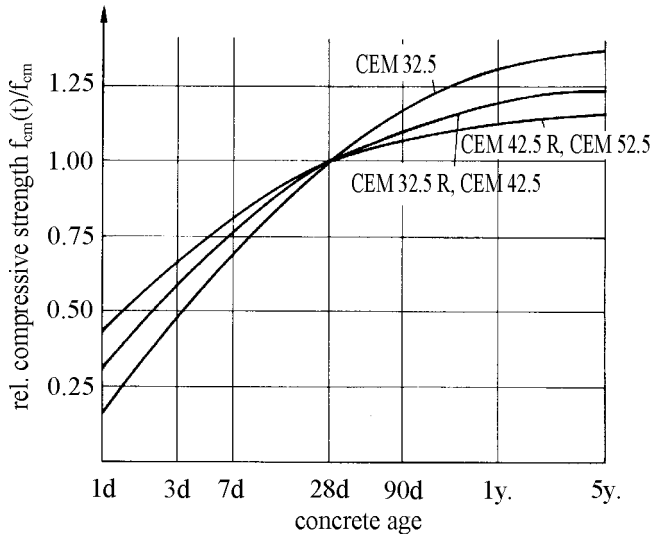

Fig. 3.1-12: Development of the concrete compressive strength with time at a temperature of 20°C

The development of *tensile strength* with time is much more difficult to predict, because it is significantly influenced by the development of shrinkage stresses which in turn depend on member size and curing conditions. Therefore, only for a concrete age larger than 28 days it may be assumed that the development of tensile strength with time is similar to that of the concrete compressive strength.

The *modulus of elasticity* of concrete develops more rapidly than does the compressive strength. $E_c(t)$ to a large extent is controlled by the modulus of elasticity of the aggregates which in turn is independent of the concrete age. This is taken into account in eqs. (3.1-13 a and b) [MC2010].

$$E_{ci}(t) = \beta_E(t) \cdot E_{ci} \qquad (3.1\text{-}13\ a)$$

with

$$\beta_E(t) = [\beta_{cc}(t)]^{0.5} \qquad (3.1\text{-}13\ b)$$

where:

$E_{ci}(t)$	tangent modulus of elasticity [MPa] at a concrete age t [days]
E_{ci}	tangent modulus of elasticity [MPa] at a concrete age of 28 days according to eq. (3.1-4)
$\beta_E(t)$	function to describe the development of the modulus of elasticity with time
$\beta_{cc}(t)$	coefficient according to eq. (3.1-12 b)
t	concrete age [days].

(2) Strength and deformation under sustained high loadings

Concrete compressive strength also depends on the duration during which it is exposed to a constant stress. This is of practical significance because for many concrete structures the live load is small compared to the total load, so that the stresses acting on a structural element may vary little with time. A sustained stress in the range of working stresses may lead to a slight increase of compressive strength, see e.g. [Awad and Hilsdorf (1974); Probst and Stöckl (1978)]. If, however, high sustained stresses act on the concrete, the process of microcracking accelerates and may eventually lead to failure. As the sustained stress decreases, the time to failure increases. The maximum stress, which the concrete can endure without failure, is referred to as *sustained load strength*. For a concrete loaded at an age of 28 days it corresponds to approximately 80 percent of its strength under short term loading.

As a result of two counteracting effects, the sustained load strength depends on the age of the concrete at the time of loading: a high sustained stress causes a strength reduction due to continued microcracking. At the same time the concrete continues to hydrate, provided that a sufficient amount of water is available resulting in a strength increase. If the rate of strength growth due to continued hydration is more pronounced than the loss of strength due to continued microcracking, then failure under the sustained load will no longer occur. This state will be reached the sooner, the younger the concrete is at the time the sustained stress has been applied. This is due to the fact that young concrete has a higher potential for continued hydration than older concrete for which hydration may have come to an end at the time of load application. This effect must be especially considered when redesigning very old concrete structures on the basis compressive strength values determined on cores.

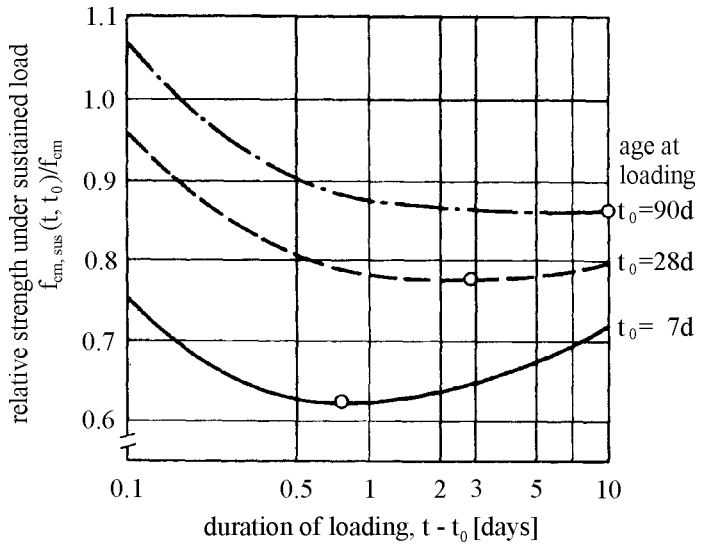

Fig. 3.1-13: Compressive strength of concrete subjected to sustained high overloads according to the relations given in MC2010

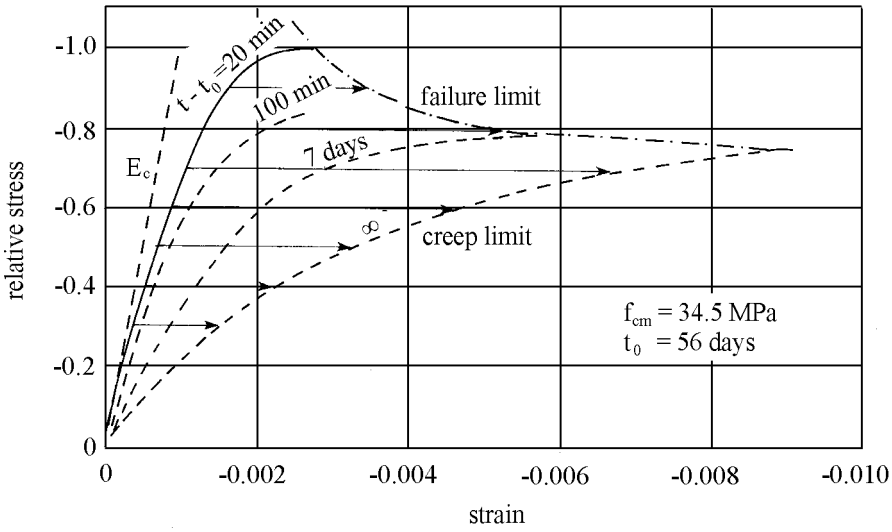

Fig. 3.1-14: Limiting strains of concrete subjected to uniaxial compression [Rüsch (1960)]

The period of time during which a concrete may fail under the action of a sustained stress is referred to as the *critical period* [Rüsch (1960)]. In MC2010 analytical expressions are given to estimate the strength of concrete under the action of a sustained load depending on the age at loading, the duration of loading and the type of cement. They are based on data from [Rüsch et al. (1962)]. Fig. 3.1-13 shows the relative strength under a sustained load as predicted by the relations given in MC2010.

Under the action of a high sustained overload the concrete strains continue to increase. In cases where failure is approached, the strains grow at an increasing rate and may eventually reach values up to 0.010 as shown in Fig. 3.1-14 [Rüsch (1960)].

It is worth noting that the parabola-rectangle stress-strain diagram often used in design, dealt with in Section 4.4.1 (3.3) and described by eqs. (4.4-1) through (4.4-3), is not a relation between a monotonically increasing strain and the corresponding stress but rather a fictitious stress-strain relation which describes the most probable stress distribution in the compression zone of a concrete member subjected to high sustained moments and/or axial forces. It takes into account both the loss of strength and the increase of strain under the action of sustained high overloads. The parabola-rectangle stress-strain diagram has been deduced from the extreme fibre strains at failure observed on prisms which were subjected to centric or to eccentric sustained high overloads. For further details refer e.g. to [Rüsch et al. (1962)].

(3) Definitions of time-dependent deformations

Time-dependent deformations may be stress-dependent or stress-independent. The stress independent strains or volume changes are mainly *shrinkage* and *swelling*. They are primarily caused by the loss or absorption of water by the concrete. They are defined as the time-dependent volume change or strains of a concrete specimen not subjected to an external stress at a constant temperature.

The time-dependent strains due to constant stresses are referred to as *creep*. Such strains are defined as the difference between the increase of strains with time of a specimen subjected to a constant sustained stress and the load independent strain observed on an unloaded companion specimen. Closely related with creep and caused by the same physical processes is *relaxation*, i.e. the time-dependent reduction of stress due to a constant imposed strain.

The total strain $\varepsilon_c(t)$ occurring at time t in a concrete member subjected to a sustained, uniaxial stress may be expressed by eqs. (3.1-14 a and b).

$$\varepsilon_c(t) = \varepsilon_{ci}(t_o) + \varepsilon_{cc}(t, t_o) + \varepsilon_{cs}(t) + \varepsilon_{cT}(t, T) \qquad (3.1\text{-}14\ a)$$

and

$$\varepsilon_c(t) = \varepsilon_{c\sigma}(t) + \varepsilon_{cn}(t) \qquad (3.1\text{-}14\ b)$$

where:

$\varepsilon_{ci}(t_o)$		stress-dependent initial strain (elastic strain) at the time of stress application
$\varepsilon_{cc}(t, t_o)$		creep strain at a concrete age $t \geq t_o$
$\varepsilon_{cs}(t)$		shrinkage or swelling at a concrete age t
$\varepsilon_{cT}(t, T)$		thermal strain at a concrete age t, refer to Section 3.1.7 (1)
$\varepsilon_{c\sigma}(t, t_o)$	$= \varepsilon_{ci}(t_o) + \varepsilon_{cc}(t)$	total stress-dependent strain at a concrete age t
$\varepsilon_{cn}(t, T)$	$= \varepsilon_{cs}(t) + \varepsilon_{cT}(t, T)$	total stress independent strain at a concrete age t.

Fig. 3.1-15 shows the total strain of a concrete specimen uniaxially loaded at the time t_0 with a constant stress $\sigma_c(t_0)$ = const. and completely unloaded at the time t_e assuming that the specimen is exposed to constant climate conditions (relative humidity RH = const. < 100%; temperature T = const.). It is visualised that the initial loading causes not only an initial elastic strain $\varepsilon_{ci}(t_0)$ but also an initial plastic strain component $\varepsilon_{cip}(t_0)$, often termed as initial set. This component results primarily from initial microcracking and is the more pronounced the lower the concrete strength. For conventional structural concrete the magnitude is below 5% of the initial elastic strain $\varepsilon_{ci}(t_0)$. Per definition $\varepsilon_{cip}(t_0)$ is considered as part of the creep strain $\varepsilon_{cc}(t, t_0)$.

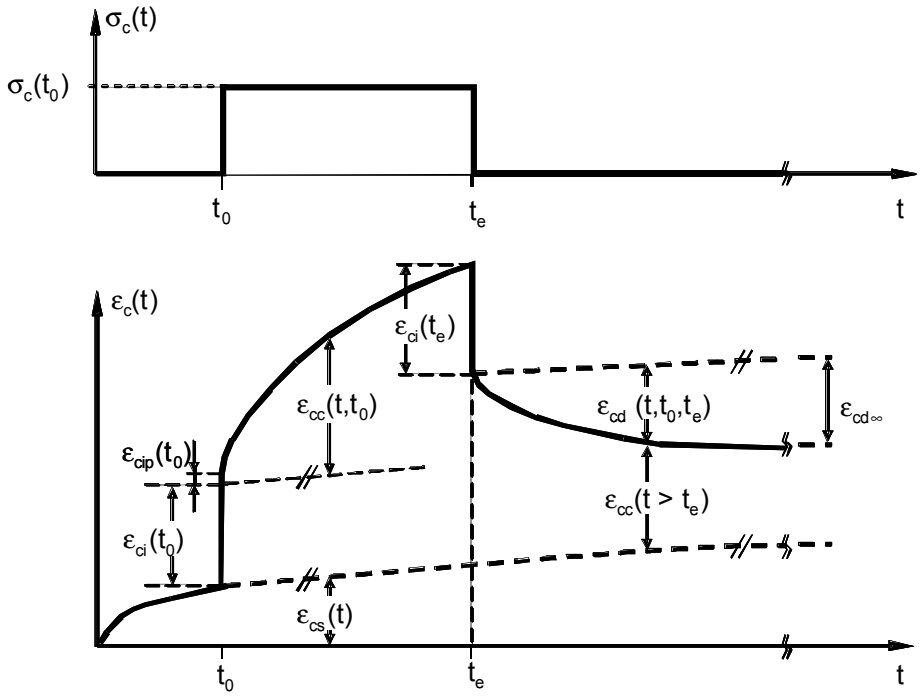

Fig. 3.1-15: Definition of the strain components of a uniaxially loaded and unloaded concrete specimen

Further Fig. 3.1-15 indicates that creep is partially reversible. The delayed elastic strain $\varepsilon_{cd}(t, t_0, t_e)$ develops after unloading and approaches a final falue $\varepsilon_{cd\infty}$. Its magnitude is usually below 50% of the initial elastic strain of a concrete at the age of 28 days.

It should be kept in mind that the distinction between creep as a stress-dependent strain and shrinkage as stress independent strain is conventional and in times useful to facilitate analysis and design. In reality, shrinkage and creep are interrelated phenomena. Further, the shrinkage of a loaded (creeping) concrete is supposed to be different to the shrinkage of an unloaded concrete. However, such a difference cannot be experimentally determined. Similar limitations are valid for the distinction between initial strain at the time of load application and creep as can be seen from Fig. 3.1-15. The behaviour of a structure is governed by the total strain at a given time.

(4) Shrinkage

(4.1) Basic considerations

The term shrinkage is generally used as the shorthand expression for drying shrinkage of hardened concrete. This deformation occurs when ordinary hardened concrete is exposed to air with a relative humidity of less than 100 percent. However, several other types of shrinkage deformations exist, such as plastic shrinkage, autogenous shrinkage and carbonation shrinkage, which may occur simultaneously and which are added up as total shrinkage.

Plastic shrinkage occurs when water is lost from concrete while it still is in its plastic state. *Autogenous shrinkage*, also called *basic shrinkage*, *self-desiccation shrinkage* or *chemical shrinkage*, is associated with the ongoing hydration reaction of the cement as shown in Section 3.1.4 (1). It occurs irrespective of the ambient medium due to chemical volume changes and internal drying. *Carbonation shrinkage* is caused by the reaction of cement stone components with carbon dioxide in the air in the presence of moisture. Among the different types of shrinkage, *drying shrinkage* is the most important type of shrinkage in concrete practice.

Using a proper concrete composition, casting and curing procedures plastic shrinkage may be avoided in most practical cases. While autogenous shrinkage is small for ordinary concrete, it is significant for high performance concretes with low water/cement ratios. Nevertheless, it appears to be reasonable to model shrinkage as the sum of autogenous (basic) and drying shrinkage for all types of concrete, refer to Section 3.1.6 (4.2).

For ordinary concrete as a first approximation water loss due to drying and shrinkage of concrete are proportional [Verbeck and Helmuth (1969)]. Since drying of concrete is a rather slow diffusion process, also the development of drying shrinkage with time is slow. The surface-near regions of a concrete section reach a state of moisture equilibrium with the surrounding environment already after a short period of time. However, with increasing distance from the concrete surfaces, the moisture content of the concrete increases so that e.g. in the centre of a concrete cylinder with a diameter of 500 mm the relative humidity in the pore system of the concrete is still above 90 percent when stored in air with a relative humidity of 60 percent over a period of several years [Philajavara (1982)]. Since the moisture distribution in the concrete section is non-uniform and the moisture content increases from the surface towards the centre, internal stresses develop. These are tensile stresses in the surface-near regions and compressive stresses in the interior regions. These tensile stresses quite often lead to surface cracks. Similar stresses do not occur for the autogenous (basic) shrinkage

component, as this deformation develops nearly uniform throughout the cross-section of a building member.

Additional internal stresses occur due to the fact that the hydrated cement paste generally shrinks much more than the stiffer aggregates. These stresses may lead to microcracks in the aggregate-paste interface. Further shrinkage stresses develop in statically indetermined structures if the average shrinkage strain of a structural member is restrained by the supports or other parts of the structure. Cracks across the entire section may be the consequence.

When estimating such shrinkage stresses, the effect of creep always has to be taken into account: since shrinkage stresses develop only gradually with time, they are substantially reduced by creep, refer to e.g. [Neville et al. (1983); Rüsch et al. (1983)].

The physical processes leading to drying shrinkage of concrete are clarified reasonably well. The primary causes are changes in capillary stresses in the pore system of the hydrated cement paste, changes in the surface energy of the hydration products due to changes of the moisture content as well as the so-called disjoining pressure between hydration products [Wittmann (1977)]. Autogenous shrinkage results from the volume reduction during the hydration of cement, i.e. the volume of the hardened cement paste is less than the sum of the volume of water and the volume of cement prior to the chemical reaction. The main reason is the higher density of the chemically bound water compared to free water. In addition, a self-desiccation within the cement paste occurs during hydration which causes internal capillary or pore stresses which result in an additional volume reduction. Though normal weight aggregates usually shrink very little, their mechanical properties and in particular their moduli of elasticity substantially influence the magnitude of shrinkage of concrete.

Total shrinkage strain after long durations of drying ranges from about 0.1 to 1 ‰. For normal strength concrete the most important parameter influencing the magnitude of shrinkage is the water loss after a given duration of drying. Shrinkage, therefore, increases with increasing water content of the concrete and decreasing relative humidity of the surrounding environment. For high performance concrete drying shrinkage is substantially reduced as the capillary porosity is very low leading to a substantial reduction of the water loss of concrete.

As a first approximation, total shrinkage is proportional to the cement paste content. Generally shrinkage of concrete increases with increasing fineness of the cement. Also the chemical composition of the cement, in particular its content of alkalis, may influence shrinkage. Shrinkage of concrete decreases with increasing modulus of elasticity of the aggregates, since stiff aggregates restrain shrinkage of the paste more effectively than soft aggregates. The size of a concrete member influences drying shrinkage in the view of the fact that, as small sections lose moisture at a much higher rate than thick sections. Therefore, they shrink much more rapidly. Even though the final value of shrinkage deformation should be independent of the member size practically a reduction of deformations with increasing member size in structural analysis and design is justified, since thick sections may reach their final shrinkage values only after several centuries. The duration of curing has little influence on the magnitude of drying shrinkage for normal strength concrete. For high performance concrete it should be kept in mind that already during the moist curing period autogenous shrinkage develops, so that total shrinkage during drying is the smaller the longer the preceding curing period. For all types and classes of concrete, curing is decisive for the resistance of a concrete against the formation of shrinkage cracks which often are caused by insufficient curing.

When subjected to alternate drying and wetting, shrinkage strains are only partially reversible so that swelling during a wetting period is substantially smaller than the preceding

shrinkage e.g. [Bažant and Wang (1985)]. With respect to the development of shrinkage with time, refer to Section 3.1.6 (4.2).

(4.2) Prediction of shrinkage

The model presented below predicts the mean time-dependent shrinkage behaviour of a plain structural concrete member which is exposed to a dry or to a moist environment after curing. It is valid for normal and for high strength concrete up to a strength of 120 MPa, moist cured at normal temperatures not exceeding 14 days and exposed to a mean relative humidity in the range of 40 to 100 percent.

It should be pointed out that similar to the models given in MC2010 also the prediction models for shrinkage as well as for creep given in the book at hand include concrete compressive strength as a major parameter to be taken into account when estimating concrete deformation properties. In reality, shrinkage and creep strains per se do not depend on concrete compressive strength but rather on parameters related to the microstructure and the concrete composition such as the water/cement ratio, the degree of hydration and the properties of the aggregates etc. However, the prediction models given in the following are aimed at assisting the designer, who in most instances at the stage of design has no knowledge of the concrete properties and composition etc. other than the required strength grade. In this case, the concrete compressive strength can serve as an indirect measure of the microstructural properties of concrete and thus is a useful parameter in prediction models.

In contrast to previous prediction models, in this new model total shrinkage is subdivided into a autogenous shrinkage (also termed basic shrinkage) and a drying shrinkage component. Such an approach was necessary, so that shrinkage of normal as well as of high strength concrete can be predicted with sufficient accuracy [Müller et al. (1999)]. The significance of autogenous shrinkage in high strength concrete becomes apparent in Fig. 3.1-16 which shows the development of the shrinkage components with time both for normal strength concrete (NSC) and for high strength concrete (HSC).

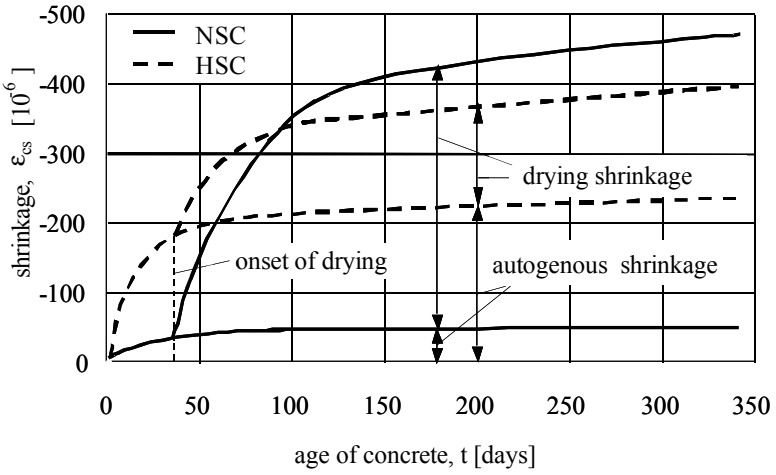

Fig. 3.1-16: Time development of autogenous shrinkage and of drying shrinkage in normal strength (conventional) concrete (NSC) and in high strength concrete (HSC)

The total shrinkage may be calculated from eqs. (3.1-15 a to c).

$$\varepsilon_{cs}(t,t_s) = \varepsilon_{cas}(t) + \varepsilon_{cds}(t,t_s) \qquad (3.1\text{-}15\ a)$$

with

$$\varepsilon_{cas}(t) = \varepsilon_{caso}(f_{cm}) \cdot \beta_{as}(t) \qquad (3.1\text{-}15\ b)$$

and

$$\varepsilon_{cds}(t, t_s) = \varepsilon_{cdso}(f_{cm}) \cdot \beta_{RH}(RH) \cdot \beta_{ds}(t - t_s) \qquad (3.1\text{-}15\ c)$$

where:

$\varepsilon_{cs}(t, t_s)$	total shrinkage at time t
$\varepsilon_{cas}(t)$	autogenous shrinkage at time t
$\varepsilon_{cds}(t, t_s)$	drying shrinkage at time t
$\varepsilon_{caso}(f_{cm})$	notional autogenous shrinkage coefficient from eq. (3.1-16 a)
$\varepsilon_{cdso}(f_{cm})$	notional drying shrinkage coefficient from eq. (3.1-17 a)
$\beta_{as}(t)$	function to describe the time development of autogenous shrinkage, from eq. (3.1-16 b)
$\beta_{RH}(RH)$	coefficient to take into account the effect of rel. humidity on drying shrinkage, from eq. (3.1-17 b)
$\beta_{ds}(t - t_s)$	function to describe the time development of drying shrinkage, from eq. (3.1-17 c)
t	concrete age [days]
t_s	concrete age at the onset of drying [days]
$t - t_s$	duration of drying [days].

Autogenous shrinkage $\varepsilon_{cas}(t)$ according to eq. (3.1-15 b) may be estimated by applying eqs. (3.1-16).

$$\varepsilon_{caso}(f_{cm}) = -\alpha_{as}\left(\frac{f_{cm}/f_{cm0}}{6 + f_{cm}/f_{cm0}}\right)^{2.5} \cdot 10^{-6} \qquad (3.1\text{-}16\ a)$$

and

$$\beta_{as}(t) = 1 - exp\left(-0.2 \cdot \left(\frac{t}{t_1}\right)^{0.5}\right) \qquad (3.1\text{-}16\ b)$$

where:

f_{cm}	mean compressive strength at the age of 28 days [MPa]
f_{cm0}	= 10 MPa
α_{as}	coefficient which depends on the type of cement:
	α_{as} = 800 for slowly hardening cements
	α_{as} = 700 for normal or rapidly hardening cements
	α_{as} = 600 for rapidly hardening high strength cements
t	concrete age [days]
t_1	= 1 day.

Note that autogenous shrinkage is independent of the ambient humidity and of the member size and develops more rapidly than drying shrinkage.

For drying shrinkage $\varepsilon_{cds}(t, t_s)$ according to eq. (3.1-15 c) the subsequent eqs. (3.1-17) may be applied.

$$\varepsilon_{cdso}(f_{cm}) = \left[(220 + 110 \cdot \alpha_{ds1}) \cdot exp\left(- \alpha_{ds2} \cdot \frac{f_{cm}}{f_{cmo}} \right) \right] \cdot 10^{-6} \qquad \text{(3.1-17 a)}$$

$$\left.\begin{aligned} \beta_{RH}(RH) &= -1.55 \left[1 - \left(\frac{RH}{RH_o} \right)^3 \right] \quad \text{for } RH < 99\% \cdot \beta_{s1} \\ \beta_{RH}(RH) &= 0.25 \qquad\qquad\qquad\quad \text{for } RH \geq 99\% \cdot \beta_{s1} \end{aligned}\right\} \qquad \text{(3.1-17 b)}$$

$$\beta_{ds}(t - t_s) = \left[\frac{(t - t_s)/t_1}{350(h/h_o)^2 + (t - t_s)/t_1} \right]^{0.5} \qquad \text{(3.1-17 c)}$$

$$\beta_{s1} = \left(\frac{3.5 f_{cmo}}{f_{cm}} \right)^{0.1} \qquad \text{(3.1-17 d)}$$

where:

f_{cm}	mean compressive strength at the age of 28 days [MPa]
f_{cmo}	= 10 MPa
α_{ds1}	coefficient which depends on the type of cement
	α_{ds1} = 3 for slowly hardening cements
	α_{ds1} = 4 for normal or rapidly hardening cements
	α_{ds1} = 6 for rapidly hardening high strength cements
α_{ds2}	coefficient which depends on the type of cement
	α_{ds2} = 0.13 for slowly hardening cements
	α_{ds2} = 0.12 for normal or rapidly hardening cements
	α_{ds2} = 0.12 for rapidly hardening high strength cements
β_{s1}	coefficient to take into account self-desiccation in high performance concretes
RH	ambient relative humidity [%]
RH_o	= 100%
t	age of concrete [days]
t_1	= 1 day
t_s	age of concrete at the beginning of shrinkage [days]
h	= 2 A_c/u notional size of member [mm], where A_c is the cross-section [mm^2] and u is the perimeter of the member in contact with the atmosphere [mm]
h_o	= 100 mm.

According to eq. (3.1-17 b) for normal strength concretes swelling is to be expected if the concrete is exposed to an ambient relative humidity equal to or above 99%. For higher strength grades swelling will occur already at lower relative humidities because of the preceding reduction of the internal relative humidity due to self-desiccation of the concrete.

(5) Creep

(5.1) Basic definitions and considerations

In the range of service stresses, i.e. $\sigma_c \leq 0.4 \cdot f_{cm}(t_0)$, where $f_{cm}(t_0)$ is the cylindrical compressive strength at the age t_0, concrete may be considered as an aging linear viscoelastic material. Hence, creep strains are linearly related to stress. The quotient of creep strain and elastic strain is called creep coefficient φ, see eq. (3.1-18).

$$\varphi(t,t_o) = \frac{\varepsilon_{cc}(t,t_o)}{\varepsilon_{ci}} \tag{3.1-18}$$

where:

$\varphi(t, t_o)$ creep coefficient
$\varepsilon_{cc}(t, t_o)$ creep strain at time t of a concrete loaded at an age t_o
ε_{ci} initial strain (elastic strain) when concrete is loaded at an age of 28 days.

Note that the creep coefficient is sometimes also defined as the ratio $\varphi^*(t,t_0) = \varepsilon_{cc}(t,t_0)/\varepsilon_{ci}(t_0)$, see e.g. [ACI 209 (2008)]. However, this definition is accompanied by the disadvantage that $\varphi^*(t,t_0)$ not only describes the time effects on creep, but also the time effects on the initial strain. As a consequence, strange results may be obtained for very young concretes, i.e. $\varphi^*(t,t_0)$ firstly increases with increasing age at loading before it decreases again. On the basis of eq. (3.1-18) the creep strain $\varepsilon_{cc}(t, t_o)$ may be expressed by eq. (3.1-19).

$$\varepsilon_{cc}(t,t_o) = \varphi(t,t_o) \cdot \frac{\sigma_c(t_o)}{E_{ci}} \tag{3.1-19}$$

where:

$\sigma_c(t_o)$ creep inducing stress, i.e. stress applied at time t_o
E_{ci} modulus of elasticity at a concrete age of 28 days either from measurement values or deduced from the compressive strength according to eq. (3.1-4).

Eq. (3.1-19) is valid as ε_{ci} may be expressed as $\varepsilon_{ci} = \sigma_c(t_o)/E_{ci}$.

The total stress-dependent strain $\varepsilon_{c\sigma}(t, t_o)$ follows from eq. (3.1-20).

$$\varepsilon_{c\sigma}(t,t_o) = \sigma_c(t_o)\left[\frac{1}{E_c(t_o)} + \frac{\varphi(t,t_o)}{E_{ci}}\right] = \sigma_c(t_o) \cdot J(t,t_o) \tag{3.1-20}$$

where:

$J(t, t_o)$ creep function or creep compliance representing the total stress-dependent strain per unit stress
$E_c(t_o)$ modulus of elasticity at the time of loading t_o.

In practice, creep of concrete under variable stresses is of particular significance. In consistence with the assumption of linearity the principle of superposition may be applied. According to this principle, the strain caused by the stress history $\sigma_c(t)$ may be obtained by decomposing the stress history to small increments $\Delta\sigma_c$ applied at times τ_i, and summing up the corresponding strains which leads to eqs. (3.1-21 a and b).

$$\varepsilon_c(t,\sigma_c) = J(t,t_o)\cdot\sigma_c(t_o) + \sum_{i=1}^{n} J(t,\tau_i)\cdot\Delta\sigma_c(\tau_i) \qquad (3.1\text{-}21\ a)$$

In eq. (3.1-21 a) $\Delta\sigma_c(\tau_i)$ may be substituted by $\frac{\partial\sigma_c(\tau)}{\partial\tau}\cdot d\tau$ if $\sigma_c(t)$ is a continuous function. Then eq. (3.1-21 a) may be expressed as follows by eq. (3.1-21 b). Note that t is the age of concrete at the moment considered and τ is the time as integration variable with $t_0 \le \tau \le t$.

$$\varepsilon_c(t,\sigma_c) = J(t,t_o)\cdot\sigma_c(t_o) + \int_{t_o}^{t} J(t,\tau)\cdot\frac{\partial\sigma_c(\tau)}{\partial\tau}\cdot d\tau \qquad (3.1\text{-}21\ b)$$

The principle of superposition describes the behaviour of concrete under variable stresses reasonably well if the stresses are within the service stress range, if there is no significant change in moisture content and moisture distribution during creep and if complete unloading does not take place.

In view of modelling the creep of concrete, different constitutive approaches for the creep function $J(t, t_o)$ or the creep coefficient $\varphi(t, t_o)$ may be adopted. Depending on the approach and the types of aging function and time development function which are included in $\varphi(t, t_o)$, different prediction accuracies for creep under constant and in particular under variable stresses are obtained. In addition, some mathematical procedures in calculating creep effects in practical applications are facilitated by a certain type of constitutive approach [CEB Bull. No. 199 (1990); Bažant (1988)].

Eq. (3.1-21 b) is a general constitutive relation for concrete which allows to calculate strains if the stresses are given or, vice versa, to calculate stresses if a strain history is considered. In the latter case, eq. (3.1-21 b) represents a Volterra integral equation which for realistic forms of $J(t, t_o)$ must be numerically solved even in the case of pure relaxation, where the stress decreases with time such that an imposed strain remains constant.

Similar to the creep coefficient $\varphi(t, t_o)$, for the case of constant stress, relaxation may be described by a relaxation coefficient $\psi(t, t_o) = \Delta\sigma_c(t, t_o)/\sigma_o$ where $\Delta\sigma_c(t, t_o)$ is the decrease of stress at time t for an age at loading t_o, and σ_o is the initial stress. Relaxation coefficient and creep coefficient are interrelated according to eq. (3.1-22).

$$\psi(t,t_o) = \frac{\varphi(t,t_o)}{1+\rho\cdot\varphi(t,t_o)} \qquad (3.1\text{-}22)$$

In eq. (3.1-22) ρ is referred to as aging coefficient. For longer durations of loading $\rho \approx 0.8$. More accurate values for ρ may be found in [CEB Bull. No. 215 (1993)]. Because of the relation between creep and relaxation the relaxation coefficient depends on the same parameters as the creep coefficient, also refer to [Bažant (1988)].

(5.2) Parameters and creep effects

Creep of concrete depends both on internal factors such as the material properties of the phases of a concrete and its composition, and on external parameters such as the ambient climate. Similar to shrinkage, creep is as a first approximation proportional to the volume fraction of the cement paste. It increases with increasing capillary porosity. Consequently, creep of concrete decreases with decreasing water/cement ratio and increasing degree of hydration at the time of loading, i.e. with increasing age at loading. Creep increases with increasing volume content of hydrated cement paste and decreasing stiffness of the aggregate, as aggregates normally do not creep and restrain the creep of the hydrated cement paste. Furthermore, creep increases with increasing moisture content of the concrete and increasing loss of moisture while subjected to loading. Consequently, creep increases with decreasing ambient humidity and decreasing thickness of a structural member. Note that there is a pronounced interrelation between the individual parameters affecting creep.

The development of creep with time is of particular practical significance. It depends on the moisture state of the concrete and its variation during the creep process. Thin concrete sections creep at a higher rate than thick sections, since they lose moisture more rapidly. As an example, Fig. 3.1-17 shows the influence of the ambient relative humidity on the magnitude and on the time development of the creep function. Here also a typical phenomenon becomes evident: if the concrete looses moisture during the creep process (RH = 50 or 70%, respectively), the observed time functions are s-shaped whereas when a moisture loss is prevented, the time function develops linear in semi logarithmic scale (strain over duration of loading), in particular for higher durations of loading.

It is still controversial whether concrete creep approaches a finite value. However, from the view point of the designer, this is of little significance because in the range of working stresses the rate of creep decreases substantially with increasing duration of loading. After a duration of loading of about 70 years the rate of creep is so low that creep is not likely to increase by more than 5% during the subsequent 70 years [CEB Bull. No. 217 (1993)]. Therefore, it is justified to base calculations, in which not the highest level of accuracy is sufficient, on a "final" creep coefficient. For structural concretes these final values are in the range of $1 < \varphi_\infty < 5$, i.e. the creep strain may be up to five times the initial strain.

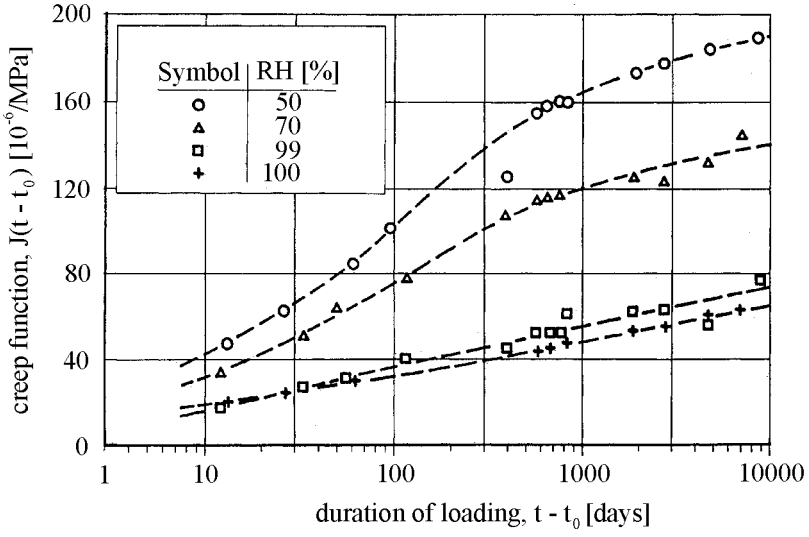

Fig. 3.1-17: Effect of the relative humidity on the time development of the creep function [Troxell et al. (1958)]

Creep of concrete is partially reversible, i.e. some part of the developed creep strain under load will be recovered upon unloading. Therefore, creep may be separated into an irreversible strain component, generally referred to as *flow,* and in a reversible strain component, the *delayed elastic strain*. Due to the significant influence of the water content of the concrete and the water loss due to drying while the concrete is under load, creep may also be separated into the components *basic creep* and *drying creep.* Basic creep is defined as the creep strain of a concrete which neither loses nor gains water while under loading. The difference of total creep of a drying concrete and basic creep is defined as drying creep. When creep is modelled, the chosen constitutive approach, which may take into account reversible/irreversible strains or basic/drying creep components, affects the prediction accuracy. Summaries and experimental results on creep and their evaluation may be found e.g. in [CEB Bull. No. 199 (1990)]. A database which contains most of the significant results on creep experiments reported in the literature has been prepared by [RILEM TC 107, SC 5 (1999)].

The causes of creep are known only to a limited extent. It is, however, generally accepted that creep of concrete is almost exclusively due to creep of the hydrated cement paste, since normal weight aggregates show little or no creep deformation. Creep of the hydrated cement paste is governed to a large extent by water within the paste. In addition to stress-dependent movements of water within the pore system of the paste, sliding and compaction processes may take place. The increase of creep at high stresses is caused primarily by a time-dependent growth of microcracks which for very high stresses may lead to failure as described in Section 3.1.6 (2). A survey of the hypotheses on the causes of creep may be found e.g. in [Wittmann (1977); Mindess and Young (1981); Neville et al. (1983)].

Creep of concrete may affect the long-term behaviour of concrete structures both in a favourable and in an unfavourable way. When subjected to a sustained load, the deformations of a concrete structure will continue to increase due to the effects of creep. According to [Rüsch et al. (1983)] the deflection of a reinforced concrete member subjected to flexure, d(t), increases with time: $d(t) \approx d_i\,[1 + 0.3\,\varphi(t, t_o)]$, where d_i is the initial deflection. In prestressed concrete members creep causes a reduction of prestressing force which may be estimated from $F_p(t) \approx F_p(t_o)/[1 + \alpha\,\varphi\,(t, t_o)]$, where $F_p(t_0)$ is the initial prestressing force, $F_p(t)$ is the prestressing force at time t and α is the stiffness ratio which is 0.5 for prestressing against rigid supports and $0.08 < \alpha < 0.20$ for conventional prestressing. In reinforced concrete sections subjected to compression, creep of concrete causes a redistribution of stresses from the concrete to the reinforcing steel which may lead even to yielding of the steel.

Creep of concrete has a favourable influence on internal stresses and stresses due to restraint which develop gradually. Such stresses may be substantially reduced by creep or never reach the magnitude which would be obtained in an analysis in which the effects of creep are not taken into account.

(5.3) Prediction of creep

In terms of the constitutive modelling two different approaches may be used to predict creep of concrete. These are the so-called *product-type formulations* and the *summation-type formulations*. The particular characteristics of both approaches and their advantages and disadvantages are discussed in [Hilsdorf and Müller (1987)]. Inherent weaknesses in both approaches which cannot be eliminated as long as linearity is maintained in modelling the creep behaviour have been summarised in [CEB Bull. No. 199 (1990)].

For the CEB-FIP MC90 preference has been given to a product-type formulation for creep. This model also has been included in the European specification EC2 [EN 1990:2002]. The prediction model subsequently presented is given in the new model code MC2010 – which represents an extension of the approach in the model code MC90 – in order to take into account the particular characteristics of high strength concretes. Hence, the model represents a linear product-type, mean cross-section prediction model which is valid both for normal strength and for high strength concrete. For background information refer to [Müller and Küttner (1996); Müller et al. (1999)].

The creep coefficient $\varphi(t, t_o)$ of a concrete at an age t which has been subjected to a constant sustained load at an age t_o follows from eq. (3.1-23).

$$\varphi(t,t_o) = \varphi_o \cdot \beta_c(t,t_o) \tag{3.1-23}$$

where:

φ_o notional creep coefficient according to eq. (3.1-24)
$\beta_c(t, t_o)$ coefficient to describe the development of creep with time after loading according to eq. (3.1-29).

The notional creep coefficient φ_o may be determined from eqs. (3.1-24) through (3.1-28).

$$\varphi_o = \phi_{RH} \cdot \beta(f_{cm}) \cdot \beta(t_o) \tag{3.1-24}$$

with

$$\varphi_{RH} = \left[1 + \frac{1 - RH/RH_o}{\sqrt[3]{0.1 \cdot h/h_o}} \cdot \alpha_1\right] \cdot \alpha_2 \tag{3.1-25}$$

$$\beta(f_{cm}) = \frac{5.3}{\sqrt{f_{cm}/f_{cmo}}} \tag{3.1-26}$$

$$\beta(t_o) = \frac{1}{0.1 + (t_o/t_1)^{0.2}} \tag{3.1-27}$$

and

$$t_o = t_{o,T} \cdot \left[\frac{9}{2 + (t_{o,T}/t_{1,T})^{1.2}} + 1\right]^{\alpha} \geq 0.5 \tag{3.1-28}$$

The time development function $\beta_c(t, t_o)$ follows from eqs. (3.1-29) and (3.1-30).

$$\beta_c(t,t_o) = \left[\frac{(t - t_o)/t_1}{\beta_H + (t - t_o)/t_1}\right]^{0.3} \tag{3.1-29}$$

with

$$\beta_H = 150\frac{h}{h_o}\left[1+\left(1.2\cdot\frac{RH}{RH_o}\right)^{18}\right]+250\alpha_3 \le 1500\alpha_3 \qquad (3.1\text{-}30)$$

The coefficients α_1, α_2 and α_3 in eqs. (3.1-25) and (3.1-30) shall be determined from eq. (3.1-31).

$$\alpha_1 = \left[\frac{3.5}{f_{cm}/f_{cmo}}\right]^{0.7};\quad \alpha_2 = \left[\frac{3.5}{f_{cm}/f_{cmo}}\right]^{0.2};\quad \alpha_3 = \left[\frac{3.5}{f_{cm}/f_{cmo}}\right]^{0.5} \qquad (3.1\text{-}31)$$

The parameters and variables in the preceding equations are defined as follows:

RH	relative humidity of the ambient environment in [%]
RH_o	= 100%
h	= $2\cdot A_c/u$
A_c	= cross section of the structural member in [mm^2]
u	= perimeter of the structural member in contact with the atmosphere in [mm]
h_o	= 100 mm
f_{cm}	mean compressive strength of concrete at an age of 28 days [MPa]
f_{cmo}	= 10 MPa
t	age of concrete in [days] at the moment considered
t_o	age of concrete at loading in [days]
$t_{o,T}$	age of concrete at loading adjusted according to the concrete temperature as given in eq. (3.1-40). For T = 20°C, $t_{0,T}$ corresponds to t_o
$t_{1,T}$	= 1 day
t_1	= 1 day
α	exponent in eq. (3.1-28) which depends on the type of cement: α = -1 for slowly hardening cement α = 0 for normal or rapidly hardening cement α = 1 for rapidly hardening high strength cement
α_i	coefficients i =1, 2 or 3 which depend on the mean compressive strength of concrete according to eq. (3.1-31).

From these relations the significant effect of compressive strength on the creep properties of concrete, particularly for the range of high strength concretes becomes apparent: for f_{cm} = 110 MPa the final value of the creep coefficient is only about 40 percent of the value obtained for f_{cm} = 35 MPa, all other conditions and parameters being identical.

Eqs. (3.1-23) to (3.1-31) are valid as long as the stresses do not exceed $\sigma_c = 0.4\cdot f_{cm}(t_o)$, where $f_{cm}(t_o)$ is the mean compressive strength at the time of load application. In some instances e.g. for prefabricated pretensioned concrete members, higher stresses may be applied at an early concrete age. Then the assumption of linearity of creep is no longer valid. Therefore, in MC2010 relations are given to take into account the effect of high stresses on creep.

(6) Fatigue

Some concrete structures such as bridges, concrete pavements, offshore structures or rail road ties may be exposed to frequently varying stresses. Under such conditions they are subjected to fatigue. State-of-Art-Reports on fatigue of concrete may be found e.g. in [CEB Bull. No. 189 (1988); ACI Committee 215 (2009)].

In experiments on the fatigue behaviour of a specific material generally a specimen is subjected to stresses fluctuating around a constant mean stress so that a certain stress history can be characterised either by the mean stress and the stress amplitude or by the minimum and the maximum stress. Failure occurs after a certain number of cycles N. The resistance of concrete against repeated loads is influenced by the same technological parameters which control the strength of concrete subjected to short term static loads. Therefore, it is useful to express the stresses applied in a fatigue test as fractions of a static reference strength, i.e. in terms of the stress levels S_{min} and S_{max}, respectively. Then the fatigue behaviour of a material may be presented in so-called S-N-relationships, where the maximum stress levels S_{max} for a given minimum stress level S_{min} are plotted versus the number of cycles, N, causing failure (Fig. 3.1-18). Such S-N-relationships may have characteristic shapes which are dealt with in Section 4.4-3 “Fatigue”.

The *fatigue strength* of a material is defined as the maximum stress which the material can sustain for a given number of load cycles. It decreases with the number of cycles and is for most materials considerably lower than the static strength. The *fatigue limit* or *endurance limit* corresponds to the maximum stress which the material can sustain for an infinite number of cycles. Whether such a limit exists for concrete is still controversial, refer to e.g. [Klausen and Weigler (1979); Grübl et al. (2001)] as well as to Section 4.4.3 and the State-of-Art-Reports listed above.

As an example, Fig. 3.1-18 shows experimental data from various investigators summarised by [Holmen (1979)]. In this diagram S-N-relationships are given for concretes subjected to concentric compression with $0.65 < S_{max} < 0.85$ at a frequency of 3 to 10 Hz and for a minimum stress level S_{min} between 0.035 and 0.050. The stress levels given in Fig. 3.1-18 exhibit substantial scatter. Therefore, often it is useful to present fatigue data as so-called S-P-N relationships where P is the probability of fatigue failure. In Fig. 3.1-18 relations for failure probabilities $P = 0.05$ and $P = 0.95$ are included. According to [Holmen (1979)] the scatter of the fatigue data corresponds to the scatter of the static compressive strength of the concretes.

In addition to the technological parameters which influence the static strength of a concrete, also the moisture content of the concrete may have a significant effect on its resistance to repeated loadings: concretes with a high moisture content and in particular water saturated concretes have a considerably lower fatigue strength than dry concretes. Since thick concrete sections dry out at a much slower rate than thin sections and, therefore, may have a much higher moisture content, there is a size effect on the fatigue resistance of concrete so that thin sections tend to have a higher fatigue strength than very large sections. Furthermore, high strength concretes generally are more sensitive to fatigue loading than are normal strength concretes.

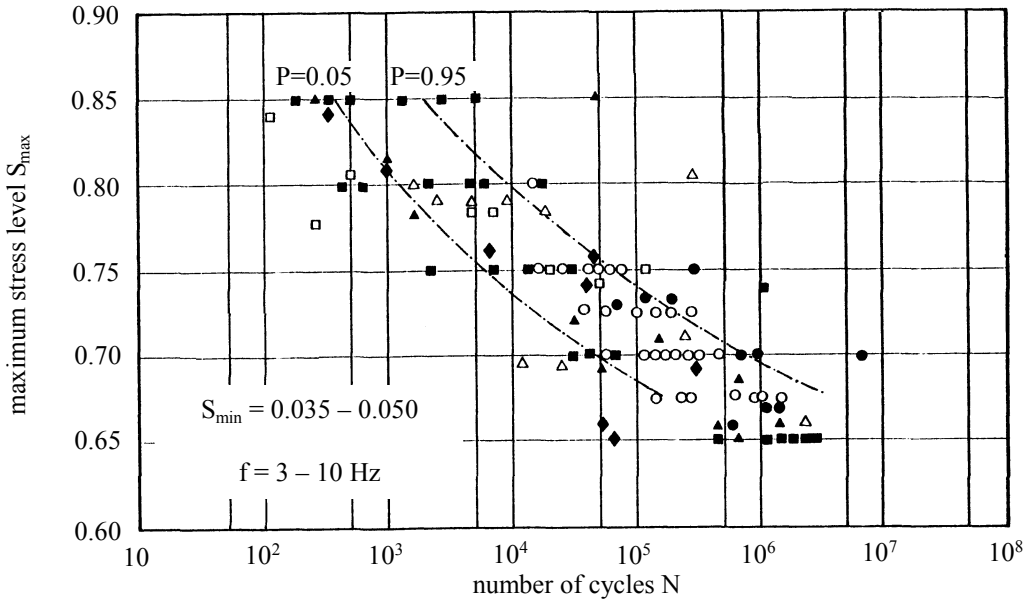

Fig. 3.1-18: S-P-N-relations for concrete subjected to compression [Holmen (1979)]

In the MC2010 analytical expressions are given to estimate the number of cycles to failure, N, for a constant minimum and maximum stress level for pure compression, compression-tension and pure tension, respectively. In these relations the maximum and minimum stress levels for compression $S_{c,max}$ and $S_{c,min}$ are defined as given in eqs. (3.1-32 a and b). There, the maximum and minimum stress levels are expressed as a fraction of the fatigue reference compressive strength $f_{ck,fat}$ which follows from eq. (3.1-32 c). In this equation the coefficient $\beta_{c,sus}(t, t_o)$ takes into account the effect of high sustained loads in cases where the mean stress during fatigue loading is high. A relation for $\beta_{c,sus}(t, t_o)$ is given in MC2010. The product $\beta_{cc}(t)\cdot\beta_{c,sus}(t, t_o)$ may also be taken from Fig. 3.1-13, i.e. $f_{cm,sus}(t,t_0)/f_{cm} = \beta_{cc}(t) \cdot \beta_{c,sus}(t,t_0)$. Eq. (3.1-32 c) also considers the increased sensitivity to fatigue loads with increasing concrete compressive strength. For an age at loading of 28 days $f_{ck,fat}$ decreases from about $0.82\cdot f_{ck}$ for a low strength grade to about $0.75\cdot f_{ck}$ for a high strength grade.

$$S_{c,\,max} = \left|\sigma_{c,\,max}\right| / f_{ck,\,fat} \qquad (3.1\text{-}32\ a)$$

$$S_{c,\,min} = \left|\sigma_{c,\,min}\right| / f_{ck,\,fat} \qquad (3.1\text{-}32\ b)$$

with

$$f_{ck,fat} = \beta_{cc}(t)\cdot\beta_{c,sus}(t,t_o)\cdot f_{ck}\cdot\left[1 - f_{ck}/(25 f_{cko})\right] \qquad (3.1\text{-}32\ c)$$

where:

$S_{c,max}$	maximum stress level
$S_{c,min}$	minimum stress level
$\sigma_{c,max}$	maximum compressive stress [MPa]
$\sigma_{c,min}$	minimum compressive stress [MPa]
f_{ck}	characteristic compressive strength [MPa] according to Table 3.1-1 and eq. (3.1-1)

$f_{ck,fat}$ fatigue reference compressive strength [MPa]
f_{cko} = 10 MPa
$\beta_{cc}(t)$ coefficient to take into account the effect of age at the beginning of fatigue loading on the compressive strength of the concrete, see eq. (3.1-12b)
$\beta_{c,sus}(t, t_o)$ coefficient to take into account the effect of high mean stresses during fatigue loading, see MC2010.

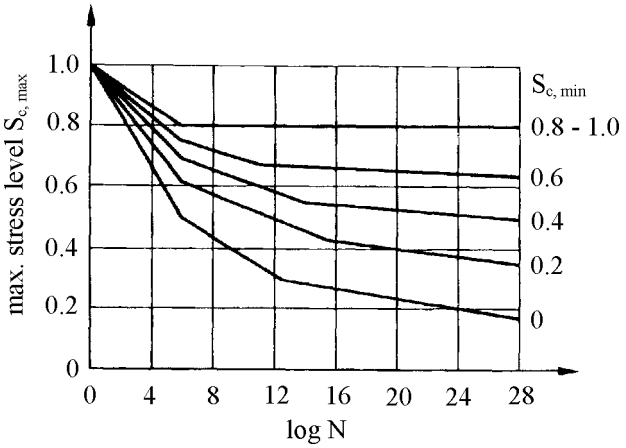

Fig. 3.1-19: S-N relations for concrete subjected to compression as obtained from the analytical expressions given in MC2010

In Fig. 3.1-19 S-N-relations for concrete subjected to compressive stresses are shown which have been obtained from the relations given in MC2010 (note Section 3.1.1). They are generally considered as rather conservative giving lower bound limits for severe loading conditions.

Structural elements are generally subjected to a spectrum of load levels which deviate considerably from the constant stress level amplitude conditions applied in laboratory experiments. To estimate the fatigue life of concrete subjected to realistic stress histories MC2010 recommends to apply the so called Palmgren-Miner summation rule as expressed by eq. (3.1-33).

$$D = \sum_i \frac{n_{Si}}{N_{Ri}} \tag{3.1-33}$$

where:

D fatigue damage
n_{Si} number of cycles applied at a given stress level and stress range
N_{Ri} number of cycles causing failure at the same stress level and stress range.

Failure occurs, if D = 1. The Palmgren-Miner rule is only a rough approximation of the actual concrete behaviour. It may over- or underestimate the actual fatigue strength of concrete subjected to varying repeated loads. For further details refer to [Holmen (1979)].

3.1.7 Effects of temperature on strength and deformation

The data given in the following section are applicable for concrete exposed to ambient temperatures below 200°C. For concrete exposed to higher temperatures or to fire refer to Chapter 6, "Design of concrete buildings for fire resistance".

(1) Thermal strains

As holds true for most materials, the volume of a concrete member increases as its temperature increases. The corresponding length change Δl depends on the initial length l, the change in temperature ΔT and the coefficient of thermal expansion α_{cT} according to eqs. (3.1-34).

$$\Delta \ell = \alpha_{cT} \cdot \ell \cdot \Delta T \qquad (3.1\text{-}34\ a)$$

and

$$\varepsilon_{cT} = \alpha_{cT} \cdot \Delta T \qquad (3.1\text{-}34\ b)$$

where:

ε_{cT} thermal strain.

The coefficient of thermal expansion α_{cT} depends on the coefficients of thermal expansion of the aggregates α_{gT} and of the hydrated cement paste α_{hpT}, on the volume fraction of the aggregates v_g and of the paste v_{hp}, as well as on the moisture state of the concrete. It may be estimated from eq. (3.1-35), refer to e.g. [Ziegeldorf et al. (1979)].

$$\alpha_{cT} = \alpha_{gT} \cdot v_g + \alpha_{hpT} \cdot v_{hp} \qquad (3.1\text{-}35)$$

The coefficient of thermal expansion of hydrated cement paste, α_{hpT} depends primarily on the moisture content of the paste and amounts to about $10 \cdot 10^{-6}$ K^{-1} for water saturated and for very dry paste with a maximum value around $20 \cdot 10^{-6}$ K^{-1} at a relative humidity of about 70 percent. Aggregates with a low coefficient of thermal expansion are e.g. limestone and blast furnace slag. As the quartz content of an aggregate increases, also its coefficient of thermal expansion increases.

Coefficients of thermal expansion of concrete range from about $5.5 \cdot 10^{-6}$ K^{-1} to about $14 \cdot 10^{-6}$ K^{-1}. Typical values for normal weight concretes in an air-dry state made of different types of aggregates are listed in Table 3.1-4. They are somewhat lower for water-saturated concrete.

type of aggregate used for concrete	coefficient of thermal expansion $\alpha_{cT} \cdot 10^{-6}$ [1/K]
quartzitic rock, sand or gravel	12 – 14
granite, gneiss	9 – 12
syenite, diorite, gabro, diabase, basalt	8.5 – 11
dense limestone	6.5 – 9

Table 3.1-4: Typical values of the coefficient of thermal expansion of concrete [Dettling (1962)]

The linearity between thermal strain and temperature change as expressed by eqs. (3.1-34 a and b) holds true only for temperatures in the range of about 0°C to 60°C. Particularly for higher temperatures the coefficient of thermal expansion increases with increasing temperature.

(2) Maturity

The rate of hydration of cement increases with increasing temperature. Consequently, the mechanical properties of concrete and their development with time are also influenced by the temperature of the concrete and of the surrounding environment. Maturity concepts generally are applied to quantify the dependence of concrete properties on temperature.

The simplest maturity function results from the assumption that there is a linear relation between the rate of hydration and the temperature as expressed by eq. (3.1-36).

$$M = \sum_{i=1}^{n} T_i \cdot \Delta t_i \tag{3.1-36}$$

where:

M maturity [°C · days] also referred to as degree-days
T_i temperature [°C] during the time interval Δt_i [days]
Δt_i time interval I where the temperature T_i prevales.

A maturity relation, initially proposed to estimate the effectiveness of steam curing and frequently used in the past, is given by eq. (3.1-37) [Saul (1951)].

$$M = \sum_{i=1}^{n} (T_i + 10) \cdot \Delta t_i \tag{3.1-37}$$

According to eq. (3.1-37) the maturity M corresponds to the integral of the time-temperature relation above a temperature of –10°C. Thus it is assumed that hydration stops at a temperature of –10°C. Particularly the assumption of linearity in eqs. (3.1-36) and (3.1-37) is only a crude approximation which contradicts thermodynamics. If the well known Arrhenius relation is applied, than a maturity function should have a general form as expressed by eq. (3.1-38) [Carino and Tank (1990)].

$$M = \text{const} \cdot \int_{t_o}^{t_i} e^{-Q/(RT)} dt \qquad (3.1\text{-}38)$$

where:

T temperature at a concrete age t [K]
Q activation energy for cement hydration [kJ/mol]
R universal gas constant [kJ/(mol·K)].

According to eq. (3.1-38) maturity increases at an increasing rate with increasing temperature. Additional maturity functions are dealt with e.g. in [Carino and Tank (1990)].

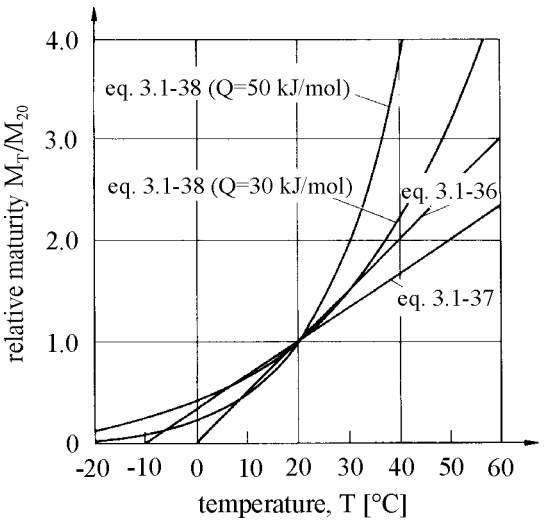

Fig. 3.1-20: Comparison of maturity functions as expressed by eqs. (3.1-36), (3.1-37) and (3.1-38)

In Fig. 3.1-20 the maturity at a given temperature M_T according to eqs. (3.1-36), (3.1-37) and (3.1-38) expressed as a fraction of the maturity M_{20} at a temperature T = 20°C is given as a function of temperature for an activation energy of 30 kJ/mol and of 50 kJ/mol, respectively. Compared to eq. (3.1-38) the linear maturity relations according to eqs. (3.1-36) and (3.1-37) underestimate the accelerating effects of elevated temperatures, particularly for high values of activation energy. Eq. (3.1-36) generally gives lower bound maturity values. The activation energy for cement hydration is in the range of $30 < Q < 65$ kJ/mol. According to [Carino and Tank (1990)] it depends not only on the type and strength class of the cement, but also on the water/cement ratio, additions and admixtures. Therefore, it should be experimentally determined, whenever accurate estimates of temperature effects are required.

As an alternative to maturity also the concrete age may be adjusted in order to take temperature effects into account: In case the concrete temperature deviates from 20°C then the *effective* or the *equivalent concrete age* corresponds to the time interval at a temperature T after which the concrete has reached the maturity which it would have at a temperature of 20°C. Eq. (3.1-39) gives a relation for the effective concrete age t_T on the basis of eq. (3.1-37).

$$t_T = \frac{\sum_{i=1}^{n} (T_i + 10) \cdot \Delta t_i}{30} \qquad (3.1\text{-}39)$$

Eq. (3.1-39) has been used e.g. in [CEB-FIP MC 78]. According to MC2010 the effective concrete age can be estimated from eq. (3.1-40) which is based on the maturity function according to eq. (3.1-38) and an activation energy for cement hydration of 33 kJ/mol.

$$t_T = \sum_{i=1}^{n} \Delta t_i \cdot \exp\left[13.65 - \frac{4000}{273 + T(\Delta t_i)/T_o}\right] \tag{3.1-40}$$

where:

t_T effective concrete age [days]
$T(\Delta t_i)$ temperature [°C] during the time interval Δt_i [days]
T_o = 1°C.

Maturity functions are suitable to estimate the effect of temperature on the time development of the degree of hydration of the cement and of some associated concrete properties in the temperature range of –10°C < T < 60°C such as creep and modulus of elasticity. They are useful tools to estimate the required duration of curing at temperatures deviating from 20°C. To some extent it may also be assumed that equal maturity is equivalent to equal strength. In this context it should be kept in mind, however, that in cases where the hydration of young concrete is accelerated by an increase of the concrete temperature the assumption of equal strength for equal maturity is valid only for an estimate of the concrete strength at the end of such a heat treatment. The compressive strength at a higher age would be substantially overestimated by such an approach.

(3) Strength, fracture and deformation properties

Excluding the effect of temperature on maturity and degree of hydration, respectively, there is a general trend that with increasing temperature at the time of loading both strength and modulus of elasticity of concrete decrease, whereas ultimate strains and plastic deformations increase.

The extent to which the *compressive strength* of concrete is influenced by *elevated temperatures* depends on the moisture state and on the drying conditions of the concrete. For a temperature range 0°C < T < 100°C, MC2010 gives empirical relations to estimate the effect of temperature on the compressive strength of concretes without moisture exchange e.g. mass concrete. From these relations it follows that for such conditions a temperature increase from 20°C to 100°C leads to a strength reduction of about 25 percent. Particularly for young concretes it is likely that continued hydration will offset this strength loss. If the concrete is allowed to dry, an increase of temperature in the range 0°C < T < 100°C generally does not cause a significant strength reduction. A further temperature increase may even lead to a strength increase due to the associated partial dehydration of the hydrated cement paste.

Elevated temperatures T > 100°C may cause phase transitions which have a significant effect on the mechanical properties of the concrete. The extent to which such changes occur depends on the temperature level and on the duration of temperature exposure, on the presence of moisture, on the type of aggregates, particularly the type of sand and on the type and amount of cement and additions. Elevated temperatures may also lead to internal stresses, if the coefficients of thermal expansion of the aggregates and of the cement paste differ significantly. However, such stresses are often overshadowed by internal stresses which develop, if the hydrated cement paste loses water and consequently shrinks during the

exposure to elevated temperatures. The temperature induced internal stresses lead to extensive microcracking and consequently to a strength reduction. However, if a concrete is subjected to sustained compressive stresses while exposed to elevated temperatures up to 600°C, no significant strength loss may occur as long as the compressive stresses are larger than the internal tensile stresses [Schneider (1982)].

If drying of the concrete during exposure to elevated temperatures is prevented, hydrothermal reactions may take place which significantly alter the structure of the hydrated cement paste and the mechanical properties of the concrete. In practice, such conditions may prevail e.g. in very thick concrete sections or in structural members with surfaces which are protected e.g. by a liner. The phase changes generally lead to a coarsening of the pore structure of the hydrated cement paste and consequently to a significant strength loss. These changes in the microstructure may be counteracted by reactions between calcium hydroxide in the paste and sand particles or additions which contain sufficient amounts of siliceous compounds. Then the strength of the concrete may even increase under the action of elevated temperatures. Therefore, concretes primarily containing limestone aggregates show significant strength losses if exposed to elevated temperatures under sealed conditions, whereas concretes containing a sufficient amount of siliceous fines particles have a high resistance to such an exposure [Seeberger et al. (1985)].

Concretes with a high compressive strength generally are more sensitive to elevated temperatures than concretes of a lower strength grade. This is due to a high vapour pressure which is generated in the remaining capillary pores of the hydrated cement paste and which reduces itself only very slowly because of the low permeability of the paste. This may also cause severe spalling of the concrete cover, see Section 6. Considering these complex circumstances, it is not possible to reliably predict the properties of a particular concrete at elevated temperatures without experimental proof.

Elevated temperatures may cause a significant reduction of the concrete *tensile strength* already at temperatures T < 100°C, depending on the moisture state and on the rate of temperature change. This behaviour is normally ascribed to internal stresses due to non-linear temperature gradients and associated non-uniform shrinkage. The effect of temperature in the range 0°C < T < 80°C on the flexural strength of concrete may be estimated from eq. (3.1-41) which is taken from MC2010.

$$f_{ct,fl}(T) = f_{ct,fl} \cdot (1.1 - 0.005\ T/T_o) \qquad (3.1\text{-}41)$$

where:

$f_{ct,fl}(T)$	flexural strength at temperature T
$f_{ct,fl}$	flexural strength at T = 20°C
T	concrete temperature [°C]
T_o	= 1°C.

From eq. (3.1-41) it follows that a temperature increase from 20°C to 80°C leads to a reduction of the tensile strength of about 30 percent.

The effect of elevated temperatures on the *fracture energy* of concrete is not sufficiently clarified yet. It is likely that the fracture energy decreases with increasing temperature because the energy of atomic bonding also decreases.

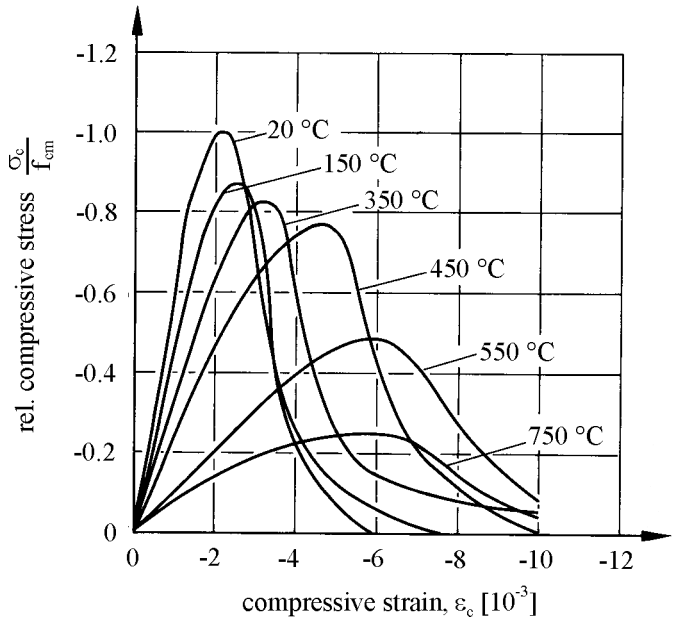

Fig. 3.1-21: Effect of concrete temperature on compressive stress-strain relations [Schneider (1982)]

Fig. 3.1-21 shows stress-strain relationships for concrete at elevated temperatures [Schneider (1982)]. As the temperature increases, the ultimate stress may increase or decrease, however, the ultimate strain generally increases. The modulus of elasticity and the slope of the descending branch decrease substantially.

For temperatures in the range of 0°C < T < 80°C the effect of the temperature on the *modulus of elasticity* may be estimated from eq. (3.1-42) [MC2010].

$$E_{ci}(T) = E_{ci} \cdot (1.06 - 0.003\ T/T_o) \qquad (3.1\text{-}42)$$

where:

$E_{ci}(T)$	modulus of elasticity at temperature T
E_{ci}	modulus of elasticity at T = 20°C
T	concrete temperature [°C]
T_o	= 1°C.

At very *low temperatures* compressive and tensile strength as well as modulus of elasticity generally are significantly higher than they are at room temperature, particularly if the concrete has a high moisture content. This is of practical significance e.g. for the design of LNG-tanks. The increase of strength and stiffness at very low temperatures is caused by the freezing of water in the pore system of the hydrated cement paste so that the frozen water acts as a load bearing solid. Repeated freezing and thawing may, however, damage the concrete [Rostasy et al. (1979)].

(4) Shrinkage and creep

As the temperature increases, the rate as well as the magnitude of *shrinkage* increase because a temperature increase accelerates the rate of drying and reduces the equilibrium moisture content of concrete thus increasing the amount of water lost during drying.

MC2010 gives relations for normal strength concrete to estimate the effect of temperature upon shrinkage for a temperature range 0°C < T < 80°C. From these relations it follows that a temperature increase from 20°C to 60°C results in an increase of final shrinkage by about 20 percent if the relative humidity stays constant at 60%. After one month of drying at 20°C, a concrete member with a cross-section 200 mm by 200 mm has reached about 30 percent of its final shrinkage value. If the temperature is increased to 60°C, this percentage increases to about 70 percent.

Of particular significance for the influence of elevated temperatures on creep of concrete are the drying conditions to which the concrete is exposed while under load as well as the moment in time at which the temperature increases. For steady and sealed conditions, i.e. the temperature is constant while the concrete is subjected to a constant sustained stress and the concrete neither loses nor gains water, an increase of temperature only accelerates basic creep as defined in Section 3.1.6 (5.2). However, if the concrete is allowed to dry, a temperature increase leads not only to an acceleration of basic creep but also to an increase and an acceleration of drying creep. For non-steady temperature conditions, i.e. a temperature change while the concrete is under load, an additional creep component, the transient thermal creep has to be taken into account which develops at the time of a temperature increase. The following example illustrates these effects: a concrete member with a cross-section 200 by 200 mm and a mean compressive strength f_{cm} = 35 MPa is subjected to a sustained stress $\sigma_c < 0.4 \cdot f_{cm}$ at an age of 28 days in air with a temperature of 20°C and a relative humidity of 60 percent. After 28 days a creep coefficient $\varphi(t, t_0) \approx 1.4$ has developed. If the temperature is increased immediately prior to loading to 60°C the creep coefficient after 28 days of loading increases to $\varphi(t, t_0) \approx 6.0$. If the temperature is increased from 20°C to 60°C while the concrete is subjected to the sustained stress, then in addition a transient creep component $\Delta\varphi \approx 0.7$ develops. Surveys on the effects of temperature on creep can be found e.g. in references [Geymayer (1972); Neville et al. (1983)].

3.1.8 Material properties influencing concrete durability

(1) Transport mechanisms

Most deterioration mechanisms of concrete require the penetration of water, ions in aqueous solutions or gases into the concrete. Therefore, it is generally accepted that concrete durability is to a large extent governed by the resistance of the concrete to the penetration of aggressive media. The paths of transport are the pore system of the hydrated cement paste as well as microcracks as dealt with in Section 3.1.4. The liquid or gaseous substances are transported by various mechanisms, in particular *permeation* such as water under a hydrostatic water pressure, *diffusion* such as the penetration of carbondioxide into the concrete or of water vapour out of the concrete, *capillary suction* or *absorption* of water or of solutions as well as combinations such as the transport of ions by moving water. The rate of transport is different for the various mechanisms. In particular the absorption of water or solutions by capillary suction is considerably more effective than the loss of moisture due to drying.

The resistance of porous materials to such processes can be described by a number of materials characteristics which are to some extent interrelated and described in the following. For further details refer to [Kropp and Hilsdorf (Ed.; 1992)].

(1.1) Permeation

Permeation is the transport of liquids or gases caused by a pressure gradient. Flow through a system of capillary pores may be either laminar or turbulent depending on the size of the pores. Only for a laminar flow the volume of transported material is proportional to the pressure gradient.

Under the assumption of laminar flow the *coefficient of gas permeability* may be expressed by eq. (3.1-43 a).

$$K_g = \eta \cdot \frac{Q \cdot \ell}{t \cdot A} \cdot \frac{2p}{(p_1 - p_2) \cdot (p_1 + p_2)} \qquad (3.1\text{-}43\ a)$$

where:

K_g coefficient of gas permeability [m^2]
η viscosity of the gas [Ns/m^2]
Q volume of the transported substance [m^3]
ℓ thickness of penetrated body [m]
A penetrated area [m^2]
p pressure at which volume Q is measured [N/m^2]
p_1 pressure at entry of gas [N/m^2]
p_2 pressure at exit of gas [N/m^2]
t time [s].

The flow of a gas through hydrated cement paste is not necessarily laminar because of the large range of pore diameters. Therefore, the coefficient of gas permeability also has been defined according to eq. (3.1-43 b). In this case K_g also depends on the transported medium and, therefore, is not a materials characteristic.

$$K_g = \frac{Q \cdot \ell}{t \cdot A} \cdot \frac{p}{p_1 - p_2} \qquad (3.1\text{-}43\ b)$$

where:

K_g coefficient of gas permeability [m^2/s].

The *coefficient of water permeability* follows from *Darcy´s law* according to eq. (3.1-44). It is not a materials characteristic and only describes the penetration of water.

$$K_w = \frac{Q \cdot \ell}{t \cdot A} \cdot \frac{1}{\Delta h_w} \qquad (3.1\text{-}44)$$

where:

K_w coefficient of water permeability [m/s]
Δh_w pressure head or height of water column [m].

(1.2) Diffusion

Diffusion is the transport of mass by random motion of free molecules or ions in the direction of and caused by a concentration gradient. The rate of flow is proportional to the concentration gradient dc/dx and the diffusion coefficient D as expressed by [m^2/s] according to *Fick´s first law* of diffusion, see eq. (3.1-45).

$$\frac{dm}{dt} \cdot \frac{1}{A} = -D \frac{dc}{dx} \tag{3.1-45}$$

where:

m	mass of substance flowing [g]
t	time [s]
A	area [m^2]
D	diffusion coefficient [m^2/s]
x	distance [m]
c	concentration [g/m^3].

The diffusion coefficient often is not a constant and may depend on the local concentration of ions or molecules, on the location x and on the temperature, so that D = f(c, x, t, T).

For non-steady diffusion *Fick´s second law* of diffusion should be applied which describes the change of concentration in a unit volume with time. In certain cases the transported substance may become immobile e.g. where chloride ions penetrate the concrete, refer to Section 3.1.8 (2.4). This may be taken into account by introducing an additional term, the sink, s, in Fick´s second law of diffusion as has been done in eq. (3.1-46).

$$\frac{\partial c}{\partial t} = \frac{\partial}{\partial x}\left(D \frac{\partial c}{\partial x} \right) - s \tag{3.1-46}$$

In cases where the sink is neglected or unknown an “apparent” or “effective” diffusion coefficient may be deduced from experiments which may depend on time and location.

(1.3) Capillary suction

Capillary suction is the take up of a liquid in a porous solid such as water in hydrated cement paste caused by the surface tension in the capillaries. The transport of a liquid through capillary suction depends on the viscosity, the density and the surface tension of the liquid.

Various theoretical relations have been deduced to describe the transport of liquids by capillary suction. Due to irregularities within the pore system the behaviour of real materials such as hydrated cement paste often deviates substantially from these theoretical relations. Therefore, empirical relations have been established to describe the absorption of a liquid by capillary suction. The most commonly used characteristic is the *rate of absorption* or the *absorption coefficient*, S, as defined by eqs. (3.1-47 a and b).

$$S = \frac{\Delta m}{A \cdot f(t)} \tag{3.1-47 a}$$

and with $f(t) = t^n$:

$$S = \frac{\Delta m}{A \cdot t^n} \qquad (3.1\text{-}47\ b)$$

where:

S	absorption coefficient [g/m^2s^n] or [m/s^n]
Δm	liquid absorbed at time t [g] or [m^3]
A	penetrated area [m^2]
f(t)	time function
t	time [s].

Though a time function $f(t) = t^{0.5}$ has been frequently proposed, often a power $n \neq 0.5$ fits experimental data better.

(1.4) Transport of ions

The transport of ions generally occurs by ion diffusion. However, also a *mixed mode* of transport may take place e.g. when chloride ions penetrate the concrete. If a non-saturated concrete comes into contact with a salt solution, chloride ions will penetrate the concrete through capillary suction of the solution at a much faster rate than by ion diffusion. Nevertheless, a mixed mode of transport by capillary suction and by diffusion occurs.

(1.5) Migration

This is the transport of ions in electrolytes due to the action of an electrical field. In this case positive ions will move preferentially to the negative electrode, and negative ions will move towards the positive electrode. These processes are of particular relevance regarding the corrosion of reinforcement bars (see also Section 3.2).

(1.6) Parameters influencing transport properties

The transport properties of concrete are influenced by microstructural (internal) as well as by environmental (external) parameters. All transport characteristics described above depend on the total amount, the size distribution and the connectivity of the pores in the hydrated cement paste as well as on cracks in the cement paste matrix or in the aggregate-paste interfaces.

As has been pointed out in Section 3.1.4 (1) the *connectivity* of the capillary pores of the hydrated cement paste is the most significant microstructural characteristic for the transport properties of a concrete irrespective of the mode of transport, unless the transport is governed by a system of continuous or nearly continuous cracks. The connectivity of the capillary pores decreases as the water/cement ratio decreases and as the degree of hydration increases. Based on computer simulations it was found, that there is a unique relationship between the *total capillary porosity* and the connectivity of the pores as shown in Fig. 3.1-22 [Bentz and Garboczi (1991)]. From this figure it also follows that there is a so-called percolation threshold at a capillary porosity of about 0.18 irrespective of the water/cement ratio and the degree of hydration of the hydrated cement paste, i.e. for a capillary porosity less than 0.18 the paste contains no interconnected pores.

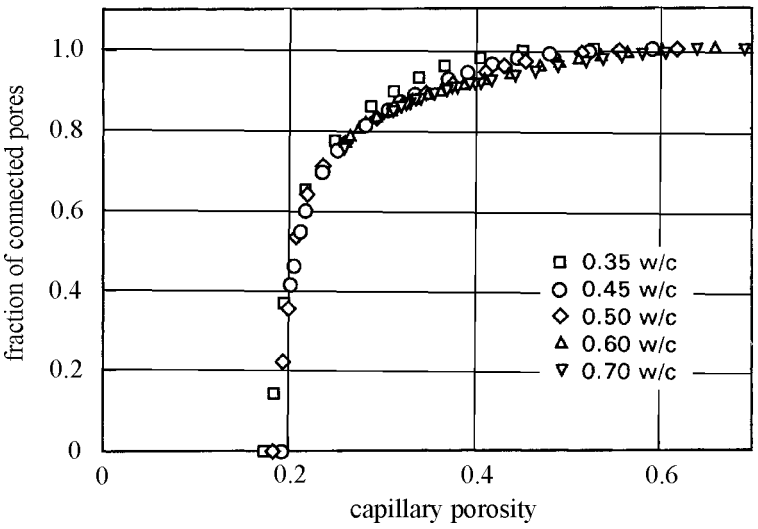

Fig. 3.1-22: Relation between connectivity of capillary pores and total capillary porosity of hydrated cement paste [Bentz and Garboczi (1991)]

The *size* of the *capillary pores* influences the various transport mechanisms in different ways. Whereas for a given total porosity in a continuous pore system water or gas permeability decrease significantly as the pores become smaller, pore size has little or no influence on e.g. ionic diffusivity. The rate of capillary suction decreases as the pores become smaller, however, the level to which water rises in a capillary increases with decreasing pore diameter. Whereas the *gel pores* are nearly impermeable against a liquid or gaseous pressure, diffusion continues in the gel pore system even if the capillary pores become discontinuous.

Of particular significance for the transport of liquids and gases in concrete is the amount and the size of the aggregates. It has been shown in several investigations that the water permeability of concrete may be considerably larger than the water permeability of the cement paste it is made from. This effect is the more pronounced the larger the aggregate particles. In addition to the already mentioned microcracks at the interface between aggregates and paste, the microstructure of the hydrated paste at the interface, which has a higher porosity than the bulk paste, should be the reason for this particular behaviour, see also Section 3.1.4 (1). Further details can be found in references [Kropp and Hilsdorf (Ed.; 1992)].

The most significant external parameter influencing the transport characteristics of concrete is the relative humidity of the surrounding atmosphere. At low relative humidities the moisture content of the concrete is reduced leading to a partial emptying of the capillary pores. Therefore, the pore space available for the transport of gases and the connectivity of the capillary pores increase. As a consequence, also gas permeability and gas diffusivity increase significantly as can be seen from Fig. 3.1-23 in which the relative gas permeability of various concretes is given as a function of the internal relative humidity of the concrete [Ollivier et al. (1992)]. An increase of the relative humidity from 60% to 95% causes a reduction of the gas permeability by almost 2 orders of magnitude. However, the diffusivity of ions dissolved in water as well as of water vapour decreases as the water content decreases.

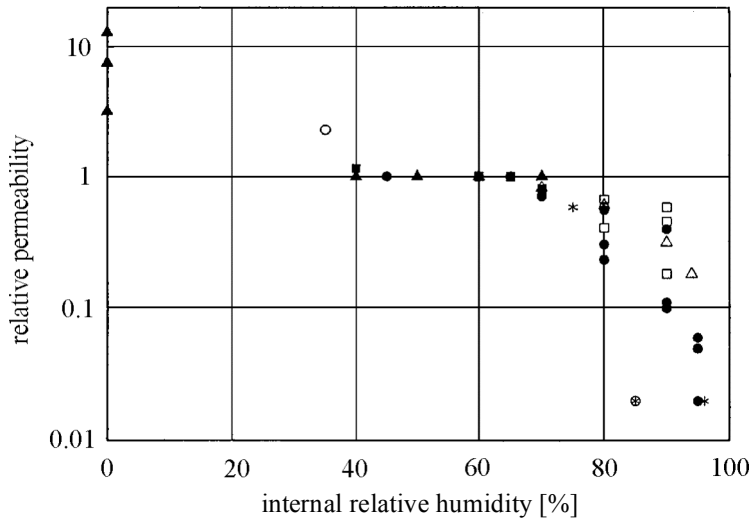

Fig. 3.1-23: Effect of the internal relative humidity upon the concrete gas permeability [Ollivier et al. (1992)]

Also capillary suction is considerably increased as the capillary pores in the concrete are emptied. In this context it should be kept in mind that under normal conditions it is only the outer skin of a concrete member up to a depth of about 30 mm where seasonal changes of the environmental conditions have a significant effect on the moisture state of the concrete.

The temperature of the ambient environment in a moderate climate has little influence on the permeability and diffusivity characteristics, however, a temperature increase leads to a significant increase of capillary suction because of the temperature dependence of the viscosity and surface tension of water [Ollivier et al. (1992)].

In MC2010 relations are given to estimate gas permeability and water permeability coefficients, diffusion coefficients for water vapour and for carbondioxide as well as water absorption coefficients depending on the strength grade of ordinary concretes.

(2) Physical processes

(2.1) Freezing and thawing

Concrete may be severely damaged by freezing and thawing if the pore system of the concrete is filled with water to such an extent that the concrete has reached a critical degree of saturation. The mechanisms leading to such damage are not entirely clarified. However, it is generally accepted that because of the surface tension in the small capillaries and because of the reduction of the freezing temperature of water in the pore system of the hydrated cement paste by dissolved substances, the water in concrete freezes at temperatures below 0°C, and the amount of frozen water increases continuously as the temperature decreases. Hydrostatic pressure in the still unfrozen water caused by the volume increase of the ice which has already formed, osmotic pressures as well as a redistribution of water in the pore system lead to internal stresses which may severely damage the concrete, particularly as the number of freeze-thaw cycles increases [Powers (1975); Setzer (1991); Fagerlund (1997)].

Concrete may be protected against the negative effects of freezing and thawing, even if the degree of water saturation is high, by air entrainment, i.e. by a system of artificial, small and dispersed air voids generated by air entraining agents as a concrete admixture. Such air voids generally do not become water saturated even after prolonged exposure to water so that they provide sufficient space for the expansion of unfrozen water in the hydrated cement paste.

The air void system in air-entrained concrete may be characterised by the so-called spacing factor which is defined as the distance of a defined point within the hydrated cement paste to the nearest air void. For a concrete with a high resistance to freezing and thawing it should not exceed 0.20 mm. In addition it has been proved that only very small pores with diameters < 0.30 mm are effective. Hence, the amount of such micropores (Ø < 0.30 mm) should not drop below a volume content of 1.5%.

The production of a concrete with a high frost resistance requires the use of suitable aggregates. Particularly porous aggregates may, if critically saturated, be damaged by frost action leading to pop-outs or other forms of damage in the concrete.

Another procedure to improve the resistance of concrete against freezing and thawing is a reduction of the capillary porosity of the hydrated cement paste by the choice of a low water/cement ratio and sufficient curing. High strength concretes with very low water/binder ratios may have such a low capillary porosity that the amount of freezable water is low enough so that concrete even without air entrainment may be damaged by frost action only after very long and continuous exposure to water [Guse et al. (1998)]. Nevertheless, questions regarding the frost resistance of high performance concretes are not completely clarified yet.

(2.2) Freezing, thawing and deicing chemicals

The resistance of concrete to freezing and thawing may be significantly reduced in the presence of deicing chemicals such as sodium chloride, calcium chloride or urea. There are several reasons for the increased damage of concrete due to freezing and thawing in the presence of deicing chemicals, e.g. an increase of the number of freeze-thaw cycles, an increase in the degree of saturation of the concrete, osmotic pressures, thermal shock and other temperature induced internal stresses and in some instances chemical attack. Since deicing salt solutions lower the freezing point of water, the freezing point in the concrete will increase with increasing distance from the exposed surface. As a consequence layers of concrete below the still unfrozen surface layer may freeze thus causing spalling of the top layer [Springenschmid (1969)]. Because of the severity of this attack the technological requirements for concretes with a high resistance to freezing, thawing and deicing chemicals are more stringent than they are for concretes with a high resistance to freezing and thawing.

Even more important in this context is that deicing salt solutions may penetrate reinforced concrete up to the level of the reinforcement leading to severe corrosion of the embedded steel, see Section 3.1.8 (2.4), 3.2.2 and 5.4.7.

(2.3) Abrasion resistance

Concrete exposed to abrasive actions has to have a sufficiently high abrasion resistance. Such conditions prevail e.g. as a result of heavy traffic acting on concrete pavements or industrial floors. Also the interior surfaces of bins or silos may suffer abrasion due to exposure to moving or dropping bulk material during charge or discharge. In hydraulic structures sand and gravel may abrade the surfaces of the structure in addition to cavitation erosion caused by the rapid flow of water.

Particles acting on a concrete surface by sliding, rolling or impact generate a multiaxial state of stress which may eventually lead to local failure [Kunterding (1990)]. In the vicinity of a particle that imposes compressive and shear stresses on a concrete surface, biaxial tension-compression stresses cause tensile cracks in the concrete surface layer. Depending on the size of the particle and its motion relative to the concrete surface, as well as on the properties

of the aggregates, fracture and thus abrasion damage is initiated either in the hydrated cement paste, in the aggregates or in the aggregate-cement paste interface. From this failure mechanism it follows that concrete abrasion resistance should correlate well with other mechanical properties such as the tensile or the compressive strength.

The abrasion resistance of concrete increases with decreasing water/cement ratio and increasing duration of curing. Consequently, it increases with increasing concrete compressive strength. Depending on the type of abrading action the effects of the type of aggregates may be of equal significance.

In Fig. 3.1-24 the abrasion depth of concretes made of various cements, additions and aggregates with the water/cement ratio and the duration of curing as additional parameters, is given as a function of the concrete compressive strength [Dhir et al. (1991)].

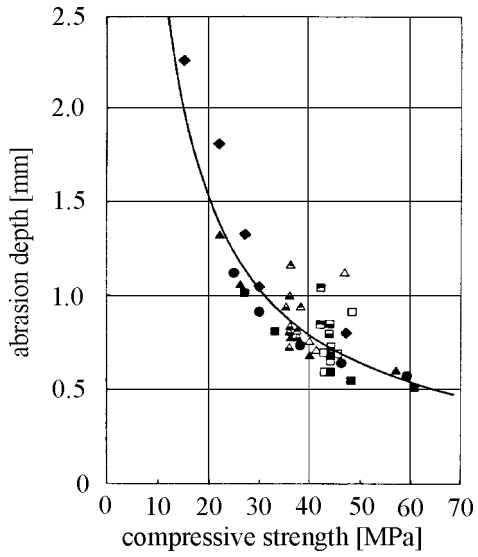

Fig. 3.1-24: Relation between abrasion and concrete compressive strength [Dhir et al. (1991)]

Even though in particular the type of aggregates as well as the moisture state of the concrete are significant parameters which do not always reflect in the compressive strength of the concrete, there is a reasonably close correlation between the abrasion depth and the compressive strength of the concrete.

High abrasion resistance may be achieved by optimising both the properties of the hydrated cement paste and of the aggregates, i.e. a low water/cement ratio, sufficient curing and aggregates with a high abrasion resistance. [Kunterding (1990)] showed that the abrasion resistance of high strength concretes containing silica fume and made with a water/binder ratio less than 0.30 was superior to all other types of concretes tested. Further information on the abrasion characteristics caused by water and rubble in hydraulic structures is given in [Vogel et al. (2009); Vogel (2010)].

(2.4) Penetration of chlorides

Depending on the environment and exposure conditions, chlorides may penetrate the concrete. Sources of chlorides are in particular sea-water and deicing salt solutions, but sometimes also plastics, when fire has occurred. Chlorides in most instances have only a minor corrosive effect on the concrete itself, however, they may destroy the passive layer on

the surface of steel bars embedded in the alkaline concrete and, therefore, may lead to corrosion of the steel as dealt with in Sections 3.2.2 and 5.4.7. This corrosion is associated with a high risk as it may develop very locally (pitting corrosion) causing no significant concrete spalling but reducing also the plastic strain potential of the reinforcement bars.

Some of the penetrating chloride ions may react with some compounds of the hydrated cement paste chemically or physically and thus become immobile. Only the concentration of free chloride ions in the pore water of the hydrated cement paste controls the possible corrosion of embedded steel. The binding capacity for chlorides, i.e. the fraction of chlorides which become demobilized, depends on the chemical composition of the cement or of additions. The binding capacity of a hydrated cement paste increases with increasing content of C_3A of the cement which combines with chlorides to form Friedel´s salt $3CaO \cdot Al_2O_3 \cdot CaCl_2 \cdot 10H_2O$. Blast furnace slag or fly ash as blending compounds of the cement or as addition are particularly effective in physically binding chloride ions [Raupach (1992)]. In this context it is important to note that various hydration products are decomposed by carbonation including the chloride bearing compounds. Thus the formerly immobilised chloride ions are set free by carbonation.

The paths of chloride penetration generally are the capillary pores in the hydrated cement paste, the aggregate-cement paste interfaces and eventually microcracks. The mechanisms of transport are ion diffusion within the pore water, capillary suction of solutions containing chloride ions with a subsequent redistribution of the chloride ions by diffusion and in rare cases permeation such as in marine structures, refer to e.g. [CEB-FIP Bull. No. 182 (1989)].

For non-steady diffusion of chloride ions Fick´s 2nd law of diffusion as expressed by eq. (3.1-46) applies. In order to take into account the chloride binding capacity of the concrete c_{bcl}, the sink s in eq. (3.1-46) should be replaced by the term $\partial c_{bcl} / \partial t$. If the sink is neglected the diffusion coefficient for chloride ions in an aqueous solution D_{Cl} may be replaced by an effective diffusion coefficient $D_{Cl,eff}$ which is no longer a constant but varies in time (t) and location (x). The effective chloride diffusion coefficient depends on the capillary porosity, i.e. water/cement ratio and degree of hydration and in particular on the type and amount of cement and additions, refer to e.g. [Raupach (1992)]. $D_{Cl,eff}$ decreases with decreasing water/cement ratio and increasing duration of curing. Because of the binding capacity of some blending compounds discussed above, $D_{Cl,eff}$ is considerably lower for blast furnace cements than it is for Portland cements. It also decreases with an increasing content of fly ash or silica fume as additions. Furthermore, the diffusion coefficient for chlorides increases significantly with increasing temperature.

In concrete pavements or bridge decks exposed to deicing salt solutions, generally a mixed mode of transport consisting of capillary suction of a chloride solution and of chloride ion diffusion takes place. In such cases, where a concrete member is repeatedly exposed to chloride solutions with intermittent periods of drying, the more effective transport by capillary suction dominates, and according to [Volkwein (1991)] the diffusion controlled transport may be almost negligible. Volkwein also found that in the penetration process of a chloride solution, the penetration front of the chlorides was lagging behind the water front. He attributed this filtration process to the binding of chloride ions by the hydration products.

Chloride profiles, i.e. the spatial distribution of chlorides in a concrete element may be calculated on the basis of Fick´s second law of diffusion as given in eq. (3.1-46). MC2010 gives the resulting error function describing time-dependent profiles depending on a so-called apparent chloride diffusion coefficient. This approach also takes into account the existence of a convective zone, where chloride penetration is not diffusion controlled.

In fact, the distribution of chlorides may be considerably complex e.g. due to mixed modes of transport as well as due to the wash-out of chlorides from the near surface regions as can be seen from Fig. 3.1-25 taken from [Weber (1983)] which shows the experimentally determined distribution of chlorides in a concrete retaining wall adjacent to a city highway which had been exposed to deicing salt solutions. Because of washout effects the maximum chloride content is about 30 mm below the concrete surface.

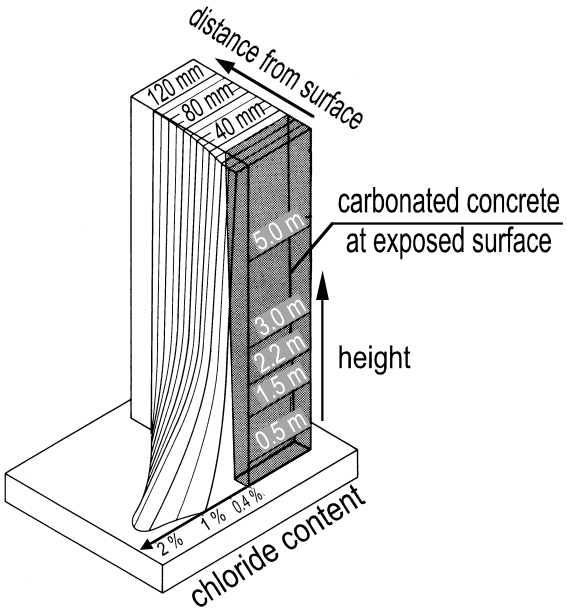

Fig. 3.1-25: Chloride distribution in a concrete retaining wall exposed to deicing salt solutions [Weber (1983)]

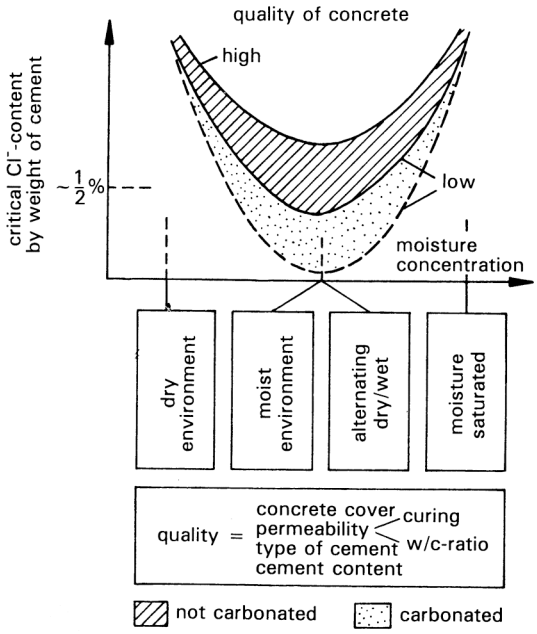

Fig. 3.1-26: Parameters influencing the critical chloride content of concrete [CEB Bull. No. 182 (1989)]

The critical chloride content of a reinforced or prestressed concrete structure exposed to chlorides is of outmost importance in estimating its prospective lifetime. A permissible chloride concentration will depend on various parameters such as the concrete composition, the permeability of the concrete cover, the depth of carbonation, the oxygen supply and the moisture state. Therefore, there is no unique value for an allowable chloride concentration. In Fig. 3.1-26 taken from [CEB Bull. No. 182 (1989)], the various parameters influencing the critical chloride content are summarised. Depending on these parameters, the critical chloride content may vary between 0% and approximately 1% by mass of the cement.

(3) Chemical processes

(3.1) Carbonation

An important chemical process which takes place in most concrete members is carbonation. Though carbonation is in most instances not harmful for the concrete itself, it may be harmful for a reinforced concrete member as it reduces the pH-value of the pore solution in the concrete to such an extent that embedded steel is no longer protected sufficiently against corrosion; also refer to Section 3.2.2 and 5.4.7.

Carbonation is caused by the penetration of carbondioxide into the concrete from the surrounding environment. The concentration of carbondioxide of the air generally is in the range of 0.03 percent by volume. It may be considerably higher in industrial areas or above parking decks etc. Carbondioxide may react with all alkaline compounds of the hydrated cement paste. However, the most significant reaction is the one with calcium hydroxide as expressed by eq. (3.1-48) taking place in the presence of moisture.

$$Ca(OH)_2 + CO_2 \rightarrow CaCO_3 + H_2O \qquad (3.1\text{-}48)$$

The rate of carbonation is controlled by the ingress of carbondioxide into the concrete and thus by the diffusion coefficient for carbondioxide through carbonated concrete. For steady state conditions the depth of carbonation at a given time can be estimated from eqs. (3.1-49 a and b) which are based on Fick´s first law of diffusion as expressed by eq. (3.1-45).

$$x^2 = \frac{2 \cdot D_{CO2} (c_1 - c_2)}{a} \cdot t \qquad (3.1\text{-}49\ a)$$

where:

x	depth of carbonation at time t [m]
D_{CO2}	diffusion coefficient for carbondioxide through carbonated concrete [m^2/s]
c_1	concentration of carbon dioxide of the surrounding environment [g/m^3]
c_2	concentration of carbon dioxide at the carbonation front [g/m^3]
a	mass of CO_2 per unit volume of concrete required to carbonate all relevant hydration products [g/m^3]
t	duration of carbonation [s].

Combining all coefficients of eq. (3.1-49 a) into a single constant C, results in the well-known relation for the progress of carbonation according to eq. (3.1-49 b):

$$x = C\sqrt{t} \qquad (3.1\text{-}49\ b)$$

Eqs. (3.1-49 a and b) are valid only as long as the diffusion coefficient for carbondioxide is a constant in time and location. Though this requirement may be satisfied to some extent when carrying out carbonation tests in the laboratory under controlled environmental conditions, it is rarely met by the conditions to which actual concrete structures are exposed, particularly because of the pronounced dependence of D_{CO2} on the moisture content of the concrete. Generally, D_{CO2} decreases with increasing moisture content of the concrete. If the capillary pores in the hydrated cement paste are filled with water, then gas diffusion ceases. Though the gas diffusivity of very dry concrete is high, carbonation progresses at a slow rate because for the chemical reactions to take place a certain amount of moisture is required for dissociation.

For the carbonation of concrete in structures exposed to the open air, distinction should be made between elements protected from rain and elements exposed to rain. Though theoretically not correct, a time function $x = C \cdot t^n$, where $0.2 < n < 0.5$, describes the progress of carbonation in structural elements permanently protected from rain sufficiently well. This does not hold true for elements exposed to alternate drying and wetting by liquid water or rain. During a period of rain the concrete takes up water rapidly by capillary suction. As a consequence carbonation ceases, until during a subsequent drying period the moisture content of the concrete decreases far enough so that a sufficient amount of carbondioxide penetrates the concrete. Under such conditions the depth of carbonation may even approach a finite value if the drying periods are too short and if the depth of carbonation is already too large so that the concrete does not dry sufficiently to allow penetration of carbondioxide at a rate which is required for further carbonation [Bakker (1988); Bunte (1993)].

MC2010 describes the progress of carbonation on the basis of eq. (3.1-49b). However, the constant *C* is replaced by various parameters taking into account environmental and execution effects, material parameters as well as effects resulting from accelerated carbonation tests.

Carbonation alters the pore structure of the hydrated cement paste. For concretes made of Portland cements the capillary porosity of the paste is significantly reduced by carbonation if the water/cement ratio is less than approximately 0.70. This may result in a significant increase of compressive strength and of surface hardness of the concrete. For concretes made of blast furnace cements, the reduction of capillary porosity decreases with increasing slag content. In addition, carbonation of blast furnace cement concretes with a high slag content results in a coarsening of the pore structure and thus in a substantial increase of the diffusion coefficient D_{CO2} and a corresponding acceleration of carbonation. This coarsening effect is mostly due to a partial decomposition of the CSH gel by carbonation [Bier (1987)].

The air permeability of concrete prior to carbonation is a good indicator of the carbonation potential of a particular concrete. This follows from Fig. 3.1-27 where the depth of carbonation after 1 year of storage at 20°C and 65 percent relative humidity is given as a function of the air permeability coefficient for concretes made of different types of cement and water/cement ratios and exposed to different durations of curing. Though a unique relation was found for most types of cement, the depth of carbonation is significantly higher for a given permeability if the concretes are made of blast furnace cements with a high slag content because of the coarsening of the pore structure of such concretes by carbonation as mentioned above.

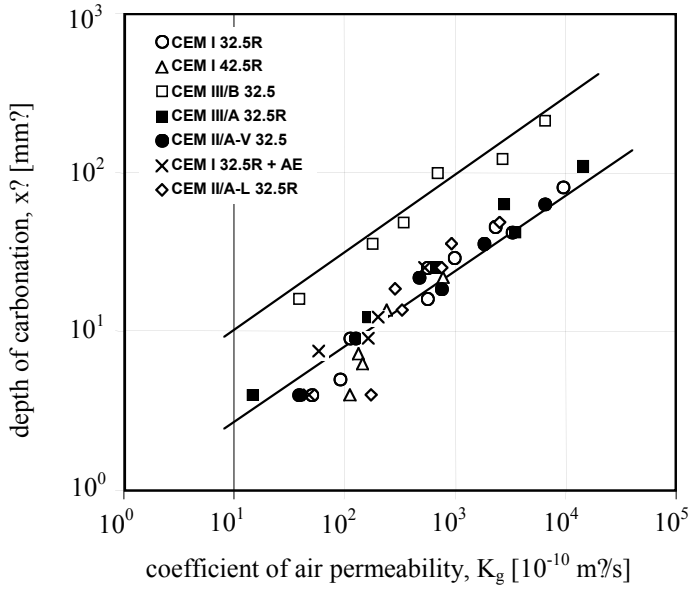

Fig. 3.1-27: Depth of carbonation after 1 year of storage in air at 20°C and 65 percent rel. humidity versus concrete air permeability at an age of 5 days [Schönlin (1989)]

According to [Nilsson and Luping (1992)] the theoretical background for the correlations shown in Fig. 3.1-27 is that the coefficient of permeability K_g and the diffusion coefficient D_g for a given gas in a given porous material are interrelated as expressed by eq. (3.1-50), where the exponent b depends on the type of gas.

$$K_g = \text{const} \cdot D_g^b \tag{3.1-50}$$

Carbonation is to some extent a reversible process. In [Bier (1987)] it has been shown that the decomposition of the CSH gel due to carbonation in concretes made of blast furnace cements with a high slag content can be healed if the carbonated concrete is exposed to an alkaline environment. This, however, does not hold true for the other carbonation products, since they have reached a lower energy level by carbonation.

(3.2) Types of chemical attack and influencing parameters

Concrete may be damaged as a consequence of chemical reactions between deleterious substances penetrating the concrete and the various phases of the hydrated cement paste and in some instances also of the aggregates. Such reactions may lead to damage either due to a dissolution of concrete compounds (leaching) or due to a volume increase (expansion) of the reaction products compared to the initial volume of the reaction partners. Table 3.1-5 gives a brief overview on the major aggressive media, the attacked components of the hardened cement paste and the types of reactions caused.

In most instances, in order for chemical attack to take place requires a high moisture content of the concrete and thus transport of moisture and of the aggressive medium to the place of reaction. Therefore – aside from its chemical composition – concrete resistance to the ingress of aggressive media again is the principal parameter controlling the resistance against chemical attack.

dissolving attack in aqueous media			expanding attack		
aggressive fluids	attacked paste components	reactions	aggressive aqueous media	attacked components	reaction products
acids (inorganic/ organic)	$Ca(OH)_2$ CSH CAH	decomposition transformation dissolution ion exchange leaching	sulfates	$Ca(OH)_2$	plaster
				aluminates	trisulfate
bases (strong)	CAH		magnesium salts	$Ca(OH)_2$	$Mg(OH)_2$
				CSH	Mg-silicate
ammonium salts	$Ca(OH)_2$		alkali hydrox-ides	reactive siliceous aggregates	alkali silicate gel
H_2S, SO_2, HCI, CO_2	$Ca(OH)_2$ CSH CAH				

Table 3.1-5: Dissolving and expanding attack on components of the hardened cement paste (CSH = calcium silicate hydrate; CAH = calcium aluminate hydrate)

The severity of chemical attack depends primarily on the nature of the aggressive medium, its composition and whether it is solid, fluid or gaseous. Additional parameters are the rate of flow and the temperature of the deleterious substance as well as an external pressure. Substances in natural water or in soils which are deleterious to concrete are in particular acids characterised by their pH-value, lime dissolving carbonic acid (CO_2), ammonium (NH_4^-), magnesium (Mg^{2-}) as well as sulphate (SO_4^{2-}) ions and to some extent soft water. In European an national standards limiting values of such substances contained in natural water or in soils are given, which may lead to slight, moderate or severe chemical attack.

(3.3) Acid attack

Acids cause leaching of all compounds of the hydrated cement paste and in particular those containing calcium. Also some aggregates, in particular limestone aggregates are vulnerable to acids. The rate of leaching increases with decreasing pH-value of the acid. Leaching occurs due to the formation of soluble salts as shown e.g. in eq. (3.1-51).

$$Ca(OH)_2 + HCl \rightarrow CaCl_2 + 2H_2O \qquad (3.1\text{-}51)$$

Inorganic acids generally are more deleterious than organic acids. If a natural water contains a surplus of CO_2, then lime dissolving carbonic acid is formed which may result in leaching of the compounds of the hydrated cement paste containing calcium.

Ion exchange between compounds of the hydrated cement paste and magnesium or ammonium salts penetrating the concrete may either lead to the formation of compounds with increased solubility and thus to leaching or to an expansion e.g. according to the reaction given in eq. (3.1-52).

$$Ca(OH)_2 + MgCl_2 \rightarrow CaCl_2 + Mg(OH)_2 \qquad (3.1\text{-}52)$$

Sea-water is characterised by a high content of dissolved salts. It may lead to leaching as well as to expansive reactions. However, because of the formation of protective coatings, sea-

water generally is less deleterious than would be expected on the basis of its salt concentrations. For further details on sea-water attack refer e.g. to [RILEM TC 32-RCA (1985)].

The degradation of concrete due to acid attack is a time-dependent process starting from the original concrete surface towards the interior parts of a member. It may be described by a function similar to eq. (3.1-49b) in case the strength of the acid is assumed to be constant and the material loss remains negligible. However, if the corroded material is removed, the corrosion rate increases. For further details see MC2010.

(3.4) Sulphate attack

Among the most important expansive reactions in concrete are those associated with sulphates contained e.g. in ground water or sea-water, soils or sewage. If sulphate ions penetrate the concrete they may react either with calcium hydroxide or with calcium aluminate hydrates, both being possible constituents of the hydrated cement paste. An ion exchange occurs when e.g. sodium sulphate reacts with calcium hydroxide:

$$Ca(OH)_2 + Na_2SO_4 \rightarrow CaSO_4 + 2NaOH \tag{3.1-53}$$

Following such a reaction, gypsum $CaSO_4 \cdot 2H_2O$ is formed. This reaction is associated with a volume increase of about 20 percent compared to the original volume of the calcium hydroxide. Since, however, gypsum is soluble in water it may be leached. Further, gypsum reacts with calcium aluminium hydrate leading to the formation of the so-called *ettringite* $3CaO \cdot Al_2O_3 \cdot 3CaSO_4 \cdot 32H_2O$. Calcium aluminate $3CaO \cdot Al_2O_3$ is one of the major compounds of Portland cement clinker. Controlled and intended ettringite formation generally occurs in the early stages of cement hydration in order to avoid early set of the fresh concrete. Though the ettringite formation is associated with a volume increase of about 220 percent it is of no harm, as long as the fresh concrete is still in a plastic state. However, severe damage, i.e. microcracking and eventually complete disintegration occurs if sulphate solutions penetrate the hardened concrete, unless suitable precautionary measures are taken. For more details refer to e.g. [Lawrence (1990)].

Volume expansion may also take place due to *secondary (or delayed) ettringite formation*. It occurs if e.g. during steam curing of prefabricated concrete members the young concrete is exposed to temperatures exceeding about 80°C. Under such conditions the ettringite formation during the early phases of hydration is either hindered, or ettringite which already has been formed, is decomposed. If liquid water penetrates such concrete elements at a later stage, ettringite will be formed in the hardened concrete leading to the associated volume expansion and severe damage. In a few cases secondary ettringite formation has also been observed in members not subject to heat treatment [Heinz and Ludwig (1987); Stark and Wicht (2001)]. Attention to this reaction should also be paid when the heat of hydration leads to concrete temperatures above 70°C due to the thickness of a member. In case a light weight aggregate concrete is used, even thinner members may attain a comparatively high temperature as this concrete has a much higher thermal insulation capacity. Further the porous light weight aggregates might store large amounts of free water, which is a prerequisite for a secondary ettringite formation.

A special type of corrosive action leading to acid and to sulphate attack is caused by *biogenic reactions* in the presence of bacteria. In such processes aggressive substances may be generated on concrete surfaces, particularly in sewage systems. The most common reaction is the formation of hydrogen sulphide H_2S from sulphate reducing or from sulphate forming bacteria in the absence of oxygen. In the presence of oxygen, sulphuric acid H_2SO_4 will be

generated resulting in acid and sulphate attack of the concrete. For further details refer to [Mullik and Chandra (1992)].

(3.5) Alkali-silicate and alkali-carbonate reactions

An alkali-silica reaction may occur in a concrete exposed to a humid environment if the aggregates contain critical amounts of amorphous or poorly crystalline silicates. Such aggregates may react with the alkali hydroxides NaOH and KOH which are contained in the hydrated cement paste and its pore solution. In natural aggregate sources such minerals may be opal inclusions in basalt, opaline sand stones, chalcedony, obsidian or flint. The reactive silicates form alkali-silicate hydrates which have the structure of a swelling gel. They take up water from their surrounding resulting in a severe and destructive expansion. At the same time the reacting aggregates may shrink and thus separate from their surrounding matrix resulting in the formation of micro-cracks and eventually in a complete disintegration of the concrete. The extent of expansion depends primarily on size and reactivity of the aggregates, on the chemical composition of the cement, in particular its content of alkalis, on the composition and alkalinity of the pore water in the hydrated cement paste, on the availability of water and on the resistance of the concrete against the penetration of water. In some instances damage due to alkali-silicate reaction became apparent only after several years or even decades. For further details on alkali-silicate reactions refer to e.g. [Swamy (Ed.) (1992), Stark and Wicht (2001)].

An expansive reaction, also referred to as *alkali-carbonate reaction* may take place due to ion exchange in dolomitic aggregates according to eq. (3.1-54).

$$CaMg(CO_3)_2 + 2\ NaOH \rightarrow CaCO_3 + NaOH + Mg(OH)_2 \qquad (3.1\text{-}54)$$

The magnesium hydroxide formed in this reaction may also have the characteristics of a swelling gel, however, it is considerably less expansive than most alkali-silica reactions.

(3.6) Precautionary measures

As shown in the preceding sections, chemical attack of concrete generally requires the presence of water, and severe damage occurs only if the aggressive media can penetrate the concrete by capillary suction, diffusion or mixed modes of transport at a sufficiently high rate. Thus the most important precautionary measures to prevent damage due to chemical attack in concrete are the protection of the structure against water by suitable structural detailing and the production of a concrete with a high resistance against the ingress of aggressive media, i.e. *a very low capillary porosity*. Consequently, high strength concretes in most instances show a significantly higher resistance against chemical attack than conventional concretes, refer e.g. to [Whiting (1987); Guse (1998)].

In addition, suitable concrete making materials have to be selected. Sulphate attack can be avoided if sulphate resistant cements with a low content of calcium aluminates are used. Also a sufficiently high content of blast furnace slag, fly ash or silica fume may increase the sulphate resistance of concrete substantially. In order to avoid damage due to alkali-silicate reactions careful preliminary testing of aggregates, for which no long-term service record is available, is inevitable. Also the use of low-alkali cements and the use of additions e.g. fly ash may be sufficient to avoid such reactions**.** In extreme cases, however, additional protective measures, such as coatings or overlays are inevitable. For further details regarding concrete

composition, concrete production and additional protective measures for concrete with a high resistance to chemical attack, see also [ACI (2009)].

3.1.9 Aspects of durability design and service life prediction

Despite of a profound knowledge on durability characteristics of concrete, the procedure for durability design of civil concrete structures according to national and international standards is based on empirical experience until today. These standards imply special deem-to-satisfy limits, e.g. on a maximum water/cement ratio and a minimum concrete cover, in connection with rough environmental classifications to ensure the durability of structures for an approximate defined minimum lifetime, e.g. 50 years according to EN 206-1:2001. The compliance of the given regulations is supposed to prevent the concrete and the reinforcement from damaging effects resulting from e.g. frost attack or chloride ingress, respectively. This design concept is termed as a *descriptive concept*.

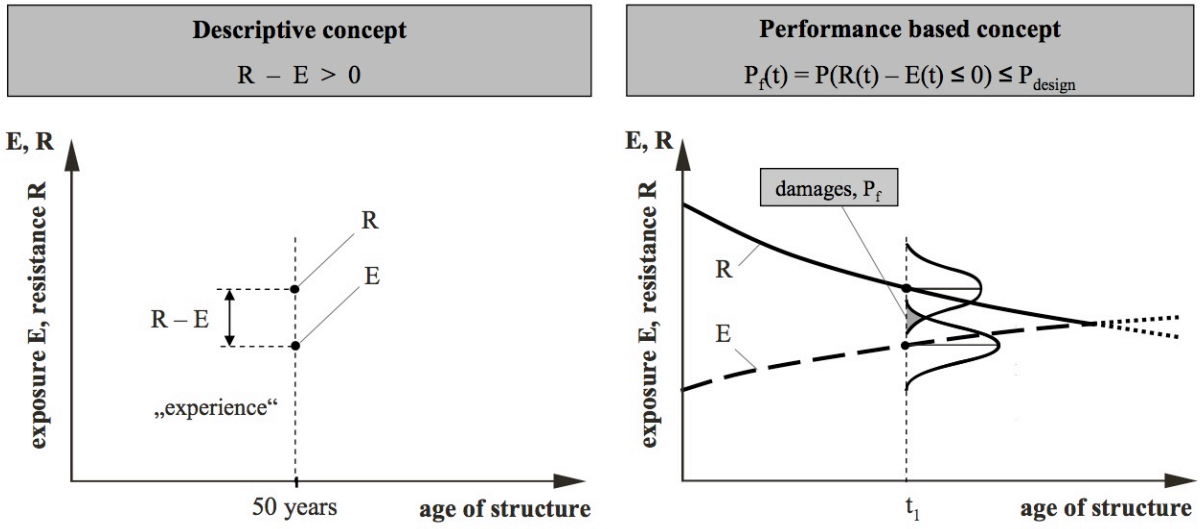

Implementation in EN 206-1

descriptive concept	exposure E	resistance R			
	environment	max. w/c	min. strength	min. cement	c
	XC4: reinforcement corrosion alternating wett and dry	0.60	C25/30	280 [kg/m³]	40 [mm]

Implementation in *fib* Model Code

physical models	
	$E = d_k(t) = \sqrt{2 \cdot k_e \cdot k_c \cdot (k_t \cdot R^{-1}_{ACC,0} + \varepsilon_t) \cdot C_S} \cdot \sqrt{t} \cdot W(t)$
	R = c = const.

Fig. 3.1-28: Action and resistance in view of the durability of concrete members. Schemata of the descriptive concept (left) and the performance concept including a probabilistic approach (right); below: implementation of the concepts for carbonation induced corrosion

It is quite evident that this descriptive approach is associated with several basic disadvantages allowing only a rather crude estimate of the durability of the structure. Neither the environmental actions nor the structural or material resistance, i.e. the different deterioration mechanisms in concrete, are considered in a realistic way. Instead of, the different environmental actions are roughly subdivided in so-called exposure classes which are associated with limiting values for the concrete composition and the concrete compressive strength. The intensity of the different exposure conditions is described in terms like “moderate humidity” or “cyclical wet and dry”. The influence of the temperature is completely neglected. This means that the difference between the action S and the resistance

R, being a measure of the failure safety, is only estimated by experience (Fig. 3.1-28, left). There is no information on the scatter of the actions and the resistance, respectively, and the effective safety margin is unknown to the designer. This descriptive concept is supposed to "guarantee" a sufficient concrete performance for a fixed service life of e.g. 50 years. Hence, it is not possible to quantify the necessary concrete properties for a specified lifetime of e.g. 20 or 100 years. In addition, it is also not possible to consider different limit states in view of damage risks, e.g. the time span until the depassivation of the reinforcement occurs.

In contrast, the *performance concept* based on a probabilistic approach is appropriate to allow for quantitative estimations of the durability of concrete structures. Hereby, the increasing damage process with time, i.e. the interaction of action and resistance, affecting the concrete structure is modelled by means of suitable deterioration time laws. Since there are several uncertainties in the action- and resistance-related parameters, it is necessary that the variability and the observable scatter, e.g. for the material parameters, are described by means of related statistical parameters. As a consequence, the safety margin between the well defined functions for the action S and the resistance R can be expressed in terms of the failure probability P_f, see the overlap region between the two curves in Fig. 3.1-28, right.

The lower part of Fig. 3.1-28 indicates the implementation of the related concepts for durability design in view of the carbonation induced corrosion. Considering the performance concept, the resistance is given by the concrete cover c, i.e. a constant over time. The action is described by the progress of the carbonation front according to the equation shown, which is also given in MC2010. The principle of this concept may be applied also for any other deterioration mechanism.

By means of the probabilistic performance concept the time-dependent increase of damage, i.e. the failure probability according to a defined unintended condition of the structure, e.g. E = R, can be calculated. It is obvious that the application of statistical methods in durability design is – in analogy to the structural design approach – an essential tool in order to quantify the performance of structural concrete. The decisive advantage of the performance concept is based on the fact that the time-dependent durability of concrete structures can be expressed in terms of failure probability or reliability indices, respectively, see in particular [*fib* Bull. No. 34 (2006)].

The quality of every quantitative durability design strongly depends on the quality and prediction accuracy of the material model applied. Considering the knowledge summarized in Section 3.1.8 and the complexity of this subject it becomes clear that for quite many relevant durability actions no adequate model exists so far. The deterioration time laws available allow for the prediction of the two most important mechanisms, i.e. carbonation and chloride attack [*fib* Bull. No. 34 (2006)]. Further some very crude information has already been published on the frost deterioration mechanism of concrete, see e.g. [Fagerlund (1997); RILEM Report No. 14 (1996)]. In addition, besides the lack of suitable deterioration time laws for many attacks on concrete, the interaction of different deterioration mechanisms is completely unknown in most cases so far.

3.1.10 Special concretes

Concrete can be classified according to various schemes, such as the compressive strength, the unit weight, the durability, the workability or aesthetical aspects, see Section 3.1.2. Due to physical and technological reasons the various classification categories cannot be arbitrarily combined (e.g. ultra high strength with minimum unit weight). Therefore

defined classification categories have been grouped into special concrete types. Among the subsequent concretes covered in this chapter are:

- *self-compacting concrete (SCC)*: a type of structural concrete which strongly deviates from ordinary concrete in the fresh state, as it de-aerates and flows without the application of additional compaction energy;
- *architectural concrete*: a type of structural concrete which fulfils high aesthetical standards in addition to technological requirements;
- *light weight concrete (LWC)*: a type of structural concrete which has a unit weight lower than 2000 kg/m³;
- *fibre reinforced concrete (FRC)*: a type of structural concrete which shows an increased ductility and a reduced microcracking due to the addition of steel or polymer fibres;
- *ultra high performance concrete (UHPC)*: a type of structural concrete with a compressive strength above 120 MPa and a very high durability, achieved by an optimized packing density of all granular raw materials.

While the composition of conventional structural concrete and its properties at the fresh state are not dealt with in detail in the preceding sections, as this is considered to be consolidated knowledge, such information will be given for special concretes where necessary. On the other hand, properties of special concretes at the hardened state are only treated when they differ significantly from those of conventional concrete.

3.1.10.1 Self-compacting concrete

(1) General

Self-compacting concrete (SCC) is a concrete that de-aerates and flows without the application of compaction energy, while staying homogenous during the whole placing process until hardening. This type of concrete was first invented in Russia and Japan in order to minimize negative effects of the placing process on the concrete properties, by omitting the external compaction process [Ozawa et al. (1990); Okamura et al. (1996)].

As pointed out in Section 3.1.3, when designing conventional concrete mixes, the aim is to maximize the aggregate content while minimizing the pore volume. At the hardened state, this ensures a direct load transfer between the aggregate grains via a thin intermediate cement matrix layer. However, at the fresh concrete state, this composition results in a very restricted workability characterized by a high viscosity.

In order to facilitate the concrete to de-aerate properly without any additional compaction work during the placing process, i.e. by flowing in the formwork at moderate shear rates, the dynamic viscosity of the mixture at these shear rates must be low enough in order for the entrapped air bubbles to rise to the concrete surface (see Fig. 3.1-3 and 3.1-4). Today, two procedures are available to achieve this:

So-called *powder type self-compacting concretes* are characterized by an approximately 30% higher paste content compared to conventional concrete. This ensures a high fluidity of the mix. The paste itself consists of cement, large amounts of mineral additives such as fly ash or limestone powder, water and chemical admixtures (above all superplasticizers). In order to prevent segregation, the water/cement ratio and water/binder ratio are kept very low, leading to high strength values at the hardened state. Due to the high paste content, powder type SCC

generally exhibits a reduced modulus of elasticity in comparison to conventional concretes of equal strength.

In contrast to powder type SCC, s*tabilizer type self-compacting concretes* have a lower paste content (approximately 10% higher than conventional concrete) but significantly higher water/binder ratio. By adding superplasticizer the viscosity of the mixes, especially at low shear rates is strongly reduced hence allowing the entrapped air to leave the concrete. At rest, however, strong segregation would occur unless this is prevented by adding stabilizing admixtures, so-called viscosity modifying agents (VMA). At the hardened state stabilizer type SCC differs only insignificantly from conventional concrete of equal strength. The increased water/binder ratio allows for the production of low and normal strength concretes with self-compacting properties.

(2) Mix design

The mix design process of SCC still is exclusively focused on ensuring self-compacting properties while neglecting other important mix design criteria, such as the compressive strength or the durability. Usually this disadvantage is accepted, as the most commonly used powder type SCC normally results in strengths $f_{cm} > 60$ MPa at very low water/binder-ratios, ensuring a high durability. However, it should be considered that exceeding the strength class projected by the designer might be associated with significant changes in the concrete's modulus of elasticity and its longtime deformation behaviour, i.e. creep and shrinkage, see [Haist and Müller (2003)].

(2.1) Powder type SCC

As has already been pointed out, by increasing the powder and thus the paste content in the concrete, its workability can be significantly improved. However, this measure alone is not sufficient to achieve the desired self-compactability. In order for the paste to flow properly and to be able to transport coarse aggregate grains, it must have a sufficient viscosity at high shear rates. On the other hand, at low shear rates the viscosity should not be too high, in order to enable sufficient de-aering and flow in common placing conditions. This behaviour is usually ensured using modern superplasticizers, which allow for a targeted adjustment of the pastes viscosity at low shear rates, without significantly influencing the flow behaviour at high shear rates. Prerequisite for such a systematical adjustment of the pastes properties is that the water/binder ratio of the paste is kept at a minimum value, the so-called water demand level. In order to prevent segregation of the concrete – i.e. sedimentation of the coarse aggregates in the paste – the grading curve of the aggregates should be adjusted to have a high fines or sand content. The sand grains hinder the coarser aggregates from sinking and thus prevent sedimentation.

Based on these principles, Okamura et al. (1995) developed a mix design procedure for powder type SCCs which is depicted in Fig. 3.1-29 for a concrete with a maximum grain size of 16 mm.

The mix design procedure is based on a three-fold approach considering the phases paste, mortar and concrete.

- estimation of the air-void content in the concrete (usually 2-3 vol.%)
- limitation of the coarse aggregate content (here: grains 4-16 mm) in the concrete to less than 50 vol.% and determination of the remaining mortar content ($V_{mortar} = V_{concrete}-V_{air}-V_{agg4/16}$)

- limitation of the fine aggregate content (here: grains 0-4 mm) in the mortar to less than 40 vol.% and determining the remaining paste content ($V_{paste} = V_{mortar} - V_{agg0/4}$)
- determining the composition of the remaining paste by defining the cement/filler volume ratio (V_{filler}/V_{cement}), experimentally measuring the water demand of the cement-filler – i.e. powder – mix β_{powder}, calculating the necessary water content $V_{water} = V_{paste} \cdot \beta_{powder}$ and powder content $V_{powder} = V_{paste} - V_{water}$
- experimental optimization of the resulting phases (paste, mortar and concrete)

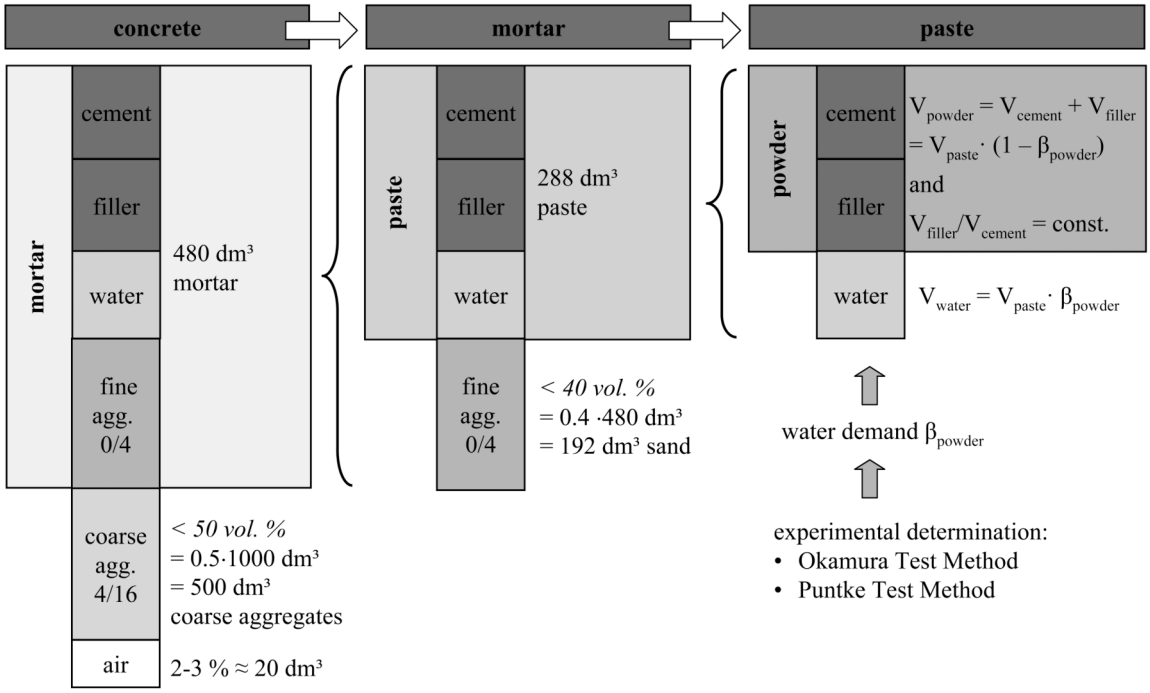

Fig. 3.1-29: Mix-design concept for self-compacting concrete according to Okamura et al. (1995)

In order to determine the water demand β_{powder} of the fines particles, two different methods can be applied. The *method by Okamura* et al. (1996) defines β_{powder} as the water content in the paste ($V_{water}/(V_{water} + V_{powder})$ at which a given paste stops to flow in the so-called mini-slump test according to EN 1015-3:2007, i.e. when no slump can be measured in the test. By plotting the volumetric water/paste ratio of pastes with identical powder content but stepwise reduced water contents over the slump flow value of each paste and using a linear regression over this data, the water β_{powder} demand can be extrapolated as the value at which no flow occurs, i.e. the slump flow equals 100 mm (diameter of the mini-slump cone). With regard to the effect of superplasticizers Okamura recommends to reduce β_{powder} by a factor of 0.8-0.9 for the application in SCC.

In contrast to the Okamura method, the so-called *Puntke method* defines the water demand β_{powder} as the water content in the paste at which the granular powder system merges from an undersaturated into a saturated state and thus into a suspension [Puntke (2002)]. Using the so-called Puntke test method, water is mixed stepwise with the dry powder and compacted thereafter. The water gradually fills up the voids between the particles while the granular system strives to reach an optimal packing density. The water content when the optimal packing density is reached and all voids are fully filled with water is referred to as the water demand β_{powder}. Exceeding this water content will lead to the formation of a shiny water film ontop of the wet powder, indicating that all voids in the powder are filled with water and the additional water added does not fit into intergranular voids. In contrast to the Okamura

method, the Puntke method allows for a direct experimental determination of the packing density of the granular system.

Instead of following all the steps listed above, a simplified mix design procedure for SCC can be applied. Hereby the paste content in the concrete is set to be approximately 36-42 vol.-%, based on experience or trial mixes. In a next step, the water demand of the powder is determined as described above. The resulting paste is mixed with aggregates, with a sand-rich grading curve. The fresh concrete behaviour is optimized by the addition of a superplasticizer.

(2.2) Stabilizer type SCC

Today, no standardized mix design procedure for stabilizer type SCC exists. This is due to the fact, that the stabilizers and superplasticizers available on the market have a highly divers working regime, which makes it very difficult to follow standardized approaches.

Stabilizer type SCC normally has a paste content of approximately 32-36 vol.% (conventional concrete 27-32 vol.%). In contrast to powder type SCC the paste usually contains a much higher water content which at the fresh state leads to a pronounced reduction of the viscosity of the mix over the total shear rate range (compare Fig. 3.1-4). In order to prevent segregation at rest and to avoid blockage of coarse aggregates in confined reinforcement layouts, stabilizing admixtures are added. These stabilizers significantly influence the concretes viscosity at low and medium shear rates.

In order to design a stabilizer type SCC the following steps should be followed:

- estimation of the air-void content in the concrete (usually 2-3 vol.%)
- specification of a sand-rich grain size distribution and limitation of the maximum grain size to 16 mm
- limitation of the aggregate content to 61-66 vol.%
- experimental adjustment of the water, superplasticizer and stabilizer content in the concrete in order to get optimal self-compacting properties

Similar to the powder type SCC the grain size distribution of stabilizer type SCC is coined by a comparatively high sand content, which helps to prevent segregation phenomena.

(3) Composition and fresh concrete properties

The final composition of a self-compacting concrete strongly depends on the mix design principle applied (see Section 3.1.10.1 (2)). As can be seen from Fig. 3.1-30, mixes based on the powder type formulation are characterized by a volumetric powder content, which is approximately twice as high as for a conventional vibrated concrete. When using fly ash as a filler, it should be noted, that in many national codes (e.g. the German DIN 1045-2:2008) only parts of this amount can be regarded as cement replacement (max. 33 mass%) and hence be attributed to the equivalent water/cement ratio (k-value = 0.4). The remaining rest of the fly ash is normally considered as pure filler, even though it reacts in the same manner as the rest of the fly ash. This explains why powder type self-compacting concretes containing fly ash usually show very high strengths and hardened properties rather corresponding to a high strength concrete than to a conventional concrete.

When using limestone or other inert mineral powders, it should be noted, that for the contents considered here, these fillers do not contribute actively to the hydration process. The

increased paste content of the concrete might therefore have negative influence on the hardened state properties and especially on the durability of the concrete (see Section 3.1.10.1 (4)). With respect to the use of limestone powders, it is recommended to use powders with low total organic contents (low TOC) and high fineness, i.e. powders of LL-quality according to EN 197-1:2004.

The maximum aggregate size for the production of self-compacting concrete should be limited to approximately 16-20 mm. In order to prevent segregation at rest and blocking behaviour during flow, the grading curve of the aggregates should be characterized by a high content in fines. It is possible to produce self-compacting concrete with rounded or crushed aggregates. In the latter case, normally a higher paste content might be required in order to get equivalent flow properties. When using aggregates sensitive to an alkali-silica-reaction it should be kept in mind that the high paste content in SCC as well as the high superplasticizer content – which may provide large amounts of alkalis – form unfavourable boundary conditions for such a concrete.

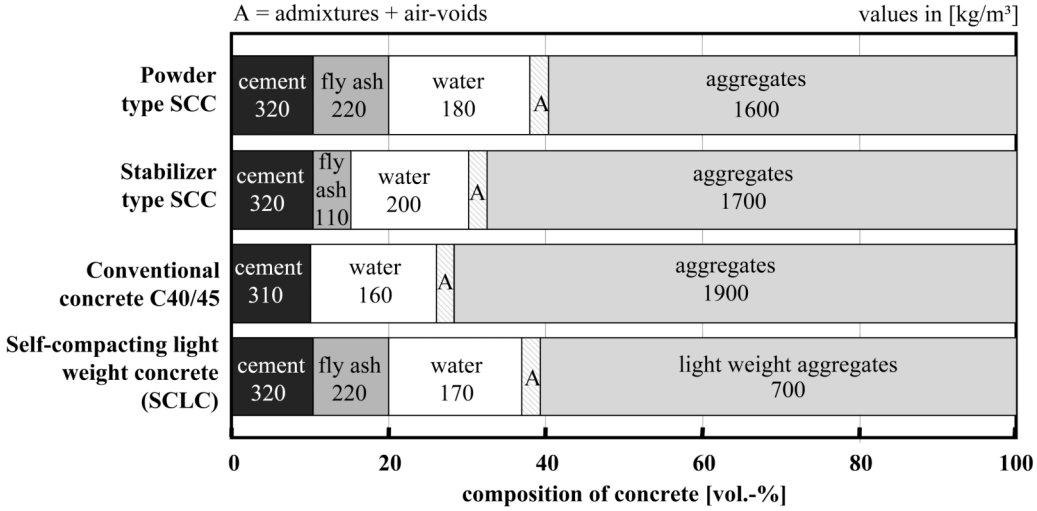

Fig. 3.1-30: Mixture composition of a powder type SCC, a stabilizer type SCC and a conventional vibrated concrete C40/45 as well as a self-compacting light weight concrete (SCLC)

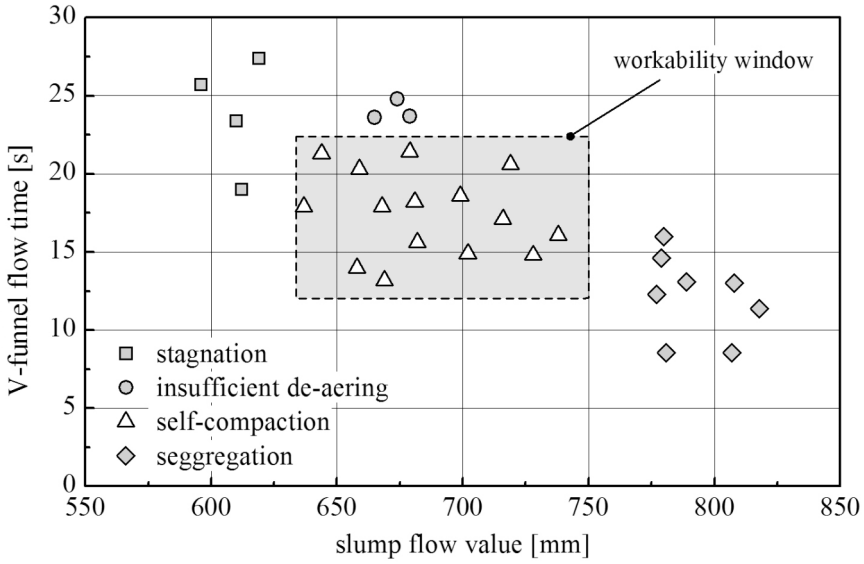

Fig.3.1-31: Workability window consisting of the slump flow value (EN 12 350-8:2008) and the V-funnel value (EN 12 350-9:2008), ensuring good self-compacting properties [Kordts (2005)]

Testing of the fresh concrete properties of SCC is, among others, covered in EN 206-9:2008. In contrast to conventional concrete the complex fresh concrete behaviour of SCC required the introduction of several new test methods, such as the slump flow test (see EN 12 350-8:2009 and EN 12 350-12:2008 with or without J-Ring), the V-funnel test (see EN12 350-9:2008-01) or the sedimentation test (see EN 12 350-11:2008).

Primary goal of the test procedure is to guarantee, that the concrete de-aerates properly, stays homogenous during flow and rest until hardening and has a suitable flow behaviour in order to fill a given formwork. The last requirement mentioned clarifies, that the required flow behaviour is a function of the formwork geometry. Before this background the flow properties must vary whether a long wall element with extensive flow passages is casted or whether a slender column is filled with SCC.

Kordts (2005) proposed a so-called workability window, consisting of at least two parameters, such as the slump flow value and the V-funnel flow time (Fig. 3.1-31). By pre-testing the boundary conditions of the workability range the workability window ensures that a concrete, which is well within the window, provides optimal self-compacting properties in the formwork. The adaptation of the workability window to the requirements of each concrete member however requires the knowledge of an experienced concrete technologist.

(4) Properties at the hardened state

The differences in the composition of self-compacting concrete in comparison to conventional (vibrated) concrete may lead to deviations in the hardened state behaviour. Especially for powder type SCC the increased paste content normally results in a reduced *modulus of elasticity* E_{cm}. From experimental results, this deviation can be estimated to be between 10-20% below the prediction of e.g. MC2010 for a conventionally compacted concrete of equal compressive strength. However, as can be seen from Fig. 3.1-32 (left), this deviation is still within the scatter band known from conventional concretes. When using puzzolanic additives like fly ash, the reduced modulus of elasticity at the age of 28 days is outweighed to some extend by an increased gain in stiffness due to the puzzolanic reaction of the fly ash and the hardening associated with this reaction. The designer should however keep in mind that for structures reacting sensitive to the deformation behaviour of the concrete, additional testing of the self-compacting concrete to be used is highly recommended.

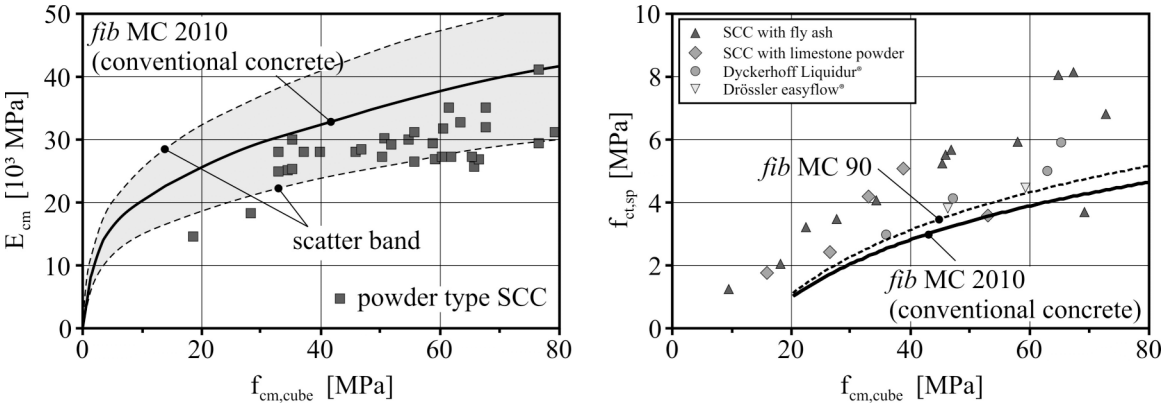

Fig. 3.1-32: Modulus of elasticity E_{cm} (left) and splitting tensile strength (right; data from [Brameshuber et al. (2001)] as a function of the mean concrete compressive (cube) strength $f_{cm,cube}$ for various self-compacting concretes

Regarding the *tensile strength* the increased binder content of SCC may lead to higher values, depending on the type of filler used (see Fig. 3.1-32, right). Note in this context, that MC2010 predicts a slightly lower splitting tensile strength $f_{ct,sp}$ for concretes of equal mean compressive strength f_{cm} than CEB/FIB MC90. This is due to the fact, that in the MC2010 the conversion factor from the tensile strength to the splitting tensile strength was changed from A = 0.9 to A = 1.0. For structures sensitive to cracking, further attention should be paid to the development of the tensile strength beyond the design age of 28 days. Especially when using large amounts of puzzolanic additives like fly ash or silica fume, a pronounced growth of the tensile strength at higher concrete ages might be observed.

Similarly to the modulus of elasticity the *creep and shrinkage behaviour* of powder type SCC is also affected by the high paste content of such concretes. The limited data regarding the shrinkage behaviour of powder type SCC indicates, that the ultimate shrinkage deformation can be expected to be approximately 20% higher than for a conventional concrete of equal strength. The same holds true for the creep behaviour of such concretes. Powder type SCC in general also exhibits an increase of approximately 10-20% in creep deformations [Müller and Kvitsel (2006)].

Both creep and shrinkage deformations of SCC are well within the scatter band e.g. of MC2010, which is defined to be ± 30%. It should be noted, however, that for structures which react sensitive to variations in the modulus of elasticity as well as the creep and shrinkage behaviour, the deviations mentioned above for SCC occur systematically. In case of doubt it is therefore highly recommended to measure the actual short and longtime deformation behaviour.

The *bond behaviour* of SCC is less dependent on the position of the rebar, i.e. whether a rebar is embedded at the top or the bottom of a formwork. The *durability* of SCC is characterized by an identical or improved behaviour than conventional concrete of equal strength regarding the *carbonation and chloride diffusion behaviour*. According to investigations by Ludwig et al. [Ludwig (2001)] the *freeze-thaw resistance* of powder type SCC strongly depends on the type of filler used. For SCC containing fly-ash an equivalent or even higher freeze-thaw resistance was detected. However, concretes containing limestone powder showed an increased weathering in the freeze-thaw test. Further it should be considered that SCC has a higher paste content which in general has a negative influence on the freeze-thaw behaviour [Brameshuber (2004)].

3.1.10.2 Architectural concrete

(1) Introduction

Concrete surfaces with particularly demanding requirements on their appearance are termed *fair-faced or architectural concrete*. This type of concrete is an important design element of modern architecture. The concept of architectural concrete is defined in guidelines and codes of practice for the construction industry, see e.g. [Deutscher Beton- und Bautechnik-Verein (Ed.; 2004); Oesterreichischer Beton- und Bautechnikverein (Ed.; 2009)]. These resources also provide valuable information and guidance relevant to building practice. However, there is no separate, comprehensive, generally applicable standard or guideline pertaining to architectural concrete that contains details with regard to design, specification and construction.

The terms "*architectural concrete*" or "*fair-faced concrete*" are used to refer to uncoated concrete surfaces the appearance of which is subject to certain requirements. There is a wide range of appearances that can be achieved. In simple terms, a distinction can be made

between untreated and finished surfaces. Untreated surfaces are characterised by the colour of the concrete and the formwork texture with its simple or structured arrangement. Finished surfaces are realised by applying stonemason techniques (such as pointing or bush hammering) or blasting (using sand particles or steel balls, for example), as well as acid washing, washing-out, grinding and polishing processes. Exposed-aggregate concrete and terrazzo are just two examples of washed or ground surfaces. The following considerations concentrate on architectural concrete with an appearance that is characterised by the formwork and it's facing (untreated surfaces).

(2) Design and specification

The production of architectural concrete is a complex construction process. In all construction phases, it therefore requires the parties involved to have a high degree of expertise and to apply utmost care. What is even more important is a close coordination between the parties. The wishes of the client regarding the appearance of the architectural concrete surface and the technical possibilities of the contractor to realize these wishes must be aligned with each other prior to the commencement of the construction work. The involvement of an experienced concrete technologist is strongly recommended if special requirements are imposed on the architectural concrete.

The creation of sample and reference surfaces is strongly recommended. They serve as samples for the contractor whilst enabling him to optimise the entire production process from a technological and economical point of view, including its logistics and the associated training of staff. These surfaces also demonstrate to the client the results that are actually achievable, depending on the alternatives chosen, if any. It is essential to ensure that the sample surfaces are, as far as possible, of a representative nature in every respect (including their positions, geometries etc.). When evaluating the architectural concrete surface produced, the parties must bear in mind, as a matter of course, that reference surfaces can never be replicated without slight deviations (see Section 3.1.10.2 (5)). When selecting the reference surface, the parties should not rely on exposed surfaces of existing buildings. The boundary conditions and determining factors that influenced the production of such surfaces are generally unknown. Moreover, the specific overall impression characterises the appearance of any surface section. Also, ageing processes result in both desired and unwanted changes in the appearance that cannot be reproduced when realising new surfaces.

The use of a testing formwork as described by [Lohaus and Fischer (2005)] makes it possible to optimise the architectural concrete system consisting of formwork facing, release agent and fresh concrete. At the same time, exposed surfaces are created that may also be used as references if required.

In addition, special attention must be paid to the quality control system. It is useful to divide the entire production of architectural concrete into several sub-processes and to define the specific tasks and responsibilities beforehand, as well as the required random samples and checks.

(3) Concrete mix design and production

The composition of the concrete mix must be as constant as possible in order to fulfil one of the main requirements for architectural concrete, i.e. its uniformity. Moreover, the raw materials used – cement, aggregates, concrete additives (including pigments) and admixtures – must adhere to the specifications included in the relevant standards whilst ensuring a quality

that fluctuates as little as possible. Even minor deviations of these parameters that do not significantly influence the technological properties of the concrete, such as strength or deformation behaviour, may result in considerable changes to the appearance of an architectural concrete surface.

There is no standard mixture recipe to produce high-quality architectural concrete. However, robust mixes with a plastic to soft workability (workability classes F2/F3 according to EN 206-1:2001) have proven to be suitable (see e.g. [Springenschmid (2007)]). The content of cement or binder paste and mortar must be sufficiently high to prevent bleeding and/or segregation while avoiding any concrete stickiness. The w/c ratio should be lower than 0.55. Water/cement ratio fluctuations of ± 0.02 may already cause significant changes in brightness or colour. As a rule, a lower w/c ratio results in a darker shade. When adhering to the mix parameters above and to a maximum aggregate size of 16 or 32 mm, it will be necessary to add a plasticizer. The addition of an air-entraining agent has proven its worth in stabilising the mix, irrespective of its effect on the frost resistance. Especially suitable for the production of highly uniform surfaces are self-compacting concretes, as by omitting the compaction process, undesirable influences on the visual properties of the concrete can be avoided.

The mixing sequence should be the same as for conventional structural concrete. If pigments are used, they should be added already to the concrete aggregates. The mixing time should rather be longer than in the case of conventional concrete, with a minimum mixing time of at least 90-120 seconds even when high performance mixers are used. Significantly longer mixing times are required for SCC. Fluctuations in the temperature of the fresh concrete (which should not exceed 25°C) should be avoided as far as possible since they may also cause colour variations.

At delivery of the concrete at the construction site, it should be noted that already minor deviations from the agreed workability may have a negative effect on the appearance of the architectural concrete surface. It is recommended to check and monitor the temperature of the fresh concrete. Architectural concrete should preferably be delivered over short haulage distances.

(4) Placement and finishing

(4.1) Formwork and release agent

Regarding the formwork, distinction has to be made between absorbent and non-absorbent facings and smooth and structured facings. The structure can range from a simple wood grain pattern to the use of form liners with height offsets of several centimetres. Most of the non-absorbent formwork panels include a plastic or phenolic resin surface layer, or they are all-plastic or all-steel. Their surface is smooth unless it is structured by form liners. Absorbent panels are mostly made of wood. Their surfaces exhibit various degrees of porosity and are partly untreated (e.g. as-sawn or planed) or lined by an additional, thin surface film.

Quite clearly, the surface properties of the formwork-facing materially influence the appearance of the architectural concrete that reflects the surface texture of the formwork. This applies to both roughness and absorption capacity. For instance, an absorbent type of formwork-facing will result in darker surfaces with fewer pores. Brighter surfaces will appear once the absorption capacity of the formwork-facing has decreased after several use cycles. Chemical reactions may occur between the formwork-facing and the constituents of the concrete. These reactions may compromise the visual appeal of the surface. For example, the highly alkaline pore water in the concrete attacks certain polymers used as formwork-facings or liners. When using untreated timber formwork for the first time, chemical reactions may

occur in the concrete edge zone that result in colour variations and sanding. A cement slurry may be applied to prevent these phenomena [Springenschmid (2007)]. Applying smooth, non-absorbent formwork-facings results in brighter surfaces. However the resulting surfaces are more susceptible to streaking, clouding and mottling. Identical formwork panels should be used to achieve a uniform surface pattern. Even an exposure of the formwork to light that varies in its intensity across certain sections or duration may have an effect on the appearance of the architectural concrete surface.

Rust stains may become visible on the surface if a steel formwork is used. Care must be taken when using steel formwork in conjunction with pigmented concrete. The commonly used metal oxide pigments show a ferromagnetic attraction to the steel, which is the reason why such panels should generally be demagnetised, if necessary.

Formwork facings can be grouped into classes allocated to the architectural concrete classes. Detailed information on the types of formwork facing, their texture characteristics, their possible effects on the architectural concrete surface and indicative frequencies of use are, for example, provided in the German or Austrian guidelines for architectural concrete [Deutscher Beton- und Bautechnik-Verein (Ed.; 2004), Oesterreichischer Beton- und Bautechnikverein (Ed.; 2009)]. This reference also includes details on panel dimensions, design elements (formwork liners etc.) and the feasibility of architectural concrete. The joints between the individual formwork elements must be sealed in such a way that neither solid matter nor water can pass through.

Release agents are used to make formwork stripping easier whilst preventing any damage to the architectural concrete surface, to render the visible surfaces more uniform and to protect the formwork itself. They consist of complex chemical compounds and mixes. No general recommendations can be made with regard to the selection of release agents. This selection must be based on the specific experience gained with such products in combination with the formwork facing chosen. However, appropriate preliminary tests are strongly recommended, using the testing formwork mentioned in Section 3.1.10.2 (2), for example.

(4.2) Execution and finishing

The methods commonly applied to place concrete in building construction (using a bucket or pump) can also be used for architectural concrete. The concrete should be poured quickly and at constant speed in layers not exceeding 50 cm. As a matter of course, formwork soiling should be prevented. Special emphasis must be put on a uniform compaction intensity adjusted to the respective workability. Even robust concrete mixes cannot compensate for irregularities and compaction flaws, which become all the more apparent in architectural concrete (such as mottling patterns or water marks). It is therefore crucially important to ensure a thorough planning and execution of concrete placement and compaction.

During finishing, too, a high degree of uniformity and consistency must be ensured. All measures to protect concrete surfaces from harmful impacts (such as temperature, soiling or loss of moisture) at the early age must be applied to an even greater extent. It is a known fact that any subsequent treatment or finishing that adds water will pose the risk of discolourations. When a protective film is applied to the concrete, any water dripping onto the concrete surface must be avoided, as well as any draughts (chimney effect). Reference [Springenschmid (2007)] includes the recommendation to remove the formwork at a relatively early stage and to ensure a subsequent humidity in excess of 85%, or to spray a hydrophobing agent onto the surface. When applying this method, however, a test must have been carried out beforehand to ensure that such an agent would not have any deleterious

effect on the appearance. This principle also applies to liquids used for subsequent protective treatment.

Local and temporal irregularities in the drying process of the surface after completion of the subsequent protective treatment may also result in staining. The weather impact during the construction and stripping of architectural concrete surfaces on the site is hard to avoid. This influence may result in a slight change to the shades of grey in which the concrete appears.

(5) Assessment

The assessment of architectural concrete surfaces is based on the criteria that were contractually agreed upon beforehand, such as the architectural concrete class or reference surfaces. It should be noted that reference surfaces cannot be replicated without deviations. Even if utmost care is taken, each element is a unique piece since some of the factors and parameters that influence the appearance cannot be controlled on the construction site. These include the weather conditions (such as temperature and humidity) prevailing during the production of architectural concrete and formwork stripping, as well as unavoidable fluctuations in the characteristics of all materials and substances used, which influence the appearance in the same way as uncontrollable deviations in concrete production and placement. Architectural concretes may be assessed only after the surface has dried evenly.

The overall impression of an exposed surface is the underlying acceptance criterion. This impression must be based on an observation under the usual lighting conditions from an appropriate distance. The latter is the distance at which the user/observer of a building would usually be located at. Individual criteria, such as porosity or colour uniformity, should be considered for the purpose of the assessment only if the overall impression of the exposed surfaces is not in line with the appearance agreed upon by the parties.

(6) Defects and remedial work

Beyond the non-compliance with criteria listed e.g. in relevant guidelines, streaks, clouding, mottling, lime bloom and discolourations constitute typical deficiencies of architectural concrete. In each specific case, an expert should be consulted to decide whether the phenomenon observed does in fact constitute a deficiency.

Streaks, clouding and mottling occur as a result of local segregation of the concrete in the transition zone to the formwork facing. These phenomena may be caused by the composition of the mix but also by the method used for concrete placement and/or compaction. The smoother and less absorbent the formwork-facing, the higher the risk for such deficiencies to occur. The darker, and in most cases smoother, areas indicate a locally reduced w/c ratio and a higher share of calcium carbonate whereas a higher amount of calcium silicates was found in the rougher and brighter zones [Strehlein and Schießl (2008)]. The surface roughness and the deposit of various compounds or crystals also leads to varying light refraction patterns, and thus to differences between bright and dark sections.

Another significant factor that promotes the occurrence of dark discolourations is the weather prevailing during architectural concrete production and formwork stripping. When architectural concrete is produced in the winter season (with low temperatures and a high relative humidity), the risk for stain-like dark discolourations to occur is significantly higher compared to the situation in the summer months [Strehlein and Schießl (2008)].

Colour variations may also be caused by the composition of the mix but also by the formwork facing and method of compaction. Any change in the type of cement used, and even a new cement batch, may influence the shade of grey. A higher degree of milling fineness, lower Calcium-Aluminate-Ferrite ratios in the cement clinker and higher w/c ratios result in brighter exposed surfaces. This also explains why brighter surfaces are created when the formwork absorption capacity decreases due to frequent use. Another typical phenomenon are darker areas that occur at formwork joints both because of the locally reduced w/c ratio and, as the case may be, the exposed aggregate. Likewise, a difference in vibration intensity that occurs, for instance, due to a variance in workability or because of an unwanted minor stiffening of the concrete may result in colour variations between the individual cast layers. Even reinforcing steel deeply embedded in the concrete may show a pattern on the surface if the vibrating cylinder got into contact with the reinforcement and triggered its vibration [Springenschmid (2007)].

Brighter areas due to lime deposits or lime bloom and sintering are created if pore water rich in calcium hydroxide penetrates into layers close to the edge or reaches the surface, followed by its evaporation and subsequent carbonation of the calcium hydroxide left on the surface. Such brightening or bloom occurs predominantly when, soon after concrete placement and formwork stripping, water is allowed to penetrate into a young concrete of (still) low strength, and is transported to the evaporation front again at a later stage. In cold weather, and thus slow hydration, the risk for brightening or bloom to occur is particularly high.

In the case of brown discolourations, metal oxides play a major role in most cases. For instance, they may originate from corroding reinforcement, and are then transported to the surface by moisture. To a lesser extent, such discolourations may be the result of pyrite-containing aggregates. Brown discolourations may also occur if formwork panels are used that are lined with phenolic resin, for example when water penetrates into the gap created by the loosening of the tie rods, or when the water condensates in this gap, which triggers a reaction with the formwork facing due to the highly alkaline environment.

Blue or green discolourations are typical of the use of cement that contains blast-furnace slag. They are created by the formation of metal sulphides. These colour phenomena do, however, disappear again when atmospheric oxygen diffuses into the edge zone and subsequently reacts with the metal sulphides to form colourless metal compounds. This usually happens within only a few weeks [Stark and Wicht (2000)].

Any work to remedy architectural concrete defects is an extremely demanding task that requires a high degree of expertise, care and craftsmanship. As a rule, the parties should evaluate whether it is actually worth undertaking such work well ahead of its commencement, and whether their benefit outweighs the associated costs. Some of the irregularities form an integral part of the appearance of the concrete or will be perceived to a lesser extent as the visible surface is aging, or will disappear altogether over time. Any substandard remedial work undertaken may result in a deterioration of the appearance. For this reason, an experienced concrete technologist should be consulted when architectural concrete is to be repaired.

The measures to be taken will depend on the type and magnitude of the visual flaw and on its root cause, which must be clarified before work starts. A distinction can be made between five methods to remedy defects: cleaning (by mechanical or chemical means), the application of stonemason techniques, the use of a filler, and concrete replacement combined with crack and/or void filling [Günter (2005)]. Prior to commencing remedial work, sample surfaces must be used to check if the selected method would achieve the intended outcome.

The concrete needs to be replaced, for instance, when existing flaws or defects that go deeper into the concrete (such as voids, gravel pockets or leaking construction joints) also compromise its durability or strength, or if local contamination occurred (for instance by penetrating oil). On the basis of appropriate preliminary testing and a mix designed specifically for the intended repair, the contractor usually succeeds in placing a repair concrete adjusted to the architectural concrete in such a way that the area of repair can be recognised only at the initial stage and when viewed at close range [Günter (2005)].

(7) Special architectural concretes

White architectural concrete is produced with a specially designed Portland cement ("white cement") and additional white pigments if required. For this purpose, the raw materials used for the Portland cement must be free of iron and manganese oxides. As regards concrete technology and production, there are no differences to cement-grey architectural concrete. However, the intended white appearance requires special care and attention. Even finest cracks, that would normally be invisible, can become very disruptive on an exposed surface appearing in white.

Coloured architectural concrete is usually produced with metal oxide powder pigments or other alkali- and light resistant particles. Their ratio is usually lower than 5 percent by weight of the cement and should be kept as low as possible since their powder nature increases the required amount of water whilst making the concrete stickier and more viscous. A brilliant and particularly uniform shade can be achieved only if white cement is used at the same time. The considerations outlined in Section 3.1.10.2 (3) apply to the production of coloured concrete. However, the mixing time should rather be increased in order to achieve the highest possible level of homogenisation.

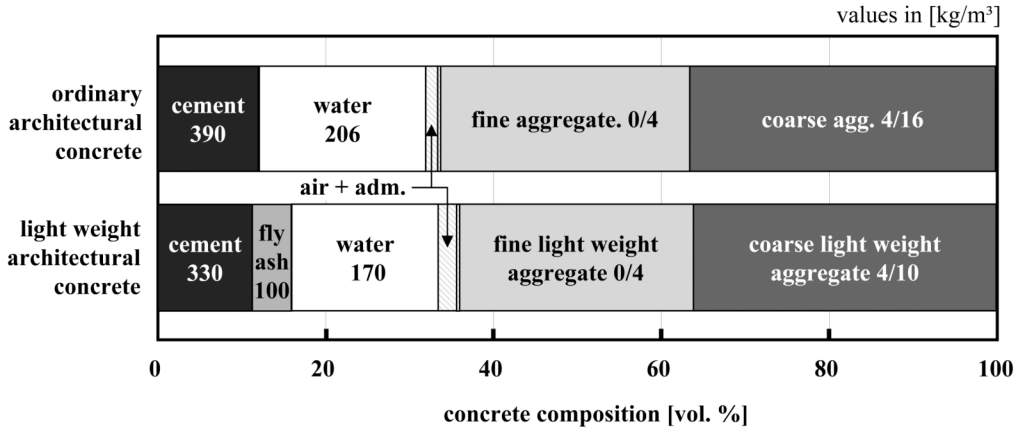

Fig. 3.1-33: Composition of a normal weight and a light weight architectural concrete with the raw materials cement, fly ash, fine and coarse aggregate, water, admixtures and the resulting air content

Light weight architectural concrete is an attractive modification of architectural concrete because this type of concrete also ensures an appropriate degree of heat insulation if designed and placed accordingly. Its production requires adherence both to the rules and standards to produce and process light weight concrete (see Section 3.1.10.3) and to the rules and standards pertaining to architectural concrete referred to above. Fig. 3.1-33 compares the composition of a light weight architectural concrete with the constituents of a normal weight architectural concrete mix. More details regarding the technology used to produce and process light weight architectural concrete and built examples are provided in [Müller and Haist (2005)].

3.1.10.3 Light weight concrete

(1) Introduction and overview

For certain applications, the relatively high unit weight and low degree of thermal insulation of conventional concrete can be disadvantageous. This fact resulted in the development of light weight concrete already at an early stage. In this process, the concrete bulk density is generally reduced by a targeted entrainment of air in the composite material. This can be achieved both by using porous light weight aggregates (*Approach 1*) or by making the cement paste matrix porous (*Approach 2*), for example by adding air-entraining or foaming agents. These two approaches can also be combined. No-fines light weight concrete is a special option (*Approach 3*) in which the volume ratio of the cement paste matrix is reduced in the composite system to such an extent that internal voids are formed between the individual aggregate particles. In this mix, the cement paste merely serves to make the aggregate particles stick to each other.

The term *structural light weight concrete* is applied to concrete grades that are produced and used as specified in EN 206-1:2001. These concretes are mainly produced in accordance with Approach 1, or using a combination of Approaches 1 and 2. Correspondingly, the surface of structural light weight concrete is characterized by a closed pore structure, which is why this type of concrete is also often referred to as light weight concrete with impermeable structure. Besides the unit weight, these concretes are classified by their compressive strength, in analogy to normal weight concrete. Whereas its durability parameters show almost no deviation from those of conventional concrete of equal strength, the mechanical characteristics differ significantly in some cases. They are closely dependent on the bulk density of the concrete and the strength of the paste matrix. The bulk density of light weight concrete in accordance with EN 206-1:2001 can range from 800 to 2 000 kg/m^3. Depending on their bulk densities, structural light weight concretes provide relatively good thermal insulation properties. However, due to the increasingly demanding requirements on the thermal behaviour of buildings, today, a separate heat insulation layer needs to be added in most cases, if usual element thicknesses are used.

This section on light weight concrete concentrates on structural light weight concrete in accordance with EN 206-1:2001, which can be used as ready-mixed concrete or in the precast industry. Beyond concrete technology, this section also refers to particular aspects to be considered in the production, application and quality control of such concretes.

(2) Structural light weight concrete

(2.1) Key characteristics

Structural light weight concrete according to EN 206-1:2001 is produced, either partially or completely, by adding light weight aggregates. The development of porosity in the paste matrix, for example by adding an air-entraining agent, generally is permissible only up to an air void content of 10 percent by volume (regulation may vary depending on country). Correspondingly, structural light weight concretes exhibit a surface structure that is mainly determined by the cement paste, and is largely equivalent to the structure of normal weight structural concrete.

The advantages offered by structural light weight concrete compared to conventional concrete include, above all, the combination of a low bulk density with a high compressive

strength and good heat insulation parameters [Faust (2003)]. Light weight concrete also shows a low degree of thermal expansion, which limits resulting imposed or internal stresses.

Further, structural light weight concrete deviates from the behaviour of conventional concrete with respect to its deformation characteristics. Due to the lower stiffness of the light weight aggregates, structural light weight concrete has a considerably lower modulus of elasticity and exhibits more significant shrinkage deformation than conventional concrete [Müller et al. (2000); Grübl et al. (2001)]. However, the lower stiffness also has a favourable effect on the development of internal and imposed stresses in elements and structures. Its lower thermal conductivity and capacity results in a higher development of hydration heat than in normal weight concrete. By taking appropriate measures, any resulting deleterious effect on the properties of the fresh concrete and the structural element can be prevented.

When producing structural light weight concrete, the accurate monitoring and management of the water content of the light weight aggregate is of particular importance. Fluctuations in the moisture content of the no-fines light weight aggregate lead to variances in the absorption capacity which, in turn, may result in significant changes in the properties of the fresh concrete.

In many cases, the compaction of light weight concrete poses problems. Due to the low bulk density of the concrete and the high porosity of the light weight aggregates used, the amount of vibration introduced by the compaction equipment is damped significantly. This effect must be countered by a much longer compaction period and a more tightly spaced vibration pattern.

(2.2) Light weight aggregate

Structural characteristics and behaviour

Aggregates to be used for the production of structural elements consisting of light weight concrete must conform to the EN 12 620:2008 and EN 13 055-1:2002 standards. In general, the following materials may be used as aggregates: pumice, foamed lava (crushed lava), expanded slag (crushed and foamed blast-furnace slag), boiler ash (processed residues of coal firing), sintered pumice (crushed agglomerates, e.g. from fly ash, tailings or clay), brick chippings (processed crushed bricks), or expanded clay, shale or glass. For all aggregates, in particular expanded glass, the principle applies that they must not be reactive to the alkaline substances of the cement paste. Aggregates preferably used to produce high strength light weight concrete include expanded clay and shale, and, to a certain extent, expanded slag and sintered pumice [Faust (2003); Müller et al. (2000)]. The area of application of light weight aggregates to produce structural light weight concrete is specified in EN 206-1:2001.

The key element to understand the properties of fresh light weight concrete is the behaviour of the light weight aggregate. In this context, the aggregate edge zone – which directly interacts with the other concrete constituents (especially water and cement) –, plays a major role. In general, a distinction must be made between light weight aggregates with an edge zone that exhibits a very low degree of porosity with small pore radii and aggregates that have a uniform pore structure across the entire section, associated with high porosity. Correspondingly, light weight aggregates can be divided into aggregates with closed and open pores. Due to the different behaviour resulting from these characteristics, each of these types of aggregate need to be treated differently during concrete production.

Light weight aggregates with closed pores

Usual light weight aggregates that are produced in an expansion or sintering process consist of a highly porous ceramic core that is characterised by an interconnected system of pores in diameters from approximately 20 to 800 μm, and is surrounded by a relatively impermeable sintered shell. This shell mainly determines the properties of the fresh and hardened concrete (Fig. 3.1-34). In this setting, the permeability of the sintered shell is not directly correlated with the bulk density of the aggregate. The radii of the shell pores range from 0.01 to 40 μm, depending on the type of aggregate used. In all expanded clay aggregates, the pores of the shell show a high degree of capillary activity due to their size.

As a result of the strong capillary effect of the shell pores, such light weight aggregates can withdraw a high amount of water or ultrafine paste from the mortar matrix of the light weight concrete. A severe workability reduction occurs if this behaviour is not countered during concrete production. A significant portion of this absorption process can be shifted to an earlier phase by wetting the aggregate in a targeted process prior to producing concrete (so-called pre-wetting), which considerably reduces changes in workability.

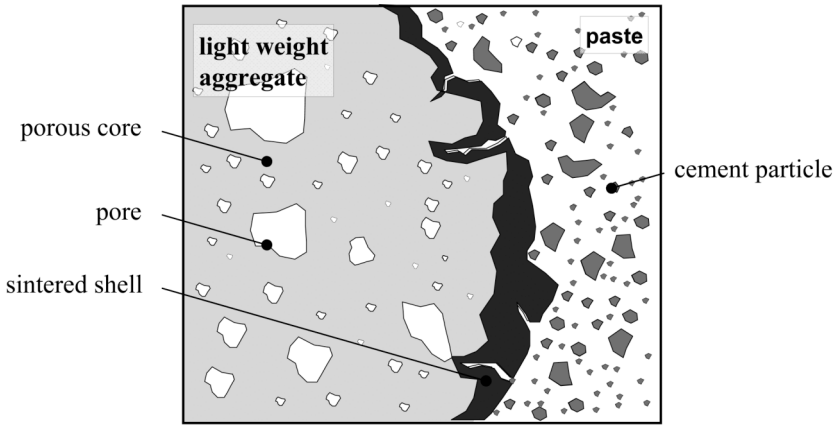

Fig. 3.1-34: Schematic cross-section of a light weight aggregate grain with sintered shell (e.g. expanded clay) suspended in cement paste

The absorption behaviour of light weight aggregates with a sintered shell is characterised by a water absorption that progresses quickly at the initial stage and slows down significantly over time. This absorption process lasts several hours. The behaviour results from the air contained in the aggregate, which cannot escape in the presence of the isotropic pressure acting on the aggregate when stored in water undisturbed. Such aggregates are therefore often wetted long before concrete production starts. In this respect, care should be taken to ensure that light weight aggregates with a wet core and dry surface absorb a significant amount of water in addition to the existing core moisture. The total of this water absorption and the existing initial moisture significantly exceeds the test value for the water absorption of oven-dried light weight aggregates determined in accordance with EN 13055-1:2002. This must be taken into account when preparing light weight aggregates for use and calculating the water to be added as pre-wetting water.

Light weight aggregates with open pores

Light weight aggregates with open pores include aggregates made of pumice, lava, expanded clay or shale sand, and boiler ash. They are characterised by their high porosity that is evenly distributed across the entire particle section. As a result they have a high capillary absorption capacity. When in contact with water or ultrafine paste, their system of pores is

saturated almost completely within seconds or only a few minutes, unlike the pores of light weight aggregates with a sintered shell. However, the absorbed water cannot be retained permanently due to the high degree of interconnection of the individual pores and the larger pore radii. For this reason, a certain portion of the water is released again during the mixing process, in particular in case of a high degree of pre-wetting. During the placement process, an uncontrolled water release may occur, especially under the impact of vibrators, and may lead to segregation. On the other hand, fluctuations in the mixing water content can be compensated by the buffer effect of the open-pore system unless the light weight aggregate is not fully saturated with water.

When selecting the aggregate to be used for the production of light weight concrete, it should be noted that aggregates with open pores have a lower particle strength than those with a sintered shell. This is a factor that limits the strength of such light weight concretes. Moreover, the fact that open-pore light weight sands usually have a higher powder content (particle diameter < 0.125 mm) must be taken into account.

Light weight aggregate preparation (pre-wetting)

Irrespective of the type of light weight aggregate, the first step of the preparation and adjustment of pre-wetting should be to determine the initial moisture in a drying test in accordance with EN 1097-5:2008. The amount of pre-wetting water required for dry aggregates with closed pores is equivalent to the water absorption test value. If the aggregate core is wet, however, the amount of pre-wetting water is equivalent to 1.3 to 1.5 times the absorbed water determined in accordance with EN 1097-6:2000 or DIN V 18 004:2004-04, less the initial moisture (core moisture) of the aggregate.

The situation is different in the case of light weight aggregates with open pores. Because of the risk of repeated water release that may occur in the case of over-saturation, a pre-wetting equivalent to approximately two thirds of the water absorption measured according to DIN V 18 004:2004-04 is recommended.

In construction practice, a defined degree of pre-wetting is adjusted by selective mixing of the weighed (wet, if appropriate) light weight aggregate with the calculated amount of pre-wetting water prior to adding the remaining concrete raw materials. To ensure a sufficient durability of the light weight concrete, the degree of pre-wetting of the aggregate should be restricted to the minimum level required for processing.

(2.3) Concrete mix

Since light weight aggregates usually have a lower compressive strength than the surrounding paste matrix in light weight concrete, an increase in concrete compressive strength can be achieved only by adjusting the water/cement ratio and the binder content to the type of aggregate used. An accurate adjustment of the bulk densities of the aggregates used in the mix is also required. Significant differences in the bulk densities of the mortar matrix and the coarse aggregate may result in segregation. For this reason, only limited options are available with regard to the selection of the types of fine and coarse aggregate and their respective ratio in the mix.

Starting from the requirements on the bulk density, mechanical characteristics and durability of the concrete, the first step of the concrete mix design must be to define the type of coarse aggregate to be used. Expressed in general terms, the higher the intended strength of the concrete, the higher the bulk density of the coarse aggregate required. To achieve the

aspired bulk density class of the concrete, it should be clarified whether this is still feasible using a natural sand matrix, or whether the natural sand needs to be partially or completely replaced with light weight sand. Fig. 3.1-35 shows the related design diagrams, which enable an estimate of the particle bulk density of the coarse aggregate, as well as of the type and composition of the fine aggregate (see [Faust (2003)]).

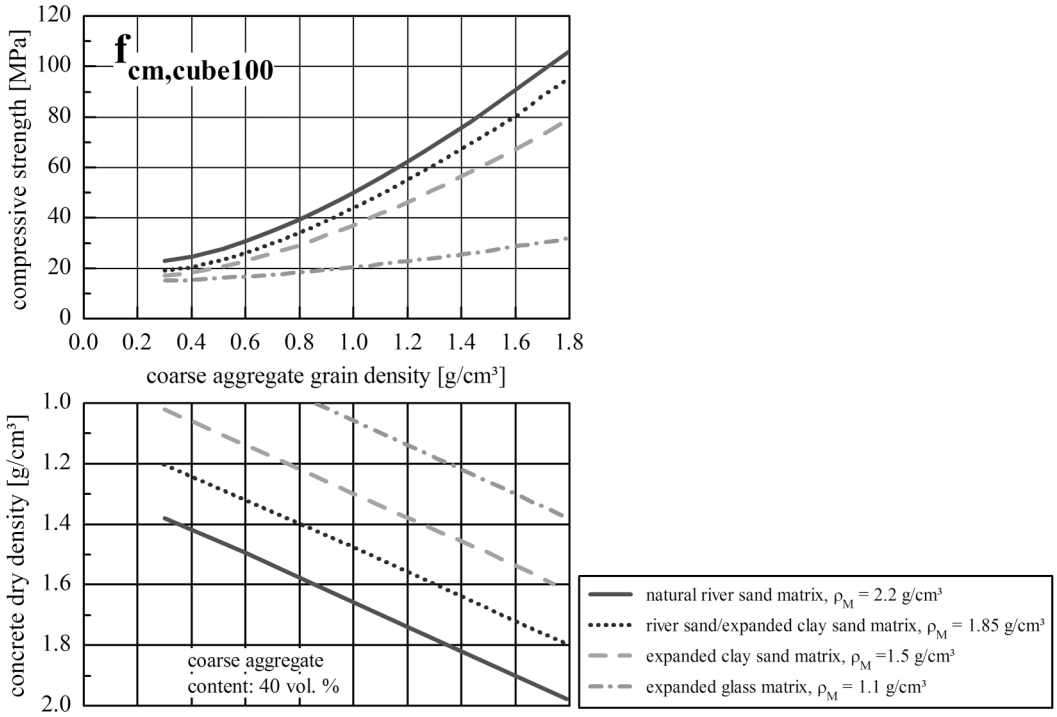

Fig. 3.1-35: Nomogram enabling the determination of the mean concrete compressive strength $f_{cm,cube,100}$ as a function of the concrete dry density and the type of aggregates used [Faust (2003)]

Following the selection of the type of coarse and fine aggregate, the cement- or binder-paste content in the concrete is determined. This content must be 1.1 to 1.2 times higher than in a conventional concrete of identical strength, and ranges from 330 to 400 dm^3 of paste per m^3 of concrete for commonly used light weight concretes.

It is far more difficult, however, to determine the required w/c ratio. Unlike in conventional concrete, the 28-day compressive strength of the concrete does not only depend on the w/c ratio and the cement grade but is also strongly dependent on the strength of the light weight aggregate. The compression failure of light weight concrete is determined by the tension failure of the light weight aggregate. Accordingly, the achievable maximum compressive strength of the concrete is limited by the type and strength of the light weight aggregate. For this reason, the diagrams used for conventional concrete, such as the Walz-diagram, cannot be applied to light weight concrete.

The design of a light weight concrete mix aims to relieve the light weight aggregate of stresses by selecting a sufficiently stiff paste matrix. This is why the w/c ratio of light weight concrete must be significantly lower than that of conventional concrete, and must be adjusted to the strength of the light weight aggregate. Fig. 3.1-36 shows a related diagram that was modified for light weight concrete [Faust (2003)].

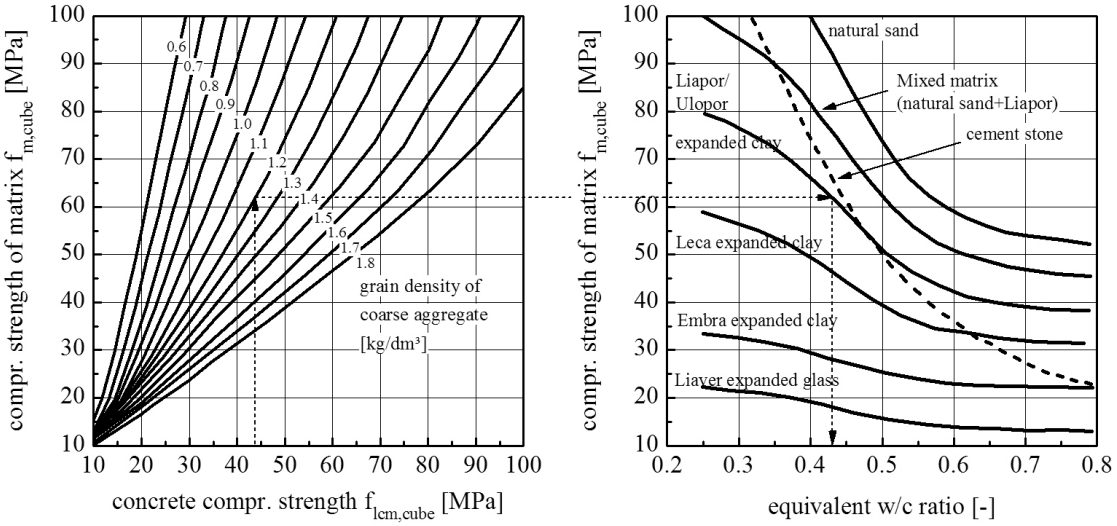

Fig. 3.1-36: Diagram for the determination of the required w/c ratio as a function of the desired concrete compressive strength $f_{lcm,cube}$, the strength of the matrix $f_{m,cube}$, the density of the coarse aggregates and the type of matrix used [Faust (2003)]

As regards the type of cement and additives to be used, structural light weight concrete is subject to the same requirements as normal weight structural concrete.

In the case of light weight concrete, special attention must be paid to the development of hydration heat. Due to the excellent heat insulation characteristics of light weight concrete, a sharp increase in temperature may occur, in particular in bulky light weight concrete elements. Among other things, this is associated with an expansion of the air contained in the aggregate, which expels the pre-wetting water absorbed by the grains. At temperatures in excess of approximately 60-70°C, further the hydration process of the cement will be disturbed resulting in unbound sulphate residues in the cement stone. In combination with the free water present in the porous aggregates this may promote an increased formation of secondary ettringite in the hardened concrete. The swelling potential of this mineral would result in massive internal damage to the concrete.

Bearing this in mind, cements that develop their strength and hydration heat slowly are generally used for the production of light weight concrete elements. Among other materials, binder mixes consisting of cement and fly ash have proven to be particularly favourable options. However, this also results in a slower hardening progress and a prolonged curing period. For this reason, the 56-day strength is often agreed upon as the parameter to verify the strength of structural light weight concrete.

Concrete additives, in particular plasticizers, are also very commonly used in light weight concrete. When selecting an appropriate plasticizer, its reaction to a possible water release by the light weight aggregates should be tested before use. In practice, robust concrete mixes are achieved by using stabilising concrete additives.

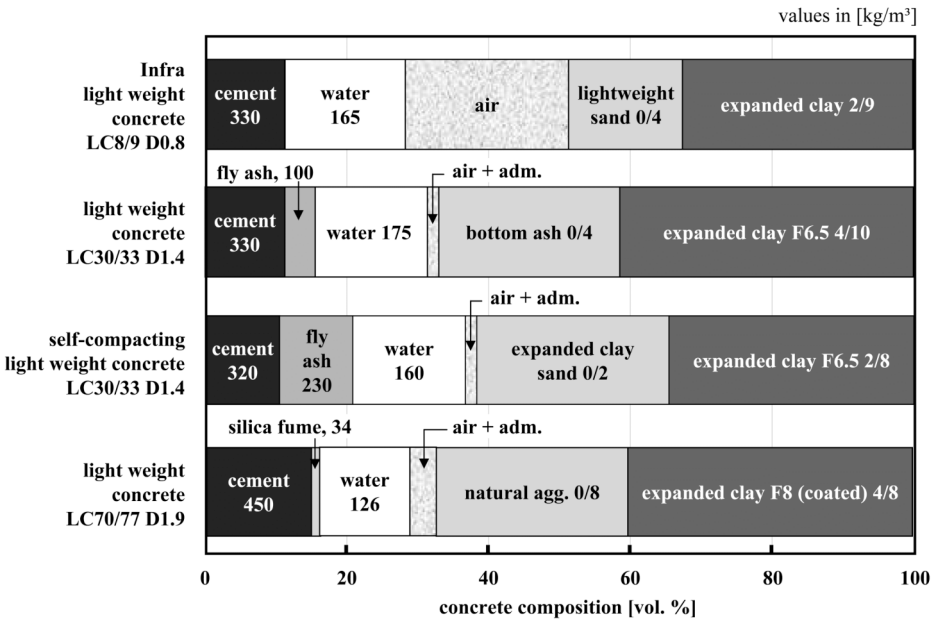

Fig. 3.1-37: Exemplary comparison of different light weight concrete compositions

As an example, Fig. 3.1-37 shows the compositions of a normal strength and high strength structural light weight concrete LC30/33 D1.4 and LC70/77 D1.9, respectively [Müller et al. (2000)], and of a self-compacting light weight concrete LiSA 1.4 (LC30/33 D1.4, SCLC) [Müller, Haist, Mechtcherine (2002)], as well as of a foamed light weight concrete (infra light weight concrete, LC8/9 D0.8) [Schlaich and El Zareef (2008)] consisting of cement (C), fly ash (FA), silica fume (SF), water, air, concrete additive (adm.) and various types of mineral aggregate (agg.). The latter mix is currently not covered by EN 206-1:2001.

(2.4) Production, transport and placement

The properties of light weight concrete in its fresh state are largely influenced by the moisture absorption behaviour of the light weight aggregate. When using dry aggregates, its water absorption capacity must be determined prior to concrete production. If wet aggregates are used, the water content must be measured prior to use. This is preferably achieved by a drying test (in accordance with EN 1097-5:2008). It is not possible to determine the moisture content of light weight aggregates automatically via sensors. Once the water content and water absorption capacity are known, the aggregate weight and the amount of water required for sufficient pre-wetting can be calculated (see Section 3.1.10.3 (2.2)).

The first step of the concrete production process is to feed the required light weight aggregate quantity into the mixer. In the next step, the calculated amount of pre-wetting water is added and mixed with the aggregate. Thereafter, appropriate quantities of cement and additives, mixing water and, if required, admixtures are added.

Following its delivery to the construction site, light weight concrete must first be thoroughly re-mixed in the truck mixer. A representative sample should then be taken and its slump measured. For structural light weight concrete, too, its adjustment to standard workability (workability class F3; slump between 42 and 48 cm) has proven to be entirely adequate. This degree of workability results in a robust placement behaviour whilst limiting the risk of over-compaction or segregation.

Structural light weight concrete must usually be conveyed by a concrete bucket since pumping is not possible as it would strongly reduce the workability or even obstruct the conveyance line. Pumping will be successful only if self-compacting light weight concrete is used (see Section 3.1.10.3 (2.6)) [Haist and Müller (2005)]. This pumping process has a favourable effect on the quality of the building element to be cast because concrete is conveyed continuously whilst the risk of separated casting layers is excluded. In both conveying processes, any air entrainment in the concrete due to excessively high free falls must be avoided. For this reason, hoppers and hoses tapering to the bottom must be used if a concrete bucket is used for casting.

Structural light weight concrete requires a more intense compaction than conventional concrete. When using an internal vibrator, this requires a more tightly spaced compaction pattern and longer immersion periods. However, any excessive compaction must be avoided as it may cause concrete segregation. Unlike in the case of conventional concrete, the spacing of the immersion zones of the vibrator should be reduced to five or six times the diameter of the vibrating cylinder, depending on the bulk density of the fresh concrete. For wall elements, the maximum height of individual cast layers should be in the range from 30 to 40 cm.

During concrete production and placement, the light weight aggregate constantly exchanges moisture with the surrounding cement paste matrix. Since an excessive water release from the pre-wetted aggregate would lead to segregation, only under-saturated aggregates may be used. If this requirement is met, the absorption capacity of the aggregate acts as a buffer to compensate slight variations in the mixing water content. This results in a significantly higher uniformity of the properties of the fresh concrete.

(2.5) Behaviour at the hardened state

The particular aspects of the behaviour of structural light weight concrete in its hardened state are primarily attributable to the load carrying behaviour and failure mechanisms of light weight concrete. While normal weight structural concrete transfers loads within the structure via the stiff aggregates, the low stiffness and strength of the light weight aggregate results in a load transfer that is almost exclusively guided through the mortar matrix. Light weight concretes also show a more brittle failure pattern, which must be taken into account for design purposes.

In addition, they exhibit a hygric deformation behaviour that significantly deviates from conventional concrete. This pattern is characterised by an initial swelling deformation that is followed by the typical shrinkage shortening only at a later age. Moreover, a drying process extending over several years is observed in light weight concrete, which often results in the formation of fine crackles on the concrete surface.

Mechanical characteristics

At an early age, the compressive strength of structural light weight concrete mainly depends on the cement paste strength, as is the case for conventional concrete. If, however, the cement paste strength approaches the aggregates strength in the course of hydration, the influence of the aggregate and the thickness of the cement paste layers increase. For this reason, the compressive strength of structural light weight concrete does no longer significantly increase with age after one week if Portland cement is used – unlike in the case of conventional concrete. By contrast, a considerable increase in compressive strength at a given testing age should be expected in line with an increase in cement content at an identical w/c ratio.

Light weight concrete requires a slightly lower effective water/cement ratio than conventional concrete to achieve a given compressive strength. Since the maximum concrete strength that can be achieved at a certain light weight concrete bulk density is determined by the strength of the aggregate, an ultimate concrete strength value can be assigned to each type of light weight aggregate, also see Fig. 3.1-36.

Although light weight concrete mostly has an identical compressive strength but a higher cement paste strength compared to conventional concrete, and the bond between aggregate and cement paste is often more effective than in conventional concrete, the low strength of the light weight aggregate ultimately leads to a lower *tensile strength* of light weight concrete. Related tests have shown that the magnitude of tensile bending strength, splitting tensile strength and concentric tensile strength is usually somewhat lower in structural light weight concrete than in a conventional concrete with an identical compressive strength. In MC2010 this is accounted for by introducing a reduction factor η_l according to eq. 3.1-55 to be multiplied with the tensile strength of normal weight concrete f_{ctm} of equal compressive strength. The factor η_l hereby depends on the oven dry density ρ of the concrete:

$$\eta_l = (0.4 + 0.6 \cdot \rho/2200) \tag{3.1-55}$$

When using the tensile strength of light weight concrete, it must be noted that the temporary reduction in tensile bending strength and concentric tensile strength can, as a result of drying, be much more significant than in conventional concrete.

The *sustained load strength* of light weight concrete reaches approximately 70 to 75% of the 28-day strength, and is thus slightly lower than that of conventional concrete (see MC2010). This more marked reduction is explained by the fact that, in general, light weight concrete shows a lower degree of longtime hardening than conventional concrete, which means that the critical period during which sustained load failure is possible is correspondingly longer [Faust (2003)].

The resistance of light weight concrete to *fatigue* compressive loading is also slightly lower than that of conventional concrete. In contrast, the *Poisson ratio* of light weight concrete is identical to conventional concrete.

The *modulus of elasticity* of light weight concrete E_{lcm} shows a significant correlation with the type of aggregate used. Its magnitude is closely correlated with the concrete bulk density ρ. For this reason, the stiffness of structural light weight concrete is estimated on the basis of the modulus of elasticity of normal weight concrete E_{cm} with the same compressive strength in accordance with MC2010 by using the equation $E_{lcm} = E_{cm} \cdot (\rho/2200)^2$.

The *stress-strain curves* of light weight concrete reflect a more significant brittleness compared to conventional concrete (Fig. 3.1-38). The ascending branch shows a linear stress behaviour up to higher loading levels. Elongation at rupture increases in line with the rise in compressive strength. It reaches 2.5 to 3.5 ‰, and is thus greater than the values for conventional concrete. A striking characteristic is the descending branch of the stress-strain curve, which shows a much sharper decline compared to conventional concrete with identical strength. This has to be taken into account in the design of reinforced or prestressed light weight concrete structures by adjusting the parabolic-rectangular diagram.

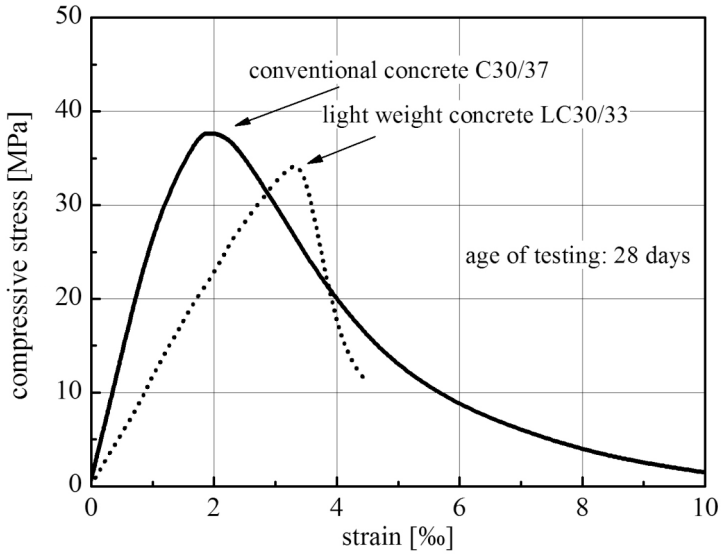

Fig. 3.1-38: Stress-strain curve for conventional concrete C30/37 and light weight concrete LC30/33

The knowledge of *fracture mechanisms* of light weight concrete is still insufficient, and the dependence of fracture energy of such concretes on different parameters (density, types of aggregates, strength etc.) must be addressed to future research. Light weight concrete is notch sensitive (most important to this sensitivity are eigen-stresses because of moisture gradients). The maximum crack opening depends on the kind of matrix and the kind of aggregates, respectively. Thus, tests to determine *fracture energy* and softening behaviour are difficult. MC2010 gives a rough estimation of the fracture energy $G_{F,l}$ as a function of the concrete tensile strength and the type of matrix (light weight or normal weight sand) used.

The *creep strain* occurring in structural light weight concrete is of the same magnitude as in normal weight concrete of the same strength class [Müller and Kvitsel (in prep.)]. Although a higher degree of creep should normally be expected to occur in light weight concrete, this is compensated by the lower creep of its stronger paste matrix due to the relatively low stiffness of the light weight aggregate. In accordance with MC2010, however, the creep coefficient $\varphi = \varepsilon_{cc}/\varepsilon_{ci,28}$ for normal weight concrete must be reduced by a factor $\eta_E = (\rho/2200)^2$, which depends on the dry bulk density ρ of the concrete, because the elastic deformation value is increased by the same factor.

Drying and hygric deformation behaviour

The *drying and hygric deformation* behaviour of light weight concrete is significantly different from conventional concrete [Rostásy et al. (1974), Kvitsel (in prep.)]. This is mainly attributed to the water absorbed by the porous light weight aggregate, which is released to the paste matrix, and then to the ambient air, only very slowly. Unlike in conventional concrete, moisture is transferred not only through the capillary pore system of the cement paste but also through the pores of the light weight aggregate.

A typical phenomenon of the hygric deformation behaviour of structural light weight concrete is the swelling deformation at an early age, which is gradually reduced by the shrinkage process only after an extended drying period, resulting in a transition to shrinkage shortening (Fig. 3.1-39). As also shown in Fig. 3.1-39, swelling deformation may be captured only if deformation measurements begin at a sufficiently early age of the concrete.

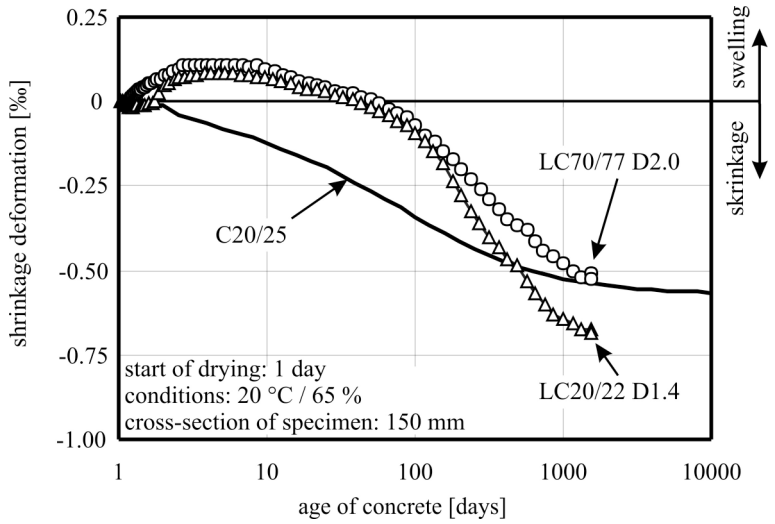

Fig. 3.1-39: Shrinkage behaviour of a normal (LC20/22 D1.4) and a high strength light weight concrete (LC70/77 D2.0) in comparison to a conventional normal weight concrete C20/25

Depending on the moisture gradient across the element section, significant local differences in deformation occur as a result of swelling and shrinkage. While the inner part of a cross section still undergoes a pronounced swelling, the surface region dries and consequently shrinks. These processes lead to eigenstresses and to cracking once the ultimate tensile strength of the concrete in the surface region is reached. Since the moisture and deformation gradients generally reach their maximum only at an age of 90 to 180 days, a thorough, long-term protective treatment alone is not sufficient for structural light weight concrete to limit cracking in the edge zone close to the surface. Rather, it is crucial to reduce the degree of pre-wetting of the light weight aggregate, and thus the core moisture of the concrete.

According to MC2010, light weight concrete shrinkage is – like conventional concrete shrinkage – the sum of basic shrinkage and drying shrinkage. The total shrinkage must be increased by a factor of 1.5 or 1.2 (for LC 20/22 and higher) compared to conventional concrete of identical compressive strength. Quite clearly, this is a simplified approximation to reflect the relatively complex shrinkage characteristics of light weight concrete. As explained above, the magnitude of the drying shrinkage will essentially depend on the moisture content of the porous light weight aggregate. Swelling will occur as long as the aggregates within a concrete element release originally absorbed water to the hydrating and drying paste matrix. This deformation process will show a transition to shrinkage only when the moisture reservoir is nearly depleted and when the drying front penetrating from the surface dominates the deformation behaviour. Investigations currently being performed still need to clarify whether the final shrinkage coefficient of light weight concrete is actually greater than that of normal weight concrete [Kvitsel (in preparation)].

Durability

The high durability of structural light weight concrete results from the dense cement stone matrix, which has a higher strength compared to conventional concrete of equal compressive strength, and the excellent bond between the matrix and the light weight aggregate. This bond is created by the interlocking of particles and matrix and as a result of the good hydration in the contact zone (different to ordinary concrete), as well as by a hydraulic or pozzolanic reaction that occurs between the particle surface and the adjacent cement paste. More recent studies confirm the high frost and freeze-thaw resistance of light weight concrete, which has also been proven in practice on buildings and structures being in use for many years under

severe weather conditions. In addition to the influencing factors mentioned above, this is also due to the porosity of the light weight aggregate. Due to the porosity of the aggregates, a sufficient volume is available for the expansion of the freezing water and crystallising salts. However, this requires a moderate degree of pre-wetting of the light weight aggregate.

No differences in comparison to conventional concrete are observed concerning the carbonation behaviour of light weight concrete. The increase in the concrete cover specified in guidelines merely accounts for the fact that an aggregate particle that comes into contact with a rebar may act as a diffusion bridge for carbon dioxide. This especially applies to concretes with a light weight sand matrix. Due to their high powder content and high porosity, these concretes are significantly more permeable than concretes with a natural sand matrix. For this reason, carbonation progresses more quickly in concretes containing light weight sand.

Thermal characteristics

According to MC2010, the thermal expansion of light weight concrete may be reduced by a factor of 0.8 compared to conventional concrete.

A major advantage of light weight concrete is its low thermal conductivity. Fig. 3.1-40 shows the thermal conductivity of light weight concrete as a function of the dry bulk density of the concrete. However, if the specified thermal conduction resistance $R \approx 1.2$ $(m^2 \cdot K)/W$ for an external wall unit (e.g. in Germany) were to be achieved without additional insulation, this would still require a wall thickness of $d = 0.48$ m at a dry bulk density of the concrete of $\rho = 0.8$ kg/dm^3.

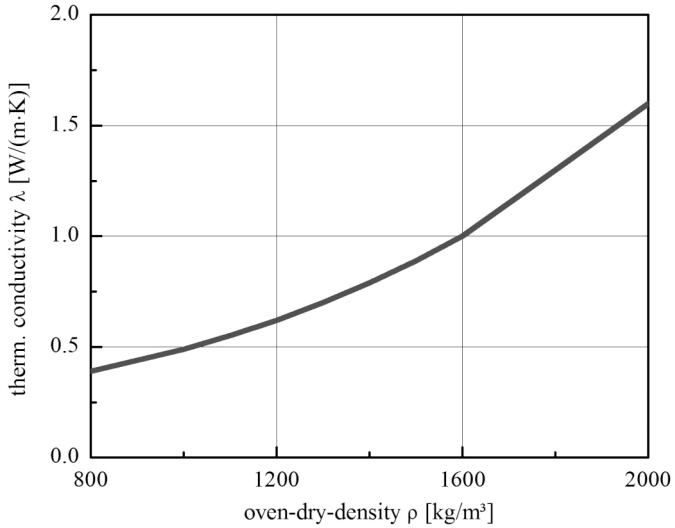

Fig. 3.1-40: Thermal conductivity of light weight concrete according to German DIN V 4108-4:2007

The fire rating of light weight concrete elements is higher than that of elements consisting of conventional concrete because of the lower thermal conductivity, lower coefficient of thermal expansion and increased ductility of light weight concrete at high temperatures [Haksever and Schneider (1982)]. Today, the spalling of light weight concrete layers during fire tests, which is caused by high water vapour pressure due to a high moisture content of the aggregate, can be countered effectively by adding polymer fibres.

(2.6) Self-compacting structural light weight concrete

Compared to conventional structural light weight concrete, the key advantages of self-compacting light weight concrete (SCLC) include, quite clearly, its robust fresh concrete properties that enable pumping in conjunction with hardened concrete properties that are comparable to conventional structural light weight concrete. In particular in the precast industry, the use of SCLC enables the production of more slender elements, which, in turn, considerably reduces the cost for transporting and erecting these elements. For construction and rehabilitation work in the context of existing structures, there are many areas of application of SCLC due to its beneficial characteristics, such as self-compaction and pumpability, low unit weight, higher strength and high thermal insulation capacity (see Müller et al. (2002)).

The composition of self-compacting structural light weight concrete is similar to normal weight SCC (see Fig. 3.1-37). It is characterised by a powder content that is approximately 100 dm^3/m^3 higher than that of a conventional structural light weight concrete (also see Table 3.1-6).

characteristic value	self-compacting light weight concrete		
	LiSA 1.3 (SCLC)	LiSA 1.4 (SCLC)	LiSA 1.6 (SCLC)
strength class	min. LC30/33		min. LC35/38
density class	D1.4		D1.6
shrinkage and creep	according to MC2010 for light weight concrete		
acceptable exposure class	X0, XC1-XC4, XD1, XD2, XS1, XS2, XF1, XA1		
thermal conductivity [W/(m·K)]	< 0,60[a)]		< 0,80[a)]
strength development	medium/fast		
density of fresh concrete [kg/dm³]	1550		1800
fresh concrete pressure	hydrostatic		

[a)] according to German technical approval Z-23.11-1244

Table 3.1-6: Characteristics of self-compacting light weight concretes according to a German technical approval

Fresh concrete tests demonstrate that SCLC has good, uncompromised self-compacting properties up to an age of two hours. The ability of the light weight aggregate to buffer fluctuations in the water content of the fresh concrete as a result of the aggregate's absorption behaviour makes these concretes highly robust in terms of their segregation resistance [Haist and Müller (2005)]. Comprehensive laboratory tests and several industrial-scale concreting jobs proved that SCLC can be easily placed via pumps. Sample elements complied with the architectural concrete quality standard [Müller and Haist (2004)].

The properties of hardened SCLC correspond to those of conventional structural light weight concrete with an identical compressive strength. SCLC elements can therefore be designed as specified in EN 206-1:2001. Today, almost every modern precast plant provides the technical prerequisites to produce SCLC. Only an initial test is required prior to producing and using these concretes. The quality control system is defined in the manual on the internal quality control of concrete.

3.1.10.4 Fibre reinforced concrete

(1) General

Fibre reinforced concrete is a type of concrete to which fibres – predominantly made of steel, alkali-resistant glass or plastic (polymer) materials – are added in order to improve its cracking and fracture behaviour. The fibres are embedded in the paste or in the mortar, i.e. in the matrix and act as reinforcement.

By integrating ductile fibres with a high tensile strength in the matrix, concrete cracking can be either inhibited or reduced, i.e. a fine cracking pattern can be achieved. In the cracked condition, the existing fibres establish a bridging of both crack edges. Provided certain requirements are met, the fibres may also resist sizeable tensile loads even in the case of larger strains (Fig. 3.1-41). In contrast, conventional concrete cannot transfer tensile stresses over a crack in the case of crack widths of 0.15 mm or larger.

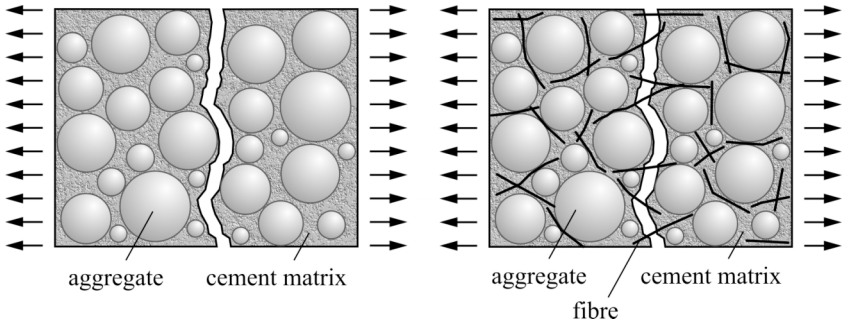

Fig. 3.1-41: Comparisson of a conventional (non-reinforced) concrete (left) and a fibre reinforced concrete (right) at the fractured state

In general, either continuous *long fibres* can be inserted in the direction of the anticipated tensile stresses (e.g. textile reinforced concrete, Ferrocement [Naaman (2000 a)]), or *short fibres* may be added to the mix and are thus randomly distributed in the concrete (see [Curbach et al. (Ed.; 1998)]). Depending on the processing conditions prevailing in the hardened concrete, the fibres may show a varying distribution pattern from a one dimensional to a random, three dimensional distribution. The information given in this Textbook, is exclusively focused on concretes, where fibres are added to the concrete during the mixing process and which therefore possess a random, three dimensional fibre distribution and orientation. However, the reader should be aware of the fact that both the fibre distribution and orientation can be strongly affected by the mixing and placing process, which in turn can lead to strong deviations in the desired material behaviour.

(2) Interaction of fibres and matrix

The interaction between the fibres and the matrix in fibre reinforced concrete can be described either by the *spacing concept*, reflecting fracture mechanics, or, as it is done here, by the *composite concept*. The later offers the key advantage, that the working principle assumed is very similar to the principles applied in the design of conventional reinforced concrete. Within this concept fibre reinforced concrete is considered as a composite consisting of two homogeneous elastic or elastoplastic materials. Each component (i.e. concrete and fibres) participate by carrying a certain portion of the external load. The fibres

are considered as a statistically distributed reinforcement. The external load is taken up by the components in accordance with their volumetric share in the concrete and their stiffness in comparison to the stiffness of the concrete.

At the *uncracked state*, the fibres are involved in the load transmission according to the ratio of the elastic moduli of both fibres and concrete. Since under tensile loadings, the elongation at rupture of the paste matrix (m) is significantly lower than the elongation at rupture of the fibre materials (f), the matrix will always crack before the ultimate strength of the fibres is reached. Further the fibre content in the concrete is limited to comparatively low values (approximately 2-3 vol.-%) in order to ensure sufficient workability at the fresh state and to limit the costs. The contribution of the fibres to the strength of the composite material, i.e. the load at which cracks in the matrix occur, therefore is low. Even if fibres with a very high modulus of elasticity such as steel or carbon fibres are used, the crack resistance level can be increased only to a limited extent.

At the *cracked state*, the fibres inhibit the advanced opening of the crack. For crack widths greater than approximately 0.15 mm it is assumed, that the force transfer over the crack by an interlocking of the aggregate particles is negligible and thus the fibres have to carry the total force accumulated over the crack length (i.e. the surface of the crack faces). As a prerequisite, the fibre must have a sufficient bond length in order to ensure that the forces can actually be transferred into and out of the fibre. Expressed as a statistical average, the existing bond length l_H amounts to only one quarter of the fibre length l.

Assuming constant bond stress levels along the fibre, the mean pull-out force $\overline{F}$ of the fibre increases proportionally to the fibre surface in the concrete. The mean bond stress τ_m can determined in tests and ranges between 1 and 10 MPa, depending on the type of fibre used [Meyer (1979)]. For a circular fibre cross-section, with a fibre radius r and a diameter d, the following equation applies (see eq. 3.1-56):

$$\overline{F} = \tau \cdot O = \tau \cdot l_H 2\pi r = \tau \cdot \frac{1}{4} \cdot l \cdot 2\pi r \tag{3.1-56}$$

The mean fibre stress $\overline{\sigma}_f$ amounts to (see eq. 3.1-57):

$$\overline{\sigma}_f = \frac{\overline{F}}{r^2\pi} = \tau \frac{l}{d} \tag{3.1-57}$$

The l/d ratio is also termed *slenderness or aspect ratio*. The fibre slenderness at which both the strength of the fibre material and the bond capacity are fully utilised is termed *critical fibre slenderness* $(l/\mathrm{d})_{\mathrm{crit}}$. This is the case if the bond stresses introduced across one half of the length ($l = 2l_H$) correspond exactly to the tensile strength of the fibre material $R_{p0.2}$ (see eq. 3.1-58 and Fig. 3.1-42):

$$\sigma_f = 2\tau \frac{l}{d} \le R_{p0.2} \rightarrow \left(\frac{l}{d}\right)_{cr} = \frac{R_{p0.2}}{2\tau} \tag{3.1-58}$$

According to eq. 3.1-58 smooth fibres with a high tensile strength result in relatively great critical fibre lengths, yet the concrete would hardly be workable anymore. For this reason, fibre l/d-values are chosen in practice that are below the critical fibre slenderness $(l/\mathrm{d})_{\mathrm{cr}}$. Although this approach prevents the full utilisation of the tensile strength of the fibres, this may also lead to positive outcomes with respect to the energy capacity of the concrete (see also Section 3.1.10.4 (5)).

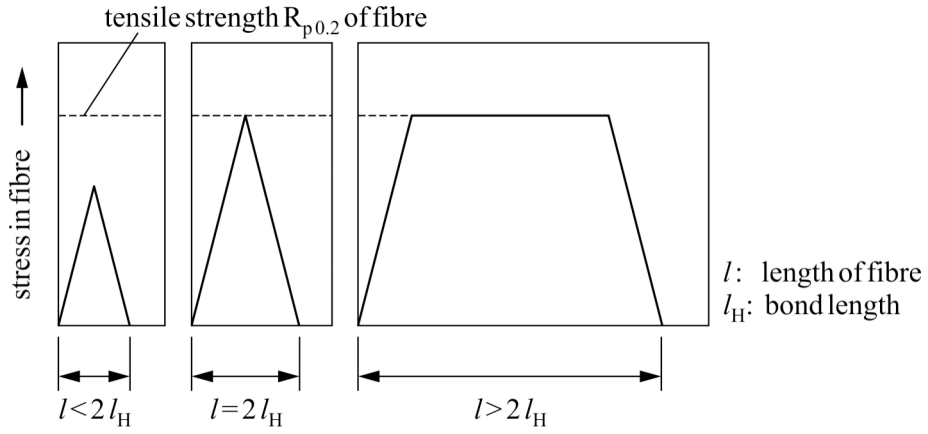

Fig. 3.1-42 Tensile loading σ_f of an embedded fibre as a function of its length l and the bond length l_H

In order to evaluate the post-cracking behaviour of concrete it is decisive to know the different failure patterns of the fibres itself and their influence on the deformation and failure of the concrete. Depending on the fibre slenderness, the failure patterns can be classified into a pull-out, i.e. bond failure, or a tensile failure of the fibre itself.

In a first step, the stress f_{fc} is calculated, which randomly distributed fibres with a certain content V_f can transfer across a crack. Hereby N gives the number of fibres crossing the crack (fibres/m²) and η accounts for the random orientation of these fibres (η = 1: fibres parallel to outer force):

$$f_{fc} = N \cdot \overline{F} = \eta \cdot V_f \frac{l}{d} \cdot \tau \tag{3.1-59}$$

where

$$N = \eta \frac{V_f}{\pi r^2} \tag{3.1-60}$$

In the following step, the critical fibre content $V_{f,cr}$ where the fibres are just able to take up the crack load can be determined. This means that the stress f_{fc} must be equivalent to the composite stress σ_c^{cr} (i.e. the stress relative to the overall section) at initial cracking (see eq. 3.1-61 a):

$$f_{fc} \equiv \sigma_c^{cr} \tag{3.1-61 a}$$

with

$$\sigma_c^{cr} = f_m \left[\frac{E_f V_f}{E_m} + (1 - V_f) \right] \tag{3.2-61 b}$$

and

$$f_{fc} = V_f \frac{l}{d} \tau \tag{3.1-61 c}$$

Accordingly, we get for a random fibre orientation:

$$V_{f,cr} = \left(\eta \cdot \frac{\tau}{f_m} \cdot \frac{l}{d} - \frac{E_f}{E_m} + 1 \right)^{-1} \approx \frac{1}{\eta} \cdot \frac{f_m}{\tau} \cdot \frac{d}{l} \tag{3.1-62}$$

E_f and E_m represent the modulus of elasticity of the fibres and the matrix, respectively. The parameter f_m denotes the tensile strength of the matrix. Fig. 3.1-43 illustrates the influence of the fibre content on the stress-strain curve under uniaxial tensile loading for the cases of a subcritical, critical and overcritical fibre content.

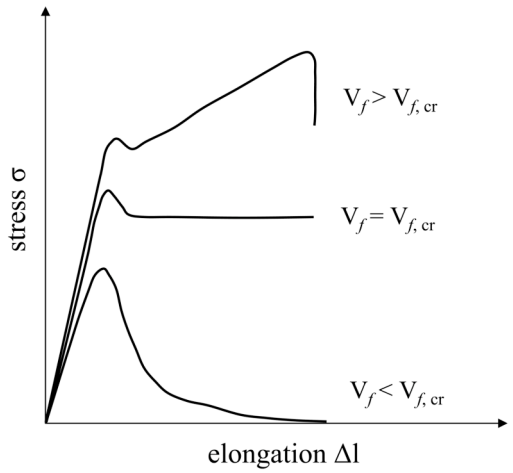

Fig. 3.1-43: Schematic stress-strain curve for fibre reinforced concrete under uniaxial tension loading at different fibre contents (subcritical $V_f < V_{f,cr}$, critical $V_f = V_{f,cr}$ and overcritical $V_f > V_{f,cr}$) using short chopped fibres [Curbach et al. (Ed.; 1998)]

The maximum transferable composite stress under tensile loading depends on the fibre content (sub- or over-critical), as does the development of the stress-strain curve from the point where the maximum stress is exceeded (Fig. 3.1-43). Beyond the first load decrease the load is primarily transferred by the fibres, whereas the load-share of the matrix suddenly reduces. If the concrete contains a sufficient amount of fibres, the load can be kept at this level ($V = V_{f,cr}$), or even increased further ($V > V_{f,cr}$).

The higher the pull-out resistance of the fibres, and the longer it is retained as the elongation increases, the slower the decrease in the transferable tensile load and the more significant the increase in concrete energy capacity. Compared to conventional concrete, the key advantage of fibre reinforced concrete is its higher energy capacity or ductility, respectively. The deformation pattern of the fibres is dependent on their elasticity, bond behaviour and end anchoring, see e.g. [Naaman (2000 b)].

Beyond the direct transfer of stresses (across the crack), the *crack arrest effect* is another significant factor describing the influence of a fibre addition to concrete. In [Bentur et al. (1985)], the cracking pattern is described in such a way that a crack that runs perpendicular to the fibre is split into a large number of smaller cracks by the fibre. Already at a distance of 10 to 40 μm from the transition zone, the crack changes its direction and runs in parallel to the fibre on both sides, and resumes its original orientation once it has passed the fibre. This can be explained considering the fact, that in the vicinity of the fibre a three-dimensional state of stress is observed, causing a re-orientation of the crack pattern, see e.g. [Cook (1986)].

(3) Types and durability of fibres

The fibres used for fibre reinforced concrete mainly consist of steel, alkali-resistant glass, polymer materials or carbon. Table 3.1-7 provides an overview on the mechanical and physical characteristics of selected fibre types in use for the production of fibre reinforced concrete. As pointed out in Section 3.1.10.4 (2) fibres with a high modulus of elasticity and high strength should be used. *Steel fibres* fulfil both these conditions while showing a high ductility and very good durability in the alkaline environment of the concrete. Due to their limited aspect ratio (i.e. thickness) the failure of steel fibres will normally be characterized by a bond failure between the fibre and the surrounding matrix. This, however, can be encountered by using corrugated or longitudinally twisted fibre types.

type of fibre	unit weight [kg/dm³]	tensile strength [MPa]	modulus of elasticity [GPa]	strain at fracture [‰]	alkali resistance [-]	max. temperature [°C]	diameter [µm]
steel	7.8	500-2600	200	5-35	high	1000	100-500
alkali-resistant glass	2.6	2000-4000	75	20-35	med./low	800	12-20
carbon	1.75-1.91	2000-4000	200-450	4-15	high	3000	15
polypropylene	0.98	450-700	7.5-12	60-90	high	150	50
polyvinyl alcohol	1.3	800-900	26-30	50-75	high	240	13-300
polyester	1.4	800-1100	10-19	8-20	med.	240	10-50
aramide	1.42	700-3600	70-130	21-40	med.	600	12

Table 3.1-7: Physical and mechanical properties of selected fibres for use in the production of fibre reinforced concrete

In the alkaline environment of the (non-carbonated) concrete steel fibres are protected against corrosion processes. In the carbonated edge zone of concrete elements, however, single fibres may corrode in the presence of moisture. Due to the slenderness of the fibres, spalling should generally not occur since experience demonstrates that the bursting pressure of the corrosion products created around the fibres is not sufficient. Hence, this corrosion does not cause any significant damage, with the exception of the visual imperfections that are created by the resulting rust stains on the surface. Exposed fibres, however, can be protected against corrosion by a polymer coating applied to the surface of the steel fibre reinforced concrete.

With regard to the modulus of elasticity *carbon fibres* seem to be an ideal alternative to steel fibres. However, the bond behaviour of these fibres is inferior to that of steel fibres. A corrugation of the carbon fibres in order to improve the bond behaviour similar to steel fibres is not possible today. In addition, carbon fibres show a pronounced brittleness and a high notch sensitivity. The mechanical wear during the mixing and placing process of the concrete therefore might lead to a derogation of the technical properties of the fibre and in turn of the concrete reinforced with these fibres.

The same holds true for *alkali-resistant glass fibres*. The reduced cost of this fibre type in comparison to carbon fibres, however, goes along with a strongly reduced modulus of elasticity and in some cases a reduced durability of the fibre in the alkaline concrete, even though termed alkali resistant.

Polymer or plastic fibres made out of *polypropylene, polyvinyl or polyester* are characterized by a sufficiently high strength, however, a very low modulus of elasticity. With regard to the working mechanism of the fibres in the concrete (see Sec. 3.1.10.4 (2)) plastic fibres are of limited use in restricting the strain and the crack-width of the concrete. The low stiffness, however, is encountered by very high ductility and energy capacity combined with a usually very good bond behaviour. Further, when the concrete is subjected to very high temperatures, e.g. during a fire loading, the plastic fibres will melt and provide room for the expanding or evaporating water in the concrete. Large scale spalling can hereby be prevented. The application of aramide fibres seems to provide an alternative to carbon fibres. According to [Johntston (2001)] this type of fibre is less sensitive to the mechanical wear during the mixing process. Similar to carbon fibres the separation of the single fibres during the mixing process poses a technical problem. The longtime durability of aramide fibres in a cement-bound matrix, however, is questionable. For uncoated multi-filament aramide strands immersed in a calcium hydroxide solution, tests showed a reduction in strength that progressed significantly in line with the increase in temperature. The deleterious effect on the fibres was less significant in specimens coated with synthetic resin [Schürhoff and Gerritse (1986)].

A more detailed overview on the types of fibres available today and their properties is given in [Müller and Reinhardt (2010)].

(4) Composition

(4.1) Concrete

The composition of the concrete mix is governed by the general rules and standards as described in Section 3.1.3. However the rod-shaped nature of the fibres requires some modifications in the standard mix design process.

The lower the *coarse aggregate ratio*, the more fibres can be incorporated without the formation of fibre agglomerations. Thicker fibres are advantageous when using coarser aggregates. To ensure a sufficient workability of fibre reinforced concrete, the maximum aggregate diameter is often restricted to 8 mm or lower. In German tunnel construction projects, in particular, using steel fibres and a maximum aggregate size of 16 mm has proven its worth [Maidl (1991)].

Especially in the case of *steel fibre reinforced concrete*, care must be taken to ensure a sufficiently high fines ratio. This is necessary for the fine mortar to enclose the fibres completely so that their effect is optimised. The paste volume should be increased by approximately 10% in comparison to conventional concrete of equal strength without fibres.

A mix with a sufficiently high fines ratio is also recommended for *glass fibre reinforced concrete*. In addition, mixes with a high aggregate ratio and a cement content that is as low as possible should be preferred to reduce shrinkage. Such mixes show quicker carbonation, and thus substantially contribute to reducing alkalinity. Thus the durability of the glass fibres is increased.

Water/cement ratios between 0.4 and 0.5 turned out to be favourable for the production of fibre reinforced concrete. A relatively high cement content is required to adhere to these values since the amount of water needed to ensure a defined workability of the concrete increases in line with the fibre content. This even more applies to mixes with a low ratio of coarse aggregates.

In practice 25 to 35 mass% of the cement may be replaced with fly ash to reduce the cement content whilst retaining the intended strength. The addition of silica fume instead of up to 10 mass% of the cement may also have a favourable effect. A higher powder ratio promotes the workability of the concrete. However, the standard values to limit the powder ratio must be adhered to. The addition of an air-entraining agent may also result in improved workability whilst increasing the frost resistance of the concrete. Today, even self-compacting fibre reinforced concrete may be produced [Nakamura et al. (2004); Gründewald (2004)].

(4.2) Fibres

The *fibre content* is usually stated in per cent by volume of the concrete. The amount of fibres which can be incorporated in the mix depends on the composition and workability of the fresh concrete, the fibre properties (type, slenderness, modulus of elasticity, density) and the mixing technology used. As mentioned above, the amount of steel fibres added to concrete in pratice ranges from 0.5 to 3.0 vol.-%. In some cases glass fibres may be added up to a content of 6 vol.-%. Fibres made of polymers are mostly applied up to a volume content of 0.1 to 1.0 vol.-% (fire protection).

The addition of fibres increases the amount of water required for the concrete mix. The *fibre aspect ratio l/d* has a critical influence on the ability of the fibres to be mixed into the concrete, and on concrete workability. In general, workability decreases as the aspect ratio increases. However, a reasonably good workability of the fresh concrete may be expected if the subsequent condition for steel fibres is fulfilled (see eq. 3.1-63).

$$V_f \cdot l/d < 100 \ldots 220 \qquad (3.1\text{-}63)$$

where

V_f is the fibre content in vol.-%; typically the diameter d < 1 mm and l/d = 30 … 80.

Normally the fibres are added to the fresh concrete in the mixer resulting in a random distribution and orientation of the fibres in the hardened concrete. Various methods have been proposed in the literature to increase the fibre content or to influence the fibre orientation, see e.g. [Lankard (1985)]. Represenatives for these types of concretes are SIFCON (i.e. Slurry Infiltrated Fibre CONcrete) or DUCON® (= DUctile CONcrete).

(5) Properties

(5.1) Behaviour under compressive stress

In general, the compressive strength of fibre reinforced concrete shows a minor increase in line with the fibre ratio (Fig. 3.1-44, left) because micro-cracking is obstructed. What is much more important, however, is the increased strain at rupture and, in particular, the increased energy capacity that results from the fact that the descending branch of the stress-strain curve

becomes increasingly flat in line with the increase in the fibre ratio. However, an increase in fibre aspect ratio may also result in a higher energy capacity (Fig. 3.1-44, right).

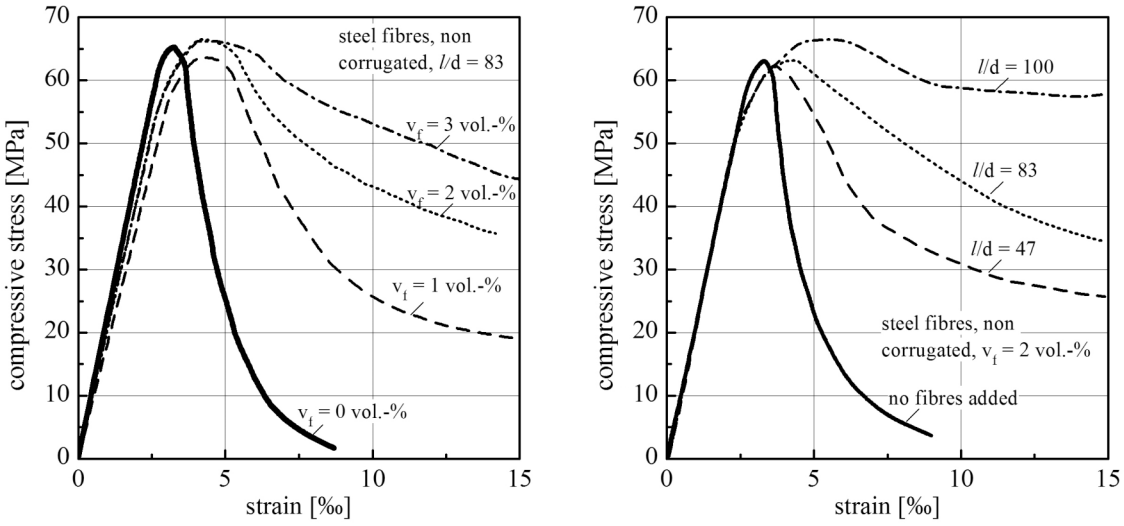

Fig. 3.1-44: Stress-strain diagram for steel fibre reinforced concrete with different fibre contents (left) and fibre aspect ratios (right) under compressive loading [ACI Committee 544 (1988)]

(5.2) Behaviour in tension and bending

The extent to which the uniaxial tensile strength and tensile bending strength can be increased by a fibre reinforcement mainly depends on whether the fibre content exceeds the critical value as referred to in Section 3.1.10.4 (2), see also Fig. 3.1-45, left.

When applying very high dosages of fibres with varying *l*/d ratios – i.e. fibre mixes – a pronounced increase in the tensile strength, the ductility and the energy capacity can be observed under tensile loading. Fig. 3.1-45 (right) shows the load/deformation behaviour of such a high performance fibre reinforced cement composite in comparison to conventional fibre reinforced concretes. As can be seen, the stress/strain and stress/crack width curve, respectively, can be divided into three sections I to III. Segment I is characterized by the load/deformation behaviour of the pure cement matrix. In segment II a pronounced contribution of fibres with corrugated or twisted pattern and end-anchors can be observed, until they are pulled out of the matrix, see segment III.

In general, the principles applied to uniaxial tensile loading are also valid for tensile bending stresses. However, provided certain geometrical conditions are met (crack widths/beam height), the non-linear relationship between stress and crack width may lead to an increase in strength also at lower fibre ratios due to the more favourable stress distribution across the section. Note that even in the case when fibres produce no increase in tensile strength but only an increase in energy capacity or ductility, respectively, the bending tensile strength will increase accordingly. Theoretically, if by the addition of fibres the material characteristics were to change from ideal elastic to ideal plastic behaviour, while the strength remains constant, the bearing capacity for pure bending is increased up to 50%. This is, besides minimizing shrinkage cracking, also a reason why fibre reinforced concrete is often applied for industrial floors or foundations.

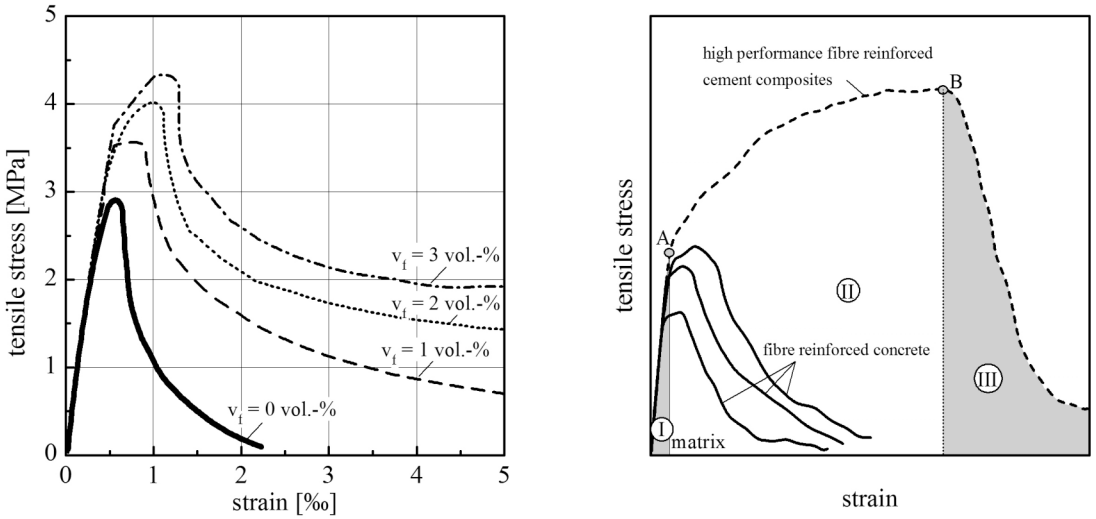

Fig. 3.1-45 Stress-strain diagram for steel fibre reinforced concrete with different fibre contents under tensile loading (left; [Soroushian and Bayasi (1987)]) and schematic drawing of the tensile stress-strain behaviour of ordinary fibre reinforced concrete and high performance fibre reinforced cement composites (right) [Naaman (2000 b)]

In several investigations, for instance, a linear correlation between the tensile bending strength and fibre content associated with increases in tensile bending strength by 10 to 20% has been established for steel fibres. However, what is always observed at a sufficiently high fibre content are higher strains at rupture or deflections under maximum loading, and in particular a significantly higher fracture energy that may increase to several times the fracture energy of non-reinforced specimens. For this reason, a significant increase in the resistance to dynamic loading and impact stress is generally also observed.

(5.3) Behaviour under shear and torsion

As is the case for concrete without fibre reinforcement, the *shear resistance* of fibre reinforced concrete is attributable to the tensile strength of the material. The explanations given in Section 3.1.10.4 (2) thus also apply to shear loading in qualitative terms.

In the shear tests described in [Barr (1987)], the addition of up to 1 vol.-% of steel or polypropylene fibres had only a very minor influence on shear resistance. In contrast, the shear resistance of the concrete could be almost doubled by adding high glass fibre dosages (approximately 4 per cent by volume). In all cases, the addition of fibres led to an increase in energy capacity, which rose proportionally to the fibre content. This phenomenon occurs because the fibres bridge the shear cracks, slow down the opening of the cracks and link the crack edges to each other. In this respect, the fibres act similarly to a shear reinforcement, but are less effective at an identical reinforcement ratio [Swamy et al. (1987)].

Compared to non-reinforced members, fibre reinforced members under torsional stress resist significantly higher levels of torsion until failure. Despite a non-existent or only relatively minor increase in the torsional moment at failure, this leads to an energy capacity to failure that is approximately 1-2 decimal powers higher than for conventional concrete [Maidl (1991)].

(5.4) Creep and shrinkage

Steel fibres only have a minor influence on the *creep deformation* of concrete since the stiffening effect of the fibres and the influence of the compaction pores frequently contained in the concrete largely balance out each other.

As the volume share of fibres in the overall volume is usually low (i.e. approximately 1 vol.-% or less), the effect of the fibres on the *shrinkage coefficients* is hardly noticeable.

In the case where *shrinkage is restrained*, the use of fibres does not prevent the formation of cracks that occur as a result of imposed and internal stresses. However, instead of few single cracks a large number of microcracks are produced and thus the crack widths can be reduced to a tolerable degree. This requires a sufficiently high stiffness of the fibres compared to the stiffness of the concrete matrix at the time of cracking, as well as a sufficiently high bond strength.

(5.5) Frost and freeze-thaw resistance

The main parameters that influence frost and freeze-thaw resistance are primarily the system of air voids and the water/cement ratio. Hence, fibre reinforced concrete shows a behaviour similar to conventional concrete when exposed to repeated freeze-thaw cycles.

(5.6) Behaviour at high temperatures

Compared to conventional concrete, steel-fibre reinforced concrete has a slightly higher resistance to high temperatures. This is achieved by the higher degree of cohesion created by the steel fibres.

Polymer or plastic fibres (especially polypropylen fibres) are added in a targeted way to increase the fire rating of high strength concrete, making use of the fact that the thermal decomposition of the fibres results in channels that relieve vapour pressure. Toxic gases that may be present as a result of high temperatures usually escape from the concrete only very slowly, which is why no critical exposure limits are reached.

(5.7) Impact and abrasion resistance

Any improvement of wear resistance by fibre addition will depend on the type of stress the concrete is exposed to. Fibre reinforced concrete shows a very favourable behaviour under impact stress. In the case of abrasive or rolling stresses, the hardness of the concrete surface and the wear resistance of the aggregates determine the abrasion rate, in particular if the fibre content is low. As a minimum, steel fibres should be added at a ratio of 0.5 per cent by volume to improve wear resistance. At a steel fibre ratio of 1.0 per cent by volume, a significant increase in impact wear resistance was observed.

3.1.10.5 Ultra high performance concrete

(1) Introduction

Ultra high performance concrete is usually defined as a concrete having a characteristic compressive strength above the strength grade C100/115. One may distinguish between two

types: the reactive powder concrete (RPC) characterised by a maximum aggregate size of approximately 0.5 mm and the ultra high performance concrete (UHPC) with coarse aggregates normally up to an aggregate size of 8 mm. The water/cement ratio of such concretes are usually below 0.25, and highly reactive additions such as silica fume have to be added to the mix. The workability of the concrete can only be ensured by applying high amounts of superplasticisers. Thus a compressive strength of approximately 200 MPa may be achieved. Depending on the type of curing, e.g. additional heat treatment without or with mechanical pressure, this concrete may reach a compressive strength up to 800 MPa, provided a proper selection of the aggregates is carried out.

No standard has been adopted yet for this type of concrete, which significantly exceeds the strength range specified in EN 206-1:2001. Nevertheless UHPC might become interesting for a broader application in practice. The reason is that the very high strength allows a significant reduction of the cross-section of members while retaining a high load bearing capacity. This is accompanied by a significant mass reduction allowing in principle a much higher span of beams as it may be realized when ordinary structural concrete is used. In addition, the saving of material has a positive effect in view of the sustainability, and makes UHPC superior to ordinary structural concrete despite of the significantly higher cement content of UHPC, see e.g. [Müller and Scheydt (2009)].

Considering the practical application of UHPC major problems result from the fact that this concrete shows a significant autogenous shrinkage during the early hardening process. As a consequence, construction in practice is realised mostly by applying precast elements. However, research is under way to overcome this deficiency e.g. by the addition of super absorbent polymers. An overview of various research activities on UHPC is given in [Fehling et al. (2008)].

(2) Mix design

UHPC is composed of aggregates, cement, water, additives and admixtures. Aggregates that may be used include the materials referred to as “aggregates for concrete” in EN 12 620:2008. The particle strength should be sufficiently high and the grain size distribution should guarantee a high packing density (see Section 3.1.3).

Regarding the cement type used in UHPC, Portland cements with a low C_3A content are recommendable, as these cements have a low water demand. This is also advantageous in view of the risk of a secondary ettringite formation in case of curing at high temperatures. The strength classes of the cements applied is 42.5 or 52.5. Blast furnace slag cement of strength class 52.5 has been successfully used. Cement contents used in UHPC normally are very high and range from 600 to 1000 kg/m^3. The fineness of the cement should be between 3000 and 4500 cm^2/g.

In order to produce UHPC, it is important to achieve the maximum possible packing density of all granular constituents. The voids between the cement particles (diameter from 1 to 20 μm) are filled by silica fume (SF) particles (0.1 to 0.3 μm). For this purpose, silica fume quantities are required that amount to 10 to 30 mass% of the cement.

The second major effect expected beyond the increase in packing density by addition of silica fume is a reduction in the amount of calcium hydroxide present in the interfacial zone between aggregate and matrix. The almost pure SiO_2 in silica fume consumes $Ca(OH)_2$, which is created during cement clinker hydration, and forms calcium silicate hydrates (CSH). The $Ca(OH)_2$ of lower strength is replaced by CSH of much higher strength and the porosity

decreases in the bulk and in particular in the interfacial zone. All these effects result in a significant increase in strength.

Quartz powder with particle sizes similar to cement is predominantly used in heat-treated UHPC. The quartz particles are inert at room temperature and together with $Ca(OH)_2$ react at high temperatures to form CSH phases.

Fresh UHPC is not workable without the addition of large quantities of high performance plasticisers (up to 5 mass% of the cement). Only the third generation of plasticisers (polycarboxylate ethers, PCE) allow to save a sufficient amount of water to make UHPC workable. Their mechanism of action relies on the adsorption of the PCE molecules to the surface of the clinker phases and hydration products, which results in a steric repulsion. This leads to a dispersion of the cement particles, which, in turn, creates the plasticising effect.

Like dense natural stone, UHPC shows an elastic and brittle behaviour. Fibres are added to the concrete to compensate this disadvantage in construction practice. It has been proven that approximately 2.5 vol.-% of steel fibres at an aspect ratio *l*/d between 40 and 60 leads to best results, both in view of fresh and hardened concrete properties. The fibre length should be adjusted to the maximum aggregate diameter. For powder type UHPC (i.e. with limited maximum grain size), the fibre length should at least be equal to ten times the maximum aggregate diameter.

The water content of the mix is the crucial parameter to ensure optimal properties. Water/binder ratios from 0.15 to 0.25 seem to ensure a reasonable balance between the flow properties of the fresh concrete and the strength of the hardened concrete.

(3) Properties of fresh concrete

UHPC is characterized by a high powder content in excess of 1000 kg/m³ in combination with high dosages of superplasticizers. It's properties at the fresh state are thus comparable to self-compacting concrete (SCC) of the powder type. For this reason, the workability of this type of concrete should rather be measured with the test set-up used for SCC, i.e. slump flow and V-funnel flow test. The slump flow of UHPC normally ranges from 650 to 800 mm and the V-funnel flow time from 15 to 40 seconds. Superplasticizers strongly reduce the flow resistance of the concrete and lead to a normalization of the dynamic viscosity over the whole shear rate range (Fig. 3.1-46).

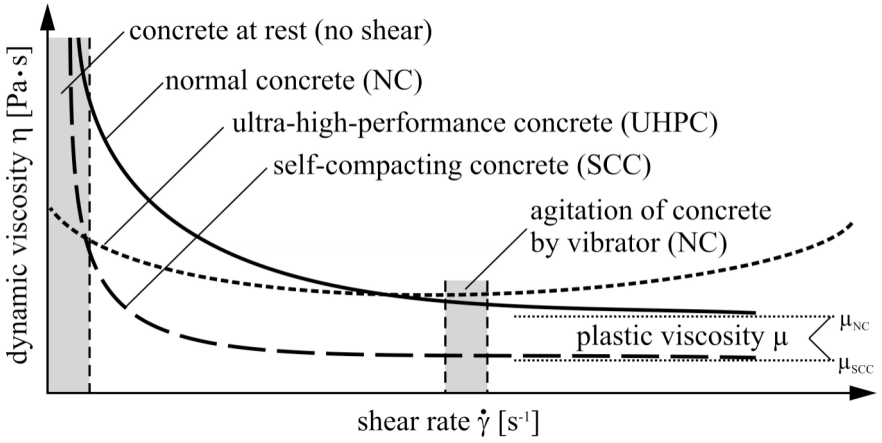

Fig. 3.1-46: Dynamic viscosity of fresh UHPC in comparison to conventional concrete and self-compacting concrete as a function of the externally applied shear rate

As can be seen from Fig. 3.1-46 the dynamic viscosity of UHPC remains nearly constant – even though at a very high level – whether the concrete is at rest or whether it is agitated for example by a vibrator. For UHPC, the de-airing process therefore cannot be enhanced significantly by vibrating the concrete. At rest, however, for concretes with a very low dynamic viscosity, sedimentation would be observed, which must be prevented in UHPC by optimizing the grain size distribution of the aggregates, thus ensuring an interlocking of the particles. At high shear rates UHPC normally shows a dilatant material behaviour, i.e. an increase of the dynamic viscosity.

The air content in UHPC ranges from 1 to 5 vol.-%, with the lower ratios observed in low viscosity mixes. In addition, there is a trend toward an air ratio increase that occurs in line with the increasing length of the steel fibres.

Plastic (capillary) shrinkage and autogenous deformation are promoted by a high cement paste content and a low water/cement ratio. For this reason, the immediate curing of UHPC is basically very important.

(4) Properties of hardened concrete

(4.1) Strength characteristics

The compressive and the tensile strength which may be achieved by UHPC depend strongly on the concrete composition, in particular with regard to the type and amount of binders and the fine aggregates (micro fillers) as well as the type and duration of curing. If an ordinary curing at room temperature of 20°C is applied a maximum *compressive strength* of UHPC of approximately 200 MPa may be achieved. If the curing temperature is increased up to 100°C the strength will reach approximately 250 MPa. A further increase of the curing temperature up to 250°C is accompanied by a strength gain leading to a maximum strength of approximately 400 MPa. A compressive strength value of 800 MPa may be achieved if additional mechanical pressure is applied [Richard (1996)].

The addition of fibres (mostly steel fibres) improves the compressive strength of UHPC only minor but may significantly affect the strain capacity of the concrete similar to ordinary fibre reinforced concrete. Summarizing the investigations on the effect of the volume content of fibres being varied up to 6 vol.-%, there seems to exist an optimum fibre content of approximately 2.5 vol.-%.

The *uniaxial tensile strength* and the *flexural tensile strength* of UHPC reach values ranging approximately from 10 to 60 MPa. When special binders and techniques are applied a tensile strength of 150 MPa may be attained [Richard and Cheyrezy (1995)]. It should be noted that different to the compression characteristics the tensile strength of UHPC may be doubled when fibres (1.5 to 3.0 vol.-%) are added to the mix. This may be attributed to a large extend to the reduction of the brittleness of non-reinforced UHPC where minor flaw and cracks may tremendously reduce the tensile strength.

Concerning the *fracture energy* and the *characteristic length* of UHPC the gained knowledge is still very insufficient. It appears that these values for UHPC made without fibres are somewhat lower than for high strength concrete. Of course the addition of fibres may increase the fracture energy up to a factor of approximately 100.

(4.2) Deformation behaviour

The *stress-strain behaviour* of non-reinforced UHPC shows a linearly elastic pattern almost up to the ultimate load level. Most of the commonly used testing equipment and specimen sizes do not allow the determination of a descending branch in the stress-strain diagram. The elastic strain energy released at fracture is too large to be consistently compensated by the fracture energy. An explosive failure exerting a strong impact on the testing equipment is obtained. In a fibre reinforced UHPC, the fibres prevent macro-cracking because they hold the crack edges together already at the micro-cracking stage and thus hinder the cracking progress. As a result a significant additional strain capacity is obtained while the increase in strength is minor. Similar to ordinary fibre reinforced concrete, the fibre content determines whether this strain results in strain softening or strain consolidation (see Section 3.1.10.4 (2)). At fibre contents in excess of the critical ratio, the strain results in consolidation, whereas strain softening occurs below this threshold. No fibre rupture occurs if the critical fibre slenderness has not been reached. The fibres are pulled out of the matrix. Theoretically, this strain softening process continues until the last fibre has been pulled out across the entire bond length in a crack.

The *modulus of elasticity* of UHPC reaches approximately 50 to 60 GPa when the compressive strength is 200 MPa. If reactive powder concrete (RPC) is produced, having a compressive strength up to 800 MPa, the modulus of elasticity may approach 75 GPa. As it holds true for conventional structural concrete the modulus of elasticity of UHPC also strongly depends on the paste content and the type of aggregates.

The *autogenous shrinkage* of UHPC is very pronounced and may reach values beyond 0.0012 (1.2 μm/mm). Often in the literature much lower values are reported. However, this is mostly due to the applied measurement technique in connection with the age of concrete at the beginning of the measurement. When such measurements start e.g. at the concrete age of one day, most of the autogenous shrinkage, which develops mainly between an age of 8 to 24 hours, has already taken place and is consequently not recorded.

Drying shrinkage of UHPC is much lower even when compared to this strain component for high strength concrete. This may be traced back to the extreme low porosity of UHPC. In studies on autogenous and drying shrinkage of different UHPC starting at the concrete age of one day, an autogenous shrinkage of 0.3 μm/mm and a drying shrinkage of 0.1 μm/mm (at a maximum) have been observed [Müller et al. (2010)]. No drying shrinkage was found when the UHPC was produced without coarse aggregates.

While autogenous shrinkage and drying shrinkage of UHPC are observed as may be expected and extrapolated from the deformation characteristics of high strength concrete this is not the case for *creep strains*. If UHPC (e.g. a C170) is loaded at an early age, e.g. $t_0 = 1$ days or $t_0 = 3$ days, final creep coefficients between approximately $\varphi = 3$ and $\varphi = 2$, respectively, are observed. Even for an age at loadings of $t_0 = 28$ days the final creep coefficient reaches approximately $\varphi = 1.5$, see e.g. [Müller et al. (2010)]. This means that the pronounced decrease of the creep capacity of concrete with the increase in strength of the hardened cement paste holds no longer true for UHPC. However, the comparatively high creep of UHPC results to some extent from the high volume content of the hardened paste matrix in UHPC, which is considerably higher than in high strength concrete.

(4.3) Physical characteristics

The physical characteristics of concrete are mainly determined by its capillary porosity. Whereas conventional concrete (C35) and high strength concrete (C100) show marked peaks in the pore size distribution between 0.01 and 0.1 μm, these peaks are nearly eliminated in the case of UHPC C200, and disappear completely in RPC C500. Absolute porosities then become so low that transport processes almost come to a halt.

As a consequence *carbonation depths* measured on UHPC are almost negligible. In a test on UHPC with a compressive strength of 170 MPa, the penetration depth after four years of outdoor exposure amounted to 0.2 mm [Roux (1997)]. This value is equivalent to a CO_2 diffusion coefficient below $0.07 \cdot 10^{-9}$ m^2/s. Water vapour diffusion was investigated in several types of concrete applying the dry-cup method specified in EN ISO 12572:2001. A value of $5 \cdot 10^{-9}$ m^2/s was documented for a C190 UHPC [Jooss et al. (2002)]. Chloride penetration was investigated in migration tests where a diffusion coefficient of $0.02 \cdot 10^{12}$ m^2/s was measured [Roux (1997)], which is about 100 times lower than the value for a C30 concrete.

The nitrogen *permeability* of UHPC decreases to a level that is ten times lower than in a high performance C100 concrete and 100 times lower than in a C30 concrete [Schmidt and Fehling (2005)]. The water permeability of a C190 UHPC was tested at three different temperatures and was found to be in a range between 4 to $5 \cdot 10^{-15}$ m^2/s, which corresponds to the permeability of dense natural stone. The same behaviour was found for capillary water absorption [Schmidt and Fehling (2005)].

(4.4) Durability

Structural concrete usually containing capillary pores is often destroyed by mechanisms triggered by *frost or freeze-thaw impact*. If no capillary pores are present, or if only a minimal amount of such pores exists, only a small amount of water can be absorbed, and no saturation will occur [Fagerlund (2002)]. Correspondingly, the concrete shows a very good behaviour when exposed to frost or freeze-thaw cycles, as demonstrated in tests. After 56 CDF cycles, the frost removal rate ranged from 50 to 200 g/m^2 whereas the tolerable rate was 1500 g/m^2 [Schmidt and Fehling (2005)]. Similarly favourable results were already reported in [Roux (1997)] and [Torrenti (1996)].

Tests in sodium sulphate solution demonstrated a very high *chemical resistance* [Roux (1997)]. No conclusive findings have been established yet with regard to the ASR issue. However, the tightness of the system appears to be one of the crucial factors that determine resistance.

Concerning the risk of the *formation of secondary ettringite,* investigations in [Schmidt and Fehling (2005)] showed that independent of the C_3A content of the cement, no adverse change of the microstructure of UHPC could be observed.

Even though UHPC is exposed to a strong *acid attack* (pH = 1 and 3) it shows a significant better performance than ordinary structural concrete [Franke and Kieckebusch (2004); Herold et al. (2006)]. Of course also UHPC will be destroyed by a long term attack of strong acids as the CSH component of the hydrated cement paste is principally dissolved by acids as a consequence of its chemical nature. However, due to the extreme low porosity of UHPC compared to ordinary structural concrete and even high strength concrete, the rate of damage is much slower leading to a significant higher durability or life time, respectively.

The *abrasion resistance* of a C200 UHPC was measured by underwater storage of the concrete. At regular intervals, the concrete was sand-blasted at an angle of 45° and a pressure of 250 kPa. This test simulates the transport of sediments in water above a concrete base. A wear resistance was found that is about four times higher than that of a C30 concrete, and roughly corresponds to the wear resistance of added hard aggregate [Roux et al. (1996)].

Initially, UHPC had not been fire-resistant since the tested material bursted and the fibres in the fibre reinforced material oxidised under heat exposure. Fire resistant UHPC could be successfully produced by adding 0.3 to 0.6 vol.-% of polypropylene fibres [Bornemann et al. (2002); Heinz et al. (2004)]. It is also helpful to replace quartz with basalt aggregate, which prevents the occurrence of the deleterious quartz conversion.

References to Section 3.1

American Concrete Institute ACI, Committee 544 (1988), *Design considerations for steel fiber reinforced concrete.* Report No. ACI 544.4R-88, ACI Structural Journal.

American Concrete Institute ACI (2009), *Manual of concrete practice.* Detroit, USA.

American Concrete Institute ACI, Committee 209 (2008), *Guide for modeling and calculating shrinkage and creep in hardened concrete*.

American Concrete Institute ACI, Committee 215 (2009, in prep.), *Considerations for design of concrete structures subjected to fatigue loading*.

Andreasen, A. H. M. (1930), *Über die Beziehung zwischen Kornabstufung und Zwischenraum in Produkten aus losen Körnern (mit einigen Experimenten)*. Kolloid-Zeitung, Vol. 50, pp. 217-228.

Awad, M. E.; Hilsdorf, H. K. (1974), *Strength and deformation characteristics of plain concrete subjected to high repeated and sustained stresses*. Abeles Symposium on Fatigue of Concrete, American Concrete Institute, SP-41, pp. 1-13.

Bache, H. H. (1981), *Densified cement/ultra-fine particle-based materials*. 2. International conference on superplasticizers in concrete, Ottawa, Canada.

Bakker, R. F. M. (1988), *Initiation period*. Corrosion of steel in concrete, Schießl, P. (Ed.), Report of the Technical Committee 60-CSC RILEM, Chapmann and Hall, London, Great Britain, pp. 22-55.

Barr, B. (1987), *The fracture characteristics of FRC materials in shear*. Fiber reinforced concrete – Properties and applications, ACI SP-105, American Concrete Institute, Detroit, USA, pp. 27-53.

Bažant, Z. P.; Oh, B. H. (1983), *Crack band theory of concrete*. Materials and Structures, Vol. 16, No. 3, pp. 155-177.

Bažant, Z. P.; Wang, T.-S. (1985), *Practical prediction of cyclic humidity effects on creep and shrinkage of concrete*. Materials and Structures, Vol. 18, No. 4, pp. 247-252.

Bažant, Z. P. (1988), *Mathematical modelling of creep and shrinkage of concrete*. John Wiley & Sons Ltd., Chichester, Great Britain.

Bentur, A.; Mindess, S. (1985), *Cracking process in steel fiber reinforced cement paste*. Cement and Concrete Research, Vol. 15, pp. 331-342.

Bentz, D. P.; Garboczi, E. J. (1991), *Percolation of phases in a three-dimensional cement paste microstructural model*. Cement and Concrete Research, Vol. 21, pp. 325-344.

Bier, T. (1987), *Influence of the type of cement and curing on carbonation progress and pore structure of hydrated cements*. MRS Symposium Microstructural development during hydration of cement, Proceedings, Vol. 85, pp. 123-134.

Bornemann, R.; Schmidt, M.; Vellmer, C. (2002), *Brandverhalten ultra-hochfester Betone*. Beton, Vol. 52, No. 9, pp. 418-422.

Brameshuber, W.; Uebachs, S.; Eck, T. (2001), *Betontechnologische Grundlagen des Selbstverdichtenden Betons*. Selbstverdichtender Beton, Bauwerk Verlag, Berlin, Germany, pp. 11-23.

Brameshuber, W. (2004), *Selbstverdichtender Beton*. Verlag Bau + Technik, Düsseldorf, Germany.

Bunte, D. (1993), *Zum karbonatisierungsbedingten Verlust der Dauerhaftigkeit von Außenbauteilen aus Stahlbeton*. Schriftenreihe des Deutschen Ausschusses für Stahlbeton, No. 436, Beuth Verlag, Berlin, Germany.

Carino, N. J.; Tank, R. C. (1990), *Maturity functions for concrete made with various cements and admixtures*. Testing during construction, Proceedings of an international RILEM workshop, Chapmann and Hall, pp. 192-206.

Chen, W. F.; Saleb, A. F. (1994), *Constitutive equations for engineering materials*. Vol. 1, Elasticity and Modelling, Revised Edition, Elsevier, Amsterdam, The Netherlands.

CEB Bulletin 156 (1983), *Concrete under multiaxial states of stress – Constitutive Equations for Practical Design*. Comité Euro-International du Béton, Lausanne, Switzerland.

CEB Bulletin 189 (1988), *Fatigue of concrete structures*. Comité Euro-International du Béton, Lausanne, Switzerland.

CEB Bulletin 182 (1989), *Durable concrete structures – CEB Design Guide*. Second Edition, Comité Euro-International du Béton, Lausanne, Switzerland.

CEB Bulletin 199 (1990), *Evaluation of the time dependent behaviour of concrete*. Comité Euro-International du Béton, Lausanne, Switzerland.

CEB Bulletin 213/214 (1993), *CEB-FIP Model Code 1990*, published by Thomas Telford Ltd., UK. ("MC90")

CEB Bulletin 215 (1993), *Structural effects of time dependent behaviour of Concrete*. Comité Euro-International du Béton, Lausanne, Switzerland.

CEB Bulletin 217 (1993), *Selected justification notes*. Comité Euro-International du Béton, Lausanne, Switzerland.

CEB-FIP *Model Code for concrete structures* (1978), Comité Euro-International du Béton, Lausanne, Switzerland.

Cook, J.; Gordon, J. E. (1986), *A mechanism of the control of crack propagation in all-brittle systems*. Proceeding of the Royal Society, Vol. A 228, pp. 508-520.

Curbach, M.; Reinhardt, H.-W. et al. (Eds.; 1998), *Sachstandbericht zum Einsatz von Textilien im Massivbau*. Deutscher Ausschuss für Stahlbeton (DAfStb), No. 488, Beuth Verlag, Berlin, Germany.

Dettling, H. (1962), *Die Wärmedehnung des Zementsteins, der Gesteine und der Betone*. Schriftenreihe des Otto-Graf-Instituts der Technischen Hochschule Stuttgart, No. 3, Stuttgart, Germany.

Deutscher Beton- und Bautechnik-Verein E. V. (Ed.) (2004), *Richtlinie Sichtbeton*. Berlin, Germany.

Dhir, R. K.; Hewlett, P. C.; Chan, Y. N. (1991), *Near-surface characteristics of concrete – Abrasion resistance*. Materials and Structures, Vol. 24, pp. 122-128.

DIN 1045-2:2008-08, *Concrete, reinforced and prestressed concrete structures - Part 2: Concrete - Specification, properties, production and conformity - Application rules for DIN EN 206-1*. Beuth Verlag, Berlin, Germany.

DIN V 4108-4:2007-06, *Thermal insulation and energy economy in buildings - Part 4: Hygrothermal design values*. Beuth Verlag, Berlin, Germany.

DIN V 18004:2004-04, *Use of building products in construction works - Test methods for aggregates according to DIN V 20000-103 and DIN V 20000-104*. Beuth Verlag, Berlin, Germany.

EN 197-1:2009-09, *Cement - Part 1: Composition, specifications and conformity criteria for common cements*. Beuth Verlag, Berlin, Germany.

EN 206-1:2001-07, *Concrete - Part 1: Specification, performance, production and conformity*. Beuth Verlag, Berlin, Germany.

EN 206-9:2008-01, *Concrete - Part 9: Additional rules for self-compacting Concrete (SCC)*. Beuth Verlag, Berlin, Germany.

EN 1015-3:2007-05, *Methods of test for mortar for masonry - Part 3: Determination of consistence of fresh mortar (by flow table)*. Beuth Verlag, Berlin, Germany.

EN 1097-5:2008-06, *Tests for mechanical and physical properties of aggregates - Part 5: Determination of the water content by drying in a ventilated oven.* Beuth Verlag, Berlin, Germany.

EN 1097-6:2005-12, *Tests for mechanical and physical properties of aggregates - Part 6: Determination of particle density and water absorption*. Beuth Verlag, Berlin, Germany.

EN 12350-8:2008-01, *Testing fresh concrete - Part 8: Self-compacting concrete - Slump-flow test*. Beuth Verlag, Berlin, Germany.

EN 12350-9:2008-01, *Testing fresh concrete - Part 9: Self-compacting concrete - V-funnel test*. Beuth Verlag, Berlin, Germany.

EN 12350-11:2008-01, *Testing fresh concrete - Part 11: Self-compacting concrete - Sieve segregation test*. Beuth Verlag, Berlin, Germany.

EN 12350-12:2008-01, *Testing fresh concrete - Part 12: Self-compacting concrete - J-ring test*. Beuth Verlag, Berlin, Germany.

EN 12620:2008-07, *Aggregates for concrete.* Beuth Verlag, Berlin, Germany.

EN 13055-1:2002-08, *Lightweight aggregates - Part 1: Lightweight aggregates for concrete, mortar and grout.* Beuth Verlag, Berlin, Germany.

EN ISO 12572:2001-09, *Hygrothermal performance of building materials and products – Determination of water vapour transmission properties (ISO 12572:2001)*. Beuth Verlag, Berlin, Germany.

Fagerlund, G. (1997), *Internal frost attack – state of the art*. Frost Resistance of Concrete, Setzer, M. J.; Auberg, R. (Eds.), Proceedings of the International Workshop, E&FN Spon, London, Great Britain, pp. 321-338.

Fagerlund, G. (2002), *Freeze-thaw resistance of high performance concrete.* 6th Int. Symp. of High Strength/High Performance Concrete, König, G.; Dehn, E.; Faust, T. (Eds.), Leipzig, Germany, pp. 45-62.

Faust, T. (2003), *Leichtbeton im Konstruktiven Ingenieurbau*. Ernst & Sohn, Berlin, Germany.

Fehling, E.; Schmidt, M.; Stürwald, S. (Eds.; 2008), *Ultra high performance concrete (UHPC)*. Proceedings of the 2nd International Symposium on Ultra High Performance Concrete, 5-7 March 2008, University of Kassel, Germany.

Feldman, R. F.; Sereda, P. J. (1968), *A model for hydrated cement paste as deduced from sorption–length change and mechanical properties*. Materials and Structures, Vol. 1, No. 6, pp. 509-520.

fib Model Code 2010 (to be published in 2010). International Federation for Structural Concrete (*fib*), Lausanne, Switzerland. ("MC2010")

fib Bulletin 34 (2006), *Model code for service life design*. International Federation for Structural Concrete (*fib*), Lausanne, Switzerland.

Franke, L.; Kiekbusch, J. (2004), *Behaviour of high performance concrete under acid attack.* Proceedings of the International Conference on Durability of High performance Concrete and Final Workshop of CONLIFE, September 2004, University of Essen, Germany, pp. 311-320.

Garboczi, E. J. (1992), *Microstructure and transport properties of concrete*. Performance Criteria for Concrete Durability, RILEM Report No. 12, E&FN Spon, London, Great Britain, pp. 198-212.

Geymayer, H. G. (1972), *Effect of temperature on creep: a literature review*. Concrete for Nuclear Reactors, American Concrete Institute, SP-34, Vol. 1, pp. 547-564.

Grübl, P.; Weigler, H.; Karl, S. (2001), *Beton, Arten – Herstellung – Eigenschaften*. Ernst & Sohn, Berlin, Germany.

Grünewald, S. (2004), *Performance-based design of self-compacting fibre reinforced concrete*. PhD thesis, TU Delft, Delft, The Netherlands.

Günter, M. (2005), *Sichtbeton - Möglichkeiten der Mängelbeseitigung und Instandsetzung*. Sichtbeton - Planen, Herstellen, Beurteilen, Müller, H. S.; Nolting, U.; Haist, M. (Eds.), 2. Symposium Baustoffe und Bauwerkserhaltung, Universitätsverlag Karlsruhe, Karlsruhe, Germany, pp. 71-80.

Guse, U.; Hilsdorf, H. K. (1998), *Dauerhaftigkeit hochfester Betone*. Schriftenreihe des Deutschen Ausschusses für Stahlbeton, No. 487, Beuth Verlag, Berlin, Germany.

Haist, M.; Müller, H. S. (2005), *Optimization of the pumpability of self-compacting light weight concrete*. Proceedings of the Second North American Conference on the Design and Use of Self-Consolidating Concrete (SCC) and the Fourth International RILEM Symposium on Self-Compacting Concrete, Sha, S. (Ed.), Chicago, USA, pp. 195-202

Haist, M.; Müller, H. S. (2006), *Selbstverdichtender Beton*. Müller, H. S., Nolting, U., Haist, M. (Eds.), 3. Symposium Baustoffe und Bauwerkserhaltung, Universitätsverlag Karlsruhe, Karlsruhe, Germany, pp. 9-22.

Haist, M. (2009), *Zur Rheologie und den physikalischen Wechselwirkungen bei Zementsuspensionen*. PhD thesis, University of Karlsruhe, Germany.

Haksever, A.; Schneider, U. (1982), *Zum Brandverhalten von Leichbetonkonstruktionen*. Deutsche Bauzeitung, Vol. 9, pp. 1279-1282.

Hansen, T. C. (1986), *Physical Structure of Hardened Cement Paste – A Classical Approach*. Materials and Structures, Vol. 19, No. 6, pp. 423-436.

Hashin, Z. (1983), *Analysis of composite materials: a survey*. Journal of Applied Mechanics, Vol. 16, pp. 481-505.

Heinz, D.; Ludwig, U. (1987), *Mechanism of secondary ettringite formation in mortars and concretes subjected to heat treatment*. Concrete Durability, Scanlon, J. (Ed.), American Concrete Institute, SP-100, pp. 2059-2071.

Heinz, D.; Dehn, E; Urbonas, L. (2004), *Fire resistance of ultra high performance concrete (UHPC) - Testing of laboratory samples and columns under load.* Ultra high performance concrete (UHPC), Schriftenreihe Baustoffe und Massivbau, Schmidt, M.; Fehling, E.; Geisenhanslüke, C. (Eds.), University of Kassel, Germany, pp. 703-716.

Helmuth, R. A.; Turk, D. H. (1966), *Elastic moduli of hardened portland cement and tricalcium silicate pastes; effect of porosity*. Special Report No. 90, Highway Research Board, Washington D.C., USA, pp. 135-144.

Herold, G.; Scheydt, J. C.; Müller, H. S. (2006), *Development and durability of ultra high performance concretes*. Betonwerk + Fertigteil-Technik, Vol. 72, No. 10, pp. 4-14.

Hillerborg, A.; Modéer, M.; Petersson, P. E. (1976), *Analysis of crack formation and crack growth in concrete by means of fracture mechanics and finite elements*. Cement and Concrete Research, Vol. 6, No. 6, pp. 773-781.

Hillerborg, A. (1983), *Analysis of one single crack*. Fracture Mechanics of Concrete, Wittmann, F. (Ed.). Elsevier Science Publishers, Amsterdam, The Netherlands, pp. 223-249.

Hilsdorf, H. K.; Müller, H. S. (1987), *Stoffgesetze für das Kriechen und Schwinden von Dischinger bis heute*. Spannweite der Gedanken, Specht, M. (Ed). Springer-Verlag, Berlin, Germany, pp. 193-212.

Hilsdorf, H. K.; Brameshuber, W. (1991), *Code-type formulation of fracture mechanics concepts for concrete*. International Journal of Fracture, Vol. 51, pp. 61-72.

Holmen, J. O. (1979), *Fatigue of concrete by constant and variable amplitude loading*. Division of Concrete Structures, The Norwegian Institute of Technology, The University of Trondheim, Norway.

Johntston, C. D. (2001), *Fiber-reinforced cements and concretes*. Advances in concrete technology, Vol. 3, Gordon and Breach Science Publishers, Canada.

Klausen, D.; Weigler, H. (1979), *Strength of concrete under constant and variable pulsating fatigue load*. Betonwerk + Fertigteil-Technik, Vol. 45, No. 3, pp. 158-163.

König, G.; Grimm R. (1996), *Hochleistungsbeton*. Beton-Kalender 1996, Vol. 2, Ernst & Sohn, Berlin, Germany.

Kordts, S. (2005), *Herstellung und Steuerung der Verarbeitbarkeitseigenschaften selbstverdichtender Betone*. Schriftenreihe der Zementindustrie, No. 66, PhD thesis, TU Berlin, Berlin, Germany.

Kropp, J.; Hilsdorf, H. K. (Eds.) (1992), *Performance criteria for concrete durability*. RILEM Report No. 12, E&FN Spon, London, Great Britain.

Kunterding, R.; Hilsdorf, H. K. (1990), *Measurement and evaluation of abrasion resistance of concrete surfaces*. Proceedings 5th International Conference on Durability of Building Materials and Composites, Nov. 1990, E&FN Spon, London, Great Britain, pp. 527-538.

Kvitsel, V. (in prep.), *Vorhersage des Schwindens und Kriechens von normal- und hochfestem Konstruktionsleichtbeton*. PhD thesis, Karlsruhe Institute of Technology (KIT), Karlsruhe, Germany.

Lankard, D. R. (1985), *Slurry infiltrated fiber concrete (SIFCON): Properties and applications*. Mat. Res. Soc., Symp. Proc. 42, pp. 277-286.

Larbi, J. A. (1993), *Microstructure of the interfacial zone around aggregate particles in concrete*. HERON, Vol. 38, No. 1, pp. 1-69.

Lawrence, C. D. (1990), *Sulphate Attack on Concrete*. Magazine of Concrete Research, Vol. 42, No. 153, pp. 249-264.

Lohaus, L.; Fischer, K. (2005), *Sichtbeton – Betonzusammensetzung, Einbau, Qualitätssicherung*. Sichtbeton - Planen, Herstellen, Beurteilen, Müller, H. S.; Nolting, U.; Haist, M. (Eds.), 2. Symposium Baustoffe und Bauwerkserhaltung, Universitätsverlag Karlsruhe, Karlsruhe, Germany, pp. 33-43.

Ludwig, H.-M. (2001), *Dauerhaftigkeit selbstverdichtender Betone*. Selbstverdichtender Beton, König, G.; Holschemacher, K.; Dehn, F. (Eds.), Bauwerk Verlag, Berlin, Germany, pp. 11-23.

Maidl, B. (1991), *Stahlfaserbeton*. Ernst & Sohn, Berlin, Germany.

Malárics, V. (2010), *Ermittlung der Betonzugfestigkeit aus dem Spaltzugversuch bei festen und hochfesten Betonen*. PhD thesis, Karlsruhe Institute of Technology (KIT), Karlsruhe, Germany.

Mechtcherine, V.; Müller, H. S. (1997), *Fracture mechanical and fractological investigations on normal and high strength concrete*. Proceedings of the Fifth International Symposium on Brittle Matrix Composites, Brand, A.M.; Li, V.C.; Marshall, I.H. (Eds.), Woodhead Publishing Ltd., Cambridge, Great Britain, pp. 231-240.

Meyer, A. (1979), *Faserbeton*. Zement-Taschenbuch 47 (1979/80), Bauverlag, Wiesbaden, Germany, pp.453-477.

Mindess, S.; Young, J. G. (1981), *Concrete*. Prentice Hall Inc, New Jersey, USA.

Mindess, S. (1984), *Relationships between strength and microstructure for cement-based materials – An overview*. Materials Research Society Symposia, Proceedings, Vol. 42, pp. 54-68.

Müller, H. S.; Küttner, C. H. (1996), *Creep of high performance concrete – Characteristics and code-type prediction model*. 4th International Symposium on Utilisation of High strength/High performance Concrete, Paris, France, pp. 377-386.

Müller, H. S.; Küttner, C. H.; Kvitsel, V. (1999), *Creep and shrinkage models for normal and high performance concrete – a unified code-type approach*. Journal of the Revue francaise du genie civil, Paris, France.

Müller, H. S.; Linsel, S.; Garrecht, H.; Wagner, J.-P.; Thienel, K.-C. (2000), *Hochfester konstruktiver Leichtbeton – Teil 1: Materialtechnologische Entwicklungen und Betoneigenschaften*. Beton- und Stahlbetonbau, Vol. 95, No. 7, pp. 392-414.

Müller, H. S.; Haist, M.; Mechtcherine, V. (2002), *Selbstverdichtender Hochleistungs-Leichtbeton*. Beton- und Stahlbetonbau, Vol. 97, No. 6, pp. 326-333.

Müller, H. S.; Haist, M. (2004), *Selbstverdichtender Leichtbeton – Erste allgemeine bauaufsichtliche Zulassung*. Betonwerk + Fertigteil-Technik, Vol. 70, No. 12, pp. 8-17.

Müller, H. S.; Haist, M. (2005), *Sichtbetone aus Leichtbeton*. Sichtbeton – Planen, Herstellen, Beurteilen, Müller, H. S.; Nolting, U.; Haist, M. (Eds.), 2. Symposium Baustoffe und Bauwerkserhaltung, Universitätsverlag Karlsruhe, Karlsruhe, Germany, pp. 57-70.

Müller, H. S.; Kvitsel, V. (2006), *Kriechen und Schwinden von Hochleistungsbetonen*. Beton, Vol. 56, No. 1+2, pp. 36-42.

Müller, H. S. (2007), *Zum Baustoff der Zukunft*. Gebaute Visionen – 100 Jahre Deutscher Ausschuss für Stahlbeton, Deutscher Ausschuss für Stahlbeton im DIN (Ed.), Beuth Verlag, Berlin, Germany, pp. 195-221.

Müller, H. S.; Kvitsel, V. (in prep.), *Kriech- und Schwindbeiwerte für normalfeste und hochfeste Konstruktionsleichbetone*. Deutscher Ausschuss für Stahlbeton (DAfStb), Berlin, Germany.

Müller, H. S.; Scheydt, J. C. (2009), *The durability potential of ultra-high-performance concretes – Opportunities for the precast concrete industry*. Betonwerk + Fertigteil-Technik, Vol. 75, No. 2, pp. 17-19.

Müller, H. S.; Reinhardt, H.-W. (2010), *Beton*. Betonkalender 2010, Ernst & Sohn Verlag, Berlin, Germany.

Müller, H. S. et al. (2010), *Time dependent behaviour of ultra high performance concrete (UHPC)*. Proceedings of the 3rd *fib* International Congress, Washington, USA, to be published in June 2010.

Mullick, A. K.; Chandra, S. (1992), *Physico-chemical, biological and thermal degradation including environmental effects*. 9th International Congress on the Chemistry of Cement, New Delhi, India, Vol. 1, pp. 695-734.

Naaman, A. (2000 a), *Ferrocement and laminated cementitious composites*. Techno Press 3000, Ann Arbor, USA.

Naaman, A. (2000 b), *Fasern mit verbesserter Haftung*. Beton- und Stahlbetonbau, Vol. 95, No. 4, pp. 232-238.

Nakamura, S.; van Mier, J. G. M.; Masuda, Y. (2004), *Self compactibility of hybrid fiber concrete containing PVA fibers*. Fibre reinforced concretes, di Prisco, M.; Felicetti, R.; Plizzari, G.A. (Eds.), 6th RILEM Symposium BEFIB 2004, Varenna, Italy, Vol. 11, pp 527-538.

Neville, A. M.; Dilger, W. H.; Brooks, J. J. (1983), *Creep of plain and structural concrete*. Construction Press, London, Great Britain.

Neville, A. M. (1996), *Properties of concrete*. Fourth Edition, Longman Scientific & Technical, London, Great Britain.

Nilsen, U. A.; Monteiro, P. J. M. (1993), *Concrete: a three phase material*. Cement and Concrete Research, Vol. 23, pp. 147-151.

Nilson, A. (1987), *High strength concrete – An overview of concrete research*. Utilization of High strength Concrete, Proceedings, Stavanger, Norway.

Nilsson, L.-O.; Luping, T. (1992), *Relations between different transport parameters*. Performance Criteria for Concrete Durability, RILEM Report No. 12, E&FN Spon, London, Great Britain, pp. 33-96.

Oesterreichische Vereinigung für Beton- und Bautechnik (Ed.; 2009), *Richtlinie Sichtbeton – Geschalte Betonflächen inkl. Gütezeichen „Fachbetrieb für Sichtbeton“*. Vienna, Austria.

Okamura, H.; Ozawa, K. (1995), *Mix design for self-compacting concrete*. Concrete Library of JSCE, Vol. 25, No. 6, pp. 107-120.

Okamura, H.; Ozawa, K. (1996), *Self compactable high performance concrete in Japan*. High performance concrete, Zia, P. (Ed.), SP-159, ACI, Farmington Hills, USA, pp. 31-44.

Ollivier, J.-P.; Massat, M.; Parrott, L. (1992), *Parameters influencing transport characteristics*. Performance Criteria for Concrete Durability, RILEM Report No. 12, E&FN Spon, London, Great Britain, pp. 33-96.

Ottosen, N. S. (1977), *A failure criterion for concrete*. Journal Engineering Mechanics Division ASCE, Vol. 103 EM4, pp. 527-535.

Ozawa, K.; Maekawa, K.; Okamura, H. (1990), *High performance concrete with high filling capacity*. Admixtures for concrete, improvement of properties, Vasquez, E. (Ed.), Chapman & Hall, London, Great Britain, pp 51-62.

Philajavara, S. E. (1982), *Estimation of drying of concrete at different relative humidities and temperatures of ambient air with special discussion about fundamental features of drying and shrinkage*. Creep and Shrinkage in Concrete Structures, Bažant, Z. P.; Wittmann, F. H. (Eds.), John Wiley & Sons Ltd., Chichester, Great Britain, pp. 87-108.

Powers, T. C.; Copeland, L. E.; Mann, H. M. (1959), *Capillary continuity or discontinuity in cement pastes*. PCA Research Bulletin No. 110, Skokie, USA.

Powers, T. C. (1960), *Physical properties of cement paste and concrete*. Proceedings of the 4th International Symposium on the Chemistry of Cement, Washington D.C., USA, Vol. 2, pp. 577-609.

Powers, T. C. (1975), *Freezing effects in concrete*. Durability of Concrete, American Concrete Institute, SP-47, pp. 1-12.

Probst, P.; Stöckl, S. (1978), *Kriechen und Rückkriechen von Beton nach langer Lasteinwirkung*. Schriftenreihe des Deutschen Ausschusses für Stahlbeton, No. 295, Ernst & Sohn, Berlin, Germany, pp. 29-66.

Puntke, W. (2002), *Wasseranspruch von feinen Kornhaufwerken*. Beton, Vol. 52, No. 5, pp. 242-248.

Raupach, M. (1992), *Zur chloridinduzierten Makroelementkorrosion von Stahl in Beton*. Schriftenreihe des Deutschen Ausschusses für Stahlbeton, No. 433, Beuth Verlag, Berlin, Germany.

Reinhardt, H.-W. (2002), *Beton*. Beton-Kalender 2002, Vol. 1, Eibl, J. (Ed.), Ernst & Sohn, Berlin, Germany, pp. 1-152.

Richard, P.; Cheyrezy, M. (1995), *Composition of reactive powder concretes*. Cement and Concrete Research, Vol. 25, pp. 1501-1511.

Richard, P. (1996), *Reactive powder concrete: A new ultra-high-strength cementitious material*. Proceedings of the 4th International Symposium on Utilisation of High-Strength/High-Performance Concrete, De Larrard, F.; Lacroix, R. (Eds.), Paris, France, pp. 1343-1349.

RILEM Report No. 14 (1996), *Durability design of concrete structures*. E&FN Spon, London, Great Britain.

RILEM TC 32 – RCA – Resistance of Concrete to Chemical Attacks (1985), *Sea water attack on concrete and precautionary measures*. Material and Structures, Vol. 18, No. 3, pp. 223-226.

RILEM TC 107, Subcommittee 5 (1999), *Data Base on Concrete Creep and Shrinkage*. Institut für Massivbau und Baustofftechnologie, University of Karlsruhe.

Rostásy, F. S.; Teichen, K.-T.; Alda, W. (1974), *Über das Schwinden und Kriechen von Leichtbeton bei unterschiedlicher Korneigenfeuchtigkeit*. Beton, Vol. 24, No. 6, pp. 223-229.

Rostasy, F. S.; Schneider, U.; Wiedemann, G. (1979), *Behavior of mortar and concrete at extremely low temperatures*. Cement and Concrete Research, Vol. 9, No. 3, pp. 365-376.

Roux, N.; Andrade, C.; Sanjuan, M. A. (1996), *Experimental study of durability of reactive powder concrete.* Journal of Materials in Civil Eng., Vol. 8, No. 1, pp. 1-6.

Roux, N. (1997), *Durabilité des bétons de poudres réactives*. Centre d'assistance technique et de documentation, St.-Rémy-lès-Chevreuse, pp. 46-58.

Rüsch, H. (1960), *Researches toward a general flexural theory for structural concrete.* Journal Proceedings, American Concrete Institute, Vol. 57, pp. 1-28.

Rüsch, H.; Grasser, E.; Rao, P. S. (1962), *Principes de calcul du béton armé sous de etats de contraintes monoaxiaux*. Comité Européen du Béton, Bulletin d'Information, No. 36, Paris, France.

Rüsch, H.; Jungwirth, D.; Hilsdorf, H. K. (1983), *Creep and shrinkage - Their effect on the behavior of concrete structures*. Springer Verlag, New York, USA.

Sargin, M. (1971), *Stress-strain relationships for concrete and the analysis of structural concrete sections*. Studies Series 4, Solid Mechanics Division, University of Waterloo, Waterloo, Canada.

Saul, A. G. A. (1951), *Principles Underlying the Steam Curing of Concrete at Atmospheric Pressure*. Magazine of Concrete Research, Vol. 2, No. 6, pp. 127-140.

Schlaich, M.; El Zareef, M. (2008), *Infraleichtbeton*. Beton- und Stahlbetonbau, Vol. 103, No. 3, pp. 175-182.

Schmidt, M.; Fehling, E. (Eds.) (2005), *Entwicklung, Dauerhaftigkeit und Berechnung Ultrahochfester Betone (UHPC)*. Schriftenreihe Baustoffe und Massivbau, No. 1, University of Kassel, Germany.

Schneider, U. (1982), *Verhalten von Beton bei hohen Temperaturen*. Schriftenreihe des Deutschen Ausschusses für Stahlbeton, No. 337, Ernst & Sohn, Berlin, Germany.

Schönlin, K. F. (1989), *Permeabilität als Kennwert der Dauerhaftigkeit von Beton*. Schriftenreihe des Instituts für Massivbau und Baustofftechnologie, No. 8, Universität Karlsruhe, Karlsruhe, Germany.

Schürhoff, H. J.; Gerritse, A. (1986), *Aramid reinforced concrete. Aramid fibres of the Twaron type, for prestressing concrete*. Swamy, R. L.; Wagstaffe, D. R.; Oakley, D. R. (Eds.), 3rd Intern. Symposium on Developments in Fibre Reinforced Cement and Concrete, RILEM Technical Committee 49-TFR, 13-17 July 1986, Vol. 1, Rochdale, Great Britain, Paper 2.6.

Seeberger, J.; Kropp, J.; Hilsdorf, H. K. (1985), *Festigkeitsverhalten und Strukturänderungen von Beton bei Temperaturbeanspruchung bis 250°C*. Schriftenreihe des Deutschen Ausschusses für Stahlbeton, No. 360, Ernst & Sohn, Berlin, Germany.

Setzer, M. J. (1991), *Interaction of water with hardened cement paste*. Conference on Advances in Cementitious Materials, Mindess, S. (Ed.), Ceramic Transactions, Vol. 16, American Ceramic Society, pp. 415-439.

Shah, S. P.; Winter, G. (1968), *Inelastic behavior and fracture of concrete*. American Concrete Institute, SP-20, pp. 5-28.

Soroushian, P.; Bayasi, Z. (1987): *Prediction of the tensile strength of fibre reinforced concrete: a critique of the composite material concept*. Fibre reinforced concrete, properties and applications. ACI SP-105, American Concrete Institute, Detroit, USA, pp 71–84.

Speck, K. (2008), *Beton unter mehraxialer Beanspruchung – Ein Materialgesetz für Hochleistungsbetone unter Kurzzeitbelastung*. PhD thesis, University of Dresden, Germany.

Springenschmid, R. (2007), *Betontechnologie für die Praxis*. Bauwerk Verlag, Berlin, Germany.

Stark, J.; Wicht, B. (2000), *Zement und Kalk. Der Baustoff als Werkstoff*, Bau-Praxis, Birkhäuser Verlag, Basel, Switzerland.

Stark, J.; Wicht, B. (2001), *Dauerhaftigkeit von Beton. Der Baustoff als Werkstoff*, Bau-Praxis, Birkhäuser Verlag, Basel, Switzerland.

Strehlein, D.; Schießl, P. (2008), *Fleckige Hell-Dunkel-Verfärbungen an Sichtbetonflächen*. Betonwerk + Fertigteil-Technik, Vol. 74, No. 1, pp.32-39.

Stroeven, P. (1973), *Some aspects of micromechanics of concrete under compressive loads*. TU Delft, Delft, the Netherlands.

Swamy, R.; Jones, R.; Chaim, T. (1987), *Shear transfer in steel fiber reinforced concrete, properties and applications*. American Concrete Institute, SP-105, Detroit, USA, pp. 565- 592.

Swamy, R. W. (Ed.; 1992), *The alkali-silica-reaction in concrete*. Blackie, Glasgow, Great Britain.

Tasdemir, M. A.; Maji, A. K.; Shah, S. P. (1990), *Crack propagation in concrete under compression*. Journal of Engineering Mechanics, ASCE, Vol. 116, No. 5, pp. 1058-1076.

Taylor, H. F. W. (1990), *Cement Chemistry*. Academic Press Limited, London, Great Britain.

Torrenti, J. M.; Matte, V., Maret; V., Richet, C. (1996), *High integrity containers for interim storage of nuc1ear wastes using reactive powder concrete.* 4th Intern. Symp. on the Utilization of High Strength/High Performance Concrete, de Larrard, F.; Lacroix, R. (Eds.), Presses ENPC, Paris, Vol. 3, pp 1407-1413.

Troxell, G. E.; Raphael, J. M.; Davis, R. E. (1958), *Long time creep and shrinkage tests of plain and reinforced concrete.* ASTM Proceedings, Vol. 58, pp. 1101-1120.

van Mier, J. G. M. (1986), *Multiaxial strain softening of concrete*. Materials and Structures, Vol. 19, No. 3, pp. 179-190.

Verbeck, G. J.; Helmuth, R. H. (1969), *Structure and physical properties of hardened cement.* Proceedings, 5th International Symposium on the Chemistry of Cement, Tokyo 1968, Vol. 3, Principal Paper III-1, Cement Association of Japan, pp. 1-32.

Vogel, M. (2010), *Schädigungsmodell zur probabilistischen Lebensdauerabschätzung abrasionsbeanspruchter Betonoberflächen im Wasserbau*. PhD thesis, Karlsruhe Institute of Technology (KIT), Karlsruhe, Germany.

Volkwein, A. (1991), *Untersuchungen über das Eindringen von Wasser und Chlorid in Beton*. Berichte aus dem Baustoffinstitut, No. 1, Technische Universität München, München, Germany.

Weber, D. (1983), *Investigations into the effect of deicing salt and carbonation of structures of the city highway Berlin.* Wittmann, F.H. (Ed.), International Colloquium Materials Science and Restoration, Technische Akademie Esslingen, pp. 215-220.

Whiting, D. (1987), *Durability of High strength Concrete*. Concrete Durability, Scanlon, J. (Ed.), American Concrete Institute, SP-100, Vol.1, pp. 819-842.

Wittmann, F. H. (1977), *Grundlagen eines Modells zur Beschreibung charakteristischer Eigenschaften des Betons*. Schriftenreihe des Deutschen Ausschusses für Stahlbeton, No. 290, Ernst & Sohn, Berlin, Germany.

Wittmann, F. H. (Ed.) (1986), *Fracture toughness and fracture energy of concrete*. Elsevier Publishers, Amsterdam, the Netherlands.

Wittmann, F. H.; Roelfstra, P. E.; Mihashi, H.; Huang, Y.-Y.; Zhang, X.-H.; Nomura, K. (1987), *Influence of age at loading, water-cement ratio and rate of loading on fracture energy of concrete*. Materials and Structures, Vol. 20, No. 2, pp. 103-110.

Ziegeldorf S.; Kleiser, K.; Hilsdorf, H. K. (1979), *Vorherbestimmung und Kontrolle des thermischen Ausdehnungskoeffizienten von Beton*. Schriftenreihe des Deutschen Ausschusses für Stahlbeton, No. 305, Ernst & Sohn, Berlin, Germany.

3.2 Reinforcement

by Rolf Eligehausen and Agnieszka Bigaj-van Vliet

3.2.1 Production of steel

(1) Steel composition

The main factors influencing steel quality are composition of steel and treatment after rolling. In general, steel is composed of iron, various impurities and alloying components that are added in different proportions to reach the required properties of the alloy. The main non-metallic component of steel is carbon (C). Phosphorus (P), sulphur (S) and nitrogen (N) are the most common impurities, whose amount has to be kept within certain limits. The main ferro-alloying components are manganese (Mn), silicon (Si), chromium (Cr), nickel (Ni), copper (Cu) and aluminium (Al). Micro-alloys, such as vanadium (V), niobium (Nb), titan (Ti) or boron (B) are often added as well. Depending on the content of alloying components steel types are divided into non-alloyed, low-alloyed and alloyed steels. As a rule non-alloy steels (also called carbon steel) contain less than 2.5% of alloying components (specifically - less than 1% manganese is required), for low-alloy steels it is less than 5% (more than 1% manganese is permitted), while for alloy steels the amount of additions may exceed 5% (proportions by volume). Steels which contain less than 0.12% of micro-alloying components are called micro-alloyed. Among the alloys a stainless steel should be mentioned: this type of steel, with high content of chromium and nickel, is corrosion resistant (see also Section 3.2.5). All types of steel for ordinary reinforcement contain in principle no substantial amount of alloying components, hence they are non-alloyed. For producing prestressing reinforcement non-alloyed and low alloyed steel can be used. The content of carbon, alloying components and steel impurities is a very important, because it influences to high extend the final strength, deformability and weldability of the alloy. Table 3.2-1 gives the indication of the effect caused by some elements on steel characteristics.

alloying component	yield stress increase [N/mm^2]	tensile strength increase [N/mm^2]	deformability
carbon (C)	28.0	70.0	worsen
silicon (Si)	5.6	9.2	worsen
manganese (Mn)	8.4	8.0	worsen
phosphorus (P)	55.0	46.0	worsen
chromium (Cr)	5.5	7.4	worsen
nickel (Ni)	4.5	3.4	improved

Table 3.2-1: Average improvement of steel characteristics due to the addition of 0,1% of alloying component (proportion by mass) [Straßberger (1976)]

Steel type (cast analysis)	Amount of alloying component [%]								
	C	Si	Mn	P	S	Cu	Cr	Ni	V
micro-alloyed for ordinary reinforcement	0,22	0,28	1,20	0,02	0,02	0,04	0,01	0,01	0,07
low alloyed for plain prestressing bars	0,72	0,60	1,40	0,02	0,02	-	-	-	0,25

Table 3.2-2: Chemical composition of micro-alloyed converter steel for ordinary reinforcement [Rußwurm and Martin (1993)] and of low alloyed steel for plain prestressing bars [Weiß (1997)], proportions by mass

In the absence of other significant amount of alloying components, the mechanical properties of steel, such as strength and deformability, its weldability and suitability to heat treatment depend nearly entirely on the carbon content which is usually 0.15-0.20% for ordinary reinforcing steel and 0,5-0,8% for prestressing steel (cast analysis). Due to the high content of carbon all types of prestressing steel are not weldable in contrast to ordinary reinforcement which in general can be welded. With a maximum carbon content in the reinforcing products of 0.24%, the maximum tensile strength of ordinary reinforcement is approximately 550 N/mm^2, while with a maximum carbon content of 0.90% in the prestressing products their maximum tensile strength amounts to about 2000 N/mm^2. An example of the chemical composition as found in cast analysis of micro-alloyed converter steel for production of ordinary reinforcement is given in Table 3.2-2, along with an example of low alloyed steel for plain prestressing bars.

(2) Production process

(2.1) Production of molten steel

Reinforcing and prestressing steel is a steel product with a circular or practically circular cross-section which is suitable to reinforce concrete. For all types of steel the first steps of production – steel making and casting - are identical. There are basically two process routes for making steel: the basic oxygen steelmaking (BOS) and the electric arc furnace (EAF). The earlier process requires a charge of molten iron, which is produced in blast furnaces. The raw materials for producing molten iron are iron ore, coking coal and fluxes (materials that help the chemical process) - mainly limestone. The carbon monoxide (CO), which is formed when oxygen in the hot air blast into the furnace combust with the coke, flows up through the blast furnace and removes oxygen from the iron ores, thereby leaving iron. The heat in the furnace melts the iron, and the resulting liquid iron (or hot metal as it is called in the industry) is transported to the steel furnace. The iron produced by the blast furnace has a carbon content of 4 to 4.5% as well as a number of other "impurities". This makes it relatively brittle. Steelmaking refines iron, amongst other things by reducing carbon content, to make it a stronger and more manipulable product.

The BOS process is the major modern process for making bulk steels. Apart from special quality steels (such as stainless steel), all flat and long products over a certain size are rolled from steel made by the BOS process, including the lighter long products such as those used to reinforce and prestress concrete. The EAF is the other modern way of making special quality steels (steels alloyed with other metals) and some ordinary (non-alloy) quality steels. The molten steel may undergo secondary steelmaking. A range of different processes of secondary steelmaking is available, such as stirring with argon, adding alloys, vacuum de-gassing or powder injection. The objective in all cases is to fine tune the chemical composition of the steel and/or to improve homogenisation of temperature and remove impurities. The semi-finished cast products are transported to the hot rolling mill for rolling into finished steel products.

(2.2) Production of reinforcing steel

(2.2.1) Hot-rolling

Before hot rolling semi-finished products are first heated in a re-heat furnace until they are red hot (around 1200°C). At a roughing stand a collection of steel rolls (or drums) applies pressure to squeeze the hot steel passing through them and arranged so as to form the steel

into the required shape. Billets used to produce reinforcing steel are processed in long product mills. Leaving the roughing stand, the billets pass through a succession of stands which do not just reduce the size of the steel, but also change its shape. After rolling the rods are often coiled up, before they are used for drawing into wire or for fabricating into bars. In all rolling processes, cooling the steel is a critical factor, since the speed at which the rolled product is cooled will affect the mechanical properties of the steel. Cooling speed is controlled normally by spraying water on the steel as it passes through and/or leaves the mill, although occasionally the rolled steel is air-cooled using large fans.

Rebars are delivered as weldable or non-weldable. The production routine for non-weldable steel is hot rolling without additional treatment. In this case, when producing ribbed bars, the ribs are formed by the last stand of the rolling mill, where two or three working rolls are provided with a series of identical intrusions which form the "mould" for the ribs. The production of weldable steel can be executed by three process routes, such as hot rolling after micro-alloying, hot rolling followed by heat treating and hot rolling followed by cold-forming.

(2.2.2) Heat treatment

Heat treatment is a thermal process performed on the steel in a solid state. The most commonly used routine to obtain good weldable reinforcing steel at acceptable costs is a finishing heat treatment in line with the rolling according to the so-called Tempcore process. In this case, after leaving the last stand of the rolling mill the bars are quenched (rapidly cooled) from a final rolling temperature of approximately 950°C. Quenching is interrupted when a surface layer has been transformed from austenitic to martensitic structure. This quenching is performed in a cooling equipment which is passed by the steel before reaching the cooling bed. The heat which remained in the core of the steel migrates towards the surface and in an automatic self-tempering process the martensitic layer is annealed at a temperature of approximately 620°C. Tempering enables partial diffusion of carbon out of the extremely brittle but strong martensite, thus reducing the inherent tensions, significantly increasing deformability and improving in this way the quality of steel. The core of the heat treated rebars is formed from the ferrite and the pearlite - more ductile, but less strong than martensite phase. Thickness of the surface (tempered) martensitic layer and the temperature of annealing is depending on chemical composition of steel, desired grade and size of the bar.

Produced in this thermal process steel, usually called Tempcore, has excellent weldability. Furthermore, while hardening and tempering results in a slight decrease of hardness and strength of steel, a significant increase of deformability is of major importance. The use of this technology allows producing very ductile steel without adding (expensive) micro-alloying components. In general the process permits the production of sizes between 8 and 50 mm (in case of large diameters a small addition of micro-alloying components is usual).

(2.2.3) Cold-forming

After hot rolling, many steel products undergo a further processing in the cold state. The so-called cold-forming is another form of further processing that is applied to semi-finished hot-rolled products in order to produce weldable reinforcing steel of required grade. The base material for this process is a non-alloy steel with carbon content lower than 0,10% and manganese content between 0,5 and 0,7%. Due to this chemical composition after hot-rolling the (semi-finished) steel rod is characterised by a relatively low tensile strength of

approximately 450 N/mm^2. The amount of cold deformation has to assure that at the final product the yield stress increased by cold-forming complies with the requirements. It is important to stress that cold-forming implicates a significant reduction of ductility, understood in terms of strain hardening of steel (ratio between tensile strength and yield stress) and its elongation at maximum load.

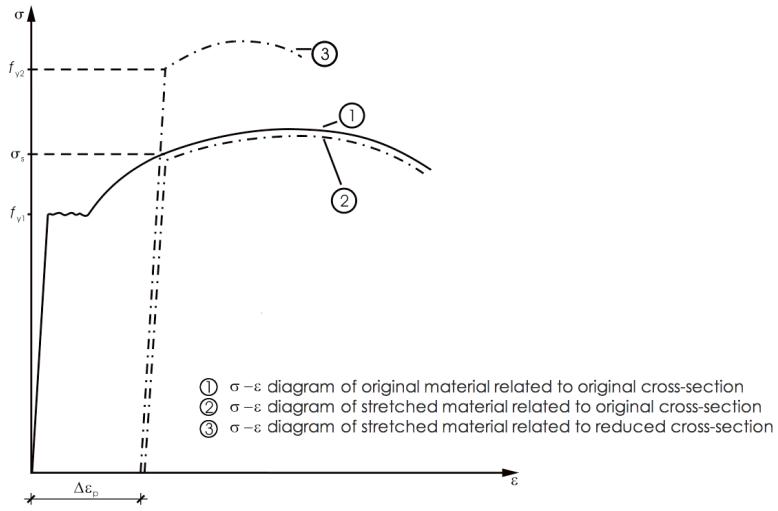

Fig. 3.2-1: Stress-strain relationship of steel before and after stretching, after Rußwurm and Martin (1993)

Stretching, drawing, twisting and cold-rolling and (or) their combinations are the most common methods of cold-forming. As indicated in Fig. 3.2-1, when stretching, the semi-finished hot-rolled rod is stressed into the strain hardening region, thereby reducing the cross section. After unloading plastic deformations remain in the material. During the subsequent reloading, "yielding" will occur at the load level reached at the first loading. If the stress is calculated based on the cross section of the original rod, the stress-strain diagram of hot-rolled steel is followed. However, if the reduced cross-section area is used, yield stress and tensile strength increase with respect to these obtained by former method. Comparing to the un-stretched hot-rolled steel, the new cold-formed material has a lower ratio between tensile strength and yield stress (so-called hardening ratio of steel) and a lower elongation at maximum load. Similar effects are reached with the cold drawing process, where the steel rod is dragged at pressure (drawn) through a series of dies which progressively reduce the circumference of the rod to produce a wire. The processes inside steel during the drawing correspond basically to that of cold-rolling (also known as cold reduction). In this case the rod is first de-coiled (uncoiled) and then passes through a series of rolling mill stands which apply pressure to the strip and progressively reduce its cross-section. Cold-rolling processes are also used to alter the surface quality of the steel, e.g. providing the rib pattern on the plain rods.

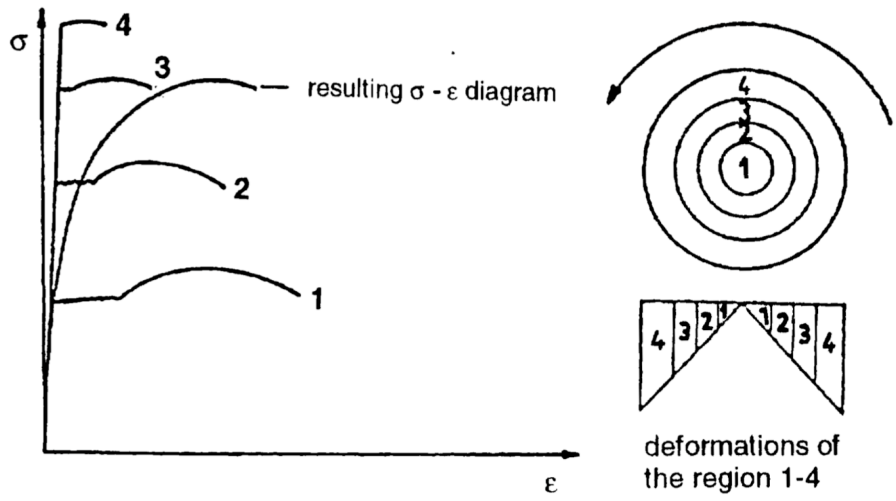

Fig. 3.2-2: Strain hardening by twisting, after Reinhardt (1973)

Contrary to stretching, drawing and cold-rolling, where the hardening is equal over the total cross-section of the bar, in the case of twisting the hardening increases from inside to outside. As shown in Fig. 3.2-2, the concentric layers 1,2,3,4 of the twisted rod have different stress-strain characteristics. As these layers can not deform independently a common (mean) stress-strain diagram of the bar results, that has no yield plateau characteristic for hot-rolled original material. In general, ageing of steel (i.e. diffusion of nitrogen out of the lattice structure to the grain boundaries) causes an increase of strength and a decrease of elongation at maximum load. Note that after ageing, twisted steel may have a yield plateau as well. Similarly to stretching, twisting substantially increases the tensile strength and reduces ductility comparing to these of the base (not-cold-formed) material. The cold working processes can be combined, as in case of cold-worked wires, where drawing is followed by cold-rolling in order to get ribbed material with the required degree of cold-reduction.

(2.2.4) Re-reeling and straightening of coiled products

In case of hot-rolling of micro-alloyed steel or heat treating in line with hot-rolling (Tempcore process), small sizes of bars (6 – 16 mm) are rolled into coils in order to achieve a high production rate. The loose reels of a semi-finished product have to be re-reeled to compacted coils. This re-reeling operation is usually combined with a small amount of cold deformation (< 5%) by stretching or similar treatments in order to obtain the desired final properties of the coiled material. Although cold forming is basically not anymore in use for bars, also this process in a simplified form with strongly reduced cold working is applied to produce small size rebars in coils. Also wires are produced in coils on the basis of wire rod, by cold working or hot-rolling process.

Rebars in coils, however, are semi-finished products, which can only be used in straightened or bent rods. This makes it necessary to straighten the coiled rebars into rods using appropriate equipment. This straightening, normally performed by fabricators, influences some essential properties of the steel. In particular the ductility values are reduced. To make sure that the decoiled product provides all required properties, the coiled (semi-finished) product has to be produced with a certain degree of over-quality. Note that this over-quality – particularly in ductility properties – is easier to obtain with hot rolled coils than with cold deformed ones.

(2.2.5) Welding of wire fabrics

Steel bars and wires can be cut, welded and otherwise prepared to form the reinforcing units. Wire fabric is the most common type of industrially fabricated two dimensional reinforcement. Basically it consists of two rows of parallel and mostly equidistant bars or wires of the same or different diameter and length which cross in right angle. At points of intersection, longitudinal and cross rebars are factory electrical resistance welded together by automatic machines in a shear resistant manner. The current is applied to this part of the rebars by conductor electrodes. The weld is produced by putting the heated and localised melting of sections under pressure. The heat necessary for the local melting of steel, needed to produce the weld without a filler metal, is obtained in the electrical resistor formed by the two reinforcing bars in contact due to the Joule effect.

Welding locally provides a heat treatment of the steel. Although the properties of the steel rebar at the weld point are influenced by this process, careful processing should guarantee that on global scale the mechanical properties of the original material are not significantly influenced. The main problem is to ensure a slow enough cooling of the heated material. If the cooling is too fast, hardening of steel with a subsequent reduction of ductility takes place. The resulting reduction of the deformability depends on the time of heating and on the chemical composition of steel (mainly content of C, N, S, P). Therefore the speed of welding (usually 50 to 120 weld points per minute) must be related to the chemical composition (and weldability) of steel chosen for producing wire meshes.

(2.3) Production of prestressing steel

(2.3.1) Hot-rolling

High steel strength is required for utilising partial or full prestressing of concrete. However, as far as production of steel is concerned up to hot rolling all production processes for prestressing steel are identical as for reinforcing steel. Billets used to produce prestressing steel are processed in long product mills in a very similar way as in the case of reinforcing steel. Accelerated cooling takes place after the rods leave the last stand of the rolling mill. At this stage of production differences between strength and ductility of semi-finished rods for production of prestressing reinforcement and that for production of ordinary reinforcement follow basically from differences in chemical composition of steel in both cases.

There is a certain variety in process routes that are used for production of prestressing steel that follow after hot-rolling and cooling. The prestressing reinforcement may undergo the following treatments, either single or in combination: quenching, tempering (or partial tempering, similar to Tempcore process), cold stretching and stress relieving. Hence, one can distinguish between hot-rolled bars, hot-rolled, stretched and tempered bars, quenched and tempered wire rods and wires, produced by cold working hot rolled rods.

(2.3.2) Heat treatment

One of the traditional ways of increasing the resistance of steel is quenching. The semi-finished hot-rolled steel rods are heated up to a temperature of 1000°C to get a homogeneous austenite. This heating is followed by a rapid quenching in a bath of oil. During this process the whole section is transformed to martensite. After quenching, martensite must be tempered to reduce its brittleness. The rod is heated to temperatures between 450 and 650°C and kept at these temperatures for some time. This enables partial diffusion of carbon (C) out of the

martensite, thus reducing the inherent tensions. The result of quenching and tempering is a slight decrease of hardness and strength, with a significant increase in deformability. Quenching and tempering are commonly used to produce prestressing wire rods. If required, ribs on this type of wire rods are produced during hot-rolling process.

Partial tempering is in principle similar to the Tempcore process, described in Section 3.2.1 (2.2.2). In production process of prestressing bars, partial tempering usually follows directly after hot-rolling and cooling, preceding stretching (described in Section 3.2.1 (2.3.3)), additional tempering (described above) and, in some cases, stress relieving (described in Section 3.2.1 (2.3.4)). The thread on the prestressing bars is either produced during hot-rolling or in a separate cold thread-rolling process.

(2.3.3) Cold-forming

Basically three of the cold-forming processes described in Section 3.2.1 (2.2.3) can be applied when producing prestressing steel: stretching, drawing and cold-rolling. While prestressing bars undergo stretching, prestressing wires are cold drawn from steel rods. The desired strength of the final product is obtained by an appropriate choice of steel composition and degree of cold deformation. After drawing, the reinforcement is given a final thermo-mechanical treatment; see Section 3.2.1 (2.3.4). Cold-rolling is also used, if desired, to improve the bonding characteristics of prestressing wires and bars: produce the indentations on prestressing wires, to perform crimping (series of regular bends in one plane of the wire) or to form a thread on the prestressing bars.

(2.3.4) Stress revealing and stabilising

Mechanical and thermal processes (e.g. cold working or hardening) cause inherent stresses in the manufactured product. By stress relieving the performance of this product can be enhanced. The procedure of stress relieving, commonly applied to prestressing wires and strands, is called stabilising. Stabilising is a combined process of low temperature heat treatment (at 400°C) and a simultaneous stretching just over 1%. Thereby the relaxation is significantly reduced and all mechanical properties are improved. Note that the influence of steel characteristics on the overall performance of prestressed concrete structures is much more pronounced than in case of reinforced concrete structures. Hence, the higher the strength of prestressing steel is, the more one has to take care on manufacturing. Only smallest mechanical defects or non-homogeneity in the crystal structure could lead to damages. Stretching, executed during the stabilising process in the plastic branch of the stress-strain diagram of steel, represents also a continuous testing procedure of prestressing reinforcement to uniaxial strain. This check reduces dramatically the probability of rupture of prestressing reinforcement on site.

(2.3.5) Stranding and compacting of strands

Prestressing wires are used to manufacture a very efficient consumer product: the prestressing strand. Generally strands consist of a straight core wire around which one or more layers are formed in helical configuration. During stranding the wires are winded around the central core wire. This is achieved by spinning bobbins holding the wire around the central axis and bending the outer wires to form parallel helices over and around the core wire. The pitch of the outer layer is constant and its lay length is usually between 14 and 18 times the nominal strand diameter. The stranding process is normally followed by a heat

treatment according to the stabilising process described in Section 3.2.1 (2.3.4), which results in a stabilised strand.

In some cases the application of prestressing steel demands that the outer diameter of the prestressing element should be as low as possible. A partial solution of this demand has been found in compacting the stabilised strand. During the compacting process the wire strand passes through a series of dies to reduce the diameter. It results in changing the shape of the wires in the outer layer, filling up the space between the individual wires thus decreasing the outer reach of the strand and increasing the steel area for a given strand diameter.

(3) Types of steel products

(3.1) Reinforcing steel products

Reinforcing steel can be basically divided into weldable and non-weldable ones. As explained in Section 3.2.1 (1), weldability of steel depends primarily on its chemical composition. In the following mainly the weldable steel grades with carbon content lower than 0.24% are referred to.

Reinforcing steel can be categorised by its strength and ductility. As demonstrated in Section 3.2.1 (2.3), besides the chemical composition of steel, both strength and ductility depend on the production process and, eventually, on the treatment after rolling. While formerly relatively low strength steel was in use in Europe (guaranteed yield stress between 220 and 350 N/mm^2), the currently produced weldable reinforcing steel has a guaranteed yield stress, which usually varies from 450 to 550 N/mm^2. The value of the characteristic yield stress in N/mm^2 denotes the so-called steel grade (e.g. steel grade 450, 480 or 500). Note that in any case an overstrength is implied with respect to the characteristic yield stress of steel, however in practice it should not exceed roughly 20% of the nominal yield stress value. In general hot-rolled micro-alloyed steel and heat-treated (Tempcore) steel are characterised by a lower strength and a higher ductility than cold-formed steel types. Based on the specific ductility characteristics reinforcing steel may also be divided into different ductility classes. See also Section 3.2.4 for a survey on the classification of reinforcing steel.

Reinforcing steel can also be distinguished by its surface geometry (dimensions, number and configuration of transverse and longitudinal ribs and other indentations, if present) by means of which bond with concrete is achieved. Rebars can be classified by their surface configuration as plain, indented or ribbed reinforcing steel. Plain reinforcing steel has a smooth surface. Indented reinforcing steel has well defined indentations uniformly distributed over the length while ribbed reinforcing steel is characterised by at least two rows of transverse ribs which are also uniformly distributed over the entire length of the rebar. In the following the main types of products used to reinforce concrete are briefly presented.

(3.1.1) Bars

Rebars are usually produced in a large range of sizes. Range and scales differ from country to country. In European standard EN 10080 the following scale is provided: 6, 8, 10, 12, 14, 16, 20, 25, 28, 32 and 40 mm. Larger sizes (50, 57 and 63 mm) are rarely produced, mostly used in piles. The common length of bars is between 12 and 18 m. Exceptional length may amount to 30 m. Delivery of steel bars takes place in bundles with a usual weight between 200 and 3000 kg. Note that for steel a density value of 7850 kg/m^3 can be used. Bars

can be produced as plain, indented or ribbed (examples of some typical rib patterns are given in Fig. 3.2-3). For hot-rolled, heat treated and cold-formed weldable steel bars, EN 10080 limit the direct use as reinforcement to ribbed bars manufactured in steel grades 450 and 500. According to these standards, plain and indented bars manufactured in steel grade 500 can be used only in lattice girders, further discussed in Section 3.2.1 (3.1.4).

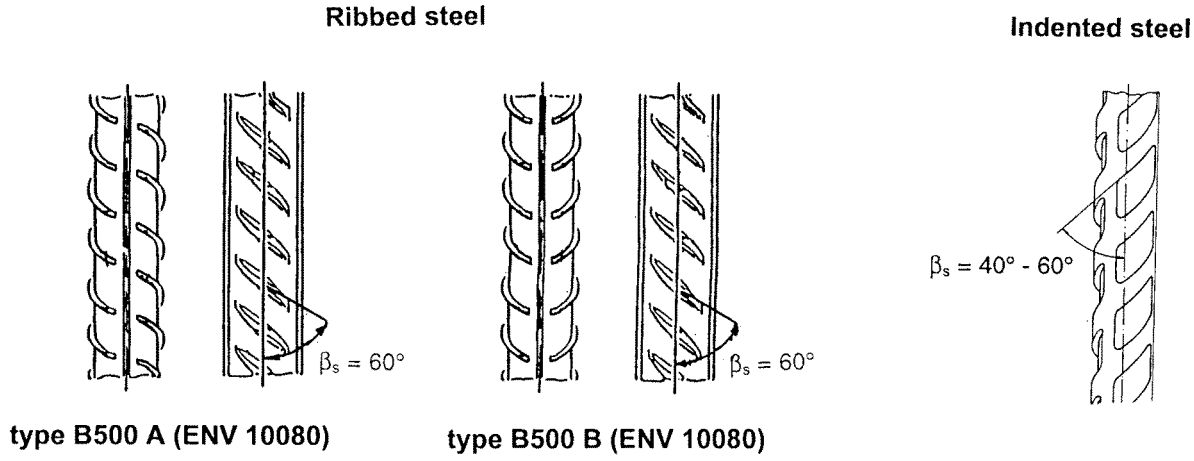

Fig. 3.2-3: Rib pattern for reinforcing steel, after ENV 10080 (1994) and Rußwurm and Martin (1993)

(3.1.2) Decoiled rods and wires

Coils are produced with rebar sizes between 6 and 16 mm (mainly 6 to 14 mm) and with wire sizes between 4 and 12 mm. For the nominal diameter of a wire, EN 10080 allow its increase with a 0.5 mm increment (i.e. 4.0, 4.5, 5.0, 5.5 mm, etc.) The usual weight of a coil is between 800 and 3000 kg, which corresponds with the diameter of the coil between 0.5 and 1.2 m. Decoiled material may be delivered in straight lengths or as cut and bent pieces. Note that in Section 3.2.1 (2.2.4) the problems of re-reeling and straightening of coiled rebars are treated. According to ENV 10080 and prEN 10080, plain, indented and ribbed weldable coiled bars and wires can be produced in steel grades 450 and 500. Similar to bars, the use of plain and indented wires is limited to lattice girders. Also MC90 limits use of plain wires: they should not be used for reinforced concrete, except as non-structural reinforcement (spacers etc.) or in form of welded fabrics.

(3.1.3) Welded wire fabrics

Wire fabrics, which consist of two rows of parallel and mostly equidistant bars or wires of the same or different diameter and length which cross in right angle, are very suitable for reinforcing slabs and similar constructions. Most commonly used are industrially fabricated welded wire fabrics; see Section 3.2.1 (2.2.5) for details of the production process. The big advantage of welded wire fabrics is that a stable element (panel) can be easily transported, stored and placed, while the position of the individual rebars remains unchanged during all operations.

Welded wire fabrics are sub-divided in two types: standard fabrics and purpose (tailor) made fabrics. While the purpose made fabrics are manufactured to user's specific requirements leaving the designer the freedom of choice with respect to rebar diameter and spacing (as long as the general design requirements are satisfied), the standard fabrics are

produced in a limited number of variations and are available from stock. The base materials for fabrication of welded fabrics are ribbed, plain or indented wires. In case of standard wire fabrics from cold deformed wires the rebar size ranges from 4 to 12 mm while in case of standard fabrics from hot rolled wires it ranges from 6 to 40 mm (normally the largest bar size is 16 mm). The grades of steel used are similar in both cases: 500 or 480 (460) for cold reduced steel wires and 500 or 450 for hot-rolled steel wires. The usual length of standard fabrics is between 4.5 and 6 m and the width between 1.9 and 2.4 m. The cross-section area of the main reinforcement usually ranges between 100 and 900 mm^2/m. Note that the minimum reinforcement may differ for the different standards. Adequate stiffness of the fabric should be ensured either by limiting the maximum spacing of the bars, or by introducing a minimum ratio between the diameter of the transverse bars and of the longitudinal bars. Preferred pitch (centre-to-centre distance) of longitudinal and transverse wires shall not be less than 50 mm. The wires in one direction may be twin wires (i.e. two wires of the same steel grade and size placed adjacently and in contact with each other as a pair).

Wire fabrics can be produced as mesh-bearing in two directions or predominantly bearing in one direction. In the latter case the cross wires are acting as load distributors. The grade of steel shall be homogenous in both directions if they are used as bearing reinforcement An interesting variation to be mentioned is an uniaxial fabric, where only the load bearing wires are made of better quality steel, often the hot-rolled ones. Using this kind of arrangement has the advantage of having an improved performance (e.g. increased ductility) in load bearing direction and of reducing costs by using cheaper steel as transverse reinforcement.

(3.1.4) Lattice girders

Another example of industrially prefabricated reinforcing systems are lattice girders. A lattice girder is a two or three-dimensional metallic structure comprising an upper chord, a lower chord and continuous or discontinuous diagonals, which are welded or mechanically assembled to the chords in order to obtain a shear bearing joint. The chords are usually made of ribbed or indented wires or bars, while the diagonals are mostly smooth. Note that while both chords usually consist of longitudinally extended wires (bars), in some systems the upper chord may be made of a profiled steel strip. The wire size starts from 4 mm and ends up at 12 mm. The chords and diagonals are produced mainly of steel grade 500. The height of the standard lattice girders ranges between 70 and 300 mm. The width ranges between 50 and 250 mm and the usual length is up to 8 m.

Lattice girders are stiff and transportable elements. They can be used directly as reinforcement. Their flexible application in double plate panels (walls) and floor slabs is of important advantage. Double plate panels in a building system with partially prefabricated elements permit the construction of external and inner load bearing walls. Lattice girders are also often used to pre-manufacture the so-called lattice girder planks for system floors - the plank encasing the lower chord of the girder may be made of concrete or concrete in a clay mould. Another type pre-manufactured construction element used for constructing floor slabs is the pre-cast lattice girder plate. If standard lattice girders are used the plate has a height between 80 and 340 mm. Lattice girder planks for system floors and pre-cast lattice girder plates allow to increase speed of placing onside and, in the latter case, reduce necessity of prop (used only during concrete casting). Fig. 3.2-4 shows some examples of lattice girder arrangements and their applications for constructing.

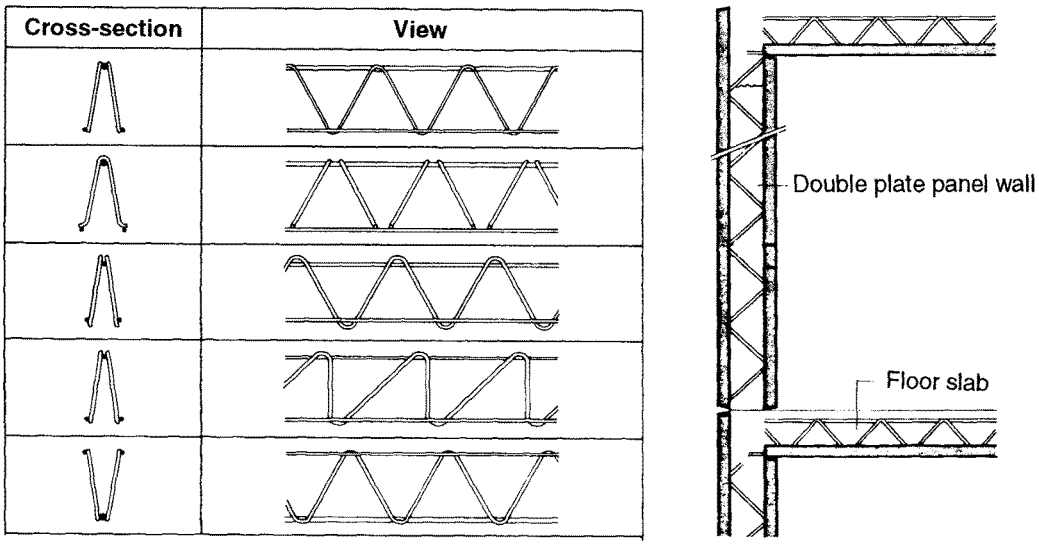

Fig. 3.2-4: Arrangement of lattice girders and their applications, after Rußwurm and Martin (1993)

(3.2) Prestressing steel products

As discussed in Section 3.2.1 (1), due to the high content of carbon (C) all types of prestressing steel are not weldable. The classification of prestressing steel is then mainly based on its strength and ductility and on relaxation behaviour. All these characteristics are directly related to the type of production process and, obviously, to the composition of steel for prestressing reinforcement. In Section 3.2.1 (2.4) the manufacturing processes of the different products and the influence of the production process on the properties of prestressing steel is discussed in general. According to their tensile strength prestressing steels can be classified in grades, ranging from 1030 to 2060 (yield stress ranges from 835 to 1820, respectively). Note that not all grades are available for each prestressing product: e.g. heat-treated bars are produced with a tensile strength from 1030 to 1230 N/mm^2 (yield stress from 835 to 1080 N/mm^2), quenched and tempered wire rods with a tensile strength from 1470 to 1570 N/mm^2 (yield stress from 1325 to 1420 N/mm^2), cold drawn wires with a tensile strength from 1570 to 1770 N/mm^2 (yield stress from 1375 to 1570 N/mm^2) and strands with a tensile strength from 1770 to 2060 N/mm^2 (yield stress from 1520 to 1770 N/mm^2). The current European standard prEN 10138 (2000) distinguishes between steel grade 1030, 1100 and 1230 for hot-rolled and processed bars, grade 1570 for quenched and tempered wire rods, grade 1570, 1670, 1770 and 1860 for cold drawn wires, grade 1860, 1960 and 2060 for stabilised 3-wire strands and grade 1770, 1860, 1960 and 2060 for stabilised 7-wire strands. Section 3.2.4 provides the survey on the classification of prestressing steel, including the steel grades distinguished in prEN 10138.

Similar to reinforcing steel, different shapes or surface characteristics are defined for prestressing reinforcement. In the following the main types of prestressing steel products are briefly presented.

(3.2.1) Bars

Bars were the very first prestressing elements used. As for other types of prestressing products, the basic materials for producing prestressing bars are non-alloyed and low alloyed steel grades. Bars are manufactured in sizes from 12 to 50 mm, though sizes 26, 32 and 36 mm are most commonly used. In prEN 10138 the following scale is provided: 15, 20, 26,

32, 36, 40 and 50 mm. Typical for prestressing bars is that they are produced in straight length. The length of the bars runs from 6 up to 30 m. The bars are produced either in smooth or ribbed configuration. In order to achieve simple handling in anchoring and forming joints the ribs form a thread. Examples of typical surface configuration of prestressing bars are given in Fig. 3.2-5. As mentioned above, although prestressing bars can be produced in different steel grades prEN 10138 distinguishes in this case between steel grade 1030, 1100 and 1230 both for hot-rolled and processed bars.

Fig. 3.2-5: Surface geometry of plain and of threaded prestressing bar (DYWIDAG)

Just as with other types of prestressing reinforcement, prestressing bars in transport and storage bars shall be protected against damage and contamination, particularly from substances or liquids which are likely to produce or encourage corrosion.

(3.2.2) Wires

Cold drawn prestressing wires are single prestressing elements delivered in coil form. The wire diameters are running from 3 to 10 mm. In prEN 10138 the following diameters are listed in relation to the steel strength, both for smooth and indented wires: 3, 4 and 5 mm for steel grade 1860, 3.2, 5 and 6 mm for 1770, 6.9, 7, 7.5 and 8 mm for steel grade 1670 and 9.4, 9.5 and 10 mm for steel grade 1570. The nominal diameter of an indented wire is the nominal diameter of a smooth wire having the same cross-section area. The diameter of the coil used for storage and transportation of the wires shall be sufficiently large to ensure that the permanent straightness of the product after decoiling is unaffected. Therefore large diameter coils are used: their inner diameter ranges from 1.2 to 2 m and the outer one from 1.5 to 2.4 m. The coils weigh between 200 and 2000 kg. Cold drawn wires can be delivered with smooth or indented surface. The indentations are produced in that way to avoid disadvantages resulting from this penetration. Therefore their depth varies within 1 to 3% of the diameter and they are positioned on the opposite sides of the wire and staggered.

Another type of prestressing product are quenched and tempered wire rods with increased resistance. Quenched and tempered wires are produced in sizes from 6 to 16 mm and delivered in coils with sizes of 1800 mm for wires diameter smaller than 8 mm and 2400 m for wires beyond 8 mm diameter. PrEN 10138 allows the following sizes of the quenched and tempered wire smooth rods: 6, 7, 8, 9.5, 10, 12 and 14 mm and for ribbed rods 6.2, 7.2, 7.5, 8, 9.5, 10, 12.2 and 14 mm. Ribbed wires are mostly used in pre-tensioning systems. In some cases end-anchors in form of rolled threads are applied. PrEN 10138 names only steel grade 1570 in case of quenched and tempered wire rods, both in case of smooth and ribbed surface configuration.

(3.2.3) Strands

Prestressing strands consist of a number of cold drawn wires spun together in helical configuration (i.e. in the same direction and with the same pitch). The pitch is appropriate to the size and type of the strand. The basic advantage of using strands is that arranged in this way number of wires can be prestressed in a single operation. This goal can be perfected if a series of strands form a cable, which can be stressed simultaneously all together. Strands behave as homogeneous units under tension and are also capable to withstand significant transverse forces without distortion. Moreover, stranding provides an excellent bond with the grout which can be improved in using indented constituent wires to produce the so-called indented strands. Strands start with two wires and normally end up with 19 individual wires, though as much as 27 wires are also used in some cases. However, most commonly used are 3-wire strands (three wires spun together over a theoretical common axis) and 7-wire strands (a straight core wire around which six wires are spun in one layer). The stabilised strands, i.e. strands that have been given a stress relieving heat treatment, have significantly reduced relaxation and generally improved mechanical properties.

Compacted strands, with reduced outer diameter, increased steel area and, hence, for given diameter larger weight per unit length must also be mentioned. In Fig. 3.2-6 cross-sections of most commonly used standard and compacted 7-wire strands are shown. Note that in case of compacted strand not only the reduced diameter of the strand is of advantage, but compacted strands are also easier to anchor in the wedge of a prestressing block due to their spherical deformed outer wires.

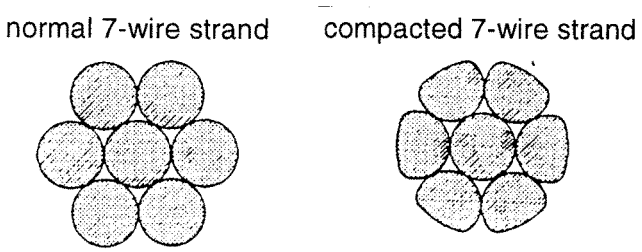

Fig. 3.2-6: Cross-section of normal and compacted 7-wire strand, after Nawy (1996)

The common strands are dispatched with coil weights from 1.5 to 8 tons. As with wires, coils shall be of such a diameter and formed in such a way that the material is held firmly by restraining bands or ties and can easily be decoiled. The inner diameter of the coils for strands is therefore 0.7 to 1.2 m; the outer one runs from 1.2 to 1.5 m. Produced with a tensile strength up to 2060 N/mm^2 (yield stress up to 1770 N/mm^2) for stabilised 3-wire strands are classified in prEN 10138 into the following steel grades: 1860, 1960 and 2060. For stabilised 7-wire strands the following is defined: steel grade 1770, 1860 and 1960. Compacted 7-wire strands may be produced in grades 1700, 1820 and 1860.

3.2.2 Essential properties of reinforcing steel

(1) European normative references for reinforcement of concrete structures

The European standards EN 10080:2005 specify general requirements for weldable reinforcing steel used for the reinforcement of concrete structures in the form of bars, de-coiled rods and wires, welded wire meshes and lattice girders. Another example of relevant international product standard is ISO 6935 (Parts 1 to 3). Note that these standards do not

apply to non-weldable reinforcing steel, galvanised or epoxy-coated reinforcing steel, and stainless reinforcing steel. Relevant international product standards for coated reinforcing steel are ISO 14645 and ISO 14657. In general, the behaviour of reinforcing steel is specified by the following properties: strength and ductility characteristics, bendability, bond characteristics, section sizes and tolerances, fatigue characteristics, weldability, shear and weld strength for welded fabrics and lattice girders. In the following these and some other essential characteristics of reinforcing steel are discussed more in detail.

(2) Behaviour under static loading

(2.1) Stress- strain behaviour

In a uniaxial tensile test the stress-strain diagram of a reinforcing steel can be obtained. The stress (σ) is normally obtained by dividing the load by the original section of the specimen at the beginning of the test. The strain (ε), which is assumed to be uniformly distributed until the stress localisation takes place (i.e. until the maximum load is reached), is obtained by dividing the measured elongation by the original (standardised) measuring length. Due to the diversity and evolution of the manufacturing process for bars and wires, various stress-strain diagrams may be encountered. Basic distinction is to be made between the stress-strain behaviour of steel produced by hot-rolling or heat treatment and that which undergone cold-forming process.

(2.1.1) Hot-rolled and heat treated steel

The shape of stress-strain diagram shown in Fig. 3.2-7 is typical for hot-rolled (micro-alloyed) steel and heat treated (Tempcore) reinforcement. This stress-strain diagram can be subdivided into different ranges: elastic range, flow range, hardening range and post-peak range.

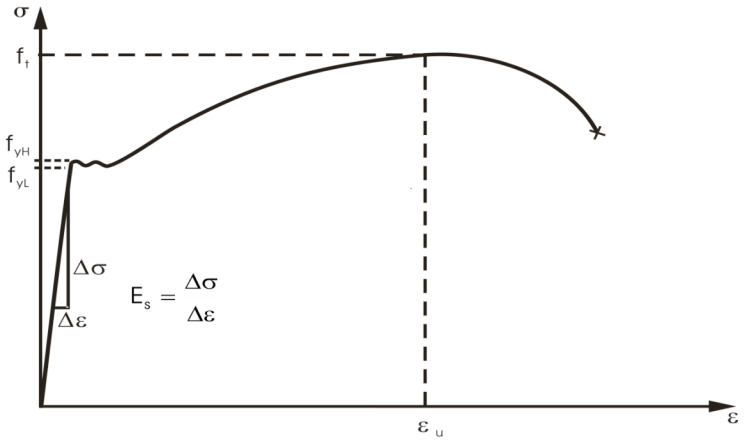

Fig. 3.2-7: Stress-strain diagram for hot-rolled and heat-treated reinforcing steel

In the elastic range the σ - ε relationship is linear i.e. deformation (strain) is proportional to stress and goes back to zero if unloaded. Hence, the Hook's law is valid:

$$\sigma = E_s \cdot \varepsilon \qquad (3.2\text{-}1)$$

where:

E_s the modulus of elasticity of steel

Modulus of elasticity of steel is a material constant and for reinforcing steel it falls between 195 000 and 210 000 N/mm^2. Due to the longitudinal elastic elongation, ε, there is a transverse contraction ε_v, which can be given by the expression:

$$\varepsilon_v = - \nu_s \cdot \varepsilon \tag{3.2-2}$$

where:

ν_s Poisson ratio (for reinforcing steel $\nu_s \sim 0.3$).

In case of hot-rolled and heat treated steel yielding takes place in a very evident way: leaving the elastic branch a more or less horizontally extended apparent flow range starts. In the flow range the stress value only slightly varies between the so-called lower and upper yield stress values (in the following denoted as f_{yL} and f_{yH}). European standards for reinforcing steel EN 10080 state that for characteristic yield stress the upper yield stress shall apply. This exact limit of elasticity is, however, difficult to measure. Therefore for practical purposes some standards allow that the stress under which the residual strain (strain after unloading) is 0.1% (also called 0.1%-proof stress and in the following denoted as $f_{0,1}$) can be taken as a limit value for the yield stress of hot-rolled or heat treated steel.

After passing the yield point plastic (irreversible) deformations occur. The strains do not go back to zero after unloading and the unloading branch is parallel with the elastic one, since only the elastic strains can be released when decreasing the load. Characteristic for hot-rolled and heat-treated steel is the sudden transition into hardening range, after a certain (characteristic) strain value has been reached. Depending on the type of steel, the strain at which so-called strain hardening starts falls approximately between 1% and 3%. In the hardening range the load can be increased again, which comes together with further increase in plastic deformations. The load increase can be obtained until the strain localisation takes place. In the pre-peak range the strain is assumed to be uniform. The steel tensile strength f_t is obtained from the maximum load measured. Strain that corresponds with that point on the stress-strain diagram, i.e. the total elongation at maximum load, defines the so-called ultimate steel strain ε_u. The value of ε_u can be determined either from direct measurement with an extensometer; from measurement after rupture of the uniform plastic elongation outside the failure zone (and corrected with the elastic – released – portion of strain at maximum load), or from the difference of two elongations measured after rupture over the rupture zone (and corrected with the elastic strain at maximum load) according to $\varepsilon_u = 2 \cdot A_{10} - A_5 + f_t / E_s$ (A_5 and A_{10} denote the strain related to the gauge length of 5 and 10 bar diameter, respectively).

The load decreases after the tensile strength has been reached – for a naked rebar in uniaxial tension - at the weakest section of the rebar. This is due to the fact that localisation of failure takes place. Local and strong contraction takes place at the zone where failure localises and the so-called necking phenomenon can be observed. This fracture localisation results in the decrease of stresses, if calculated on the basis of the original cross-section of unloaded bar. Note that if the stresses are calculated with the real (smaller) area in the region where failure occurs, an increasing trend is observed, despite the load decreases. Necking of steel is followed by rupture which takes place when the total deformation capacity of the material has been exhausted in the most stressed section. The stress-strain relationship of most types of hot-rolled and heat-treated steel under compression is almost symmetrical to the relationship under tension and yield stress and compression strength are nearly corresponding. The shear strength is approximately 0.71 of the tensile strength.

(2.1.2) Cold-worked steel

While for small (elastic) strains behaviour of hot-rolled, heat-treated and cold-formed steel is identical, significant differences occur as soon as plastic strains start to arise. Contrary to the earlier types of steel, cold-formed material shows no distinct yield phenomenon (yield plateau), but a continuous transition from elastic to plastic behaviour is observed. In the typical stress-strain diagram of cold formed steel, shown in Fig. 3.2-8, only three characteristic ranges can be defined: elastic range, plastic (pre-peak) range and post-peak range.

The stress-strain relationship of cold-formed steel in the elastic range can be described as well with Hook's law and with the same value of modulus of elasticity E_s as in case of hot-rolled of heat treated steel, see eq. (3.2-1). Since the point of passing from the elastic range to the plastic range is difficult to be distinguished, a convention is necessary to give a definition for yielding. For cold-formed reinforcing steel a value is taken that represents the stress (or the load) where the residual plastic elongation is equal to 0.2% or where the total extension reaches 0.5%. They are called 0.2%-proof stress (in the following denoted $f_{0.2}$) and 0.5%-proof stress (in the following denoted $f_{t0.5}$), respectively, Note that while the ratio $f_{0.1}/f_{0.2}$ is ~ 0.95 for hot-rolled and heat treated steel, it might be much smaller for cold-worked steel. This means that for the same value of yield strength, plastic deformation will occur at lower load level when using cold worked steel than in case of hot rolled steel. Just as for hot-rolled and heat treated steel, until the maximum load has been reached deformations are uniformly distributed over the whole length of the tensioned specimen. After strain localisation took place, the load carrying capacity starts to decrease and a descending branch is observed in the stress-strain diagram, if the stress is derived using the original cross-section area of the bar. Visible necking, i.e. strong strain concentration in the most exhausted section, precedes rupture of the steel.

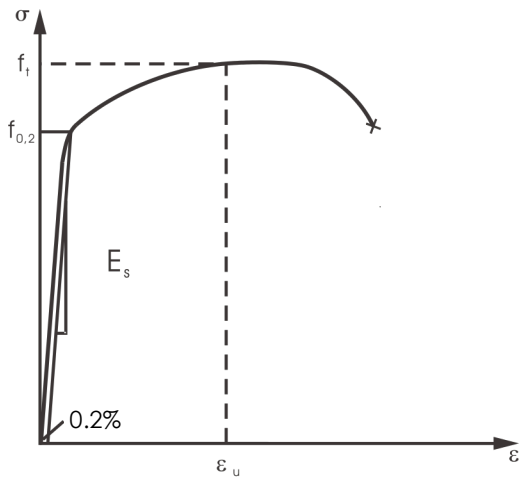

Fig. 3.2-8: Stress-strain diagram for cold-worked steel

For high strength steels, the stress-strain diagram is non-symmetrical in compression and in tension. For reinforcing steels totally or partially cold-worked by means of axial tension, it will generally be the case that the actual yield stress f_{yc} for compression and tension f_y are not equal. The value of f_{yc} to be used in a calculation should therefore be stipulated in the approval documents. Moreover, some cold-worked steels have a lower modulus of elasticity in compression than in tension. The difference is, however, not important in practice.

(2.2) Modelling behaviour under static loading

MC90 allows, as a simplification, to replace the actual stress-strain diagram of steel by an idealised characteristic diagram according to Fig. 3.2-9, assuming a modulus of elasticity E_s equal to 200 000 MPa. The actual diagram for a particular steel may be used if it is duly verified by the producer. The characteristic properties of reinforcement are defined by 5% fractile. For design the partial safety factors shall be used when modelling stress-strain behaviour.

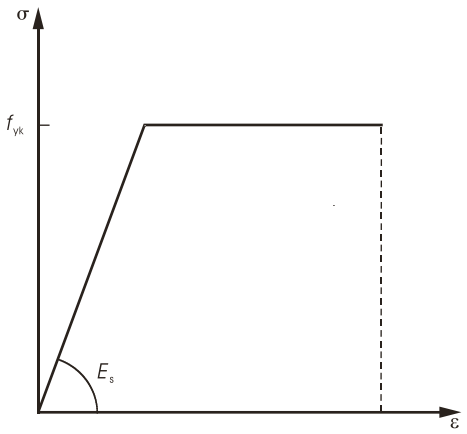

Fig. 3.2-9: Idealised stress-strain diagram of steel according to MC90

(2.3) Strength characteristics

The tensile properties of reinforcing steel shall comply with the requirements given in the material standards. For quality control purposes and design calculations, the strength characteristics of a product given in these standards, i.e. the values of yield stress f_y and tensile strength f_t are referred to the nominal cross-section of the product. Note that the nominal diameter is defined as the diameter of a plain circular cylinder of the same weight per unit length as the bar. Note that MC90 considers reinforcing steel only up to grade 500. For grades higher than 500 the validity of the rules given in MC90 should be reconsidered.

The accurate approximation of strength characteristics is crucial, since on these values the design of reinforced concrete is directly based. It is however very important that the designer is aware of the fact that values of characteristic tensile properties given in the standards are defined as fractiles. Moreover, defined in this way values are just the minimum requirement for the steel quality to be guaranteed by the producer and only in case of very ductile steel for seismic applications the upper bound values are limited (in this case the actual yield stress must not exceed 1.2 (according to EN 10080) or 1.3 (according to Eurocode 2 and MC90) times the characteristic yield stress value. These are the reasons why the yield strength of the reinforcement used in a structure is normally higher than the nominal value assumed in design. This so-called steel overstrength is of special interest considering that while the force distribution along a member is calculated under the assumption of a design (or characteristic) material characteristics, the real distribution of forces at the ultimate limit state can be significantly different than assumed in the design. This can lead to the overestimation of the anchorage capacity of staggered bars and as consequence to a bond failure before reaching the design load. While in continuous beams the distribution of shear loads is not significantly influenced by steel overstrength, this is not the case for frames. The behaviour of frames may be

negatively influenced by steel overstrength if a redistribution of moments from the corner into the girder is assumed in design: if the frame is reinforced with steel having an overstrength, the assumed moment redistribution from the frame corner into the girder will not occur and the higher than assumed plastic bending moment in the frame corner must be taken up by the columns, of which bearing capacity may be reduced significantly.

(2.4) Ductility

The stress-strain characteristics of reinforcing steel have a major influence on the deformability of reinforced concrete members. Ductility of reinforcing steel is a basic requirement of various design procedures and some engineering approaches, which can be used only when the reinforced members are sufficiently ductile. The plastic deformation capacity of reinforced members is indispensable for:

- warning before failure of statically determinate and indeterminate structures by large deflections
- linear elastic analysis, which demands a certain ductility in plastic areas, because the actual distribution of moments differs from the assumed distribution for elastic behaviour due to concrete cracking and the subsequent change in distribution of stiffness along the member
- linear elastic analysis with moment redistribution, which requires a rotation capacity in the plastic areas to allow for the assumed degree of redistribution
- elasto-plastic analysis, which is based on the assumption of indefinite plasticity of the member
- equilibrium methods which are valid only if compatibility of displacements can be achieved (e.g. truss models, strut and tie models) – to apply these models the reinforcement needs to be ductile enough to allow for the change from elastic stress distribution to that assumed by the models (particular demand of ductility for shear reinforcement)
- resistance against imposed deformations (e.g. due to temperature, support settlement, shrinkage, creep), which requires plastic adaptability of the structure to avoid unacceptable stresses
- ability to withstand unforeseen local impact and accidental loading without collapse (robustness)
- redistribution of internal forces in statically indeterminate structures under fire attack
- energy dissipation under cyclic (e.g. seismic) loading

Considering big differences in the behaviour of reinforced concrete structures that can arise due to the variation in mechanical properties of steel, standards classify reinforcing steel with respect to its ductility. The main characteristics used in MC90 to judge ductility of steel are the uniform elongation at maximum load, i.e. the total (elastic and plastic) deformation obtained at maximum load just before necking starts (and the load decreases) ε_u and the ratio between tensile strength and yield stress i.e. the so-called hardening ratio of steel f_t/f_y. Based on minimum specified values for the characteristic value of these two parameters three ductility classes are defined in MC90 as follows:

- steel class B (low ductility steel) $(f_t/f_y)_k \geq 1.05$ and $\varepsilon_{uk} \geq 2.5\%$
- steel class A (normal ductility steel) $(f_t/f_y)_k \geq 1.08$ and $\varepsilon_{uk} \geq 5.0\%$
- steel class S (high ductility steel) $(f_t/f_y)_k \geq 1.15$ and $\varepsilon_{uk} \geq 6.0\%$

Note that ductility of reinforced concrete depends on other characteristics of steel as well. In particular bond behaviour and the shape of the stress-strain diagram are important influencing factors. Consequently, the ductility requirements given above for ductility classes B, A and S are valid only for ribbed reinforcement with a rib pattern according to EN 10080, as further discussed in Section 3.2.2 (2.1). With respect to the influence of the shape of the stress-strain diagram it has been shown that the required ductility of reinforced concrete structures can be achieved using reinforcing steel characterised by various combinations of f_t/f_y and ε_u and a lower value of f_t/f_y can be substituted by a higher value of ε_u and vice versa. Hence, in general it is not quite appropriate to judge ductility of steel in terms of two separated terms but rather a combination parameter should be used, see Cosenza et al (1992).

The minimum requirements on steel ductility follow from the ductility demand of the structure, which in turn directly depends on the method of static analysis. For the ductility classes defined in MC90, the following methods of structural analysis are acceptable:

- linear elastic design without redistribution for beams, frames and slabs
  - steel classes B, A and S may be used.
- linear elastic design with moment redistribution (without explicit check on the rotation capacity) for continuous beams and slabs
  - steel class B may be used with moment redistribution up to 10%
  - steel class A may be used with moment redistribution up to 20%
  - steel class S may be used with moment redistribution up to 30%
- plastic design for beams, frames and slabs
  - steel classes A and S may be used

In the past the rupture elongation (i.e. residual change of length after failure of the specimen related to the original measuring length measured over the rupture zone) was used to estimate the strain capacity of steel. Note that the value of the rupture elongation increases with decreasing measuring length and therefore the measuring length must be stated as well when giving values for the rupture elongation. Nowadays this parameter is not used anymore, since contrary to the pre-peak branch of the stress-strain diagram of steel the descending (post-peak) branch is neglected in design. This is done mainly due to the fact that the stress-strain characteristics of reinforcing steel beyond the peak stress are not well defined or not easy to assess. Hence, the post-peak deformation capacity of steel is used only as a safety margin, in particular to accommodate imposed deformations. The advantage of this approach is that in general imposed deformations do not have to be taken into account when designing for the ULS.

More information on the topic can be found in CEB Bulletin d'Information No.242 "Ductility of Reinforced Concrete Structures".

(3) Behaviour at extreme temperatures

The strength and deformation behaviour discussed until now is valid for the normal ambient temperature (20°C). Eurocode 2 allows using the properties of reinforcing steel valid for the normal ambient temperature in the temperature range between -40°C and 100°C. However, under elevated temperatures (for example fire) the stress-strain diagrams of steel change significantly (Fig. 3.2-10). The increase of deformations at constant loads and the decrease of stress values are observed (Fig. 3.2-11).

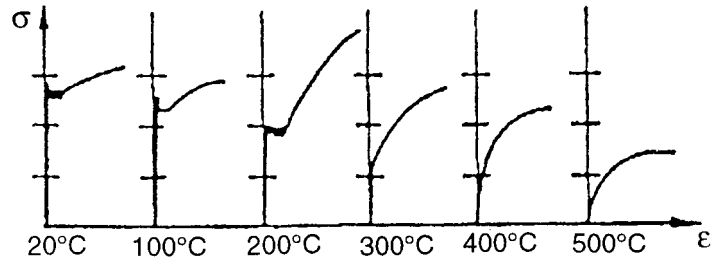

Fig. 3.2-10: Influence of high temperatures on stress-strain behaviour of steel, after Reinhardt (1973)

Therefore already at service load level plastic deformations can be expected which under certain circumstances may lead to the collapse of a structure. Note that after a cooling down period, modern types of reinforcing steel may recover their original strength nearly to 90%. More information on design aspects of steel behaviour under elevated temperatures is provided in Section 6.3.3, on design of concrete buildings for fire resistance steel.

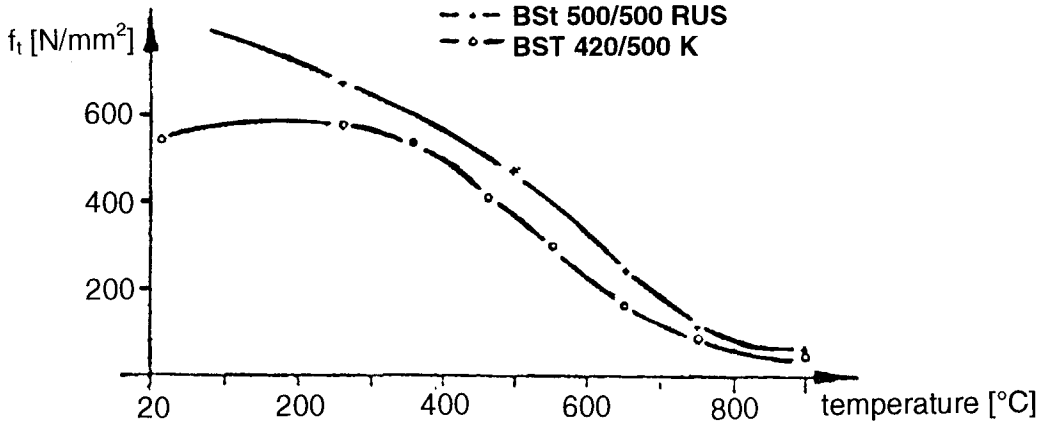

Fig. 3.2-11: Influence of high temperatures on tensile strength of steel, after Reinhardt (1973)

Under low temperatures (< 0°C) steel usually shows an increase of strength and after, an initial slight decrease, an abrupt drop of deformation capacity (Fig. 3.2-12).

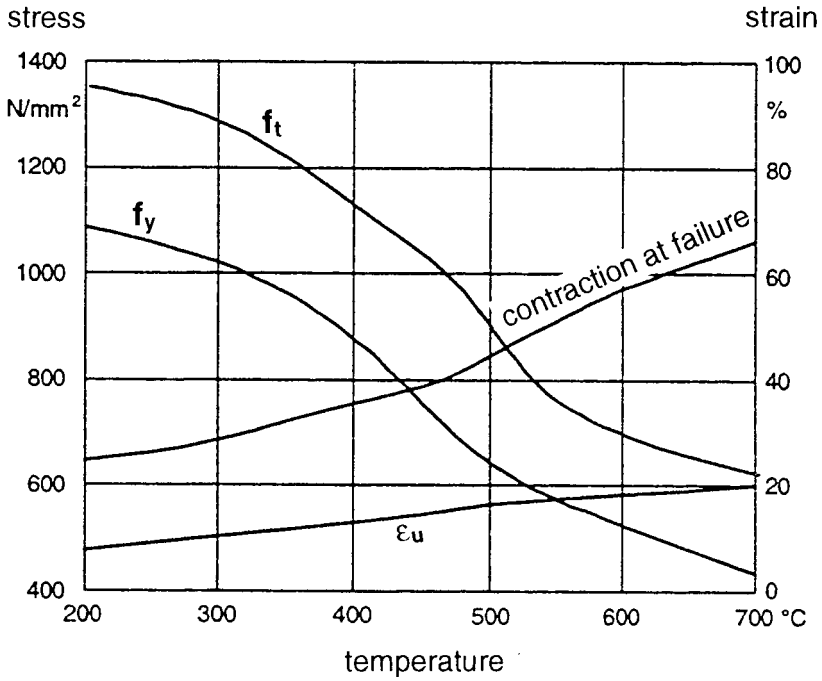

Fig. 3.2-12: Influence of low temperatures on the strength and deformation behaviour of steel, after Reinhardt (1973)

(4) Behaviour under impact loading

The deformations preceding failure of steel are time dependent. Plastic deformations occur slower than elastic deformations. Therefore increase of loading rate (decreasing time until failure) leads to a decrease of deformations and increase of strength, as shown on an example in Fig. 3.2-13. This is the reason why under impact loading with very high loading rates, such as explosions or impact of hard objects, brittle failure of steel may often occur.

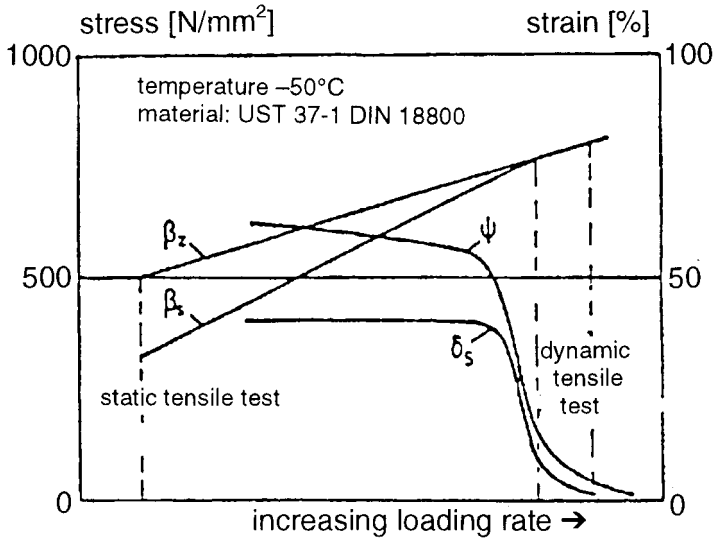

Fig. 3.2-13: Influence of loading rate on the strength and deformation behaviour of steel, after Reinhardt (1973)

(5) Fatigue behaviour

Many reinforced concrete structures are loaded not only by sustained loads (dead weight) but also by repeated loading, usually with changing load intensity and frequency (e.g. traffic). To judge fatigue performance of reinforcing steel the stress which can be endured for an indefinite number of load cycles is used. This so-called fatigue strength of steel is significantly lower than the static strength. However, as discussed more in detail in Chapter 4.4, Section 4.4.3 (4.1) on Fatigue - Fatigue Resistance of Steel, the fatigue is a rather complex phenomena. As a first step it has to be clarified which type of dynamic loading must be regarded: e.g. random loading, loading with a constant stress amplitude and a constant mean stress level, loading with a variable stress amplitude and a constant mean stress level or a low cycle fatigue. The last mentioned phenomenon occurs when the upper load of the oscillation is higher than yield load. Normally such a case will not take place with reinforcement, eventually under seismic loading. The most common yet most complicated case is random loading. For comparison, it was proposed to study the case where loading is conducted with a constant stress amplitude and a constant mean stress level, and the load changes in each cycle sinusoidal between upper and lower values.

The number of cycles until failure is recorded in series of so-called one-step-tests which are performed for the same mean stress level with various constant stress amplitudes (i.e. upper stress on different levels). When the number of cycles until failure is plotted as a function of the stress amplitude, it results in the well-known S-N-curves (also called Wöhler-lines). An example of such an experimentally obtained S-N-curve is shown in Fig. 3.2-14. Note that the upper load and the frequency of testing have an influence on the S-N-curve.

Note that the test conditions in a one-step-test differ from the conditions found in practice. Therefore multiple-steps-tests are sometimes performed in which the real loading conditions are modelled as closely as possible.

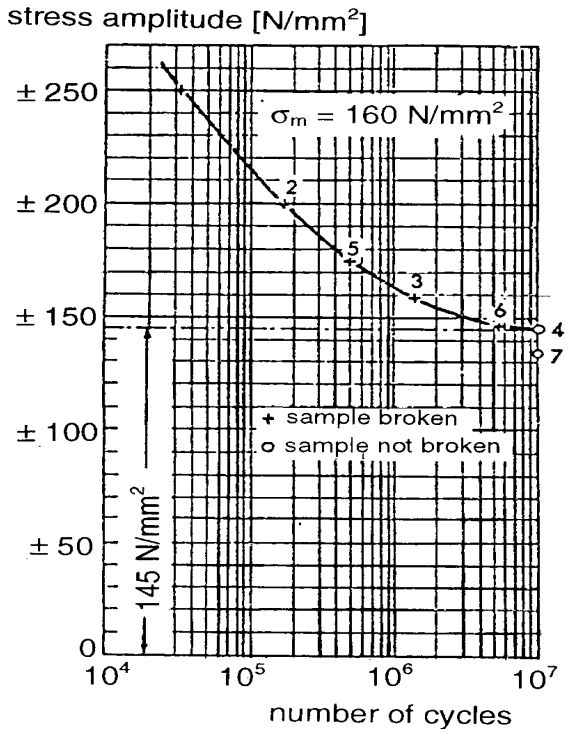

Fig. 3.2-14: Typical fatigue strength curve (S-N-curve, Wöhler-line) of a deformed reinforcing bar, after Reinhardt (1973)

The fatigue failure mechanism of reinforcing steel can be described in a simplified form as follows: at points of high stresses (e.g. mechanical notch, corrosion notch, material imperfection) a first short crack occurs which gradually grows into the material. The surface of this crack is smooth and fine. The crack grows until a suddenly failure of the remaining (reduced) cross section occurs. Therefore fatigue failure is brittle and there is no warning in a structure by large deformations. A typical example of a reinforcing bar that failed in fatigue is shown in Fig. 3.2-15.

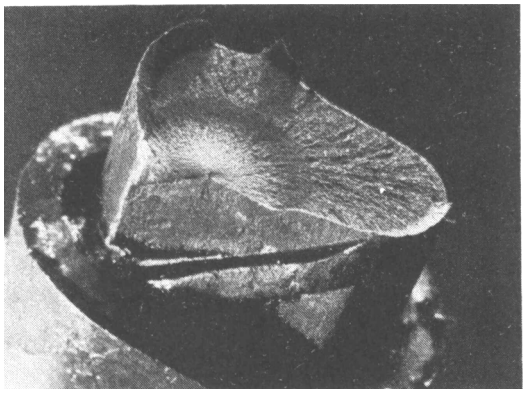

Fig. 3.2-15: Fatigue failure of a deformed reinforcing bar, after Reinhardt (1973)

As further discussed in Chapter 4.4, Section 4.4.3 (4.1) on fatigue – fatigue resistance of steel, there is a considerable scatter of fatigue strength in the tests. The fatigue behaviour of steel depends on different factors such as steel composition and production process, bar size, rib geometry, bending of bars and welded connections, thus making it difficult to give generalised S-N-curves. Experiments prove that fatigue strength is lower for specimens with ribs or notches than for smooth specimens and tends to decrease with increasing bar diameter. Furthermore, bent reinforcing steel has lower fatigue resistance than straight bars and the smaller the diameter of the mandrel the stronger the reduction of the fatigue resistance. It is experimentally shown that with a mandrel diameter of 5 times the bar diameter a reduction of fatigue strength with respect to that of a straight bar by 52-68% follows, while it is roughly the third of this ratio if the mandrel diameter is increased to 15 times the bar diameter (reduction of fatigue strength by 16-22% with respect to that of a straight bar). Moreover, while the static strength should not be negatively influenced by welding, it is unavoidable that the fatigue strength of reinforcing steel is significantly reduced due to the welding process. Finally, corrosion effects, as encountered in hazardous environments (i.e. in marine environment) negatively influence fatigue resistance of reinforcement.

The crucial question with respect to the analysis of reinforced concrete structures is whether the test results obtained on naked steel can be directly applied to embedded rebars. Experiments prove that the characteristic fatigue strength of steel embedded in concrete is 40 to 70% lower than its material fatigue strength. This reduction of fatigue strength is mainly caused by fretting corrosion effects.

The MC90 approach to modelling of fatigue behaviour and the characteristic fatigue strength curves given in MC90 are treated in Chapter 4.4, Section 4.4.3 (4.1) on fatigue – fatigue resistance of steel. Designers should draw their attention to the fact that the fatigue strength of the base material is changed if joints or anchors are applied. The fatigue resistance of joints can not be easily concluded from the fatigue resistance of the reinforcement. Some

developments of anchorages with high fatigue resistance have been done by means of resin and steel ball bearings. More information on this topic can be found in CEB Bulletin d'Information No.188 "Fatigue of Concrete Structures".

(6) Bond properties of reinforcing steel

(6.1) Surface characteristic of reinforcing steel

Steel can easily be provided with different surface configuration. Three shapes or surface characteristics of reinforcing steel are defined: plain, indented and ribbed. Plain reinforcement has smooth surface with no extrusions or indention. Indented reinforcing steel has well defined indentations uniformly distributed over the length. Normally at least two equally distributed rows of indentations are present and the indentations form an inclination with the bar axis of 40 to 60°. Most commonly used ribbed reinforcement has two or more rows of parallel transverse ribs equally distributed around the perimeter with a uniform spacing over the entire length. Longitudinal ribs may be present or not. The mainly used rib patterns are two or three rows of oblique ribs which are well rounded at their base. An appropriate shape of the rib is not only important to maintain bond but also for other mechanical and technological properties of reinforcing steel. Both bendability and fatigue strength of reinforcement depend to a certain extent on the rib geometry. The notch effect of ribs has to be reduced so that the bendability and fatigue strength are sufficiently assured. Therefore it is required that the transverse ribs have a crescent shape and merge smoothly into the core of the product (unless the same product properties can be achieved by other special surface configurations). The projection of the ribs shall extend over approximately 80% of the periphery of the product, which shall be calculated from the nominal diameter. The European standard EN 10080 require rib flank inclination α_s not less than 45° and radiused at the transition to the core of the product. The angle of rib inclination β_s shall be between 35° and 75°. The rib height h_s shall be 0.05Ø to 0.10Ø, the rib spacing c_s shall be 0.5Ø to 1.0Ø (Ø denotes the nominal diameter of the bar). Where longitudinal ribs are present, their height shall not exceed 0.15Ø.

Note that the arrangement of transverse ribs can be used for identification of steel classes: e.g. according to EN 10080 low ductility steel shall have two or more series of parallel transverse ribs and one (in case of two or three rib series) or two (in case of four rib series) of these series shall be at a contrary angle to the others, normal ductility steel shall have two or more series of parallel transverse ribs and the same direction for each series and high ductility steel shall have two or more series of parallel transverse ribs and one (in case of two or three rib series) or two (in case of four rib series) shall be at a contrary angle to the others. Some examples of typical rib patterns are given in Fig. 3.2-3.

(6.2) Relative rib area

Bond is the key to an optimisation of reinforcing action. Chapter 3.3, Section 3.3.2 on Bond Behaviour provides a detailed description of bond behaviour of reinforcing steel. As discussed in Chapter 3.3, Section 3.3.2 (1.1.6) on Influence of Reinforcement Geometry, the rebar geometry governs to a high degree the general bond behaviour and determines the bond resistance. Though even a plain surface of a rolled steel has enough surface roughness to guarantee some minimum adhesion, higher shear bond can be reached only with well optimised ribs or indentations. In particular the height of the ribs or indentations and their spacing are found to be the most important parameters in this respect. A coefficient has been

proposed that combines both influences and that reasonably describes the influence of the deformation pattern on the local bond behaviour, see Rehm (1961). The so-called projected rib area f_R is regarded as the ruling criterion for the bond performance of ribbed and of some indented products. The related rib area f_R is defined as the quotient of the axial projected area of the rib and the circumferential area of the bar. It has been proven that rib height and rib distance can be considerably changed without much influencing bond behaviour as long as the related rib area reminds approximately constant. With an increasing value of related rib area, bond strength and bond stiffness increase. It should be noted, however, that since the ultimate bond strength is reached at decreasing slip values, the bond becomes more brittle for increasing f_R. Also the splitting ability increases considerably with increasing values of related rib area.

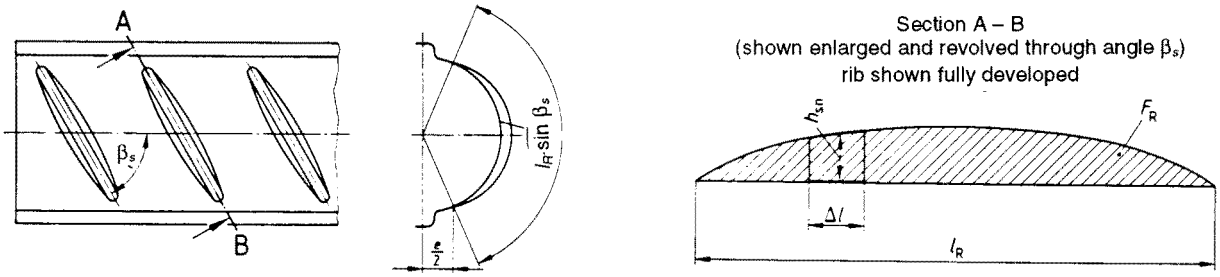

Fig. 3.2-16: The rib geometry and the method to calculate the relative rib area f_R for ribbed bars according to EN 10080

A more refined method to calculate the relative (or projected) rib area f_R provided in the European standard EN 10080 for ribbed bars makes use of the following formula (see also Fig. 3.2-16):

$$f_R = \frac{1}{\pi \cdot Ø} \cdot \sum_{n=1}^{k} \frac{\frac{1}{m} \sum_{l=1}^{m} F_{R(n,1)} \cdot \sin \beta_{s(n,1)}}{c_{s(n)}} + \frac{1}{j \cdot Ø} \cdot \sum_{n=1}^{i} h_{l(n)} \qquad (3.2\text{-}3)$$

where:

$Ø$	the bar diameter
β_s	the transverse rib inclination, i.e. the angle between the centre line of the transverse rib and the longitudinal axis of the bar
c_s	the transverse rib spacing, i.e. the distance between the centres of two consecutive transverse ribs measured parallel to the axis of the bar
h_l	the longitudinal rib height, i.e. the distance from the highest point of the rib to the surface of the core measured normal to the axis of the bar
j	the length of the pitch of the longitudinal rib on a twisted bar
k	the number of rows of transverse ribs around the perimeter
m	the number of transverse ribs in one row over the distance considered
i	the number of longitudinal ribs
p	the number of segments on the transverse rib considered
F_R	the cross-section area of a transverse rib in the plane of the rib axis defined as (Fig. 3.2-16):

$$F_R = \sum_{n=1}^{p} (h_{sn} \cdot \Delta l) \tag{3.2-4}$$

where:

h_s the transverse rib height, i.e. the distance from the mid-point of the considered segment on the rib to the surface of the core measured normal to the axis of the bar

Δl the rib length increment measured along the rib axis

Note that in the simplest form the value of the relative rib area f_R can be calculated as follows:

$$f_R = \gamma \cdot h_s / c_s \tag{3.2-5}$$

where:

γ bar geometry dependent constant, which should be provided by the producer (in usual cases ≈ 0.5)

h_s the maximum transverse rib height, i.e. the distance from the highest point of the rib to the surface of the core measured normal to the axis of the bar

c_s the transverse rib spacing

Ribbed bars or wires are considered as high bond bars if they satisfy the conditions and requirements imposed on the value f_R by the relevant standards or by approval documents. Bars not satisfying these requirements should be treated as plain bars with respect to bond. For indented bars and wires, which cannot be considered as high bond bars, reference should be made to relevant standards or technical approvals. The requirements for f_R as a function of the nominal diameter are given in Table 3.2-3 according to EN 10080.

Nominal diameter Ø [mm]	5 to 6	6,5 to 8,5	9 to 10,5	11 to 40
f_R	0,039	0,045	0,052	0,056

Table 3.2-3: Minimum required values of relative rib area f_R according to EN 10080

(6.3) Optimisation of bond

There is a clear link between the research done to determine the effect of rib geometry on bond and the requirements for currently produced ribbed steel bars. The limit values for the relative rib area which are given in the material standards for reinforcing steel (see Table 3.2-3) are optimised from the point of view of bond resistance and splitting ability in normal strength concrete and evolved from the extensive research on required performance of reinforced concrete structures under service load. Consequently, the research done in earlier times was restricted to the bond performance at serviceability limit state: short development and anchorage lengths were aimed at and small crack openings and overall deformations were secured.

However there are more requirements on bond than that considered in these studies. Currently more attention is dedicated to bond in ultimate limit state, which is significant for the ductility of the structure and e.g. the deformation capacity of plastic hinges. With respect to deformation capacity of structural members it is required that bond should ensure a high structural stiffness and small cracks under service loads, generate small splitting forces and allow full utilisation of reinforcement ductility at ultimate limit state. All these aspects can be influenced by changing the bond properties of reinforcing bars.

Since the requirements on bond partially contradict each other an optimisation of bond properties of reinforcing bars both in the elastic and in the plastic range of steel strains is necessary. This may require development of new types of rib pattern. In this optimisation process the unfavourable top bar effect on the bond behaviour and the fatigue strength of reinforcement must be considered. Since tension stiffening of small ribbed bars is very pronounced at large steel strains and may reduce significantly the ductility of a structure, special attention is needed for small bar diameters.

(7) Bendability

The essential difference between steel reinforcement and all other types of reinforcement (glass or carbon fibre etc.) is the plastic behaviour of steel. As to be seen from the stress-strain diagram, the elastic branch is not followed by a brittle rupture, but large plastic deformations can be developed. This not only ensures a ductile behaviour of reinforced concrete members but also enables bending and rebending of reinforcing steel.

Bendability is of high importance for normal reinforcing steel. All reinforcing steel must be suitable for bending at ambient temperatures. Particularly small diameter bars, which are used as stirrups must be capable to be bent on small mandrels. Bending is a local cold deformation and, hence, a reason for locally increased strength and locally reduced ductility. There is a large variety of tests to check bendability of reinforcement: some standards require a simple bend test while according to other specifications a rebend test should be executed with an artificial ageing before bending back. The European standard ENV 10080 order to check suitability for bending by the behaviour of a reinforcing product in a rebend test, where the material is bent through approximately 90° over a mandrel, aged and then bent back at least 20°. The required mandrel diameter for this rebend test varies with the bar diameter from 5Ø for diameter Ø = 4 to 16 mm, 8Ø for diameter Ø = 16 to 25 mm, up to 10Ø for diameter Ø = 25 to 40 mm.

The currently produced reinforcing steel usually provides the user the necessary capacity to sustain bending to a radius not less than specified in standards. For that reason reinforcing bars should not be bent to a radius less than that required by material codes for the relevant rebend tests. In several cases and at some types of continuity sets rebending to straight bars is done. This rebending is generally possible if the radius of the previous bending pin is increased by a factor 1.5 and rebending is carefully performed. Note that bending and rebending at increased temperature results in a reduction of strength.

Bending of wire fabric is possible under the condition that at least a minimum distance between weld and the beginning of the bend is kept. Bends at welds should be omitted, though if large radii are used (>100Ø) rebars can be bent at welds as well. For more details see Chapter 4.5, Section 4.5.2 (6) on Detailing Principles – Allowable Mandrel Diameter.

(8) Weldability

Most of the reinforcing steels are weldable. This is in some cases necessary, because their production process includes welding (wire fabrics, lattice girders). On the other hand the aptitude for welding is very useful in prefabricating cages and other reinforcement. The weldability of steel is mainly governed by its chemical composition, in particular the content of carbon (C) and of steel impurities, such as sulphur (S), phosphorus (P) and nitrogen (Ni). Therefore most standards for reinforcing steel define the grades as weldable depending on the content of these chemical elements and other alloying components. In this respect the carbon equivalent value C_{eq} is introduced. It can be computed with the following formula:

$$C_{eq} = C + \frac{Mn}{6} + \frac{Cr + Mo + V}{5} + \frac{Ni + Cu}{15} \tag{3.2-6}$$

where the symbols of the chemical elements indicate their content in percent by mass (C – carbon, Mn – manganese, Cr- chromium, Mo – molybdenum, V – vanadium, Ni – nitrogen, Cu – copper).

Various standards differ in limiting the value of C_{eq} for weldable steel. Table 3.2-4 specifies the maximum content of major components in weldable reinforcing steel according to EN 10080. Note that not only the equivalent carbon value is limited, but also the contents of carbon (C), sulphur (S), phosphorus (P) and nitrogen (Ni) are restricted (higher nitrogen (Ni) contents are permissible if sufficient quantities of nitrogen binding elements are present). The steel is considered weldable provided the values specified by the standards are not exceeded. This suitability applies for example for arc welding, flash welding, friction welding and electrical resistance welding. Note that in general, depending on the type of reinforcement used, the methods for welding may be restricted, since every welding method requires specific quality of steel. For instance reinforcing steels can be welded by flash butt welding if carbon (C) content is lower than 0.60%, sulphur (S) and phosphorus (P) contents are in total lower than 0.12% and silicon (Si) content is lower than 0.60%.

Type of analysis	Equivalent carbon C_{eq} [%]	Carbon (C) [%]	Sulphur (S) [%]	Phosphorus (P) [%]	Nitrogen (Ni) [%]
Cast analysis	0.50	0.22	0.050	0.050	0.012
Product analysis	0.52	0.24	0.055	0.055	0.013

Table 3.2-4: Chemical composition of weldable reinforcing steel according to EN 10080 (max. content in proportions by mass)

(9) Corrosion resistance of reinforcing steel

Just as iron can only be found in the form of oxides in nature, all unprotected carbon-steel products under normal conditions tend to form more stable oxides as well. Concrete provides to some extend protection of reinforcement against corrosion. As discussed more in detail in Chapter 5 on Durability, due to high alkalinity of non-carbonated concrete steel in concrete is protected against corrosion by passivation, i.e. by a microscopic oxide layer (so-called passive layer) which is formed on the steel surface if the pH–value of the pore-water is sufficiently high. This passive layer impedes the dissolution of iron. Therefore corrosion of reinforcement is

impossible, even if all other preconditions for corrosion are met. If due to carbonation or by the action of chloride-ions the pH-value drops locally or over greater surface areas of the reinforcement below 9, or if the chloride (Cl) content exceeds a critical value, the passive layer and the corrosion protection get lost. Consequently, corrosion of reinforcement is possible, if sufficient moisture and oxygen are available.

All aspects related to physical and chemical processes in concrete and their influence on corrosion process as well as protective measures to prevent severe effects of corrosion are extensively treated in Chapter 5.

Note that corrosion of steel not only results in a reduction of the steel cross-section and hence, a reduced load bearing capacity of rusted bars. The fatigue strength and deformation capacity of steel under static loading are even more sensitive to corrosion than the load bearing capacity. Last but not least, occurrence of splitting cracks due to volume increase of corrosion products may cause longitudinal splitting cracks in the bar anchorage zone and lead to the bond failure, with all its structural consequences.

The corrosion resistance of rebars can be increased by modifying the chemical composition of the steel or by applying a metallic or organic coating on their surface. Three types of reinforcing bars with a higher corrosion resistance than the common carbon-steel can be used as a preventive method under conditions of high environmental aggression, or when a long service life is requires: the stainless steels, the galvanised steel and the epoxy-coated rebars. Characteristic properties of these specific products are discussed in Section 3.2.6.

(10) Thermal expansion

If steel is heated or cooled down it extends or, respectively, contracts in all directions. The temperature strain ε_{sT} is in both cases given by the expression:

$$\varepsilon_{sT} = \alpha_{sT} \Delta T \tag{3.2-7}$$

where:

α_{sT} coefficient of thermal expansion of steel
ΔT temperature increment

From the temperature strain ε_{sT} the temperature elongation Δl_T over the length l can be computed according to:

$$\Delta l_T = \varepsilon_{sT} l \tag{3.2-8}$$

Within the temperature range from –20 to 180°C the coefficient of thermal expansion of steel may be taken as $\alpha_{sT} = 10 \cdot 10^{-6}$ m/(m°C). Note that the value of coefficient of thermal expansion of steel corresponds with that of concrete, which for the purpose of structural analysis may be taken as well as $\alpha_{cT} = 10 \cdot 10^{-6}$ m/m°C. Conductivity for heat of steel can be taken as $\lambda^R = 60$ W/m°C.

(11) Influence of straightening

The Eurocode 2 requirements on properties of steel apply to the product in the condition in which it is placed in the hardened concrete. If site operations can affect the properties of the reinforcement, then those properties shall be verified after such operations. For instance in case of coiled rods, the requirements apply to the material after straightening. The characteristic values of tensile strength f_{tk}, yield stress f_{yk} and total elongation at maximum load ε_u are meant in this respect. Note that the over-quality of semi-finished coiled products is required to reach desired characteristics of the product after straightening, see Section 3.2.1 (2.2.4). Furthermore, poor straightening of ribbed bars and wires from coils can significantly reduce the projected rib area and thus the bond properties of the straightened bars or wires.

3.2.3 Classification of reinforcing steel

(1) CEB-FIP Model Code 1990

MC90 classifies reinforcing steels on the basis of their size, characteristic yield stress f_{yk}, ductility properties, surface type (and bond characteristics) and weldability. The steel grade according to MC90 denotes the value of the specified characteristic yield stress in N/mm^2. MC90 contemplates reinforcing steel up to grade 500. Table 3.2-5 gives an overview of classification of the reinforcing steel provided in MC90.

Property	Classification
size (nominal diameter Ø)	Unlimited
characteristic yield stress f_{yk}	up to 500 N/mm^2
grade	up to 500
ductility	class A: $(f_t / f_y)_k \geq 1.08$ and $\varepsilon_{uk} \geq 5.0\%$ class B: $(f_t / f_y)_k \geq 1.05$ and $\varepsilon_{uk} \geq 2.5\%$ class S: $(f_t / f_y)_k \geq 1.15$ and $\varepsilon_{uk} \geq 6.0\%$
surface conditions	plane indented ribbed
bond properties	high bond bars: $f_R \geq f_R$ prEN 10080, ENV 10080 plain bars: $f_R < f_R$ prEN 10080, ENV 10080 indented bars
weldability	weldable non-weldable

Table 3.2-5: Classification of reinforcing steel according to MC90

(2) European normative regulations

The mechanical and technological properties of reinforcing and prestressing steels are defined by specific material standards and are generally secured by certification schemes and certificates of compliance. In general the European standards base the classification of steel

on similar parameters. Note that the exact definitions of the parameters may slightly different, as already discussed in the preceding sections.

Property	Class A	Class B	Class C
size (nominal diameter d)	4 to 16 mm	6 to 40 mm	6 to 40 mm
yield strength R_e	500 N/mm^2	500 N/mm^2	450 N/mm^2 and $R_{e,act} / R_{e,\,nom} \leq 1.20$
grade	500	500	450
ratio R_m / R_e	≥ 1.05	≥ 1.08	≥ 1.15 and ≤ 1.35
total elongation A_{gt}	2.5%	5.0%	8.0%
surface conditions	ribbed indented plain	ribbed	ribbed
required projected rib area f_R for ribbed surface	0.039 to 0.056		
fatigue stress range for ribbed rebars $2\sigma_A$	150	150	100

Table 3.2-6: Required properties of reinforcing steels, after EN 10080

Property	Class A	Class B	Class C
size (nominal diameter Ø)	unlimited (> 5 mm)		
yield strength f_{yk} or $f_{0,2k}$	400 to 600 MPa		
grade	400 to 600		
ratio $k = (f_t / f_y)_k$	≥ 1.05	≥ 1.08	≥ 1.15 and < 1.35
total elongation A_{gt}	2.5%	5.0%	7.5%
surface conditions	ribbed		
minimum related rib area f_R	0.035 to 0.056		
fatigue stress range (for N ≥ $2 \cdot 10^6$ cycles) with an upper limit of $\beta\, f_{yk}$	≥ 150 for bars and de-coiled rods ≥ 150 for wire fabrics		

Table 3.2-7: Required properties of reinforcing steels after Eurocode 2 (the values of f_{yk}, fatigue stress range with an upper limit of βf_{yk} and β for use in a Country may be found in its National Annex; the recommended value of β is 0.6)

The European standards for steel for reinforcing and prestressing of concrete are still under discussion. The referred to EN 10080 for reinforcing steel reflect the most recent State-of-Art in the field of standardisation of steel production. They specify the requirements for weldable reinforcing steel used for the reinforcement of concrete in form of bars and coils, welded fabrics and lattice girders. Table 3.2-6 provides an overview of major properties of reinforcing steel as defined in EN 10080. Table 3.2-7 provides an overview of major properties of reinforcing steel as defined in Eurocode 2. It specifies the requirements for ribbed weldable reinforcing steel used for the reinforcement of concrete in form of bars and de-coiled rods and welded fabrics and lattice girders made with ribbed bars. Note that the steel class indications and symbols used in Eurocode 2, EN 10080 and MC90 may differ. For comparison of symbols used in European standards and in the MC90 see Table 3.2-A1 at the end of this Chapter.

3.2.4 Essential properties of prestressing steel

(1) European normative references for prestressing steel for concrete structures

Besides chemical composition, geometrical properties and similar mechanical and technological properties as in the case of reinforcing steel, European standard prEN 10138 (2000) for prestressing steel requires to additionally determine special properties such as isothermal stress relaxation, deflected tensile resistance and stress corrosion resistance. Test methods to determine these characteristics shall be in accordance with ISO 15630 (tensile properties, bending, reverse bending) and prEN 10138 (fatigue and special properties of prestressing steel). In the following main characteristics of prestressing steel are discussed in detail.

(2) Behaviour under static loading

(2.1) Stress-strain behaviour

Depending on the production process the shape of the stress-strain diagram of prestressing steel in tension resembles either this of hot-rolled or heat treated steel or that of the cold–formed ordinary reinforcing steel, both discussed in Section 3.2.2 (1.1.1). Examples of stress-strain diagrams for different prestressing steel types are given in Fig. 3.2-17.

As in case of ordinary reinforcing steel, Hook's law describes the tress-strain relationship of prestressing steel in the elastic range of strains. Note that the modulus of elasticity of prestressing reinforcement differs from that of ordinary reinforcing steel. In case more precise information is not available, the modulus of elasticity E_p may be taken as 205 000 N/mm^2 for bars and wires and 195 000 N/mm^2 for prestressing strands.

Though in some cases for lower strength prestressing steel (e.g. grade 1030 in Fig. 3.2-17) transition from elastic to plastic steel strain range takes place with some distinct yielding, the length of the yield plateau is never significant and hardening starts almost immediately after yielding. The knowledge of the first deviation from the elastic stiffness is of high importance for design, e.g. with respect to creep and relaxation phenomena. For prestressing steel it is most usual to use the 0.1%-proof stress $f_{p0.1}$ (i.e. stress at a plastic deformation of 0.1%) as a conventional value that defines yielding of prestressing steel. The value of 0.2%-proof stress $f_{p0.2}$ (i.e. stress at a plastic deformation of 0.2%) can also be used to characterise deformation behaviour of reinforcing steel. For convenience in presentation, the relevant for the used type of

steel conventional value of $f_{p0.1}$ or $f_{p0.2}$ is often denoted as f_{py}. The characteristic tensile strength f_{pt} is derived from the characteristic failure load using the nominal diameter of the reinforcement.

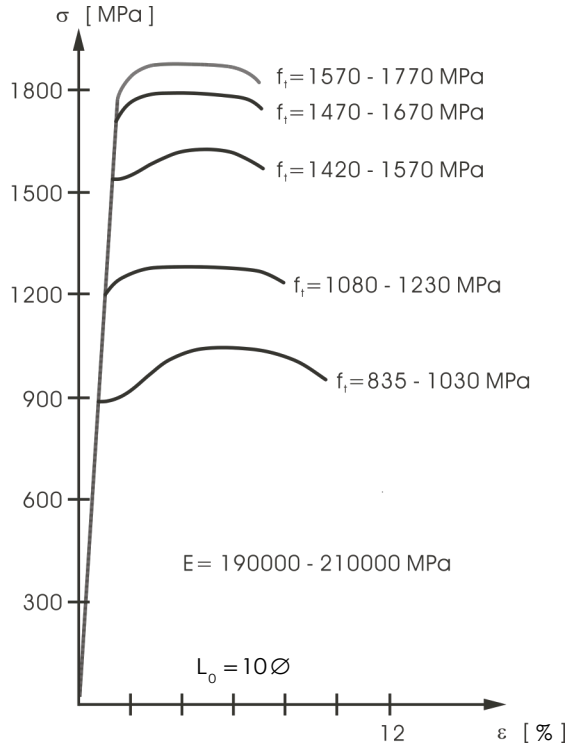

Fig. 3.2-17: Stress-strain diagram for different types of prestressing steel, after Leonhardt (1980)

Just as for ordinary reinforcing steel, after the maximum load has been reached necking takes place and the stress, calculated on the basis of the original cross-section decreases. Rupture of prestressing steel takes place when the strain capacity of the material in the most exhausted section is reached.

(2.2) Modelling behaviour under static loading

MC90 allows for calculation purposes to replace the actual stress-strain diagram of prestressing steel by an simplified schematic diagram according to Fig. 3.2-18, assuming a modulus of elasticity E_p equal to 205 000 N/mm^2 for prestressing wires or 195 000 N/mm^2 for prestressing strands. The simplified bi-linear diagram shown in Fig. 3.2-18 is valid for temperatures from –20 to 100°C. Note that MC90 permits as an alternative to the idealised stress – strain relationship to use the duly factored actual stress-strain diagram of prestressing steel.

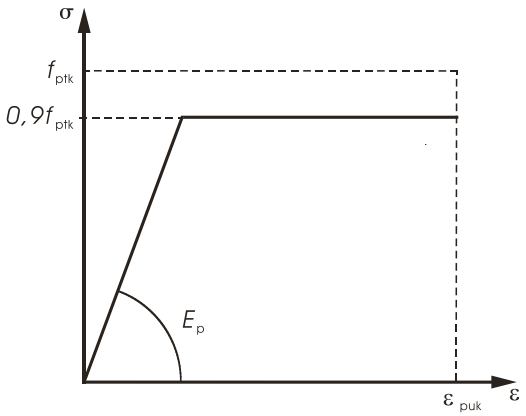

Fig. 3.2-18: Schematic stress-strain diagram for prestressing steel, after MC90

The tensile properties of prestressing steel shall comply with the requirements given in material standards. For quality control purposes and design calculations, the strength characteristics of a product given in these standards, (i.e. tensile strength f_{pt} maximum load $F_{p,max}$ characteristic 0.1% proof load $F_{p0.1}$ and characteristic proof load $F_{p0.2}$) are referred to the nominal cross-section of the product. Note that for all types of prestressing reinforcement the nominal diameter is defined as the diameter of a plain circular cylinder of the same weight per unit length as the prestressing unit.

MC90 uses the values of the characteristic tensile strength f_{pt} (which also defines the grade of prestressing steel) and the value of the characteristic 0.1% proof-stress $f_{p0.1}$ to classify prestressing steel. Characteristic values are denoted f_{ptk} and $f_{p0.1k}$, respectively, and correspond to the 5% fractile. MC90 requires that the condition $f_{p0.1k} \geq 0.80\ f_{ptk}$ should be fulfilled. The value of $0.9\ f_{pt}$ is generally assumed to be a good estimate for $f_{p0.1}$. For design purposes $0.9\ f_{pt}$ may even be used to estimate $f_{p0.1}$, though MC90 differentiates between cold-drawn stress-relieved wires and stress-relieved strands giving the indicative values of the ratio $f_{p0.1} / f_{pt}$ equal to 0.86 and 0.85 for wires and strands, respectively. Indicative force – strain diagrams for prestressing wires and strands postulated in MC90 are given in Fig. 3.2-19.

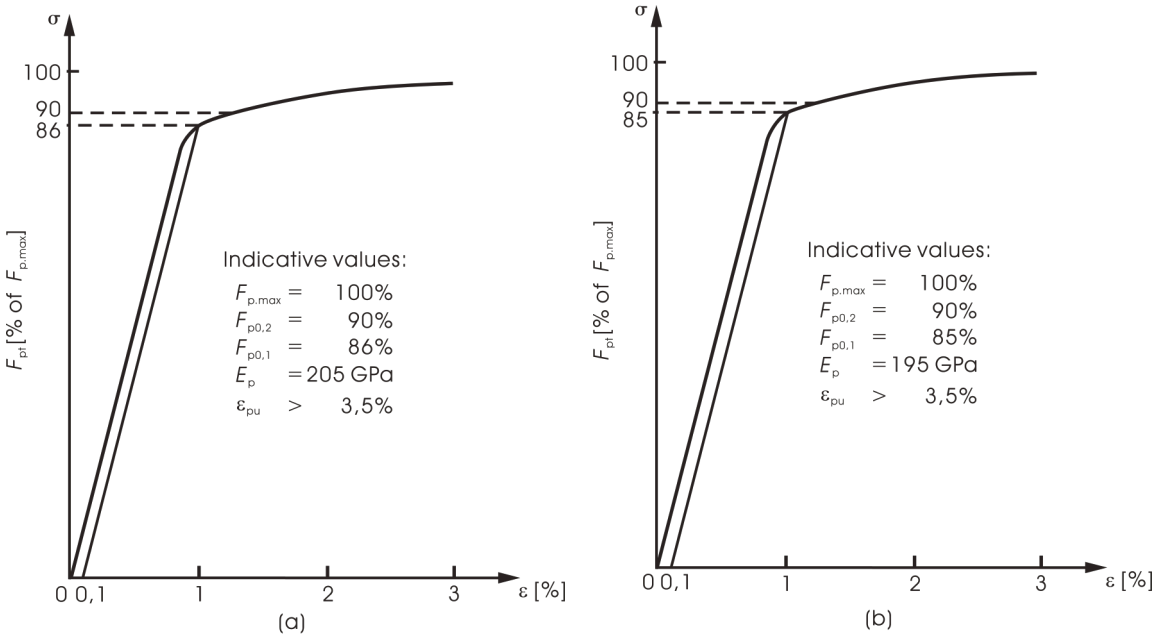

Fig. 3.2-19: Provided in MC90 indicative force-strain diagram a) for cold-drawn stress-relieved wires b) for stress-relieved strands

(2.3) Ductility

Though for prestressing steel bending shall be avoided and stress limit is kept below yielding, a certain robustness of prestressing reinforcement is required. The ductility of prestressing steel must enable curving of the prestressing tendons to the radius chosen and allow anchoring of prestressing steel with rolled threads and wedges. Note that if curvatures are necessary, the radius has to be so large that steel remains in an elastic condition. Both prEN 10138 and MC90 demand, as indicated in Fig. 3.2-19, that the unit elongation of prestressing steel at maximum load ε_{uk} for each type of reinforcement shall be at least equal to 0.035 and, hence, a ductile break shall be visible to the unaided eye. Moreover, for quality control purposes bend tests (for bars) and reverse bend tests (for wires) are common practice. These tests permit a good estimation of the ductility of prestressing steel though not being used as performance characteristics. The minimum number of reverse bends required by MC90 equals 4 for smooth wires and 3 for indented wires. Last but not least, the behaviour of prestressing steel under multiaxial stresses must be adequately good, as discussed more in detail in the following Section.

(2.4) Behaviour under multiaxial stresses

Multiaxial stresses occur in the area of bent or anchored prestressing steel, in particular at deviators, at saddles or in sharply curved bundles of wires. The extent of these combined stresses depends on the design and the grouping of the tendons. In order to judge the behaviour of prestressing reinforcement – specifically strands –prEN 10138 and MC90 require that a so-called deflected tensile test is executed. In this test a piece of strand is deflected through an angle of 20° over a grooved mandrel approximately half way along its length and is subjected to a tensile load until fracture of at least one wire occurs. The load at fracture is compared with that obtained on an (unbent) uniaxial tensile test. In the evaluation of the test results the deflected tensile load coefficient D is used, which is calculated as:

$$D_i = \left(1 - \frac{F_a}{F_{mm}} \right) \cdot 100 \qquad [\%] \tag{3.2-9}$$

and

$$D = \sum_{i=1}^{n} \frac{D_i}{n} \qquad [\%] \tag{3.2-10}$$

where:

D	the mean value of n individual results D_i from at least 5 tests
D_i	the deflected tensile load coefficient of an individual test piece
F_a	the maximum load measured at the active side during a deflected tensile test
F_{mm}	the mean value of at least two individual results F_m
F_m	the maximum load in the uniaxial tensile test

PrEN 10138 requires that the maximal D-value of the deflected tensile test for 7-wire strands ≥ 12.5 mm and for compacted strands under normal application shall not be more than 28%. For stay cables and other special applications a maximum D = 20% is permitted.

(2.5) Long-time loading

(2.5.1) Creep

The strength and deformation behaviour obtained in static short time tests may not be valid for long time loading. One of the time-dependent effects is creep, i.e. the increase of deformations under a constant load (compare references related to concrete). Fig. 3.2-20 shows schematically the increase of strain as a function of time for different values of tensile stress. Under permanent tensile stresses and in relation to the ambient temperatures creep deformations occur and the strength is reduced to the so-called endurance strength, i.e. the stress which a material can endure under a certain temperature over an infinite long period of time.

For prestressing steel, however, the difference between endurance strength and short time strength is negligible for normal ambient temperatures (20°C). Moreover, under normal temperature considerable creep deformations can occur only for stresses larger than yield stress.

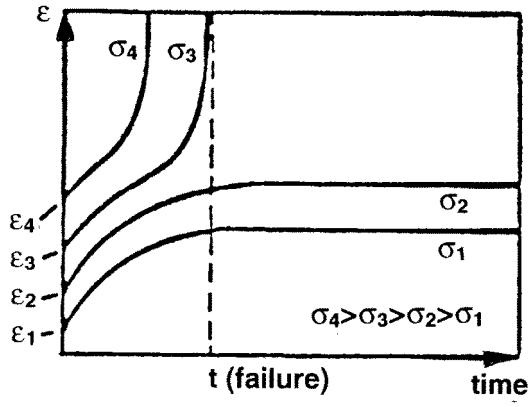

Fig. 3.2-20: Increase of strain as a function of load duration; parameter is the permanent tensile stress, after Leonhardt (1980)

(2.5.2) Relaxation

If an induced deformation is kept constant, the stress (load) decreases with time. This effect is called relaxation. Though a characteristic for all types of steel, the relaxation behaviour is interesting especially for prestressing reinforcement. While nowadays it is a common convention to use relaxation behaviour to describe the time dependent change in length and stress of prestressing steel, in former times the creep behaviour has been tested instead. Note that both approaches are not quite realistic to be applied to prestressed concrete, since in practice there is neither a deformation nor a stress being kept constant.

The relaxation is expressed in a percentage loss of the initial stress (load). The closer the initial stress approaches f_{py} the higher the relaxation. A second very important influence on the relaxation behaviour of steel is the temperature. The relaxation increases substantially with increasing temperatures. This has to be taken into consideration if prestressed concrete elements are subjected to a high temperature (e.g. by sunshine or fire). The influence of the initial stress and the temperature on stress decrease in time (relaxation) is shown in Fig. 3.2-21.

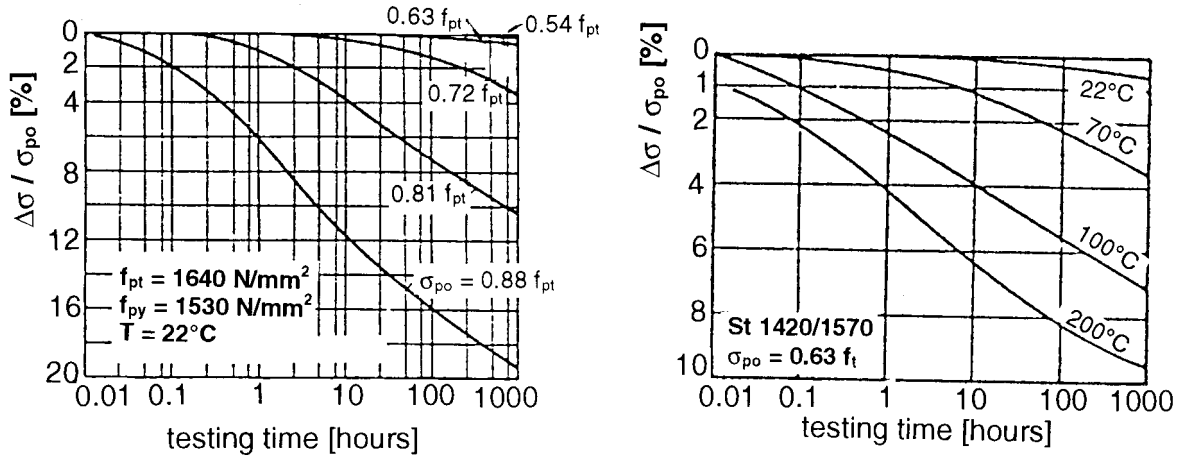

Fig. 3.2-21: Decreases in time of stress $\Delta\sigma$ related to the initial stress σ_{po}, after Leonhardt (1980):
a) as influenced by the initial stress σ_{po},
b) as influenced by the ambient temperature ϑ

The relaxation behaviour of prestressing reinforcement is tested under well defined conditions in a relaxation test. The test is carried out by subjecting a specimen of prestressing steel to an initial load. The load is applied in several steps. The strain as a reaction of the initial load and the temperature are maintained constant for the prescribed duration of the test. Normal tests last for 1000 hours. The loss in load is expressed as a percentage of the initial load and as a function of time. In Fig. 3.2-22 it can be seen how strong the influence of the initial stress on the relaxation is.

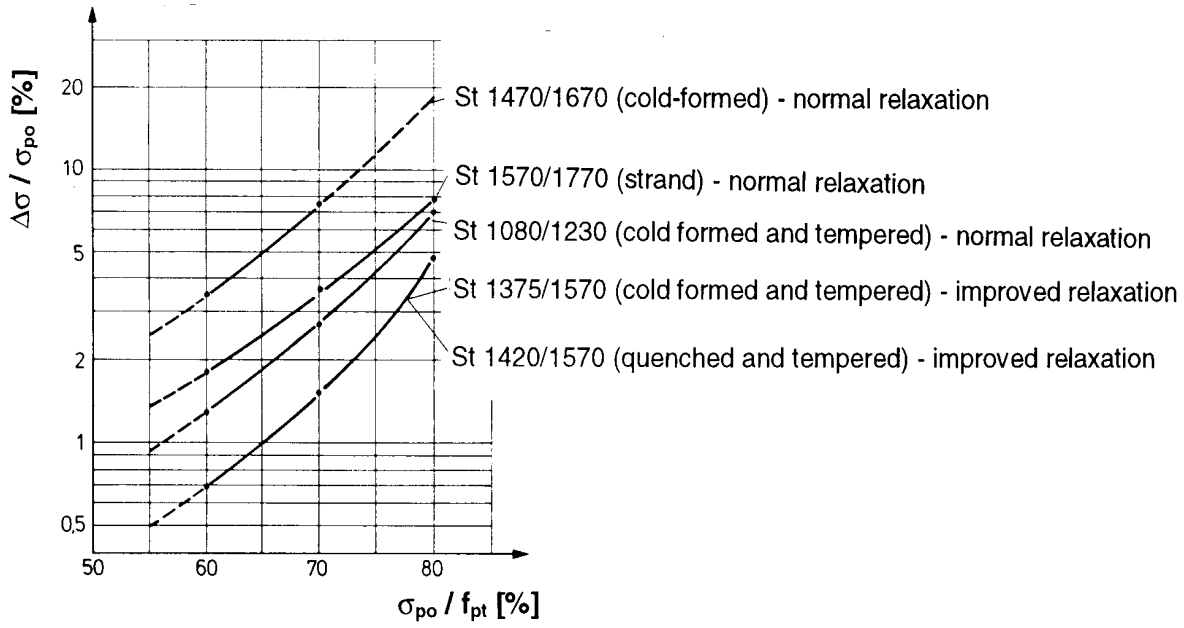

Fig. 3.2-22: Decreases of stress $\Delta\sigma$ after 1000 hours related to the initial stress σ_{po} as a function of initial stress σ_{po} related to f_{pt} for different types of prestressing steel, after Leonhardt (1980)

An indication of how relaxation varies with time is given in Table 3.2-8.

Time in hours	1	5	20	100	200	500	1000
Relaxation losses related to the loss at 1000 hours	0.25	0.45	0.55	0.70	0.80	0.90	1.00

Table 3.2-8: Relationship between relaxation losses and time, after MC90

Prestressing steel is usually classified in relaxation classes according to test results obtained at 1000 hours, an initial load of 0.6, 0.7 or 0.8 of the actual rupture load and at a constant temperature of 20°C. For design purposes MC90 distinguishes between three relaxation classes, defined as follows:

- class 1: normal relaxation characteristics for wires and strands
  loss of stress corresponding to 0.6, 0.7 and 0.8 f_{ptk} of not more than 4, 8 and 12%, respectively
- class 2: improved relaxation characteristics for wires and strands
  loss of stress corresponding to 0.6, 0.7 and 0.8 f_{ptk} of not more than 1, 2 and 5%, respectively
- class 3: relaxation characteristics of bars
  loss of stress corresponding to 0.6, 0.7 and 0.8 f_{ptk} of not more than 2, 4 and 7%, respectively

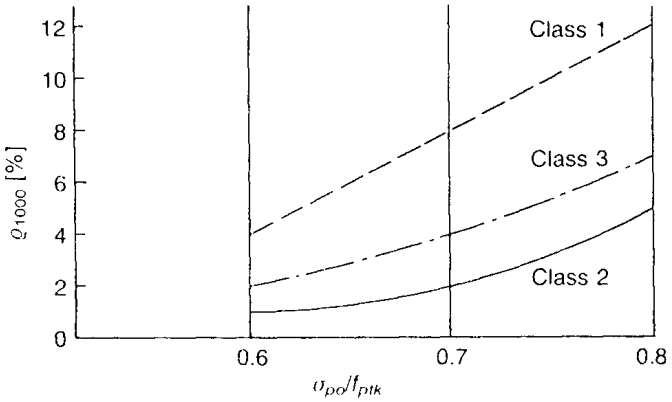

Fig. 3.2-23: Relaxation losses for different relaxation classes as a function of initial stress level after 1000 hours and at temperature of 20°C, according to MC90 (design values)

Fig. 3.2-23 shows the corresponding permanent design stress - relaxation curves, as given in MC90. Normally, the long-term values of the relaxation losses are taken from long-term tests. However, for an estimate of the relaxation up to 30 years the following formula may be applied:

$$\rho_t = \rho_{1000}\left(\frac{t}{1000}\right)^k \qquad (3.2\text{-}11)$$

where:

ρ_t the relaxation after t hours

ρ_{100} the relaxation after 100 hours

ρ_{1000} the relaxation after 1000 hours

$k \approx \log(\rho_{1000} / \rho_{100})$

In the absence of more exact information the value of the coefficient k can be taken as 0.12 for relaxation class 1 and 0.19 for relaxation class 2 (classification according to MC90). Note that MC90 allows assuming that the relaxation after 50 years and more is approximately three times the relaxation after 1000 hours.

(3) Behaviour under extreme temperatures

The mechanical properties of prestressing steel such as the strength, yield point, proportionality limit and elastic modulus do not change appreciably when the ambient temperature various over a reasonable range.

(4) Fatigue behaviour

For all structures in reinforced or prestressed concrete which are submitted to dynamic loads (stresses) it is important to know the behaviour of both steel and concrete under repeated loading. Just as in case of reinforcing steel, discussed in detail in Section 3.2.2 (1.3), fatigue resistance of prestressing reinforcement is defined by a number of cycles of a dynamic load which lead to rupture of a specimen, even if the maximum stress does not exceed the yield stress. In order to provide the designer with sufficient information a lot of parameters must be taken into account.

MC90 approaches modelling of fatigue performance of prestressing reinforcement in a similar way as in case of reinforcing steel. The characteristic fatigue strength curves (i.e. the so-called S-N-curves) are proposed that can be described by the same function as in case of ordinary reinforcement, see Chapter 4.4, Section 4.4.3 (4.1) on Fatigue - Fatigue Resistance of Steel. Obviously, due to the different steel composition, deformation behaviour and geometry of the prestressing products, the values of parameters used to define the exact shape of the S-N-curves change. As mentioned in Section 3.2.2 (1.3), the characteristic fatigue strength (stress range) in case of embedded reinforcement is lower than that measured for the basic material in naked conditions. The characteristic fatigue strength of naked prestressing reinforcement for $2 \cdot 10^6$ cycles, with a maximum stress being $0.7 f_{ptk}$ is shown in Table 3.2-9, as given in MC90 for different types of prestressing products.

Basic material	$\Delta\sigma$ [N/mm^2]
Smooth bars	200
Ribbed bars	180
Wires (cold-drawn or hot-rolled) - smooth - indented	 200 180
Strands - from smooth wires - from indented wires	 190 170

Table 3.2-9: Characteristic fatigue strength of naked prestressing reinforcement for $2 \cdot 10^6$ cycles, with a maximum stress of $0.7 f_{ptk}$, after MC90

Note that the lower values of the characteristic fatigue strength provided for curved tendons compared with that given for straight tendons take into account the effect of fretting corrosion which results from the lateral pressure and slip between prestressing strands and/or ribs of the steel sheaths.

(5) Bond properties of prestressing reinforcement

While discussing bond properties of reinforcing steel, distinction should be made between post-tensioned and pretensioned prestressing steel, since the two types of reinforcement significantly differ with respect to the prestress transfer and the force anchorage mechanism. Note that while the efficiency of pretensioned reinforcement fully depends on the bond between tendon and concrete, the post-tensioned reinforcement only partially relies on the bond between tendon and grout matrix or are unbonded. Examples of bonded and unbonded tendons are given in Fig. 3.2-24. Note that pretensioned and post-tensioned tendons differ with respect to the transverse deformations (Poisson effect). Implications of the level of stress in prestressing reinforcement on its bond behaviour are discussed in detail in the Section 3.3.2 (1.1.7) on Bond Behaviour and Models - Influence of Stresses Level in the Reinforcing Unit.

With respect to force transfer mechanism of bonded prestressing reinforcement it should be distinguished between ribbed prestressing bars and wires, indented or smooth bars and wires, and indented or smooth strands. Smooth, indented and ribbed prestressing steel behave in principle similar to ordinary reinforcement with the same type of surface deformation. Somehow different is the behaviour of prestressing strand with helical outer wires. Unlike in the case of ribbed reinforcement, where bond relies mainly on rib bearing, bond of prestressing wire strands with no lugs or indents can mainly be ascribed to friction that is activated after loss of initial bond. Contrary to smooth reinforcement, however, radial compressive stress connected to friction is additionally caused by: wedging action due to irregular shape of the strand (lack of fit as a result of the larger diameter of centre wire, varying pitch) and pitch effect (change of pitch when steel stress changes is prevented by the surrounding concrete, both when steel stress is decreased or increased). When the roughness of the tendon is increased (e.g. by means of indents or lugs) a transition between the frictional mechanism of plain wires and strands and the rib bearing mechanism of ribbed bars can be assumed as far as the bond mechanism is considered. More detail discussion of Bond of Prestressing Strands is to be found in Chapter 3.3 Section 3.3.2 (1.1.5) on Bond Behaviour and Models.

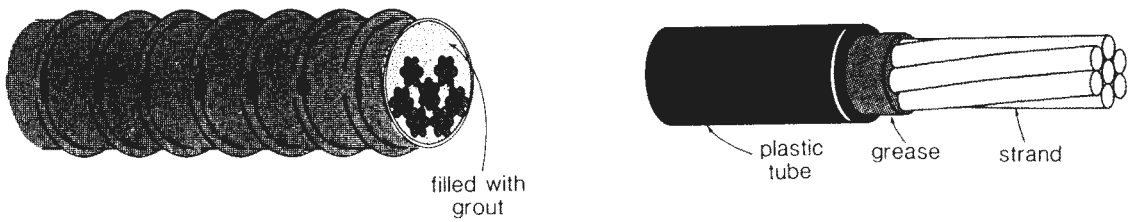

Fig. 3.2-24: Example of bonded and unbonded tendons, after Collins and Mitchell (1991)

(6) Corrosion resistance of prestressing steel

(6.1) Stress corrosion

Besides the generally known corrosion, discussed in Section 3.2.2. (4) in relation to ordinary reinforcement, a particular phenomenon has been repeatedly observed in prestressing steel under certain circumstances: the so-called stress corrosion. Note that though discussed with respect to prestressing steel, virtually all alloys are susceptible to stress corrosion by a specific corrodent under a specific set of conditions. However, not every alloy cracks in every environment. There are specific material-environment combinations that may produce stress corrosion cracking. In case of carbon steels these are e.g. NaOH solutions, nitrate solutions, H_2SO_4/HNO_3 mixtures, HCN solutions and H_2S environments.

Stress corrosion cracking is a progressive fracture mechanism in metals that is caused by the simultaneous interaction of a corrosive environment and a sustained tensile stress. Corrosion film characteristics (i.e. passivation) and local anodic attack (i.e. depassivation) serve as controlling factors in stress corrosion crack initiation and growth. In most cases, stress corrosion cracking is associated with the process of active path corrosion whereby the corrosive attack or anodic dissolution initiates at specific localised sites and is focused along specific paths within the material. Hence, localised corrosion can promote stress corrosion. The tensile stresses necessary for stress corrosion can either be applied (e.g. external load) or can be residual stress in the metal (e.g. due to production process or heat treatment). Stress corrosion cracking in prestressed concrete is especially insidious. Structural failure due to stress corrosion is often sudden and unpredictable. Steel may rupture without any warning or previous deformation after as little as a few hours of exposure, or after months or even years of trouble-free service. It is frequently encountered in the absence of any other obvious kinds of corrosive attack.

A particularly dangerous type of stress corrosion of prestressing steel is the cathodic stress corrosion, well known as hydrogen damage. Hydrogen attack of steel is a damage mechanism in which hydrogen atoms migrate into the steel and at imperfections in the matrix (e.g. grain, boundaries or dislocations) cause microcracks that weaken the material and can lead to structural failure. Common forms of hydrogen damage are hydrogen embrittlement (i.e. loss of ductility and tensile strength in a steel, as a result of penetration (absorption) of hydrogen into it) and hydrogen stress cracking (i.e. a cracking process that results from the presence of hydrogen in a metal in combination with a tensile stress).

Stress corrosion proves to be strongly affected by chemical composition of steel, the concentration of specific corrodent species and the stress intensity. Moreover the higher the tensile strength of prestressing steel, the lower the test lifetime. Hence, the prestressing steel with overstrength is more sensible to corrosion damage than steel with no overstrength. This offers one of the protection possibilities for prestressing steel: it is better to prestress a steel with lower tensile strength at a higher level as to use prestressing steel with exaggerated high tensile strength even with a moderate strain. Furthermore, designers should be aware of all of the constituents in the service environment of prestressed steel, since stress corrosion problems are often induced by a concentration or a deposit of impurities. These aspects are also treated in Section 3.2.3 (2.2.2) devoted to the delivery conditions of prestressing steel.

One of the objectives of the research done in the field of stress corrosion has been to establish a selective accelerated corrosion test which allows the producer/user to check the susceptibility of prestressing steel for that type of corrosion. European standard prEN 100138

specifies the procedure of the stress corrosion test with ammonium thiocyanate NH_4 SCN. The test method determines the time of fracture of a test piece immersed in a pre-defined test solution of NH_4 SCN. The test is maintained at a constant tensile force equivalent to 80% of the (characteristic) maximum load in the tensile test (0.8 F_{ptk}) and at a constant temperature of 50°C. The test is completed either on fracture of the test piece or at an agreed time. In case of strands the test lifetime is reached when at least one wire is fractured. Note that fracture in this test is caused by a hydrogen induced stress corrosion cracking. Hence, it provides only comparative data and does not reflect practical corrosion attack. Therefore it is not possible to extrapolate test results to indicate lifetime in practice. The test lifetime, however, is a very practical measure to compare different prestressing steel grades concerning their stress corrosion susceptibility. In order to assess stress corrosion susceptibility of prestressing steel some requirements are fixed in prEN 10138, as listed in Table 3.2-10. MC90 gives slightly different recommendations for the lowest values of exposure time in similar stress corrosion tests, see Table 3.2-11.

Product	Diameter [mm]	Minimum lifetime in stress corrosion test [h] in individual test	median of all tests
Bar	< 25 25 – 50	20 100	30 400
Wire	all	1.5	4
3-wire strand	all	1.5	4
7-wire strand	all	1.5	4

Table 3.2-10: Require lifetime of prestressing steel in stress corrosion test with ammonium thiocyanate, after prEN 10138

Product	Diameter [mm]	Lowest exposure time to failure [h]	Exposure time to failure of 50% of test samples [h]
Bar	< 12 12 – 25 25 – 40	20 60 100	50 250 400
Wire	4 – 10	1.5	4
Strand	all	1.5	4

Table 3.2-11: Recommended lowest values of exposure time of prestressing steel in stress corrosion test with ammonium thiocyanate, after MC90

(6.2) Surface conditions at delivery

In context of corrosion susceptibility and its interaction with fatigue and brittleness, all prestressing steel has to be packed, transported and stored with care. Prestressing steel should be free of corrosion when it is used. The rust may be a thin film removable by rubbing with a dry cloth. The steel surface must appear – judged by the naked eye – to be smooth and absolutely free of pits. In the same way prestressing steel must be free of surface defects which may influence the performance characteristics. The surface of wires and strands may be covered by thin film of a drawing lubricant. This is not harmful. The same is valid for the layer of scale which covers normally the bars.

Coating with anti-corrosion oil may be used for bars and can be applied on wires and strands before coiling. Note that the coating material used should be seriously checked that it does not contain additives which are harmful to the prestressing steel. Due to evaporation temporary corrosion protection starts to vanish after its application. Hence, it is effective only for some months. Thick layers of coating shall be avoided since they may negatively influence bond.

(7) Thermal expansion

Within the temperature range from –20 to 100°C the coefficient of thermal expansion of prestressing steel may be taken as $\alpha_{sT} = 10 \cdot 10^{-6}$ m/m°C.

3.2.5 Classification of prestressing steel

(1) CEB-FIP Model Code 1990

MC90 distinguishes between different types and sizes of steel for prestressing and classifies prestressing steels on the basis of characteristic tensile strength f_{ptk}, characteristic 0.1% proof-stress $f_{p0.1k}$ and relaxation behaviour. The grade of prestressing steel according to MC90 denotes the value of the characteristic tensile strength in N/mm^2. Table 3.2-12 gives an overview of the classification of prestressing steel provided in MC90.

Property	Classification
type	wire strand bar
size (nominal diameter Ø)	Unlimited
characteristic tensile strength f_{ptk}	Unlimited
grade	Unlimited
characteristic 0.1% proof-stress $f_{p0.1k}$	unlimited under the condition $f_{p0.1k} \geq 0.80\, f_{ptk}$
relaxation	class 1: normal relaxation characteristics for wires and strands class 2: improved relaxation characteristics for wires and strands class 3: relaxation characteristics for bars

Table 3.2-12: Classification of prestressing steels according to MC90

(2) European normative regulations

prEN 10138 specifies requirements for high tensile strength steel products, used for the prestressing of concrete as well as for other applications in the construction field such as e.g. ground anchors, load lifting, suspension and stay cables of bridges. According to prEN 10138, the value of the characteristic tensile strength in N/mm^2 denotes the grade of prestressing steel. Table 3.2-13 to 3.2-16 summarises the required performance characteristics of various

types of prestressing reinforcement. Distinction is made between prestressing wires, strands, bars and quenched and tempered rods. Symbols used in the MC90 and in prEN 10138 are compared in Table 3.2-A2.

Property	Steel name and number			
	Y1860C 1.1353	Y1770C 1.1352	Y1670C 1.1351	Y1570C 1.1350
size (nominal diameter *d*)	3 to 5 mm	3.2 to 6 mm	6.9 to 8 mm	9.4 to 10 mm
tensile strength R_m	1860 N/mm^2	1770 N/mm^2	1670 N/mm^2	1570 N/mm^2
grade	1860	1770	1670	1570
characteristic max. load F_m	13.1 to 36.5 kN	14.2 to 50.0 kN	62.4 to 83.9 kN	109 to 123 kN
maximum of max. load F_{mm}	15.0 to 41.8 kN	16.2 to 56.9 kN	71.0 to 95.4 kN	124 to 140 kN
characteristic 0.1% proof-load $F_{p0.1}$	11.3 to 31.4 kN	12.2 to 43.0 kN	53.7 to 72.2 kN	90.4 to 102 kN
max. relaxation at 1000 hours - corresponding to 70% R_m - corresponding to 80% R_m	2.5% 4.5%			
fatigue stress range $2\sigma_A$ - for smooth wires - for indented wires	200 N/mm^2 180 N/mm^2			

Table 3.2-13: Required properties of prestressing wire, after prEN 10138

Property	Steel name			
	Class A		Class B	
	Y1960S3 1.1361	Y1860S3 1.1360	Y2060S3 1.1362	Y1960S3 1.1361
size (nominal diameter *d*)	5.2 mm	6.5 to 7.5 mm	5.2 mm	6.5 mm
tensile strength R_m	1960 N/mm^2	1860 N/mm^2	2060 N/mm^2	1960 N/mm^2
grade	1960	1860	2060	1960
characteristic max. load F_m	26.7 kN	39.2 to 54.0 kN	28.0 kN	41.4 kN
maximum of max. load F_{mm}	30.5 kN	44.9 to 61.7 kN	32.1 kN	47.3 kN
characteristic 0.1% proof-load $F_{p0.1}$	22.9 kN	33.8 to 46.4 kN	24.1 kN	35.6 kN
max. relaxation at 1000 hours - corresponding to 70% R_m - corresponding to 80% R_m	2.5% 4.5%			
fatigue stress range $2\sigma_A$ - for smooth wires - for indented wires	190 N/mm^2 170 N/mm^2			

Table 3.2-14: Required properties of prestressing 3-wire strand, after prEN 10138

Property	Steel name and number				
	Class A		Class B		
	Y1860S7 1.1366	Y1770S7 1.1365	Y2060S7 1.1368	Y1960S7 1.1367	Y1860S7 1.1366
size (nominal diameter *d*)	7 to 13 mm	15.2 to 18 mm	7.0 mm	9.0 mm	15.2 to 16 mm
tensile strength R_m	1860 N/mm^2	1860 N/mm^2	2060 N/mm^2	1960 N/mm^2	1860 N/mm^2
grade	1860	1770	2060	1960	1860
characteristic max. load F_m	56 to 186 kN	248 to 354 kN	62 kN	98 kN	260 to 279 kN
maximum of max. load F_{mm}	65 to 213 kN	282 to 403 kN	71 kN	112 kN	298 to 319 kN
characteristic 0.1% proof-load $F_{p0.1}$	48 to 160 kN	213 to 304 kN	53 kN	84 kN	224 to 240 kN
max. relaxation at 1000 hours - corresponding to 70% R_m - corresponding to 80% R_m	2.5% 4.5%				
fatigue stress range $2\sigma_A$ - for smooth wires - for indented wires	190 N/mm^2 170 N/mm^2				

Table 3.2-15: Required properties of prestressing 7-wire strand, after prEN 10138

Property	Steel name and number		
	Class A		
	Y1860S7G 1.1372	Y1860S7G 1.1371	Y1700S7G 1.1370
size (nominal diameter *d*)	12.7 mm	15.2 mm	18.0 mm
tensile strength R_m	1860 N/mm^2	1860 N/mm^2	1860 N/mm^2
grade	1860	1820	1700
characteristic max. load F_m	209 kN	300 kN	380 kN
maximum of max. load F_{mm}	238 kN	342 kN	436 kN
characteristic 0.1% proof-load $F_{p0.1}$	180 kN	258 kN	327 kN
max. relaxation at 1000 hours - corresponding to 70% R_m - corresponding to 80% R_m	2.5% 4.5%		
fatigue stress range $2\sigma_A$ - for smooth wires - for indented wires	190 N/mm^2 170 N/mm^2		

Table 3.2-16: Required properties of prestressing 7-wire compacted strand, after prEN 10138

3.2.6 Special products with improved corrosion resistance

(1) Galvanised reinforcement (zinc-coated reinforcement)

Ordinary carbon-steels will gradually rust when exposed to air. However, the steelmaker can nowadays improve the corrosion resistance of steel by further processing it in the factory prior to delivery to the end-user. Such processing includes among the other coating with zinc, normally called galvanising.

The zinc can be applied either electrolytically (which gives a thinner coating) or by dipping the steel in a bath of molten zinc. The latter method, also called hot-dip-galvanising, is applied when producing zinc-coated reinforcement. The best steels for galvanising are those containing less than 0.15% carbon (C). During the hot-dip-galvanising process a thick coating of zinc is produced by immersing reinforcing steel in a molten bath of zinc maintained at a temperature of about 450°C. The coating is actually a coating of several distinct layers, where the layers closest to the steel surface are composed of iron-zinc compounds, while the outer layers consist mainly of zinc. The main layers are the four following ones: connection-layer (γ-layer between steel and zinc with up to 28% iron), palisade-layer (layer with a lower iron rate - up to 11%), γ-layer (with 6% iron) and pure-zinc-layer. The positive effect of galvanising depends very much on the quality of these layers. The thickness of the coating varies greatly with bath temperature, immersion time, and withdrawal rate from the bath. For reinforcing steel the thickness of the zinc coating should be at least 100 µm and it should not exceed 150 µm. Note that since hydrogen evolution is possible on galvanised bars, galvanising is not recommended as a protective measure for steel susceptible to hydrogen embrittlement (i.e. for prestressing steel).

Zinc is has excellent protective properties including its relatively high corrosion resistance in a natural environment. Therefore zinc-coated-steel bars can be used as a preventive measure to control corrosion in reinforced concrete structures exposed to carbonation or mild contamination with chlorides, such as chimneys, bridge structures, tunnels and coastal buildings. The passive film of galvanised bars is stabile even in mild acidic environment, so that the zinc coating remains passive even when the concrete is carbonated. Note that as long as the zinc layer is passive, it can only reduce the corrosion rate in the areas of the steel that are properly coated. Therefore, when constructing with galvanised reinforcement the forming processes should be reduced to a minimum, cracks in the zinc coating must be avoided and macroscopic defects have to be repaired prior to casting.

The corrosion rate of galvanised bars remains negligible in carbonated concrete even if a low content of chloride is present. However, in chloride-contaminated concrete, galvanised steel may be affected by pitting corrosion. In general, a critical chloride level in the range of 1-1.5% by mass of cement is assumed for galvanised steel, compared to the value of 0.4-1% normally considered for carbon-steel reinforcement. More detailed information is given in Nuernberger &. Buel (1991).

The proper execution of the galvanisation process should guarantee that the temperature and the time of galvanisation do not negatively affect the mechanical properties of the steel bar. However, bond between galvanised-steel bars and concrete at early age (the first days after casting) may be worse than that of the normal steel bars, due to the hydrogen evolution at the interface and the dissolution of the superficial layer of the zinc coating, which delays the hydration of the interfacial cement paste. However, after a few weeks the galvanised steel

adheres well and the bond strength for ribbed black steel and galvanised-steel bars is essentially the same.

Galvanised-steel may be welded, but lost of the zinc coating may take place in the welded zone; the application of a zinc-rich paint should be recommended after cleaning of the welded area. In combination with other steel products contact between galvanised and non galvanised steel should be reduced to small areas e.g. cross points. Contact between galvanised and prestressed steel must be avoided. Combination of galvanised and stainless steel is possible with no restrictions. Note that special cement should be used due to the sensitivity of zinc corrosion process to the alkalinity of concrete. More detailed information on corrosion resistance of galvanised reinforcement is given in Bertolini et al. (2004).

(2) Epoxy-coated reinforcement

Besides metallic coatings, such as zinc, organic coatings (plastic and paint) can also be applied to extend the steel's service life, while at the same time giving it an attractive appearance. Epoxy coated reinforcing bars were introduced in the 1970s in North America for protection of reinforcing steel against corrosion. Although recently doubts have arisen about their long-term durability of epoxy-coated reinforcement in heavily chloride contaminated and hot environments, particularly where the concrete is frequently wetted [K.C.Clear Effectiveness of epoxy-coated reinforcing steel, Concrete International 1992, 5, 58-62], in many cases this protective technique proved to be very effective in preventing corrosion of reinforcement in carbonated or chloride contaminated concrete.

The epoxy coating is impermeable and an electrical insulator. It resists corrosion of reinforcement by providing a physical barrier to the oxygen and moisture necessary for the corrosion reaction, and by interrupting electrical continuity of the corrosion cell. Accordingly, effective corrosion protection depends to a great extension on the integrity of the coating. In fact any damage will expose bare metal to the aggressive environment. In the case of chloride-contaminated concrete, the attack tends to penetrate below the coating and widens the area affected. In carbonated concrete, on the other hand, the attack tends to remain in the region of the defect. Therefore the coating must cover the reinforcement uniformly, be well adherent and flexible enough to allow bending of the reinforcement without rupturing. Accordingly, considerable concern has been expressed about the vulnerability of a coated bar to flaws in the coating caused by damage during fabrication or construction, however proper application and quality control permit to avoid this problem. It now appears to be generally accepted that although an epoxy coating cannot provide 100% protection against corrosion, it does enhance durability of reinforced concrete construction. A typical situation where a very high corrosion rates may occur in the vicinity of defects in the coating is the presence of macro cell, for instance when the epoxy-coated reinforcement in contact with chloride-contaminated concrete is coupled to non-coated reinforcement embedded in concrete that is uncontaminated or contains a level of chlorides below the critical level. For this reason, design and application rules require that the coated bars be electrically isolated from each other and from the uncoated reinforcement. More detailed information on corrosion resistance of epoxy-coated reinforcement is given in Bertolini et al (2004).

Reinforcement for coating may be individual bars, welded wire fabric, or prefabricated reinforcement cages. Prestressing strands may also be coated. Although epoxy powder may be applied by spray or by fluidised bed dipping techniques, current standards cover only electrostatic or tribostatic spray application to individual bars or to fabric. The process of coating individual rods comprises the following stages: cleaning by grit/shot blasting or

chemical pre-treatment, heating to a temperature of around 240°C (heating technique shall not impair cleanliness of the bar), application of the coating powder to the hot bar by a spray technique (the electrically charged particles are attracted to the earthed bar), curing of the coating by the residual heat of the bar, followed by water quenching. Prefabricated reinforcement cages are coated using the fluidised bed method. The cages are first fabricated by welding bars at all intersections before dipping in a tank containing a fluidised bed of epoxy powder. This method gives a greater but less uniform coating thickness, which tends to smooth out bar deformations. Mechanical interlock of bar ribs with concrete can then not be relied on for transfer of force (bond and anchorage are instead provided by welded transverse bars).

Coating of reinforcement does not effect mechanical properties of reinforcement, such as strength or ductility, to any significant extend. Re-heating of steel to the temperatures used in the coating process does not remove the effects of quenching or tempering of steel. Grit/shot blast removing the mill scale tends to smooth sharp re-entrant angles at the base of the ribs, reducing stress concentrations – this provides slight fatigue endurance of coated reinforcement, though of not meaningful magnitude.

The strongest influence of coating on performance characteristics of reinforcing steel is found with respect to bond between reinforcement and concrete. In fact, to avoid changes in the structural design procedures, it is necessary to obtain levels of bond strength with epoxy-coated bars comparable to those of bare reinforcement. As already mentioned, the surface texture of an epoxy coating is much smoother and chemically inert than the normal mill scale surface of a reinforcing bar. Firstly, chemical adhesion and friction between bar and concrete are reduced. Plain round bars, which rely on adhesion and friction for bond, are thus not suitable for coating, except where it is intended that bond be destroyed (e.g. for dowel bars in carriageway construction) or where other means of force transfer are to be used (e.g. by welded cross wires in fabric). Subject to some restrictions on geometry of bar deformations, spray methods of coating are capable of providing a uniform coating thickness, and therefore do not significantly alter rib geometry. Changes in bond properties are then entirely attributable to the different surface texture of the coated bar. On the contrary, when using the fluidised bed method bar deformations are smoothen out. In this case bond is affected by both the change in surface text and the change in rib geometry and the effectiveness of the interlock of bar ribs with surrounding concrete maybe severely impaired.

MC90 considers only the ordinary “black” (i.e. not-coated) reinforcement. If similar design rules are to be applied for structures reinforced with fusion bonded epoxy coated reinforcement they need to be altered. For recent proposals, reference is made to *fib* Bulletin 10 (2000).

(3) Stainless steel reinforcement

Various types and grades of stainless steels have been developed and used over the years. All of them are iron-chrome or iron-chrome-nickel alloys. The four main classes of stainless steels, designated in accordance with their metallurgical structure, are ferrite, martensitic, austenitic and austenitic-ferrite (duplex) steel. The high degree of toughness and excellent corrosion resistance of austenitic and duplex stainless steel allow its application as preventative technique for reinforcing concrete structures in aggressive environment as well as in the repair of corroding structures. Note that in some countries also clad bars, i.e. bars with a carbon-steel core and an external layer of stainless steel are used for similar purpose.

The stainless steels used for production of corrosion resistant reinforcement are iron-chrome-nickel alloys with a chrome (Cr) content between 17 and 30% and a nickel (Ni) content between 7 and 35%. The mechanism of corrosion resistance of these types of steel is based on oxidation protection delivered by chrome (Cr) which is not in reaction with carbon (C) or nitrogen (N). Hence, the higher-nickel alloys are more resistant to the corrosion process than lower-nickel compositions. The addition of molybdenum (Mo) greatly improves the resistance to corrosion in reducing conditions, such as dilute sulphuric acid, and to pitting in solutions containing halides. A typical composition of the three types of stainless steel most utilised for reinforcing bars is given in Table 3.2-17.

Amount of alloying component [%]								
Steel types	C (max)	Cr	Ni	Mo	S (max)	Si (max)	Mn (max)	P (max)
340L	0.03	17.0-19.5	8.0-10.5	-	0.003	1	2	0.045
316L	0.03	16.5-18.5	10.5-13.0	2.5-3.5	0.015	1	2	0.045
318 duplex	0.03	21.0-23.0	4.5-6.5	2.5-3.5	0.015	1	2	0.045

Table 3.2-17: Typical ranges of chemical composition (proportions by mass) of the three types of stainless steel most utilised for reinforcing bars after Bertolini et al (2004)

The austenitic stainless steel reinforcement is generally used in a hot-rolled or cold-formed (cold-drawn) condition. Just as in case of ordinary reinforcement, cold forming is used to increase the strength of the material. Strength values of stainless reinforcing steel are high, in particular for cold-drawn bars. Yield stress and tensile strength fall in the range 500 to 750 N/mm^2 and 700 to 900 N/mm^2, respectively. Due to the type of crystal structure of the austenitic steel, it is the most deformable microstructure of all steels. The strain capacity of this type of steel proves to be high and fairly uniform for the same technological process. Uniform elongation values for hot-rolled bars fall above 8%, while in case of cold-drawn bars they are usually not less than 5%. The combined strength and ductility characteristics give the austenitic stainless reinforcement an interesting quality that could be considered even for seismic applications.

Compared with other types of corrosion-resistant reinforcement, such as epoxy-coated or galvanised steel, corrosion resistance is a bulk property of stainless steel. Therefore, the integrity of stainless steel is unaffected if its surface is cut or damaged by handling. Stainless steel remains passive in carbonated concrete and due to its excellent resistance to chloride-induced corrosion it is particularly suitable for use in chloride contaminated concrete. Actually, pitting is the only form of corrosion expected, in practice, on stainless steel in concrete. Note that in some austenitic stainless steels, cold-forming can produce martensite, largely increasing their susceptibility to hydrogen embrittlement. Fabrication can also produce residual stresses that may result in stress corrosion cracking even without externally applied stresses. Besides, increased susceptibility to stress corrosion cracking is often found at welds of stainless steel. On the other hand, stress corrosion may take place only under conditions of high temperature, carbonated concrete, and heavy chloride contamination, which are very unlikely to occur concomitantly. Different available types of stainless steel allow the engineers to select the most suitable in the terms of strength and corrosion resistance. More detailed information on corrosion resistance of stainless reinforcement and practical information on applicability of diverse types of stainless steel are given in Bertolini et al (2004).

The weldability of stainless steel depends on its chemical composition: it is improved by decreasing the carbon content and increasing the nickel content. Although stainless-steel bars are usually weldable, welding is not recommended under site conditions unless adequate control is maintained. In fact, welding may have some negative consequences with regard to mechanical properties and corrosion resistance, as mentioned above. Particular measures should be taken when coupling stainless steel with carbon steel. Stainless steel with welding oxide or with black scale formed at high temperature can increase the risk of galvanic corrosion of carbon steel induced by coupling with stainless-steel bars. However, this risk can be avoided by removing the scale. In fact, the combined use of stainless-steel and carbon-steel bars is encouraged in order to reduce cost, referring to an "intelligent" use of stainless steel, see Bertolini et al (2004).

Particular property of austenitic stainless steel is its non-magnetic behaviour, which can be useful for specific applications. Furthermore, the thermal conductivity of austenitic stainless steel is much lower than that of carbon steel and thus the increase in temperature throughout the steel is delayed.

3.2.7 Prestressing systems and anchorages

(1) Anchorage systems for post-tensioned reinforcement

Pretensioning and post-tensioning represent two groups to which most prestressing techniques belong. In post-tensioning the tendons are stressed and anchored at the ends of the concrete member after the member has been cast and has attained sufficient strength. Commonly, a mortar-tight metal tube or duct (also called sheath) is placed along the member before concrete casting. The tendons may have been pre-placed loose inside the sheath prior to casting or could be placed after hardening of the concrete. After stressing and anchoring, the void between each tendon and its duct is filled with a mortar grout, which subsequently hardens. The tendons generally used in post tensioning are made of wires, strands or bars, as described in Section 3.2.1 (3.2).

There are four common types of tendon systems to be distinguished: monostrand tendons, single-bar tendons, multi-wire tendons and multi-strand tendons. Each tendon needs an active anchorage which can be used for stressing: at this anchorage a jack can be placed to stress the tendon. While bars are tensioned one at a time, wires and strands can be tensioned singly or in groups. In one of the Freyssinet systems 12 wires or strands forming a tendon can be pulled simultaneously. Up to 170 thin wires can form a single tendon in the BBR system and up to 31 strands can form a single tendon in VSL system. Most common tensioning systems are mechanical. Hydraulic jacks are normally used and, with the tendons and anchorages, they all are often an integral part of the post tensioning system. The basic principles used in various systems are few and essentially similar, though the details of different patented systems vary. Some of the typical anchorage systems are based on the principle of direct bearing. These include threaded bars anchored with nut and plate such as for the Dywidag system or wires with pre-formed end buttons bearing on a plate through an anchor head such as the BBR system. In the buttoned wires system sufficient accuracy is needed in estimating the exact length of the tendons before and after tensioning. Such difficulty is overcome if an anchor system based on wedge action or wedge and grip action is used. The wedge may accommodate simultaneously several wires or strands on its outer periphery such as in the Freyssinet system, or it may grip in sandwich a single bar or strand as in the monostrand VSL system.

The passive (or dead-end) anchors are also available. They are encased directly in the concrete and are generally used in short members when tensioning is needed at one end only. Dead-end anchors can be similar in construction as the live-end or can be a bond anchorage which is buried in the concrete. In this case the post tensioning force is transmitted to the concrete by bond over the exposed length of the strands and by the splayed or plate forms at their ends. Note that the specific technical data and in some cases also design aids of various systems are frequently available from manufacturers. Apart from tendon force, other considerations that may influence the choice of tendon type and anchorage device include: the compactness of jacking and anchorage system (characteristic for monostrand tendons), the ease of coupling and anchoring (characteristic for threaded bars), the versatility and economy (characteristic for multi-strand systems).

(2) Stressing anchorage of pretensioned reinforcement

In pretensioning the prestressing tendons are stretched to a predetermined tension and anchored to fixed bulkheads or molds. Subsequently the concrete is poured around the tendons, cured, and upon hardening the tendons are released. Also in case of pretensioned reinforcement the tendons are generally made of wires, strands or bars. As mentioned above, most common tensioning systems are mechanical and in such cases in order to stretch the tendons hydraulic jacks are generally used. Once the predetermined elongation is reached, the tendons are anchored to the bulkhead using patented anchors similar to those described for post-tensioning. Anchors for individual strands are frequently achieved using so-called jaw systems.

3.2.8 Connections of reinforcing steel

(1) Welding

(1.1) Welding methods for reinforcing bars

The main aim of the weld is to connect two steel parts in such a way that the required stresses can be transmitted from the reinforcing bars which are connected in this way. These stresses may be limited to those of the assembly, positioning and handling of the reinforcement - in this case the weld fixes the steel very well giving the reinforcement great rigidity. When the weld also has to transmit in-service stresses then the welded sections must have mechanical properties close to those of the reinforcement itself. Welding of reinforcement for concrete is carried out mainly by metal arc welding, by electric resistance welding and by electric flash welding (only in factories). The other welding processes, such as gas pressure welding, friction welding, pulse welding or thermit welding may only be used in accordance with special recommendations and after preliminary tests.

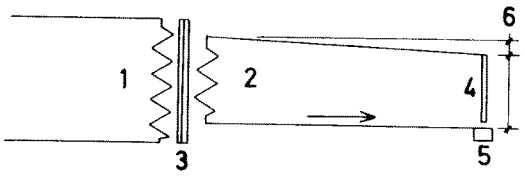

Electric flash welding

1. jaws (one fixed, the other mobile)
2. reinforcement bar
3. weld
4. transformer

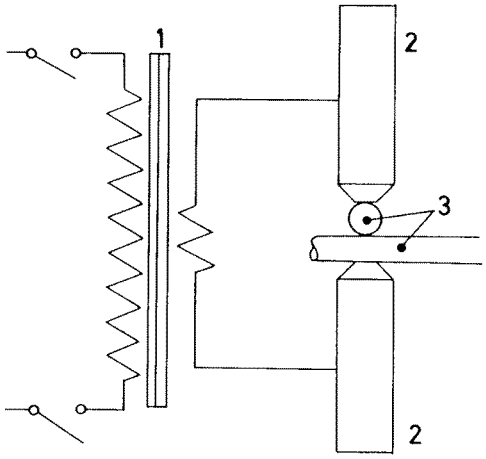

Metal arc welding

1. primary
2. secondary
3. transformer
4. electrode
5. item to be welded
6. voltage drop (1 to 3 V)

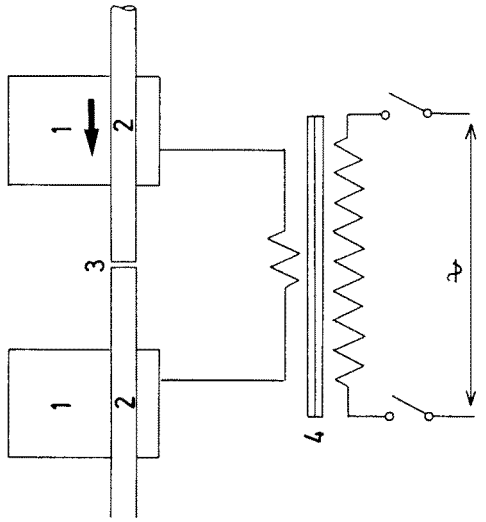

Electric resistance welding

1. Transformer
2. Electrodes
3. Crossed reinforcing bars to be welded

Fig. 3.2-25: Principle of major welding methods, after CEB Application Manual on Concrete Reinforcement Technology (1983)

Metal arc welding allows joining by localised melting of the bar ends and deposited metal (principle shown in Fig. 3.2-25). The melting heat is obtained by an electric arc, which is struck between the electrode and the bars to be welded. The electrode is either coated or bare. In the first case the electrode, when burning, supplies molten metal to the joint and provides the protection necessary for the melting operation. In the second case, the electrode itself constitutes the source of the metal deposited and a gas shroud provides the protection. Welding using this method can be performed either in normal atmosphere (so-called non shielded metal arc welding) or under a specific inert gas shield (so-called gas-shielded metal arc welding). Note

that the coated (covered) electrode metal arc welding is more expensive than gas-shielded metal arc welding, the latter being furthermore faster and more reliable though relatively difficult on site.

In case of electric resistance welding the heat necessary for the local melting to produce the weld without a filler metal is due to the Joule effect in the electrical resistance formed by the two reinforcing bars in contact (Fig. 3.2-25). The current is applied to this part of the bars by conductor electrodes. The weld is produced by putting the localised sections heated in this way under pressure. In general this process is used only for joining crossed bars (e.g. when producing welded wire fabrics, see Section 3.2.1 (2.2.5)).

Electric flash welding (and in particular electric flash butt welding) is carried out by the following succession of operations (Fig. 3.2-25). The two reinforcing bars to be welded are gripped in a device with jaws which aligns the ends and is connected directly to the terminals of the secondary winding of a transformer. At this moment the ends to be spliced are not in contact or are in imperfect contact without pressure. After the transformer is switched on the bars are brought together slowly with the aid of a mobile device and come into contact under weak pressure. The secondary electric circuit is thus closed by a few points of contact where the current density is very high. The intense heat emitted rapidly melts the metal at these points. During this so-called sparking phase in the operation permanent contact between the faces is maintained by mobile table advances as material is expelled. When the sparking movement is completed, the ends to be spliced have reached the welding temperature. Subsequently the welding current is switched off and, by a rapid movement of the mobile table, the ends are strongly applied to each other forming a butt joint.

Finally, the pressurised gas butt welding process is as autogenous welding method for all steel grades. The operation runs through the following phases. The ends of the bars to be welded are gripped in jaws, in alignment, while maintaining a certain distance between the sections. The torches (annular nozzles) are pointed at the space between the bars, lit and burn until the two end sections melt. With the aid of a mobile device, the jaws move together and the two end sections are compressed together forming a butt joint.

In general, welded assemblies may be classified into two types: load bearing assemblies which may be taken into account for calculation purposes and non-load bearing assemblies (e.g. tack welds), which must not be taken into account in the calculations. In general two types of welded joints are met: longitudinal joint (either butt or lap, direct or indirect using a plate) and cruciform joint. For this latter type the distinction is made between a joint capable of sustaining shear stresses at the welded node and one which is not. Additionally, joints between rebar and structural steel shall be distinguished. Examples of simple and double lap joint, butt joint and cruciform joint are given in Fig. 3.2-26.

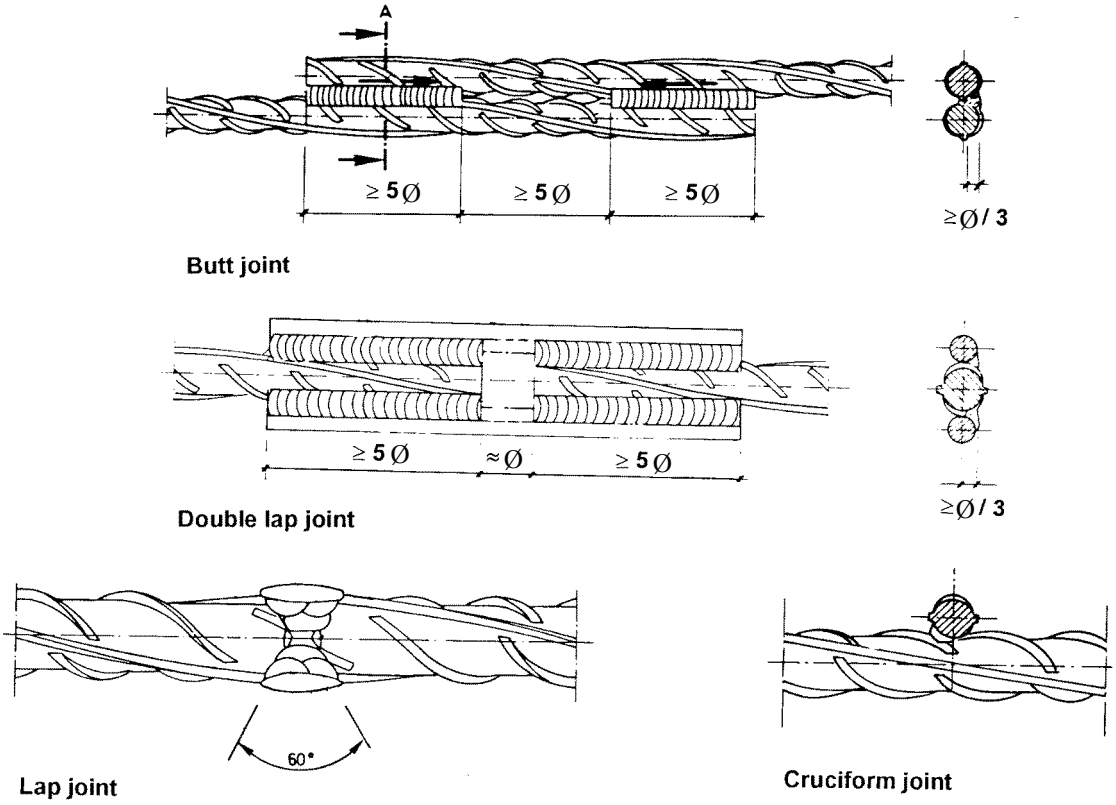

Fig. 3.2-26: Typical welded joints of reinforcing bars, after CEB Application Manual on Concrete Reinforcement Technology (1983)

(1.2) Influence of welding on the steel quality and recommendations

The mechanical properties of the original material should not be influenced significantly by welding process. However, the welding operation introduces additional stresses into the joint and the base material. Because of this ductility and strength are generally decreased and brittleness increased. The main problem with respect to limiting negative influence of welding process on steel properties is to ensure a slow enough cooling of the heated material. If the cooling is too fast, hardening of the steel with a subsequent reduction of ductility takes place. As an example Fig. 3.2-27 shows the comparison of the cooling rates of electrical and gas pressure welding. One can see that for electric flash butt welding less energy is dissipated per unit time on the greater area than in case of metal arc welding. With respect to types of joints, an extreme high difference of temperature is achieved in case of non load bearing cruciform welding and since in this case the heated area is very small compared to the large mass of the base material, the danger of increased brittleness is very high.

Note that the resulting reduction of the deformability depends on chemical composition of steel (mainly content of C, N, S, P) and time of heating as well. Another major source of the reduction of the deformability of steel is the residual stresses. During welding the heated base material expands in all directions and after welding shrinks as a result of cooling. In the same way, the weld beads shrinks to a smaller volume. If the deformations are restrained (e.g. by the unheated base material) residual stresses will occur. The amount of residual stresses can be reduced by structural measures (little restraint) and by suitable welding order. Possible measures to reduce unfavourable effects due to the hardening or the residual stresses are the preheating of the material to temperatures between 300 and 400°C (in order to increase the

cooling time and to reduce the cooling rate) or heat treatment after welding (in order to reduce the residual stresses). Besides residual stresses and local hardening caused by the weld heat, metallurgical disturbances, local deformations (cracks and eccentricities) must also be considered when discussing change of steel quality due to welding process. In the following different welding methods are evaluated from the point of view of quality of the joint and the base material after welding.

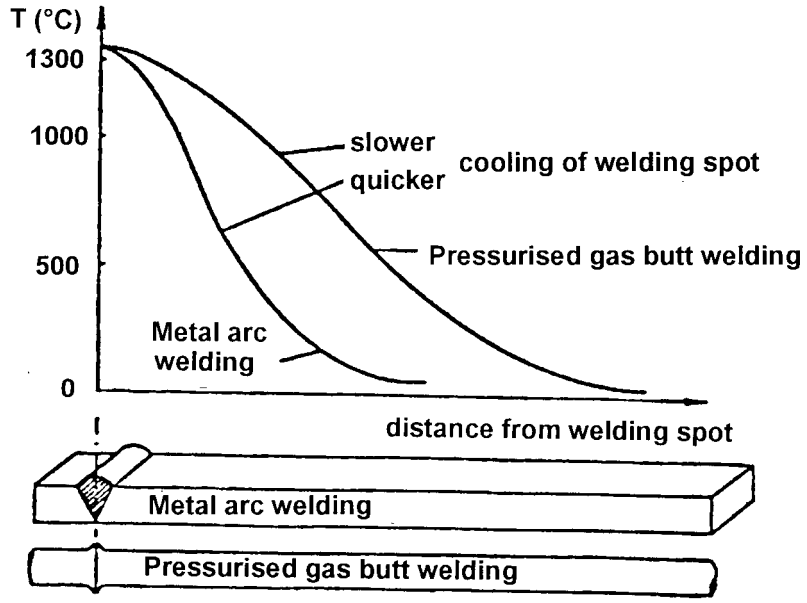

Fig. 3.2-27: Comparison of the cooling rates of electrical arc and gas pressure welding, after CEB Application Manual on Concrete Reinforcement Technology (1983)

In case of metal arc welding process, because of the heat released from the electric arc the parts of the base metal near the molten pool are subject to very high thermal stresses. Temperatures are reached at which certain crystalline changes altering the characteristics of the steel may take place and in addition the sections of the joint undergo a relatively sudden cooling. Thus fairly extensive local hardening must be expected when the amount of carbon (C), manganese (Mn), silicon (Si), chromium (Cr), nickel (Ni) and other elements exceed a certain value (in particular the nitrogen (N) content should not exceed the value of about 0.01%). In addition, for cold worked bars with diameter less than 12 mm a decrease in strength is generally noted in the zone subjected to the welding heat that may unfavourably affect strength of the welded splice in this case.

All steels described as weldable steels may be joined by electric resistance welding. One of the great advantages of this process is the possibility to obtain high quality welds with only slight penetration. Even with low-alloy steels, with a carbon (C) content less than 0.15% and nitrogen (N) content less than 0.012%, welding may be carried out without problems. The bar diameters which can be joined by this process depend on the power of the equipment, though joining of bars with widely different diameter should be excluded.

Also when using electric flash butt welding, the risk of local hardening of steel is slight as a result of the favourable thermal effect on standard composition steels. On the contrary certain precautions must be taken when welding steels with a normal carbon (C) and manganese (Mn) content, but containing in addition other elements such as chromium (Cr), nickel (Ni) etc. This

process is not longer applicable once the silicon (Si) content reaches about 1% or when content of phosphorus (P) and sulphur (S) are larger than 0.06% and 0.05%, respectively. For cold worked steels flash welding with preheating is not advised.

In case of gas but welding the quality of steel in weld is closely related to the operating duration of the torch. If the torch is cut off too early, it allows the formation of an oxidised film in the weld zone, which does not enable a reliable weld to be obtained. On the contrary an unnecessarily long operation of the torch only makes the weld harden without there being any technical advantage. For cold worked reinforcing bars too long period of heating may cause a degradation in the mechanical properties of the steel.

As already mentioned, for a given steel type and the welding process, the degradation in steel quality depends also on the type of joint, as can be seen from Fig. 3.2-28 where the fatigue strength of welded connections is compared for different types of joints. Note that in general the fatigue strength of welded joints is much lower than for the base material, because of the presence of notches, embrittlement, residual stresses and eccentricities. Therefore more stringent requirements are necessary for fatigue loading than for static loading.

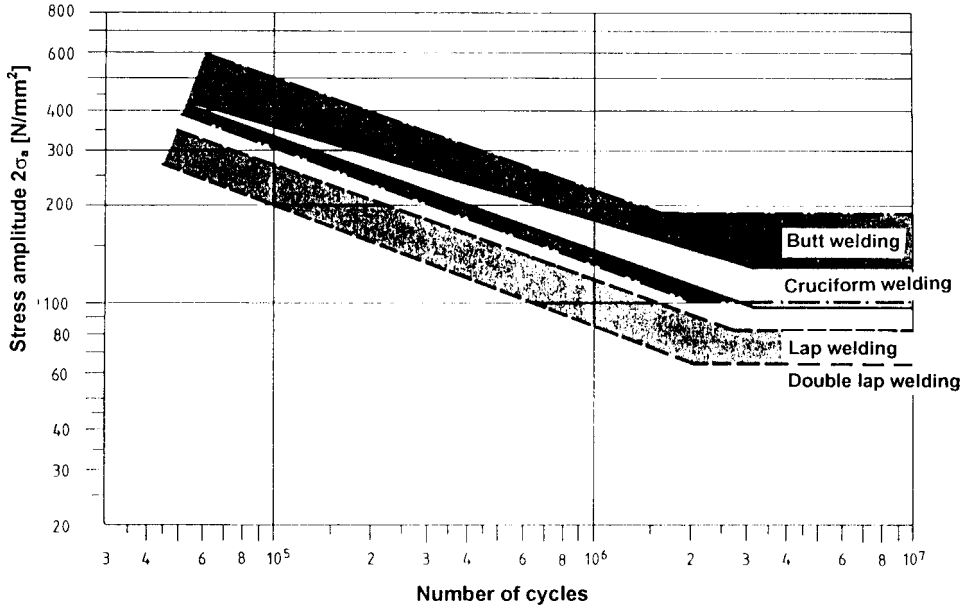

Fig. 3.2-28: Comparison of the fatigue strength of welded connections for different types of joints, after CEB Application Manual on Concrete Reinforcement Technology (1983)

Considering the above mentioned, one must ensure that welding of reinforcing bars is made only if weldability of used steel is guaranteed and if sufficient performance of welded joint is ensured by the method used, which must be as indicated in the relevant Approval. Obviously, the preconditions for good practice, the suitability of the material and the skill of the work force must be checked. For details on weldability of steel see Section 3.2.2 (2.3). The welding procedures which can be employed to form different types of joints suitable for static loading are listed in the Table 3.2-18. All splices may be used both in tension and in compression. Pressurised gas butt welding is generally considered only for reinforcement of diameters larger than or equal to 16 mm.

In case of fatigue loading butt joints are recommended and the welding methods preferred are electric flash welding, pressurised gas welding (for bar diameter larger than 14 mm) and metal arc welding (for connections in compression only and for bar diameter larger than 20 mm).

In design load bearing welded connections can be taken into account for calculation purposes by assuming a certain strength of the welded connection. On the contrary the load bearing capacity of non load bearing connections which serve to fix rebar to rebar (e.g. cruciform tack welding) must not be taken into account for calculation purposes. For full bearing connections under static loading it is required that $f_{t,w} / f_t \geq 0.95$ and $\varepsilon \geq 2.5\%$, where $f_{t,w}$, f_t and ε denote ultimate tensile strength of the welded bar, ultimate tensile strength of reference bar and uniform elongation at maximum load, respectively. For cruciform joints under static loading it is required that $\eta \geq 0.3\, f_y$, where η and f_y denote shear strength of the weld and nominal characteristic yield stress of reference bar, respectively. If the weld is liable to fatigue loading tests under the appropriate conditions must be performed if fatigue data (Wöhler-lines) are not available.

Type of joint	Welding procedure applicable	
	Load bearing	Non load bearing
Butt joint	Pressurised gas welding Non shielded metal arc welding Gas shielded metal arc welding Electric flash welding	—
Lap joint	Non shielded metal arc welding Gas shielded metal arc welding	Non shielded metal arc welding Gas shielded metal arc welding Electric resistance welding
Cruciform joint	Non shielded metal arc welding Gas shielded metal arc welding Electric resistance welding	Non shielded metal arc welding Gas shielded metal arc welding Electric resistance welding
Indirect butt and lap joint	Non shielded metal arc welding Gas shielded metal arc welding	—
Joint between rebar and structural steel	Non shielded metal arc welding Gas shielded metal arc welding	—

Table 3.2-18: Permissible welding methods for static loading and their application, after Recommendations for Welded Splices in Reinforcing Bars (in Contributions to Technology and Quality Control of Reinforcement), CEB (1988)

(2) Mechanical connections of reinforcing bars

There is a wide variety of mechanical splice devices on the market. They can be classified into different groups, according to their main characteristics. Thus, one can speak about connections needing additional materials (e.g. filling materials) or those in which end preparation of the bars is necessary (e.g. threading). From the designer's point of view, mechanical connections can be divided into two categories: compression-only connections and tension-compression connections. The types of connections available in both categories are specified in Table 3.2-19 and examples of some of them are given in Fig. 3.2-29.

Threaded sleeves are internally threaded to provide the thread-like action that allows in the splice to transfer stress from the bar to the sleeve. Basically two types of these connections shall be considered: steel sleeves specially threaded for bars with threads rolled on their total length and threaded sleeves for bars with any type of surface configuration and with purpose threaded bar ends (Fig. 3.2-29). A particular variation of threaded sleeve connection is obtained using taped-threaded steel coupler. This type of splice device is similar to the threaded sleeve with threaded bar ends, but the couplers and the ends of the bars are taper threading. By this means the possibility of cross-threading or jamming before getting the full thread engagement is avoided.

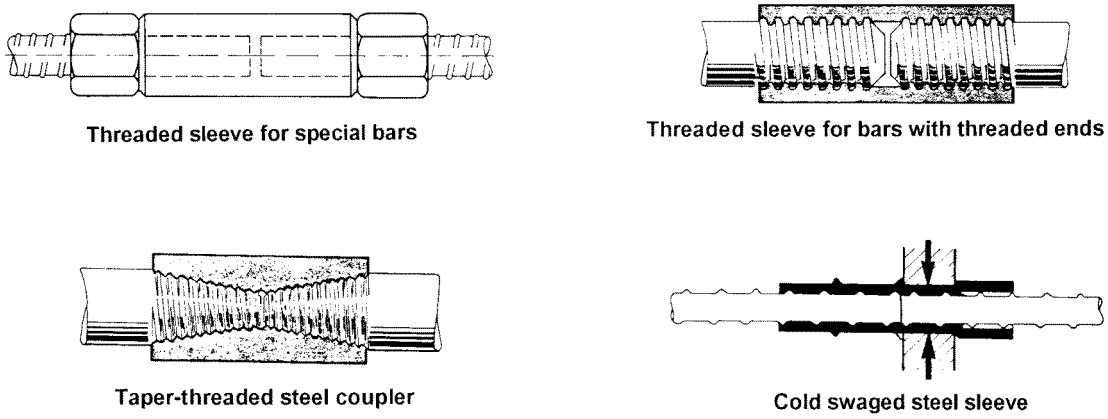

Fig. 3.2-29: Examples of mechanical connections of reinforcing bars, after Rußwurm and Martin (1993)

Type of load transfer	Type of connection
Tension-compression	Threaded sleeve connections • threaded sleeve for special bars • threaded sleeve for bars with threaded ends • taper-threaded steel coupler
	Material-filled sleeve connections • metal-filled sleeve • mortar-filled sleeve
	Deformed-sleeve connections • forged steel sleeve • cold swaged steel sleeve • cold swaged steel sleeve with threaded ends
Compression-only	Threaded sleeve connections • threaded sleeve for special bars • threaded sleeve for bars with threaded ends
	Wedge-locking sleeve connections
	Bolted steel sleeve connections • solid type • strap type
	Metal-filled sleeve connections

Table 3.2-19: Classification of mechanical connections of reinforcing bars, after Recommendations for Mechanical Splices of Reinforcing Bars, CEB (1990)

Material-filled sleeve connections need additional filler material that is poured into the sleeve after it has been placed round the connecting bar ends. In this type of sleeve, stress is transferred in the splice to the sleeve via the filler material and interior deformations in the sleeve. There are different types of filler material, depending on the use of the splice. In case of metal-filled sleeve the metallic filler is used that is ignited to become a molten metal before it is poured into the sleeve to fill the space between the bar and the sleeve, and also between the bar ends. In case of mortar-filled sleeve the filler is a special non-shrinkable mortar grout of high strength. Note that dimensions of mortar-filled sleeves are usually larger than that of metal-filled ones.

In the group of deformed-sleeve connections at least two main types have to be distinguished: forged steel sleeve and cold swaged steel sleeve (Fig. 3.2-29). Forged steel sleeve essentially consists of a cylindrical shell made of a special malleable steel that is clamped on the bar using the hydraulic press after heating it to a sufficiently high temperature. On the contrary, in the case of cold swaged steel sleeve no pre-heating of the sleeve is required. In this case a cylindrical seamless steel tube that forms the shell of the sleeve is deformed in cold state over the ribs of the bars using hydraulic press and adapts to the rib configuration while swaging. One speaks about cold swaged steel sleeve with threaded ends when two cylindrical sleeves that are interconnected by the threaded stud are used instead of one long sleeve shell. In this case the connection is completed when each cylindrical sleeve is pressed on the non-threaded portion of the bars and when the interconnecting stud is threaded to both swaged sleeves.

In case of wedge-locking sleeve the concentric bearing of the bars is assured by lateral clamp action of the sleeve when the wedge is driven into it (not that the bars have to be square cut). In bolted steel sleeves lateral clamping is produced by the bolt tightening. While in the solid type of bolted steel sleeve the shell has a cylindrical shape with the bolts in a flange, in the strap type of bolted steel sleeve is a half-cylindrical shell with several straps that enter in corresponding slots in the shell and are bolted to its flange.

Slicing devices, such as sleeves, are to be designed to work in the elastic region until the yield of the connected bars. This requirement is satisfied when the following conditions are met:

$$\Delta l \le \varepsilon_s \, l_o + 0.10 \text{ mm} \qquad \text{(3.2-12 a)}$$

and

$$\Delta l_{pl} \le 0.10 \text{ mm} \qquad \text{(3.2-12 b)}$$

where:

Δl the measured elongation between points at both sides of the splice under service load (i.e. under load corresponding to stress in the bar $\sigma_s = 0.6 f_{yk}$)

ε_s the elastic unit elongation of bar to be spliced corresponding to $\sigma_s = 0.6 f_{yk}$ (measured on reference bar or calculated according to σ_s / E_s with $E_s = 200\,000$ N/mm^2)

l_o the distance between measuring points

Δl_{pl} the residual elongation after unloading from $\sigma_s = 0.6 f_{yk}$

Furthermore, spliced joints shall have an ultimate load at rupture not lower than the corresponding guaranteed tensile ultimate load of the reinforcement bars to be applied. Where inelastic performance may be anticipated, as in seismic structures, the coupler must not significantly limit ductility of the reinforcing bars being spliced. Specifically, the connection should not introduce significant notch effects in the reinforcing bars at the end of the coupler where the bars must be considered fully effective. These requirements are satisfied when the following conditions are met:

$$R_{joint} \geq A_s f_{tk} \quad \text{or} \quad R_{joint} \geq 0.95\, A_s f_t) \tag{3.2-13 a}$$

and

$$\varepsilon_u \geq 2.5\% \tag{3.2-13 b}$$

where:

R_{joint} the ultimate load of the spliced joint
A_s the area of the smaller bar connected in the joint
f_{tk} the characteristic tensile strength of the rebars
$A_s f_t$ the actual rupture load of the smaller bar in the joint, tested on two samples adjacent to that one
ε_u the uniform elongation of one of the spliced rebars measured close to the joint under maximum load

It is also essential that the long term deformations under service load are limited, especially to mortar-filled sleeves.

For practical details on detailing provisions for splices of reinforcing bars using mechanical connections reference is made to in Chapter 4.5, Section 4.5.5 (4) on Detailing Principles – Splices by Mechanical Devices.

3.2.9 Industrialisation of reinforcement

The industrialisation of reinforcement is possible way to reduce cost of labour for preparing and placing the reinforcement. The possible solutions are presented in Chapter 4.5, Section 4.5.8 on Detailing Principles – Industrialisation of Reinforcement.

Characteristics of non-prestressed reinforcement	MC90	prEN 10080 ENV 10080
Nominal diameter	Ø	d
Cross-sectional area	A_s	S_o
Projected rib area		f_R
Yield stress	f_y	R_e
Upper yield stress		R_{eH}
Actual value of yield stress	$f_{y,act}$	$R_{e,act}$
Nominal value of yield stress	$f_{y,nom}$	$R_{e,nom}$
0.2%-proof stress (non-proportional extension)	$f_{p0.2}$	$R_{p0.2}$
0.5%-proof stress (total extension)		$R_{t0.5}$
Tensile strength	f_t	R_m
Strain hardening ratio	f_t/f_y	R_m/R_e
Percentage total elongation at maximum force	ε_u	A_{gt}
Modulus of elasticity	E_s	
Fatigue strength (specified range of stress)	$\Delta\sigma_{Rs}$	$2\sigma_A$

Table 3.2-A1: Comparison of symbols used in the CEB-FIP Model Code 1990 (MC90) and in the European standards EN 10080 for steel reinforcing steel

Characteristics of prestressed reinforcement	MC90	prEN 10380
Nominal diameter	Ø	d
Cross-sectional area	A_p	S_o
Yield stress	f_{py}	R_e
0.1%-proof stress (non-proportional extension)	$f_{p0.1}$	
0.1%-proof load (non-proportional extension)	$F_{p0.1}$	$F_{p0.1}$
0.2%-proof stress (non-proportional extension)	$f_{p0.2}$	
0.2%-proof load (total extension)	$F_{po.2}$	
Tensile strength	f_{pt}	R_m
Tensile load	F_{pt}	F_m
Percentage total elongation at maximum force	ε_{pu}	A_{gt}
Modulus of elasticity	E_p	
Relaxation after 1000 hours	ρ_{1000}	R_{r1000}
Fatigue strength (specified range of stress)	$\Delta\sigma_{Rs}$	$2\sigma_A$

Table 3.2-A2: Comparison of symbols used in the CEB-FIP Model Code 1990 (MC90) and in the European standards prEN 10380 for prestressing steel

References to Section 3.2

Bertolini L., Elsner B., Pereferri, P., Polder, R.P. (2004) *Corrosion of steel in concrete*, WILEY-VCH Verlag GmbH & Co. KGaA, Weinheim.

CEB Bulletin 140 (1983), *Concrete Reinforcement Technology*. Comité Euro-International du Béton, Lausanne, Switzerland.

CEB Bulletin 164 (1985), *Industrialization of Reinforcement in Reinforced Concrete Structures*. Comité Euro-International du Béton, Lausanne, Switzerland.

CEB Bulletin 186 (1988), *Contributions to Technology and Quality Control of Reinforcement - Recommendations for Welded Splices in Reinforcing Bars*. Comité Euro-International du Béton, Lausanne, Switzerland.

CEB Bulletin 188 (1988), *Fatigue of Concrete Structures.* Comité Euro-International du Béton, Lausanne, Switzerland.

CEB Bulletin 201 (1990), *Recommendations for Mechanical Splices of Reinforcing Bars.* Comité Euro-International du Béton, Lausanne, Switzerland.

CEB Bulletin 213/214 (1993), *CEB-FIP Model Code 1990*, published by Thomas Telford Ltd., UK. ("MC90")

CEB Bulletin 242 (1998), *Ductility of Reinforced Concrete Structures.* Comité Euro-International du Béton, Lausanne, Switzerland.

Collins, M.P., Mitchell, D. (1991), *Prestressed Concrete Structures*. Englewood Cliffs, Prentice-Hall.

Cosenza, E., Greco, C., Manfredi, G. (1992), *Remarks on defining the concept of equival steel*, Technical Report n.29, Structural Division, Instituto di Ingegneria Civile, Universita di Salerno,.

prEN 10138 (2000), *Prestressing steels.*

ENV 10080 (2005), *Steel for reinforcement of concrete.*

fib Bulletin 10 (2000), *Bond of reinforcement in concrete.* International Federation for Structural Concrete (*fib*), Lausanne, Switzerland.

Illston, J. M. (1994), *Construction Materials - Their Nature and Behaviour.* London, Second Edition.

ISO 15630-1 (2002), *Steel for the Reinforcement and Prestressing of Concrete – Test Methods – Part 1: Reinforcing bars, wire rod and wire.*

Leonhardt, F. (1980), *Vorlesungen über Massivbau, Teil 5 – Spannbeton*. Springer Verlag.

Leonhardt, F., Mönnig, E. (1984), *Vorlesungen über Massivbau, Teil 1 – Grundlagen zur Bemessung im Stahlbetonbau*. Springer Verlag.

Naaman, A.E. (1982), *Prestressed Concrete Analysis and Design: Fundamentals*. New York: McGraw-Hill.

Nawy, E.G. (1996), *Prestresses Concrete: a Fundamental Approach*. Upper Saddle River, Prentice-Hall.

Nuernberger U., Buel, W. (1991), *Einfluss einer feuerverzinkung und pvc-beschichtung von bewehrungsstaehlen und von inhibitoren auf die korrosion von stahl in gerissenem beton*. Materials and Corrosion, 42, 1991, pp. 537-546.

Nürnberger, U. (1995), *Korrosion und Korrosionsschutz im Bauwesen*. Bauverlag.

Paulucci, G.M., Siviero, E., Rasera, S., Barba, G. (1993), *Ductility of Stainless Steel Rebars*, in CEB Bulletin 218, *Ductility – Reinforcement*.

Reinhardt, H. W. (1973), *Ingenieurbaustoffe.* Wilhelm Ernst & Sohn, Berlin.

Rehm, G. (1961), *Über die Grundlagen des Verbundes zwischen Stahl und Beton*, DAfSb, Heft 138, Beuth Verlag, Berlin.

Rußwurm, D., Martin, H. (1993), *Betonstähle für den Stahlbetonbau, Eigenschaften und Vewrwendung*. Bauverlag, Berlin.

Taylor, G. D. (1991), *Construction Materials*. Longman Scientific & Technical, UK.

3.3 Composite behaviour

3.3.1 Composite behaviour of uncracked state

by Rolf Eligehausen, Agnieszka Bigaj-van Vliet, Luis J. Lima

(1) Stress and strain of uncracked composite sections

(1.1) Introduction

Cross-sections of structures like frames or beams are often composed of three types of materials: concrete, non-prestressed steel and prestressed reinforcement. In some cases, concrete of more than one type is applied in one cross-section as for example in T-sections where the web is pre-cast and the flange is cast in situ. Non-homogeneous composite sections may be analyzed using an approach similar to that applied to the analysis of homogeneous cross-sections. First, plane cross-sections must be assumed to remain plane after deformation, thus the strains in concrete and steel are assumed equal at any fibre. Second, perfect bond must be assumed between concrete and steel. Finally, when analyzing uncracked sections tensile stresses in concrete must not be neglected. In the following the cross-sections are considered to have one axis of symmetry and are subjected to bending or bending and an axial force.

(1.2) Strain, stress and curvature in composite cross-section

The key problem in the analysis of composite sections is often to find the location of the neutral axis, using Bernoulli's compatibility condition and Hooke's law. The method proposed utilises the concept of the transformed section. According to this concept the actual area A_i of any part i can be replaced by a transformed area with different that actual value and arbitrary chosen reference modulus of elasticity. In reinforced and prestressed concrete cross-sections, the reference modulus is taken to be equal to E_c, the modulus of elasticity of concrete. Hence, the area of the rebars is to be transformed.

(1.2.1) Area of transformed composite cross-section

In the following the method is explained to transform a composite cross-section to an equivalent homogeneous cross-section. As an example, a reinforced concrete cross-section under uniform stresses is used (e.g. cross-section tensioned before cracking or compressed). Based on the assumption that perfect bond exists between concrete and reinforcement, the rebar strain ε_s should be equal to the concrete strain at the rebar level ε_c:

$$\varepsilon_s = \varepsilon_c \tag{3.3-1}$$

Applying Hooke's law for steel and concrete, $\sigma_s = \varepsilon_s E_s$ and $\sigma_c = \varepsilon_c E_c$, gives:

$$\sigma_s = \frac{E_s}{E_c}\sigma_c = \alpha_e \sigma_c \tag{3.3-2}$$

where:

σ_c concrete stress at the rebar level
σ_s stress in the rebar
E_c modulus of elasticity of concrete
E_s modulus of elasticity of steel
α_e the ratio of the modulus of elasticity of the reinforcement E_s to the modulus of elasticity of concrete E_c.

It can be demonstrated that in a uniformly strained homogeneous material the value of the normal internal resistance force N is equal to the geometric area of its normal section A multiplied by the stress corresponding to the applied strain σ. In a reinforced (composite) section under the similar uniform conditions the normal force N can be written as:

$$N=A_c\sigma_c + A_s\sigma_s = A_c\sigma_c + \alpha_e A_s\sigma_s =(A_c+\alpha_e A_s)\sigma_c=A_{eq}\sigma_c \qquad (3.3\text{-}3)$$

where:

A_{eq} the transformed (or homogenised) area of reinforced section.

This means that the rebar area A_s can be transformed into a concrete area $\alpha_e A_s$, as long as the rebar stress σ_s is simultaneously converted to the concrete stress σ_c. The transformation of the rebar area to a concrete area has a profound significance. The cross-section, which is made up of two materials, reinforcement and concrete, can now be thought of as a homogeneous elastic material made of concrete only. A cross-section with the transformed rebar area is shown in Fig. 3.3-1.

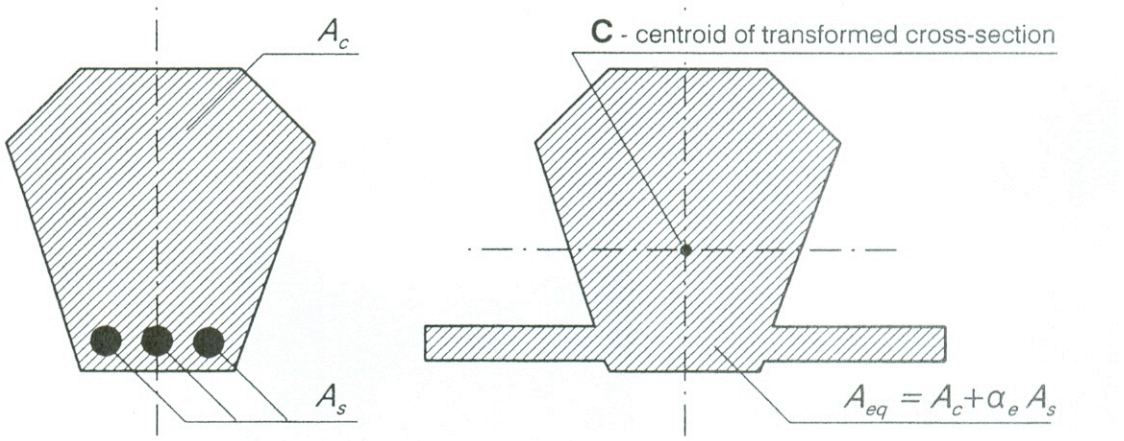

Fig. 3.3-1: Cross-section of reinforced concrete element with one axis of symmetry (left) and corresponding transformed homogeneous cross-section (right), after Dabrowski et al. (1982)

In general case, for the composite cross-section made of m materials with different elasticity moduli the following definition of the transformed cross-section is to be applied:

$$A_{eq} = \sum_{i=1}^{m} \left(\frac{E_i}{E_{ref}} A_i \right) \qquad (3.3\text{-}4)$$

$$A_i = \int b(\zeta) d\zeta = 0 \tag{3.3-5}$$

where:

A_i	the area of the *i*-th part of the cross-section
E_i	modulus of elasticity of the *i*-th part of the cross-section
E_{ref}	reference modulus of elasticity
i	*i*-th part of the composite cross-section
m	total number of the parts of the cross-section
ζ	co-ordinate of any fibre, with respect to the reference axis
$b(\zeta)$	width of cross-section at the distance ξ from the reference axis.

(1.2.2) Centroid of transformed composite cross-section

For a transformed homogeneous elastic section subjected to simple bending (Fig. 3.3-1), the neutral axis coincides with the centroidal axis. Hence, instead of solving the neutral axis from the three fundamental equations of equilibrium, compatibility and constitutive laws, one can now locate the neutral axis using the simple and well-known method of finding the centroid C of a homogeneous cross-section. In other words, the first static moment B of the stressed area of the transformed homogeneous cross-section about the centroidal axis must be equal to zero:

$$B_{eq} = \zeta \int \zeta b(\zeta) d(\zeta) \tag{3.3-6}$$

where:

B_{eq}	first static moment of the transformed homogeneous cross-section.

Note that the position of the centroidal axis for the composite cross-section made of m materials with different elasticity moduli can be derived omitting the evaluation of shape and area of the homogeneous cross-section, transformed from the composite one. Under the condition that the reference axis corresponds with the centroidal axis of the transformed cross-section the first static equivalent moments of the composite section about this axis equals zero. The following definition of the first static moment of the transformed cross section is to be applied in general case:

$$B_{eq} = \sum_{i=1}^{m} \left(\frac{E_i}{E_{ref}} B_i \right) \tag{3.3-7}$$

$$B_i = \int \zeta b(\zeta) d(\zeta) \tag{3.3-8}$$

where:

B_i	first static moment of the ith part of the cross-section.

(1.2.3) Transformed composite cross-section subjected to bending and normal force

To show a general way of analyzing the stresses and strains in a composite cross-section subjected to bending and normal force, the cross-section subjected to a force N normal to the section and situated at any point on the symmetry axis is assumed. Such a force is statically equivalent to a system composed of a normal force N at the reference point O on the axis of symmetry and a bending moment M, as shown in Fig. 3.3-2.

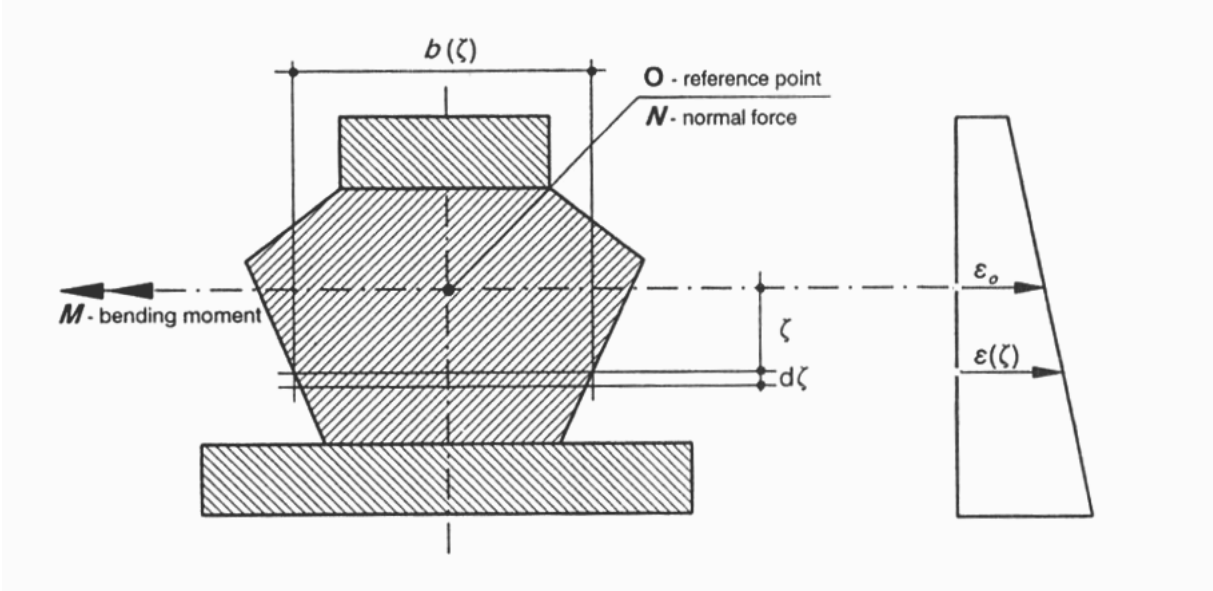

Fig. 3.3-2: Cross-section of composite element composed of m different materials and having an axis of symmetry, subjected to normal force N at the reference point O on the axis of symmetry and a bending moment M (left) and strain distribution over the section height (right), after Dabrowski et al. (1982)

In case of the cross-section composed of m different materials and having an axis of symmetry the following relationships hold. At any fibre dζ, at a distance ζ from the reference point O, the strain equals:

$$\varepsilon(\zeta) = \varepsilon_0 + 1/r\zeta \tag{3.3-9}$$

where:

ε_0 strain at the reference point
$1/r$ curvature.

When the fibre considered is in the *i*-th part (i = 1 … m) of the composite section, the stress at the fibre at a distance ζ from the reference point O is:

$$\sigma(\zeta) = E_i(\varepsilon_0 + 1/r\zeta) \tag{3.3-l0}$$

where:

E_i the modulus of elasticity of the material in the *i*-th part of the composite cross-section.

Integration of the stress over the area of the cross-section and taking the moment about an axis through O performed for all m parts of the cross-section gives:

$$N = \sum_{i=1}^{m} \int \sigma(\zeta) b(\zeta) d(\zeta) = \varepsilon_o \sum_{i=1}^{m} E_i \int b(\zeta) d(\zeta) + 1/r \sum_{i=1}^{m} E_i \int \zeta b(\zeta) d\zeta \tag{3.3-11}$$

$$M = \sum_{i=1}^{m} \int \sigma(\zeta) \zeta b(\zeta) d(\zeta) = \varepsilon_o \sum_{i=1}^{m} E_i \int \zeta b(\zeta) d(\zeta) + 1/r \sum_{i=1}^{m} E_i \int \zeta^2 b(\zeta) d\zeta \tag{3.3-12}$$

The transformed cross-sectional area A_{eq} is defined according to eq. (3.3-4), its first static equivalent moment B_{eq} is defined according to eq. (3.3-7), and the second static equivalent moment I_{eq} of the composite section about an axis through O has the following definition:

$$I_{eq} = \sum_{i=1}^{m} \frac{E_i}{E_{ref}} I_i \tag{3.3-13}$$

$$I_i = \int \zeta^2 b(\zeta) d(\zeta) \tag{3.3-14}$$

With these definitions the integral of the stress over the area of the cross-section and the moment about an axis through O for the composite cross-section reads in the matrix form:

$$\begin{Bmatrix} N \\ M \end{Bmatrix} = E_{ref} \begin{bmatrix} A_{eq} & B_{eq} \\ I_{eq} & A_{eq} \end{bmatrix} \begin{Bmatrix} \varepsilon_0 \\ 1/r \end{Bmatrix} \tag{3.3-15}$$

This equation may be used to find N and M when the axial strain ε_0 and the curvature 1/r are known. When N and M are known the equation may be solved for ε_0 and 1/ r:

$$\begin{Bmatrix} \varepsilon_0 \\ 1/r \end{Bmatrix} = \frac{1}{E_{ref}(A_{eq} I_{eq} - B_{eq}^2)} \begin{bmatrix} I_{eq} & -B_{eq} \\ -B_{eq} & A_{eq} \end{bmatrix} \begin{Bmatrix} N \\ M \end{Bmatrix} \tag{3.3-16}$$

The equations most commonly used in calculations of stress, strain and curvature are generally based on the assumption that the reference point is taken at the centroid C of the transformed section. This condition imposes that the first static moment about an axis through reference point B_{eq} equals zero (see Section (1.2.2)). Hence, if the reference point is chosen at the centroid C of the transformed section, the relationship to determine the axial strain ε_0 at reference point C and the curvature 1/r becomes:

$$\begin{Bmatrix} \varepsilon_0 \\ 1/r \end{Bmatrix} = \frac{1}{E_{ref}} \begin{Bmatrix} N/A_{eq} \\ M/I_{eq} \end{Bmatrix} \tag{3.3-17}$$

(2) Load level dependence of strain and stress in RC and PC sections

As discussed in Section (1), in reinforced and prestressed concrete cross-sections, the reference modulus taken to transform a composite cross-section into homogenised one is equal to E_c, the modulus of elasticity of concrete. More specifically, when performing the transformation the values of secant modulus of elasticity shall be applied both for concrete

and steel. However, the secant modulus of concrete $E_{c,sec}$ is a function of the strain magnitude, as shown in Fig. 3.3-3. Similar concern applies to reinforcing steel - also in this case of secant modulus of elasticity $E_{s,sec}$ changes as soon as yielding of steel is reached. Table 3.3-1 shows how the ratio $\alpha_{e,sec}$ of the secant modulus of elasticity of the reinforcement $E_{s,sec}$ and the secant modulus of elasticity of concrete $E_{c,sec}$ changes with the change of strain magnitude. In this example concrete with f_{cm} = 30 MPa and steel with f_{yk} = 400 MPa is used, both modelled according to the MC2010 approach.

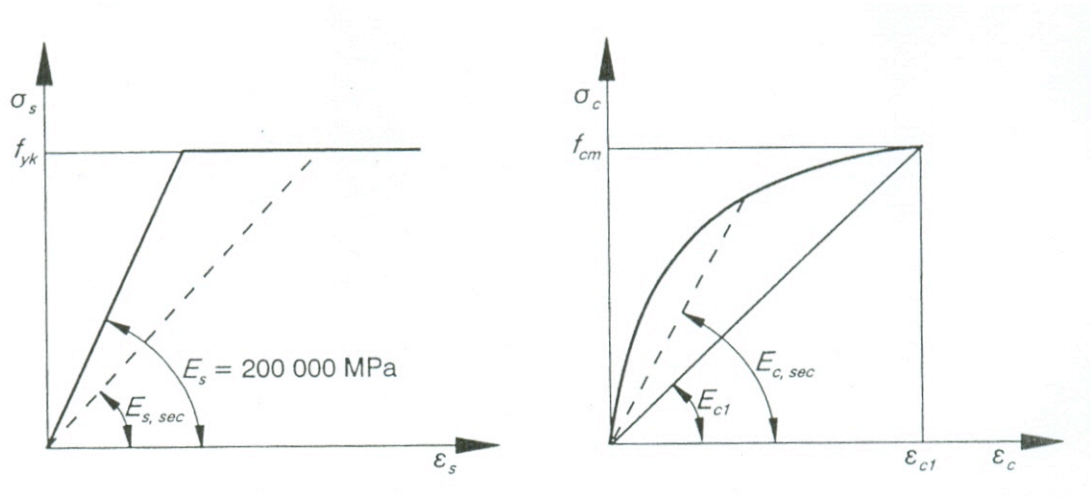

Fig. 3.3-3: Secant modulus of steel $E_{s,sec}$ (left) and concrete $E_{c,sec}$ (right) as a function of the strain magnitude

The variability of $\alpha_{e,sec}$ is a direct reason for the change of the area of the transformed composite cross-section A_{eq} and, hence, for the corresponding change in position of the centroidal axis of the homogenised cross-section. Consequently, it influences the eccentricity of normal force, which turns not to be constant but varies with the applied load change. If a prismatic element with asymmetric reinforcement is axially loaded, the eccentricity of the external load - defined as the distance between its application point and the centraid of the section - changes when the value of this force changes. So, the eccentricity of a normal external load has a variable value and must be arbitrarily defined to facilitate simplified section design.

ε (m/m)	0	0.0005	0.0010	0.0015	0.0020	0.0022
σ_c (MPa)	0	13.1	22.1	27.5	29.9	30.0
$E_{c,sec}$ (MPa)	31 000	26 300	22 100	18 300	14 900	13 600
$E_{s,sec}$ (MPa	200 000	200 000	200 000	200 000	200 000	182 000
$\alpha_{e,sec}= E_{s,sec}/ E_{c,sec}$	6.5	7.6	9.0	10.9	13.4	13.4

Table 3.3-1: Relationship between applied compressive strain ε and the ratio $\alpha_{e,sec}$ of the secant modulus of elasticity of the reinforcement $E_{s,sec}$ and the secant modulus of elasticity of concrete $E_{c,sec}$ calculated according to the MC90 approach for concrete with f_{cm} = 30 MPa and steel with f_{yk} = 400MPa

Suppose that as illustrated in Fig. 3.3-4, the eccentricity of a normal force applied in a section with asymmetl1c reinforcement is referred to the centroid of the transformed section determined using e.g. the arbitrary chosen value of $\alpha_{e,sec}$ equal to 15. In such a situation, due to load level dependence α_e of, a normal force which is in theory applied without any eccentricity has actually already at the initial state of loading a certain eccentricity. Hence, the element is not uniformly strained and must deflect.

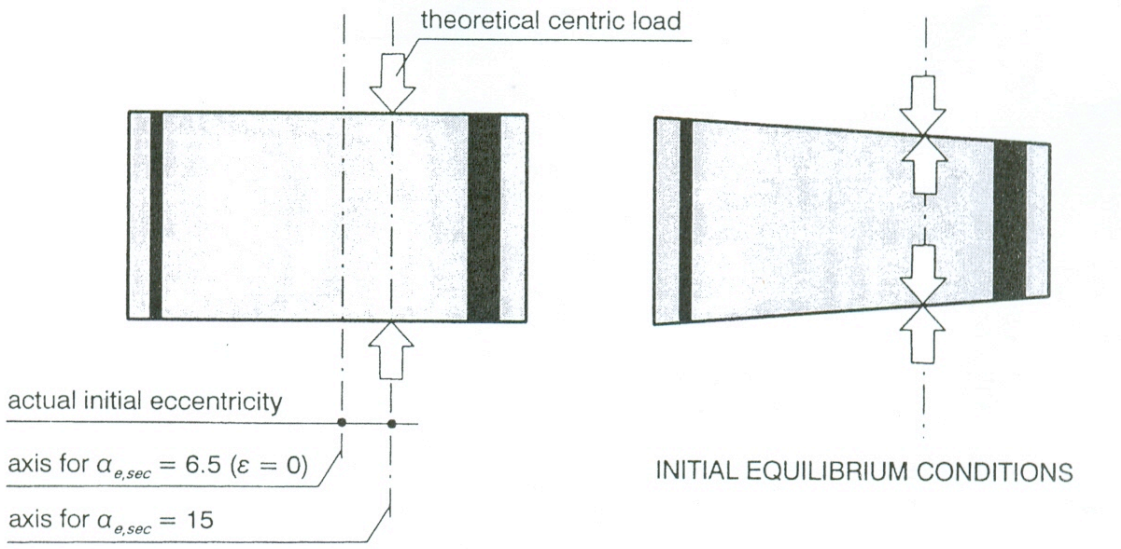

Fig. 3.3-4: Cross-section of reinforced concrete element with asymmetric reinforcement and the eccentricity of a normal force with respect to the centroid of the transformed section as influenced by value $\alpha_{e,sec}$, after Lima (1998)

(3) Time-dependence of strains and stresses in RC and PC sections

(3.1) Basic considerations

The stresses and strains in reinforced or prestressed structures are subjected to change for a long period of time, during which creep and shrinkage of concrete and relaxation of the steel (in particular prestressing steel) develop gradually. Due to this time-dependent behaviour, which is discussed in detail in Section 3.1 on Concrete and in Section 3.2 on Reinforcement, the components forming one section tend to have different strains, though the difference in strain is restrained because of the bond. Note that, for the sake of simplification, when analyzing the effect of load time-history on stresses, strains and deformations it is assumed that elongations or end rotations of a member are not restrained by the supports or by continuity with other members. Hence, the time-dependent effects change the distribution of stress and strain in the section but do not change the reactions and the induced stress resultants (values of the axial force or bending moment acting on the section).

In order to analyze the time-dependent strains and the stresses in a composite cross-section as in Fig. 3.3-5, loaded at age t_0 and subjected to loading during the period $(t - t_0)$ the following quantities must be known: the cross-section dimensions and the reinforcement areas, the magnitudes of applied loads (e.g. inc1uding prestressing), the modulus of elasticity of concrete E_c (t_0) at the age to, the shrinkage $\varepsilon_{cs}(t, t_0)$ that would occur at any fibre if it were free, the creep coefficient $\varphi(t, t_0)$ and the ageing coefficient $\chi(t, t_0)$. When applicable, the intrinsic relaxation of steel $\Delta\sigma$ that occurs during the period $(t - t_0)$ must be also known.

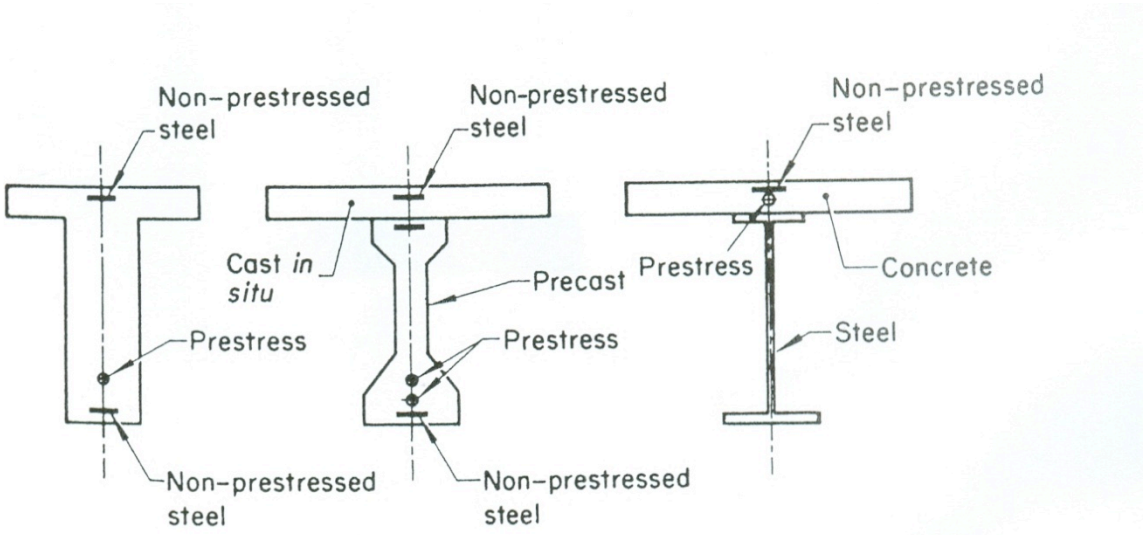

Fig. 3.3-5: Examples of composite cross-sections used to analyse the time-dependent strains and the stresses, after Ghali and Favre (1994)

(3.2) Instantaneous stresses and strains at age t_0

As it is known from the basics of reinforced concrete, the axial strain and curvature at time t_o (e.g. immediately after prestressing) are given by:

$$\begin{Bmatrix} \varepsilon_0(t_0) \\ 1/r(t_0) \end{Bmatrix} = \frac{1}{E_{ref}(A_{eq}I_{eq} - B_{eq}^2)} \begin{bmatrix} I_{eq} & -B_{eq} \\ -B_{eq} & A_{eq} \end{bmatrix} \begin{Bmatrix} N \\ M \end{Bmatrix}_{equivalent} \tag{3.3-18}$$

where:

A_{eq}	area of the transformed section at time t_0
B_{eq}	first static moment of the transformed section at time t_0
I_{eq}	second static moment of the transformed section at time t_0
$N_{equivalent}$	equivalent normal force at a reference point, which – when applicable – combines the external normal load and the prestressing forces
$M_{equivalent}$	equivalent moment at a reference point, which – when applicable – combines the external moment load and the moment from prestressing forces
E_{ref}	reference modulus of elasticity, which may be chosen as the modulus of elasticity E_k (t_0) of a material in the *k*-th part of the cross-section at age to (e.g. modulus of elasticity of concrete E_c (t_0) at age t_0).

Corresponding strains $\varepsilon_c(\zeta, t_0)$ and stresses $\sigma_c(\zeta, t_0)$ at time to in any fibre of concrete in the ith part of the cross-section:

$$\varepsilon_c(\zeta, t_0) = \varepsilon_0(t_0)+1/r(t_0)\zeta \tag{3.3-19}$$

and

$$\sigma_c(\zeta\, t_0) = [E_c(t_0)]_i \cdot [\varepsilon_0(t_0)+1/r(t_0)\zeta] \tag{3.3-20}$$

where:

$\varepsilon_0(t_0)$	strain at the reference point at time t_0
$1/r(t_0)$	curvature at time t_0
ζ	distance between the reference point and the layer considered
I	number of the part of the composite cross-section considered
$[E_c(t_0)]_i$	modulus of elasticity of the concrete in the *i*-th part of the cross-section at time t_0.

For non-prestressed steel the following holds:

$$\sigma_s(\zeta,t_0) = [E_s(t_0)]_i + [\varepsilon_0(t_0)+1/r(t_0)\,\zeta\,] \qquad (3.3\text{-}21)$$

where:

$[E_s(t_0)]_i$	modulus of elasticity of the non-prestressed steel in the *i*-th part of the cross-section at time t_0.

In the case of pretensioning, the stress in the prestressed steel immediately after transfer equals:

$$\sigma_p(\zeta,t_0) = \sigma_p(\zeta)_{initial} + [E_p(t_0)]_i + [\varepsilon_0(t_0)+1/r(t_0)\;\zeta\,] \qquad (3.3\text{-}22)$$

where:

$[E_s(t_0)]_i$	modulus of elasticity of the prestressing steel in the ith part of the cross-section at time t_0
$\sigma_p(\zeta)_{initial}$	represents the stress in prestressed steel before transfer.

In the case of post-tensioning the stress in the tendon is the same immediately before and after transfer, hence:

$$\sigma_p(\zeta,t_0) = \sigma_p(\zeta)_{initial}$$

(3.3) Changes in stresses and strains during the period t_0 to t

Creep, shrinkage and relaxation of steel result in stress redistribution between the various materials involved. From the assumptions of plane sections remaining plane after deformation and that of perfect bond between steel and concrete it follows in which way the time dependent changes in one material will affect the other parts of the cross-section. The change in strain during the period t_0 to t is defined by the increments $\Delta\varepsilon_0$ and $\Delta l/ r$ in the axial strain at reference point and curvature. To determine these, the following procedure is taken. At first the change of strain due to creep and shrinkage of concrete and relaxation of steel is artificially restrained by application of an axial force ΔN at the reference point and a bending moment ΔM. On releasing of this restrain by application of equal and opposite forces on the composite section the following changes in axial strain at the reference point and in curvature result from the relationship analogue to that given in Section (3.2):

$$\begin{Bmatrix} \Delta\varepsilon_0 \\ \Delta l/r \end{Bmatrix} = \frac{1}{\overline{E}_{ref}(\overline{A}_{eq}\cdot\bar{I}_{eq} - \overline{B}_{eq}{}^2)} \begin{bmatrix} \bar{I}_{eq} & -\overline{B}_{eq} \\ -\overline{B}_{eq} & \overline{A}_{eq} \end{bmatrix} \begin{Bmatrix} -\Delta N \\ -\Delta M \end{Bmatrix} \tag{3.3-24}$$

where:

$\overline{E}_{ref}$ an age-adjusted reference modulus of elasticity, which may be chosen as the modulus of elasticity $\overline{E}_k(t,t_0)$ of material in the *k*-th part of a cross-section (e.g. age-adjusted modulus of elasticity of concrete $\overline{E}_c(t,t_0)$.
Note that changing the value of E_c in time will result in a change of the area and of the location of the centroid of the transformed cross- section as well as its other static characteristics)

$\overline{A}_{eq}$ the age-adjusted area of the transformed section

$\overline{B}_{eq}$ the first static moment of the age-adjusted transformed section

$\bar{I}_{eq}$ the second static moment of the age-adjusted transformed section.

The restraining forces must be calculated as a sum of three terms:

$$\begin{Bmatrix} \Delta N \\ \Delta M \end{Bmatrix} = \begin{Bmatrix} \Delta N \\ \Delta M \end{Bmatrix}_{creep} + \begin{Bmatrix} \Delta N \\ \Delta M \end{Bmatrix}_{shrinkage} + \begin{Bmatrix} \Delta N \\ \Delta M \end{Bmatrix}_{relaxation} \tag{3.3-25}$$

Considering that if creep were free to occur and assurning that all loads are applied at the age to, the axial strain and curvature would increase in the period (t - t_0) by the amounts φ(t, t_0) c(to) and φ(t, t_0) 1/ r(t_0). In such case, the forces restraining these deformations may be determined from the following relationship

$$\begin{Bmatrix} \Delta N \\ \Delta M \end{Bmatrix}_{creep} = \sum_{i=1}^{m} \left\{ \overline{E}_c \phi \begin{bmatrix} A_c & B_c \\ B_c & I_c \end{bmatrix} \begin{Bmatrix} \varepsilon_0(t_0) \\ 1/r(t_0) \end{Bmatrix} \right\}_i \tag{3.3-26}$$

where:

A_{ci} the area of concrete in the *i*-th part of the cross-section

B_{ci} the first static moment about an axis through the reference point of concrete in the *i*-th part of the cross-section

I_{ci} the second static moment about an axis through the reference point of concrete in the *i*-th part of the cross-section

$\overline{E}_{ci}$ an age-adjusted reference modulus of e1asticity of concrete $[\overline{E_c}\ (t, t_0)]_i$ in the *i*-th part of the cross-section

φ_i the creep coefficient of concrete $[\varphi\ (t, t_0)]_I$ in the *i*-th part of the cross-section.

The forces required to prevent free shrinkage $\varepsilon_{cs} = \varepsilon_{cs}\ (t, t_0)$ for the period of time (t - t_0) are as folows:

$$\begin{Bmatrix} \Delta N \\ \Delta M \end{Bmatrix}_{shrinkage} = \sum_{i=1}^{m} \left\{ \overline{E}_c \varepsilon_{cs} \begin{bmatrix} A_c \\ B_c \end{bmatrix} \right\}_i \tag{3.3-27}$$

Finally, the forces needed to prevent the strain due to relaxation of steel (in particular prestressing reinforcement) result from:

$$\begin{Bmatrix} \Delta N \\ \Delta M \end{Bmatrix}_{relaxation} = -\sum_{i=1}^{n} \begin{Bmatrix} A_p \Delta\overline{\sigma}_{pr} \\ A_p \cdot \zeta \Delta\overline{\sigma}_{pr} \end{Bmatrix}_i \tag{3.3-28}$$

where:

A_{pi} the area of prestressed steel in the ith part of the cross-section (i.e. in the *i*-th layer of prestressing reinforcement)

$\overline{\sigma}_{pr}$ the reduced relaxation during the period $(t - t_0)$.

Assuming that all loads are applied at the age to, the stress in concrete required to prevent creep and shrinkage $\sigma_{restrained}(\zeta)$ at any fibre of the ith part of the cross-section located at the distance s from the reference point follows from the equation:

$$\sigma_{restrained}(\zeta) = -[\overline{E}_c\ (t,t_0)]_i\ [\varphi(t,t_0)]\varepsilon_c(\zeta,t_0) + \varepsilon_{cs}] \tag{3.3-29}$$

where:

$\varepsilon_c(\zeta,t_0)$ is the strain at fibre considered at time to, determined according to eq. (3.3-19)

The stress increments that develop during the period $(t - t_0)$ are as follows. In concrete, at any fibre in the *i*-th part:

$$\Delta\sigma_c(\zeta) = \sigma_{restrained}(\zeta) + [\overline{E}_c\ (t,t_0)]_i \cdot [\Delta\varepsilon_0 + \Delta 1/r \cdot \zeta] \tag{3.3-30}$$

In non-prestressed steel in the ith part of the cross-section:

$$\Delta\sigma_s(\zeta) = [E_s]_i\ [\Delta\varepsilon_0 + \Delta 1/r \cdot \zeta] \tag{3.3-31}$$

In the prestressed steel in the ith part of the cross-section:

$$\Delta\sigma_p(\zeta) = \overline{\sigma}_{pr} + [E_p]_i\ [\ [\Delta\varepsilon_0 + \Delta 1/r \cdot \zeta].$$

The last equation gives the change in prestress due to creep, shrinkage and relaxation.

The time-dependence of strain and stress in reinforced and prestressed sections as well as their load level dependence discussed in Section (2) have consequences for the physical meaning of the so called axis of reinforced or prestressed element. Contrary to homogeneous materials, in composite elements there is not a general definition of the axis of the element with the same unique meaning. This is a direct consequence of the fact that the position of the centroid of the composite section changes with the magnitude of an external load and with time. One must be aware of the fact that assuming constant position of an axis of the element gives only the approximate solution in case of repeated or sustained loads and that the first load application must be analysed with special care in some particular cases.

References to Section 3.3.1

Bruggeling A. S. G. (1991), *Structural concrete: Theory and its application.* A.A. Balkema, Rotterdam.

CEB Bulletin 213/214 (1993), *CEB-FIP Model Code 1990*, published by Thomas Telford Ltd., UK. ("MC90")

Dabrowski, K., Stachurski, W., Zielinski J.L. (1982), *Concrete structures.* Arkady, Warsaw.

fib Model Code 2010 (to be published in 2010). International Federation for Structural Concrete (*fib*), Lausanne, Switzerland. ("MC2010")

Ghali, A, Favre, R. (1994), *Concrete Structures: Stresses and Deformations.* E&FN Spon, an imprint of Chapman & Hall, London.

Hsu, T.T.C. (1993), *Unified theory of reinforced concrete.* CRC Press Inc., Boca Raton, Florida.

3.3.2 Bond behaviour and models

by Rolf Eligehausen and Agnieszka Bigaj-van Vliet

(1) Bond of steel to concrete

(1.1) Force transfer mechanism

(1.1.1) Introduction

A fundamental issue for reinforced concrete is the bond between reinforcement and concrete. Bond covers various phenomena related to the resistance against pulling (or pushing) a reinforcing unit through the concrete, where it has been placed before hydration and hardening of the matrix. To outline bond behaviour two important aspects have to be considered, i.e. the force transfer mechanism between reinforcement and surrounding concrete and the capacity of concrete to resist these forces. It is a generally accepted view that the transfer of forces between a reinforcing unit and concrete is caused by chemical actions, forces from capillary source, friction and other mechanical actions that are activated at different stages of loading. The contribution of each of these mechanisms strongly depends on the surface texture of the reinforcement and its geometry. In the following these various mechanisms are discussed in relation to the different stages in bond behaviour and different types of reinforcement.

(1.1.2) Bond by adhesion

For all types of reinforcement when bond between a reinforcing unit and concrete is activated for very low bond stress values bond efficiency is assured by adhesion forces (the first stage in Fig. 3.3-6, 3.3-7 and 3.3-9). The designation adhesion stands here for the contributions to elastic bond, which refers to the deformation of the cementitious layer around the bar. It consists of both chemical and physical adhesion and interlocking between cement-stone and the microscopically rough steel surface. Failure of adhesive bond occurs at a very small relative displacement and therefore adhesion plays minor part in practice.

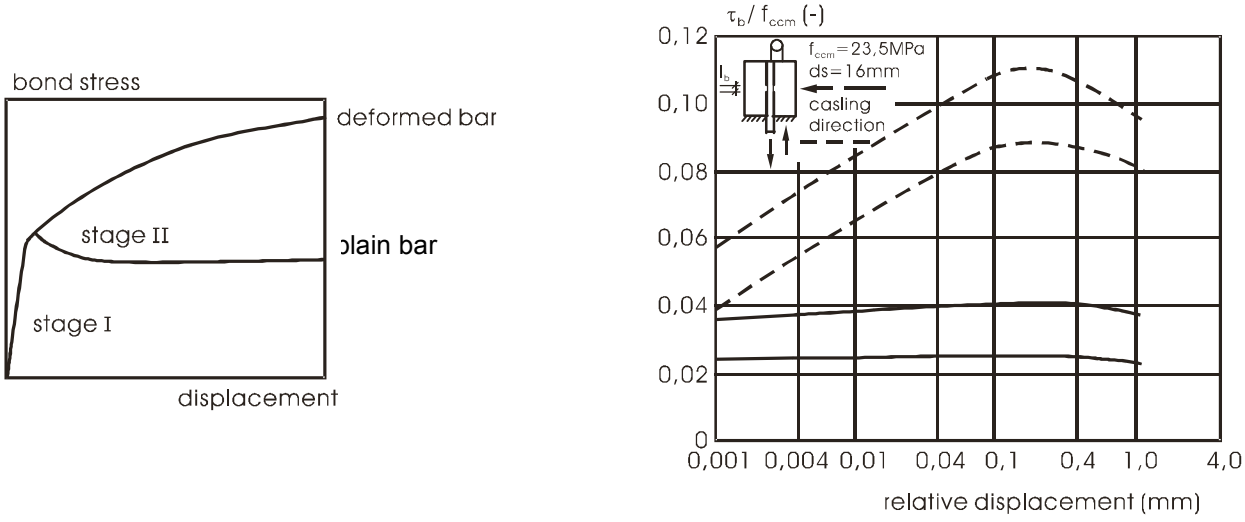

Fig. 3.3-6: Basic bond stress – slip relation for plain bars as a function of casting direction; schematic diagram and results of pull-out tests after Rehm (1961)

(1.1.3) Bond of plain bars

In case of plain bars (Fig. 3.3-6) after breakage of adhesive bond (debonding), in the following stage force transfer is provided by dry friction, i.e. the resistance against a parallel displacement between two surfaces that are kept in contact by a compressive force perpendicular to the contact plane (Stage II). The sliding plane is found to coincide with the steel-to-concrete interface for very smooth steel surfaces and to run through the cementitious layer around the bar when a certain threshold value of the roughness is passed. The radial compressive stress connected to this friction is caused by shrinkage, roughness of the sliding plane and wedging of cement-stone particles. Due to wear of the sliding plane the radial compressive stress diminishes with increasing slip, and so does the bond stress.

(1.1.4) Bond of ribbed bars

In case of ribbed bars (Fig. 3.3-7), after the stage of adhesive bond (Stage I), the force transfer is mainly governed by bearing of the ribs against the concrete. In the following stage (Stage II), for higher bond stress values, the concentrated bearing forces in front of the ribs cause the formation of cone-shaped cracks starting at the crest of the ribs. The resulting concrete keys between the ribs transfer the bearing forces into the surrounding concrete, but the wedging action of the ribs remains limited. In this stage the displacement of the bar with respect to the concrete (slip) consists of bending of the keys and crushing of the concrete in front of the ribs. The bearing forces, which are inclined with respect to the bar axis, can be decomposed into directions parallel and perpendicular to the bar axis. The sum of the parallel components equals the bond force, whereas the radial components induce circumferential tensile stresses in the surrounding concrete, which may result in longitudinal radial (splitting) cracks. The origin of the Stage III is marked by the formation of the first radial cracks. In this stage bond strength and stiffness are assured by the wedging action of the ribs on the concrete.

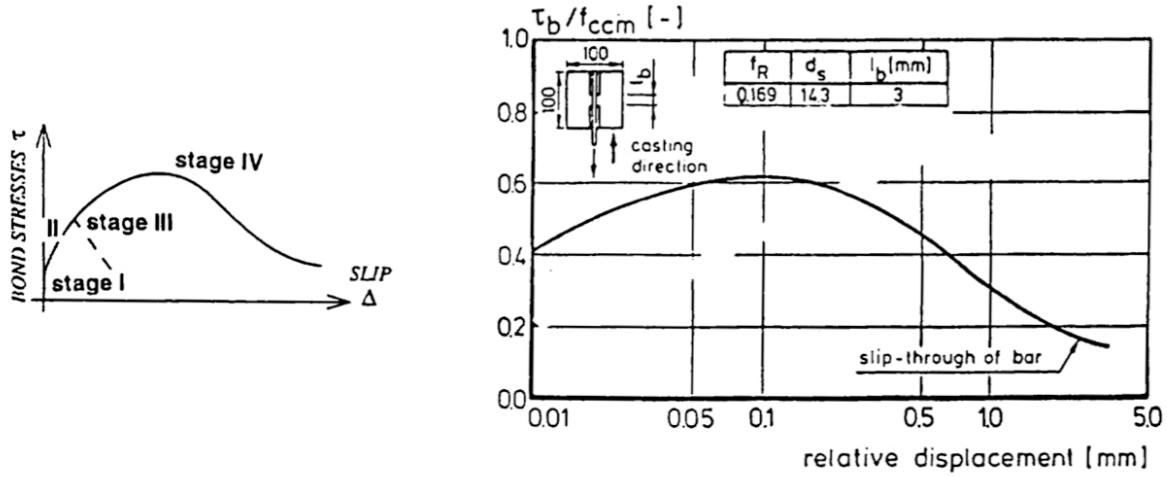

Fig. 3.3-7: Basic bond stress – slip relation for ribbed bar in case of pull-out failure; schematic diagram and result of pull-out test after Rehm (1961)

Finally, in the Stage IV, two failure modes can be considered (Fig. 3.3-8). If the radial cracks propagate through the entire cover bond splitting failure is decisive. In that case the maximum bond stress follows from the maximum concrete confinement, which is reached when the radial cracks have penetrated the cover for about 70%. Further crack propagation results in a decrease of the confining stresses. At reaching the outer surface these stresses are strongly reduced, which results in a sudden drop of the bond stress. Yet, the load bearing mechanism remains the same as in the previous stage. On the other hand, when the confinement is sufficient to prevent splitting of the concrete cover, bond failure is caused by pull-out of the bar. In that case the concrete keys are sheared off and a sliding plane around the bar is created. Thus, the force transfer mechanism changes from rib bearing to friction. The shear resistance of the keys can be considered as a criterion for this transition. It is attended by a considerable reduction of the bond stress. Under continued loading the sliding surface is smoothed due to wear and compaction, which will result in a further decrease of the bond stress, similar to the case of plain bars.

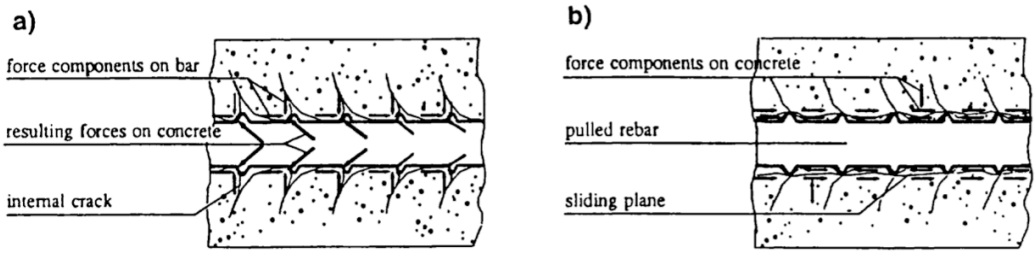

Fig. 3.3-8: Deformations around the bar, after Den Uijl and Bigaj (1996)
a) for splitting bond failure
b) for pull-out bond failure

(1.1.5) Bond of prestressing strands

Distinction should be made between the post-tensioned and the pretensioned prestressing steel, since the two types of reinforcement significantly differ with respect to the prestress transfer and the force anchorage mechanism. While the efficiency of the pretensioned reinforcement fully depends on the bond of the tendon to concrete, the post-tensioned reinforcement only partially relies on the bond between tendon and the grout matrix (description of various prestressing systems is given in Chapter 3.2 on Reinforcement). In addition, what is of particular importance for bond behaviour, both types of tendons differ with respect to the deformation in the transverse direction (Poisson effect): while in case of pretensioned tendon expansion is observed along the development length and contraction in the anchorage zone, in case of post-tensioned reinforcement contraction is found both along the development and anchorage length. Implications of this fact are discussed in detail in the Section 3.3.2 (1.1.7), devoted to the influence of level of stress in the reinforcing unit on its bond behaviour.

The following discussion mainly uses the results from research on bond of pretensioned prestressing reinforcement, however the description of force transfer mechanism to very high extent applies to the post-tensioned reinforcement as well (i.e. with respect to the bond between the tendon and the grout matrix). Smooth and ribbed prestressing steel behave in principle similar to the ordinary reinforcement with the same type of surface deformation (Fig. 3.3-9). Somehow different is the behaviour of a prestressing strand with helical outer wires. When such strand (e.g. seven wire strand) is moved through the concrete matrix the

helical concrete ribs are formed, which reminds of the concrete keys that form between the ribs of a ribbed steel bar. Contrary to the latter case, however, helical concrete ribs around the strand are never sheared off and a strand that is moved through the concrete follows the pre-shaped channel. Hence, rib bearing does not play a dominant role in case of a prestressing wire strand. Instead, other phenomena contribute to the mechanical bond action in this case. Bond of a prestressing wire strand with no lugs or indents can mainly be ascribed to friction, that is activated after rupture of the initial bond (adhesion, mechanical interlocking of cement stone into microscopically rough strand surface). This debonding occurs at a very small relative displacement (slip) and the bond force transmitted before debonding is small compared to the prestressing force. Besides factors discussed in case of plain bars, in the case of prestressing strands the radial compressive stress connected to friction is additionally caused by: wedging action caused by irregular shape of a strand (lack of fit due to the larger diameter of the centre wire, varying pitch), Poisson effect (strand diameter changes inversely proportional to local steel stress) and pitch effect (change of pitch when steel stress changes is prevented by surrounded concrete, both when steel stress is decreased and increased).

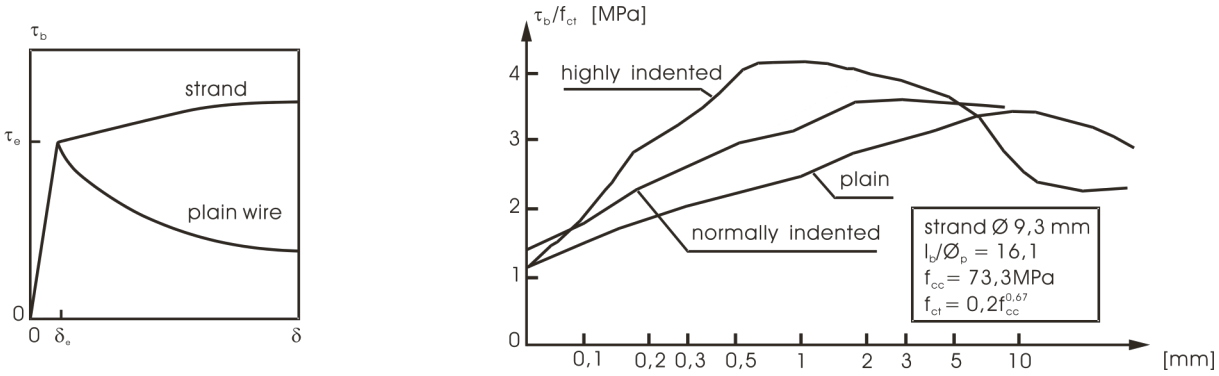

Fig. 3.3-9: Basic bond stress – slip relationships for prestressing steels; schematic diagram of plain wire and plain seven-wire strand and results of pull-out tests after Karlsson (1985) for plain and indented strand

When the roughness of the tendon is increased (e.g. by means of indents or lugs) a considerable amount of force is transferred through normal compressive stresses in the contact areas in the manner similar to that described in case of ribbed bars (Fig. 3.3-9). As far as the bond mechanism is considered, a transition between the frictional mechanism of plain wires and strands and the rib bearing mechanism of ribbed bars can be assumed. An indented wire strand presents a stronger splitting action than a plain wire strand since the bearing stresses are inclined with respect to the tendon axis, thus generating circumferential tensile stresses. Alike for ribbed bars this may result in bond splitting. Provided sufficient confinement is available to prevent bond splitting the concrete keys between the lugs are sheared off, which may lead to pull-out failure.

(1.1.6) Influence of reinforcing unit geometry

The general bond behaviour and the bond splitting action are directly dependent on geometrical parameters, characterising the reinforcement. Comparing different types of reinforcement with respect to their bond behaviour shows that in case of strands the bond splitting action is very limited, due to the low radial displacement of the sliding plane. Indented wire strands present a stronger splitting action than plain wire strands. On the contrary, with ribbed bars much greater splitting forces are generated, which may require

larger cover or considerable confining reinforcement to prevent bond splitting or to limit the crack width. However, the bond behaviour that can be improved by indenting the surface or providing it with ribs will result into a reduction of the transfer length and, hence, crack spacing and crack opening (see also Section 4.3).

The geometry of a reinforcing unit plays an important role in determining the force transfer mechanism and, hence, the bond performance. The effect of increased surface roughness in case of prestressed tendons has been already mentioned. Different indent shapes are used in practice. Some have a flat bottom and a steep edge; others have a circular longitudinal cross-section, resulting in a small slope of the edge. No information is found about the influence of the shape of indents on bond strength and bond splitting of indented tendons. Some investigations have been performed of the geometrical influences on bond of seven-wire strands. The frictional bond resistance of a seven-wire strand is thought to be enhanced by geometrical properties that contribute to the wedging effect and by the pitch effect. The geometrical characteristics involved are the ratio between the diameter of the outer wires and the diameter of the centre wire and the pitch with which the outer wires are laid around the centre wire (higher bond strength values are found for increasing ratio of outer wire to centre wire diameter and for decreasing pitch values). The currently produced seven-wire strands do not show a very large variation of the geometrical characteristics and in this case the variation of the bond strength attributed to this influence can be in general disregarded. However, for quite different (new) geometries this may not be the case anymore. Therefore warning is given that the relations given by MC90 are valid for a strand geometry as defined in the current material code for reinforcing steel (see Chapter 3.2 on Reinforcement).

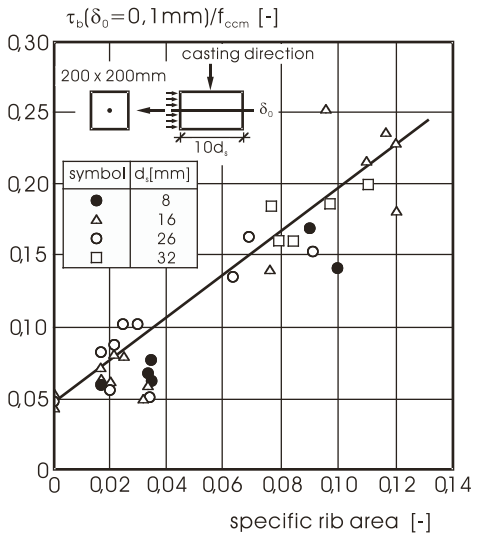

Fig. 3.3-10: Bond stress as function of the relative (specific) rib area; results of pull-out tests after Rehm (1969)

In case of ribbed steel bars the bar geometry governs to a high degree the general bond behaviour and determines the bond resistance. In particular the height of the ribs and their spacing are the most important parameters in this respect. A coefficient has been proposed that combines both influences and that reasonably describes the influence of the deformation pattern on the local bond behaviour. The relative rib area f_R is defined as the quotient of the axial projected area of the rib and the circumferential area of the bar, see also Section 3.2, section 3.2.2 (6) on bond properties of reinforcing steel. Note that rib height and rib distance

can be considerably changed without much influencing the bond behaviour as long as the related rib area reminds approximately constant. With increasing the value of the related rib area the bond strength and the bond stiffness increase (Fig. 3.3-10 and Fig. 3.3-11). It should be noted, however, that since the ultimate bond strength is reached at decreasing slip values, the bond becomes more brittle for increasing f_R. Also the splitting ability increases considerably with increasing values of the relative rib area. There is a clear link between the research done to determine the effect of rib geometry on bond and the requirements for the currently produced ribbed steel bars. The limit values for the relative rib area which are given in the material code for reinforcing steel (see Section 3.2 on Reinforcement) are optimised from the point of view of bond resistance and splitting ability in normal strength concrete and evolve from the required performance under service load (limited crack opening and deflections, restricted splitting cracking with normal concrete cover).

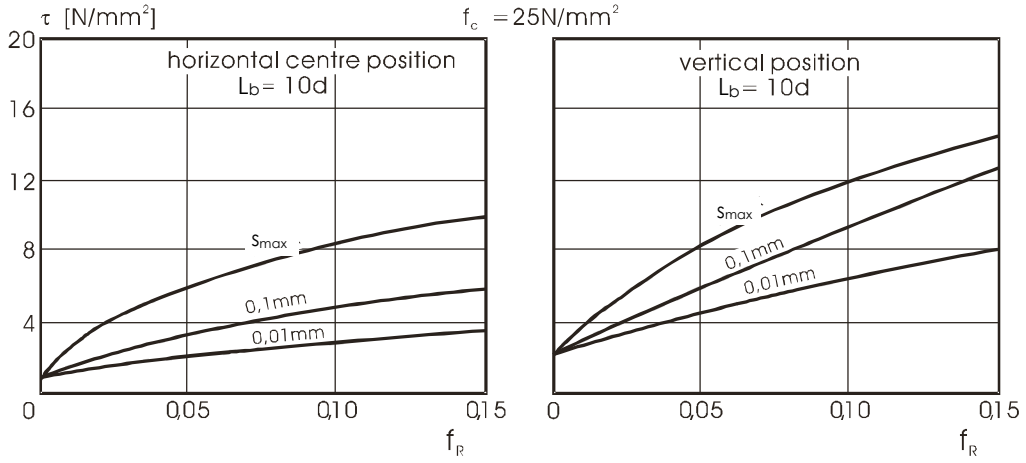

Fig. 3.3-11: Influence of specific rib area on the bond stress at a certain displacement at the free end of the bar; results of pull-out tests after Martin and Noakowski (1978)

(1.1.7) Influence of stresses level in the reinforcing unit

Last but not least aspect, that has to be discussed with respect to the force transfer from reinforcing unit to surrounding concrete, is the stress level in the bar. In general, the stress in the bar is considered to have a negligible influence on the bond resistance of ribbed bars. As long as rib bearing is the force transferring mechanism (splitting bond failure) this can be justified, considering that the transverse deformation coupled with the local steel stress change (Poisson effect) is small in comparison with the rib height. When the force transfer mechanism changes from rib bearing to friction (pull-out failure), the local transverse deformation of the bar cannot be disregarded anymore, since the roughness of the sliding plane is of much smaller magnitude than the rib height. This transverse deformation may considerably influence the development of the radial compressive stress and, hence, the frictional bond stress. The contraction of the bar coupled with an increasing steel stress will result in a reduction of the bond stress, which may become pronounced when the bar starts to yield (Fig. 3.3-12). Similar effects are to be expected for plain reinforcing bars as well. To certain extend MC90 implicitly takes the effect of bar contraction into account assuming the variable bond stress-slip relation along the transfer length (bond stress reduction in the vicinity of the crack), see the following section.

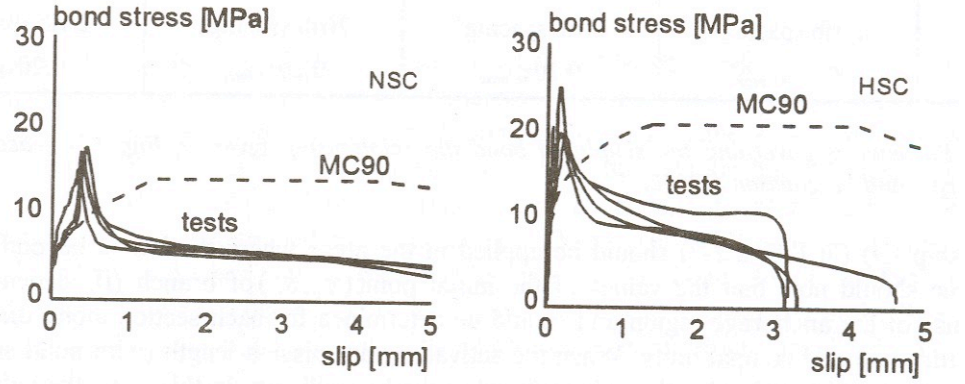

Fig. 3.3-12: Bond stress-slip relationship derived from pull-out tests on 20 mm diameter bars with long embedment length: (left) f_{cm} = 28 MPa; right) f_{cm} = 95 MPa, after Bigaj (1999)

The Poisson effect influences also the bond stress in case of prestressing strands. As already mentioned transverse deformation of the prestressing tendon depends on the situation (transfer length of anchorage zone) and differ for pretensioned and post-tensioned reinforcement. When the external force is released the diameter of pretensioned tendons increases, which generates a radial compressive stress and, hence, contributes to the frictional bond resistance. Due to this effect the bond resistance of a tendon is strongly reduced when the steel stress is increased. This influence is related to the local change in the longitudinal steel stress, since the transverse contraction is proportional to the stress level. As a consequence two different bond situations can be distinguished. Along the transfer length the steel stress is reduced at transfer, which causes an increase of the tendon diameter and, hence, contributes to the bond resistance. On the other hand, under flexural loading the steel stress in a cracked section is increased, which results in a reduction of the tendon diameter and a lower bond resistance. As far as post-tensioned reinforcement is concerned the influence of tendon contraction due to the Poisson effect can be explained in the similar way as done above for the ordinary reinforcement. Obviously the magnitude of this effect depends on the roughness of the tendon surface, which is usually considerably lower than in case of ordinary ribbed reinforcement. It should be remembered, however, that the stress level in the prestressing steel (and, hence, the related transverse deformation) is normally much higher than in ordinary reinforcement. The effect of stress level in reinforcement on its bond behaviour is explicitly recognised in MC90 by considering a lower bond strength beyond the transfer length than along the transfer length in case of pretensioned tendons.

(1.2) Resistance against bond forces

(1.2.1) 'Action' and 'reaction' forces

In the preceding section the 'action' part of the bond phenomenon has been extensively treated. Similar attention must be given to the 'reaction' part as well. Discussion of the force transfer between the bar and the surrounding concrete shows that the equilibrium is required between radial components of the concentrated anchorage forces, which radiate from the bar into the concrete, and between circumferential tensile forces activated in the concrete and additional confinement (such as transverse reinforcement and external forces). Hence, the confining capacity of reinforced concrete surrounding the bar (i.e. resistance against bond forces) affects the magnitude of the ultimate bond stress and the mode of bond failure to the same extend as the 'action' forces. In the following the most important parameters influencing the resistance against bond forces are discussed.

(1.2.2) Influence of concrete quality

Importance of concrete quality follows directly from the discussion of fracture propagation around the pulled bar. The local hardness of the concrete layer in contact with ribs of indentations is obviously important for the rib bearing mechanism. The local concrete hardness is however difficult to evaluate and can only to some extend be represented by the strength of concrete in compression. In normal strength concrete it can be shown that for small and medium displacements the influence of the compressive strength on the local bond resistance is approximately proportional (Fig. 3.3-13).

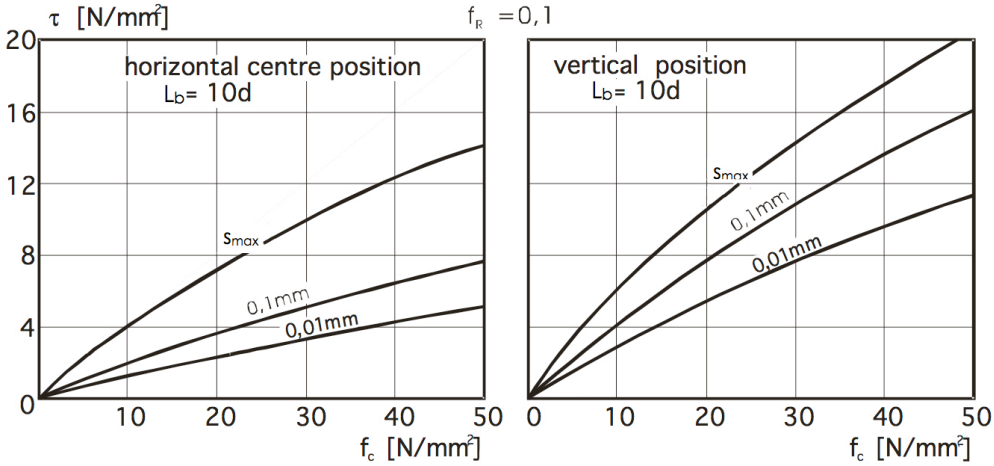

Fig. 3.3-13: Influence of the concrete compressive strength on the bond resistance; results of pull-out tests after Martin and Noakowski (1978)

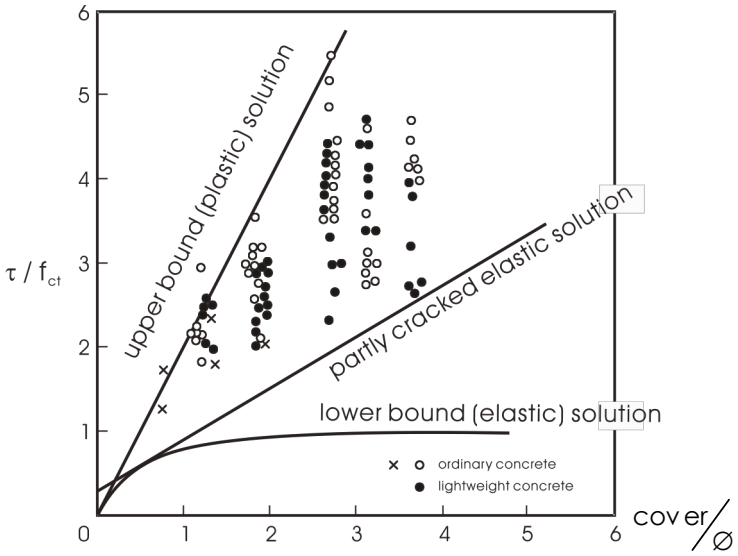

Fig. 3.3-14: Bond capacity of the pull-out specimens failed in longitudinal splitting as a function of tensile strength of concrete and relative thickness of concrete cover; test results and analytical solutions evaluated by Tepfers (1979)

It should, however, be remembered that in a multi-dimensional stress field the compressive strength of concrete is limited by its tensile strength (see Chapter 3.1 on Concrete). The fact that bond depends on the tensile strength of concrete is not always realised by engineers. If bond failure is caused by splitting the strength of concrete in tension is of major importance since (for constant cover thickness) it defines the concrete cover splitting criteria (Fig. 3.3-14). In fact the splitting of concrete due to the action of the bond is similar to the tensile splitting test of plain concrete, with one fundamental difference that while the tensile stresses are almost uniformly distributed in a splitting test specimen, they are very unevenly distributed around an anchored bar.

The position of bars during casting significantly influences the quality of the concrete layer surrounding the reinforcement and, hence, the bond behaviour. Settling of fresh concrete and accumulation of porous mortar under the reinforcing bars installed perpendicular to the casting direction (horizontally cast bars) or beneath the ribs of bars which are parallel to the casting direction (vertically cast bars) are the main reasons for this effect. Its magnitude depends on the casting direction with respect to reinforcement axis, depth of the concrete below the bar (for horizontally cast bars) and loading direction (for vertically cast bars). When a horizontal bar is placed only a few centimetres above the bottom of a mould, the local concrete quality around the bar is much better than in the case of the horizontal top position. Horizontally cast bars show a lower local concrete quality than vertically cast bars. Hence, bond strength and bond stiffness are highest for bars cast in vertical position and loaded against the settling direction of concrete or for bars cast in horizontal position not much above the bottom of the specimen, respectively. Bars cast in vertical position and loaded in setting direction of the concrete and bars cast in horizontal position well above the bottom of the framework respectively show an inferior bond behaviour compared to the first group (Fig. 3.3-15). Since the described here effect is related to the settlement of fresh concrete around the bar, the properties of fresh concrete itself (e.g. represented by slump) are also very important for the change in bond capacity due to the casting position.

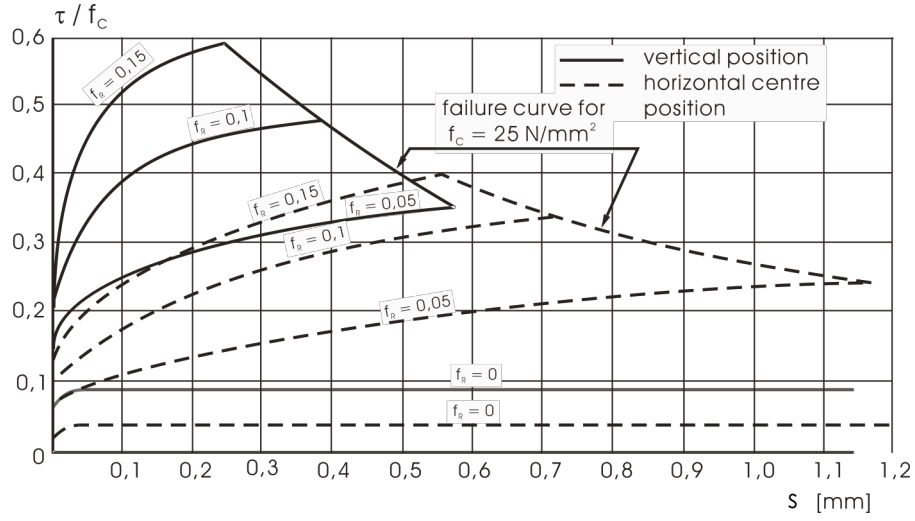

Fig. 3.3-15: Influence of the position of the bar during casting on the bond resistance; test results after Martin and Noakowski (1978)

(1.2.3) Influence of state of stress in the surrounding concrete

Tensile forces transverse to the anchored reinforcement reduce the ability of concrete to resist splitting tensile forces and quicken the onset of splitting failure. On the contrary, the failure due to splitting forces can be delayed if there are compressive forces transverse to the anchored reinforcement. These compressive forces are added to the tensile ones, where the directions are the same and compensate each other. Moreover it increases the frictional force on the steel-to-concrete or concrete-to-concrete failure surface.

Tensile stresses can be created in structural elements not only as result of external loading or dowel forces but also due to shrinkage of concrete or temperature effects. Since these tensile stresses increase the tensile splitting stresses around the bar, the bond strength is found to decrease rapidly with increasing lateral tensile stress, becoming zero at the lateral tensile stress equal to concrete tensile strength (Fig. 3.3-16). This may result in decreased ultimate resistance of the anchorage. In this respect it should be reminded that only a part of the tensile strength (the effective tensile strength) is available for structural purposes. The designer should estimate the proportion which is affected by uniform and non-uniform shrinkage, by temperature and by different types of external constraint. He should also examine the consequences of a possible error of judgement; see also Chapter 3.1 on Concrete.

Discussing the effect of lateral compression on bond behaviour of bars in real structures distinction should be made between passive and active confinement, since they contribute to the lateral confinement in a different way. The passive confinement due to the clamping action of the concrete surrounding the bar and that delivered by transverse reinforcement is activated when a certain relative displacement of bar the takes place with respect to the surrounding concrete. Hence, it depends on concrete dilatancy connected to the radial stress at the concrete-to-steel interface. The active confinement results from loads transverse to the bar, i.e. resulting from a support or from the column force in a beam-column joint. Its effect does not depend on the mobilised bond stress. Therefore the active confinement is more efficient than the passive one. In practice often both active and passive confinement are present.

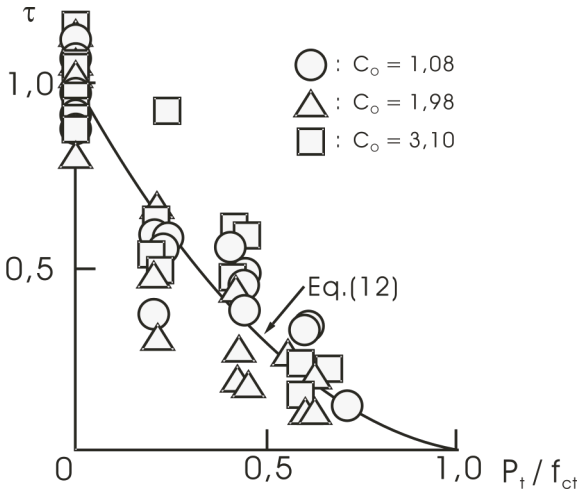

Fig. 3.3-16: Influence of lateral tensile stress, p_t, on bond strength for different relative concrete cover, c_o; test results after Nagatomo and Kaku (1992)

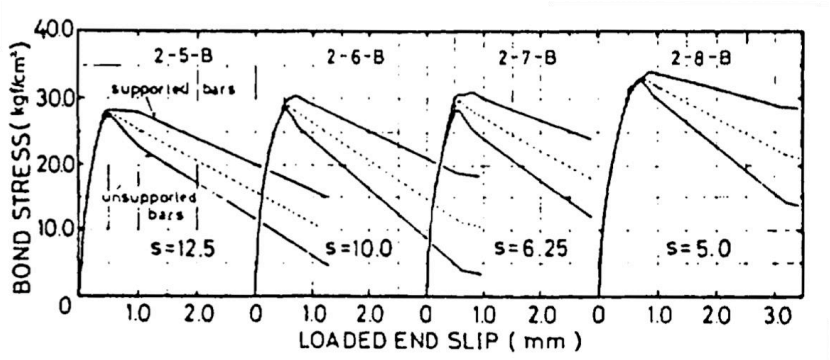

Fig. 3.3-17: Effect of stirrups on bond strength of bars –bond stress versus slip for decreasing stirrup spacing, s (increasing confining reinforcement); test results after Morita and Fuji (1982)

The influence of passive confinement depends on the bond failure mode. An increase of bond strength proportional to the confining stress delivered by the transverse reinforcement is observed in case of bond splitting failure (Fig. 3.3-17). Confining reinforcement is most effective when it crosses splitting cracks; therefore its effectiveness depends on its position in respect to the bar and on the kind of reinforcement, e.g. straight bars, stirrups of coils. As far as the pull-out failure is concerned it is usually assumed that once the transition from rib bearing to friction has taken place the bond strength cannot be increased by transverse reinforcement. Similar effect is observed with respect to concrete cover on the bar: in case of splitting an increase of ultimate bond resistance is found with increasing concrete cover thickness, which is not effective anymore as soon as pull-out failure mode takes over. On the contrary, active confinement contributes to bond strength in both failure modes, significantly increasing ultimate bond strength and reducing values of slip at a particular load (Fig. 3.3-18).

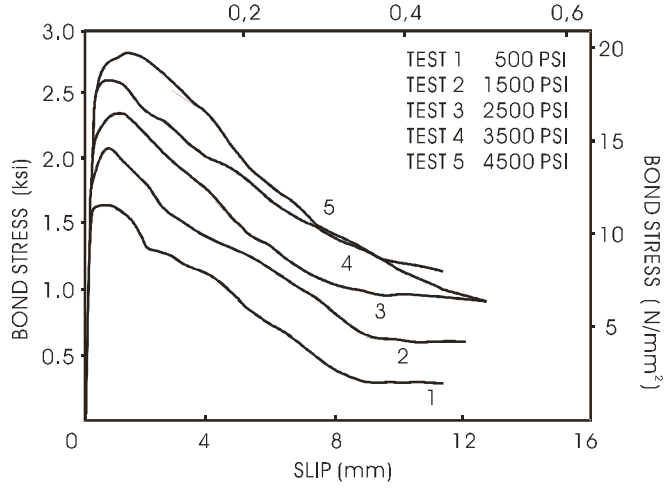

Fig. 3.3-18: Effect of increasing lateral pressure on bond behaviour; complete bond stress – slip curves after Malvar (1992)

It has been acknowledged in MC90 that the degree of confinement of a bar affects both the magnitude of the ultimate bond stress and the bond stress-slip relation. Both characteristics have been defined as a function of the confining conditions: bond in "unconfined concrete" or "confined concrete". However, the bond stress-slip relation is not a continuous function of the degree of confinement, but is given for upper and lower limits only: splitting failure in unconfined concrete and pull-out failure in confined conditions.

(1.2.4) Influence of boundary restraint (concrete cone pull-out)

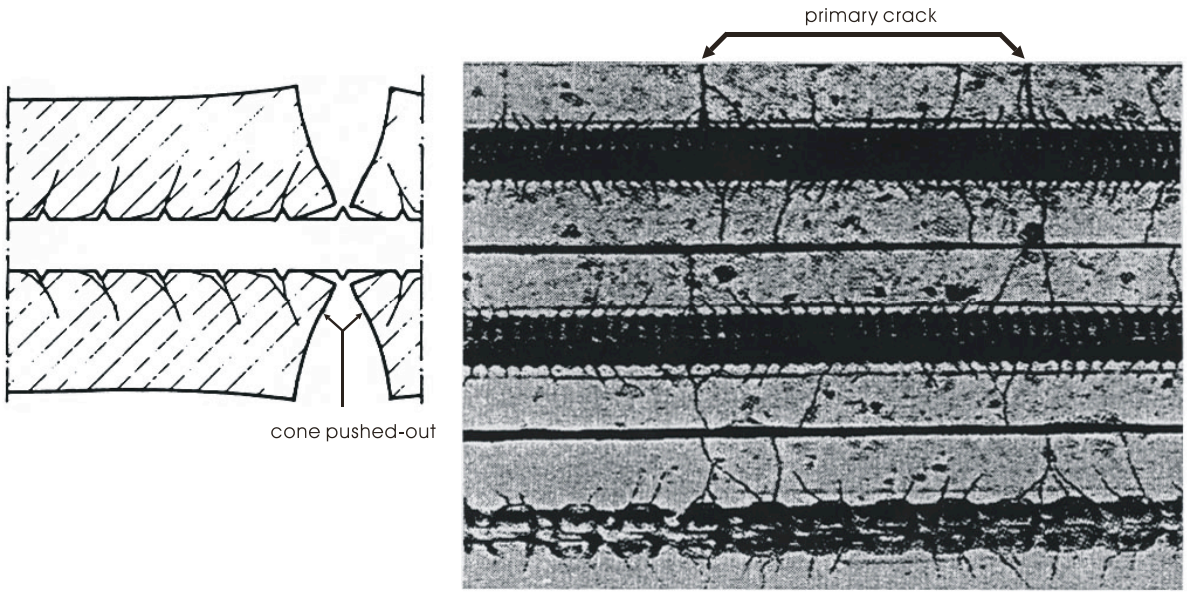

Fig. 3.3-19: Formation of the cone-shaped piece of concrete when the first rib is located near the crack; schematic drawing and picture of internal cone-shaped cracks around ribbed bar after Goto and Otsuka (1978)

The local bond stress-slip response is affected by the state of stress in the surrounding concrete. Since this state of stress significantly differs with boundary conditions and distance from the boundaries, it is not surprising that differences in bond stress-slip relations along the transfer length of an embedded bar may occur. Pull-out loading with relative displacement into the direction of the free edge will result in an earlier occurrence of radial cracks due to lack of restraint near the end of a concrete member or near a crack. In those cases often a concrete cone is pulled out (Fig. 3.3-19). Both the occurrence of radial cracks and cone pull-out are connected with a considerable reduction of bond stress. This effect is often taken into account by assuming an unbonded length at the free edge. MC90 accounts in a different way for the influences related to the introduction of bond forces near the entrance plane: it assumes the reduced bond stress-slip envelopes that are sized proportional to the distance from the entrance plane.

(1.3) Influence of load time history

Preceding discussion of bond behaviour focused mainly on the effect of monotonically increasing short term loading. In practical cases, however, a fraction of the working load will act permanently or repeatedly on a structure. Because the load repetition, rate and frequency influence the behaviour of concrete under tension and compression, they can be expected also to influence the bond stress-slip relationship. Hence, there must be an analogy between the laws governing the behaviour of compressed concrete with respect to failure criteria, creep, high cycle and low cycle fatigue and the laws of bond behaviour. As described in the preceding sections, three types of bond failure can be distinguished: failure due to excess of shear strength between the bar and the concrete (chemical or friction type), failure due to excess of tensile strength of concrete (with eventual effect of additional confinement) in an ultimate splitting failure, failure due to excess of shear strength of concrete in concrete corbels formed around ribbed bars in case of pull-out bond failure.

In view of the above, bond strength due to fatigue must depend on how each of these three strengths is affected by alternating or sustained loads. While first type of the failure has hardly been investigated from the fatigue point of view, much more is known about the bond fatigue in case of splitting failure. If the loads are repeated the splitting strength of concrete is affected by fatigue to the same extend as it has been observed for concrete under compression or tension, see Chapter 3.1 on Concrete. The fatigue resistance for bond can be then represented in the form of Wöhler curves, as shown in Fig. 3.3-20.

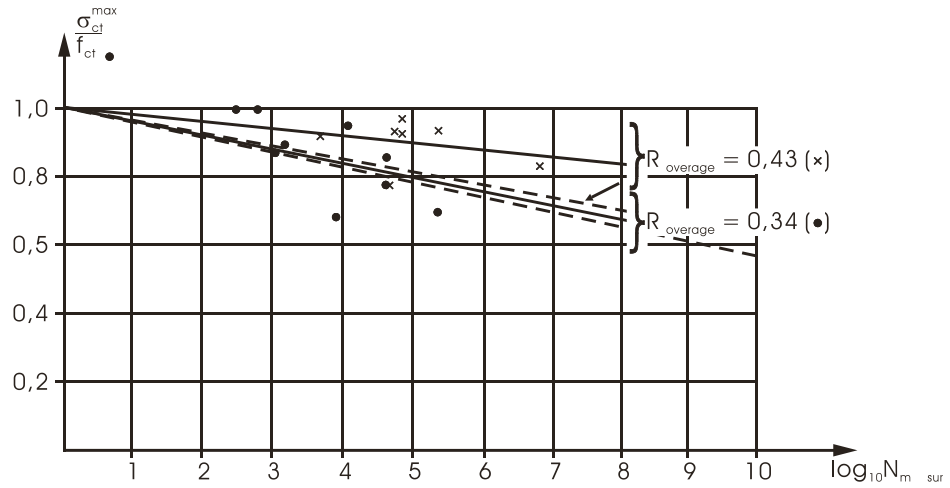

Fig. 3.3-20: Wöhler-curves for the tensile strength of concrete in ultimate failure pattern for spliced ribbed bars; evaluation of test results after Tepfers (1973)

In case of pull-out bond failure – the most resistant type of bond fatigue – it has been generally agreed that a repeated bond force of the same sign has about the same influence on deformation and failure of the concrete as has been observed for concrete uniaxially loaded in compression. Hence, the fatigue strength of bond under repeated loading, both for low cycle fatigue (high load intensity but low number of cycles) and high cycle fatigue (high number of cycles but low load intensity), corresponds to the fatigue strength of centrally loaded concrete (Fig. 3.3-21). The greater the peak load (slip) or the greater the load (slip) amplitude and the more load cycles applied the greater bond deterioration is to be expected.

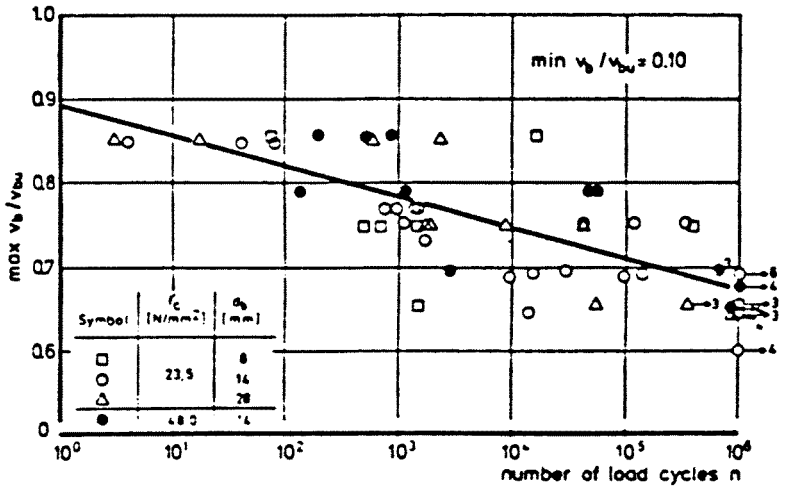

Fig. 3.3-21: Influence of the bond stress upper load, max v_b, related to the static bond strength, v_{bu} at constant lower load on the service life; test results after Rehm and Eligehausen (1979)

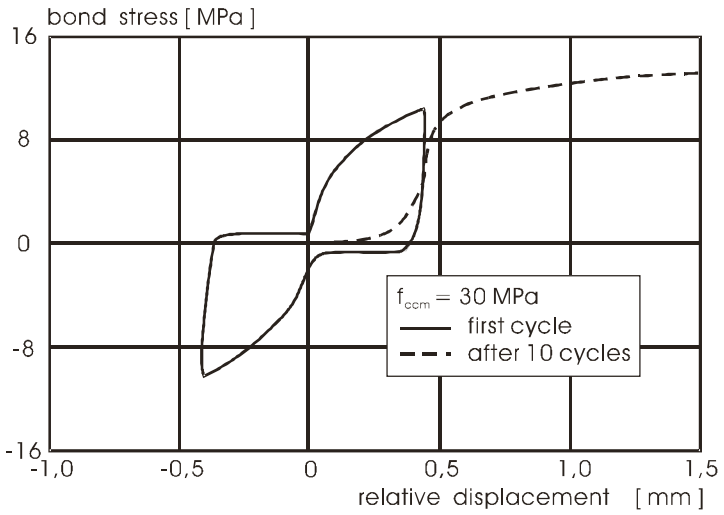

Fig. 3.3-22: Bond stress as a function of relative displacement when cycling between slip of ±0.44mm; test results after Eligehausen et al. (1983)

Cycles between relatively low bond stresses or corresponding low slip values (lower than fatigue limit of bond) deteriorate the bond during cycling, but do not affect the bond behaviour at ultimate load and the monotonic bond stress-slip relationship is reached again during reloading (Fig. 3.3-22). On the contrary, cycling between slip limits larger than that corresponding to a bond stress of approximately 80% of the static bond strength produces a pronounced deterioration of bond resistance at slip values smaller than the peak slip value and has a distinct effect on the bond stress-slip behaviour at larger slip values (so-called bond 'shake down') (Fig. 3.3-23). In this case the monotonic bond stress-slip curve cannot serve as an envelope curve, and the hysteresis loops are reduced with respect to the first load cycle. Cycles with reverse loading produce a degradation of bond strength and bond stiffness which is more severe than for the same number of cycles with unidirectional loading.

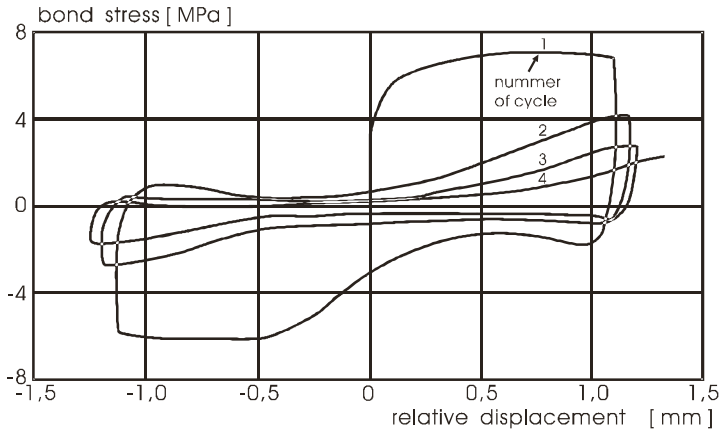

Fig. 3.3-23: Bond stress – slip curves for fully reversing relative displacement; test results after Eligehausen et al. (1981)

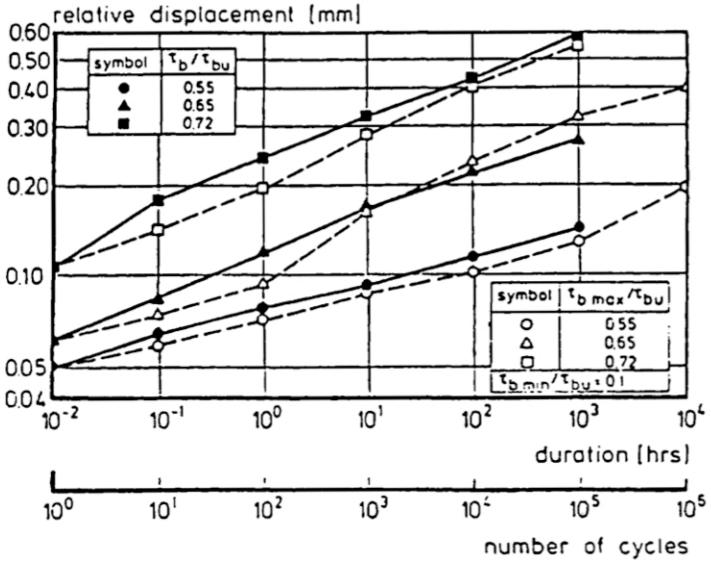

Fig. 3.3-24: Comparison between the curves obtained by Franke (1976) and Eligehausen and Rehm (1977)

Fig 3.3-24 demonstrates the analogy between the effect of sustained and of repeated loads on the increase of slip. In fact, as far as deterioration of bond is concerned, repeated loading can be considered as a time accelerator compared to sustained load. This is not surprising since in both cases creep of concrete under the ribs in the working load range causes an increase in slip between steel and concrete. The experimentally observed bond stress-slip curves under sustained load fall into the area bounded by the curves for $t = t_o = 0$ and for $t = \infty$.

(1.4) Further influencing factors

Concrete mix, size of maximum aggregate, bar spacing, number of bars in a layer, bar diameter and, last but not least, type of material used in reinforcing units (e.g. glass, FRP) all influence the bond resistance both in the case of splitting failure and in the case of bar pull-out. For more detail information on the influence on bond behaviour of these and other heretofore mentioned factors reader is referred to Eligehausen et al. (1983), Eligehausen and Rehm (1977), Franke (1976), Goto (1979), Goto and Otsuka (1978), Karlsson (1985), Malvar (1992), Morita and Fuji (1982), Nagatomo and Kaku (1992), Noakowski et al. (1979), Rehm (1961), Rehm (1969), Rehm and Eligehausen (1979), Tepfers (1973) Tepfers (1979), Den Uijl (1992a), fib (2000) and Mayer (2001).

(2) Measurement of bond performance

(2.1) Bond test specimens

To rationally describe the bond behaviour one should know the distribution of bond stresses and the possible slip between the reinforcing unit and concrete as well as stresses and strains in the surrounding concrete. Before the behavioural laws regarding the main influential parameters can be formulated tests need to be performed in order to attain necessary data for formulation of empirical relationships or for verification of analytical models.

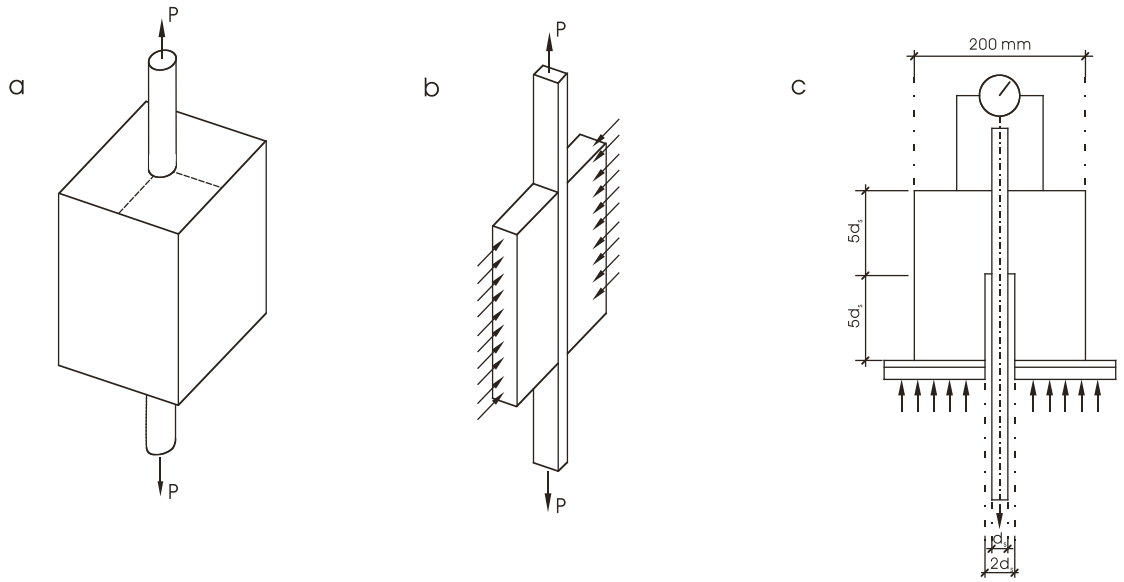

Fig. 3.3-25: Various types of bond test specimens (a, b) and set-up of pull-out test with short embedment length according to RILEM/CEB/FIP standard (c)

There are various methods to obtain the bond stress vs. slip relationship in an experimental way. In a conventional bond test a steel bar is embedded in the centre of the cross section of a concrete specimen and is pulled/pushed from both/single ends, Fig. 3.3-25a. With this type of specimen, it is possible to measure variation of steel strain and hence the bond stress distribution and the slips at the two ends. However, it is generally very difficult to measure local slips, strain distributions in the surrounding concrete and the extent of radial cracks. Another type of test specimen (Fig. 3.3-25b), with a strip of steel sandwiched between two plates of concrete facilitates in a better way the measurements of local slip, strains in the concrete and propagation of radial cracks (e.g. by means of Moire method). However, in this type of specimen the tensile tangential stresses, normally present in concrete surrounding the bar, are zero. In addition, the radial stress is constant along the length of the specimen and does not depend on the stress in the steel, as it is the case in reality. In order to avoid the difficulties in evaluation of bond stress non-uniformly distributed along the embedded length another type of test specimen has been introduced. Fig. 3.3-25c shows the specimen of RILEM/CEB/FIP standard pull-out test, which is devised to recreate a uniform distribution of the bond stress along a bar. To this end the short bonded length is adopted. To limit the boundary restraint the bonded length is moved away from the central region and an anti-friction rubber pad is inserted between the specimen and the bearing plate. Measurement of pull/push force and of the free-end displacement of the embedded bar depict uniformly distributed bond stress and local slip. This test set up is very suitable for investigating the effect of various parameters on bond behaviour. For instance the influence of active and passive confinement can be studied using transverse reinforcement (Fig. 3.3-26) or applying external pressure (in this case a cylindrical specimen is usually used).

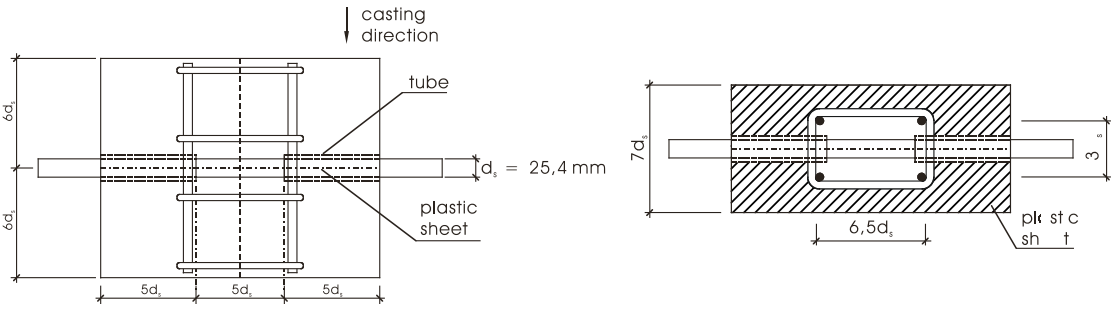

Fig 3.3-26: Test specimen used by Bertero et al. (1981)

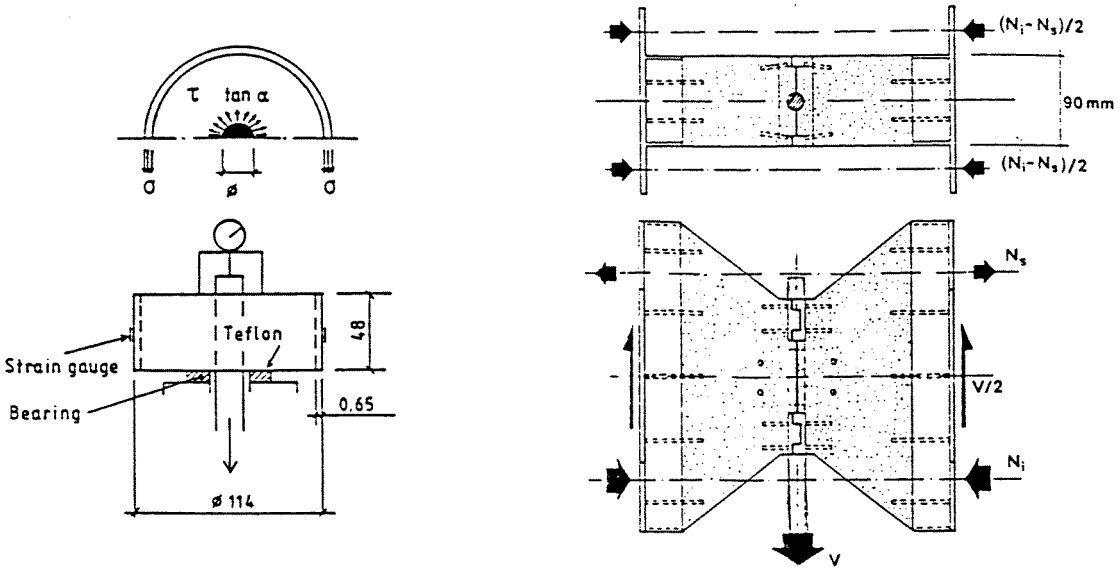

Fig. 3.3-27: Typical unsplit specimen in ring test (left) used by Tepfers and Olsson (1992) and presplit pull-out specimen (right) used by Gambarova et al. (1989)

A great variety of test specimens are used to study the bond-splitting interaction. In general they can be divided into initially unsplit (i.e. solid) and pre-split specimens; see examples in Fig. 3.3-27. Results of former tests provide information about the degradation of bond during the splitting process of uncracked concrete while the latter represent bond behaviour in concrete split due to e.g. bar corrosion, concrete shrinkage or previous severe loading. Due to the short embedded length of the bar for normal concrete grades and for normal type of reinforcing steel, yielding of the steel does not occur in tests described above. Pull-out tests with long embedment length or pull-pull load arrangement in set up similar to that given in Fig. 3.3-25a are used to investigate bond of yielded steel.

(2.2) Evaluation of test results

For the evaluation of test results it is important to realise that testing conditions influence the measurements to a very high extend. Size of the specimen, boundary restraint or state of stresses in concrete surrounding the bar introduced by the loading set up influences the bond behaviour. Therefore test results must be treated with caution since they are representative for a specific set of conditions and not generally valid. Furthermore it should be realised that in different regions of the reinforced concrete structure bond conditions do significantly differ, see example in Fig. 3.3-28.

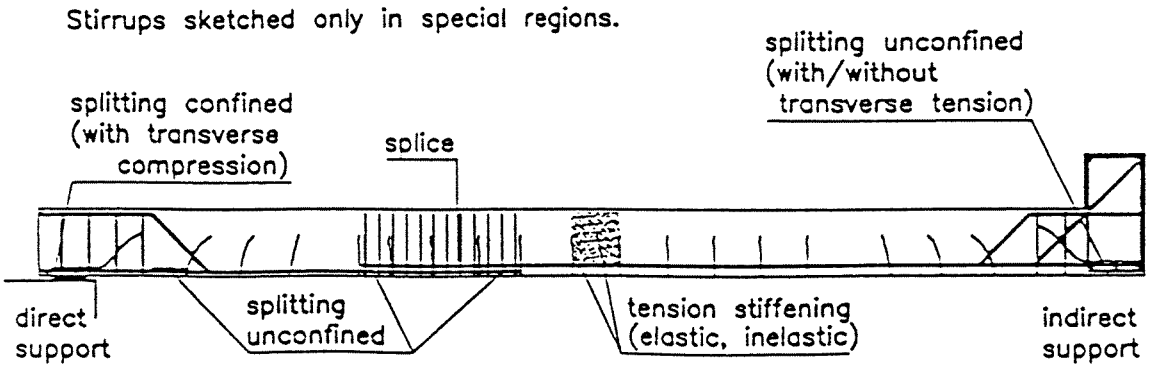

Fig. 3.3-28: Typical bond problems in reinforced concrete beam, after fib Bulletin 10: Bond of reinforcement in concrete, State-of-art report prepared by Task Group Bond Models (former CEB TG 2.5), (2000)

It is therefore necessary to simulate bond behaviour in these regions referring to the appropriate set of experimental data. For more information on test techniques to assess bond behaviour under different conditions (hence, representative for different member regions) reader is referred to the literature given in the preceding section as well as to the following references: Bertero et al (1981), Gambarova et al. (1989), Tepfers and Olsson (1992), RILEM/CEB/FIP Recommendations on Test and Specifications of Reinforcements for Reinforced and Prestressed Concrete (1970) and *fib* Bulletin 10: Bond of reinforcement in concrete, State-of-art report prepared by Task Group Bond Models (former CEB TG 2.5), (2000).

(3) Modelling of bond

(3.1) Idealisation and simplifying assumptions in modelling of bond

Research results provide the basis for improved understanding of the effects on bond performance of critical parameters such as confinement, spacing of bars, material properties etc. However, for practical reasons a certain degree of idealisation and simplification is required. In any case bond models should include in some way the following aspects: the type of collapse (through splitting, pull-out with/without partial splitting), the type of loading (monotonic/cyclic loads, pulsating/reverse loads), the confining action (active/passive confinement), the concrete type, and the specific requirements of prestressed concrete.

An approach to the modelling of bond must fit the total philosophy of design used for reinforced concrete structures. While in capacity design approaches (e.g. ACI code) designing for bond is considered to be a question of providing adequate strength along the bar anchorage for development of the bar yield force, in performance-based design approaches (e.g. MC90) considerations about deformation demand and supply are the main concern, since for this design strategy not only the strength of an anchorage must be assessed but also the level of deformation must be known that has to develop in order for the given strength to be realised. Hence, out of the two co-ordinates in the load-deformation response recorded in the bond/anchorage test the capacity design approach focuses only on the load capacity side, while the performance-based approach requires modelling of the complete load-deformation envelope of the bond-slip response.

(3.2) MC90 approach to modelling of bond

(3.2.1) Simplified bond stress–slip relationship

MC90 supplies the designer with a simplified local bond stress-slip relationship that may be used in practical applications. This relationship is often referred to as a constitutive law for bond. Note that this term is necessarily used loosely in this context, as bond is not an intrinsic physical property but the mechanical response of the bar-concrete assembly under certain specific boundary conditions. The bond model is based on experimental results and the provided bond stress-slip relationship should be considered as a statistical mean curve that can be applied as an average formulation for a broad range of cases. Therefore further reliability handling is needed to derive design bond stress-slip curves, at least in the cases where a more accurate design is considered. It must be kept in mind that for a given value of slip the coefficient of variation of the bond stress as high as 30% is frequently found in laboratory test series.

The model illustrated in Fig. 3.3-29 uses a non-linear law to relate the applied bond stress, τ, to bar slip, s. Model parameters: the bond strength, τ_{max}, and the residual bond capacity, τ_f, as well as the characteristic slip values, s_1, s_2 and s_3, depend on the state of confinement of concrete (and, hence, on the presumed mode of bond failure), concrete strength and quality of bond that is thought to be present, and, last but not least on the geometry of reinforcing bars. Table 3.3-2 summarises mean values of characteristic model parameters in all cases considered in MC90. The same bond stress – slip relationship is assumed regardless of whether the bar is pulled or pushed.

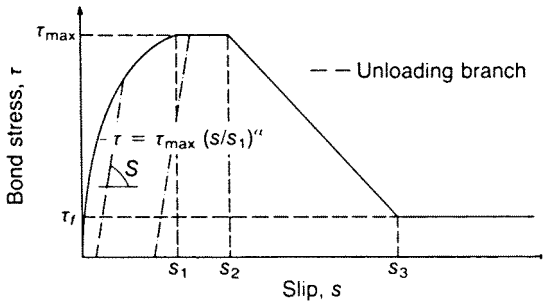

Fig. 3.3-29: Analytical bond stress –slip relationship (monotonic load) according to CEB-FIP Model Code 1990

No single bond stress – slip relationship is provided for pretensioned reinforcement, which is due to the fact that in this case significantly different bond situations should be considered due to the transverse deformations of the tendon (a push-in along the transmission length combined with tendon expansion at release and pull-out along the anchorage length with tendon contraction when the stress is increased due to loading). Nevertheless, the influence of loading case is considered when defining the design bond strength, as discussed in the sequel.

With respect to the influence of quality of bond and state of confinement, the bond characteristics are not defined as a continuous function of these influences but, for sake of simplicity, are given only for the upper and lower limits. Such a restriction has consequences for the accuracy of the estimated bond behaviour, but is acceptable from the practical point of view. Hence, distinction is made between unconfined and well confined concrete only. Concrete is defined as unconfined when the minimum concrete cover on the bar and the minimum transverse reinforcement are used (exact values given in MC90). Concrete is

defined as well confined when either concrete cover on the bars is larger than 5 times bar diameter Ø, and clear spacing is larger than 10Ø (or closely spaced transverse (enclosing) reinforcement is provided) or high transverse pressure is present (exact values given in MC90). It is assumed that in the earlier case bond failure by splitting of concrete takes place, while in the latter case pull-out bond failure prevails.

Reinforcement type		Confining conditions	Bond conditions	s_1	s_2	s_3	α	τ_{max}	τ_f	Remarks
ordinary reinforcement	ribbed reinforcing steel	unconfined concrete	good	0.6	0.6	1.0	0.4	$2.0\sqrt{f_{ck}}$	$0.30\sqrt{f_{ck}}$	$s_1 = s_2$
			poor	0.6	0.6	2.5	0.4	$1.0\sqrt{f_{ck}}$	$0.15\sqrt{f_{ck}}$	$s_1 = s_2$
		confined concrete	good	1	3	clear rib spacing	0.4	$2.5\sqrt{f_{ck}}$	$1.0\sqrt{f_{ck}}$	s_3 - bar dependent
			poor	1	3	clear rib spacing	0.4	$1.25\sqrt{f_{ck}}$	$0.5\sqrt{f_{ck}}$	s_3 - bar dependent
	smooth cold drawn wire	confined and unconfined concrete	good	0.01	0.01	0.01	0.5	$0.1\sqrt{f_{ck}}$	$0.1\sqrt{f_{ck}}$	$s_1 = s_2 = s_3$ $\tau_{max} = \tau_f$
			poor	0.01	0.01	0.01	0.5	$0.05\sqrt{f_{ck}}$	$0.05\sqrt{f_{ck}}$	$s_1 = s_2 = s_3$ $\tau_{max} = \tau_f$
	smooth hot rolled bars	confined and unconfined concrete	good	0.01	0.01	0.01	0.5	$0.3\sqrt{f_{ck}}$	$0.3\sqrt{f_{ck}}$	$s_1 = s_2 = s_3$ $\tau_{max} = \tau_f$
			poor	0.01	0.01	0.01	0.5	$0.15\sqrt{f_{ck}}$	$0.15\sqrt{f_{ck}}$	$s_1 = s_2 = s_3$ $\tau_{max} = \tau_f$
post-tensioned reinforcement	ribbed prestressing steel	similar to bond stress – slip relation for ordinary ribbed bars of the same diameter: for a given value of slip the value of bond stress an ordinary bar is multiplied by a reduction factor $\eta_p = 0.6$								
	strands	similar to bond stress – slip relation for ordinary ribbed bars of the same diameter: for a given value of slip the value of bond stress an ordinary bar is multiplied by a reduction factor $\eta_p = 0.4$								
	smooth prestressing steel	similar to bond stress – slip relation for ordinary ribbed bars of the same diameter: for a given value of slip the value of bond stress an ordinary bar is multiplied by a reduction factor $\eta_p = 0.2$								

Table 3.3-2: Bond model parameters in MC90

To derive the local bond stress-slip curve in cases that fall between that defined as unconfined and confined concrete linear interpolation can be used. Notice that a change in stiffness of the ascending branch of the bond stress-slip curve with changing confinement is neglected. Also the dependence of bond properties upon concrete compaction and curing is only globally covered by division into good and poor bond conditions.

With respect to the influence of concrete strength on bond behaviour, both τ_{max} and τ_f are defined as a continuous function of concrete compressive strength (i.e. proportional to the square root of f_{ck}). For example, for ribbed reinforcing bars the bond strength varies from $2.5\sqrt{f_{ck}}$ for good bond conditions in confined concrete (failure by shearing of concrete between the ribs) to $1.0\sqrt{f_{ck}}$ for poor bond conditions in unconfined concrete (failure by splitting of concrete). Much lower values hold for smooth bars. It is reminded that model parameters that describe the bond behaviour of ribbed reinforcement are valid for a rib geometry according to relevant material standards (in ENV 10080 the limit values for related rib area f_R are given) and that for other types of ribs or indentations the validity of the model must be checked.

Significant difference in the shape of bond stress-slip curves is found for splitting and pull-out bond failure, and only in the latter case (confined concrete) the bar slips at constant stress once the bond strength is attained up to a value of slip s_2 (in unconfined concrete $s_1 = s_2$). Beyond that point in both cases the bond resistance decays with increasing bar slip and it reaches a residual value of τ_f at a slip value s_3. The unloading branch of the bond stress-slip relationship is linear and valid for the ascending and horizontal part of the diagram. The slope of the descending branch is assumed to be independent of the slip value and estimated by an average value of $S = 200$ N/mm^3.

With respect to load time history, the influence of sustained and repeated loading on bond behaviour is considered. Since creep is found to reduce the slope of the ascending branch of the bond stress-slip relationship isochrone curves are used to describe the creep displacements due to the sustained or repeated loading. Restricting the validity of this procedure to the ascending branch of the bond stress-slip diagram the slip $s_{n,t}$ that includes creep displacement can be calculated as:

$$s_{n,t} = s\,(1 + k_{n,t}) \qquad (3.3\text{-}33)$$

where:

$k_t = (1 + 10\,t)^{0.080} - 1$ for sustained loading with known load duration t [in hours]
$k_n = (1 + n)^{0.107} - 1$ for repeated loading with known number n of load cycles

While a number of influential factors are explicitly included in the postulated bond model some others are neglected for sake of simplicity. Although in reality the stiffness of the ascending branch of the bond stress-slip curve differs from confined to unconfined concrete, in the postulated model the same value for the coefficient α is used in both cases to define the ascending branch of bond stress – slip relation according to the same function $\tau = \tau_{max}\,(s/s_1)^{\alpha}$. Moreover, the effect of the related rib area on bond strength and bond stiffness is not included, and as already mentioned the validity of the model is limited to steel bars with a geometry that is conform with the relevant material standards. Finally the dependence of bond properties upon concrete compaction and curing is only globally considered.

(3.2.2) Distance from the crack

To account for the influence of boundary restraint (concrete cone pull-out) in MC90 it is assumed that the reduced bond stress-slip envelopes may be used in relevant situations. Therefore, the values given in Table 3.3-2 for ribbed bars are valid for those parts of the bars which are at a distance x larger than 5 times the bar diameter Ø from the crack, hence in the regions where the influence of boundary restraint is found to be negligible. For those parts of the reinforcing bars which are in a distance from the transverse crack smaller than 5Ø, the bond stress τ and the slip s are to be reduced by the factor λ, which is proportional to the distance from the crack according to eq. (3.3-34):

$$\lambda = 0.2\frac{x}{Ø} \leq 1 \qquad (3.3\text{-}34)$$

(3.2.3) Differential equation of bond

The MC90 design bond model is a global, hand-calculation approach. It can be applied to predict crack formation and elongation of the reinforced concrete tie or to study anchorage of reinforcement. In the uncracked state it assumes equal strains in concrete and steel due to the compatibility conditions of full bond. After a crack has occurred tensile force acting on the bar is considered to be transmitted from the steel to the concrete by bond. At a distance equal or greater than the transfer length, l_t, the compatibility conditions of the uncracked state are assumed to be maintained again. The influence of bond is evaluated by considering the free body equilibrium of a segment of the anchored reinforcing bar (Fig. 3.3-29).

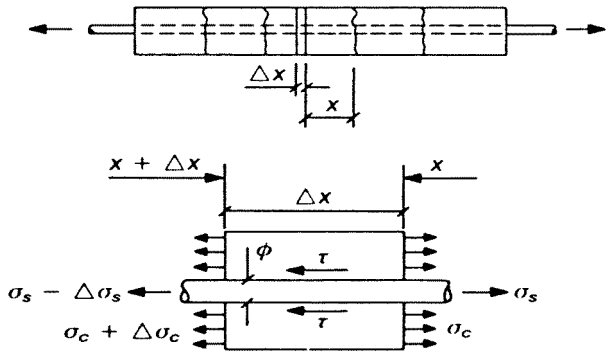

Fig. 3.3-29: Illustration for the differential equation of bond: bond stress – slip model applied to reinforced concrete tie

The critical section is at one end of the segment, at which point the applied bar stress is known. A distribution of bond stresses along the segment is obtained from local bond stress-slip relationships, postulated on the basis of experimental results as described above. The force in the other end of the bar segment is obtained directly from equilibrium considerations. If the characteristic stress-strain relationship of steel have a positive definite tangent stiffness throughout the strain range, then it is also possible to obtain the deformations along the anchored bar in addition to the distribution of stresses. The local decrease of the relative displacement along the transfer length l_t is characterised by the strain difference between steel and surrounding concrete.

Hence, the differential equations governing the behaviour of a single bar embedded in concrete can be summarised as follows.

reinforcing bar equilibrium:

$$A_s \frac{d\sigma_s}{dx} + \Sigma_o \tau(s) = 0 \tag{3.3-35}$$

strain – displacement relation:

$$\varepsilon_s - \varepsilon_c = \frac{ds}{dx} \tag{3.3-36}$$

reinforced concrete equilibrium:

$$A_c \frac{d\sigma_c}{dx} + A_s \frac{d\sigma_s}{dx} = 0 \tag{3.3-37}$$

where:

A_s	the reinforcing bar area
A_c	the concrete cross-sectional area
Σ_o	the reinforcing bar circumference
$\tau(s)$	the bond stress as a function of relative slip s
σ_s	the steel stress
σ_c	the concrete stress
ε_s	the steel strain
ε_c	the concrete strain on the area A_c

(3.2.4) Design bond stress

The distribution of bond stress over transfer length is non-linear and can be computed using the differential equation of bond and postulated bond stress-slip relationships. However for practical applications it is suitable to use mean bond stress value constant. For all but pretensioned types of reinforcement one mean bond stress value constant over the whole transfer length can be used. This principle is applied to analysis of anchorage of ordinary and pretensioned reinforcement as well as to designing the transmission (development) zones in the latter case.

For ordinary reinforcement the design value of the mean bond stress, in the following called design bond stress, f_{bd}, is given by:

$$f_{bd} = \eta_1 \eta_2 \eta_3 f_{ctd} \tag{3.3-38}$$

where:

η_1 a geometry factor (2.25 for ribbed bars and welded mesh made up of plain or indented wires - provided there is a sufficient number of welded cross bars in the anchorage zone, 1.4 for indented bars, 1.0 for plain bars)

η_2 an orientation factor for bond dependent on the position of bar during concreting (1.0 when good bond conditions are obtained, 0.7 in the other case)

η_3 bar size factor (1.0 for bars not larger in diameter than $Ø = 32$ mm, otherwise taken as $(132 - Ø)/100$)

f_{ctd} the lower design concrete tensile strength at 28 days ($= f_{ctk,min} / 1.50$)

In case of pretensioned prestressing tendons the bond strength depends on the loading case, as already discussed. Along the transmission length, where the tendons become thicker at release, higher bond strength should be taken into account that beyond that length, where the lower bond strength along the anchorage length should represents the effect of tendon contraction when the steel stress is increased due to loading. In MC90 it is considered by including a bilinear diagram for the embedment length that is required to develop the design steel stress. Hence, the design value of the bond strength for pretensioned prestressing tendon is given by:

$$f_{bpd} = \eta_{p1} \eta_{p2} \ f_{ctd} \qquad (3.3\text{-}39)$$

where:

η_1 a geometry factor (1.4 for indented or crimped wires, 1.3 for 7-wire strands)

η_2 an orientation factor for bond dependent on the position of bar during concreting (1.0 when good bond conditions are obtained, 0.7 in the other case)

f_{ctd} the lower design concrete tensile strength, for the transmission length taken at the time of release and for the bond strength along the anchorage length taken at 28 days

According to MC90 Section 1.6.4.1, the design bond stress given in Section 6.9.3 is valid for static and fatigue loading. This provision is based on the following considerations. The fatigue strength of bond agrees reasonably well with the fatigue strength of concrete in compression. Therefore the fatigue bond strength for $2 \cdot 10^6$ load cycles is about 0.6 – 0.65 times the static bond strength. This means, that with the partial safety factors assumed in MC90 ($\gamma_{global} = 2{,}1$ for bond failure), no fatigue failure of bond is to be expected during the service life of a structure. If no fatigue failure occurs, the bond strength in a subsequent test to failure agrees with the monotonic bond strength without proceeding load cycles. However, the safety against a fatigue failure of bond is rather low. This was considered as acceptable, because in most codes rather conservative fatigue loads were given. However, in the meantime in codes the fatigue loads are described very realistically. Therefore in case of fatigue loading the design bond stress given in Section 6.9.3 should be reduced according to the provisions valid for concrete in compression (see MC90, Section 2.1.7).

(3.2.5) Basic transfer lengths

Using the mean bond stress approach MC90 defines the basic transfer lengths for different types of reinforcement and different loading cases. The basic anchorage length of ordinary

reinforcement, l_b, i.e. the length that is needed to transfer the yield force of a bar is given by eq. (3.3-40):

$$l_b = \frac{Ø}{4}\frac{f_{yd}}{f_{bd}} \tag{3.3-40}$$

where:

$Ø$	the bar diameter
f_{yd}	the bar design yield stress
f_{bd}	the design bond strength of concrete

The design anchorage length $l_{b,net}$ can be derived from the basic anchorage length taking into account the beneficial effects of various factors such as shape of the anchored bars, transverse reinforcement, confinement, amount of reinforcement etc. Details of determining required anchorage length are discussed and in Section 4.5.3 (1.2).

The basic anchorage length of an individual pretensioned tendon, $l_{bp,}$ i.e. the length that is required to develop the full strength in an untensioned tendon or, in other words, the length that is needed to anchor a non-pretensioned tendon is given by:

$$l_{bp} = \frac{A_{sp}}{Ø\pi}\frac{f_{ptd}}{f_{bpd}} \tag{3.3-41}$$

where:

A_{sp}	the tendon cross-section
$Ø\pi$	the tendon perimeter (for circular cross-section $\frac{A_{sp}}{Ø\pi} = \frac{Ø}{4}$)
f_{ptd}	the tendon design yield stress (=f_{ptk} / 1.15)
f_{bpd}	the corresponding design bond strength of concrete

The transmission length of a pretensioned tendon, l_{bpt}, i.e. the length needed to introduce the prestressing force is given by:

$$l_{bpt} = \alpha_8\alpha_9\alpha_{10}\ l_{bp}\frac{\sigma_{pi}}{f_{bd}} \tag{3.3-42}$$

where:

α_8	a release factor (1.0 for gradual release, 1.25 for sudden release)
α_9	an action effect factor (1.0 for calculation of the anchorage length when moment and shear capacity are considered, 0.5 for calculation of transverse stresses in the anchorage zone)
α_{10}	a geometry factor (0.7 for indented or crimped wires, 0.5 for strands)
σ_{pi}	the stress just after release
l_{bp}	the corresponding basic anchorage length

The design anchorage length l_{bpd} can be derived from the basic anchorage length according to procedure discussed in detail in Section 4.5.3 (2.1).

(3.3) Advanced analytical bond models

The traditional approach to modelling the bond behaviour which is followed in MC90, uses the experimental data to represent the observed trends by the rules. These approaches are very practical and effective in large scale computations where complete structural systems must be modelled. However, they have clear limitations, implicit in empirical models. Many of these limitations and influences on the observed bond behaviour which are caused by the experimental set-up could be avoided if the analytical models of the bond in concrete could be used to supplement the experimental studies. A number of such a models have been developed, that take a more fundamental approach to the mechanics of bond. In such models, the local bond stress – slip relationship is no longer input property but rather a result of the computations that take into account the prescribed geometry, material properties and global boundary conditions. Hence, some of the mechanics-based bond models express the local bond stress – slip relationship as a function of the crack opening in split concrete. Plasticity models for bond use an alternative analytical approach, where bond stress and slip are fully coupled with the radial confinement stress and dilatation. Fracture mechanics applied to estimation of concrete confining capacity allows for more exact classification of the deformation mechanisms that contribute to bond slip (i.e. elastic deformation, secondary cone shaped cracking, radial cracking and concrete crushing). Last but not least, finite element idealisations can successfully be applied to analysis of bond behaviour. In particular 3-D finite element analysis are likely to provide most comprehensive solutions, however their computational demands render them impractical for large scale modelling of complete structural systems. Nevertheless, this concern, which in general applies to many refined analytical approaches, do not depreciate their value as a pertinent tool to derive characteristic bond stress – slip relations for global models, as it was done in the past with experimental results.

(3.4) Significance of bond for structural performance

Bond of reinforcing bars to concrete influences the behaviour of reinforced concrete structures in many respects. In an obvious way bond plays an important role in the cracking behaviour (crack widths and crack spacing) and the tension stiffening. It can be a key element for the ultimate load-carrying capacity of a reinforced concrete structures since it affects the anchorage of bars and the strength of lap splices. Moreover the deformation capacity of the members and, hence the redistribution capacity in statically indeterminate structures is directly influenced by bond: the length of a plastic hinge, which is of importance for the rotation capacity of reinforced concrete members, depends among other things on the force transfer from reinforcement to concrete between subsequent bending cracks. For that reason appropriate modelling of bond behaviour is of great importance. Design approach to bond must enable determining the performance of reinforced concrete structures under load with desired accuracy and safety. These aspects are discussed more in detail in the following Chapters. For more information on modelling of bond reader is referred to Ciampi et al. (1982), McCabe and Patazopoulu (1998), Rehm (1957), Rots (1989), Tepfers (1979), Den Uijl (1992b), Bigaj (1999), *fib* (2000) and Mayer (2001).

References to Section 3.3.2

Betrero, V.V., Ciampi, V., Eligehausen, R., Popov, E.P. (1981), *Analytical model for deformed bar bond under generalized excitations.* IABSE Colloquim, Delft, The Netherlands.

Bigaj, A.J., (1999), *Structural dependence of rotation capacity of plastic hinges in RC beams and slabs*. PhD Thesis, Delft University of Technology.

CEB Bulletin 213/214 (1993), *CEB-FIP Model Code 1990*, published by Thomas Telford Ltd., UK. ("MC90")

Ciampi, V., Eligehausen, R., Popov, E.P. (1982), *Analytical model for concrete anchorages of reinfortced bars under generalized excitations.* Report No.UCB/EERC82/23, University of California.

Den Uijl, J.A. (1992a), *Bond and splitting action of prestressing strand.* Proceedings of International Conference Bond in Concrete, Riga.

Den Uijl J.A. (1992b), *Background of the CEB-FIP Model Code 90 clauses on anchorage and transverse tensile actions in the anchorage zone of prestressed concrete members*. CEB Bulletin 212.

Eligehausen, R., Popov, E.P., Bertero, V.V. (1983), *Local bond stress – slip relationships of deformed bars under generalized excitations.* Report No.UCB/EERC83/23, University of California.

Eligehausen, R., Rehm, G. (1977), *Einfluss einer nicht ruhenden Belastung auf das Verbundverhalten von Rippenstählen*, Betonwerk+Fertigteil-Technik, Vo.43, No.6.

fib Bulletin 10 (2000), *Bond of reinforcement in concrete*. fédération internationale du béton, Lausanne, Switzerland.

Franke, L. (1976), *Einfluss der Belastungsdauer auf das Verbundverhalten von Stahl in Beton.* Deutscher Ausschuss für Stahlbeton, Heft 268.

Gambarova, P.G., Rosati, G.P., Zasso, B. (1989), *Steel-concrete bond after concrete splitting: (I) test results; (II) constitutive laws and interface deterioration.* Materials and Structures, RILEM (22).

Goto, Y. (1970), *Cracks formed in concrete around deformed tension bars.* Journal of the American Concrete Institute, Proceedings Vol.68, No.4.

Goto, Y., Otsuka, K. (1978), *Internal cracks formed in concrete around deformed tension bars.* Proceeding of the twenty-first Japan congress on materials research, Kyoto.

Karlsson, D. (1985), *Bond between strands and concrete in hollow-core slabs.* Nordic Seminar: Bond and Anchorage of reinforcement in Concrete, Chalmers University.

Malvar, J.L. (1992), *Confinement stress dependent bond behaviour.* In: Proceedings of the International Conference on Bond in Concrete, Riga.

Mayer, U. (2001), *Zum Einfluss der Oberflachengestalt von Rippenstahlen auf das Trag- und Verformungsverhalten von Stahlbetonbauteilen.* PhD Thesis, Stuttgart University.

McCabe, S.L., Pantazopoulu, S.J. (1998), *Evaluation of bond performance in Reinforced concrete structures.* ACI 1997 Symposium on Bond, Seattle.

Morita, S., Fuji, S. (1982), *Bond capacity of deformed bars due to splitting of surrounding concrete.* Proceedings of International Conference Bond in Concrete.

Nagatomo, K., Kaku, T. (1992), *Bond behaviour of deformed bars under lateral compressive and tensile stress.* Proceedings of International Conference Bond in Concrete, Riga.

Noakowski, P., Martin, H., Rehm, G. (1970), *Einfluss der Profilierung und des Betons auf die Verbundqualität von Stahl in Beton.* Technische Hochschule München, Report No.2203.

Rehm, G. (1957), *The fundamental law of bond.* RILEM, Symposium on bond and crack formation, Stockholm.

Rehm, G. (1961), *Über die Grundlagen des Verbundes zwischen Stahl und Beton.* Deutscher Ausschuss für Stahlbeton, No. 138.

Rehm, G. (1969), *Kriterien zur Beurteilung von Bewehrungsstäben mit hochwertigem Verbund.* Festschrift Rüsch.

Rehm, G., Eligehausen, R. (1979), *Bond of ribbed bars under high cycle repeated loads.* ACI Journal.

RILEM/CEB/FIP (1970), *Test and Specifications of reinforcements for reinforced and prestressed concrete. Four recommendations of the RILEM/CEB/FIP Committeee 2: Pull-out test.* Materials and Structures, RILEM, Vol.3, No.15.

Rots, J. (1989), *Bond of reinforcement*, Chapter 12 in *Fracture mechanics of concrete structures – from theory to applications.* RILEM (Editor: L.Elfgren).

Tepfers, R. (1973), *A theory of bond applied to overlapped tensile reinforcement splices for deformed bars.* Chalmers University, Publication 73:2.

Tepfers, R. (1979), *Cracking of concrete cover along anchored deformed reinforcing bars.* Magazine of Concrete Research, Vo.31, No. 106.

Tepfers R., Olsson, P.A. (1992), *Ring test for evaluation of bond properties of reinforcing bars.* Proceedings of International Conference Bond in Concrete, Riga.

3.3.3 Tension stiffening

by Joost C. Walraven

(1) Introduction

Fig. 3.3-30b shows a centrically reinforced prismatic concrete bar, loaded in centric tension. Under the influence of the tensile force the concrete is cracked and a more or less regular crack pattern is observed. Fig. 3.3-30a shows the load- mean strain relationship, where the mean strain has been obtained by dividing the extension by the length of the bar. Regarding the whole relationship, a number of stages can be distinguished.

- In stage 1 the concrete has not been cracked yet: the stiffness of the reinforced concrete tensile member is relatively large.
- In stage 2 cracks appear in the concrete under the influence of the increasing tensile force. The more the concrete is cracked, the more the load-strain relationship approaches the line of the unembedded steel (dotted line).
- In stage 3 the yield stress in the steel has been reached, so that the tensile force cannot increase anymore.

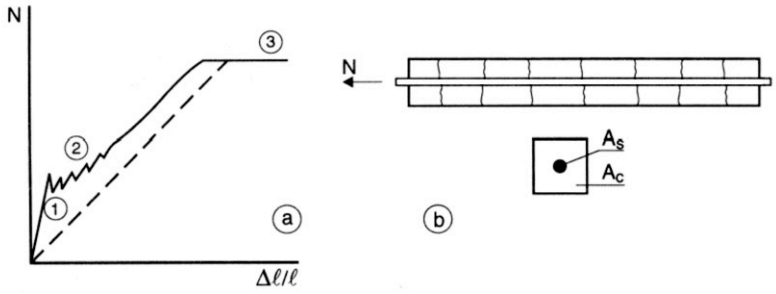

Fig. 3.3-30: Load-strain relationship for a centrically loaded tensile member

In stage 2 the pieces of concrete between the cracks contribute to the tensile stiffness of the element. This mechanism is often mentioned as *tension stiffening*. Fig. 3.3-31 shows the mechanism: between two cracks the concrete is activated by bond between steel and concrete.

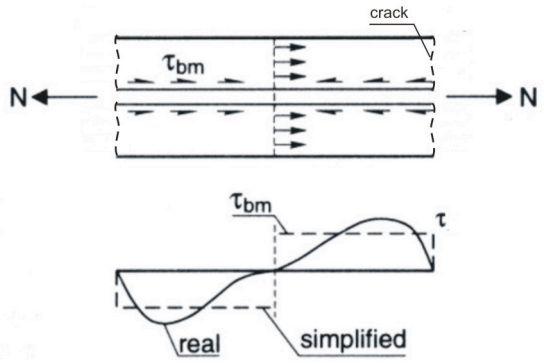

Fig.3.3-31: Load transmission from steel to concrete between two cracks

(2) Behaviour of a centrically reinforced concrete bar subjected to imposed deformations

The distribution of the bond stress along the bar is nonlinear. Since the distances between the cracks vary, it is quite laborious to calculate the average contribution of the concrete in an exact way (see also Section 4.3.2 on crack width control). In order to simplify the calculation, the analysis will be based on an averaged, constant bond stress along the bar (dotted line in Fig. 3.3-31). This means that the further calculation is based on a bond-slip relationship as shown in Fig. 3.3-32.

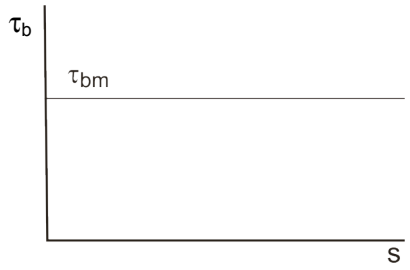

Fig. 3.3-32: Assumed bond stress - slip relationship

As a further simplification it is assumed that the tensile strength of the concrete does not vary over the length of the bar. Using the assumptions as stated before, the behaviour of the member under imposed deformations is analyzed. In the stage where the concrete is still uncracked, the strains in the steel and the concrete are equal. Hence, the contributions of concrete and steel to the equilibrium are:

$$N_c = \varepsilon \cdot E_c \cdot A_c \qquad \text{(for the concrete)} \qquad (3.3\text{-}43)$$

and

$$N_s = \varepsilon \cdot E_s \cdot A_s \qquad \text{(for the steel)} \qquad (3.3\text{-}44)$$

The equilibrium equation is then:

$$N = \varepsilon \cdot E_c \cdot A_c \, (1 + \alpha_e \, \rho) \qquad (3.3\text{-}45)$$

where

$\alpha_e = E_s/E_c$ and

$\rho = A_s/A_c$

When, however, the imposed deformation further increases, the tensile stress in the concrete reaches the tensile strength. The first crack will occur in an arbitrary cross-section, (Fig. 3.3-33 a). At the location where the concrete is cracked, the concrete tensile stress is $\sigma_{ct} = 0$. So at this place the steel has to transmit the full tensile force N. By virtue of the bond stresses between steel and concrete, at both sides of the crack, the concrete is again activated to carry a part of the tensile force. The length at both sides of the crack, where a transmission of forces from steel to concrete occurs, is called a *discontinuity region*. Outside of such a discontinuity region, the undisturbed situation applies, where the strains in the steel and the concrete are equal.

The distance, necessary to re-introduce the full tensile force in the concrete, lost by the appearance of a crack, depends on the bond strength. Here the mechanism shown in Fig. 3.3-33 b applies. As a consequence of the assumption of a constant bond stress along the steel bars (Fig. 3.3-32), the development of the concrete stress and the steel stress over the transmission length is linear (Fig.3.3-33 c and 3.3-33 d).

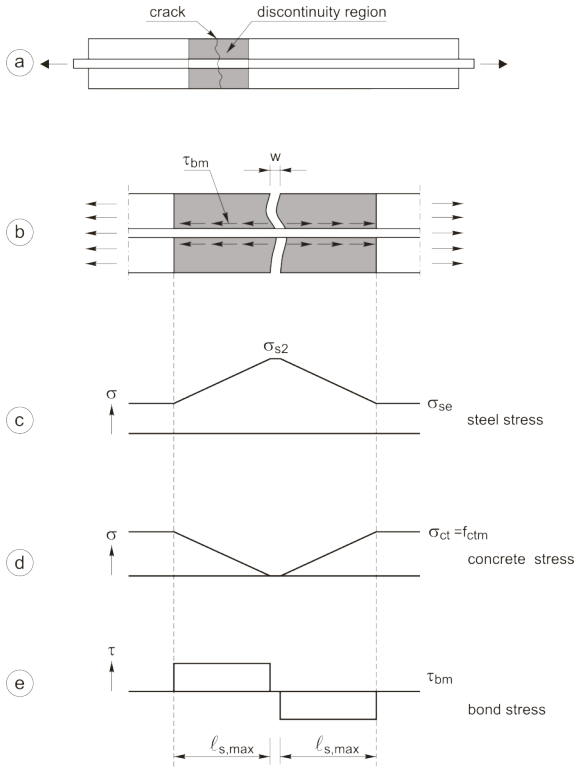

Fig. 3.3-33: Development of steel – and concrete stresses in a region disturbed by a crack
a. centrically reinforced tensile member with crack
b. discontinuity region
c. steel stress development in discontinuity region
d. concrete stress development in discontinuity region
e. development of bond stress in discontinuity region

When the bar is subjected to a steadily increasing elongation, the force in the bar will drop after the occurrence of the first crack. This can be explained on the basis of the fact that, by the generation of a discontinuity region, the total stiffness of the bar is reduced. When the total strain of the bar during cracking remains constant (principle of imposed deformation) as a consequence the force must drop from $N_{r,1}$ to N_0 (Fig. 3.3-34, right).

With increasing deformations the tensile force increases again, but it cannot exceed the cracking tensile force in the member, because the formation of new cracks will prevent this. Also around new cracks discontinuity regions occur (Fig. 3.3-34, left). The phase, in which new cracks are formed, so that the axial tensile load cannot exceed the cracking force N_r, is called the *crack-formation stage.* At distance $\ell_{s,max}$ from the crack, the tensile strength of the concrete is reached again (Fig. 3.3-33 d).

An important conclusion here is that a new crack will never occur within distance $\ell_{s,max}$ from a crack, simply because the tensile strength of the concrete cannot be reached in this region. The value $\ell_{s,max}$ is therefore important for the calculation of the contribution of tension stiffening.

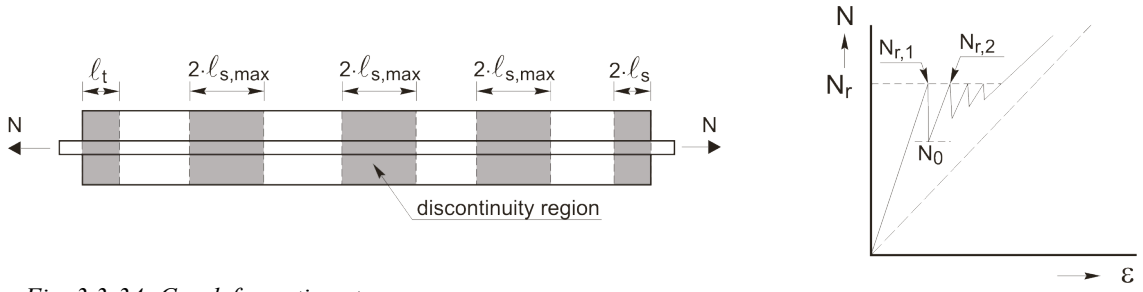

Fig. 3.3-34: Crack formation stage

At the onset of the formation of a new crack the stress in the concrete in the undisturbed region will be equal to f_{ctm}, and the tensile cracking force is

$$N_r = A_c f_{ctm} (1 + \alpha_e \rho) \tag{3.3-46}$$

The stress σ_{s2} in the steel, in a crack, is then:

$$\sigma_{s2} = \sigma_{sr2} = \frac{N_r}{A_s} = \frac{f_{ctm}}{\rho}(1 + \alpha_e \rho) \tag{3.3-47}$$

The steel stress σ_{sE} in the undisturbed areas between the discontinuity regions, where now bond slip occurs, reaches a maximum value under the force N_r which is equal to:

$$\sigma_s = \alpha_e \, f_{ctm}$$

Since the concrete stress at the crack is 0 and at distance $\ell_{s,max}$ from the crack it is equal to f_{ctm}, the force which has to develop over the length $\ell_{s,max}$ must be:

$$N = A_c \, f_{ctm} \tag{3.3-48}$$

Over the transmission length $\ell_{s,max}$, by virtue of the action of the bond stress τ_{bm} a force

$$N = \tau_{bm} \, \ell_{s,max} \, \Sigma U \tag{3.3-49}$$

is generated, where ΣU is the total perimeter of the rebars. Equating the values N from eq. (3.3-48) and eq. (3.3-49) yields:

$$\ell_{s,max} = \frac{f_{ctm}}{\tau_{bm}} \cdot \frac{A_s}{\Sigma U} \cdot \frac{1}{\rho} \tag{3.3-50}$$

For a number of n bars the total cross-section of the reinforcing steel is $A_s = \frac{n\pi\varnothing^2}{4}$ and the total perimeter is $\Sigma U = n\pi\varnothing$. Substitution those values in eq. 3.3.50 it gives:

$$\ell_{s,max} = \frac{f_{ctm}}{4\tau_{bm}} \cdot \frac{\varnothing}{\rho} \tag{3.3-51}$$

With gradual increase of axial deformation further cracks are formed. The cracking continues until the whole bar consists of overlapping discontinuity regions.

The smallest possible crack distance is found, where just at the end of a discontinuity region, a new crack has appeared. So the maximum crack distance applies, where the next crack is formed at a distance just smaller than $2\ell_{s,max}$: the remaining length is then just too short for the concrete tensile stress to reach the tensile strength again. The crack distance varies therefore between $\ell_{s,max}$ and $2\ell_{s,max}$. When finally the bar only exists of discontinuity regions, the *crack formation stage* is completed.

At further increase of the imposed deformation the steel stress σ_{s2} in the crack exceeds the value $\sigma_{sr2} = N_r/A_s$ (Fig. 3.3-34). The force in the concrete between the cracks cannot increase anymore, since the bond stress has reached its maximum value, Fig. 3.3-32. The contribution of the concrete between the cracks to the stiffness is therefore constant in the *stabilized cracking stage*. Hence the N – Δl/l line, as observed in experiments is about parallel to the line of the unembedded steel (phase 2, Fig. 3.3-35). See further details in Section 4.3.2 on crack width control.

(3) Derivation of a simplified load-elongation relationship

Fig.3.3-35 shows the simplified behaviour of the reinforced tension member.

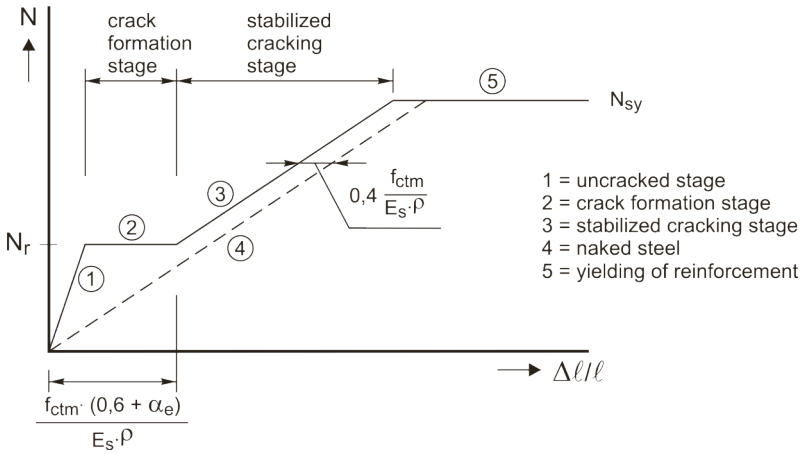

Fig. 3.3-35: Load - deformation relationship for a centrically reinforced member subjected to tension

In the first, linearly increasing branch (1) of the relationship, the concrete is still uncracked. When the cracking load has been reached the *crack formation stage* (2) starts: with increasing deformation the force N at first cannot exceed the cracking force N_r (the individual drops of the load, as seen in Fig. 3.3-30, have not been drawn here). At the end of the cracking stage, the *stabilized cracking stage* is entered: the tensile force increases steadily with increasing deformation. The dotted line represents the N-$\Delta\ell/\ell$ relationship for a the theoretical case that the reinforcement would be unembedded. The line for the response of the cracked tension member is almost parallel to the line of the unembedded bar. The distance between these two lines is important, since this represents tension stiffening. In order to calculate this contribution, it is assumed that the average distance between the cracks is $1.5\ell_{s,max}$. The corresponding representative unit of the member is shown in Fig. 3.3-36.

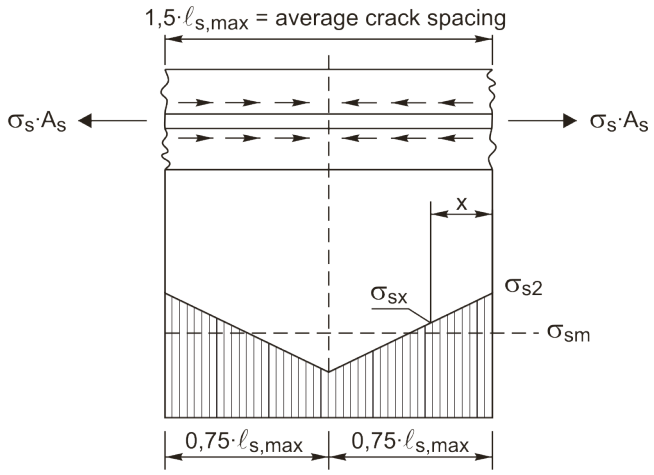

Fig. 3.3-36: Steel stress development in a representative unit

The stress in the steel at a distance of $x = 0.75\ell_{s,max}$ from the crack is

$$\sigma_{sx} = \sigma_s - \frac{0.75\, l_{s,max}\tau_{bm}\pi \varnothing}{\frac{1}{4}\pi \varnothing^2} \tag{3.3-52}$$

Substituting $\ell_{s,max}$ from eq. 3.3-51 this equation becomes

$$\sigma_{sx} = \sigma_s - 0.75\frac{f_{ctm}}{\rho} \tag{3.3-53}$$

The average steel stress is then

$$\sigma_{sm} = \sigma_s - 0.375\frac{f_{ctm}}{\rho} \tag{3.3-54}$$

and the average strain is

$$\varepsilon_{sm} = \frac{\sigma_s}{E_s} - \frac{0.375\, f_{ctm}}{E_s\,\rho} \cong \varepsilon_s - 0.4\frac{f_{ctm}}{E_s\,\rho} = \varepsilon_s - \varepsilon_{ts} \tag{3.3-55}$$

The last term in this equation represents tension stiffening for the stabilized cracking stage. For long term effects MC90 (Ch. 3.2.3) prescribes a factor 0.25 instead of 0.40. Using Fig. 3.3-35 it is now possible to determine the strain where the cracking pattern can be regarded as completed. The horizontal branch (2) can be described with

$$N_r = A_c\, f_{ctm}(1+\alpha_e\rho) \tag{3.3-56}$$

whereas the subsequent inclined branch (3) can be described with

$$N = E_s\, A_s\left(\frac{\Delta\ell}{\ell} - 0.4\frac{f_{ctm}}{E_s\rho}\right) \tag{3.3-57}$$

By equating eq. 3.3.56 and 3.3.57 it is found that the strain at the intersection point is

$$\frac{\Delta\ell}{\ell} = \frac{f_{ctm}\left(0.6+\alpha_e\rho\right)}{E_s\rho} \approx \frac{0.6\,f_{ctm}}{E_s\rho} \tag{3.3-58}$$

If the strain of the tensile member is smaller than this value, this means that the crack pattern is still in the crack formation stage. For larger values of the strain it can be assumed that the crack pattern has been stabilized.

The relationship shown in Fig.3.3-35 is a simplified representation of reality. The first plateau, occurring after first cracking is horizontal due to the assumption of a constant concrete tensile strength along the bar. This simplification is transparent for use in calculations, since it shows a clear transition from the crack formation stage to the stabilized cracking stage. The crack formation stage applies generally for the case of imposed deformations, whereas the stabilized cracking stage applies for imposed loads. In reality, however, there will not be a plateau after first cracking but an inclination, since the tensile strength in the structural element will be prone to scatter and subsequent cracks will occur at increasing loads. This was already shown in Fig. 3.3-30. An improved agreement with test results can be simply obtained by assuming that the first crack occurs at a tensile load of N_r and the last crack at a load of 1.3 N_r. Fig. 3.3-37 shows the comparison of the load-deformation relationship obtained in this way with test results of two tensile members.

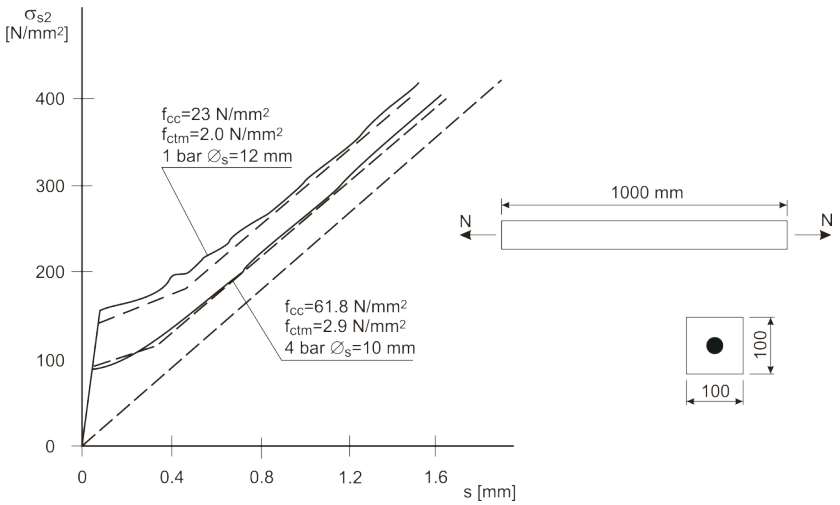

Fig. 3.3-37: Comparison of theoretical load-deformation relation with test results [Stroband (1991)].

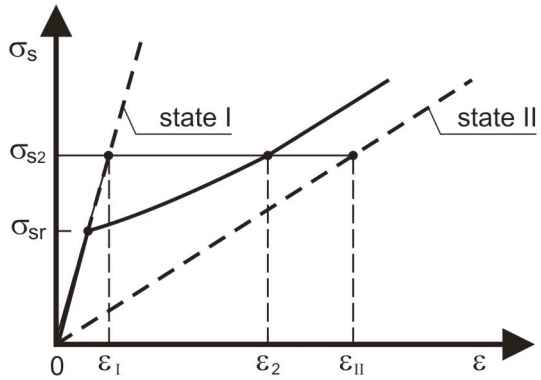

Fig. 3.3-38: Tension stiffening formulated with a parabolic curve [Favre, 1985]

It is also possible to use a parabolic formulation to describe the tension stiffening effect (Fig. 3.3-38). In this figure two limit situations are considered: the uncracked state of the reinforced prismatic bar (State I: full tension stiffening) and the fictitious case of the unembedded reinforcement (State II: no tension stiffening). Tension stiffening can then be expressed by

$$\xi = 1 - \beta(\sigma_{sr} / \sigma_{s2})^2 \tag{3.3-59}$$

where

σ_{s2} steel stress in crack under external load N_E ($\sigma_s > \sigma_{sr}$)
σ_{sr} steel stress in a crack if the bar is subjected to the cracking load N_r (σ_{sr} is the maximum possible stress in the steel in the crack formation stage)
β 1,0 for single short-term loading
0,5 for sustained loads or repeated loading

For any steel arbitrary stress σ_{s2} in the crack in state II the corresponding strain ε_2 follows from Fig. 3.3-38:

$$\varepsilon_2 = \xi \cdot \varepsilon_{II} + (1 - \xi)\varepsilon_I \tag{3.3-60}$$

This allows a simple calculation of the deformation of the member in the cracked state.

References to Section 3.3.3

CEB Bulletin 158 (1984), *Design Manual Cracking and Deformation*.

CEB Bulletin 213/214 (1993), *CEB-FIP Model Code 1990*, published by Thomas Telford Ltd., UK. ("MC90")

Stroband, J. (1991), *Experimental research into the bond behaviour of reinforcing bars in lightweight and normal weight concrete.* Delft University of Technology, Report 25.5-91-3/VF C, (in Dutch).

3.3.4 Moment-curvature relationship

by Joost C. Walraven

The moment-curvature relationship is a basic tool for the calculation of the deformation of structural members.

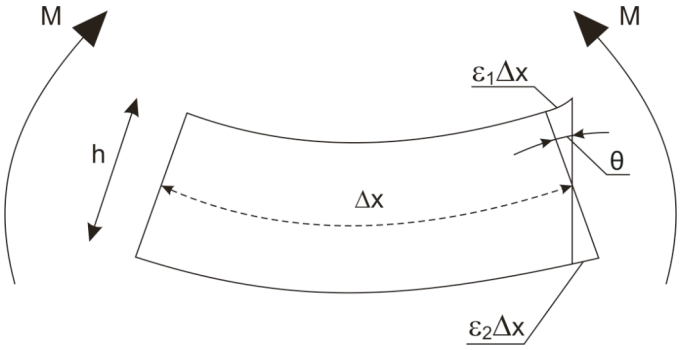

Fig. 3.3-39: Curvature of a bar increment with length Δx

If a bar increment with length Δx is subjected to a bending moment M, the strain in the upper fibre is

$$\varepsilon_1 = \frac{-M \cdot \frac{1}{2} h}{EI} \qquad (3.3\text{-}61\ a)$$

and the strain in the lower fibre is

$$\varepsilon_2 = \frac{+M \cdot \frac{1}{2} h}{EI} \qquad (3.3\text{-}61\ b)$$

the angular rotation is then

$$\Delta\theta = \frac{\left(|\varepsilon_1| + \varepsilon_2\right)\Delta x}{h} \qquad (3.3\text{-}62)$$

and the curvature, defined as the angular rotation per unit length of the member, is

$$\frac{1}{r} = \frac{\Delta\theta}{\Delta x} = \frac{|\varepsilon_1| + \varepsilon_2}{h} \qquad (3.3\text{-}63)$$

substituting ε_1 and ε_2 from eq. (3.3-61) in eq. (3.3-63), the well-known relationship

$$\frac{1}{r} = \frac{M}{EI} \qquad (3.3\text{-}64)$$

is found.

If a reinforced concrete member is subjected to a bending moment, the following stages are observed (Fig.3.3-40).

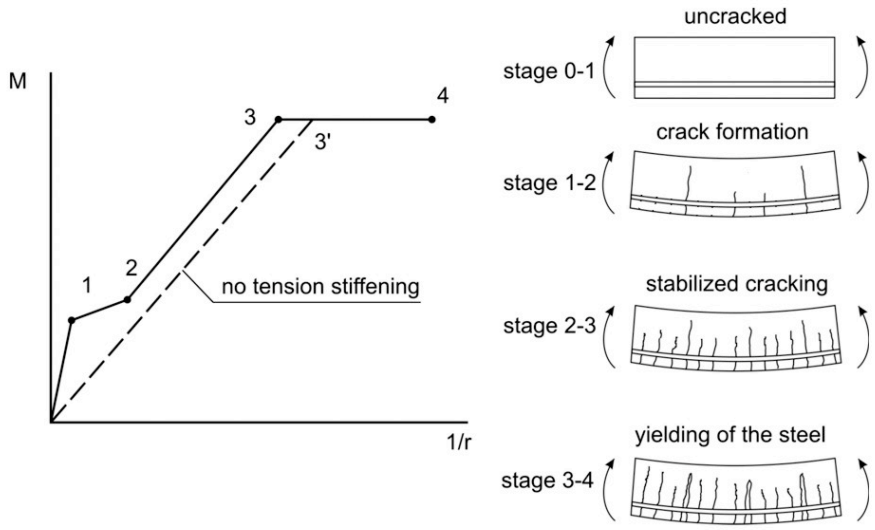

Fig. 3.3-40: Basic stages in the moment-curvature relation

- *Stage 0 - 1*: the uncracked stage
  In this stage the role of the reinforcement can be neglected
- *Stage 1 - 2*: the crack-formation stage.
  The first cracks deeply penetrate into the compression area. The subsequent cracks will have smaller lengths, because the cross-section is not fully stressed, due to the influence of the first cracks. Further cracks will occur, which are limited to the reinforcement area.
- *Stage 2 - 3*: stabilized cracking stage
  No new cracks appear any more. The existing cracks widen.
- *Stage 3 - 4*: yielding stage
  The reinforcing steel yields. The curvature strongly increases, whereas the increase of the bending moment is only slight. The bending moment increases by virtue of a small increase of the inner lever arm. Finally the concrete in the compression area fails (point 4).

The M-1/r relationship can be constructed using the characteristic points, shown in Fig. 3.3-40. In order to calculate the (M,1/r) combinations for these points, material data have to be supplied. Fig. 3.3-41 gives the stress-strain relationships for concrete and steel. In the diagram for the concrete, for the modulus of elasticity E_c a short-term or a long-term value may be chosen. Furthermore, the tensile strength of the concrete should be known (f_{ct}). Also here a short-term or a long-term value can be taken. Since the behaviour in bending is considered, the flexural tensile strength applies, which depends on the height of the cross-section.

A relationship was given in Section 3.1.4 (2.3), by eq. (3.1-6) with $\alpha_{fl} = 1.5$:

$$f_{ct,fl} = f_{ctm} \cdot \frac{(1+\alpha_{fl}\,(h/h_0)^{0.7}}{\alpha_{fl}\,(h/h_0)^{0.7}}$$

where h is the beam depth, $h_0 = 100$ mm and α_{fl} is a fracture mechanics parameter which depends on the characteristic length (eq. 3.1-10). In MC90 for α_{fl} a value 1,5 has been proposed, although 2,0 seems to be more in agreement with test results.

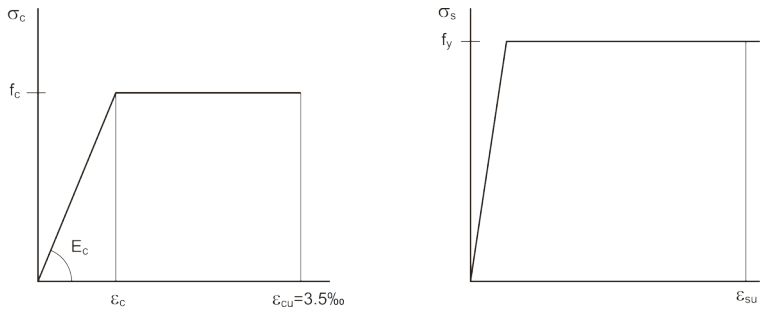

Fig. 3.3-41: σ-ε relations for concrete (left) and steel (right)

Now the characteristic points in Fig. 3.3-40 will be considered. At first the easiest ones, 1, 3′ and 4 are considered.

Point 1: Cracking moment

The flexural cracking moment is

$$M_r = W_1 \cdot f_{ct,fl} \tag{3.3-65}$$

where W_1 is the section modulus in state I (uncracked), and $f_{ct,fl}$ is the flexural tensile strength. At the onset of cracking, the strain in the lower fibre is $\varepsilon_r = f_{ct,fl}/E_c$. For a rectangular cross-section the curvature is then

$$\frac{1}{r} = \frac{\varepsilon_r}{h/2} \tag{3.3-66}$$

Point 1 in Fig. 3.3.40 is defined by equations. 3.3-65 and 3.3-64.

Point 3′: Y*ielding moment without tension stiffening*

Point 3’ marks the end of the dotted line in Fig. 3.3-40. The dotted line is a theoretical line, for the case that concrete is not able to carry tension. So in this case the reinforcement is regarded to be unembedded (no tension stiffening) (Fig. 3.3-42).

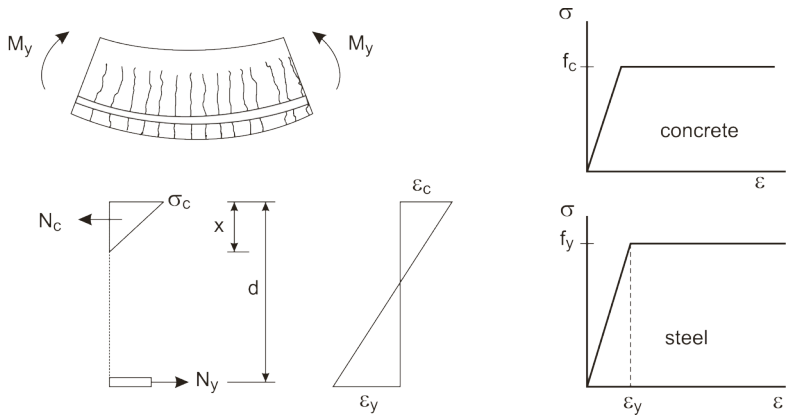

Fig. 3.3-42: Situation at the onset of yielding of the steel

For the sake of simplicity it is assumed, that the stress in the concrete in the compression area has not yet reached the value f_c.

Compatibility of deformations requires:

$$\frac{\varepsilon_c}{\varepsilon_y} = \frac{x}{d-x} \tag{3.3-67}$$

and because of equilibrium of forces:

$$\tfrac{1}{2}\sigma_c \cdot x \cdot b = f_y \cdot A_s \tag{3.3-68}$$

or

$$\tfrac{1}{2}E_c \cdot \varepsilon_c \cdot x \cdot b = f_y \cdot A_s \tag{3.3-69}$$

From eq. (3.3-68) and eq. (3.3-69) it is found that

$$\frac{x}{d} = -\alpha_e\rho + \sqrt{(\alpha_e\rho)^2 + 2\alpha_e\rho} \tag{3.3-70}$$

Now the yielding moment follows from

$$M_y = A_s f_y (d - \tfrac{1}{3}x) = \rho b d^2 f_y (1 - \tfrac{1}{3}x/d) \tag{3.3-71}$$

and the corresponding curvature follows from

$$\frac{1}{r} = \frac{\varepsilon_y}{d-x} \tag{3.3-72}$$

Point 4: Ultimate moment

The ultimate moment is reached, when the strain in the concrete reaches the ultimate value ε_{cu}=3.5‰ (Fig. 3.3-43).

The condition of equilibrium is now:

$$\left.\begin{aligned} N_c &= \alpha b x f_c \\ N_s &= A_s f_y \end{aligned}\right\} N_s = N_c \tag{3.3-73}$$

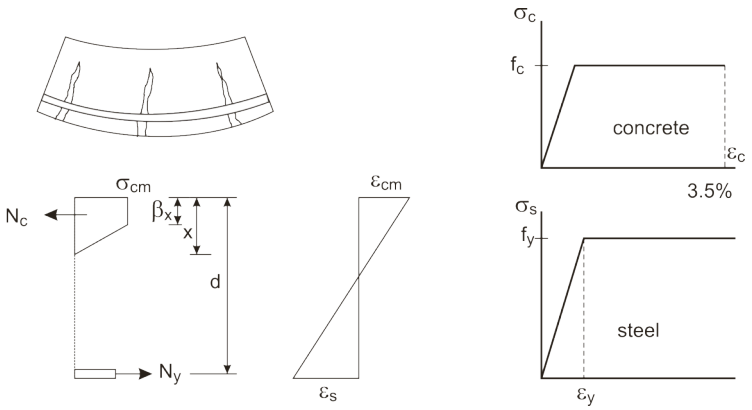

Fig. 3.3-43: Situation at the onset of crushing of the concrete

so:

$$x = \frac{A_s f_y}{\alpha b f_c} = \frac{\rho d f_y}{\alpha f_c} \tag{3.3-74}$$

where α = area factor for compression diagram. The ultimate bending moment is

$$M_u = (d - \beta x)\, A_s\, f_y \tag{3.3-75}$$

and the corresponding curvature is

$$\frac{1}{r} = \frac{\varepsilon_{cu}}{x} \tag{3.3-74}$$

Now a part of the relationship is known (Fig. 3.3-44a)

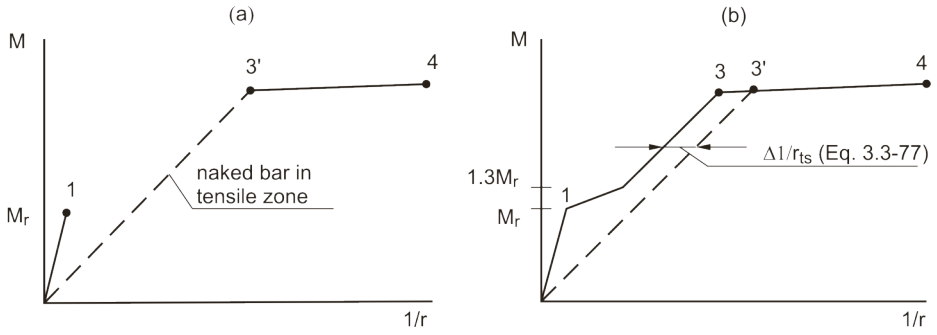

Fig. 3.3-44: M-1/r relation being constructed

The question is now how the connection between the points 1 and 3' can be found. If the member is cracked in bending, the concrete between the cracks add to the stiffness of the tension tie, as treated in Section 3.3.3. The situation occurring is shown in Fig. 3.3-45.

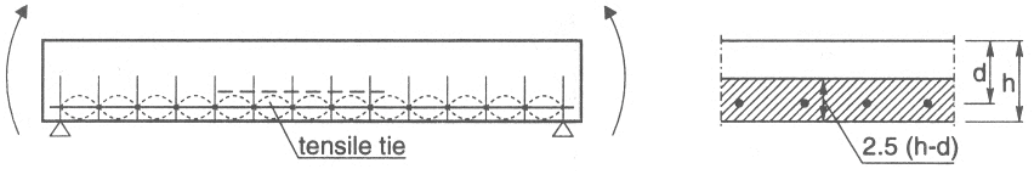

Fig.3.3-45: Tensile tie as a part of a structural members subjected to bending

Through FEM-analysis it was found that the height of the effective tensile tie is about 2.5 (h-d). If the stress σ_s in the reinforcement is known, the effect of tension stiffening can be found from Fig. 3.3-35, with

$$\Delta\varepsilon_{ts} = \frac{0.4\, f_{ctm}}{E_s\, \rho_{s,ef}} \tag{3.3-77}$$

where $\rho_{s,ef}$ follows from

$$\rho_{s,ef} = \frac{A_s}{A_{c,ef}} = \frac{A_s}{b \cdot 2.5(h-d)} \tag{3.3-78}$$

The strain in the compression zone of the member is hardly influenced by the effect of tension stiffening in the tensile zone. The average strain-distribution over the cross-section is therefore corrected in the way as shown in Fig. 3.3-46.

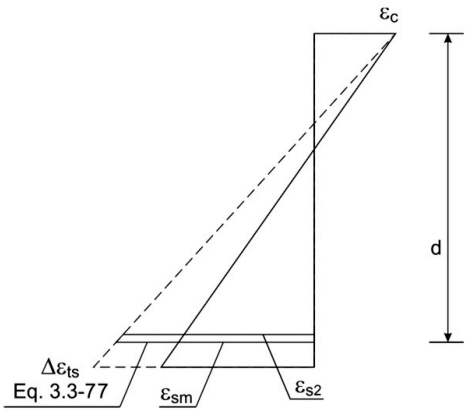

Fig. 3.3-46: Correction of strain distribution for the effect of tension stiffening

For a member subjected to bending, the corresponding shift for the curvature is

$$\Delta(1/r) = \Delta\varepsilon_{ts} / d \tag{3.3-79}$$

This shift is applied in Fig. 3.3-46b. If it is furthermore assumed that, from the first bending crack, the bending moment is increased with approximately 30% before reaching the stabilized cracking state, the diagram of Fig. 3.3-44, right, can be completed.

In MC90, Ch. 3.6, the moment curvature relation is described in an empirical way. The most important part is the cracked state (state II). For this state the tension stiffening effect is formulated as

$$\frac{1}{r_{ts}} = \left(\frac{1}{r_{2r}} - \frac{1}{r_{1r}}\right)\beta\left(\frac{M_r}{M}\right) \qquad (3.3\text{-}80)$$

where:

$1/r_{1r}$ is the curvature in the uncracked state, at the cracking moment M_r.
$1/r_{2r}$ is the curvature in state II-naked, at the cracking moment M_r .
M is the acting bending moment
β is the general reduction factor for concrete tensile strength, for the effects of shrinkage, sustained loading, etc.

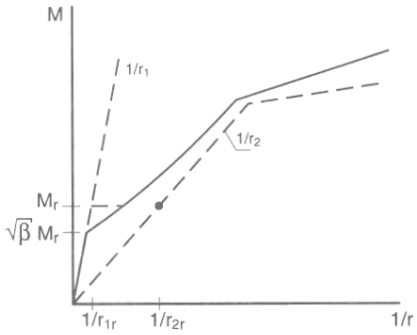

Fig. 3.3-47: Moment-curvature relationship according to MC90, Ch. 3.6

Fig. 3.3-48 shows an example, for an element with b=1000 mm, h=250 mm, d=225 mm, ρ=0.5%, f_c=32 MPa, f_{ctm}=2.6 MPa, $f_{ct,fl}$=3.6 MPa subjected to bending

It can be seen, that for ρ = 0.5%, the influence of tension stiffening is limited, if M>1.3 M_r. As an approach, for ρ > 0.5% and M>1.3 M_r the naked stiffness can be used as a reasonable approach. With $EI_2 = M_y/(1/r)_y$ and eq. (3.3-71) and eq. (3.3-72) it is found that

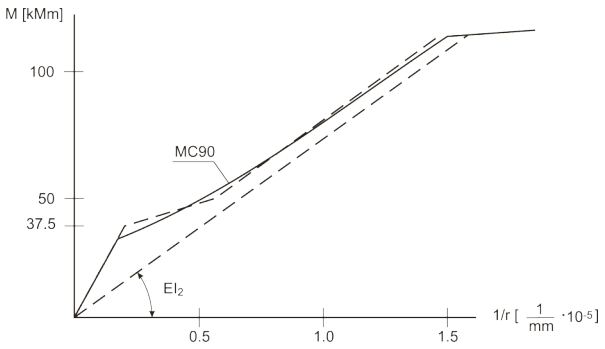

Fig. 3.3-48: Comparison between the approach of MC90 repeated here by eq. (3.3-80) and the method, described in this chapter

$$EI_2 = \rho b d^3 E_s \left(1 - \frac{1}{3}\frac{x}{d}\right)\left(1 - \frac{x}{d}\right) \qquad (3.3\text{-}81\ a)$$

where x/d can be found from eq. (3.3-70). For the sake of illustration, eq. (3.3-81 a) is written as

$$EI_2 = \psi \rho b d^3 \qquad (3.3\text{-}81\ b)$$

where $\psi = E_s \left(1 - \frac{1}{3}\frac{x}{d}\right)\left(1 - \frac{x}{d}\right)$ (3.3-81 c)

and x/d follows from eq. (3.3-70). Fig. 3.3-49 shows the dependence of ψ on the parameters ρ and α_e.

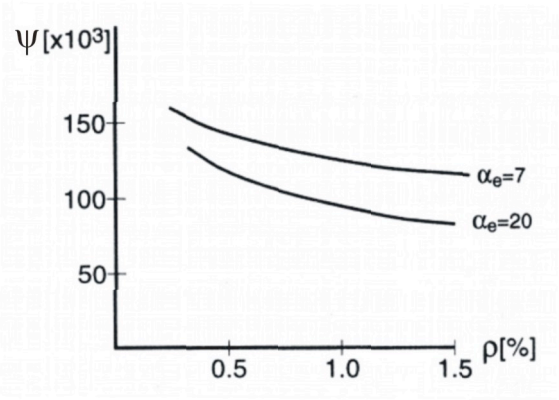

Fig. 3.3-49: Dependence of ψ on αe and ρ

As a rule of thumb, eq. (3.3-81 b) a can be simplified to

$EI_2 = 1.3 \rho_0 b d^3 \cdot 10^3$ for short term loading (3.3-82 a)

$EI_2 = 1.0 \rho_0 b d^3 \cdot 10^3$ for long term loading (3.3-82 b)

where $\rho_o = 100\ A_s/bd$.

For $M<1.3\ M_r$ the stiffness in the cracked stage can be much larger than given by eq. (3.3-82 a and b). This applies for instance to slabs in buildings, which will often only reach the crack formation state, even at the maximum service load.

If the member is subjected to a normal compressive force and subsequently loaded in flexure, the behaviour is different. The flexural cracking moment is then

$$M_r = W_1\left(f_{ct,fl} - \frac{N}{A_c}\right) \tag{3.3-83}$$

Contrary to the case of bending without normal force, no simple relationship for the curvature $1/r_2$ in the state II-unembedded can be derived. Due to the action of N the relationship is non-linear and should be calculated for any particular case.

The tension-stiffening effect, expressed by $\Delta 1/r_{ts}$, is the same as for the case of non-compressed members, and follows from eqs. (3.3-79) and (3.3-80).

The moment-curvature relationship for bending with axial compression is schematically shown in Fig. 3.3-50.

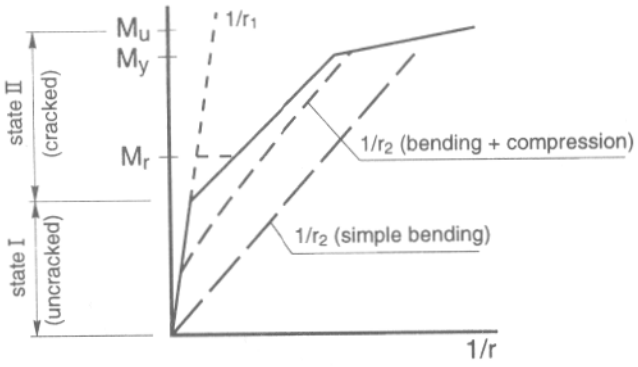

Fig. 3.3-50: M-1/r relationship for bending with axial compression

3.3.5 Confining action of reinforcement

by Joost C. Walraven

(1) Mechanism of confinement

In order to understand the confining action of reinforcement, it is necessary to consider the failure mechanism of concrete more in detail.

Normal concrete consists of about 75% aggregate particles. These particles are of various sizes, composed to obtain optimum packing, Fig. 3.3-51. The particles are the hard components of the concrete and the compression forces seek their way from particle to particle (Fig. 3.3-51 a). Equilibrium of forces is only possible if there are lateral forces, as shown in Fig. 3.3-51 b. These lateral forces occur by virtue of the bonding action of the cement paste. At a certain load the maximum capacity of the bond is reached and microcracks occur at the interface between aggregate particles and cement paste (Fig. 3.3-51 c). Those microcracks grow together to macrocracks and the specimen fails showing a characteristic crack pattern, parallel to the axial load. It is clear that a confining action (Fig. 3.3-51 d.) adds to the effect of the bond, and results in a higher strength. If the confining action is generated by reinforcement it is as well active for larger lateral displacements and improves therefore the ductility of the specimen as well. Fig. 3.3-52 shows the increase of the strength of a specimen, as a function of a confining radial stress $\sigma_2 = \sigma_3$

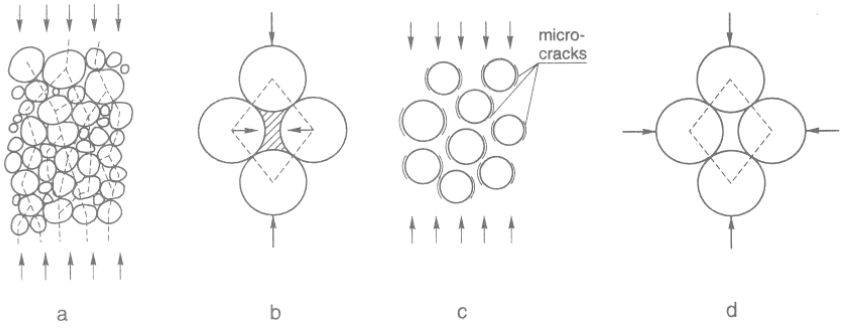

Fig. 3.3-51: The bearing capacity of concrete in compression explained
a. force paths through aggregate particles
b. transmission of forces from particle to particle
c. occurrence of interface cracks by axial loading
d. effect of confining action

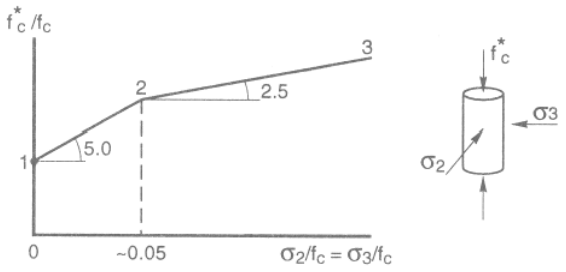

Fig. 3.3-52: Linearized approximation of compressive strength under triaxial axisymmetric loading

The failure envelope shown in Fig. 3.3-52 is the 2-D intersection of the 3-D envelope shown in Fig. 3.1-8 and can be described by the following formulation:

$$f_c^* = f_c\left(1.000 + \frac{5.0\sigma_2}{f_c}\right) \qquad \text{for} \quad \frac{\sigma_2}{f_c} < 0.05 \tag{3.3-84}$$

or

$$f_c^* = f_c\left(1.125 + \frac{2.50\sigma_2}{f_c}\right) \qquad \text{for} \quad \frac{\sigma_2}{f_c} > 0.05. \tag{3.3-85}$$

(2) The effect of a confining reinforcement

If a concrete cylinder is wrapped in spiral reinforcement, and this cylinder is axially loaded until the steel starts to yield, the radial stress $\sigma = \sigma_2 = \sigma_3$ (Fig. 3.3-53) can be formulated as

$$\sigma = \frac{2A_s f_y}{bs}. \tag{3.3-86}$$

where s = spacing between the hoops.

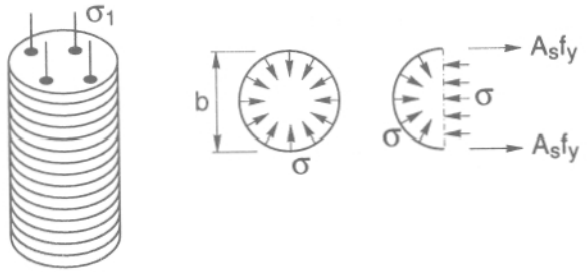

Fig. 3.3-53: Radial stresses generated by yielding of spiral reinforcement

The volumetric ratio of the confining steel is

$$\omega_V = \frac{\pi b A_s}{1/4\,\pi b^2 s} = \frac{4A_s}{bs} \tag{3.3-87}$$

The volumetric mechanical ratio is

$$\omega_w = \omega_V \cdot \frac{f_y}{f_c} = \frac{4A_s}{b_s}\frac{f_y}{f_c} \tag{3.3-88 a}$$

From eq. (3.3-87) and eq. (3.3-88a) it is found that:

$$\frac{\sigma}{f_c} = 0.5\,\omega_w \tag{3.3-89}$$

Concrete in a rectangular column can be also confined. In that case a combination of rectangular hoops is used anchored in their corner behind longitudinal bars (Fig. 3.3-54).

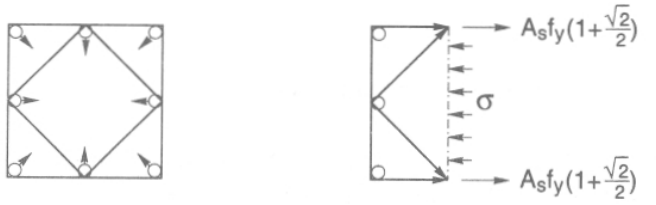

Fig. 3.3-54: Confinement of rectangular column by hoops

Now the radial stress is

$$\sigma = \frac{\left(2+2\frac{\sqrt{2}}{2}\right)A_s f_y}{bs} = \frac{3.415\,A_s f_y}{bs} \tag{3.3-90}$$

The volumetric mechanical ratio of the confining steel is

$$\omega_w = \frac{\left(4+4\frac{\sqrt{2}}{2}\right)bA_s}{b^2 s}\frac{f_y}{f_c} = \frac{6.83\,b\,A_s}{bs}\frac{f_y}{f_c} \tag{3.3-88 b}$$

and therefore also here eq. 3.3-89 can be applied.

By inserting the result of eq. (3.3-88) and (3.3-89) in eq. (3.3-84) or eq. (3.3.85), the increased strength f_c^* can be calculated. However, there is a complication: eqs. (3.3-88) and (3.3-89) are based on a uniformly distributed radial stress σ, and in a number of cases this is only approximately true. Therefore, eq. (3.3-89) is extended to

$$\frac{\sigma_2}{f_c} \approx \frac{\sigma_3}{f_c} = 0.5\,\alpha_n \alpha_s \omega_w \tag{3.3-91}$$

where:

α_n is a reduction factor expressing the effective concrete area in plan (depending on the hoop pattern in the cross-section)

α_s is a reduction factor expressing the effective concrete area in elevation (depending on the spacing of the hoops).

The factor α_n is defined in Fig. 3.3-55 for the case of a rectangular cross-section. In this case the longitudinal bars act as supporting points for arches (dotted lines), enclosing the confined 'core' of the cross-section. The depth of such an arch is about 0.25 b_1.

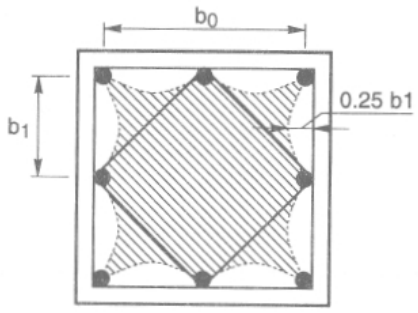

Fig. 3.3-55: Effectively confined area in rectangular cross-section (shaded): $\alpha_n = A_{core}/A_{net}$

The effectively confined area is therefore:

$$A_{core} = b_0^2 - n\left(\frac{2}{3}\cdot 0.25\, b_1 \cdot b_1\right) = b_0^2 - n\left(\frac{b_1^2}{6}\right) \qquad (3.3\text{-}92)$$

where n is the total number of the supporting longitudinal bars.

The reduction factor α_n is therefore for the case considered:

$$\alpha_n = \frac{A_{core}}{A_{net}} = \frac{b_0^2 - n\left(\frac{b_1^2}{6}\right)}{b_0^2} = 1 - \frac{n}{24} \qquad (b_1 < 200 \text{ mm}). \qquad (3.3\text{-}93)$$

Similar considerations apply for the reduction coefficient α_s vertically.

Fig. 3.3-56 shows a vertical section over a column with a non-uniform distribution of the confining stresses. Also here arches are built with a depth of about 0.25s.

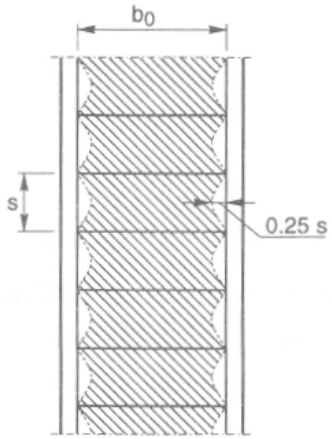

Fig. 3.3-56: Vertical cross-section over column with non-uniform distribution of confining stresses

The effectively confined core is, therefore, (for the smallest horizontal cross-section)

$$A_{core} = ¼\pi\ (b_0 - 2 \cdot 0.25s)^2 = ¼\pi\ (b_0 - 0.5s)^2 \qquad (3.3\text{-}94)$$

The reduction factor α_s is then:

$$\alpha_s = \frac{A_{core}}{A_{net}} = \frac{\frac{1}{4}\pi\left(b_0 - 0.5_s\right)^2}{\frac{1}{4}\pi b_0^2} = \left(1 - \frac{s}{2b_0}\right)^2 \qquad \text{for} \qquad s < \frac{b_0}{2} \qquad (3.3\text{-}95)$$

With eqs. (3.3-92) - (3.3-95) the increased strength can be easily calculated, using Fig. 3.3-52 or eqs. (3.3-84) and (3.3-85).

(3) Complete stress-strain relationships for confined concrete

For basic work in this field, reference is made a.o. to Ahmad, Shah (1982) and Mander, Priestly, Park (1988). If more precise calculations are not required, the following approximation may be used, see also Fig. 3.3-57.

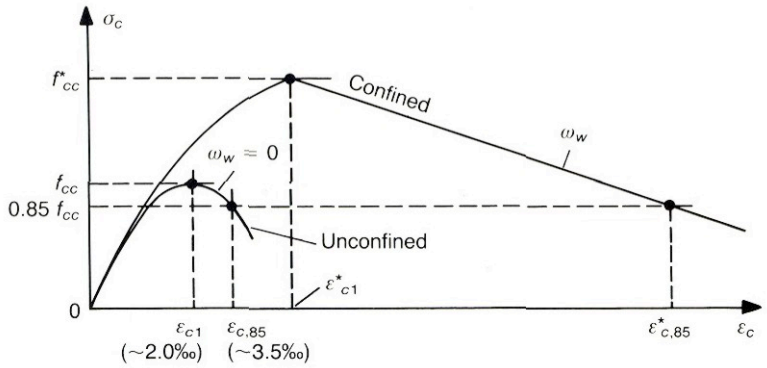

Fig. 3.3-57: Approximation for the stress-strain relationship under triaxial symmetric conditions

$$\varepsilon_{cl}^{*} = \varepsilon_{cl} + \left(\frac{f_{cc}^{*}}{f_{cc}}\right)^2 \qquad (3.3\text{-}96)$$

$$\varepsilon_{c,85}^{*} = \varepsilon_{c,85} + 0.1\alpha\,\omega_w \qquad (3.3\text{-}97)$$

where $\alpha = \alpha_n \cdot \alpha_s$

For calculations a σ-ε diagram with a horizontal axis is more appropriate. With a safety factor γ_c=1.5 and a long term factor 0.85 the diagram shown in Fig. 3.3-58 can be obtained.

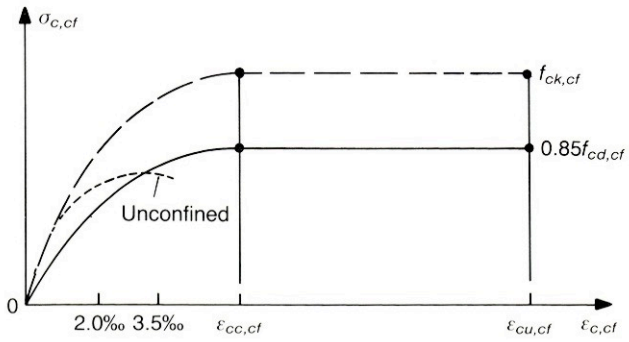

Fig. 3.3-58: Design σ - ε diagram for confined concrete

$$f_{ck,cf} = f_{ck}\left(1.00 + 5.0\frac{\sigma_2}{f_{ck}}\right) \qquad \text{for} \qquad \sigma_2 < 0.05\,f_{ck} \tag{3.3-98 a}$$

$$f_{ck,cf} = f_{ck}\left(1.125 + 2.50\frac{\sigma_2}{f_{ck}}\right) \qquad \text{for} \qquad \sigma_2 > 0.05\,f_{ck} \tag{3.3-98 b}$$

$$\varepsilon_{cc,cf} = 2.0\cdot 10^{-3}\left(\frac{f_{ck,cf}}{f_{ck}}\right)^2 \tag{3.3-98 c}$$

$$\varepsilon_{cu,cf} = 3.5\cdot 10^{-3} + 0.2\,\frac{\sigma_2}{f_{ck}} \tag{3.3-98 d}$$

where σ_2 ($=\sigma_3$) is the effective lateral compression stress at the ULS due to confinement. Simplified models for the evaluation of σ_2 may be used, i.e.

$$\frac{\sigma_2}{f_{ck}} = 0.5\,\alpha_n\alpha_s\omega_{wd} \tag{3.3-99}$$

For α_n and α_s reference is made to eq. (3.3-93) and eq. (3.3-95).
ω_{wd} is the design mechanical volumetric ratio of the confining reinforcement

$$\omega_{wd} = \frac{V_{s,trans}}{V_{c,cf}}\cdot\frac{f_{yd,trans}}{f_{cd}} \tag{3.3-100}$$

where

$V_{s,trans}$ is the volume of the closed stirrups or cross-ties
$V_{c,cf}$ is the volume of the confined concrete
$f_{yd,trans}$ is the design yield stress of the transverse reinforcement
f_{cd} is the design strength of unconfined concrete for uniaxial compression.

Some examples of the calculation of ω_{wd} are given in Fig. 3.3-59.

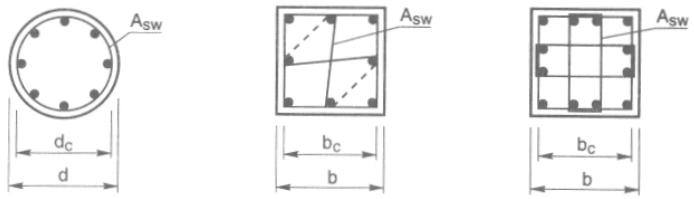

Fig. 3.3-59: Examples for the calculation of ω_{wd}

References to Section 3.3.5

Ahmad, S.H. and Shah, S.P. (1982) *Stress-strain curves of confined concrete by spiral reinforcement.* ACI Journal, Vol. 79 (6), pp. 484-490.

Mander, J.M., Priestly, M.N. and Park, R. (1988) *Theoretical stress-strain model for confined concrete.* Journal of the Structural Division, ASCE, Vol. 114 (8), pp. 1804-1826.

3.3.6 Biaxial behaviour of cracked reinforced concrete

by Joost C. Walraven

(1) General

When a concrete structural member cracks, its behaviour will turn from approximately isotropic to distinctly anisotropic. This means that the principal strain directions will change as a result of cracking and redistribution of forces will occur. In shear loaded areas, the roughness of the crack faces allows a rotation of the compression struts, so that a larger portion of the shear reinforcement is activated. The capacity of cracks to transmit shear forces is a basic condition in a number of advanced shear models, which allow a rotation of the concrete compression strut (Fig. 3.3-60). In areas where structures are discontinuous, cracks may occur in very unfavourable directions. An example is a silo with rectangular cells. The material stored in the cells of the silo causes axial tension in the walls, and shear forces perpendicular to the walls. If a crack occurs at the junction of the walls, it has to transmit the whole shear force, so that considerable reliability is imposed on its shear friction capacity (Fig. 3.3-61).

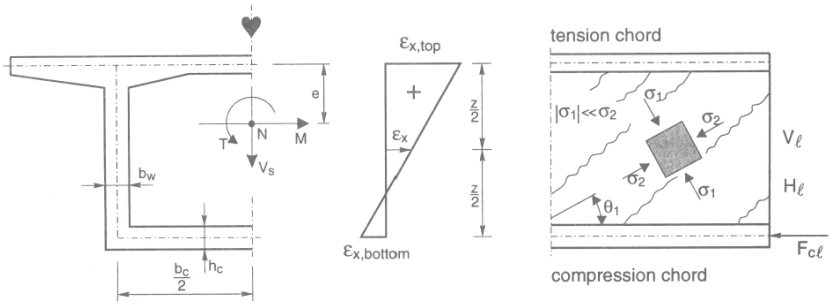

Fig. 3.3-60: Stress distribution in the web of a box girder

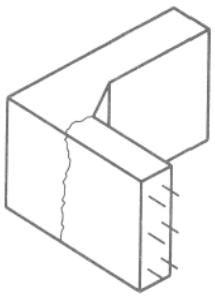

Fig. 3.3-61: Axial tension and shear in a wall of a rectangular silo

Very often the behaviour of cracked elements is concerned, subjected to biaxial in-plane loading, where the direction of principal compression deviates from the direction of the cracks (Fig. 3.3-62).

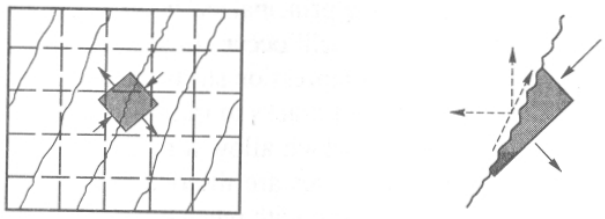

Fig. 3.3-62: Stresses in a cracked reinforced concrete panel

Since the transmission of forces across a crack is of significant importance, a number of basic mechanisms will be treated first, like dowel action of the reinforcing bars, aggregate interlock in cracks in plain concrete and shear friction in cracks crossed by reinforcement. Finally the failure criterion for reinforced cracked panels will be discussed.

(2) Dowel action

Dowel action occurs, when a steel bar in a crack is subjected to a shear displacement (Fig. 3.3-63 a). Dowel action can consist of bending, shear and kinking (Fig. 3.3-63 b). If there is sufficient cover on the reinforcing bar, a complex triaxial state of stress occurs in the concrete adjacent to the bar.

The effect of shear (Fig. 3.3-63 b) is of minor importance, because the concrete under the bar near to the crack is significantly damaged, and even spalled-off, so that the resulting dowel forces at both sides of the crack have a large eccentricity, which results in yielding of the steel due to bending.

Kinking is a mechanism which occurs when plastic hinges have formed at some distances at both sides of the crack. At large shear displacements of the crack faces the normal tensile force in the bar between the plastic hinges has a component parallel to the crack, perpendicular to the original bar direction. This mechanism is only of significance at very large shear displacements of the crack faces.

In the following considerations the effect of shear and kinking is neglected.

Fundamentally, the dowel force-shear displacement relationship is nearly linear until approximately 0.4 $F_{u,dow}$, and is for higher dowel forces nonlinear with a gradually decreasing inclination, because the concrete under the bar is progressively destroyed under the steel bar at the crack. Because of the triaxial state of stresses, the local pressure can significantly exceed the axial compressive strength f_c. For the first part of the relationship, with $F_d < 0.4\ F_{u,dow}$, the theory of beams on elastic foundation gives good results. For the subsequent part the local damage of the concrete should be considered in the modelling. The expressions used here are based on the mechanism shown in Fig. 3.3-63 c. The original description was developed by [Rasmussen (1962)] and improved by [Pruijssers (1988)].

The expression for the ultimate dowel force is:

$$F_{u,dow} = 1.35(\sqrt{1+9\varepsilon^2} - 3\varepsilon)\,ø^2\sqrt{f_y \cdot f_{c,cube}}\,\sqrt{1-(\frac{\sigma_s}{f_y})^2} \qquad (3.3\text{-}101)$$

where $\varepsilon = \frac{e}{ø}\sqrt{\frac{f_{c,cube}}{f_y}}$ (3.3-102)

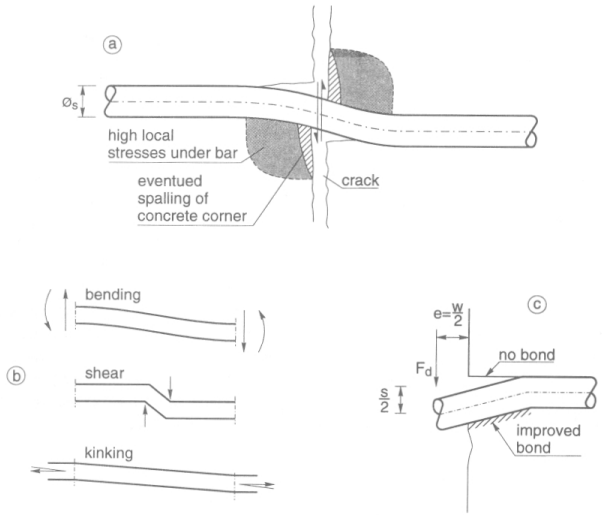

Fig. 3.3-63: Dowel action of the reinforcement
a. common representation
b. behavioural aspects bending, shear and kinking
c. failure mechanism according to Rasmussen (1962)

The factor $\sqrt{1-\left(\frac{\sigma_s}{f_y}\right)^2}$ in eq. (3.3-101) takes into account that a longitudinal stress in the dowel bar reduces its dowel capacity, because the maximum bending moment in the plastic hinges is reduced. If dowel action develops in a rough crack, always a tensile stress will develop in the steel bar, because the crack tends to open at shear sliding.

The dowel capacity will be reduced, when the crack is inclined to the bar (Fig. 3.3-64 a) or when the cover on the bar is small (Fig. 3.3-64 b).

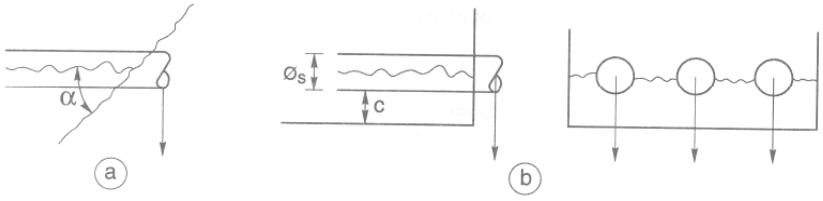

Fig. 3.3-64: Reductions to dowel capacity
a: Reduction of dowel capacity for α < 90°
b: Reduction of dowel capacity due to small cover c

For those cases reference is made to Pruijssers (1988) and Dei Poli, di Prisco, Gambarova (1993).

(3) Aggregate interlock in plain cracks in concrete

The principle of transmission of shear forces across cracks in concrete is often explained as shown in Fig.3.3-65a. As a result of the roughness of the crack faces, a type of wedging action occurs when a shear force is applied, so that the parts at both sides of the crack are driven apart. By virtue of this dilatation, the reinforcement intersecting the crack is stressed, so that it does not only counteract the crack opening, but also the relative shear displacement of the crack faces. Although Fig. 3.3-65a gives a reasonable explanation for the shear friction mechanism, the real behaviour is different: in concrete with not too high strength, the cracks intersect the cement matrix, but propagate around the relatively strong aggregate particles. Therefore, a better representation of the behaviour is shown in Fig. 3.3-65b: if the crack faces are subjected to a relative shear displacement, the strong aggregate particles are pushed into the weaker matrix, and a transmission of forces is generated at numerous contact points. At those points both compressive and frictional sliding forces are generated.

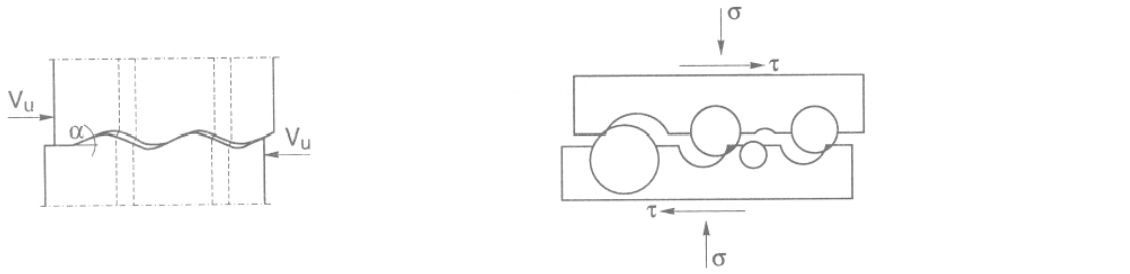

a. simplified representation of shear friction behaviour

b. Realistic aggregate interlock mechanism for cracks in concrete with normal strength.

Fig. 3.3-65: Representation of shear friction and aggregate interlock

If a crack in plain concrete is subjected to a relative shear displacement, at a constant crack with w, the number and size of the contact areas increase: so both the shear stress and the normal stress perpendicular to the crack increase. In other words, in order to keep the crack width constant during shear sliding, the normal compressive stress on the crack must proportionally increase. The shear stress τ and the normal compressive stress σ depend on the crack width w, the shear slip s, the concrete strength, the grading curve and the maximum particle diameter. If the influence of the latter two is neglected, the following relations approximately apply [Walraven (1981)]:

$$\sigma = -\frac{f_{c,cube}}{30} + \left(1.80w^{-0.8} + \left(0.234w^{-0.71} - 0.20\right)f_{c,cube}\right)s \qquad (3.3\text{-}103\ a)$$

$$\sigma = -\frac{f_{c,cube}}{20} + \left(1.35w^{-0.63} + \left(0.191w^{-0.55} - 0.15\right)f_{c,cube}\right)s \qquad (3.3\text{-}103\ b)$$

These relationships are shown in Fig. 3.3-66 (dotted lines for various crack widths). The solid lines correspond to the results of a fundamental model, based on a probabilistic evaluation of the contact areas, see also [Walraven (1981)].

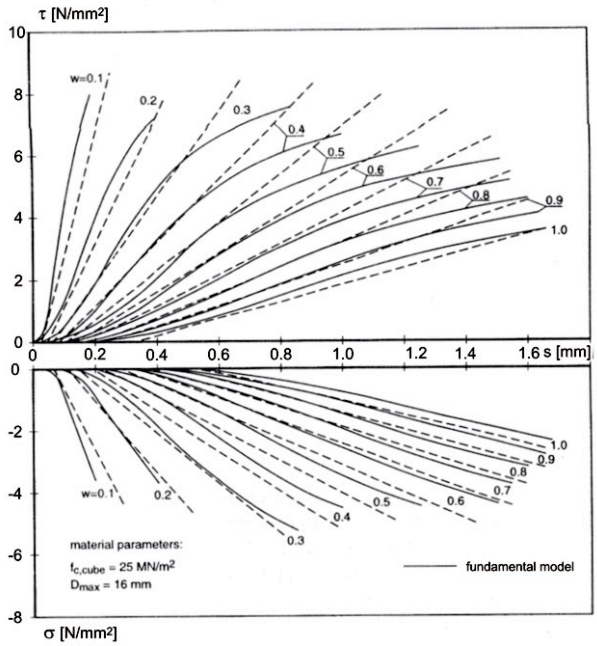

Fig. 3.3-66: Shear and normal forces in the crack as a function of crack width and shear displacement (dotted lines representing eq. 3.3-103)

The relations are principally valid for unbroken aggregate particles. For glacial Rhine-gravel, this holds true up to cube strengths of about 75 N/mm^2. If high strength concrete is regarded, particle fracture reduces both the τ- and σ-values. For this case reference is made to [Walraven, Stroband (1993)].

(4) The shear friction principle

In the previous section it was shown, that at shear sliding a crack tends to open. If reinforcing bars intersect the crack, this reinforcement is stretched during sliding and will finally reach its yield stress. In this way the reinforcement contributes in a double way to the shear capacity:

- by dowel action
- by clamping the crack together and as such providing a shear resistance.

Fig. 3.3-65 shows, that during shear sliding of the crack faces the crack tends to open, so that the reinforcing bars which intersect the crack are subjected to a combination of axial tension and bending. The formulation of the ultimate dowel capacity, eq. (3.3-101), therefore contains a reduction factor depending on the axial steel stress σ_s: the higher is the steel stress σ_s, the lower is the dowel capacity. A similar argument applies to the axial tensile force in the reinforcing bars, holding the parts at both sides of the crack together, Fig. 3.3-65a and b. Since the bars are subjected to bending due to dowel action, they are not able to develop their full axial tensile capacity $\sigma = \rho f_y$. The equilibrium in a reinforced crack can, therefore, be represented as shown in Fig. 3.3-67.

Fig. 3.3-67: Shear transmission in a reinforced crack

The forces in Fig. 3.3-67 are:

V_u is the ultimate shear force to be transmitted across the crack
N_s is the axial tensile force in reinforcement
V_d is the shear force transmitted by dowel action
D_{ai} is the diagonal force by aggregate interlock
V_{ai} is the vertical component of D_{ai}
N_{ai} is the horizontal component of D_{ai}.

The values V_d and V_{ai} are both approximate functions of $\sqrt{\rho f_y}$ and $\sqrt{f_c}$, so

$$V_u = c_1\sqrt{\alpha_1\rho f_y}\cdot\sqrt{f_c}\ A_c + c_2\sqrt{\rho f_y}\cdot\sqrt{f_c}\cdot\alpha_2 A_s \qquad (3.3\text{-}104)$$

In eq. 3.3-104 the first and the second term represent the contribution of aggregate interlock and dowel action, respectively.

The coefficients α_1 and α_2 are reduction factors taking into account that both the restraining force N_s and the dowel force V_d cannot fully develop because of the combination of axial stress and bending moment in the reinforcing bars. It was shown by tests that the normal restraining force in the steel can be 30 - 50% lower than the yielding force because of dowel action [Mishima, Susuki, Shinoda, Maekawa (1955)] and [Randl (1997)].

Since both aggregate interlock and dowel action are functions of $\sqrt{\rho f_y}\ \sqrt{f_c}$, it is not surprising that the combined action of both components can be expressed by a simple formula. In [Mau, Hsu, 1988] it was shown that a simple and accurate expression is obtained by:

$$\frac{\tau_u}{f_c'} = 0.66\sqrt{\omega} < 0.3 \qquad (3.3\text{-}105)$$

where

$$\omega = \frac{\rho f_y}{f_c'}$$

ρ = reinforcement ratio = A_s / A_c

In comparison to 60 experimental results on push-off specimens, with cube strengths ranging from 15 to 75 MPa, this expression showed a ratio $\tau_{u,exp} / \tau_{u,calc} = 1.00$ with a coefficient of variation of only 0.11. This means that a characteristic lower bound expression is obtained with

$$\tau_{uk} = 0.48\sqrt{\rho f_y}\sqrt{f_c} < 0.3 f_c \qquad (3.3\text{-}106)$$

In MC90 a design expression is given by eq. (3.9-3) which is based on the equation

$$\tau_{uk} = 0.40 f_c^{2/3}\left(\sigma + \rho f_y\right)^{1/3} \qquad (3.3\text{-}107)$$

In this equation the effect of an external compressive stress σ has been considered to be equivalent to the effect of yielding reinforcement. This is not completely logical, since yielding of the reinforcement occurs at a crack width w ≅ 0.3-0.4 mm, whereas in the case of an external compressive stress this value occurs already at w = 0.0-0.1 mm. Fig. 3.3-68 shows a comparison between eqs. (3.3-106) and (3.3-107). It turns out that the equation (3.3-107) is less conservative. This might be caused by the type of tests results used in the evaluation. For eq. (3.3-106) only specimens with ρf_y have been used, whereas eq. (3.3-107) is predominantly based on tests with σ.

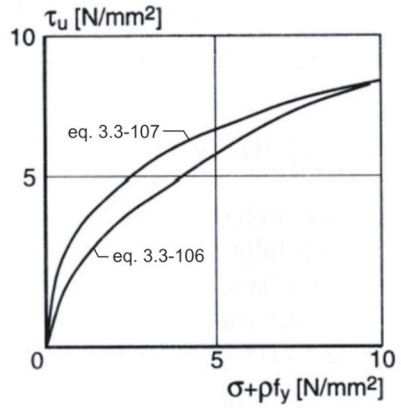

Fig. 3.3-68: Comparison of the shear friction eqs. (3.3-106) and (3.3-107) for fc=30 N/mm2

In MC90 also an idealized shear stress-shear slip relationship is given. This relationship is shown in Fig. 3.3-68. The ultimate design shear friction capacity, according to eq. 3.3-107 is used as reference.

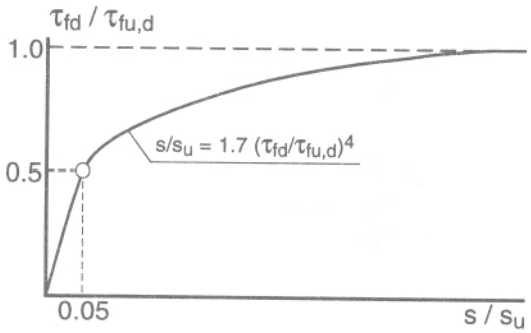

Fig. 3.3-68: Shear stress τfd as a function of shear slip s, based on su=2.0 mm

(5) Biaxial crushing criterion for cracked reinforced concrete elements under biaxial loading

In a cracked concrete member the concrete stress will be initially more or less parallel to the direction of the cracks. Due to the action of the reinforcement, intersecting the struts between the cracks, tensile stresses, due to bond of the reinforcement, will act into the direction perpendicular to the struts. The reinforcement will also cause splitting action (Fig. 3.3-70).

Due to these detrimental effects, another stress-strain relation, with a lower peak value, applies in the principal compression direction. The reduction of the peak depends on the degree of disturbance. A number of parameters have an influence, such as the diameter of the bars and their bond properties, the distance between the bars, their orientation with regard to the crack direction and the strain in the bars.

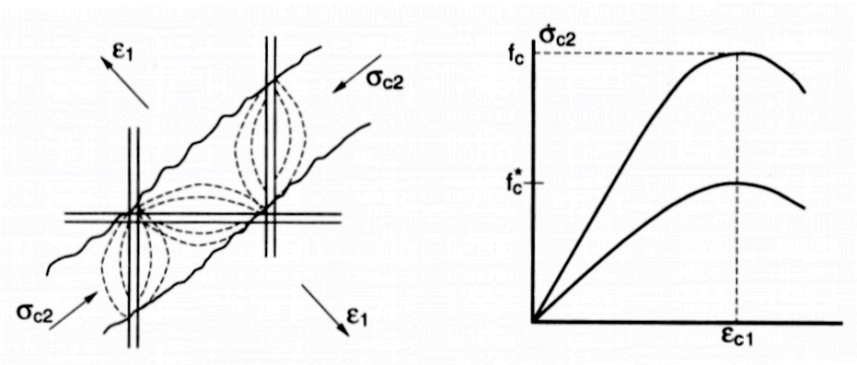

Fig. 3.3-70: Reducing action of the transverse reinforcement on the crushing capacity of the concrete struts

Quite a number of authors have investigated this mechanism and various proposals have been formulated to quantify the strength reduction of the struts. Based on a large number of panel tests, the following expression was proposed [Vecchio, Collins (1986)]:

$$\frac{f_c^*}{f_c} = \frac{1}{0.8 + 0.34\dfrac{\varepsilon_1}{\varepsilon_{c1}}} \qquad (3.3\text{-}109)$$

where ε_1 is the strain in the principal tension direction and ε_{c1} is the concrete strain corresponding to f_c under axial loading (Fig. 3.3-70). If $\varepsilon_{c1} = 2‰$, eq. (3.3-109) simplifies to

$$\frac{f_c^*}{f_c} = \frac{1}{0.8 + 170\varepsilon_1} \qquad (3.3\text{-}110)$$

During the application of the load, however, redistribution of forces can occur, resulting in a rotation of the principal compression direction. The principal compressive stresses have now to be transmitted across the cracks, inclined to the strut direction (Fig.3.3-71).

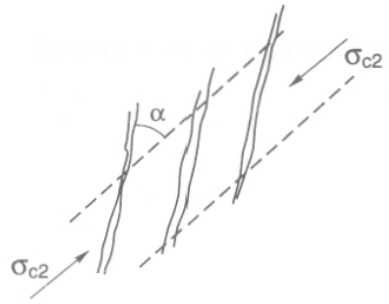

Fig. 3.3-71: Concrete strut with inclined cracks

It can be expected that, due to the action of the inclined cracks, a further reduction of the crushing capacity occurs, which is the more significant, the larger is the angle α. Values of α up to 20° are common for practical structures. In [Roos (1995)] this influence was quantified on the basis of selected test results (Fig. 3.3-72).

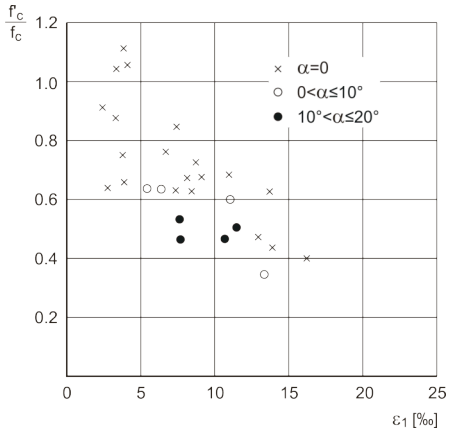

Fig. 3.3-72: Influence of cracks, inclined to the compression strut direction, [Roos (1995)]

MC90 gives the following formulation (Ch. 3.4, eq, 3.4-3): "For cracking parallel to the direction of applied compression, the reduced design concrete strength due to transverse tension can be taken as

$$f_c^* = f_c\left(1+\frac{k\varepsilon_1}{\varepsilon_{c1}}\right) \qquad (3.3\text{-}111)$$

in which ε_1 is the average (smeared) tensile strain of cracked concrete normal to the direction of applied compression, and k a coefficient which depends on the surface roughness and the diameter of the bars. For medium diameter deformed bars, k can be taken equal to 0.1, whereas for small diameter smooth welded wire mesh, k is approximately equal to 0.2"

In Fig. 3.3-73 the various formulations are compared.

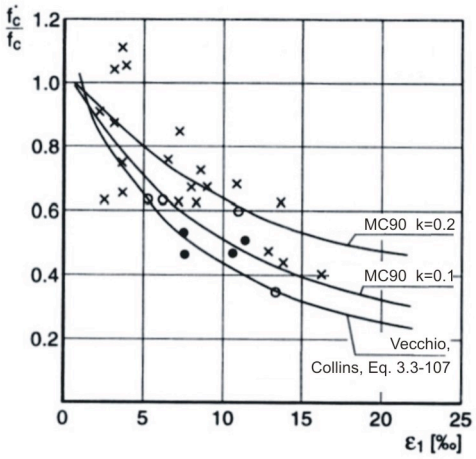

Fig. 3.3-73: Comparison of various formulations

References to Section 3.3.6

CEB Bulletin 213/214 (1993), *CEB-FIP Model Code 1990*, published by Thomas Telford Ltd., UK. ("MC90")

Dei Poli, S., di Prisco, M., Gambarova, P.G. (1993), *Cover and stirrup effects on the shear response of dowel bar embedded in concrete*. ACI Structural Journal, Vol. 90, pp. 441-450.

Mau, S.T., Hsu, T.C. (1988), Discussion contribution in PCI-Journal, Vol. 33, No. 1, pp. 166-170.

Mishima, T., Suzuki, A., Shinoda, Y., Maekawa, K. (1995), *Non elastic behaviour of axial reinforcement subjected to axial and slip deformation at the crack surface*. Journal of the American Concrete Institute, ACI, Vol. 92, No. 3, pp. 380-395.

Pruijssers, A.F. (1988), *Theoretical and experimental analysis of the behaviour of cracked concrete under monotonic and cyclic shear loading*. Heron 33, pp. 5-72.

Randl, N. (1997), *Untersuchungen zur Kraftübertragung zwischen Alt-und Neubeton bei unterschiedliche*, Fugenrauhigkeiten, Dissertation, University of Innsbruck.

Rasmussen, B.H. (1962), *Strength of transversely loaded bolts and dowels cast into concrete*. Laboratoriet for Bugningastatik, Denmark Technical University.

Roos, W. (1995), *Zur Druckfestigkeit des gerissenen Stahlbetons in scheibenförmigen Bauteilen bei gleichzeitig wirkender Querzugbelastung*. Berichte aus den Konstruktiven Ingenieurbau, TU München, 2/95.

Vecchio, F.J., Collins, M.P. (1986), *The modified compression-field theory for reinforced concrete elements subjected to shear*. ACI-Journal/March-April 1986, pp. 219-231.

Walraven, J.C. (1981), *Fundamental analysis of aggregate interlock*. Journal of the Structural Division, Proceedings of the ASCE, Vol. 107, 2245-2270.

Walraven, J.C., Stroband, J. (1993), *Shear friction in high strength concrete*. ACI-Special Publication 149-17, pp. 311-330.

Annex: List of notations

Roman lower case letters:

$1/r$	curvature of a section of an element
$1/r_{(g)}$	curvature due to g
$1/r_{(g+q)}$	curvature due to g and q
$1/r_{0(g+q)}$	instantaneous (initial) curvature due to g and q
$1/r_1$	curvature of an uncracked concrete section (state I)
$1/r_{1r}$	curvature in state I under cracking moment
$1/r_2$	curvature of a cracked concrete section (state II)
$1/r_{2r}$	curvature in state II under cracking moment
$1/r_{ts}$	tension stiffening correction for curvature
a	deflection; aggregate content in concrete
a_c	elastic deflection (calculated with rigidity $E_c I_c$)
b	breadth of compression zone or flange
b_{red}	reduced breadth of web
b_x	smaller side dimension of a rectangular section
b_y	greater side dimension of a rectangular section
b_w	breadth of web
c	concrete cover; concentration of a substance in a volume element; cement content in concrete
c_1	column dimension parallel to the eccentricity of the load
c_2	column dimension perpendicular to the eccentricity of the load
c_{min}	minimum concrete cover
c_{nom}	nominal value of concrete cover (= c_{min} + tolerance)
c_s	the transverse rib spacing, i.e. the distance between the centres of two consecutive transverse ribs measured parallel to the axis of the bar
d	effective depth to the centroid of main tension reinforcement
d’	effective depth to compression reinforcement
d_{max}	maximum aggregate size
e	load eccentricity
e_0	first order eccentricity (= M_{Sd} / N_{Sd})
e_{01}	smaller value of the first order eccentricity at one end of the considered element
e_{02}	greater value of the first order eccentricity at one end of the considered element
e_{tot}	total eccentricity
f_{bd}	design value of bond stress
f_c	cylinder compressive strength of concrete
f_c*	cylinder compressive strength of concrete under triaxial loading (confined strength), reduced concrete strength due to transverse tension
f_{cc}	cylinder compressive strength of concrete under uniaxial stress
f_{cd}*	design compressive strength of concrete under triaxial loading (confined strength), reduced design concrete strength due to transverse tension
f_{cd}	design value of f_c
f_{cd1}	average design strength value in an uncracked compression zone
f_{cd2}	average design strength value in a cracked compression zone
$f_{cd,fat}$	design fatigue reference strength of concrete under compression

f_{ck}	characteristic value of f_c
$f_{ck,cf}$	value of f_{ck} of confined concrete
$f_{ck,cube}$	characteristic value of cube compressive strength of concrete
$f_{ck,fat}$	fatigue reference compressive strength
f_{cm}	mean value of compressive strength f_c at an age of 28 days
f_{ct}	axial tensile strength of concrete (determined according to RILEM CPC 7)
f_{ctd}	design value of f_{ct}
f_{ctk}	characteristic value of f_{ct}
f_{ctm}	mean axial tensile strength
$f_{ct,fl,m}$	mean flexural tensile strength (at T = 20°C)
$f_{ct,sp,m}$	mean splitting tensile strength
f_d	design value of strength
$f_{p0,1}$	0,1% proof stress of prestressing reinforcement
$f_{p0,2}$	0,2% proof stress of prestressing reinforcement
$f_{p0,1k}$	characteristic 0,1% proof stress
$f_{p0,2k}$	characteristic 0,2% proof stress
f_{pt}	tensile strength of prestressing reinforcement
f_{ptd}	design tensile strength of prestressing reinforcement
f_{ptk}	characteristic tensile strength of prestressing reinforcement
f_{py}	tension yield stress of prestressing reinforcement
f_{pyd}	design value of tension yield stress of prestressing reinforcement
f_{pyk}	characteristic value of tension yield stress of prestressing reinforcement
f_R	relative (or projected) rib area
f_t	tensile strength of non- prestressing reinforcement
f_{tk}	characteristic value of tensile strength of non- prestressing reinforcement
f_y	tension yield stress of non- prestressing reinforcement
f_{yc}	yield strength of steel in compression
f_{ycd}	design strength of steel in compression
f_{yd}	design value of tension yield stress of non- prestressing reinforcement
f_{yk}	characteristic value of tension yield stress of non- prestressing reinforcement
g_d	design value of distributed permanent load
h	overall depth of member, total height; notional size of a member (2 A_c/u; u: perimeter in contact with the atmosphere)
h_b	depth of beam
h_f	depth of flange
h_l	the longitudinal rib height, i.e. the distance from the highest point of the rib to the surface of the core measured normal to the axis of the bar
h_s	the transverse rib height, i.e. the distance from the mid- point of the considered segment on the rib to the surface of the core measured normal to the axis of the bar
Δh_w	height of water column
i	radius of gyration, number of longitudinal ribs
j	the length of the pitch of the longitudinal rib on twisted bar
k	the number of the rows of the transverse ribs around the perimerer
l	design span, effective span, length of an element, thickness of a penetrated section
Δl	measured elongation between two measuring points
l_0	design lap length; effective length (of columns); distance between measuring points
l_b	basic anchorage length

l_{bp}	basic anchorage length of pretensioned reinforcement
l_{bpd}	design anchorage length of pretensioned reinforcement
l_{bpt}	transmission length of pretensioned reinforcement
$l_{b,min}$	minimum anchorage length
$l_{b,net}$	design anchorage length
l_{ch}	lever arm characteristic length (fracture parameter)
l_p	development length for prestressing reinforcement
l_{pl}	plastic length (region in which tensile strain is larger than yield strain)
Δl_{pl}	residual elongation after unloading
$l_{p,max}$	length over which the slip between prestressing steel and concrete occurs
$l_{s,max}$	length over which the slip between steel and concrete occurs
l_t	transmission length
m	moment per unit width (out-of-plane loading); mass of substance flowing; degree of hydration; the number of transverse ribs in one row over the distance considered
n	number of bars, number of load cycles; force per unit width (in-plane-loading)
n_{Ri}	number of cycles leading to failure at stress levels $S_{i,min}$ and $S_{i,max}$, respectively
n_{Si}	number of cycles applied at constant minimum and maximum stress levels $S_{i,min}$ and $S_{i,max}$, respectively
p	local gas pressure; the number of segments on transverse rib considered
q	distributed variable load
q_d	design value of distributed variable load
r	radius
s	slip (relative displacement of steel and concrete cross-sections); shear slip (at interfaces); spacing of bars; coefficient which depend on the strength class of cement
s_{max}	maximum bar spacing
s_r	distance between cracks; radial spacing of layers of shear reinforcement
s_{rm}	mean spacing between cracks
t	time, age, duration; thickness of thin elements
t_0	age at loading
t_s	concrete age at the beginning of shrinkage or swelling
t_T	effective concrete age
u	length of a perimeter; component of displacement of a point
u_0	length of the periphery of the column or load
u_l	length of the control perimeter for punching
u_{ef}	length of the perimeter of A_{ef}
u_n	length of the control perimeter for punching outside a slab zone with shear reinforcement
v	shear force per unit width (out-of-plane loading), component of displacement of a point
w	crack width; component of displacement of a point, water content in concrete
w_c	crack width for $\sigma_{ct} = 0$
w_k	calculated characteristic crack width
w_{lim}	nominal limit value of crack width
x	depth of compression zone, distance
z	internal

Greek lower case letters:

α	coefficient, reduction factor
α_e	modular ratio (E_s / E_c)
α_E	coefficient which depends on the type of aggregete
α_{es}	coefficient which depends on the type of cement
$\alpha_{e,p}$	modular ratio (E_p / E_c)
$\alpha_{e,sec}$	secant modular ratio ($E_{s,sec}$ / $E_{c,sec}$)
α_{sT}	coefficient of thermal expansion for steel
α_T	coefficient of thermal expansion in general
β_1	coefficient characterizing the bond quality of reinforcing bars
$\beta_c(t,t_0)$	coefficient to describe the development of creep with time after loading
$\beta_{as}(t)$	function to describe the development of autogenous shrinkage
$\beta_{RH}(RH)$	coefficient to take into account the effect of rel. humidity on drying shrinkage
$\beta_{ads}(t-t_s)$	function to describe the time development of drying shrinkage
β_s	transverse rib inclination i.e. the angle between the centre line of the transverse rib and the longitudinal axis of the bar
γ	safety factor
γ_c	partial safety factor for concrete material properties
$\gamma_{c,fat}$	partial safety factor for concrete material properties under fatigue loading
γ_F	partial safety factor for actions
γ_G	partial safety factor for permanent actions
γ_Q	partial safety factor for variable actions
γ_s	partial safety factor for the material properties of reinforcement and prestressing steel
$\gamma_{s,fat}$	partial safety factor for the material properties of reinforcement and prestressing steel under fatigue loading
δ_{ii}	node displacement
ε	strain
ε_c	concrete compression strain
ε_c*	concrete compression strain under triaxial stress
ε_{cm}	average concrete strain within $l_{s,max}$
ε_{c0}	concrete strain at peak stress in compression
$\varepsilon_{cc}(t)$	concrete creep strain at concrete age $t > t_0$
$\varepsilon_{ci}(t_0)$	stress dependent initial strain at the time of stress application
$\varepsilon_{cn}(t)$	total stress independent strain at a concrete age t (= $\varepsilon_{cs}(t) + \varepsilon_{cT}(t,T)$)
$\varepsilon_{cs}(t,t_s)$	total shrinkage or swelling strain at concrete age t (t in days)
$\varepsilon_{cs}(t,t_s)$	total shrinkage or swelling strain at concrete age t (t in days)
$\varepsilon_{cas}(t,t_0)$	autogenous shrinkage at time (t in days)
$\varepsilon_{cds}(t,t_0)$	drying shrinkage at time (t in days)
$\varepsilon_{caso}(f_{cm})$	notinal autogenous shrinkage coefficient
$\varepsilon_{cds}(f_{cm})$	notinal drying shrinkage coefficient
$\varepsilon_{c\sigma}(t)$	total stress dependent strain at a concrete age t (= $\varepsilon_{ci}(t_0) + \varepsilon_{cc}(t)$)
ε_{ct}	concrete tensile strain
$\varepsilon_{cT}(t,T)$	thermal strain at a concrete age t
ε_{cu}	ultimate strain of concrete in compression
ε_{d0}	strain of prestressed reinforcement corresponding to P_{d0}
ε_{pu}	total elongation of prestressing reinforcement at maximum load

ε_r strain at the onset of cracking
ε_s steel strain
ε_{s1} steel strain in uncracked concrete
ε_{s2} steel strain in the crack
ε_{sm} mean steel strain
$\Delta\varepsilon_{sr}$ increase of steel strain in cracking state
ε_{sr1} steel strain at the point of zero slip under cracking forces
ε_{sr2} steel strain in the crack under cracking forces (σ_{ct} reaching f_{ctm})
ε_{sT} thermal strain of steel
ε_{su} ultimate strain of non- prestressing reinforcement at maximum load
$\Delta\varepsilon_{ts}$ increase of strain by the effect of tension stiffening
ε_u total elongation of reinforcing steel at maximum load
ε_{uk} characteristic total elongation of reinforcing steel at maximum load
ε_{yd} design yield strain of non - prestressing reinforcement (= f_{yd} / E_s)
ε_ν transverse contraction
ζ ratio of bond strength of prestressing steel and high-bond reinforcing steel
η viscosity
θ angle between web compression and the axis of a member; rotation
θ_f angle between inclined compression in a flange and the axis of the member
λ slenderness ratio (= l_0 / i); span/depth ratio
μ coefficient of friction, relative bending moment
ν relative axial force
ν_c Poisson's ratio of concrete
ν_s Poisson's ratio of steel
ν_{Sd} relative design axial force (= N_{Sd} / $A_c f_{cd}$)
ρ ratio of (longitudinal) tension reinforcement (= A_s/bd)
$\rho_{s,ef}$ effective reinforcement ratio (= $A_s/A_{c,ef}$)
ρ_t relaxation after t hours
ρ_w ratio of web reinforcement (= $A_{sw}/b_w s \cdot \sin\alpha$)
σ stress
$\chi\ (t,t_0)$ ageing cooeficient
$\sigma_1,\sigma_2,\sigma_3$ principal stresses
σ_c concrete compression stress
σ_{cd} design concrete compression stress
σ_{ct} concrete tensile stress
$\sigma_{c,cf}$ compression stress of confined concrete
$\sigma_{c,max}$ maximum compressive stress
$\sigma_{c,min}$ minimum compressive stress
$\sigma_{p0}\,(x)$ initial stress in prestressing reinforcement at a distance x from anchorage device
$\sigma_{p0,max}$ maximum tensile stress in prestressing reinforcement at tensioning
σ_{pcs} tendon stress due to prestress after all losses (due to creep and shrinkage)
σ_{pd} tendon stress under design load
$\Delta\sigma_{Rsk}(n)$ stress range relevant to n cycles obtained from a characteristic fatigue strength function
σ_s steel stress
σ_{s2} steel stress in the crack
σ_{sE} steel stress at the point of zero slip

σ_{sr2} steel stress in the crack under crack loading (σ_{ct} reaching f_{ctm})
$\Delta\sigma_{Ss}$ steel stress range under the acting loads
$\Delta\sigma_p$ loss of prestress
σ_{sw} stirrups stress
τ_b local bond stress
τ_{bm} mean bond stress
$\tau_{fu,d}$ ultimate design shear friction capacity
τ_{max} maximum value of bond stress
τ_{Rd} resistance to shear stress (design value)
τ_{Sd} applied shear stress (design value)
$\psi(t,t_0)$ relaxation coefficient
ω mechanical reinforcement ratio
ω_{sw} mechanical ratio of stirrup reinforcement
ω_v volumetric ratio of confining reinforcement
ω_w volumetric mechanical ratio of confining reinforcement
ω_{wd} design volumetric mechanical ratio of confining reinforcement

Roman capital letters:

A total area of a section or part of a section (enclosed within the outer circumference)
A_1 section area in state I (taking into account the reinforcement)
A_c area of concrete cross section or concrete compression chord
$A_{c,ef}$ effective area of concrete in tension
A_{core} effectively confined area of cross-section in compression
A_{ef} area enclosed by the centre-lines of a shell resisting torsion
A_p cross-sectional area of prestressing reinforcement
A_s cross-sectional area of reinforcement
A_s' cross-sectional area of compressed reinforcement
A_{sh} cross-sectional area of hoop reinforcement for torsion
A_{sl} cross-sectional area of longitudinal reinforcement
A_{st} cross-sectional area of transverse reinforcement
A_{sw} cross-sectional area of shear reinforcement
$A_{s,cal}$ calculated cross-sectional area of reinforcement required by design
$A_{s,ef}$ cross-sectional area of reinforcement provided
$A_{s,min}$ minimum reinforcement area
C_{eq} the equivalent carbon value
D fatigue damage, diffusion coefficient
$D^{el}(t)$ system of deformations in the associated elastic problem
D_{lim} limiting fatigue damage
E modulus of elasticity
E_c modulus of elasticity for concrete
$E_c(t_0)$ modulus of elasticity at the time of loading t_0
E_{ci} tangent modulus of elasticity at a stress σ_i (at T = 20°C)
$E_{c,sec}$ secant modulus of elasticity at failure for uniaxial compression ($E_{c,sec} = f_{cm}/|\varepsilon_{c0}|$)
E_p modulus of elasticity of prestressing steel
E_s modulus of elasticity of steel
$E_{s,sec}$ secant modulus of elasticity of steel
F force, applied load or load effect

F_b	bond force transmitted along the transmission length
F_c	strut force (compression force)
F_d	design value of action
F_{pt}	tensile load of prestressed reinforcement
$F_{p0,1}$	characteristic 0,1% proof -load
$F_{Sd,ef}$	effective concentric load (punching load enhanced to allow for the effects of moments)
F_t	tie force (tension force)
F_{ud}	ultimate dowel force
G	permanent action
G_F	fracture energy of concrete
G_{F0}	base value of fracture energy (depending on maximum aggregate size)
G_{inf}	favourable part of permanent action
G_{sup}	unfavourable part of permanent action
H	horizontal force, horizontal component of a force
I	second moment of area
I_1	second moment of area in state I (including the reinforcement)
I_2	second moment of area in state II (including the reinforcement)
I_c	second moment of area of the uncracked concrete cross-section (state I)
$J(t,t_0)$	creep function or creep compliance representing the total stress dependent strain per unit stress
K_g	coefficient of gas permeability
K_w	coefficient of water permeability
L	span, length of an element
M	bending moment; maturity of concrete
M_r	cracking moment
M_{Rd}	design value of resistant moment
M_{Sd}	design value of applied moment
M_u	ultimate moment
M_y	yielding moment
N	axial force, number of cycles to failure (fatigue loading)
N_r	axial cracking force
N_{Rd}	design value of resistance to axial force
N_{Sd}	design value of applied axial force
P_{d0}	design value of prestressing force (initial force)
$P_{k,inf}$	lower characteristic value of prestressing force
$P_{k,sup}$	upper characteristic value of prestressing force
P_m	mean value of prestressing force
Q	variable single action
$R(t, t_0)$	relaxations function
R	resistance (strength); bending radius; universal gas constant
R_d	design resistance
RH	ambient relative humidity
RH_0	100% relative humidity
S	load effect (M, N, V, T); absorption coefficient
ΔS_{cd}	stress range under fatigue loading
$S_{cd,max}$	design value of maximum compressive stress level (fatigue loading)

$S_{cd,min}$ design value of minimum compressive stress level (fatigue loading)
$S_{c,max}$ maximum compressive stress level (fatigue loading)
$S_{c,min}$ minimum compressive stress level (fatigue loading)
S_d design value of load effect (M, N, V, T)
$S^{el}(t)$ system of stresses in the associated elastic problem
T temperature, torsional moment
ΔT temperature change
T_{Rd} design value of resistance to torsional moment
T_{Sd} design value of applied torsional moment
$T_{Sd,eff}$ effective design value of applied torsional moment
V shear force; volume of gas or liquid
V_{Rd} design value of resistance to shear force
V_{Sd} design value of applied shear force
$V_{s,trans}$ volume of closed stirrups or cross-ties
V_u ultimate shear force
W_1 section modulus in state I (including the reinforcement)
W_2 section modulus in state II (including the reinforcement)
W_c section modulus of the uncracked concrete cross-section (state I)
$W_{c,cf}$ volume of confined concrete
W_e external work
W_i internal work

<u>others:</u>

ø nominal diameter of steel bar
$ø_n$ equivalent diameter of bundles containing n bars
$ø_p$ diameter of prestressing steel (for bundles equivalent diameter)
$\phi\ (t,t_0)$ creep coefficient
ϕ_0 notional creep coefficient
Θ_{pl} plastic rotation capacity
$\sum U$ total perimeter of rebars

fib *– fédération internationale du béton – the International Federation for Structural Concrete – is grateful for the invaluable support of the following National Member Groups and Sponsoring Members, which contributes to the publication of* ***fib*** *technical bulletins, the Structural Concrete Journal, and* ***fib****-news.*

National Member Groups

AAHES – Asociación Argentina delHormigón Estructural, Argentina
CIA – Concrete Institute of Australia
ÖVBB – Österr. Vereinigung Für Beton und Bautechnik, Austria
Belarussian Nat. Techn. University
GBB – Groupement Belge du Béton, Belgium
ABCIC – Associação Brasileira da Construção Industrializada de Concreto, Brazil
ABECE – Associação Brasileira de Engenharia e Consultoria Estrutural, Brazil
Université Laval, Département du Génie Civil, Canada
CCES – China Civil Engineering Society
Hrvatska Ogranak ***fib***-a (HOFIB) – Croatian Group of ***fib***
Cyprus University of Technology
Ceska betonarska spolecnost, Czech Republic
Dansk Betonforening DBF – Danish Concrete Society
Suomen Betoniyhdistys r.y. – Concrete Association of Finland
AFGC – Association Française de Génie Civil, France
Deutscher Ausschuss für Stahlbeton, Germany
Deutscher Beton- und Bautechnik-Verein e.V. – dbv, Germany
Technical Chamber of Greece
Hungarian Group of ***fib***, Budapest Univ. of Tech. & Economics
The Institution of Engineers (India)
Management and Planning Organization, Iran
IACIE – Israeli Association of Construction and Infrastructure Engineers
Consiglio Nazionale delle Ricerche, Italy
JCI – Japan Concrete Institute
PCEA – Prestressed Concrete Engineering Association, Japan
Administration des Ponts et Chaussées, Luxembourg
Betonvereniging – ***fib*** Netherlands
New Zealand Concrete Society
Norsk Betongforening – Norwegian Concrete Association
Chancellery of the Polish Academy of Sciences
Committee of Civil Engineering, Concrete Structures Section, Poland
GPBE – Grupo Portugês de Betão Estrutural, Portugal
Socety For Concrete and Prefab Units of Romania
Technical University of Civil Engineering, Romania
Association for Structural Concrete (ASC), Russia
Association of Structural Engineers, Serbia

Slovak Union of Civil Engineers
Slovenian Society of Structural Engineers
ACHE – Asociacion Cientifico-Técnica del Hormigon Estructural, Spain
Svenska Betongföreningen, Sweden
Délégation nationale suisse de la ***fib***, IS-BETON, EPFL, Switzerland
ITU – Istanbul Technical University, Turkey
Research Inst. of Build. Constructions, Ukraine
fib UK Group
ASBI – American Segmental Bridge Institute, USA
PCI – Precast/Prestress. Concrete Institute, USA
PTI – Post Tensioning Institute, USA

Sponsoring Members

Preconco Limited, Barbados
Liuzhou OVM Machinery Co., Ltd., China
CONSOLIS TECHNOLOGY Oy Ab, Finland
Fachverband Beton- u. F. B.-W. e. V., Germany
FIREP Rebar Technology GmbH, Germany
Larsen & Toubro Ltd ECC Division, India
Sireg S.P.A., Italy
FKK Kyokuto Kogen Concrete Shinko Co. Ltd., Japan
FUJI P. S. Corporation Ltd., Japan
KAJIMA Corporation, Japan
OBAYASHI Corporation, Japan
ORIENTAL Construction Co.Ltd., Japan
P. S. Mitsubishi Construction Co., Ltd., Japan
PC BRIDGE Company Ltd., Japan
SE Corporation, Japan
SUMITOMO MITSUI Construct. Co.Ltd., Japan
BBR VT International Ltd., Switzerland
SIKA Services AG, Switzerland
VSL International Ltd, Switzerland
PBL Group Ltd., Thailand
CCL Stressing Systems Ltd., United Kingdom
Strongforce Engineering PLC, United Kingdom

fib Bulletins published since 1998

N°	Title
1	Structural Concrete – Textbook on Behaviour, Design and Performance; Vol. 1: Introduction - Design Process – Materials Manual - textbook (244 pages, ISBN 978-2-88394-041-3, July 1999)
2	Structural Concrete – Textbook on Behaviour, Design and Performance Vol. 2: Basis of Design Manual - textbook (324 pages, ISBN 978-2-88394-042-0, July 1999)
3	Structural Concrete – Textbook on Behaviour, Design and Performance Vol. 3: Durability - Design for Fire Resistance - Member Design - Maintenance, Assessment and Repair - Practical aspects Manual - textbook (292 pages, ISBN 978-2-88394-043-7, December 1999)
4	Lightweight aggregate concrete: Extracts from codes and standards State-of-the-art report (46 pages, ISBN 978-2-88394-044-4, August 1999)
5	Protective systems against hazards: Nature and extent of the problem Technical report (64 pages, ISBN 978-2-88394-045-1, October 1999)
6	Special design considerations for precast prestressed hollow core floors Guide to good practice (180 pages, ISBN 978-2-88394-046-8, January 2000)
7	Corrugated plastic ducts for internal bonded post-tensioning Technical report (50 pages, ISBN 978-2-88394-047-5, January 2000)
8	Lightweight aggregate concrete: Part 1 (guide) – Recommended extensions to Model Code 90; Part 2 (technical report) – Identification of research needs; Part 3 (state-of-art report) – Application of lightweight aggregate concrete (118 pages, ISBN 978-2-88394-048-2, May 2000)
9	Guidance for good bridge design: Part 1 – Introduction, Part 2 – Design and construction aspects. Guide to good practice (190 pages, ISBN 978-2-88394-049-9, July 2000)
10	Bond of reinforcement in concrete State-of-art report (434 pages, ISBN 978-2-88394-050-5, August 2000)
11	Factory applied corrosion protection of prestressing steel State-of-art report (20 pages, ISBN 978-2-88394-051-2, January 2001)
12	Punching of structural concrete slabs Technical report (314 pages, ISBN 978-2-88394-052-9, August 2001)
13	Nuclear containments State-of-art report (130 pages, 1 CD, ISBN 978-2-88394-053-6, September 2001)
14	Externally bonded FRP reinforcement for RC structures Technical report (138 pages, ISBN 978-2-88394-054-3, October 2001)
15	Durability of post-tensioning tendons Technical report (284 pages, ISBN 978-2-88394-055-0, November 2001)
16	Design Examples for the 1996 FIP recommendations *Practical design of structural concrete* Technical report (198 pages, ISBN 978-2-88394-056-7, January 2002)

N°	Title
17	Management, maintenance and strengthening of concrete structures Technical report (180 pages, ISBN 978-2-88394-057-4, April 2002)
18	Recycling of offshore concrete structures State-of-art report (33 pages, ISBN 978-2-88394-058-1, April 2002)
19	Precast concrete in mixed construction State-of-art report (68 pages, ISBN 978-2-88394-059-8, April 2002)
20	Grouting of tendons in prestressed concrete Guide to good practice (52 pages, ISBN 978-2-88394-060-4, July 2002)
21	Environmental issues in prefabrication State-of-art report (56 pages, ISBN 978-2-88394-061-1, March 2003)
22	Monitoring and safety evaluation of existing concrete structures State-of-art report (304 pages, ISBN 978-2-88394-062-8, May 2003)
23	Environmental effects of concrete State-of-art report (68 pages, ISBN 978-2-88394-063-5, June 2003)
24	Seismic assessment and retrofit of reinforced concrete buildings State-of-art report (312 pages, ISBN 978-2-88394-064-2, August 2003)
25	Displacement-based seismic design of reinforced concrete buildings State-of-art report (196 pages, ISBN 978-2-88394-065-9, August 2003)
26	Influence of material and processing on stress corrosion cracking of prestressing steel – case studies. Technical report (44 pages, ISBN 978-2-88394-066-6, October 2003)
27	Seismic design of precast concrete building structures State-of-art report (262 pages, ISBN 978-2-88394-067-3, January 2004)
28	Environmental design State-of-art report (86 pages, ISBN 978-2-88394-068-0, February 2004)
29	Precast concrete bridges State-of-art report (83 pages, ISBN 978-2-88394-069-7, November 2004)
30	Acceptance of stay cable systems using prestressing steels Recommendation (80 pages, ISBN 978-2-88394-070-3, January 2005)
31	Post-tensioning in buildings Technical report (116 pages, ISBN 978-2-88394-071-0, February 2005)
32	Guidelines for the design of footbridges Guide to good practice (160 pages, ISBN 978-2-88394-072-7, November 2005)
33	Durability of post-tensioning tendons Recommendation (74 pages, ISBN 978-2-88394-073-4, December 2005)
34	Model Code for Service Life Design Model Code (116 pages, ISBN 978-2-88394-074-1, February 2006)
35	Retrofitting of concrete structures by externally bonded FRPs. Technical Report (224 pages, ISBN 978-2-88394-075-8, April 2006)
36	2006 *fib* Awards for Outstanding Concrete Structures Bulletin (40 pages, ISBN 978-2-88394-076-5, May 2006)

N°	Title
37	Precast concrete railway track systems State-of-art report (38 pages, ISBN 978-2-88394-077-2, September 2006)
38	Fire design of concrete structures – materials, structures and modelling State-of-art report (106 pages, ISBN 978-2-88394-078-9, April 2007)
39	Seismic bridge design and retrofit – structural solutions State-of-art report (300 pages, ISBN 978-2-88394-079-6, May 2007)
40	FRP reinforcement in RC structures Technical report (160 pages, ISBN 978-2-88394-080-2, September 2007)
41	Treatment of imperfections in precast structural elements State-of-art report (74 pages, ISBN 978-2-88394-081-9, November 2007)
42	Constitutive modelling of high strength / high performance concrete State-of-art report (130 pages, ISBN 978-2-88394-082-6, January 2008)
43	Structural connections for precast concrete buildings Guide to good practice (370 pages, ISBN 978-2-88394-083-3, February 2008)
44	Concrete structure management: Guide to ownership and good practice Guide to good practice (208 pages, ISBN 978-2-88394-084-0, February 2008)
45	Practitioners' guide to finite element modelling of reinforced concrete structures State-of-art report (344 pages, ISBN 978-2-88394-085-7, June 2008)
46	Fire design of concrete structures —structural behaviour and assessment State-of-art report (214 pages, ISBN 978-2-88394-086-4, July 2008)
47	Environmental design of concrete structures – general principles Technical report (48 pages, ISBN 978-2-88394-087-1, August 2008)
48	Formwork and falsework for heavy construction Guide to good practice (96 pages, ISBN 978-2-88394-088-8, January 2009)
49	Corrosion protection for reinforcing steels Technical report (122 pages, ISBN 978-2-88394-089-5, February 2009)
50	Concrete structures for oil and gas fields in hostile marine environments State-of-art report (36 pages, IBSN 978-2-88394-090-1, October 2009)
51	Structural Concrete – Textbook on behaviour, design and performance, vol. 1 Manual – textbook (306 pages, ISBN 978-2-88394-091-8, November 2009)

Abstracts for *fib* Bulletins, lists of available CEB Bulletins and FIP Reports, and an order form are available on the *fib* website at www.fib-international.org/publications.